

Functional Assessment of Task-Based Brain Networks Detectable with fMRI

Chantal M. Percival^{1,2}, Hafsa B. Zahid^{1,2}, Leonardo Arreaza^{1,2}, Lily Yip^{1,2}, Ava Momeni^{1,2}, Jenn Huo^{1,2}, Melody Li^{1,2}, Nima Toussi^{1,2}, Crystal Han^{1,2}, Mehar Singh^{1,2}, Judy Cheng^{1,2}, Dayana Stamboliyska^{1,2}, Jillian Rodger^{1,2}, and Todd S. Woodward^{1,2}

¹BC Mental Health and Substance Use Services

²Department of Psychiatry, University of British Columbia

Functional Assessment of the fMRI-derived Auditory Attention-for-Response Network

Jenn Huo^{1,2}, Judy Cheng^{1,2}, Todd Woodward^{1,2}

¹BC Mental Health and Substance Use Services

²Department of Psychiatry, University of British Columbia

Abstract

Task-based functional magnetic resonance imaging (fMRI) techniques have provided further insight into the reverse inference challenge, which proposes conclusions about active cognitive processes inferred from observation of brain activity (Poldrack, 2006). Several prototype task-based functional brain networks have previously been identified by averaging over replicating studies that performed constrained principal component analysis for functional magnetic resonance imaging (fMRI-CPCA) (Percival et al., 2020). However, the specific cognitive function associated with each network remains undefined. The current study aimed to characterize the specific functions of the Auditory Attention for Response (AAR) network by comparing hemodynamic response (HDR) patterns across studies where the AAR configuration emerged. Recruitment of the AAR network involves activation in the bilateral superior temporal gyrus, supplementary motor area, left precentral gyrus, bilateral insula and thalamus (Lavigne et al., 2016; Percival et al., 2020). While the current analysis is more exploratory in nature, based on cognitive tasks that revealed engagement of the AAR network in previous studies (Lavigne et al., 2016; Lavigne & Woodward, 2018), it is hypothesized that the AAR shows activation when an individual attends to auditory sounds and a motor response to a specific auditory stimulus is expected, and that AAR suppression is associated with intensive monitoring of visual details. An example is the situation where an individual that is visually monitoring their phone is less likely to hear what someone else is saying to them. For the current study, the activation of the AAR network was compared across 8 studies for which its activation has already been identified, and interpretation of the AAR network involved comparing anatomical patterns and HDR plots in each of the studies to determine an interpretation that fits all studies.

Table of Contents

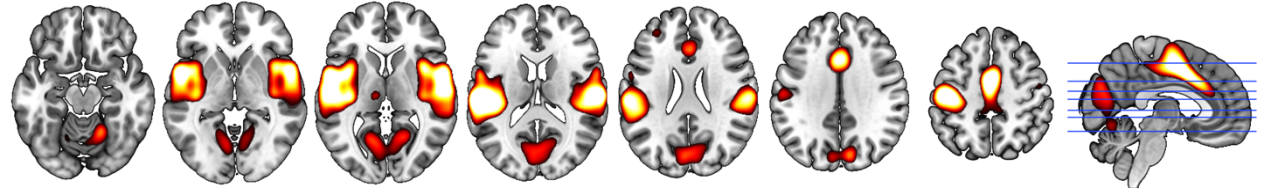
<i>Introduction</i>	4
<i>Results.....</i>	6
1a. Auditory Oddball (AO).....	6
1b. Auditory Oddball (AO); fBIRN HBM Merge	8
2a. Thought Generating Task (TGT); fBIRN HBM Merge:	9
2b. Thought Generating Task (TGT); Sanford 4-task Merge.....	10
3. Human Connectome Project Social Task	12
4. FISH Task.....	14
5. Raven's Standard Progressive Matrices Task (RSPM)	17
6. Lexical Decision Task (LDT)	20
7. Working Memory Task (WM); Sanford 4-task Merge.....	23
8. Spatial Capacity Task (SCAP); Sanford 4-task Merge.....	27
9. Task-Switch Inertia task (TSI); Sanford 4-task Merge	30
10. Source Monitoring (SM)	34
11. Semantic Integration (SI).....	36
<i>Discussion</i>	38
<i>References.....</i>	41

Introduction

While the field of neuroimaging has progressed immensely in recent years, many challenges of human brain mapping remain to be addressed. One of these is the reverse inference problem, which proposes conclusions about active cognitive processes inferred from observation of brain activity (Poldrack, 2006). By manipulating cognitive tasks and analyzing brain activity across several neural networks, different aspects of cognition can be predicted based on whole-brain patterns of neural activity. Twelve prototype task-based functional brain networks have previously been identified by averaging over replicating studies that performed constrained principal component analysis for functional magnetic resonance imaging (fMRI-CPCA) (Percival et al., 2020). However, the specific cognitive function associated with each network remains undefined. The current study will investigate the Auditory Attention for Response (AAR) network and its role in various task-based fMRI studies. Past studies have suggested that the AAR network is involved in the active monitoring of auditory information (Lavigne et al., 2016; Lavigne & Woodward, 2018). Recruitment of the AAR network is mainly characterized by activation in the bilateral superior temporal gyrus, supplementary motor area, left precentral gyrus, bilateral insula and thalamus (Lavigne et al., 2016; Percival et al., 2020) (Figure 1). While the current study is more exploratory in nature, based on cognitive tasks that showed engagement of the AAR in previous studies (Lavigne et al., 2016; Lavigne & Woodward, 2018), it is hypothesized that the AAR network is activated when an individual pays close attention to auditory sounds and a motor response to a specific auditory stimulus is expected. Conversely, the AAR is expected to show deactivation during intensive monitoring of visual details. An example is the situation where an individual that is visually monitoring their phone is less likely to hear what someone else is saying to them. As such, it is expected that AAR activity will show some overlap with the Auditory Perception (AUD) network, active when an individual listens to speech (Sanford et al., 2020). The current study compared

activation of the AAR network across 11 task-based fMRI studies for which its activation had already been identified and aims to provide an interpretation of the network that fits all studies.

Figure 1. Brain slices showing activation of the Auditory Attention for Response network (Percival et al., 2020).



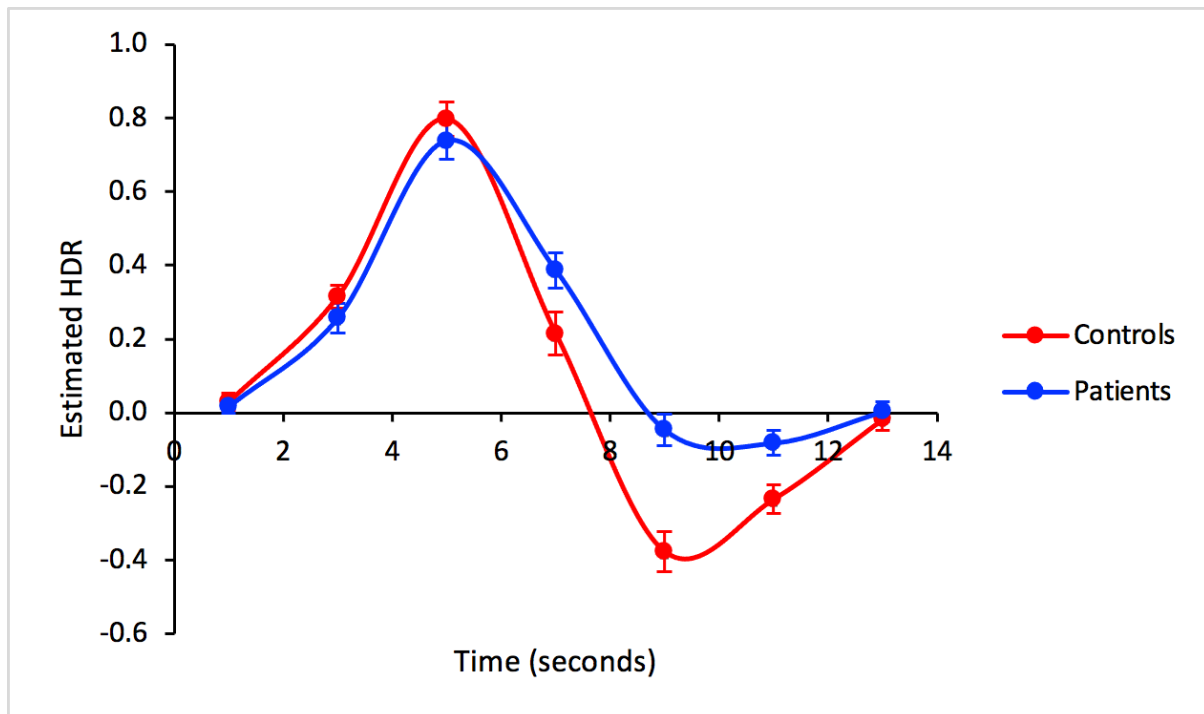
Results

1a. Auditory Oddball (AO)

AAR network was active during identification of the deviant auditory stimuli, and the HDR shape peaked at timebin 3. Mixed ANOVA revealed a significant main effect of Time, $F(6, 636) = 154.126, p < 0.001$. The Time factor was dominated by timebins 2-3 and 3-4 for increases to peak, and 3-4, 4-5, and 6-7 for decreases from peak ($p < 0.001$).

Mixed ANOVA also showed a significant main effect of Group, $F(1, 106) = 7.674, p < 0.01$ and a significant interaction of Group \times Timebin, $F(6, 636) = 7.210, p < 0.001$. Controls showed a sharper HDR decrease between timebins 3 and 4, $F(1, 106) = 8.507, p < 0.01$. Controls continued to show sharper HDR decrease and reached a lower minimum than patients from timebins 4 and 5, $F(1, 106) = 6.599, p < 0.05$ (Figure 2). Controls increased between timebins 5 and 6 while patients remained consistent, $F(1, 106) = 9.173, p < 0.01$, and controls also showed a greater HDR increase than patients between timebins 6 and 7, $F(1, 106) = 8.659, p < 0.01$. Overall, AAR is activated for both groups when listening to deviant tones. Patients showed more sustained activation of the AAR network during completion of the task, and healthy controls showed a sharper decline as indicated by more deactivation when returning to baseline.

Figure 2. HRF HDR for Auditory Oddball task averaged over Group (Healthy_Schizophrenia).

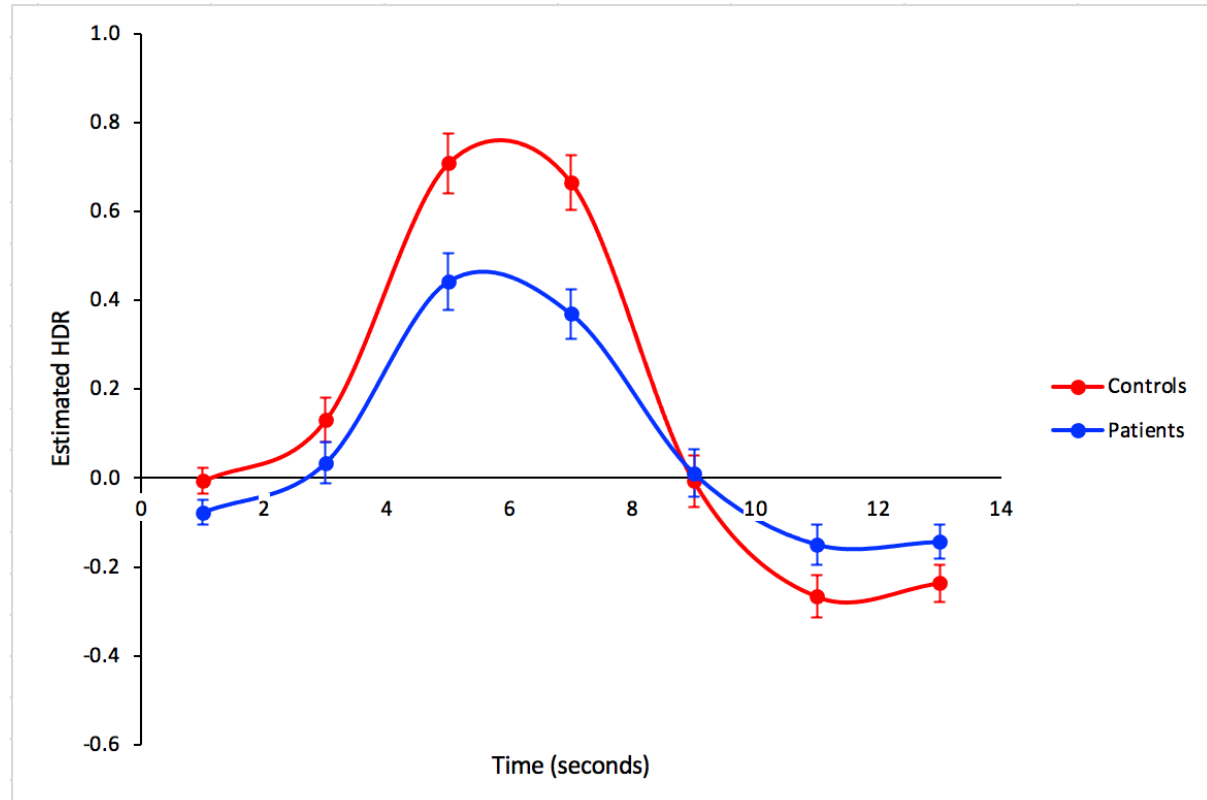


1b. Auditory Oddball (AO); fBIRN HBM Merge

Mixed ANOVA revealed significant main effect of Time, $F(6, 636) = 103.364, p < 0.001$, which was dominated by contrasts 1-2 and 2-3 for increases to peak and contrasts 4-5 and 5-6 for decreases from peak, $p < 0.001$.

Although there was no significant main effect of Group ($p = 0.081$), there was a significant interaction between Group \times Timebin, $F(6, 636) = 6.775, p < 0.001$. Controls increased faster than and reached a higher peak than Patients between timebins 2 and 3, $F(1, 106) = 7.693, p < 0.01$. Controls also decrease more sharply than Patients between timebins 4 and 5, $F(1, 106) = 18.900, p < 0.001$ (Figure 3). Similar to previous Auditory Oddball analysis, there was also AAR activation in both groups to deviant auditory stimuli, with faster activation, a higher peak, and sharper deactivation in controls.

Figure 3. HRF HDR averaged over Group (Controls_Patients) for Auditory Oddball task.

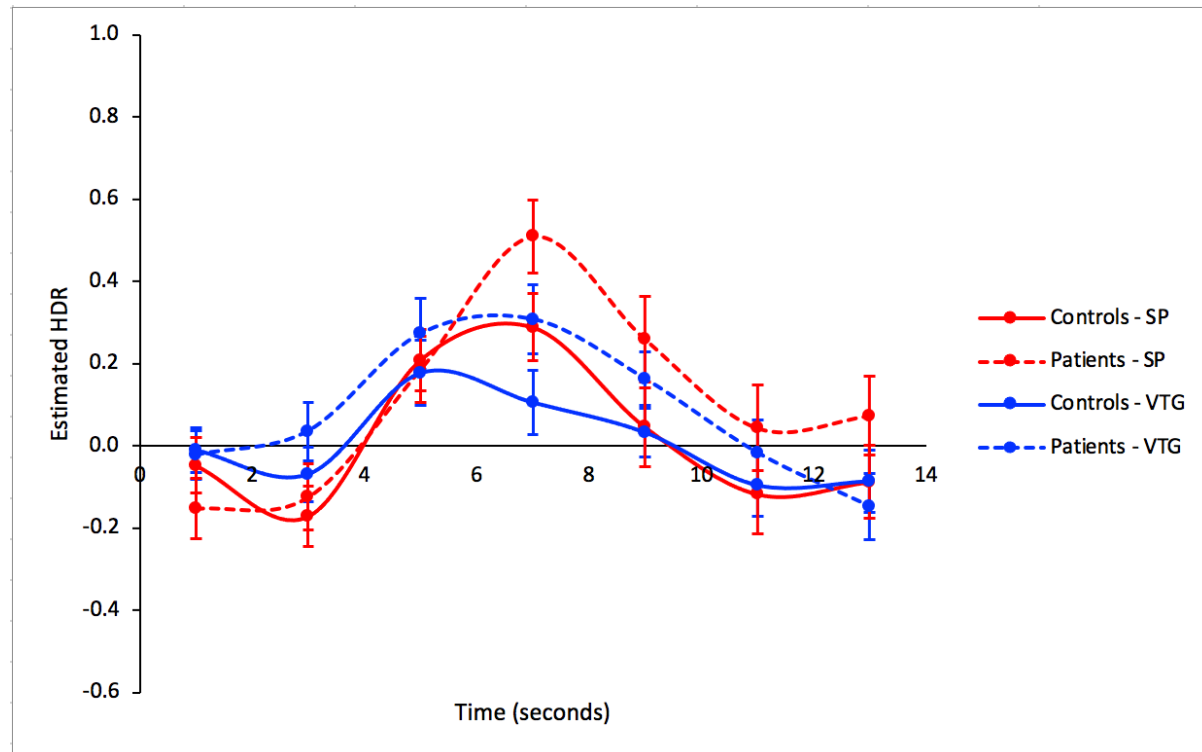


2a. Thought Generating Task (TGT); fBIRN HBM Merge:

AAR activation was observed. Mixed ANOVA revealed significant main effects of Time, $F(6, 288) = 15.125, p < 0.001$. The Time factor was dominated by timebins 2 to 3 for increases peak and timebins 4 to 5 and 5 to 6 for decreases from peak ($p < 0.001$).

The main effect of Group was also significant, $F(1, 48) = 4.255, p < 0.05$. Patients exhibited greater mean activation than Controls, revealing mean predictor weights of 0.099 and 0.013, respectively (Figure 4). Ultimately, the increase to peak in Speech Perception of the Thought Generating Task could be explained by the AAR's overlap with the primary auditory perception network.

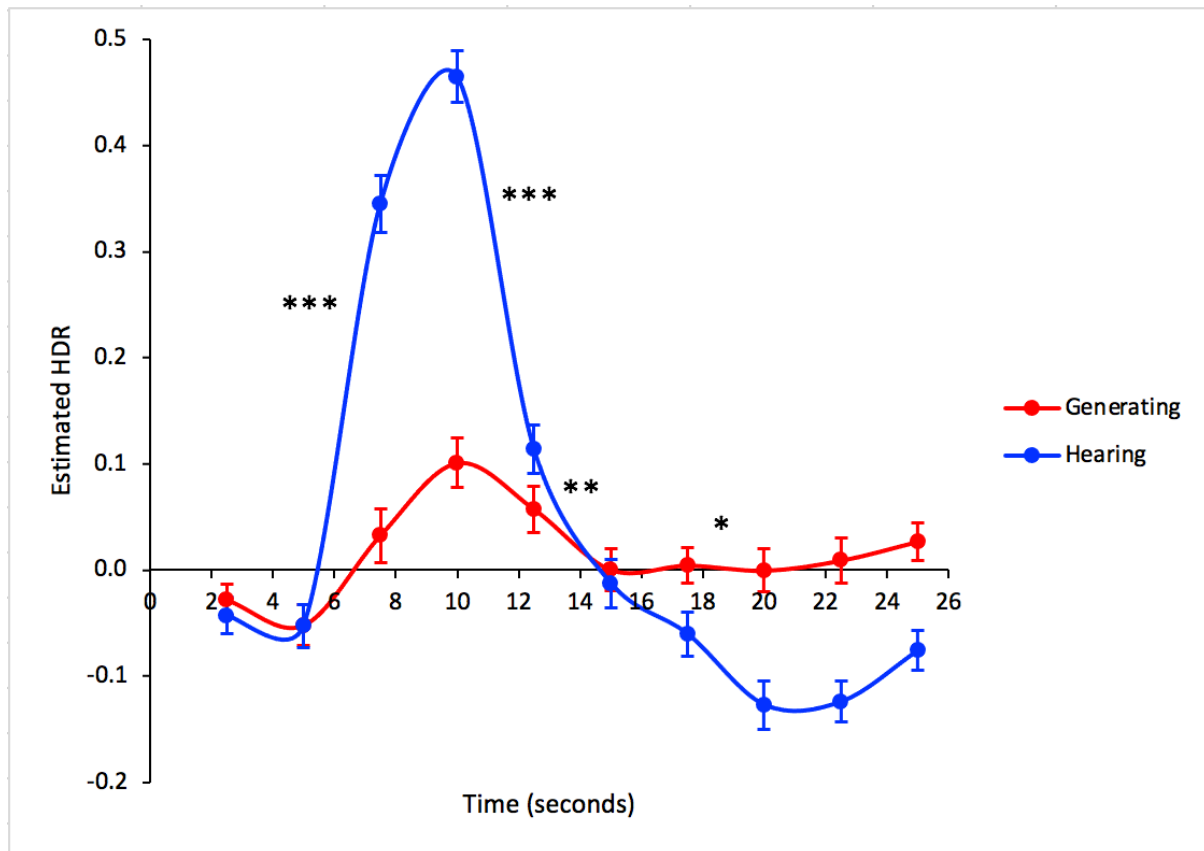
Figure 4. HRF HDR of Thought Generating Task for Group (Controls_Patients), Condition (SP_VTG), and Time.



2b. Thought Generating Task (TGT); Sanford 4-task Merge

Mixed ANOVA revealed significant main effects for Time, $F(9, 522) = 58.533, p < 0.001$, and Task Condition, $F(1, 58) = 45.638, p < 0.001$. Task Condition was dominated by substantially greater mean activation for Hearing than Generating. There was also a significant interaction between Task Condition \times Time, $F(9, 522) = 34.763, p < 0.001$. Hearing increased much more sharply than Generating between timebins 2 and 3, $F(1, 58) = 124.180, p < 0.001$ (Figure 5). Hearing reached a higher peak at timebin 4 and then decreased much more sharply between timebins 4 and 5, $F(1, 58) = 86.159, p < 0.001$. Hearing continued to decrease more than Generating between timebins 5 and 6 and 7 and 8, $p < 0.05$, and reached a lower peak suppression. In the Thought Generating Task, AAR showed much greater activation in the Hearing condition, likely due to activation of the superior temporal gyrus and other overlapping areas of the primary auditory network.

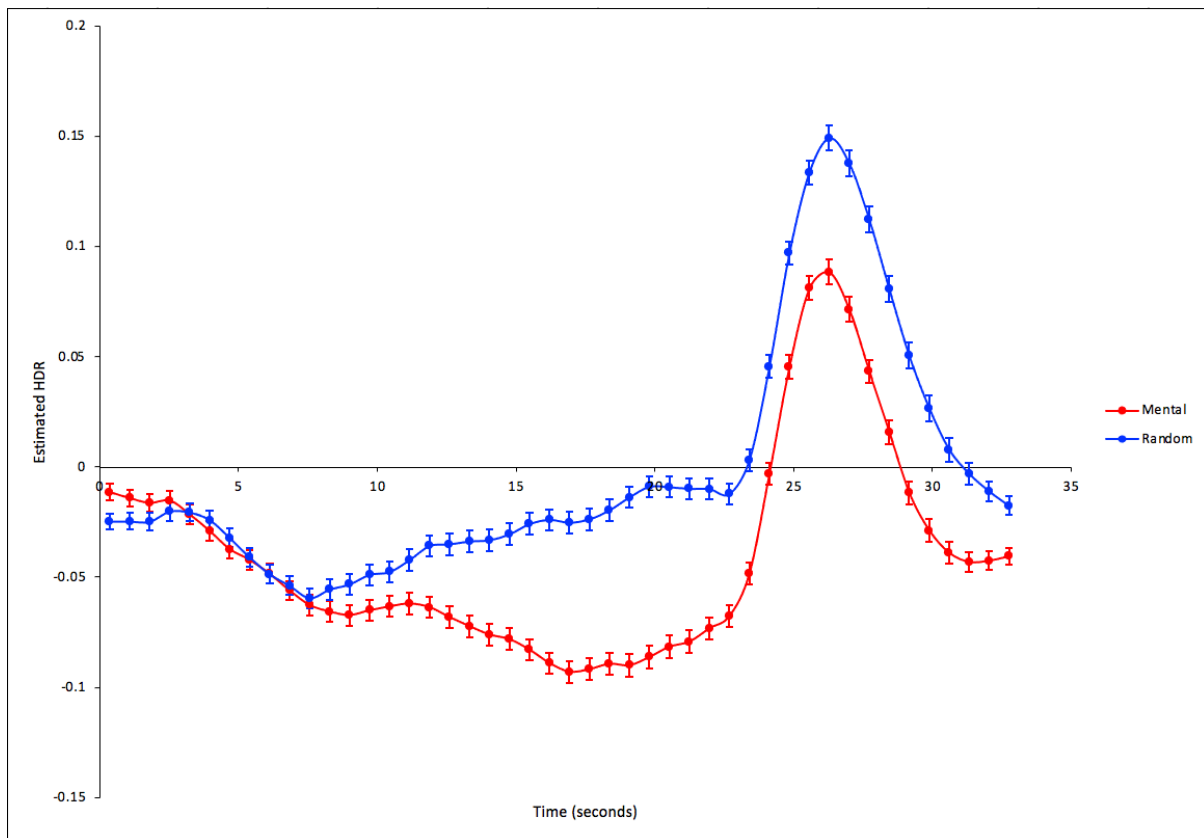
Figure 5. Varimax HDR for TGT (Hearing_Generating) \times Time, averaged over Group (Healthy_Schizophrenia).



3. Human Connectome Project Social Task

AAR suppression was observed for both conditions during the Social Task. Repeated measures ANOVA revealed significant main effects of Time, $F(45, 22455) = 261.973, p < 0.001$ and Condition, $F(1, 499) = 348.720, p < 0.001$. Significant interaction was observed for Condition \times Timebin, $F(45, 22455) = 41.124, p < 0.001$, where greater suppression was seen by Mental (Figure 6). The Mental condition showed prolonged AAR suppression, as demonstrated by greater HDR decrease, than Random from timebins 11 to 12, $F(1, 499) = 7.593, p < 0.01$. Mental continued to show HDR decrease while Random showed HDR increase between timebins 16 to 23, $p < 0.05$. The same pattern was found between timebins 26 and 27, where Mental decreased and Random increased, $F(1, 499) = 7.584, p < 0.01$. AAR suppression decreased, as shown by an increase in HDR activity, by Mental between timebins 30 and 31, $p < 0.01$. Random increased much more sharply than Mental and reached a higher peak between timebins 36 and 37, $F(1, 499) = 7.295, p < 0.01$. Random continued to decrease sharply to baseline between timebins 42 and 46, $p < 0.05$. In general, both Mental and Random showed sustained AAR suppression, but Mental remained deactivated longer while Random increased earlier and reached a higher peak HDR (Figure 6). AAR was more deactivated when participants focused on visual stimuli showing social interactions relative to when stimuli move randomly. Interpreting social interaction between the shapes requires more visual focus and attention. This is consistent with the notion that AAR is suppressed when an individual is intensely engaged in a visual task and is not prepared to attend to external auditory stimuli.

Figure 6. Varimax HDR for the Social Task for Condition (Mental_Random) and Time.



4. FISH Task

The negative loadings of component 3 in the FISH task were best matched to the AAR network; therefore, the HDR shape displays index deactivations. AAR suppression is seen in all groups and for all conditions during completion of the task. Mixed ANOVA revealed significant main effects of Strength of Evidence, $F(1, 109) = 60.150, p < 0.001$, and Time, $F(9, 981) = 80.410, p < 0.001$. Significant interactions were observed between Match Status \times Timebins, $F(9, 981) = 2.570, p < 0.01$, dominated by a sharper HDR increase in Non-match than Match between timebins 1 and 2, $F(1, 109) = 10.004, p < 0.01$, and a sharper HDR decrease in Non-match than Match between timebins 7 and 8, $F(1, 109) = 10.189, p < 0.01$ (Figure 7). There was stronger initial AAR deactivation in the Non-match condition. Mixed ANOVA also revealed significant interaction between Strength of Evidence \times Timebins, $F(9, 981) = 8.818, p < 0.001$. Strong increased more sharply than Weak from timebins 1 and 2, $F(1, 109) = 6.910, p < 0.05$, but Weak increased more sharply than Strong between timebins 2 and 3, $F(1, 109) = 11.466, p < 0.01$. Weak continued to increase more sharply and reached a higher HDR peak than Strong between timebins 4 and 5, $F(1, 109) = 9.007, p < 0.01$ (Figure 7). Strength of Evidence \times Timebin interaction was also dominated by a sharper decrease in Weak between timebins 6 and 7 and timebins 8 and 9, $p < 0.05$. Overall, Strong had greater initial AAR deactivation, but Weak showed much stronger AAR deactivation later on and reached a greater peak deactivation than Strong.

Although main effect of Group was not significant, a significant interaction of Strength of Evidence \times Group was observed, $F(1, 109) = 5.158, p < 0.05$. Controls had a larger difference between Strong and Weak mean predictor weights than patients, dominated by greater HDR activity in Weak (Figure 8). Ultimately, AAR is generally more deactivated when the strength of evidence is weak and during non-match status, since weak evidence requires more visual attention to correctly categorize the visual stimulus into one of the two lakes, and

leads to a reduction in the capability to attend to auditory stimuli. Additionally, controls showed greater suppression during weak evidence conditions, suggesting that healthy participants show the most AAR suppression when focusing on the quantities of fish in the two lakes in the task.

Figure 7. HRF HDR of Match Status (Match_Nonmatch and Strength of Evidence (Strong_Weak) for the FISH task, averaged across Group (Controls_Patients).

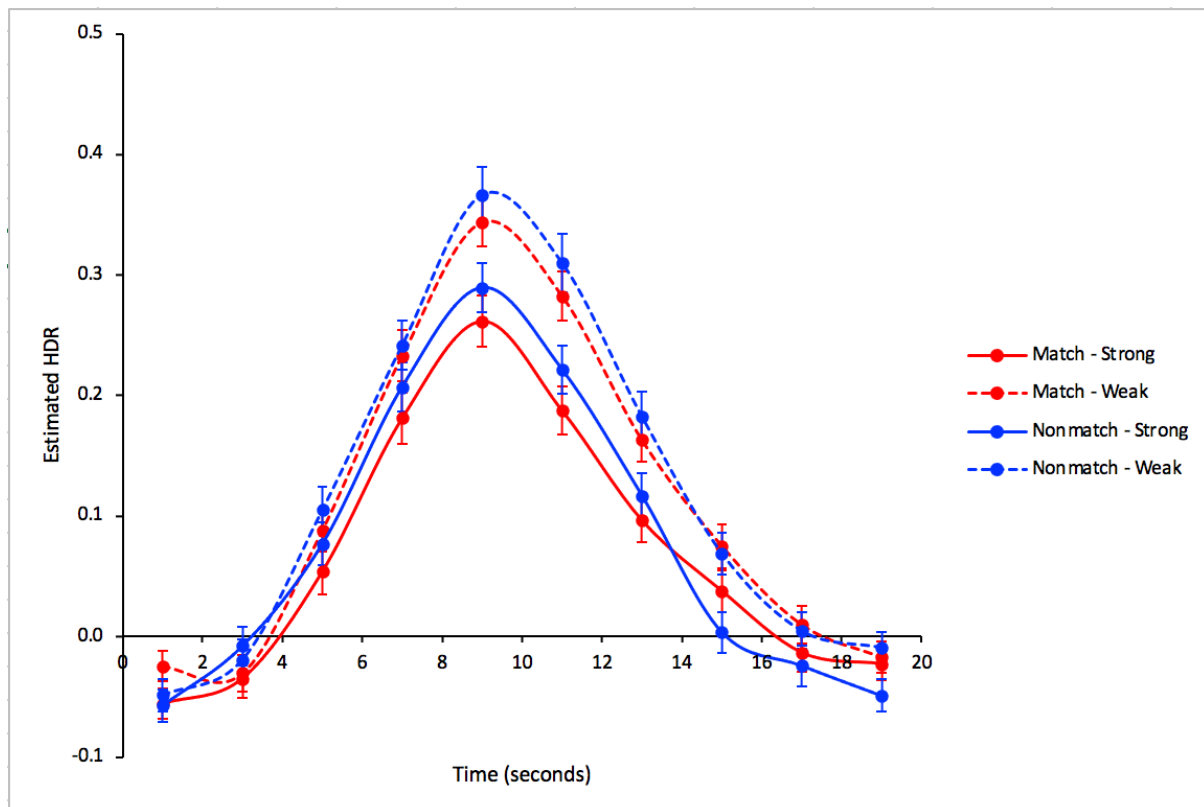
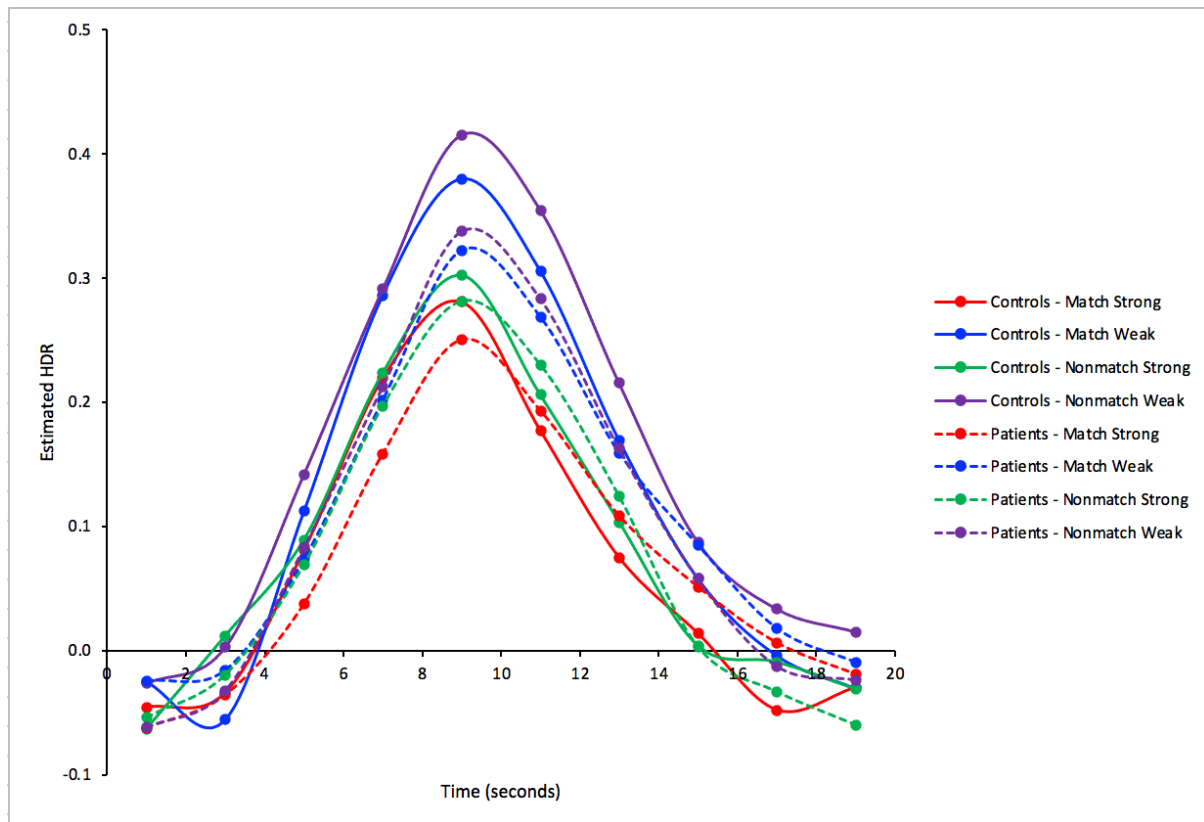


Figure 8. HRF HDR of Group (Controls_Patients), Match Status (Match_Nonmatch), and Strength of Evidence (Strong_Weak) for the FISH task.



5. Raven's Standard Progressive Matrices Task (RSPM)

Like the FISH task, the RSPM task also revealed recruitment of the AAR network when negative loadings were matched to positive patterns; therefore, higher activity in the HDR plot indicates greater AAR deactivation. Mixed ANOVA showed a significant main effect of Time, $F(9, 360) = 13.873, p < 0.001$, which was dominated by timebins 2 to 4 for increases to peak and timebins 4-5, 7-8, and 9-10 for decreases from peak, $p < 0.05$ (Figure 9).

A significant three-way interaction was revealed between Difficulty \times Timebin \times Group, $F(18, 720) = 2.313, p < 0.01$, where Bipolar showed a decrease in HDR for Medium while Control showed an increase in HDR between timebins 9 and 10, $F(1, 40) = 4.593, p < 0.05$ (Figure 10 and Figure 11). Overall, AAR network showed deactivation during the initial phase of the RSPM task and eventually returned to baseline. This suggests that the AAR is deactivated when participants focus on the visual features of the shape patterns presented in the RSPM task and pay less attention to auditory stimuli.

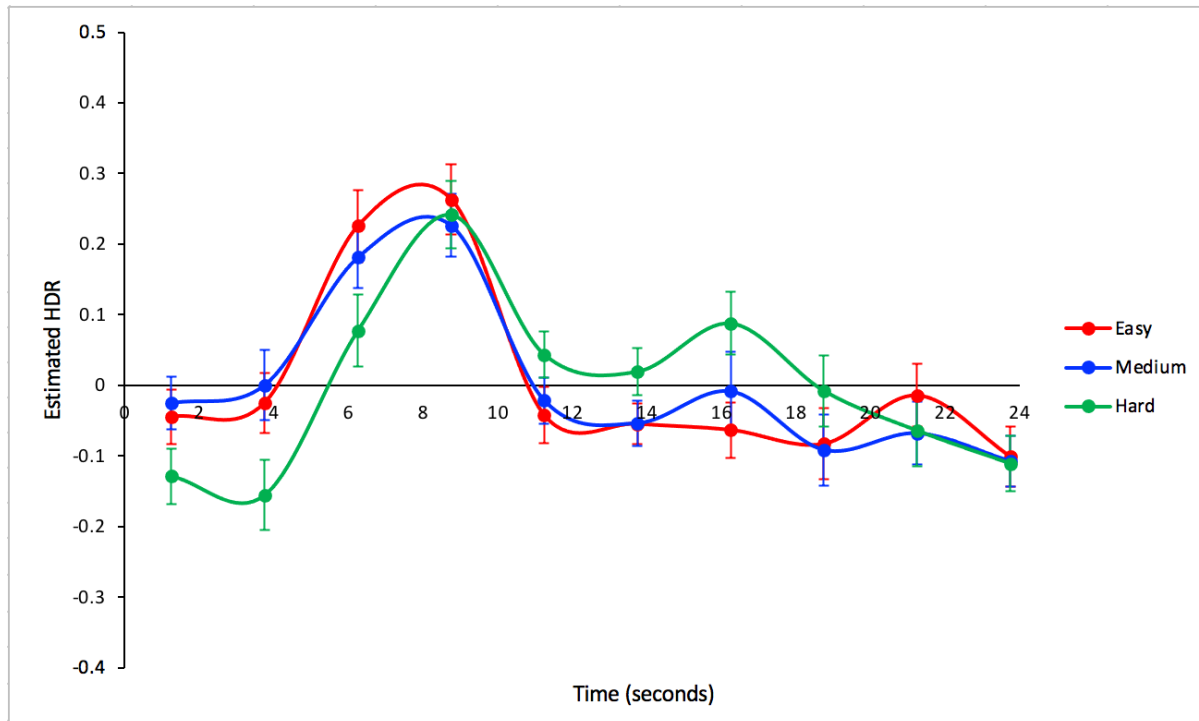
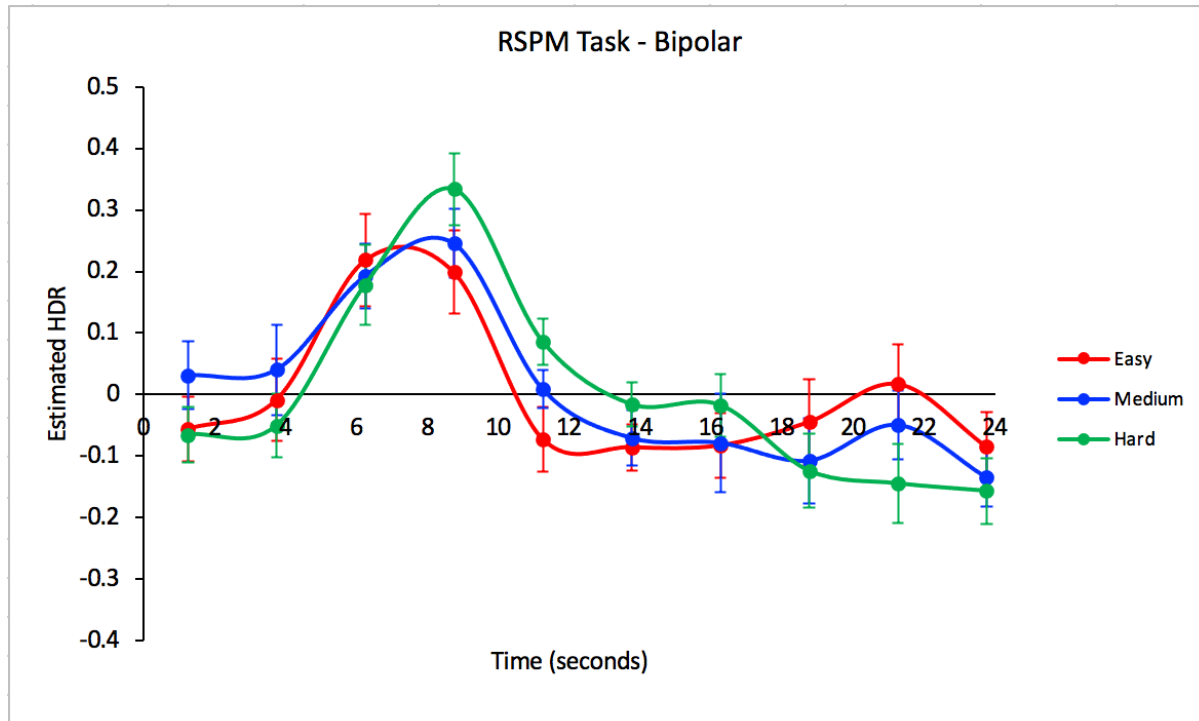
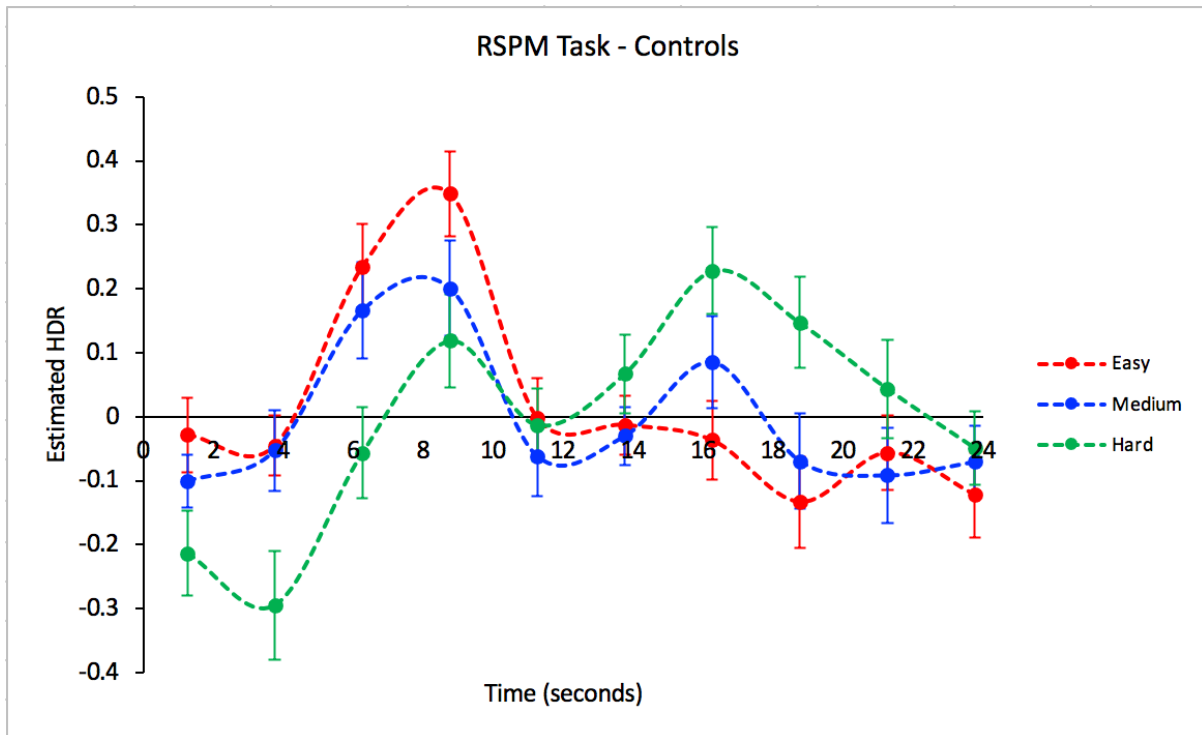
Figure 9. Varimax HDR for RSPM, averaged across Group (Controls_Bipolar).**Figure 10.** Varimax HDR for Bipolar for RSPM.

Figure 11. Varimax HDR for Controls for RSPM.



6. Lexical Decision Task (LDT)

AAR deactivation was observed. A significant main effect emerged for Time, $F(9, 360) = 10.172, p < 0.001$, which was dominated by an initial increase followed by sustained deactivation of AAR. A significant interaction was also observed between Word Type \times Timebin, $F(9, 360) = 2.229, p < 0.05$, where Word increased more sharply than Non-word between timebins 3 and 4, $F(1, 40) = 7.908, p < 0.01$ (Figure 12). AAR deactivation is stronger when interpretation involves semantic meaning.

A significant three-way interaction emerged for Difficulty \times Timebin \times Group, $F(9, 360) = 2.541, p < 0.01$. Controls showed a much sharper HDR decrease than Bipolar in Easy between timebins 2 and 3, $F(1, 40) = 4.345, p < 0.05$. Additionally, Controls increase in Hard while Bipolar decreases in Hard between timebins 2 and 3, $F(1, 40) = 4.345, p < 0.05$ (Figure 13 and Figure 14). Overall, controls show initial AAR activation in easy conditions, but an earlier deactivation of AAR in hard conditions of the Lexical Decision Task (Figure 14). Ultimately, the AAR network shows earlier initial deactivation in hard trials of LDT for controls and greater deactivation when interpreting words than non-words for both groups. This is consistent with the theory that AAR suppression is also dependent on the amount of visual attention, with greater and sharper deactivation for task conditions requiring greater visual attention and surveillance. AAR suppression is also stronger for those conditions involving semantic interpretation.

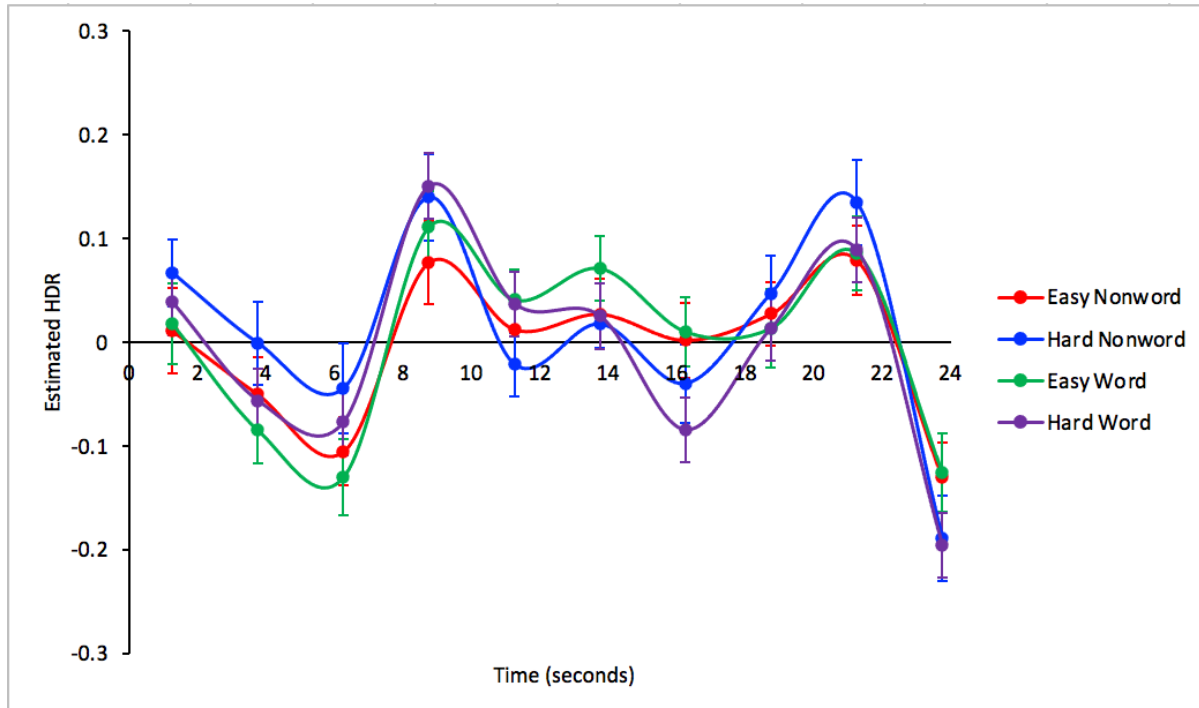
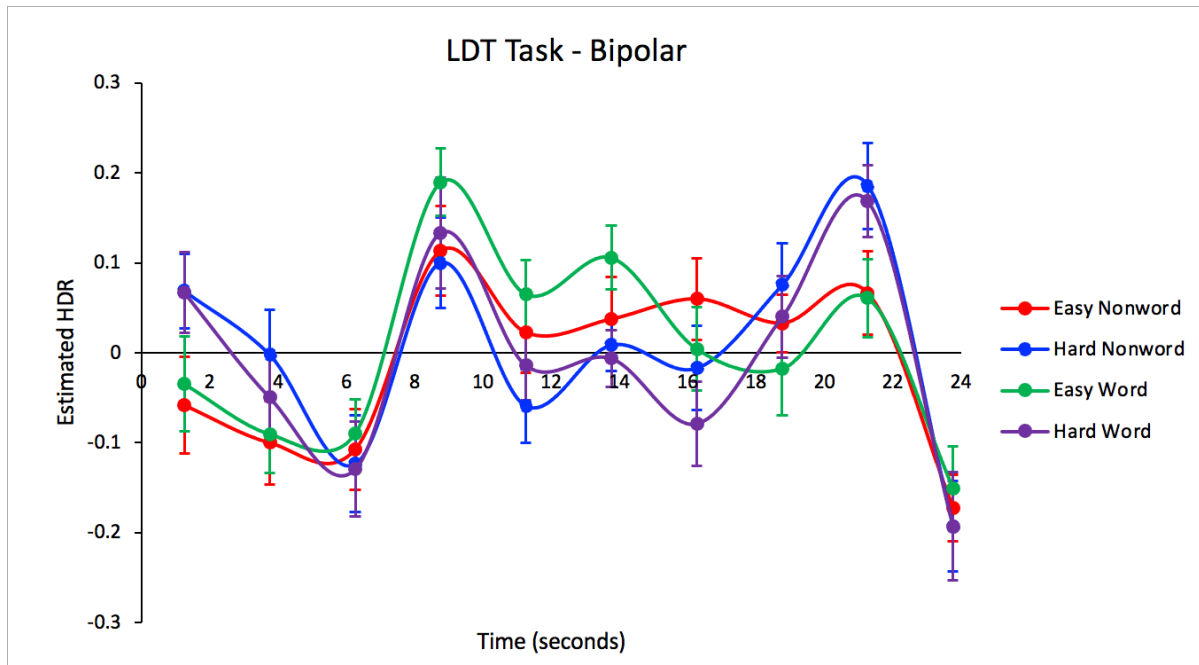
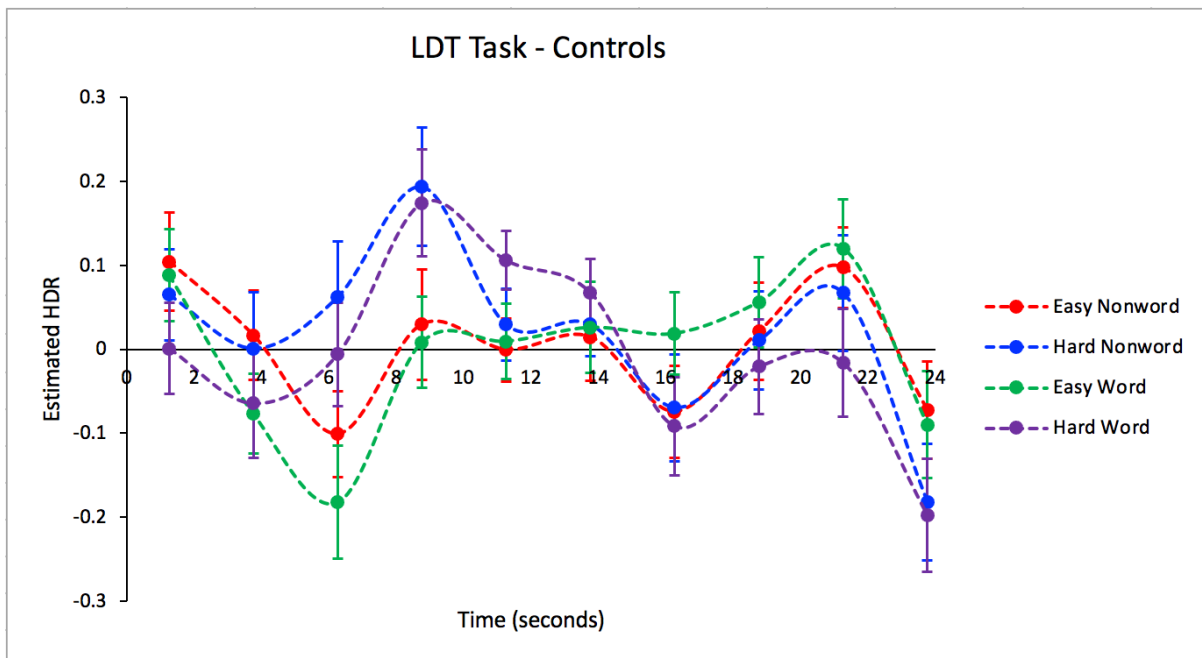
Figure 12. Varimax HDR for LDT, averaged across Group (Controls_Bipolar).**Figure 13.** Varimax HDR for Word Type (Nonword_Word) and Difficulty (Easy_Hard), for Bipolar.

Figure 14. Varimax HDR for Word Type (Nonword_Word) and Difficulty (Easy_Hard), for Controls.



7. Working Memory Task (WM); Sanford 4-task Merge

AAR in the Working Memory task is characterized by initial deactivation during the encoding period followed by an increase in HDR activity that parallels the motor response delay period (Figure 15). Mixed ANOVA revealed significant main effects of Delay, $F(1, 52) = 8.836, p < 0.01$; Load, $F(1, 52) = 4.011, p = 0.050$; and Time, $F(9, 468) = 42.390, p < 0.001$. The main effect of Delay was due to greater mean activation in 4s Delay than in 0s Delay (Figure 16). The main effect of Load was due to greater mean activation in the 4-letter condition than in the 6-letter condition (Figure 17). ANOVA also revealed significant interaction between Delay \times Time, $F(9, 468) = 66.551, p < 0.001$. The 0s Delay increased to peak beginning at timebin 4, peaked at timebin 6, and decreased to baseline. The 4s Delay condition increased to peak starting at timebin 6, peaked at timebin 8, and then returned to baseline (Figure 16). Since AAR also includes parts of the supplementary motor areas and the left precentral gyrus, the difference in these HDR plots can be explained by the delay in motor response between the 2 conditions.

There was also a significant three-way interaction between Delay \times Time \times Group, $F(9, 468) = 2.993, p < 0.05$, which was dominated by the differences from timebins 4 to 7 and between timebins 8 and 9, $p < 0.05$. Healthy participants showed a sharper increase in HDR activity than schizophrenia patients in 0s Delay between timebins 4 and 5, reached a higher peak, and decreased more sharply between timebins 6 and 7 (Figure 18). Schizophrenia patients decreased more than healthy participants in 0s Delay between timebins 8 and 9, $F(1, 52) = 4.409, p < 0.05$. Additionally, healthy participants decreased more sharply than schizophrenia patients in 4s Delay between timebins 8 and 9, $F(1, 52) = 4.409, p < 0.05$. In general for the WM task, AAR initially showed slight suppression in all four conditions due to focus on the visual stimulus at the start of the task. The HDR increased in activation as participants prepared for motor action during the response period for all conditions, with a 4-

second delay in peak for the 4s Delay condition due to a maintenance phase. Less AAR activation was observed for 6-letters, as more letters requires more visual focus and less auditory attention. Moreover, the presence of a delay required greater attention in preparation for responding to a stimulus, recruiting the supplementary motor area of the AAR which is responsible for planning of complex movements.

Figure 15. Varimax HDR for Working Memory task averaged over Group (Healthy_Schizophrenia).

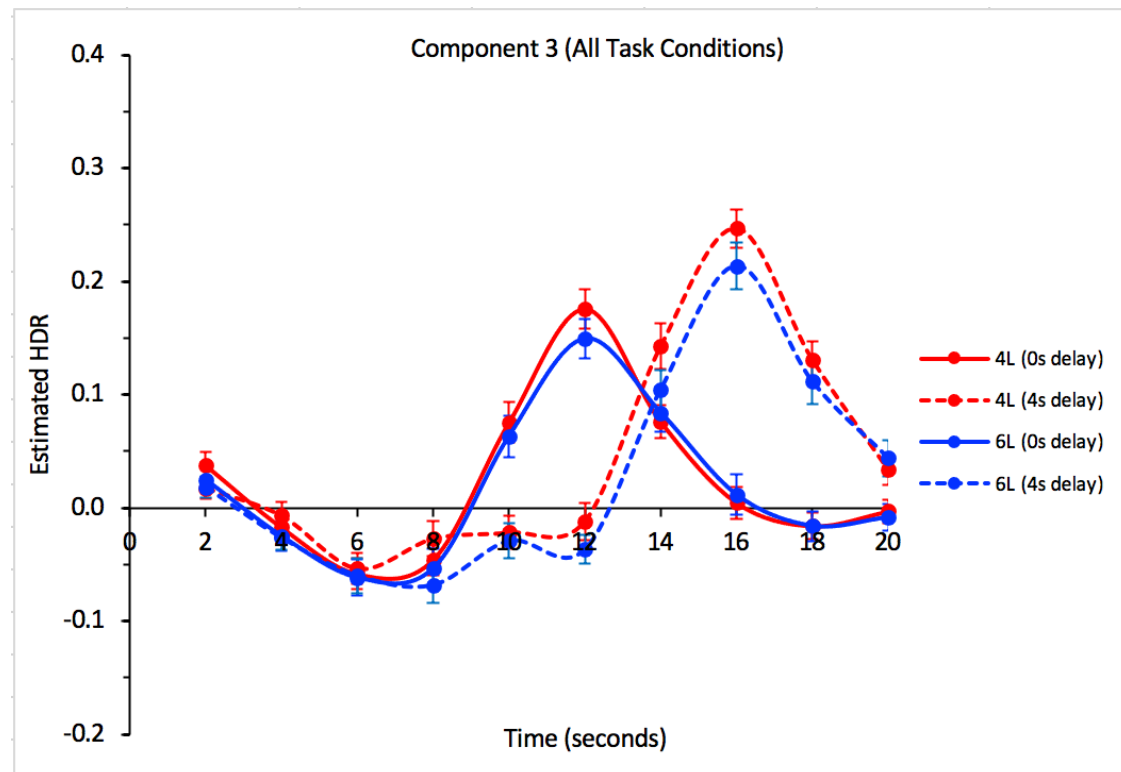


Figure 16. Varimax HDR for Delay (0s_4s) \times Time, averaged over Load (4letter_6letter) and Group (Healthy_Schizophrenia).

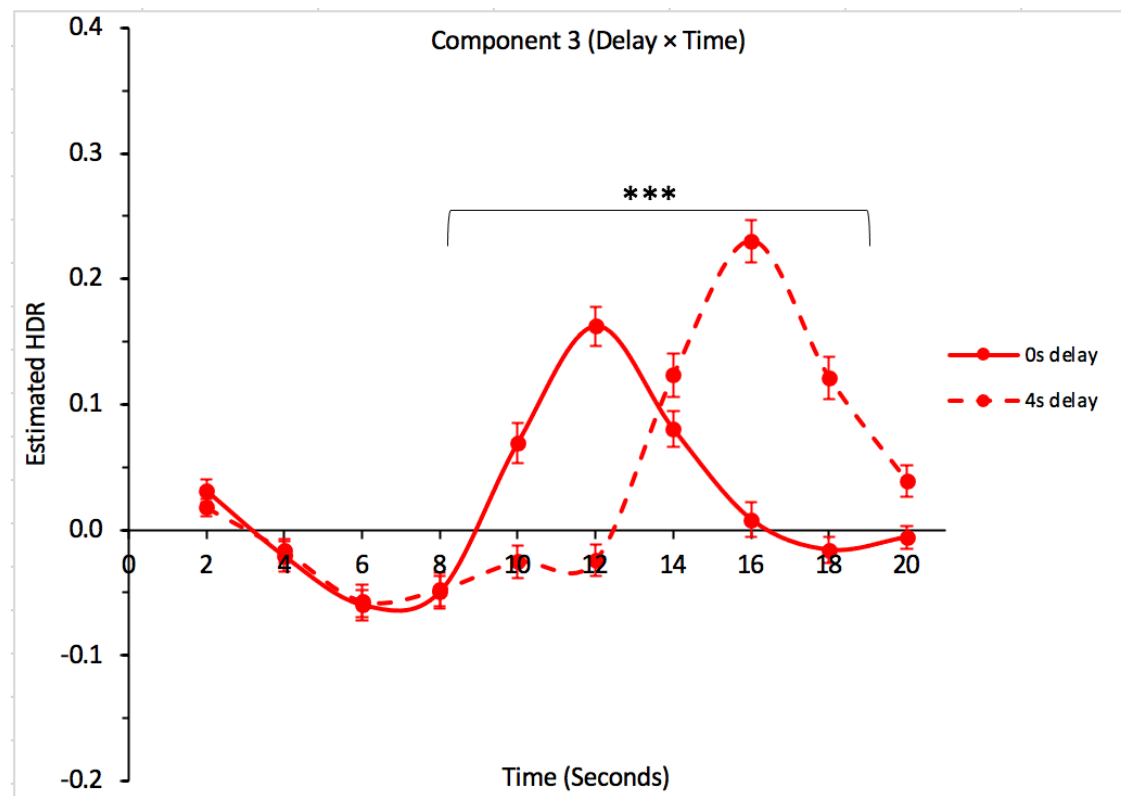


Figure 17. Varimax HDR for Load (4letter_6letter) \times Time, averaged over Delay (0s_4s) and Group (Healthy_Schizophrenia).

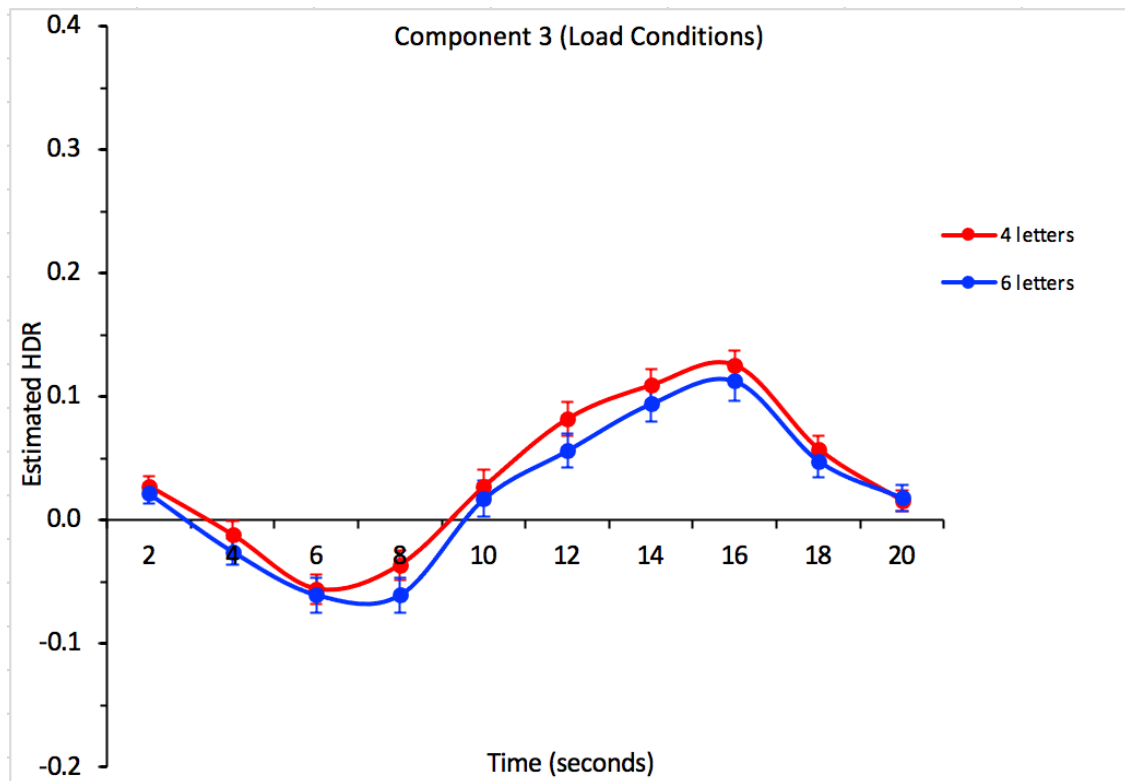
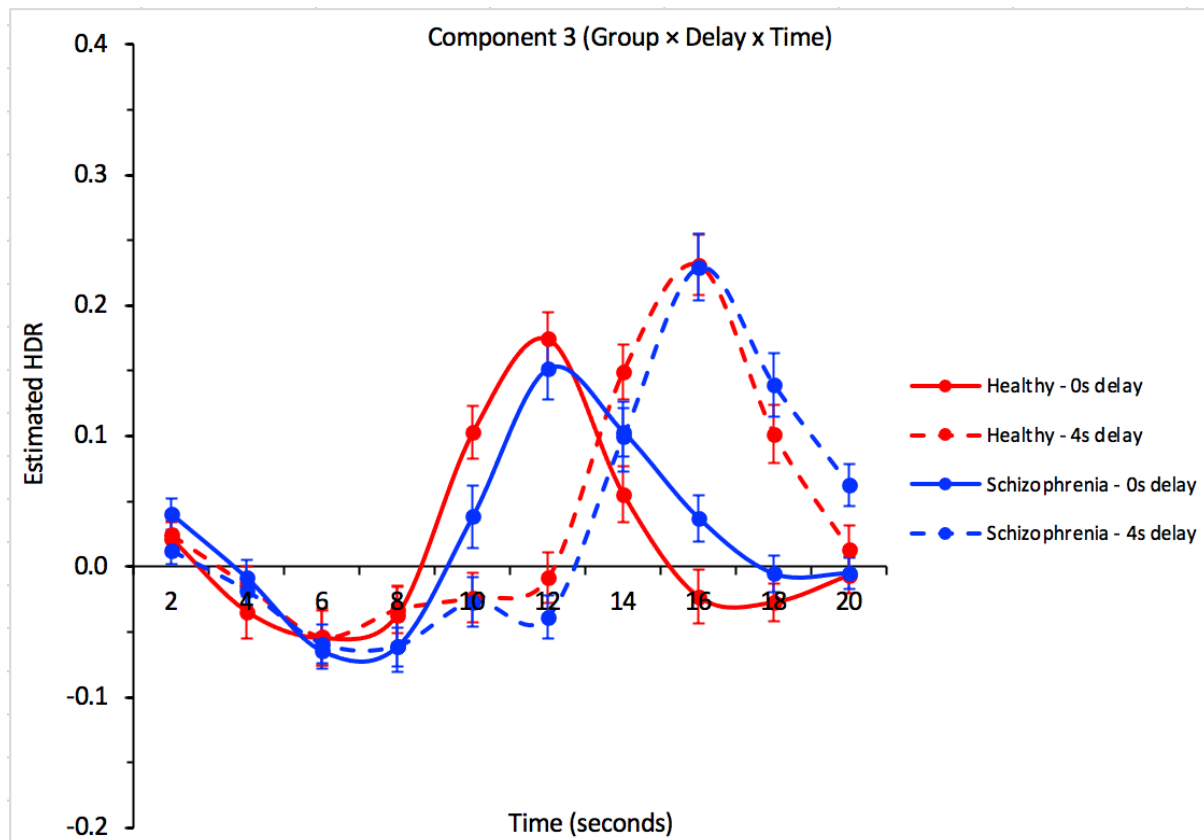


Figure 18. Varimax HDR for Group (Healthy_Schizophrenia) \times Delay (0s_4s) \times Time, averaged over Load (4letter_6letter).

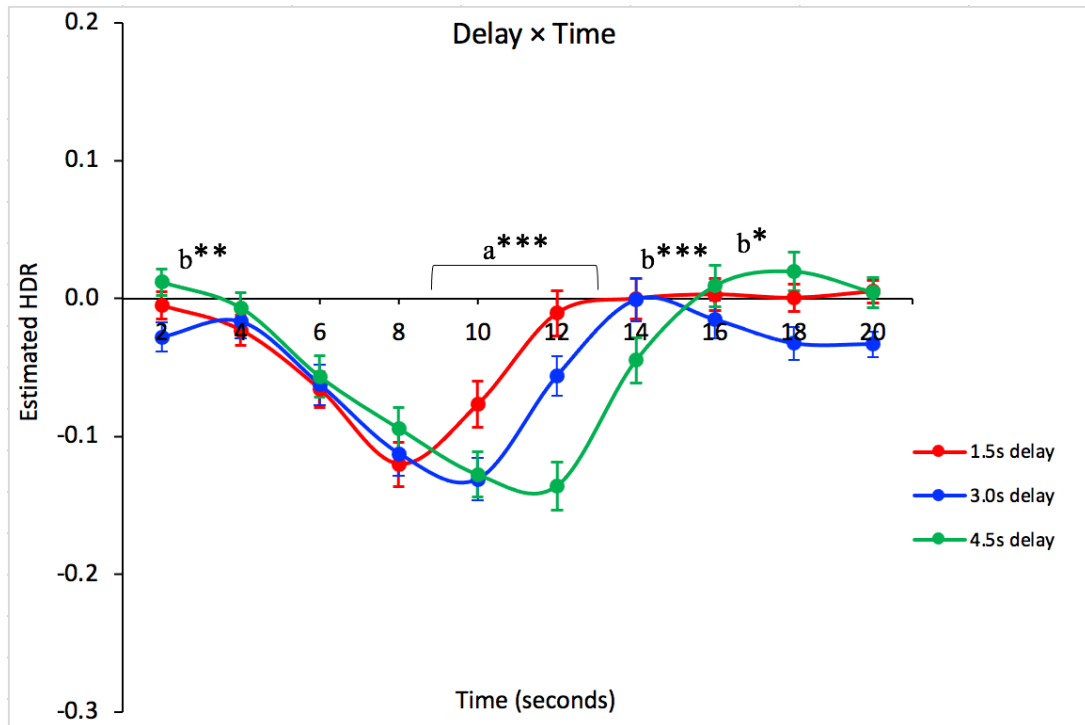


8. Spatial Capacity Task (SCAP); Sanford 4-task Merge

AAR deactivation was observed in the Spatial Capacity task. Mixed ANOVA revealed significant main effects of Load, $F(3, 258) = 12.159, p < 0.001$; Delay, $F(2, 172) = 8.203, p < 0.001$; and Time, $F(9, 774) = 27.779, p < 0.001$. The main effect of Load was dominated by a significant decrease in activity between 1-dot and 3-dots, $F(1, 86) = 21.203, p < 0.001$ (Figures 20). The main effect of Delay was dominated by a significant decrease in activity between 1.5-seconds and 3-seconds, $F(1, 86) = 15.857, p < 0.001$ (Figures 20). ANOVA also revealed significant interactions between Load \times Delay, $F(6, 516) = 3.496, p < 0.01$; Load \times Time, $F(27, 2322) = 5.167, p < 0.001$; Delay \times Time, $F(18, 1548) = 12.217, p < 0.001$; and Load \times Delay \times Time, $F(54, 4644) = 2.408, p < 0.001$. Delay \times Time was dominated by the increases between timebins 4 and 8, $p < 0.001$. AAR deactivation was lifted in order of delay condition; 1.5s Delay returned to baseline the earliest, followed by 3s Delay and then 4.5s Delay (Figure 19). This HDR pattern was seen across all load conditions for the interaction between Load \times Delay \times Time (Figure 22).

There were no significant main effect of group ($p = 0.514$) or any group interactions. Overall, the SCAP task revealed AAR suppression during the encoding and maintenance periods, when more visual and less auditory attention is required, followed by an increase in AAR activity during the response period. AAR deactivation varied depending on the delay condition, with prolonged deactivation matching the duration of the delay condition itself. The significant decrease in AAR activity between the 1-dot and 3-dots condition, as well as the 1.5s and 3.0s delay conditions, suggests that AAR deactivation is also dependent on cognitive load and duration of the maintenance period of visual stimuli.

Figure 19. Varimax HDR for Delay (1.5s_3s_4.5s) \times Time, averaged over Load (1dot_3dot_5dot_7dot) and Group (Healthy_Schizophrenia).



Figures 20-21. Main Effects of Load (20) and Delay (21) for SCAP task.

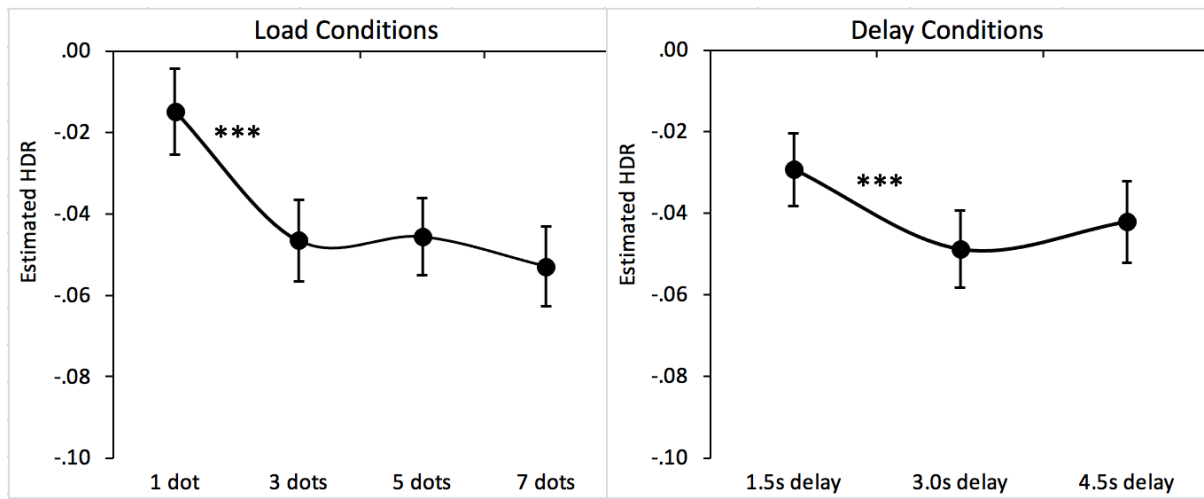
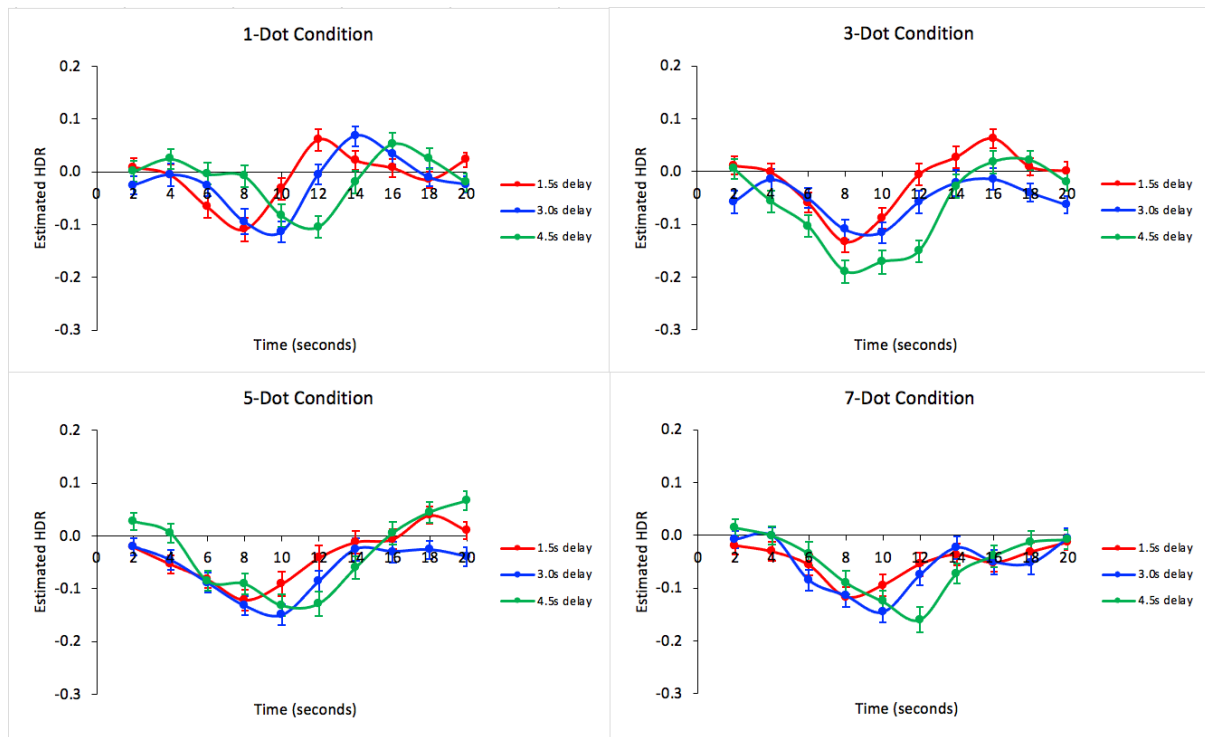


Figure 22. Varimax HDRs for Load \times Delay \times Time, separated by Load Conditions (1dot_3dot_5dot_7dot).



9. Task-Switch Inertia task (TSI); Sanford 4-task Merge

AAR activation was observed. Mixed ANOVA revealed significant main effects of Stimulus Congruency, $F(1, 52) = 15.862, p < 0.001$, and Time, $F(9, 468) = 5.548, p < 0.001$. The main effect of Stimulus Congruency can be explained by a greater mean activation for Word Neutral than Word Incongruent trials, an effect which emerged early in the HDR (Figure 25). Significant interactions were also observed between Congruency \times Task-Switch, $F(1, 52) = 10.427, p < 0.01$; Congruency \times Task-Switch \times Time, $F(9, 468) = 9.354, p < 0.001$; Task-Switch \times Time, $F(9, 468) = 3.683, p < 0.01$; and Congruency \times Time, $F(9, 468) = 12.586, p < 0.001$. The interaction between Congruency \times Task-Switch can be explained by differences in mean activation in trials following an incongruent trial. Word Incongruent showed greater deactivation following a previously incongruent trial, while Word Neutral showed an increase in HDR, $F(1, 52) = 10.427, p < 0.01$ (Figure 23). More visual attention is required for the more cognitively-taxing incongruent trials following an already difficult incongruent trial. Task-Switch \times Time interaction was dominated by HDR decrease following incongruent trials and HDR increase following neutral trials between timebins 1 and 2, $F(1, 52) = 4.842, p < 0.05$. Perhaps the more demanding transition from incongruent trials dominated the AAR suppression (Figure 24). Moreover, Congruency \times Time interaction was dominated by the increases in Word Incongruent and decreases in Word Congruent between timebins 6 and 9, $p < 0.01$ (Figure 25).

ANOVA also revealed an interaction between Time \times Group, $F(9, 468) = 2.807, p < 0.05$. Healthy participants showed an earlier increase in HDR than schizophrenia patients and also showed a steeper decrease and lower peak deactivation (Figure 26). This interaction was dominated by the increase in Schizophrenia between timebins 3 and 4, $F(1, 52) = 6.240, p < 0.05$, and the sharper decrease in HDR activity in Healthy between timebins 4 and 5, $F(1, 52) = 8.193, p < 0.01$. Ultimately, the TSI task is consistent with interpretation of AAR because

more attention on visual details, such as discrimination of color from word, is required in the WI trials and would therefore induce greater deactivation of the AAR network. Activation later in the HDR curve results from participants' preparation to respond to the presented stimulus via button press.

Figure 23. Varimax HDR for Stimulus Congruency (WN_WI) \times Task-Switch Condition (cn_ci).

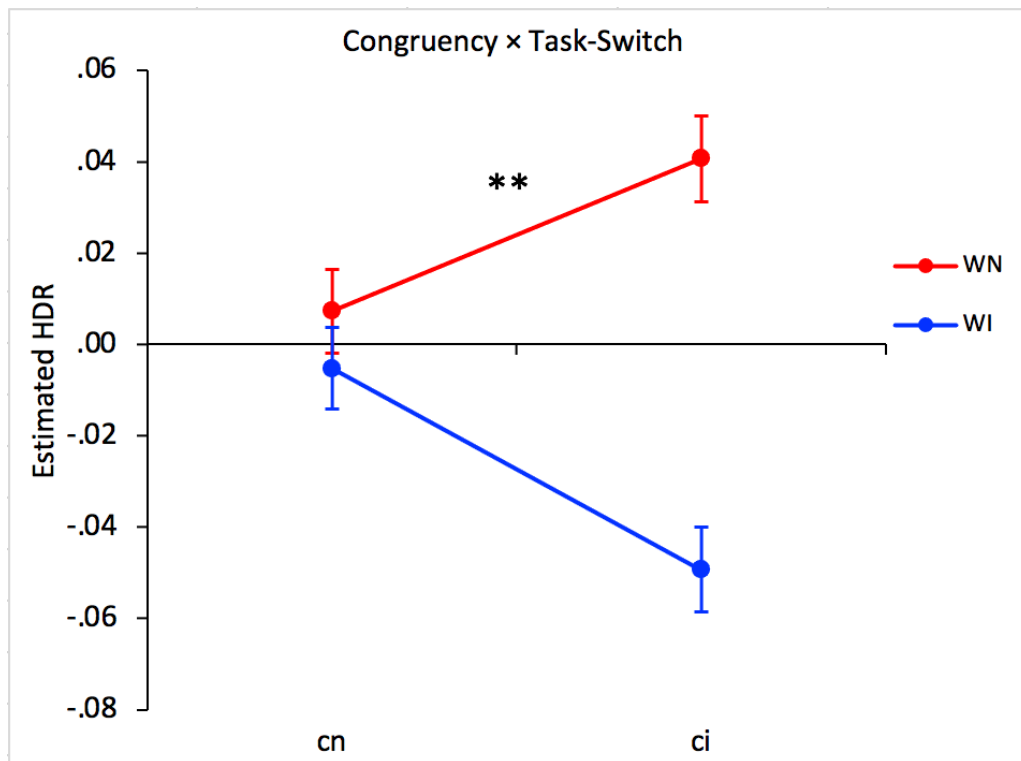


Figure 24. Varimax HDR for Task-Switch (cn_ci) \times Time, averaged over Stimulus Congruency (WN_WI) and Group (Healthy_Schizophrenia).

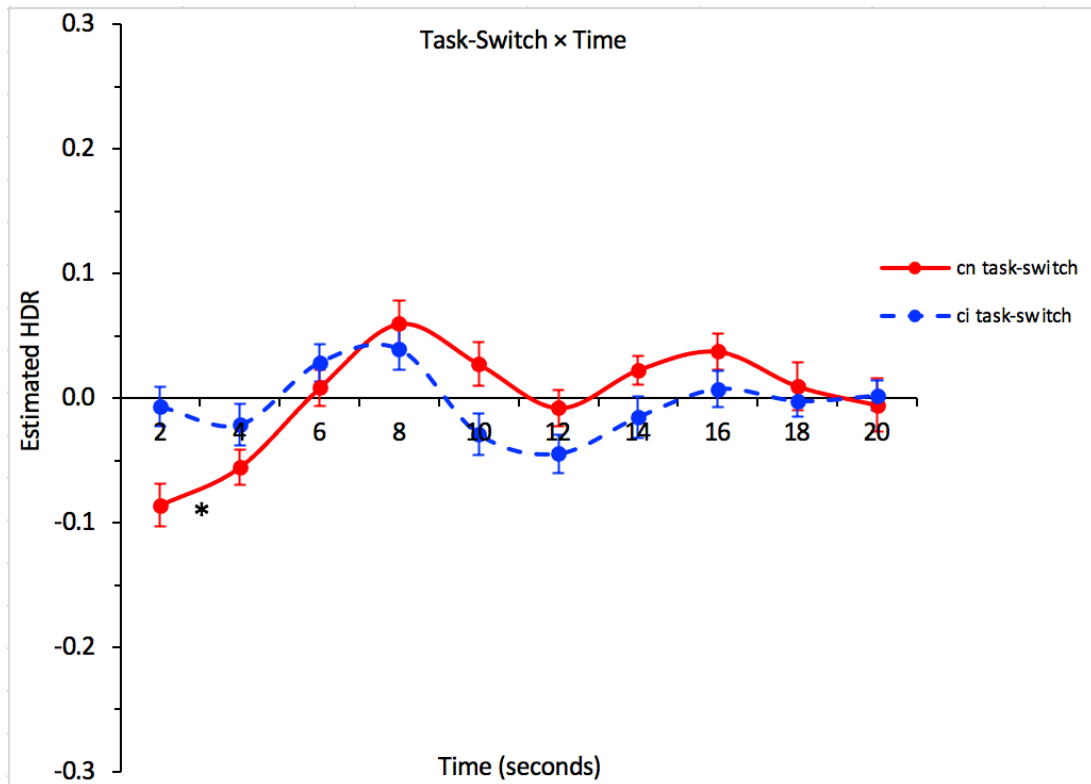


Figure 25. Varimax HDR for Stimulus Congruency (WN_WI) \times Time, averaged over Task-Switch (cn_ci) and Group (Healthy_Schizophrenia).

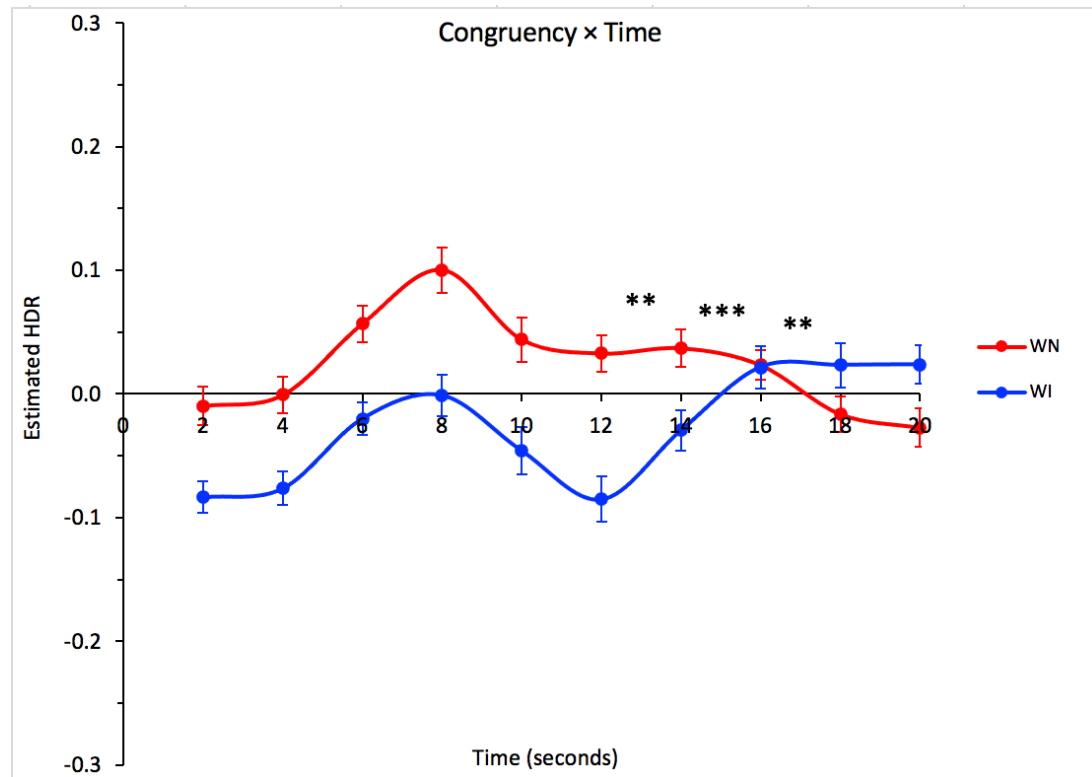
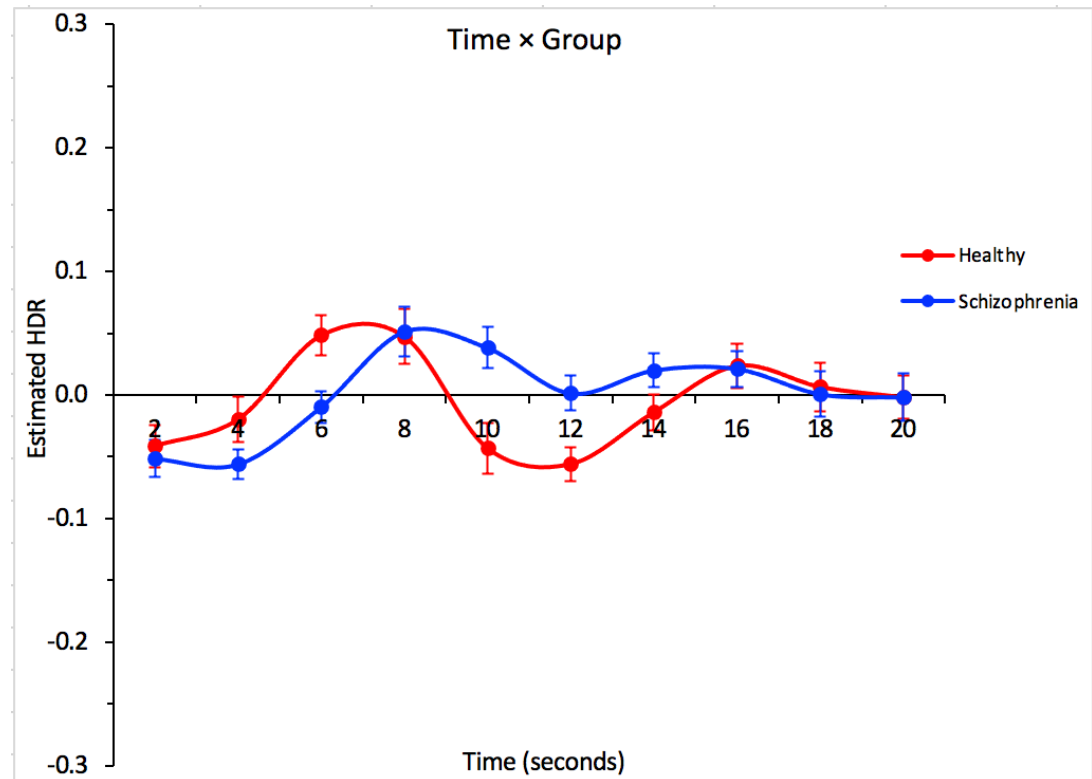


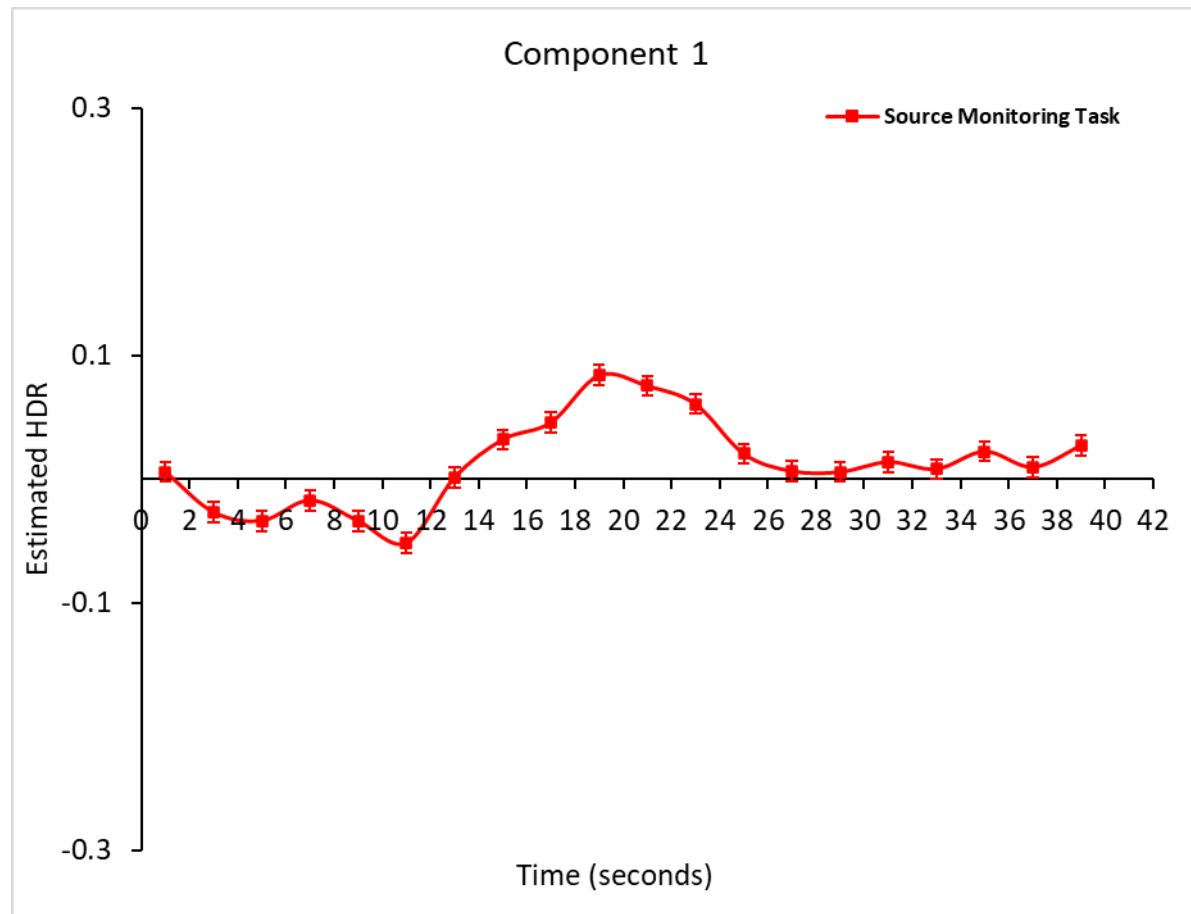
Figure 26. Varimax HDR for Group (Healthy_Schizophrenia) \times Time, averaged over Stimulus Congruency (WN_WI) and Task-Switch (cn_ci).



10. Source Monitoring (SM)

AAR in Source Monitoring is characterized by initial deactivation followed by an increase in HDR (Figure 27). A significant main effect was found in Difficulty, which was dominated by greater mean activation in Easy than Hard, $F(1, 43) = 4.92, p < .05$. There was also a main effect of Time, $F(19, 817) = 7.10, p < .001$, dominated by timebins 6-7 and 9-10 for increases to peak, and 12-13 for decreases from peak, $p \leq 0.001$. No other interactions or group effects were found. Greater activation of the AAR network in easier to recall trials (i.e., Association and Self) relative to more difficult to recall trials (i.e., Reading and Other) is due to greater AAR deactivation in tasks requiring greater cognitive effort and intensive monitoring of visual stimuli. The difficult conditions of the Source Monitoring task require high effort to monitor and recall target words, leading to less AAR activity. After initial deactivation in all conditions, the increase in activity could be due to participants' motor response by key press, or participants' ability to shift their attention from the task's intensive monitoring of visual stimuli to other cognitive processes including attention to auditory stimuli, such as noises in the scanner.

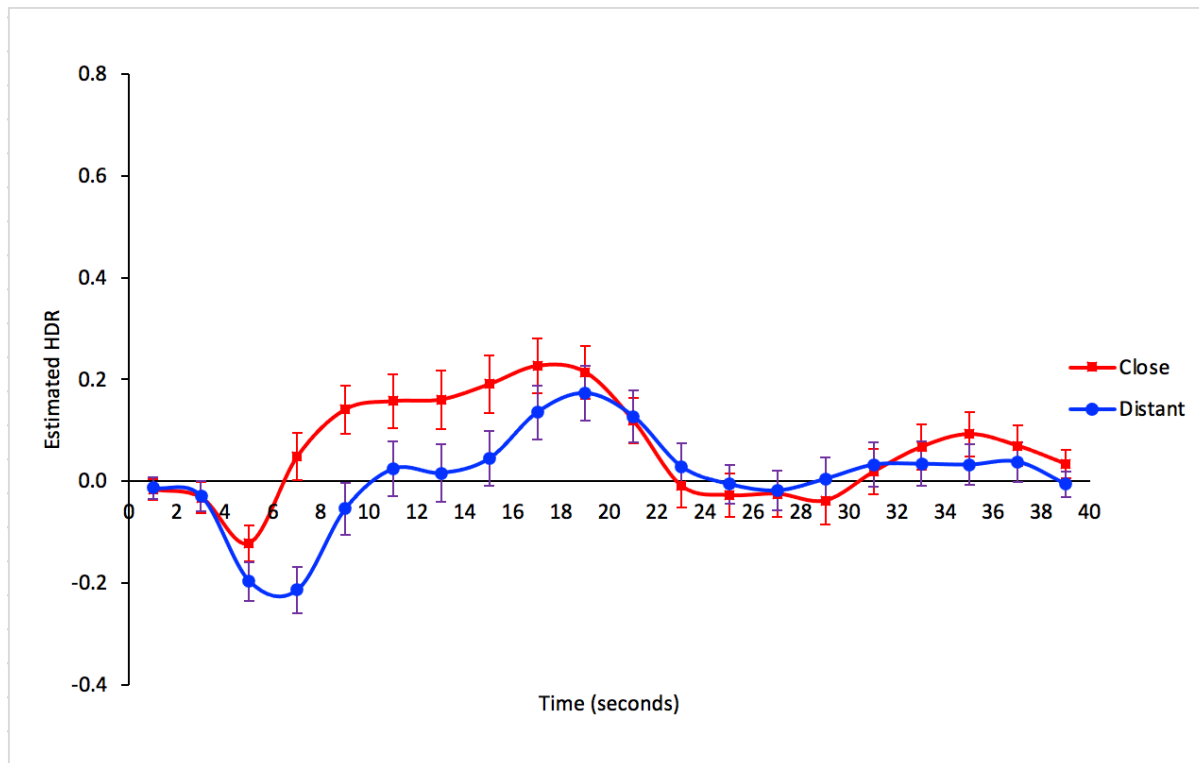
Figure 27. Varimax HDR averaged over Task (TM_SM), Difficulty (Easy_Hard), and Group (Healthy_Schizophrenia).



11. Semantic Integration (SI)

Mixed ANOVA revealed significant main effects of Condition, $F(1, 43) = 32.980, p < 0.001$, and Time, $F(19, 817) = 4.374, p < 0.001$. The main effect of Condition is explained by higher mean activation for Close than Distant. There was also a significant interaction observed between Condition \times Timebin, $F(19, 817) = 11.215, p < 0.001$. Distant decreases much more sharply than Close between timebins 2 and 3, $F(1, 43) = 10.293, p < 0.01$. Distant continues to decrease while Close increases between timebins 3 and 4, $F(1, 43) = 48.795, p < 0.001$, and Distant reaches a lower peak deactivation at timebin 4 (Figure 28). Due to prolonged and greater peak deactivation, Distant shows an increase later in the HDR and increases more sharply than Close between timebins 4 and 6 and timebins 8 and 9, $p < 0.05$. Overall, AAR showed initial deactivation in the Semantic Integration task, which was much more pronounced for conditions with distantly-related words. Greater cognitive effort is required to monitor distantly related word pairs, so there is decreased capacity to attend to auditory stimuli. Increases later in the HDR could be explained by activation of the response patterns of this component, specifically the pre- and postcentral gyrus.

Figure 28. Varimax HDR for Condition (Close_Distant) \times Time, averaged across Group (Healthy_Schizophrenia).



Discussion

By integrating the hemodynamic response curves for the Auditory Attention-for-Response network across multiple studies, we can formulate an overall understanding of this network's role in different task-based activities. Three main factors that correlate with AAR activity include presence of auditory stimuli, motor response and planning for response, and level of visual attention required. AAR activity increased in response to auditory stimuli in the Auditory Oddball and Thought Generating Task, but decreased in activity during tasks that required intensive visual focus, such as the Spatial Capacity, FISH, and Bipolar Merge tasks. Moreover, the motor areas of AAR explain activation in tasks such as Working Memory, Semantic Integration, and Source Monitoring—where a motor response is required after the initial deactivation due to visual stimuli.

AAR activation is observed when discriminating deviant auditory stimuli (Lavigne et al., 2016). In accord with previous literature, areas of the AAR—such as the superior temporal gyrus, precentral gyrus, insula, and superior frontal gyrus—are active during the Auditory Oddball task (Kim et al., 2009; Lavigne et al., 2016). In both the individual task analysis and merge, there was a significant interaction between the time and group factors, indicating there may be a difference in the functional connectivity of this network between healthy controls and schizophrenia patients. Additionally, AAR is active for both external noises and internal word and thought generation, but the network proves more active for external auditory stimuli, as shown through the Thought Generating Task (Lavigne & Woodward, 2018).

The AAR network seems to have a somewhat inverse relationship between auditory and visual stimuli; as cognitive demand for visual attention increases, AAR activity decreases. Additionally, AAR deactivation for visual tasks seems to be dependent on cognitive load and duration of maintenance period. This is shown in the Working Memory task, where there was decreased activity for 6-letters compared to 4-letters, suggesting that increased visual stimuli

hinders AAR activity in working memory tasks. AAR deactivation is greater for exclusively visual stimuli, like in SCAP and RSPM, as compared to visual stimuli that may involve internal letter or word generation, like in WM, TSI, and LDT. Although increased visual attention leads to a decrease in AAR activity, there is still some AAR activity for those visual tasks that involve some aspect of internal word, letter, or thought generation—such as LDT, WM, and TGT. Another finding in regards to visual attention is that AAR deactivation is greater when utilizing problem-solving logic and extracting presence of social interaction, as shown in the FISH and Social Tasks, respectively. AAR deactivation for visual-based problem-solving logic is also shown in RSPM and SI.

The third factor that correlates with AAR activity is attention directed toward motor response and the response itself. AAR activity increases as the allocated attention to motor response increases, as exhibited through duration of maintenance period. The Working Memory revealed a significant main effect of delay, where a 4-second delay between the encoding and response periods led to an increase in AAR activity. Source Monitoring and Semantic Integration tasks also showed AAR activation for motor response in the scanner. Overall, AAR is active when detecting external auditory stimuli and during internal thought and word generation, but decreases in activity when intensive visual attention and focus is required, with greater deactivation associated with cognitive load and semantic problem-solving. Attention for motor response also leads to an increase in AAR activity.

These findings provide valuable information in regard to the reverse inference problem, and the results suggest that activation of the AAR brain regions occurs when an individual is presented with a cognitive task involving auditory stimuli and a simultaneous motor response. It may also be inferred that deactivation of this network will signify instances when an individual exhibits strong attention to visual stimuli. Through fMRI-CPCA, voxel-based classification and subsequent analysis of the HDR plots in each of the studies, reverse inference

of cognition from brain activity was achieved. However, more tasks that include deviant auditory stimuli, similar to the auditory oddball task, but also involve manipulation of a simultaneous motor response are needed to distinguish the precise differences between the AAR and the AUD. Ultimately, with a clear understanding of the functional connectivity and task-relevance of AAR, we can better mediate symptoms that lead to disruptions and aberrant activity in this network and tasks related to those ones in this paper.

References

- Balota, D. A., Yap, M. J., Hutchison, K. A., Cortese, M. J., Kessler, B., Loftis, B., . . .
- Treiman, R. (2007). The English Lexicon Project. *Behavior Research Methods*, 39(3), 445-459. doi:10.3758/bf03193014
- Barch, D. M., Burgess, G. C., Harms, M. P., Petersen, S. E., Schlaggar, B. L., Corbetta, M., . . . WU-Minn HCP Consortium. (2013). Function in the human connectome: Task-fMRI and individual differences in behavior. *NeuroImage (Orlando, Fla.)*, 80, 169-189. doi:10.1016/j.neuroimage.2013.05.033
- Kim, D. I., Mathalon, D. H., Ford, J. M., Mannell, M., Turner, J. A., Brown, G. G., Belger, A., Gollub, R., Lauriello, J., Wible, C., O'Leary, D., Lim, K., Toga, A., Potkin, S. G., Birn, F., & Calhoun, V. D. (2009). Auditory Oddball Deficits in Schizophrenia: An Independent Component Analysis of the fMRI Multisite Function BIRN Study. *Schizophrenia Bulletin*, 35(1), 67–81. <https://doi.org/10.1093/schbul/sbn133>
- Lavigne, K. M., Menon, M., & Woodward, T. S. (2016). Impairment in subcortical suppression in schizophrenia: Evidence from the fBIRN oddball task. *Human Brain Mapping*, 37(12), 4640-4653. doi:10.1002/hbm.23334
- Lavigne, K. M., & Woodward, T. S. (2018). Hallucination- and speech-specific hypercoupling in frontotemporal auditory and language networks in schizophrenia using combined task-based fMRI data: An fBIRN study. *Human Brain Mapping*, 39(4), 1582-1595. doi:10.1002/hbm.23934
- Percival, C. M., Zahid, H. B., Woodward, T. S. (2020). *Task-Based Brain Networks Detectable with fMRI [fMRI image]*. Github.com. https://github.com/CNoS-Lab/Woodward_Atlas/tree/main/Network_Images
- Poldrack, R. (2006). Can cognitive processes be inferred from neuroimaging data? *Trends in Cognitive Sciences*, 10(2), 59-63. doi:10.1016/j.tics.2005.12.004

Sanford, N. A. (2019). Functional brain networks underlying working memory performance in schizophrenia: A multi-experiment approach [Doctoral dissertation, University of British Columbia]. Retrieved from

<https://open.library.ubc.ca/collections/ubctheses/24/items/1.0387449>

Sanford, N., Whitman, J. C., & Woodward, T. S. (2020). Task-merging for finer separation of functional brain networks in working memory. *Cortex*, 125, 246-271.
doi:10.1016/j.cortex.2019.12.014

Functional Assessment of the fMRI-derived Re-Evaluation Network

Leonardo Arreaza^{1,2}

¹BC Mental Health and Substance Use Services

²Department of Psychiatry, University of British Columbia

Abstract

Task-based Functional Magnetic Resonance Imaging (fMRI) and Constrained Principal Component Analysis (CPCA) have previously been used to identify twelve fMRI-derived functional brain networks. One of these is the Cognitive Evaluation Network (CEN). It is hypothesized that the activity of this network increases when a participant evaluates their response to a cognitive task. The fMRI BOLD response was analyzed for this network across several fMRI task-based studies to test this hypothesis and gain further insight into the function of this network. Starting with a set of fMRI tasks with previously extracted components, a network classification was done with Matlab to determine which of the twelve network templates each component best matched with. SPSS Repeated Measures Analysis of Variance (ANOVAs) was used to determine the mean hemodynamic response plot (HDR) for each group, either controls or patients with schizophrenia, and for each task condition. These HDR plots provided a temporal profile of CEN network activity, which was compared with the activity of the External Attention and Response Networks. The presence of the CEN peak after either the External Attention or Response network in all the studies supported the initial hypothesis. To gain further insight into the function of this network, canonical correlation analyzes were used to explore possible relationships between CEN activity and the activity of other networks elicited by the same task. CCAs were also conducted between CEN activity and the results of the Signs and Symptoms of Psychotic Illness scale (SSPIs), and results of the Beck Cognitive Insight Scale (BCIS) for the participants of each study. The results suggest that there may be a negative relationship between CEN activity and the severity of the delusions, as well as the ability to receive feedback from others.

Keywords: Functional magnetic resonance imaging, constrained principal component analysis, canonical correlation analysis, cognitive evaluation network.

Preface

The collection of fMRI data, and the extraction of task components using CPCAs was done by members of the Cognitive Science of Schizophrenia Lab (CNoS) prior to this investigation. I completed some of the network classifications using Matlab, and conducted the SPSS Repeated Measures Analysis of Variance (ANOVAs) to obtain the mean hemodynamic response (HDR) plots for each study. Additionally, I carried out the Baseline to Peak Analysis, and the Canonical Correlation Analysis with the results from the Signs and Symptoms of Psychotic Illness scale (SSPIs), and the elements of the Beck Cognitive Insight Scale (BCIS).

Glossary

CEN Cognitive Evaluation Network

CPCA Constrained Principle Component Analysis

ANOVA Analysis of Variance

CCA Canonical Correlation Analysis

ITP Increase to Peak

RTB Return to Baseline

BCIS Beck Cognitive Insight Scale

SSPI Signs and Symptoms of Psychotic Illness

HDR Hemodynamic Response Plot

TSI Task Switch Inertia

SA Semantic Association

MS Metrical Stress

TGT Thought Generation Task

BADE Bias Against Disconfirmatory Evidence

ABADE Animal BADE

sc Social Cognition

FUNCTIONAL ASSESSMENT OF THE FMRI-DERIVED COGNITIVE EVALUATION NETWORK

HCP Human Connectome Project

Chapter 1: Introduction to the Cognitive Evaluation Network (CEN)

The Cognitive Evaluation Network (CEN) is the first of the twelve task-based networks.

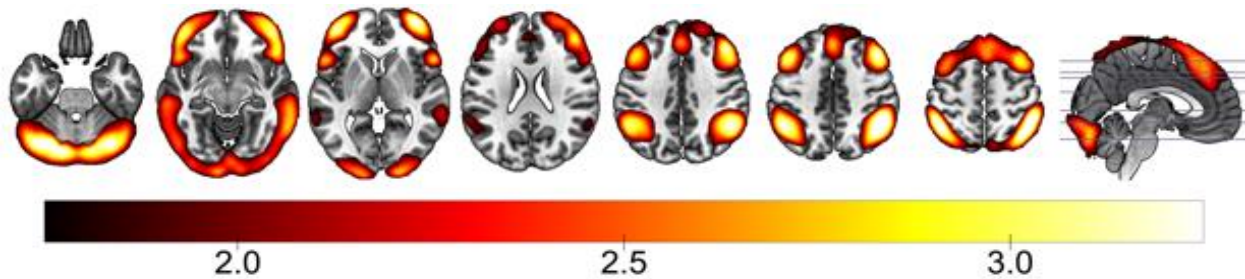
The CEN was observed in a previous published study on the functional networks underlying evidence integration and delusional ideation (Lavigne et al., 2015). In this study, the CEN showed activity in the rostral prefrontal and orbitofrontal cortices (BAs 10, 11, 47), bilateral frontal gyrus (BAs 6, 38), and the superior parietal cortex (BAs 2, 40) (Lavigne et al., 2015) as seen in Figure 1.

The dominant intercorrelated brain regions associated with this network are also depicted in Figure 1. One region that showed an increase in activity as part of this network is the rostrolateral prefrontal cortex. This area is hypothesized to be involved in higher level cognitive functions such as the evaluation of self-generated information (Christoff et al., 2003). An example of self-generated information in most fMRI-tasks is the participant's response to the task. Previous studies have confirmed that activity in the CEN decreases in patients with schizophrenia experiencing delusions compared to controls while integrating disconfirmatory evidence (Lavigne et al., 2020). These results suggest that there may be a relationship between activity in the CEN and the severity of delusions.

Many of the brain regions that comprise the CEN are also part of the lateral frontoparietal resting state network (Yeo et al., 2010). The frontoparietal network is important for coordinating behavior in a rapid, accurate and goal-driven manner (Yeo et al., 2010). The frontoparietal network acts as a functional hub both globally and specifically in terms of distributed connectivity. Fluid intelligence has also been correlated with the degree to which the frontoparietal network's coupling is distributed to other brain networks. The frontoparietal

network has also been shown to play a role in instantiating and flexibly modulating cognitive control (Marek, 2018).

Figure 1. Dominant component loadings for the Re-Evaluation Network. Images are displayed in neurological convention. Red/yellow are positive loadings.



Chapter 2: Tasks Eliciting CEN activity

Chapter 3: Results

The top seven task, or task merged studies, with CPCAs extracted components best matching the CEN template were analyzed and the Fischer Z score reported. Any significant interactions from the Repeated Measures or Mixed ANOVAs are also reported.

Task Switch Inertia (TSI)

The TSI task tested for the cognitive interference from switching between reporting different dimensions of a stimuli. For this task, participants were presented with a color naming block followed by a word reading block. The task was only conducted on a group of healthy individuals.

Component 3 of the TSI task, corresponding to 7.92% of the variance, was classified as the CEN with a Fischer Z score of 1.46. It was the highest Z score for component from any task in the CNoS fMRI task database.

For the word reading block, only the incongruent task condition elicited CEN activity, as seen in Figure 3.1. The Repeated Measures ANOVAs showed that there was a main effect for the word reading and color naming Task Conditions. For word reading, the activity in the incongruent condition was significantly higher than that in the neutral condition with average predictor weights of 0.05 and -0.05, respectively, $F(1,26) = 1.95$, $p < 0.05$. A main effect was also found for Timebins, $F(7,182) = 2.94$, but no main effect was found for the word reading block.

Significant interactions were found for Task Condition \times Timebins, for both word reading and block. As shown in Figure AAA, the interaction between Word Reading \times Timebins, $F(7,182) = 7.31$, $p < 0.001$ was dominated by timebins 2 to 4 for the increase to peak, and 5 to 6 for the return to baseline. The interaction between color naming and timebins, $F(7, 182) = 2.67$, $p < 0.05$, was dominated by timebins 2 to 3 in the increase to peak, as seen in Figure BBB. There were no significant interactions between the word reading and color naming conditions, and no significant three way interactions with timebins.

Figure 3.1. Varimax HDR for the Word Reading Block from the Task Switch Inertia task for cohort of healthy participants.

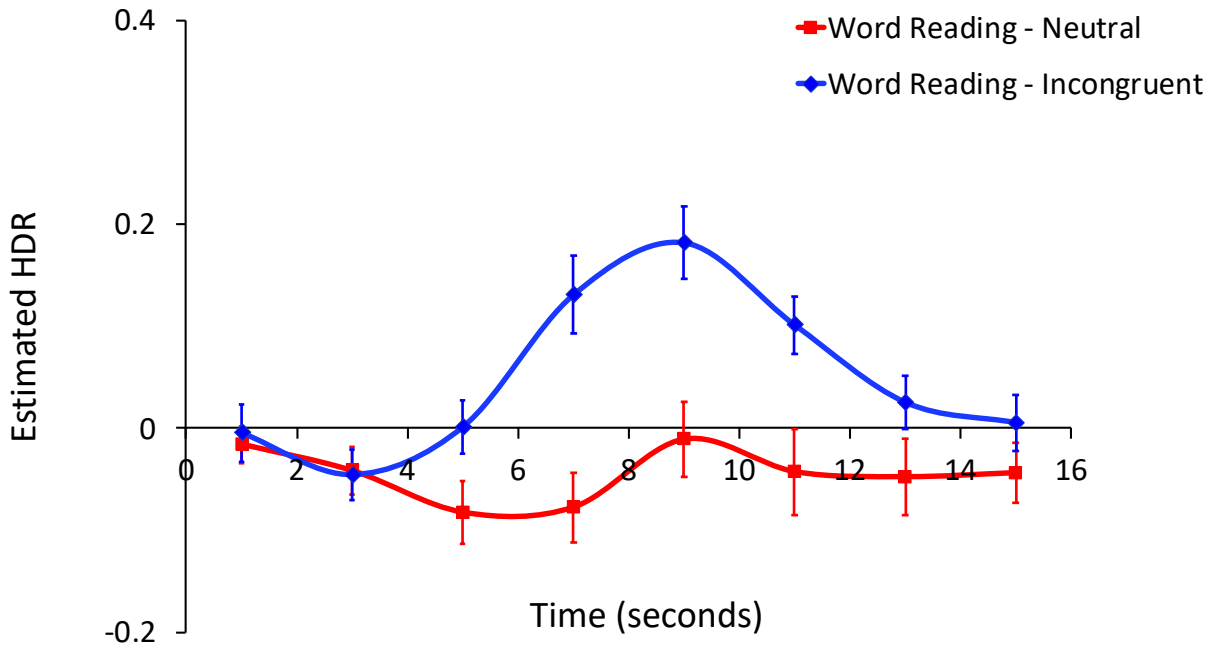
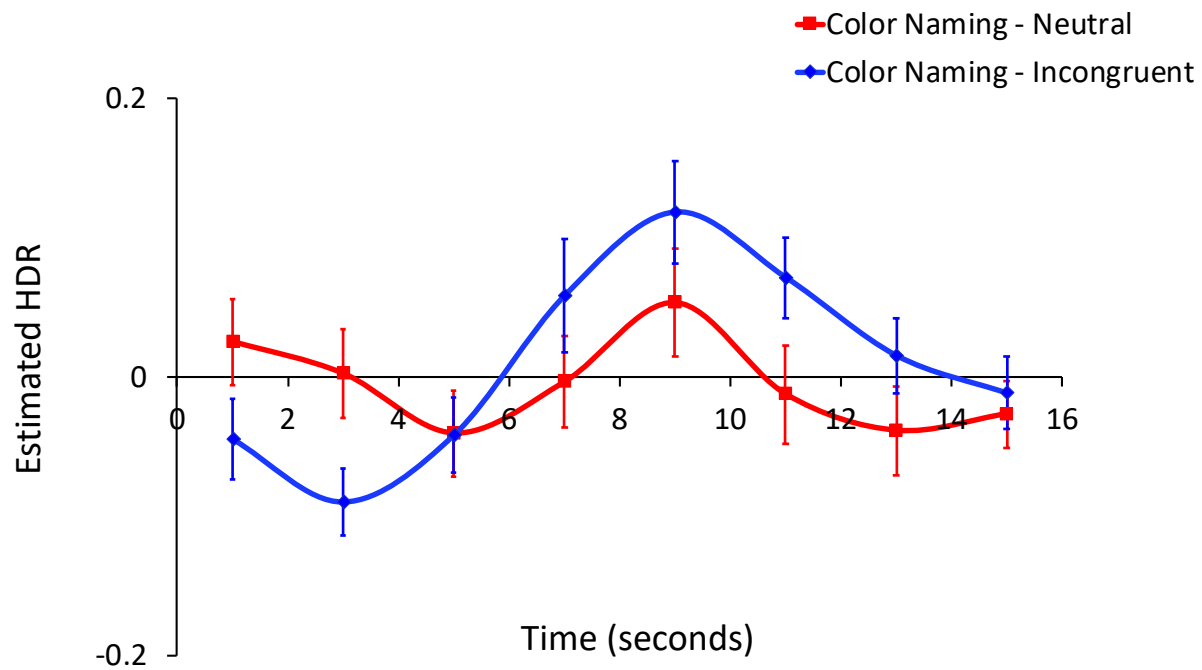


Figure 3.2. Varimax HDR for Color Naming Block from the Task Switch Inertia task for a cohort of healthy participants.



Metrical Stress and Semantic Analysis (MS-SA) Merge

For tasks where several networks exhibit similar activity over time, the low spatial and temporal resolution of fMRI can lead to the network activity of the different networks blending (Sanford et al., 2020). A proposed solution for this has been to incorporate datasets of two or more different tasks to select out specific cognitive processes (Sanford et al., 2020). In this case, the subject data sets corresponding to the semantic association and metrical stress tasks were combined and ran through the CPCA together. Predictor weights were extracted for each subject so that the estimated HDR curve for each task condition and group can be determined separately. It is important to remember that since the predictor weights depend on the components extracted with CPCA, the estimated HDR plot for a task from a merged study is different than the HDR plot corresponding only to that task.

The third component, containing 4.92 % of GC variance, was identified as the REN with a Fischer's Z score of 1.27. This study included a cohort of healthy participants and a cohort of patients with schizophrenia. As seen in the Figure 3.3, the peak of the CEN network occurred at the fourth timebin for the control cohort, but at the fifth timebin for patient cohort. Mixed ANOVAs revealed that there was a main effect of task conditions, with the average activity of the semantic condition higher than that of the Phonological condition with means of 0.05 and 0.03 respectively, as shown in Figure 3.1. There was also a main effect for Timebins, $F(9,414) = 25.95$, $p < 0.001$. No main effects were found between the cohort of healthy participants and patients with schizophrenia. A significant interaction was found for Task Condition \times Timebins, $F(9,414)=2.50$, $p<0.01$, as shown in Figure 3.3. This interaction was dominated by contrasts between Timebins 1-2, 2-3, and 3-4 for the peak increase and timebins 5-6, and 6-7 for the return to baseline. No three-way interactions with groups were found.

Figure 3.3. Varimax Rotation? HDR for Metrical Stress task from MS-SA Merge averaged over Group (Healthy_Schizophrenia).

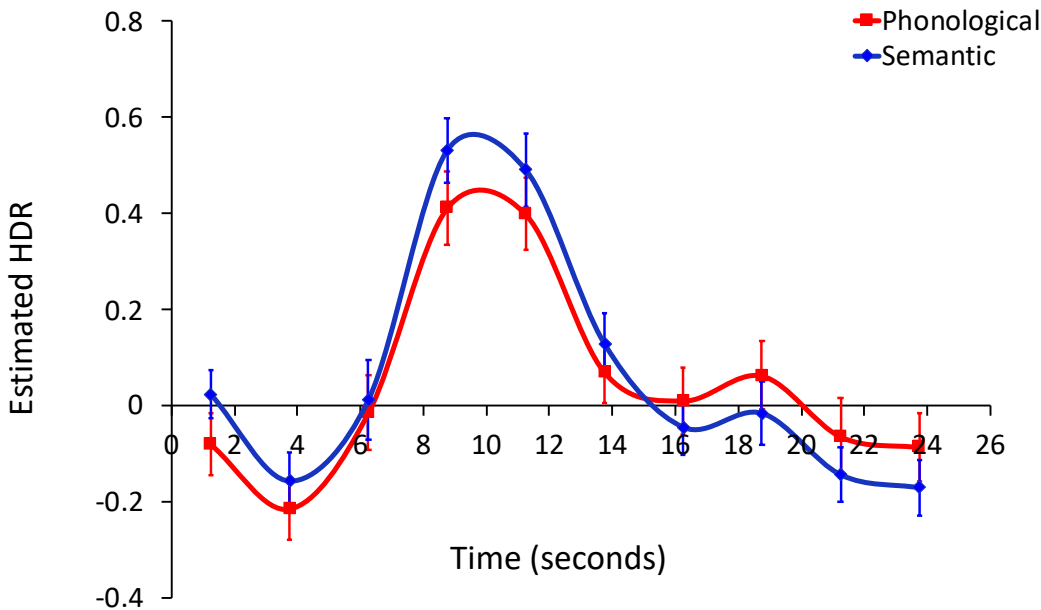
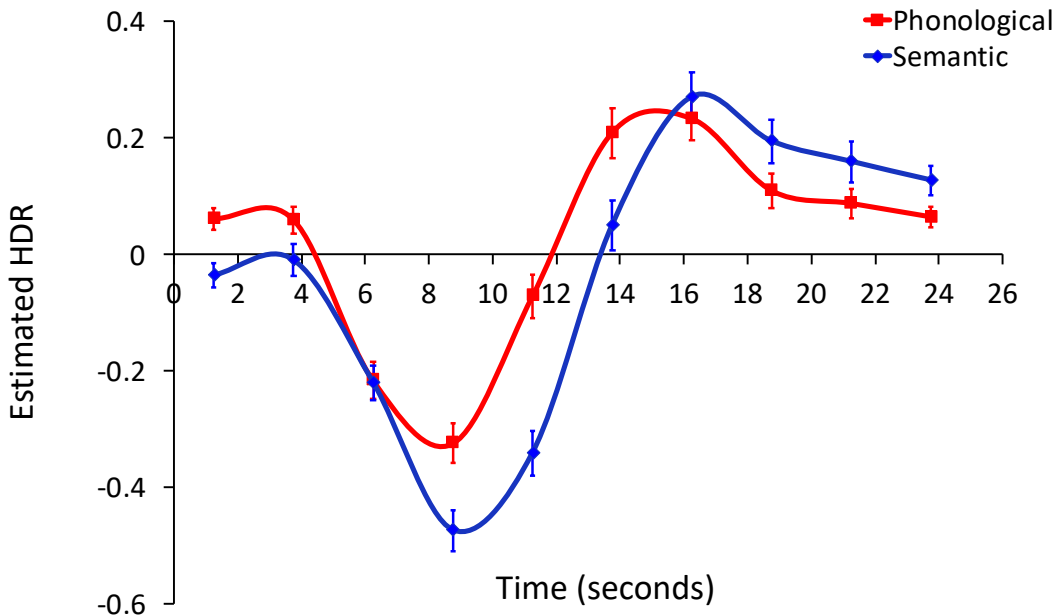


Figure 3.3 shows the estimated HDR for the SA task. In this case, an initial suppression of the network was observed for all conditions and for both the control and patient groups. The greatest suppression occurred at around the fourth timebin. Network activity then increased although to a lower amplitude than the Metrical Stress (MS) task near the seventh timebin for all groups and conditions.

For the SA task, mixed ANOVAs revealed a main effect of Timebins, $F(9,462) = 62.19$, $p < 0.001$, and of Task Condition, $F(1,55) = 11.70$, $p < 0.01$. No main effect was found between the healthy and patient cohorts. A significant interaction was found between Task Condition \times Timebins, $F(9,495) = 27.00$, $p < 0.001$ as shown in Figure 3.4. Significant increase occurred between timebins 2 to 3, $F(1,55) = 14.09$, $P < 0.005$, 3 to 4, $F(1,55) = 47.91$, $P < 0.005$, 4 to 5, $F(1,55) = 28.16$, $P < 0.005$, 5 to 6, $F(1,55) = 18.58$, $P < 0.005$, and 6 to 7, $F(1,55)$

$= 56.75$, $P < 0.005$. No significant interactions with Group or three-way interactions were found.

Figure 3.4.. Varimax HDR for Semantic Association task from MS-SA Merge averaged over Group (Healthy_Schizophrenia).



Task Switch Inertia and Thought Generating Task (TSI-TGT)

The fourth component extracted from a merged analysis of the TSI task and the Thought Generation Task (TGT) task was classified as the REN with a Fischer Z score of 1.19. This component accounts for 6.41 % of GC variance. Unlike the first TSI dataset, the TSI-TGT merge dataset included both healthy and patient cohorts.

Figure 4.4 shows the HDR response curves for each group and task condition corresponding to the TSI portion. Like the results for the TSI task alone, as seen in Figure 2.1, only task switching from any color block to a word incongruent condition elicited network activity. In this case, the dashed red curve represents the average of the neutral color naming and incongruent color naming conditions. Comparing the HDR curves between the control and

patient groups for the word incongruent condition showed that both peaked at timebin 5, with the control group having a higher activity compared to patients.

For the TGT task, CEN peaks occurred earlier, and were higher for the generating condition compared to the hearing condition for both control and patient cohorts. As shown in Figure 4.5, the peak of the generating condition occurred at timebin 4 for the generating condition and timebin 5 for the hearing condition. A significant increase was found between Condition \times Timebins, $F(7,413) = 0.85$, $p < 0.05$), but not between Condition \times Timebins \times Group. The interactions between the hearing and generating conditions were significant between timebins 2 and 3, and 4 and 5.

Presenting the OTTBADe results – make it clear exactly how this is different

Bias Against Disconfirmatory Evidence Task – One Time Testing

Bias Against Disconfirmatory Evidence Task (BADE) LAVIGNE PREPOST 3

The third component of the Bias Against Disconfirmatory Evidence (BADE) Prepost study, accounting for 4.88 % of the task related (GC) variance, was classified as the CEN with a Fischer Z score of 1.04. This study included only patients with schizophrenia. Figure 4.6 shows the HDR curves for each task. Both confirm condition (Yes-Yes (YY), No-No (NN)), and both disconfirm conditions (Yes-No (YN) and No-Yes (NT)), showed a peak in REN activity at the eighth timebin. Higher activity was observed for the two disconfirming conditions compared to the confirm conditions. Between the disconfirm condition, the No-Yes condition exhibited higher activity compared to the disconfirm condition, Yes-No condition. The Repeated Measures ANOVAs revealed a main effect for the confirm vs. disconfirm condition with activity in the disconfirm condition significantly higher ($M=0.10$) than in the confirm condition ($M=0.05$), $F(1,57)=19.07$, $p<0.001$. A significant main effect was also found for the yes first vs.

no first conditions, showing that on average, there was higher activity for yes first ($M=0.09$) compared to no first ($M=0.06$). There was also a main effect for the timebins, $F(9,513)=93.41$, $p<0.001$.

Figure 3.4. Varimax HDR for Bias Against Disconfirming Evidence Task, averaged over First Expected Response

(YesFirst_NoFirst) for a cohort of schizophrenia patients only.

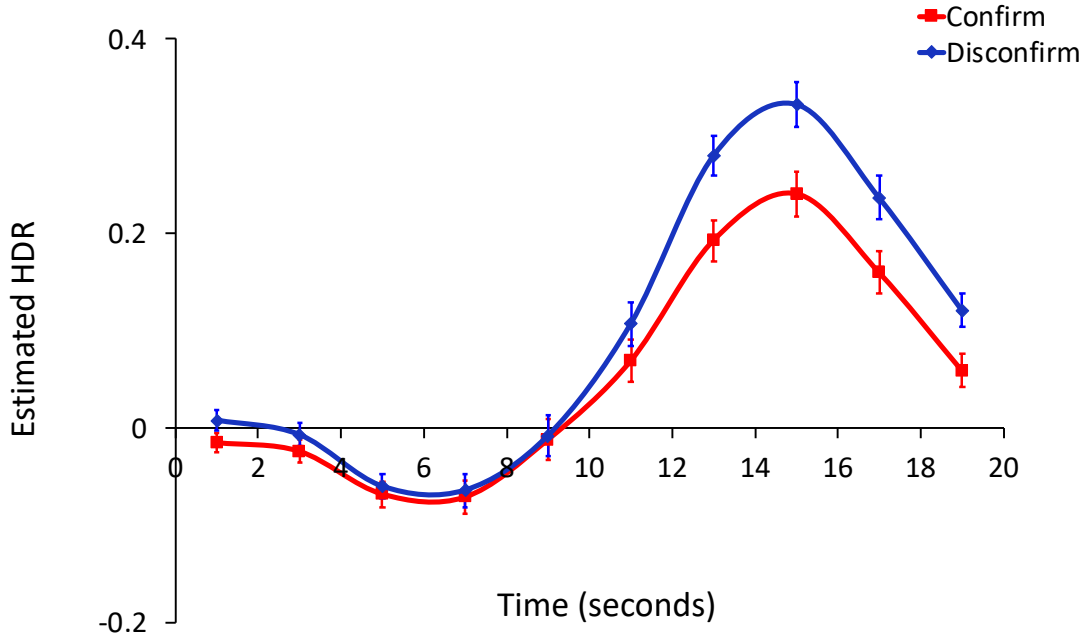
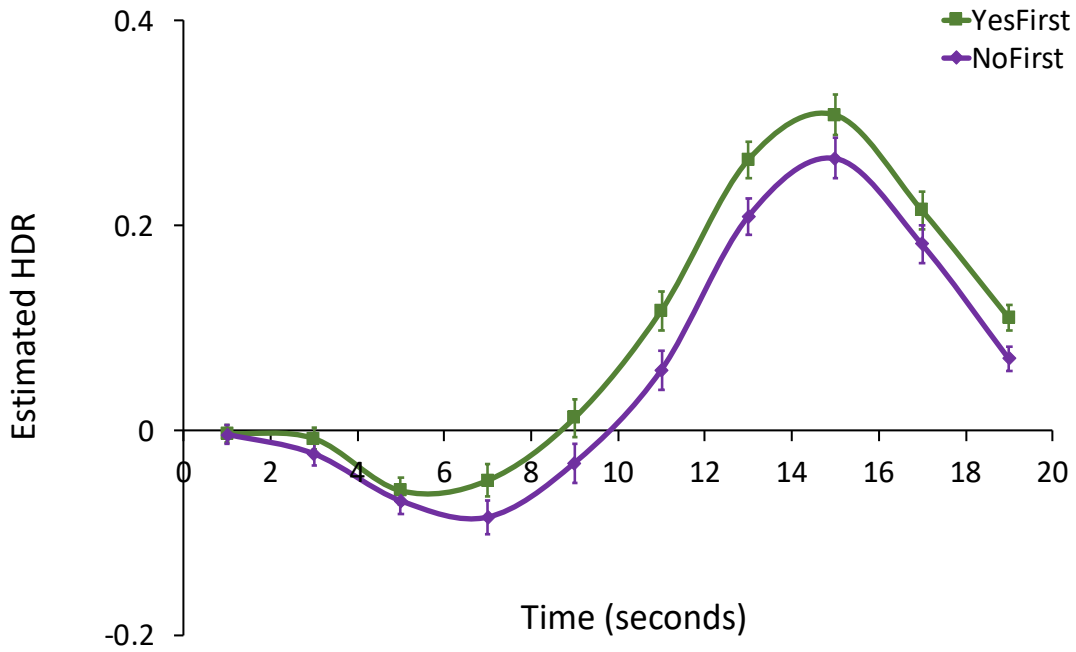


Figure 3.4. Varimax HDR for Bias Against Disconfirming Evidence Task, averaged over Response Condition

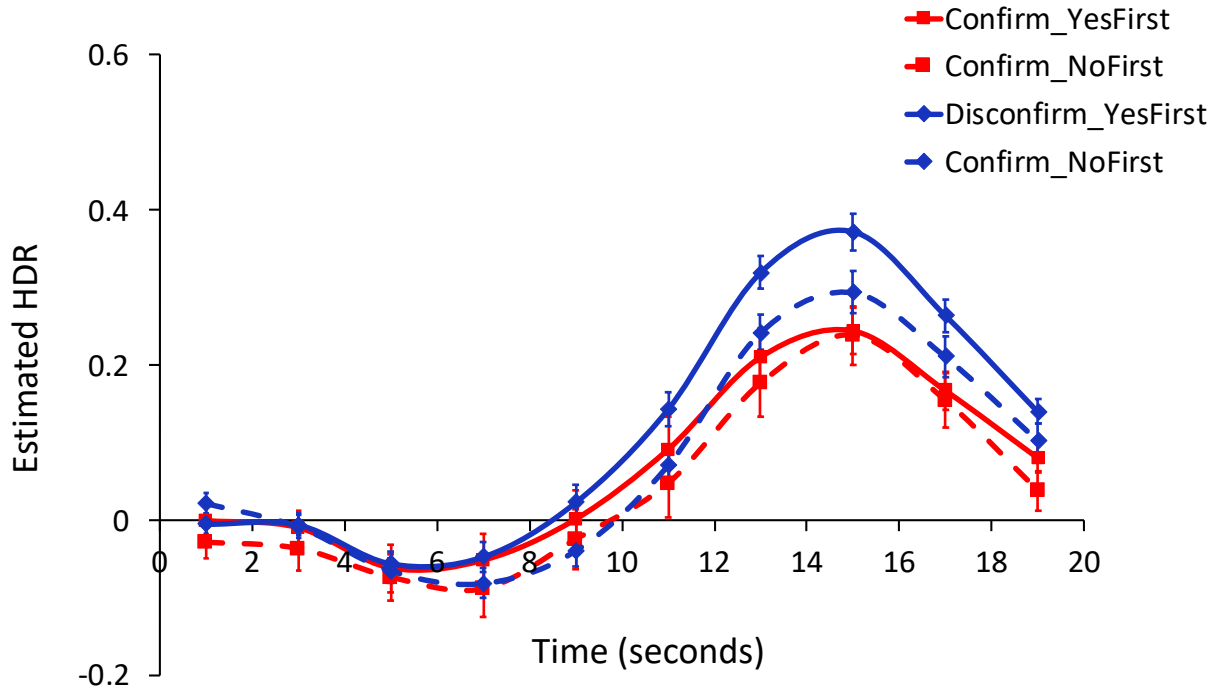
(Confirm_Disconfirm) for a cohort of schizophrenia patients only.



Significant interactions were found for Conditions \times Timebins, $F(9,513)=5.06$, $p<0.001$ which was dominated by activity between timebins 5 and 6, and 6 and 7.

There was also a significant interaction for Expected First Response \times Timebins, $F(9,513)=3.26$, $p<0.001$, which was dominated by activity between timebins 3 and 4. There was a three-way significant interaction between Task Condition \times Expected First Response \times Timebins, $F(9,513)=2.90$, $p<0.01$.

Figure 3.4. Varimax HDR for Bias Against Disconfirming Evidence Task for a cohort of schizophrenia patients only.



Animal BADE Task (ABADE)

The first component of the Animal BADE (ABADE) task conducted on a cohort of healthy controls was classified at CEN with a Fischer Z score of 1. It accounts for 10.88 % of the task related (GC) variance. This study included only healthy controls.

The HDR plot for task version A, is shown in Figure 4.7, and for task version B in Figure 4.8. Version B of the task was designed to separate between the processes involved in visual processing and those responsible for the integration of disconfirmatory evidence (Lavigne et al., 2015). The peaks in CEN activity occurred at timebin 7 for the confirm condition, and timebin 8 for the small and disconfirm conditions. For version B, a smaller peak was seen between timebins 5 and 6, followed by a larger peak at timebin 8 for all conditions. In both cases, the disconfirm condition was found to have a higher peak compared to the both the confirm and small change conditions.

Significant interactions were found between Conditions \times Timebins, $F(22,748) = 6.29$, $p < 0.05$, and between Groups \times Timebins, $F(11,374) = 47.47$, $p < 0.05$. The interaction between response conditions and timebins was significant between the small and confirm conditions from timebins 9 to 10, $F(1,34) = 5.46$, $p < 0.05$, and 10 to 11, $F(1,34) = 12.99$, $p < 0.05$. Between the confirm and disconfirm response conditions, significant interactions were found between timebins 4 and 5, $F(1,34) = 6.87$, $p < 0.05$, 6 and 7, $F(1,34) = 5.33$, $p < 0.05$, 8 and 9, $F(1,34) = 19.59$, $p < 0.001$, 9 and 10, $F(1,34) = 12.99$, $p < 0.05$.

Thought Generation Task and Semantic Analysis Task Merge (TGT-SA)

The next merged study that was analyzed was the merge of TGT and SA tasks. Component 4 of this task accounted for 4.19% of the task related variance and was classified as the CEN with a Fischer Z score of 0.93. This study included both a control cohort, and a cohort of patients with schizophrenia.

For the TGT, the CEN peak occurred between timebins 3 and 4, as seen in Figure 4.9, which is slightly earlier than the peak observed for the TSI-TGT merge, in Figure 4.5, where the peak was reached between timebin 4 and 5. A similarity between the TGT response from both merges is that there are no conclusive differences between the control and patient groups. However, in both cases, the generating condition elicited earlier and stronger CEN activity.

Main effects?

Significant interactions were found for Conditions \times Timebins, but not between Conditions \times Timebins \times Groups. These interactions showed a significant increase between timebin 2 and 3, $F(1,47) = 31.98$, $p < 0.001$, 3 and 4, $F(1,47) = 16.06$, $p < 0.001$, 4 and 5, $F(1,47) = 19.59$, $p < 0.001$, 5 and 6, $F(1,47) = 12.82$, $p < 0.005$, and 7 and 8, $F(1,47) = 13.41$, $p < 0.005$.

The SA task showed late peaks relative to stimulus presentation, and this was comparable to the results from the MS-SA merged in Figure 2.3. While there were no major differences between the control and patient groups, there was a greater and more delayed response for the CEN for the low condition, where the words presented were distantly related to the prompt word, compared to the high condition, where the words were closely related. Significant interactions were found for conditions x timebins, $F(9,495) = 36.04$, $p < 0.001$.

From this task merge, we found significant correlations between CEN network activity in the TGT task and the severity of delusions for the patient cohort, SSPI7, as indicated by the SSPI scale ($CV4, R = -0.56$, $p < 0.05$). The largest contribution for the CEN came from the generating condition ITP (canonical loading = -0.66) and the RTB (canonical loading = 0.40) variables.

A significant correlation between CEN activity in the SA task and the Beck Cognitive Insight Scale statement 10 BCIS 0 was also found for the patient cohort ($CV1, R = 0.52$, $p < 0.05$). The largest contribution for the CEN activity came from the ITP for the high condition (canonical loading = -0.61), and the RTB from the low condition (canonical loading = 0.75). According to the makers of the scale, this statement is testing for an individual's resistance to accepting feedback from others (Beck et al., 2004). This suggests a possible negative relationship between CEN activity and the ability to receive feedback from others.

Social Cognition Task

The third component of the SC task from the 100 subject HCP study, accounting for 6.18% of the task related (GC) variance, was the last component analyzed. This study only included a healthy control cohort.

For the SC 8task, the CEN peaks were late relative to stimulus presentation for both the mental and random conditions. Significant interactions were found between Conditions \times Time, $F(45,22410) = 69.53$, $p < 0.05$. The first significant range was between timebins 4 and 6 ($p < 0.05$), timebins 7 and 14 ($p < 0.05$), timebins 16-23 ($p < 0.05$), timebins 28-30 ($p < 0.005$), timebins 32 to 38 ($p < 0.005$), and timebins 41-45 ($p < 0.05$). The last two ranges correspond to the increase from baseline to peak and return to baseline, respectively. This indicates that the slope of the curves for the mental and random condition where significantly different between these time periods. Since the HCP was a study on healthy human participants, there was no data on SSPIS or BCIS and so no correlations were conducted for this study.

Chapter 4: Discussion and Analysis

The top seven task or task merged studies with CPCA extracted components best matching the spatial template of the CEN were selected and analyzed. Their predictor weights were used to generate HDR curves for each condition and group in the study. This offered a quantitative measure to compare the CEN activity over time after stimulus presentation. In this section, the results of each task are interpreted and any relevant insights into the function of the CEN are reported. Afterwards, the results from all the studies are evaluated together to see if they support or contradict the initial hypothesis. Comparing the timing of CEN activity with other networks elicited by these tasks, such as the External Attention Network and the Response Network, provides important temporal information for answering this question.

5.0.1 Task Switch Inertia (TSI)

For this study, an increase in CEN was only observed when switching to a incongruent word reading block. A previous study on the network on this task considered that the increase of this network could be potentially due to it playing a role in a stimulus conflict detection process (Sanford, 2019). However, as argued by that author, this is unlikely considering the peak of the CEN occurs relatively late compared to the Response Network. If the CEN worked in term of bottom-up processing, where the perception of the stimuli is based on the sensory input, and not based on cognition, then this network should have been active earlier on (Sanford, 2019). This evidence first supported the idea that the CEN could potentially active after the participant has responded to the cognitive task. It supports the idea that the network may be active while an individual evaluates their response to the task.

5.0.2 Metrical Stress and Semantic Association (MS-SA)

The CEN peak for the MS task occurred at roughly the same time and intensity for both groups and both conditions. The similarity in CEN activity between the phonological and semantic conditions suggests that the role played by the network is not specific to the cognitive processes involved in phonological or semantic association.

In the SA, the HDR curves were similar for all groups and conditions, with the peak occurring at timebin 7. One distinction between this task response compared to all others analyzed here is that CEN network activity showed a noticeable suppression in the right at the onset of the task. This suppression seems to occur as Language Network activity begins to increase, possibly suggesting some relationship between the two networks.

The first network elicited in the response to the MS task was External Attention Network which peaked at timebin 6 for all groups and conditions. While the specific role of the External Attention network is not fully understood, it is believed to be involved in attending to external stimuli (Lavigne et al., 2015). By comparing the timing of the peak of the CEN and the External Attention network, it was determined that CEN activity occurs after the participant's attention is sustained on the external stimuli.

Significant correlations between CEN network activity and SSPI were found for the SA task. In this case, they may suggest a weak negative relationship between CEN activity and SSPI 5: Insomnia, and SSPI 8: Hallucinations. However, the regions of brain typically involved in the control of sleep and wakefulness (Boksa, 2009) also do not seem to be involved in the CEN, and as a result, changes in CEN network activity are not expected while experiencing insomnia. Additionally, it is not expected that the activity of this network should change with hallucinations, since the regions of the brain that have been indicated as potentially playing a

role in hallucinations, namely the primary auditory cortex, and superior and medial temporal gyrus (Boksa, 2009) are not involved in the CEN.

5.0.3 Task Switch Inertia and Thought Generation Task Merge (TSI-TGT)

The observed CEN activity for the TSI portion was very similar to the analysis done on the TSI alone, as shown in Figure 4.1. The results from the TGT seen in Figure 4.5, indicate that an earlier and stronger CEN response was elicited in the generating condition compared to the hearing condition, but that no significant differences were found between controls and patients with schizophrenia.

In this case, the higher activity in the generating condition could potentially be attributed to the fact that the cognitive processes involved with self-generated information (Christoff et al., 2003) are more strongly involved in the generating condition compared to the hearing condition. This is likely the case since in the generating condition participants must come up with a definition to a given word, while in the hearing condition they simply must listen to it. This would also support the existing hypothesis that the network is involved in the evaluation of the task response.

Since the TSI task required participants to report a response, one of the CPCA extracted components for this merge was classified as the Response Network. The Response Network is hypothesized to be active when the participant is responding to the task. It demonstrates single or bilateral activity depending on if the response is done with one or both hands (Lavigne et al., 2015). While comparing the relative timing of the Response Network and CEN peak could offer valuable insights into the function of CEN, the HDR plot for the TGT task showed that for this task, the Response Network was only suppressed, making it difficult to make any conclusions about the relative timing of the networks. However, for the TSI task, where a response network

peak was observed, this peak occurred at timebin 4 for all conditions which was earlier than the CEN peak at timebin 5. These finding support the idea that the CEN plays a role a process that occurs after the participant has responded to the cognitive task. In this case, that process could be the evaluation of whether they reported the right color after task-switching.

Significant canonical correlations were found between CEN activity and Language Network activity for the control group for both tasks. This seems to suggest a possible relatively strong negative relationship between CEN and Language Network activity. This would mean that as the activity of one network increases, the activity of the other is expected to decrease. However, in other tasks where the language network was also elicited, no significant correlations were found between these two networks, so it is difficult to tell if a relationship exists at this point. A significant correlation was also found with the Focus on Visual Features Network potentially indicating a negative relationship with the CEN but only for the patient cohort.

5.0.4 Bias Against Disconfirmatory Evidence (BADE)

The results of the BADE study indicate that CEN network activity has a late peak and is larger in amplitude for the disconfirming condition in patients. This result may suggest that the network could play a specific role in dealing with information that goes against a person's current belief. However, it could also suggest that network activity increases during the response evaluation period and is more active for conditions where the participant may have more reason to question their response. This would be the case for the disconfirming condition since the participant would be more likely to question and reconsider their second response based on their answer to the first. While the participant is asked to respond to task stimuli twice, only one CEN peak is observed. A previous study on the CEN in schizophrenia patients showed reduce

network activity in patients when processing disconfirmatory evidence relative to controls, with this being most evident for the delusional group (Lavigne et al., 2020). For this reason, the finding that there were no significant correlations for symptoms was surprising. However, this may be due to the fact that a more complicated relationship exists between the onset of symptoms, and that contributions from the other networks should also be considered. Therefore, correlations using the multiple-set canonical correlations should be performed for this study to see if any relationships exist between the severity of symptoms and two or more of the networks elicited by this task.

5.0.5 Animal BADE (ABADE)

The CEN activity peaks looked slightly differently for the two versions of this task. Task version B was designed to separate the processes involved in visual processing from those related to the task response (Lavigne et al., 2020). As seen in Figure 4.8, this task showed an additional smaller and earlier peak in CEN activity. The presence of a significant interaction between for version x timebins suggests that the HDR curve depended on the version of the task and each condition (Lavigne et al., 2020).

The presence of the small peak seen at timebin 5 for the ABADE task version B, shown in Figure 2.8B, but not in task version A, shown in Figure 2.8A, suggests that slight increase in CEN activity may occur when the participants respond to the first image, but that this activity is only observed when the cognitive processes responsible for responding to the task are isolated from the visual attention processes.

When comparing the onset of the CEN peak to the other networks elicited by the ABADE task, it is evident that CEN activity peaked 4-5 timebins later than the one-handed response network. It is believed that this response network is elicited as participants respond to

the task which in this case is done by pressing a button with one hand (Lavigne et al., 2020).

The presence of the response network activation several timebins before the peak of CEN activity supports the initial hypothesis that the network could play a role in process of evaluating the response to the task.

A significant correlation was also found between CEN activity and the Focus on Visual Features Network. In this case, a positive relationship between the activity of the two networks. This contradicts the findings of the TSI-TGT merge and so no conclusions can be made about any possible relationship between CEN and the Focus on Visual Features network.

5.0.6 Thought Generating Task and Semantic Association Task Merge (TGT-SA)

For the TGT the response curves were like those observed in the TGT-TSI Merge. One distinct difference between the SA HDR response between the TST-TGT Merge and this TGT-SA Merge is that there was no initial suppression seen in CEN activity. This may suggest that the suppression was not part of the response to the SA task but simply a result of merging the TSI and TGT data sets together.

This task also elicited both the CEN network and the Response Network with the Response Network peak occurring before the CEN peak for all conditions and groups. As explained above, this supports the functional hypothesis for this network. The canonical correlations revealed two interesting results for this task. A significant interaction was found between CEN activity and the severity of delusions. This supports findings from a previous study where patients experiencing delusions exhibited lower levels of CEN activity [16]. The other significant correlation was found between CEN activity and BCIS 10 which tests for an individual's ability to receive feedback from others. The results from this correlation suggest a

negative relationship between CEN activity and the ability to receive feedback from others. This could be supported by previous research on the integration of disconfirmatory evidence (Lavigne et al., 2020), because the inability to accept feedback from others could be related to a bias for rejecting evidence that goes against one's current beliefs.

5.0.7 Social Cognition Task

Responding to the mental condition elicited higher CEN activity compared the random condition, suggesting that the network may be more active when recognizing social interactions. Past studies have shown that multiple brain regions are involved in the regulation of social behaviors and in the formation of social recognition memory (Tanimizu et al., 2017). Two of these regions are the medial prefrontal cortex and the amygdala which are involved in the regulation of social behaviors. While these regions are not highly involved in the CEN, the distinct roles of different brain regions in the consolidation of social recognition memory remain unclear (Tanimizu et al., 2017), and it is possible that some of the regions associated with the CEN could be involved. However, the relative timing of the CEN peak may contradict this idea.

Considering the initial hypothesis, the presence of a late peak of activity for both conditions supports the fact that this network could be involved in the task response evaluation process. Strengthening this argument is the fact that the External Attention Network, which is typically elicited as an individual responds to the task, showed a peak in activity about 20 timebins, or approximately fifteen seconds before the CEN. As described for previous tasks, the relative timing of these two peaks suggests that the processes that the CEN is involved in occur after task stimulus presentation.

Overall Trends and Link to Function

Comparing the timing of the CEN peak and other networks elicited by the task provides important information for testing our hypothesis. Of particular interest is comparing the peak of the CEN network with the External Attention Network and the Response Network. The External Attention Network is believed to be active when an individual directs their attention to an external stimulus (Lavigne et al, 2015). Therefore, while it does not provide information on whether the individual has responded to the task, it does provide a relative sense of when the participant began to attend to the stimulus. The Response Network is hypothesized to be active as the participant responds to the task. The timing of this network is even more important for evaluating the hypothesized function of the CEN since we can determine if CEN activity constantly occurs after the participant has responded to the task.

For the tasks that did not elicit the Response Network or where the activity of this network was suppressed, comparisons were made between the relative timing of the CEN and the External Attention network. The HDR plots for these studies are shown in Figure 2.1, and include the MS and SA tasks from the MS-SA task merge, the TGT from the TSI-TGT merge and from the TGT-SA merge, the BADE task, and the SC task. Figure 3.1 also shows indicates when the External Attention network peaked (dashed line), and when the CEN peaked (solid line). For all the tasks analyzed, the External Attention Network peaked before the CEN, suggesting the CEN is always involved in processes that occur after attending to the task stimulus. The difference in time between the two peaks varied for each task and requires further analysis for better understanding possible implication with respect to network function. Since each task elicited several specific cognitive processes, it is difficult to make general

conclusions. The length of the stimulus presentation could also play a role in the corresponding network activity.

Conclusion

Key Findings

For all the tasks were both the CEN network and the Response Network was elicited, the peak of CEN always occurred after the peak of the Response Network. This finding supports the hypothesis that the CEN activity increases after the participant has responded to the cognitive task, and likely while they are evaluating their response to the task.

The CCA revealed several possible relationships between CEN activity and that of the Language Network and the Focus on Visual Features Network. However, none of these proved to be conclusive. Since the function of the Language and Focus on Visual Features Network is only hypothesized, this also made it more difficult to interpret what the results meant in terms of the underlying cognitive operations. It may be worthwhile to study these relationships with a different method than CCA to see if any conclusions can be reached.

The results of the CCA for the TGT task from the TGT-SA suggest that there is negative relationship between CEN activity and the severity of delusions. This supports earlier research looking at CEN activity during evidence integration in patients with schizophrenia, experiencing delusions [4].

In the TGT task from the TGT-SA merge, a significant negative relationship was also found between network activity and the severity of delusions. A negative relationship with BCIS 10 was also found suggesting that CEN there may be lower CEN activity in people who have more trouble receiving feedback from others. While the results were only found in one task, the correlations with BCIS were only done in done in 3 of the seven tasks due to time and data constraints. These correlations should be computed for the remaining tasks to determine if there is a relationship present.

Limitations

There are several limitations to task-state fMRI research. The first is the temporal limitations of fMRI. This is since the hemodynamic response occurs a few seconds after the neurophysiological event, and therefore there is usually a delay in the response of 4-6 seconds (Buckner, 1998). Since this study is based on comparing the temporal profiles of the HDR, it is important to keep this limitation in mind when interpreting the BOLD response.

The interpretation of canonical correlation analyses is also straight forward and issues and therefore better methods should be implemented to better test the relationships found in this study (Wang et al., 2020).

Lastly, the BCIS is a self-reporting questionnaire which always introduces the possibility of self-bias. This should be considered when making interpretations for these results.

Future direction

Further studies will include using a behavioural CPCA method to further the relationships found between network activity and SSPI and BCIS elements. EEG task-based studies could also be planned to obtain a better temporal resolution for network activity.

Figures

Figure 1.1: Visual representation of the activation of the Cognitive Evaluation Network. The yellow, lighter regions represent more dominant intercorrelated regions, while the red, darker regions are less intercorrelated regions. The areas of the brain relevant to this network include the orbitofrontal cortex, inferior frontal gyrus, and the parietal cortex.

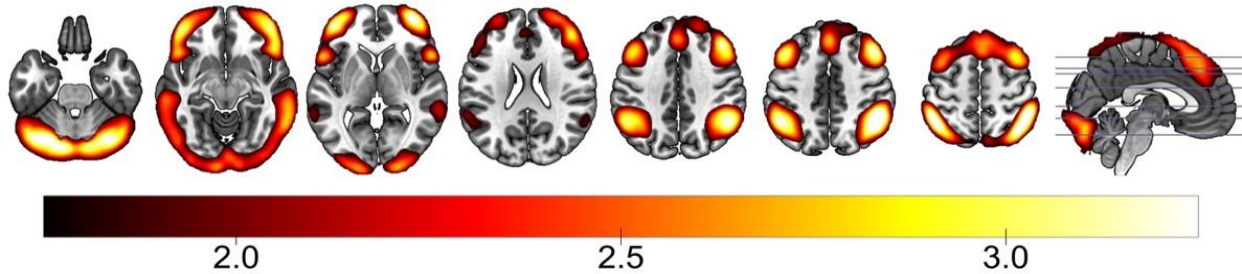


Figure 2.1: Hemodynamic response plot for the Task Switch Inertia (TSI) task for a healthy cohort divided by group and task condition.

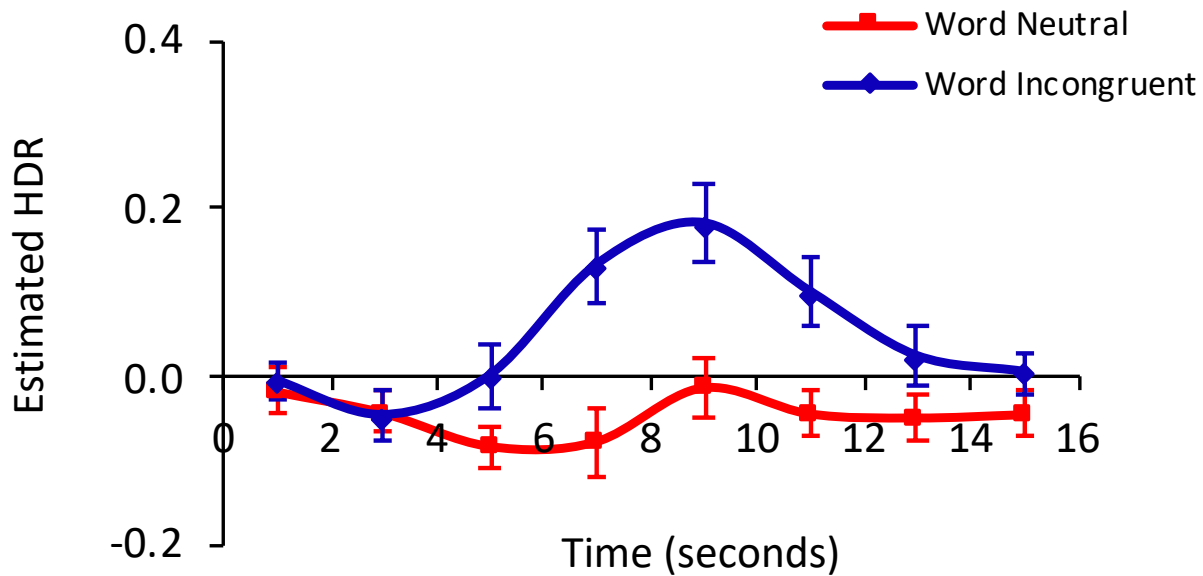


Figure 2.2: Hemodynamic response plot for the Metrical Stress task from the MS-SA merge, divided by group and condition.

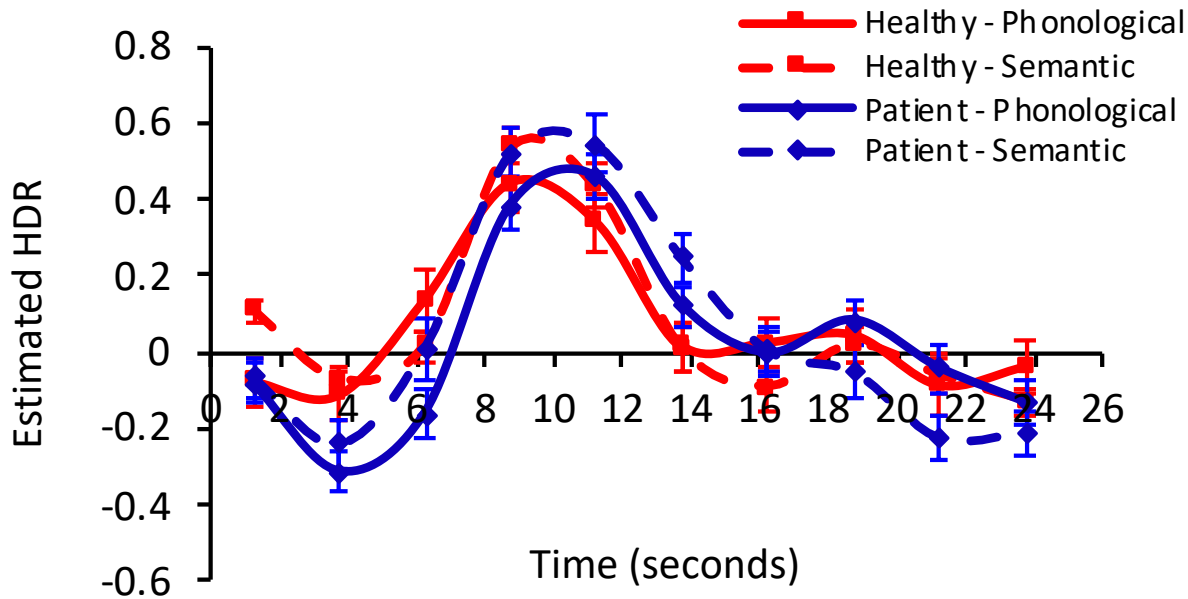


Figure 2.3: Hemodynamic response plot for the Semantic Association task from the MS-SA merge, divided by group and condition.

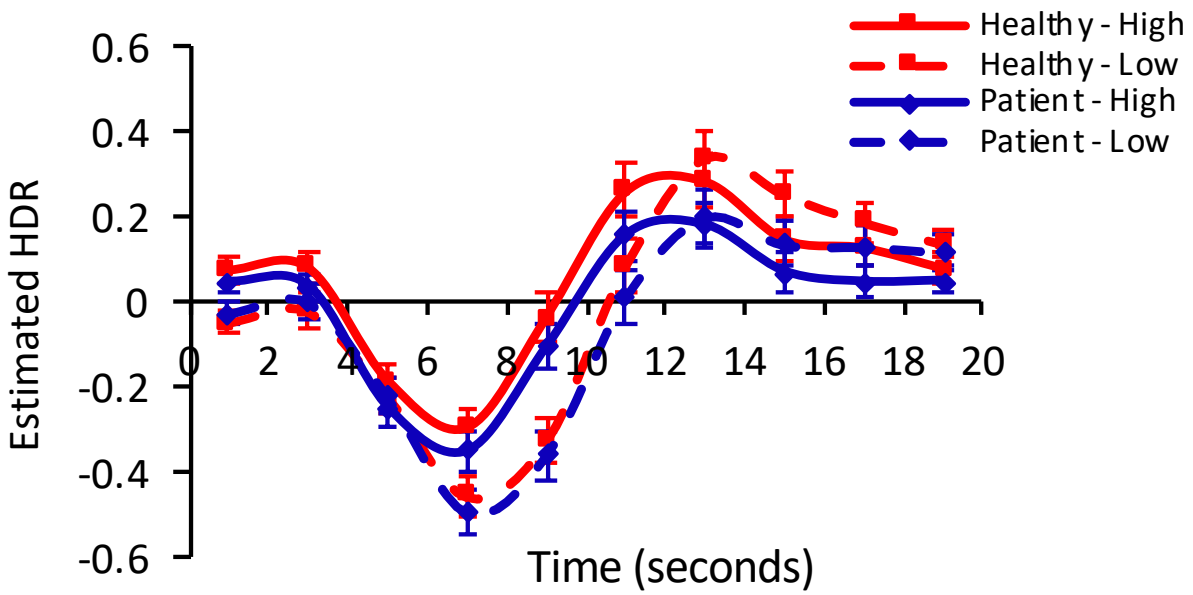


Figure 2.4: Hemodynamic response plot for the Thought Generation Task from the TSI-TGT merged study, divided by group and condition.

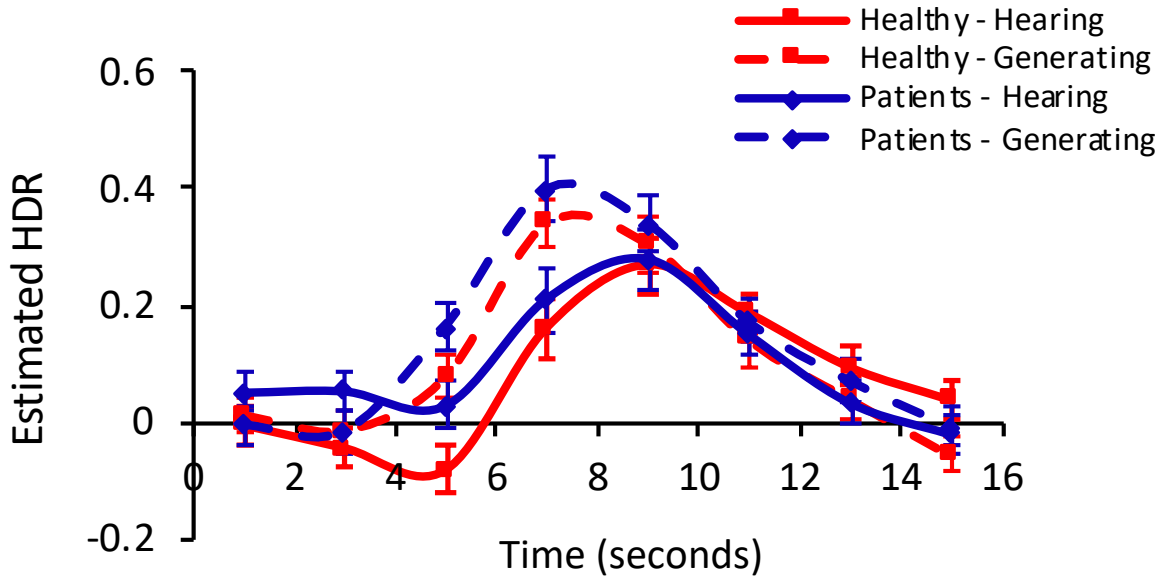


Figure 2.5: Hemodynamic response plot for the Task Switch Inertia task from the TSI-TGT merged study, divided by group and condition.

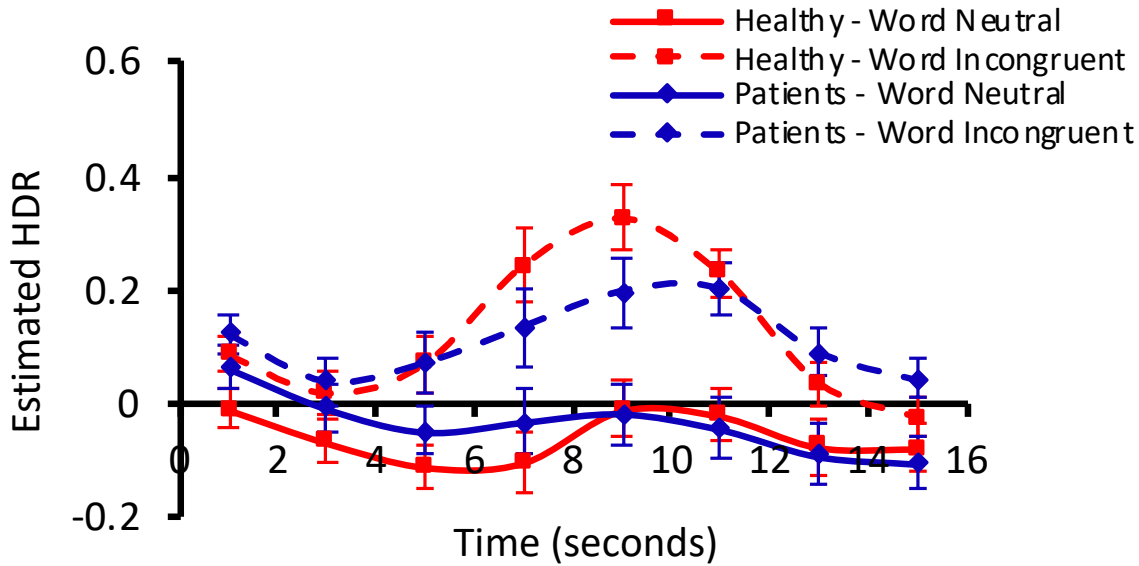


Figure 2.6: Hemodynamic response plot for the Bias Against Disconfirmatory Evidence (BADE) task divided by task condition for a cohort of patients with schizophrenia.

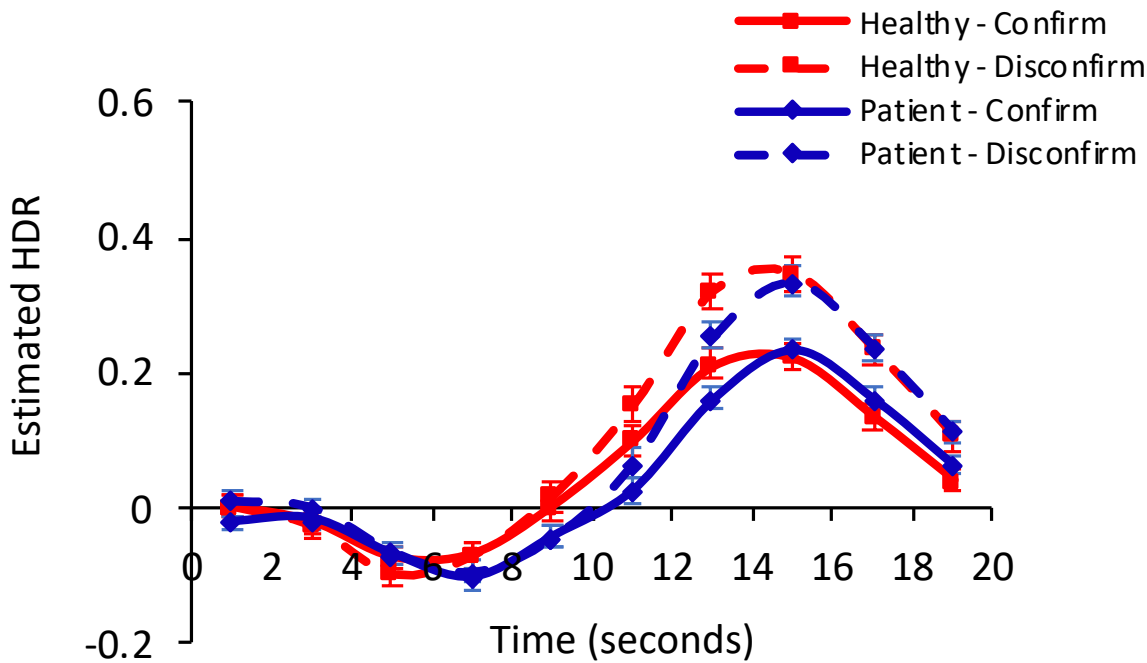


Figure 2.7: Hemodynamic response plot for the Bias Against Disconfirmatory Evidence (OTTBADE) task divided by task condition for a cohort of patients with schizophrenia.

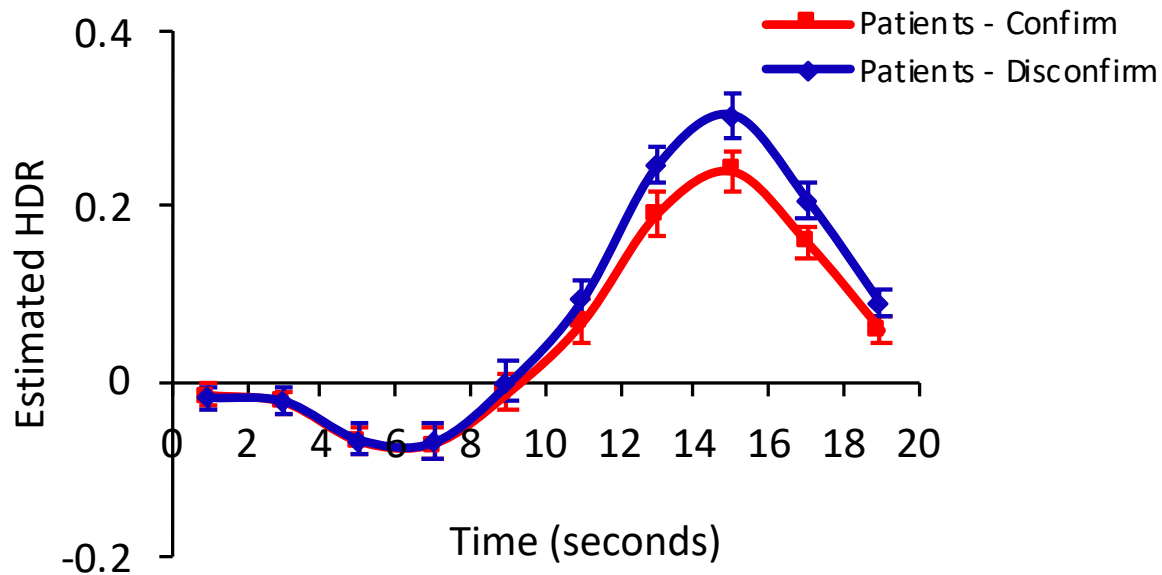


Figure 2.8A: Hemodynamic response plot for the Animal Bias Against Disconfirmatory Evidence (ABADE) task Version A divided by task condition for a cohort of healthy participants.

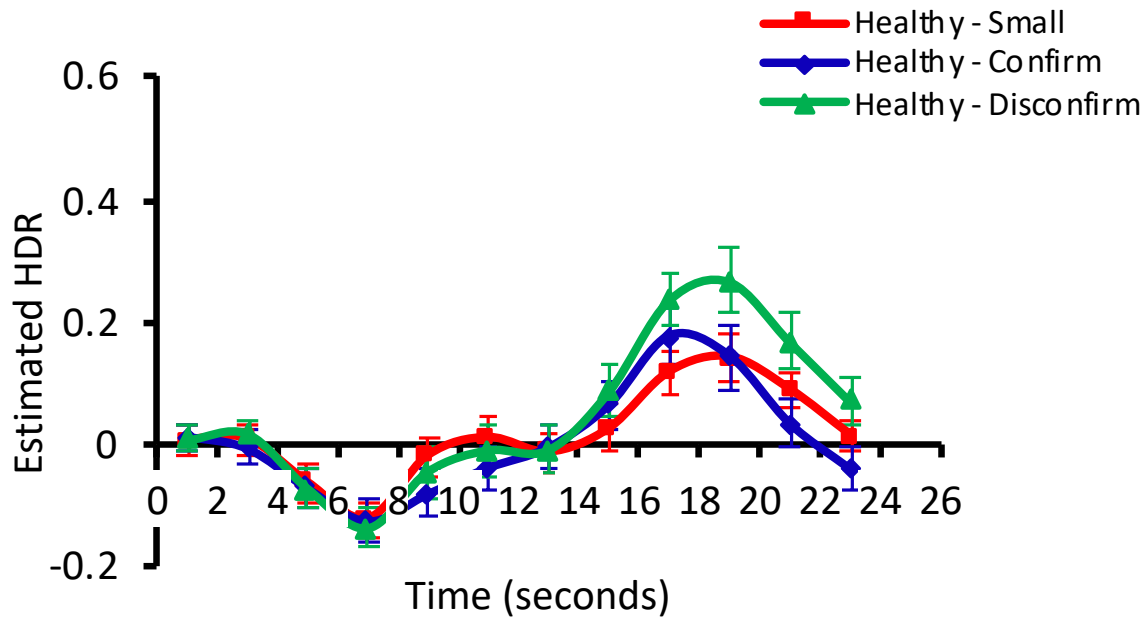


Figure 2.8B: Hemodynamic response plot for the Animal Bias Against Disconfirmatory Evidence (ABADE) task Version B divided by task condition for a cohort of healthy participants.

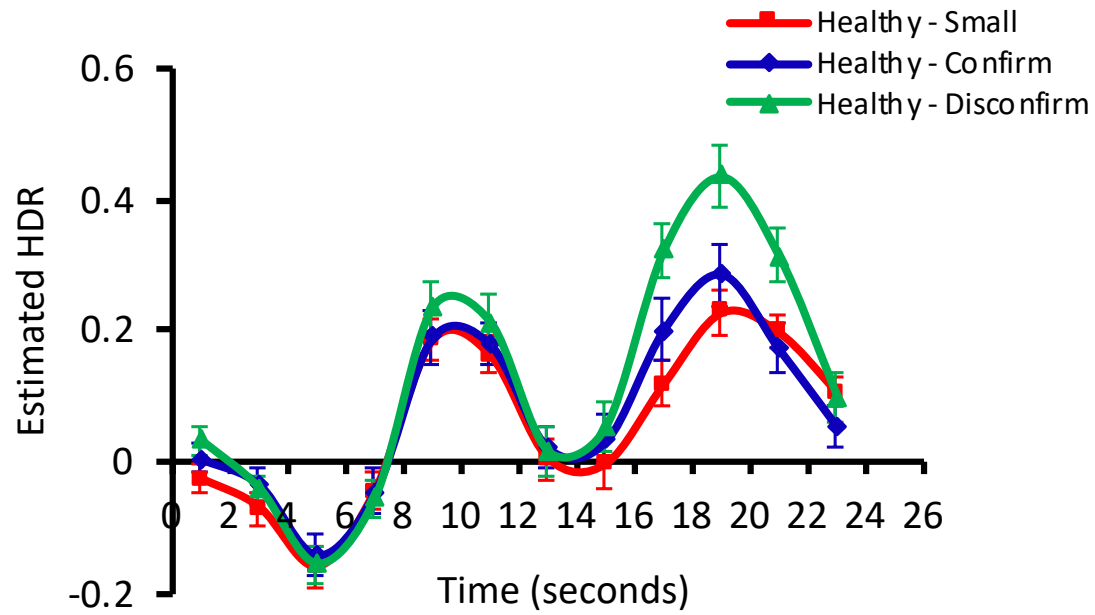


Figure 2.9: Hemodynamic response plot for the Thought Generation Task (TGT) from the TGT-SA Merge divided by task condition for a cohort of healthy participants.

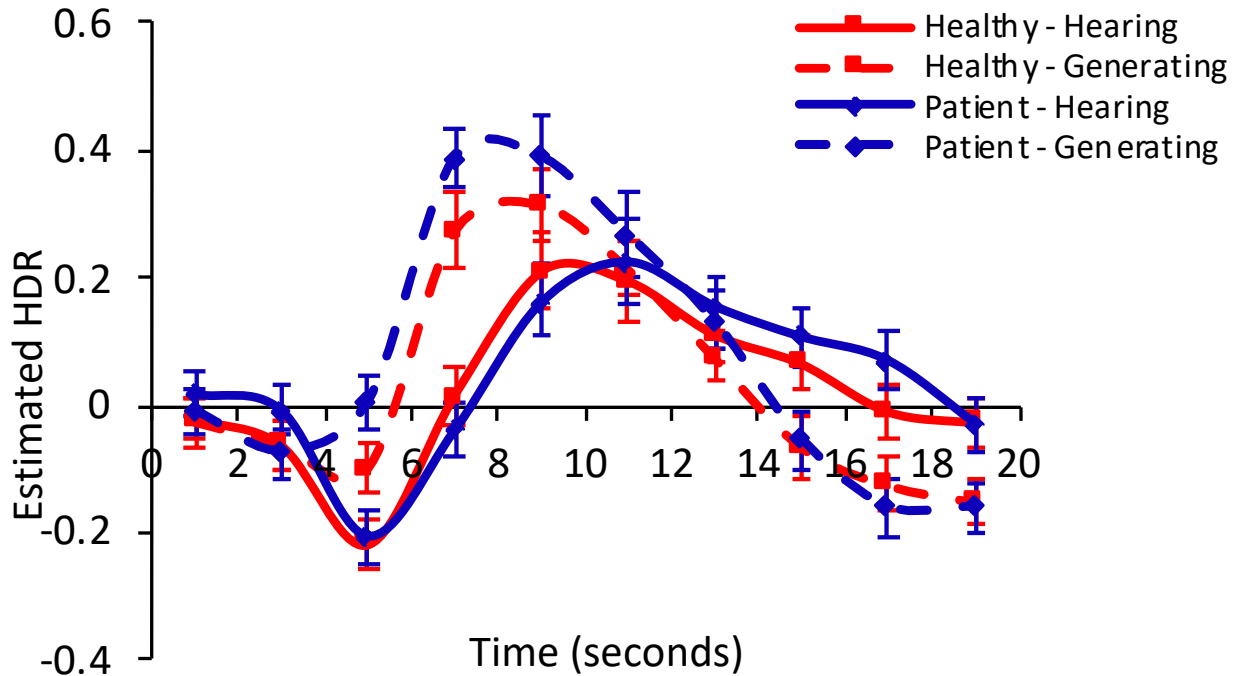


Figure 2.10: Hemodynamic response plot for the Semantic Association (SA) task from the TGT-SA Merge, divided by task condition for a cohort of healthy participants.

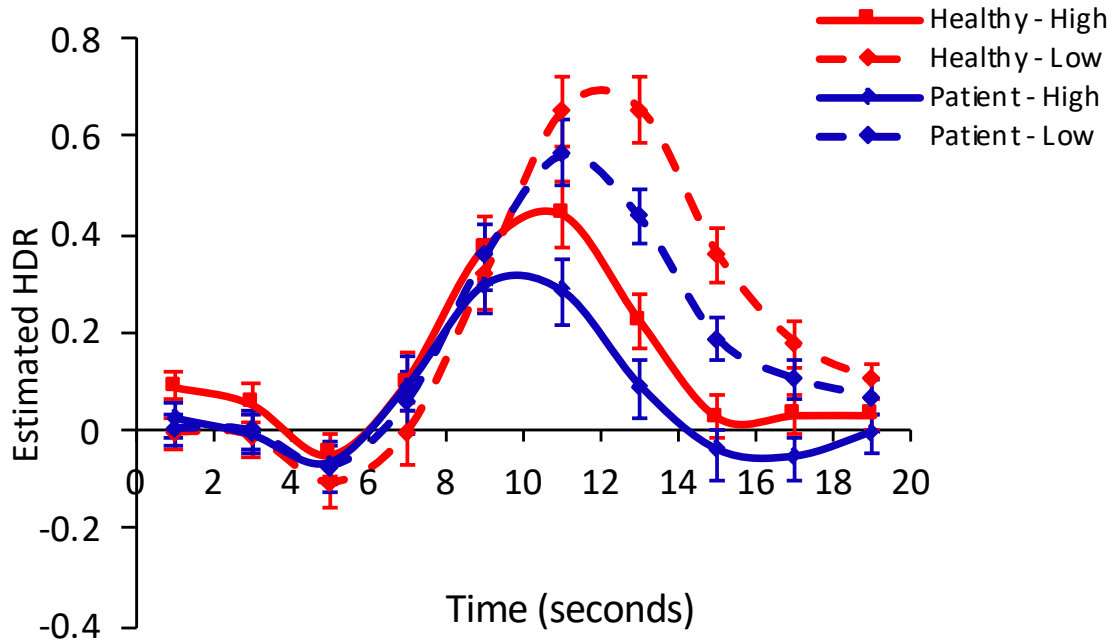


Figure 2.11: Hemodynamic response plot for the Social Cognition (SC) task from the Human Connectome Project 100 subject study, divided by task condition for a cohort of healthy participants.

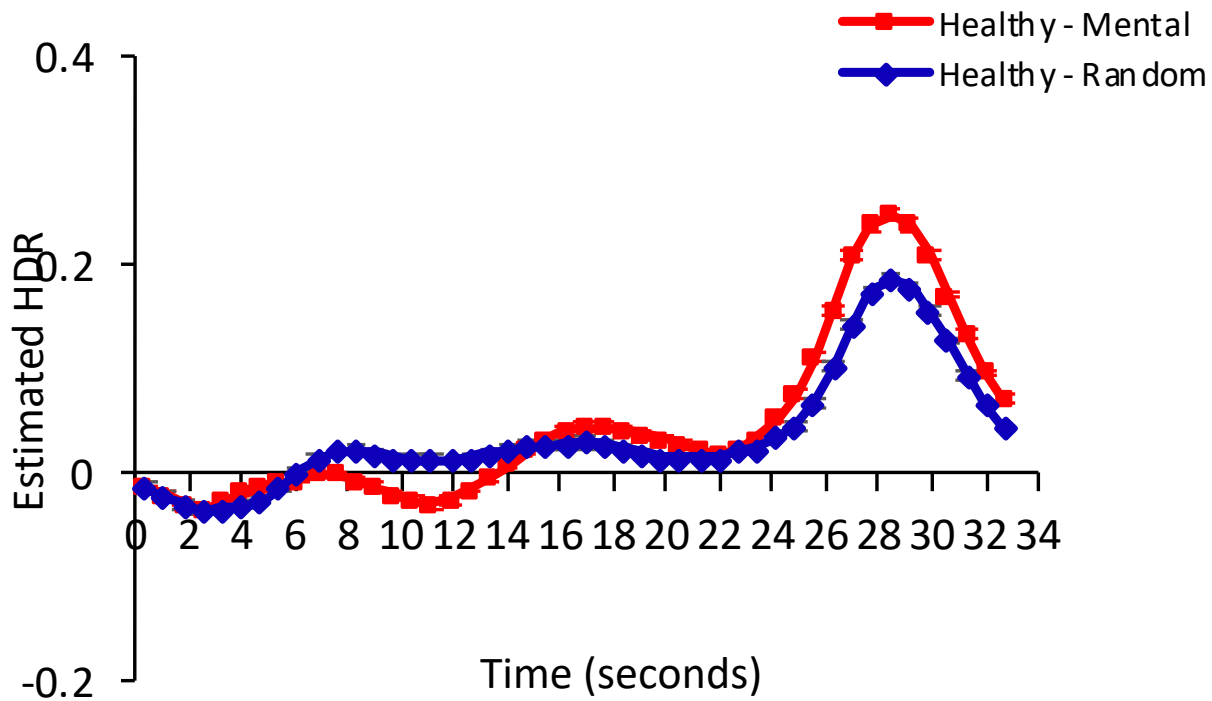


Figure 3.1: HDR plots for tasks where the External Attention Network was elicited before the CEN. The dashed and solid grey lines indicate the time of the External Attention Network peak, and the CEN peak, respectively. A) HDR plot for the ms task from the MS-SA merge with the External Attention peak at timebin 3 and CEN peak at timebin 4 or 5 depending on condition. B) HDR plot for sa task from MS-SA merge with the External Attention peak at timebin 4 or 5 depending on condition, and CEN peak at timebin 7. C) HDR plot for the TGT task from the TSI-TGT merge showing an External Attention peak at timebin 4, and the CEN peak at timebin 4 or 5 depending on task condition. D) HDR plot for the BADE task, with an External Attention peak at timebin 5, and CEN peak at timebin 8. E) HDR plots for the TGT task from the TGT-SA merge, with the External Attention peak at timebin 4 and the CEN peak at timebin 5. F) HDR plot for the sc task, with External Attention peak at timebin 21, and CEN activity peak at timebin 40.

FUNCTIONAL ASSESSMENT OF THE FMRI-DERIVED COGNITIVE EVALUATION NETWORK

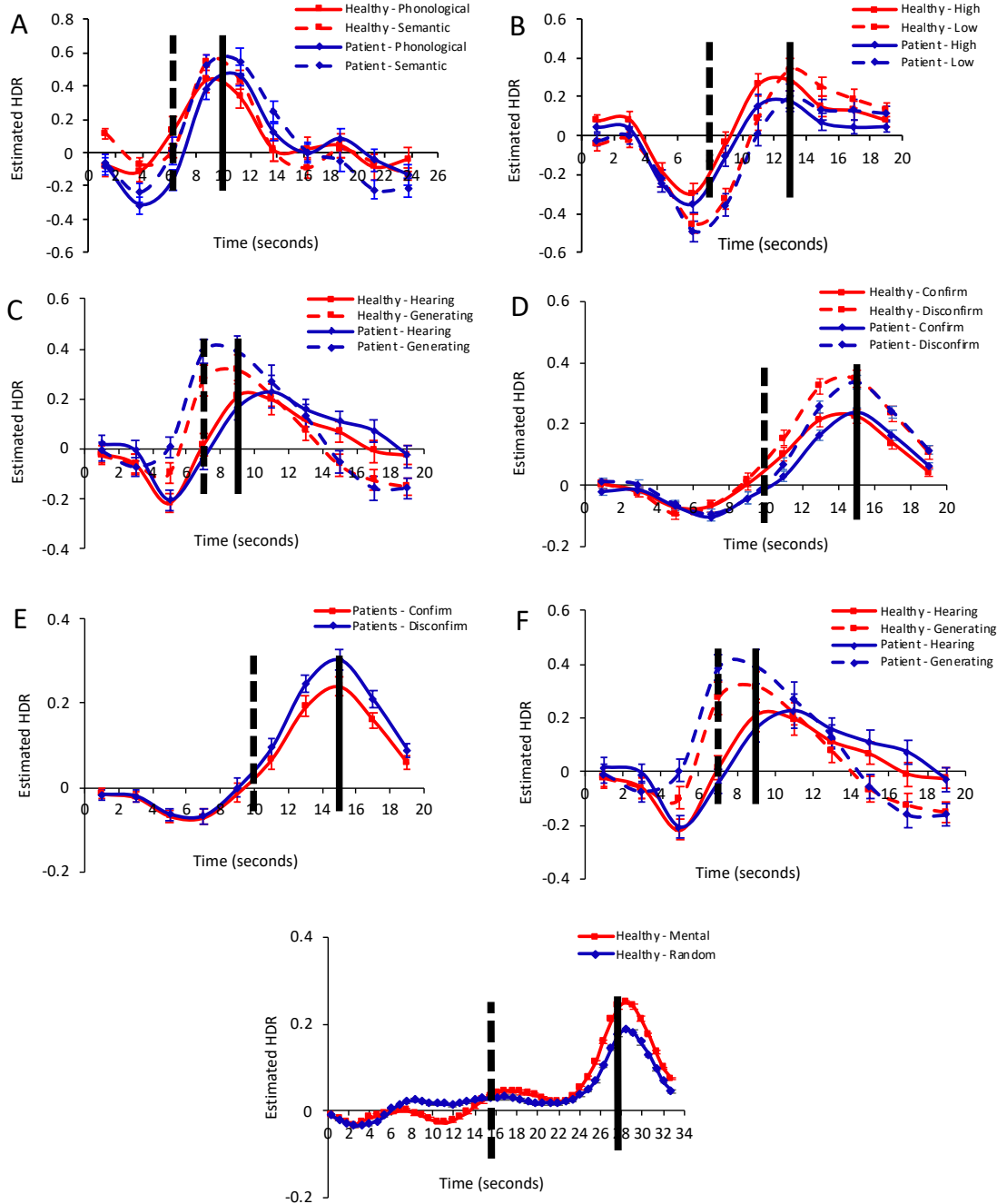
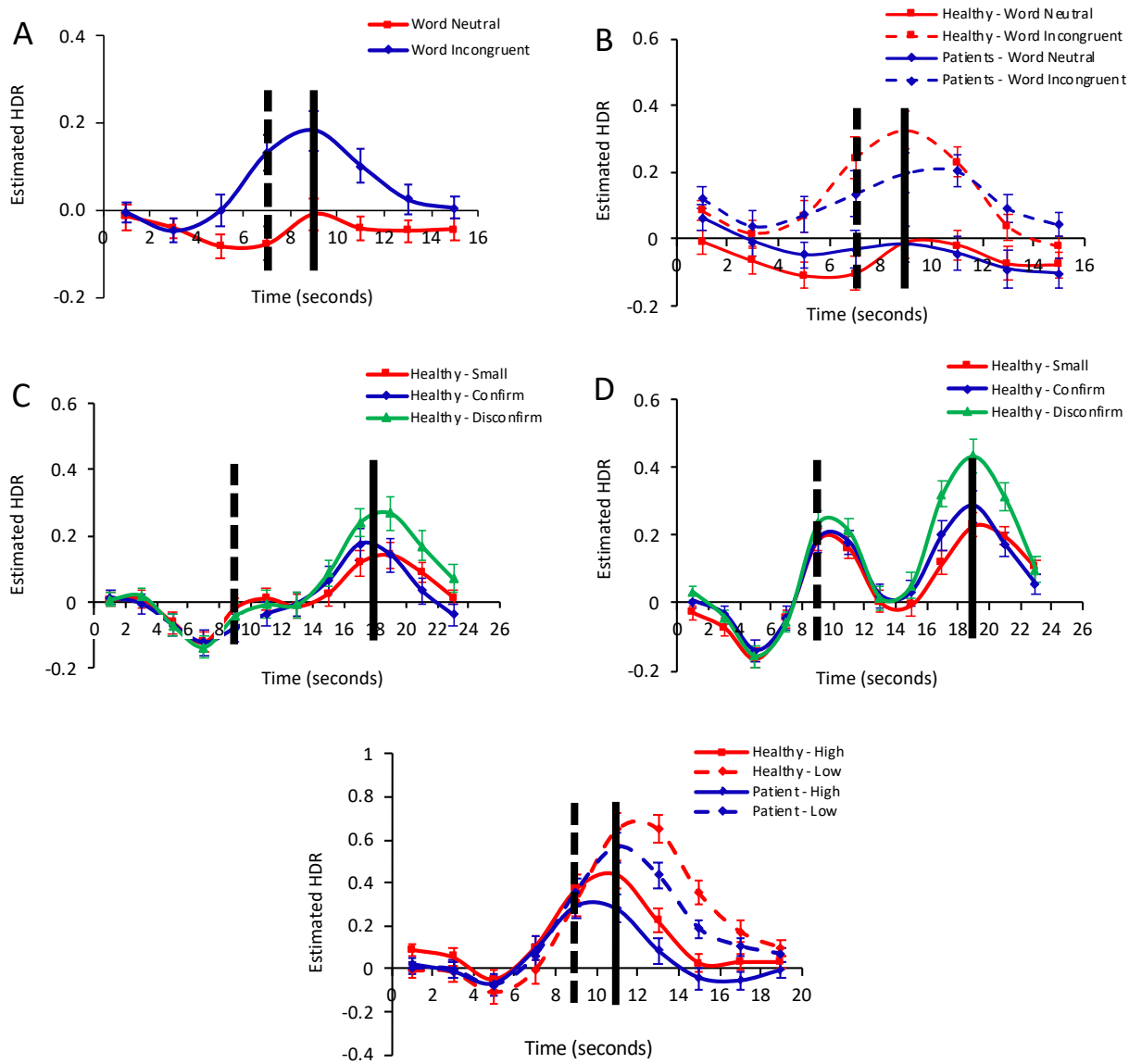


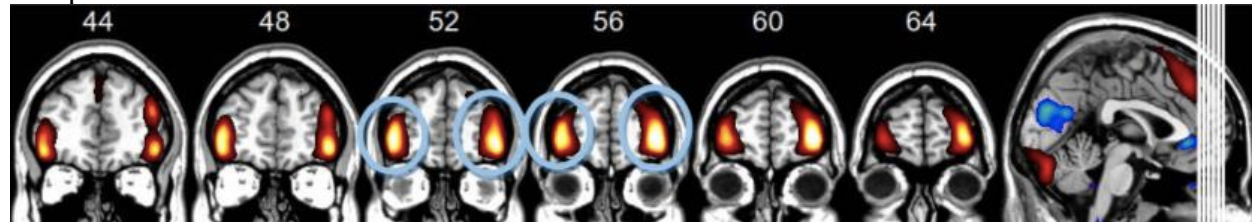
Figure 3.2: HDR plots for tasks where the Response Network was elicited before the CEN. The dashed line indicates timing of Response Network peak, and solid line indicates timing of CEN peak. A) HDR plot for TSI task only, with Response Network peak at timebin 4, and CEN activity at timebin 5. B) HDR plot for TSI task from the TSI-TGT merged study. The Response Network peak at timebin 4 and CEN peak at timebin 5. C) HDR plot for the ABADE task, version A, with the Response Network peak at timebin 5, and the CEN peak between timebins 9 and 10 depending on task condition. D) HDR plot for ABADE task, version A, with the Response Network peak at timebin 5, with CEN peak occurring at timebin 10. E) HDR plot for the SA task from TGT-SA merge. Response Network peak occurs at timebin 5, and CEN occurs at timebin 6.



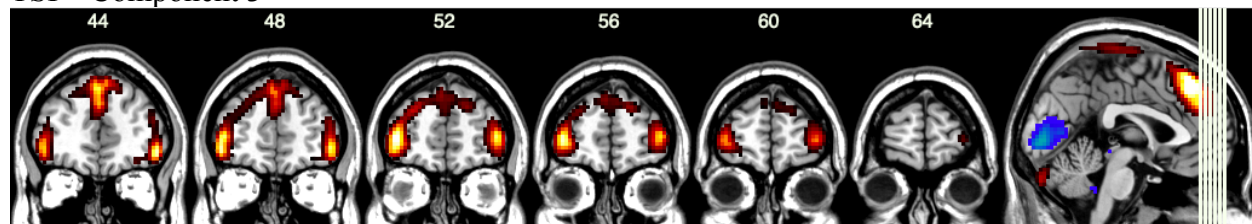
Cognitive Evaluation Network

Bilateral Eyeball Sitters: 170, 174, 178, 182, 186, 190

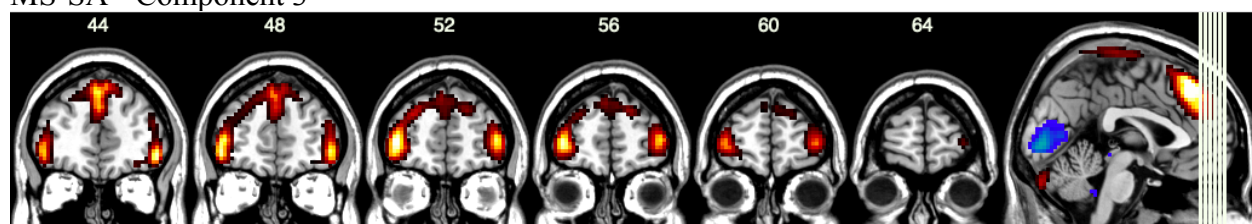
Template



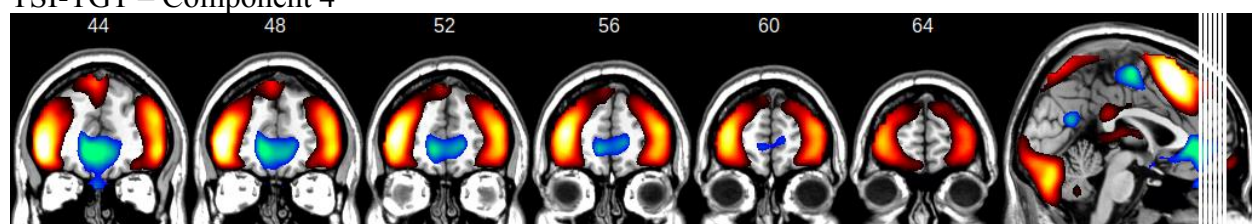
TSI – Component 3



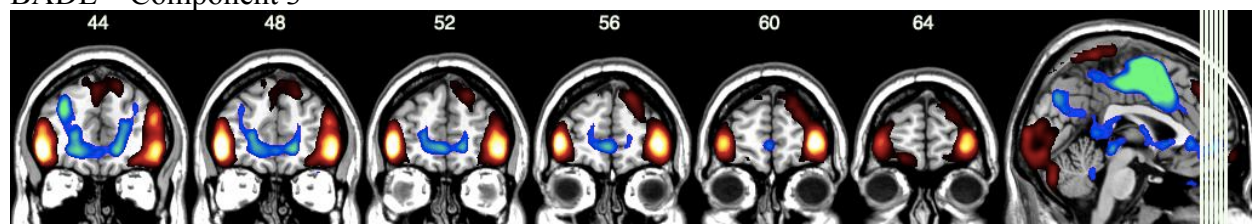
MS-SA - Component 3



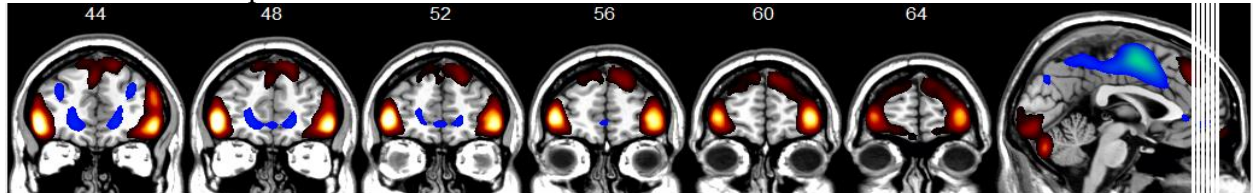
TSI-TGT – Component 4



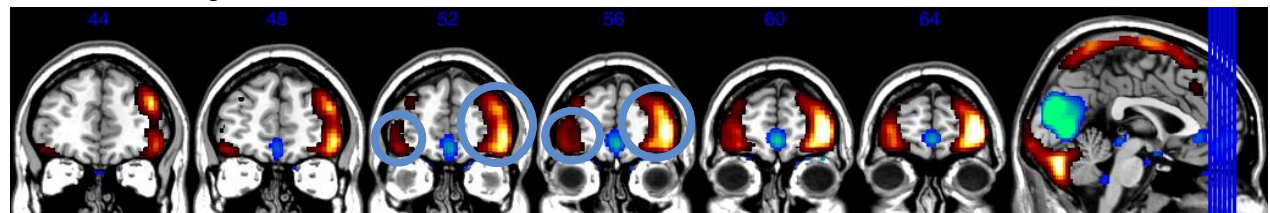
BADE – Component 3



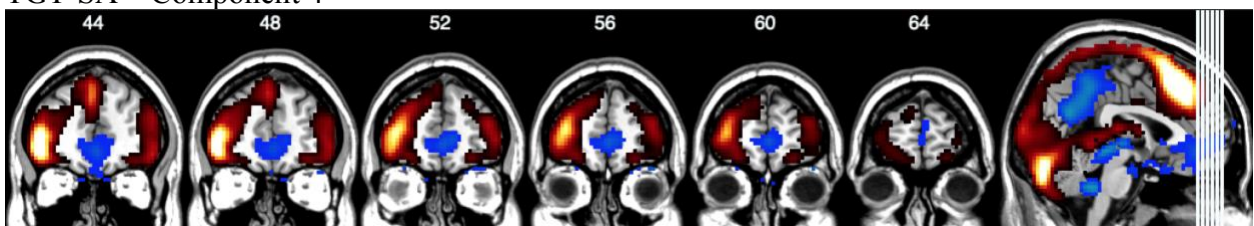
OTTBADE – Component 3



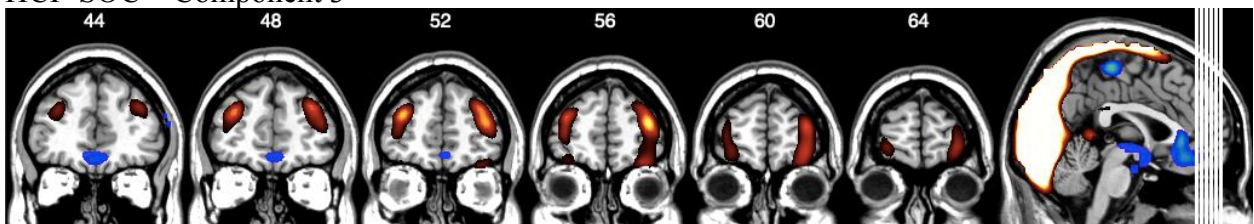
ABADE – Component 1



TGT-SA – Component 4

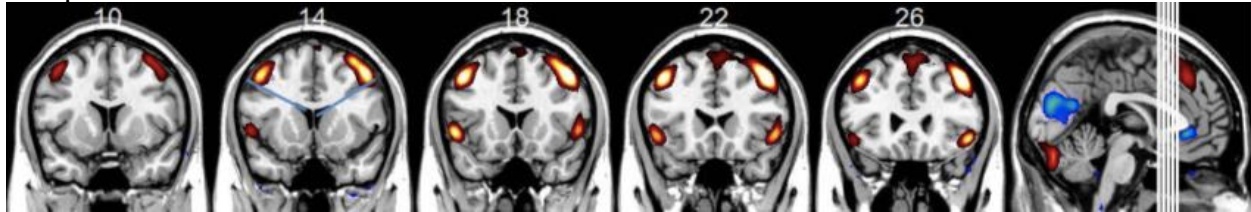


HCP-SOC – Component 3

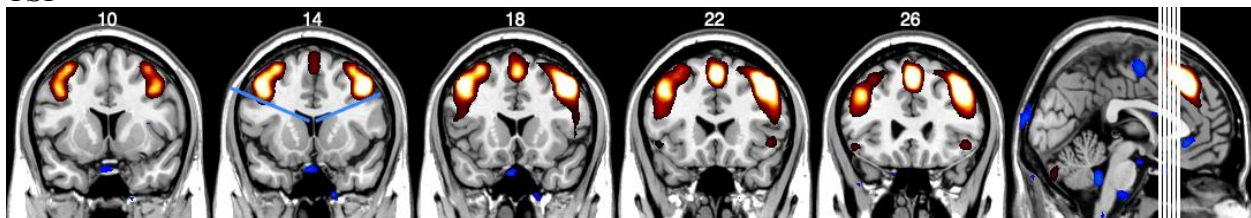


Bilateral Space Invader Shooters: 136, 140, 144, 148, 152

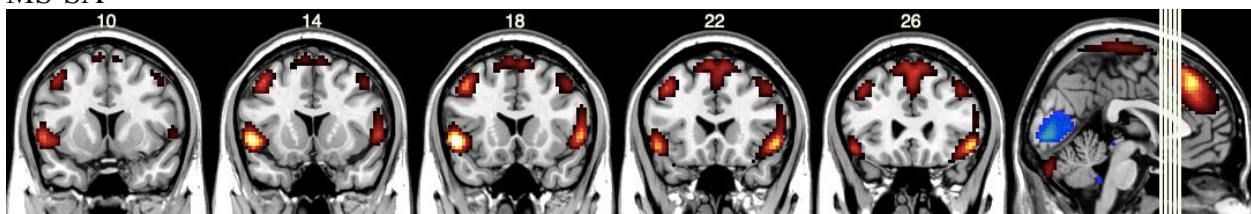
Template



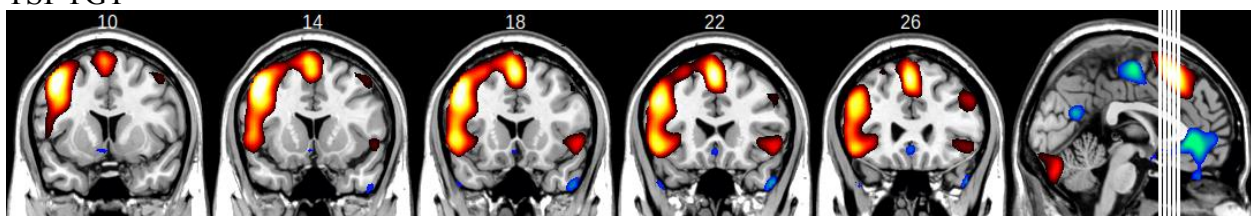
TSI



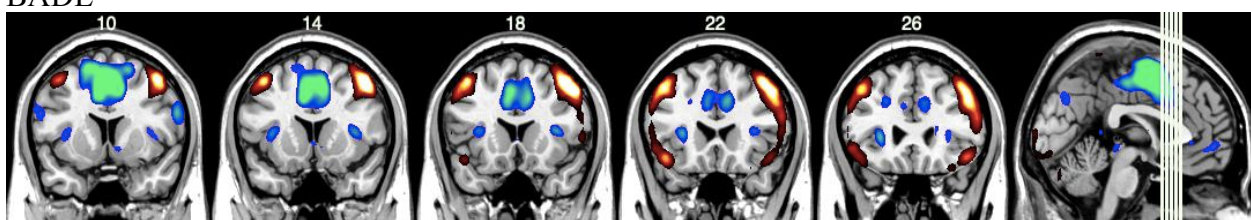
MS-SA



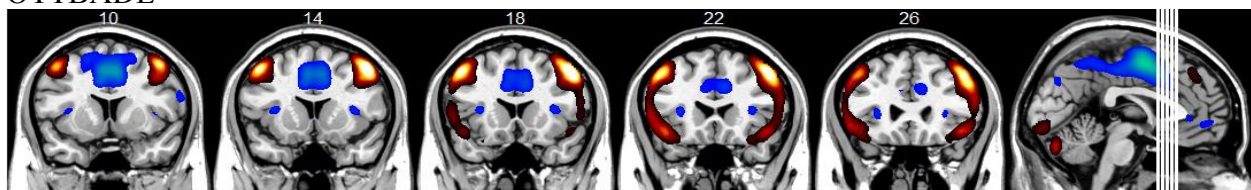
TSI-TGT



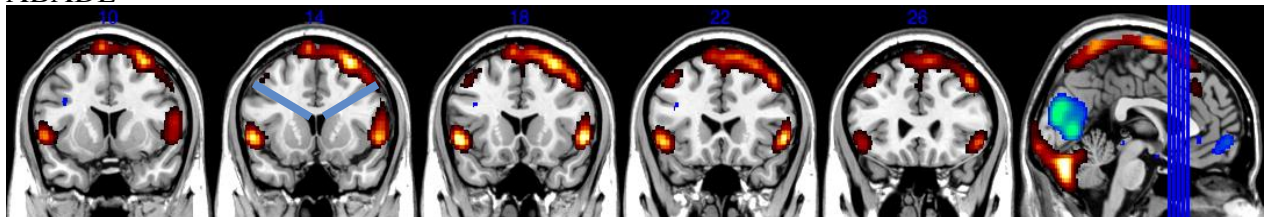
BADE



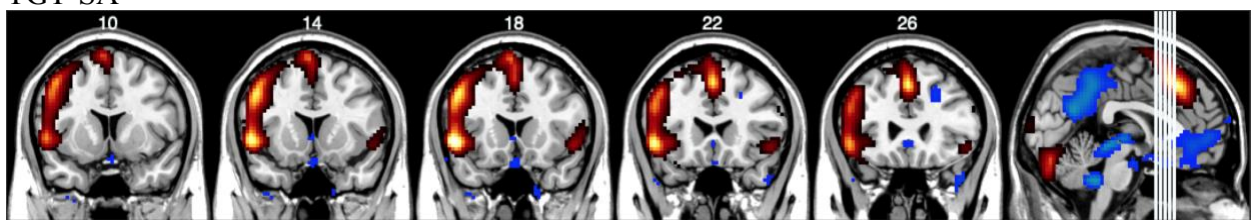
OTTBADE



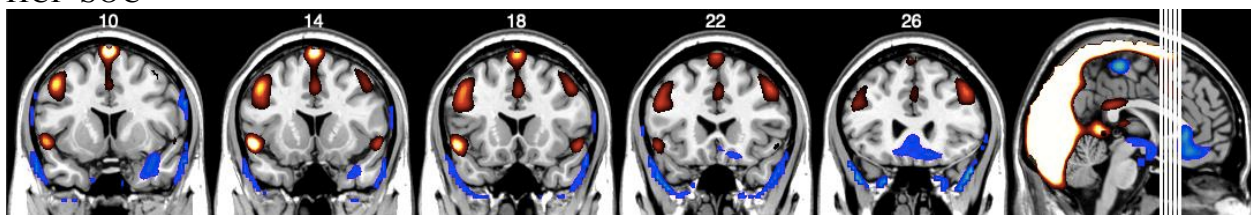
ABADE



TGT-SA

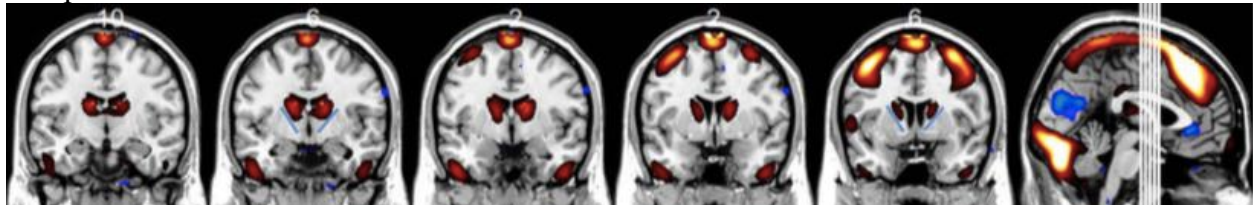


HCP-SOC

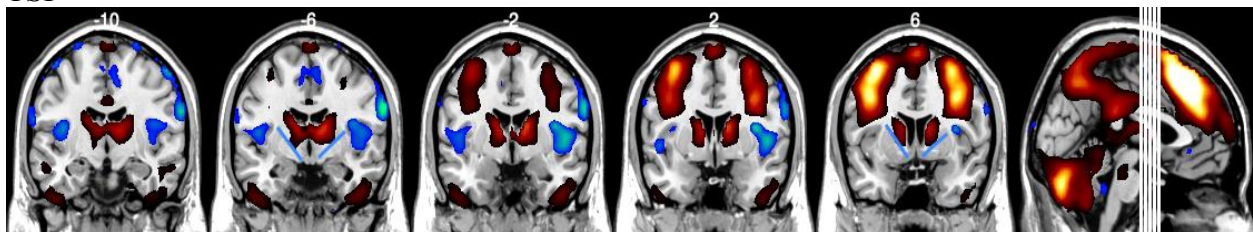


Above the line: 116, 120, 124, 128, 132

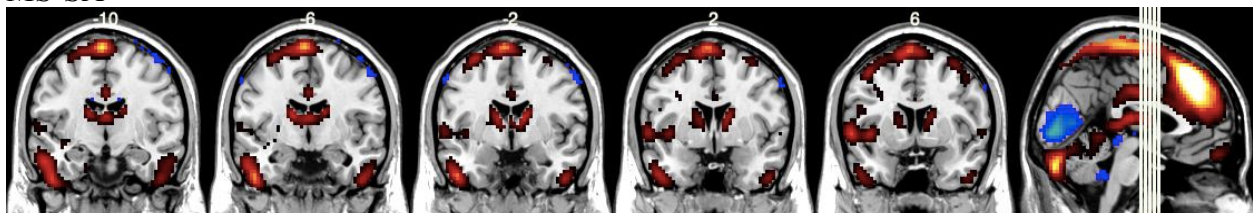
Template



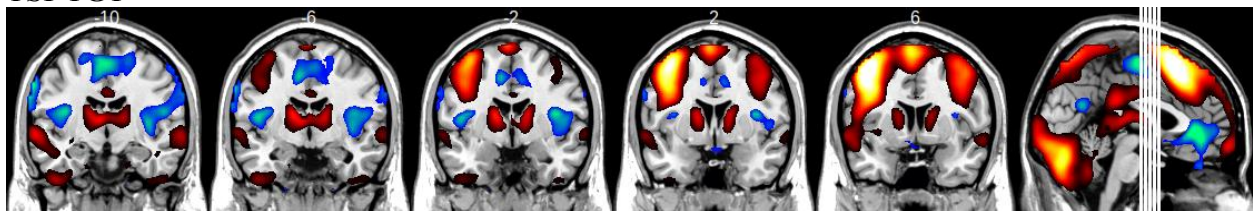
TSI



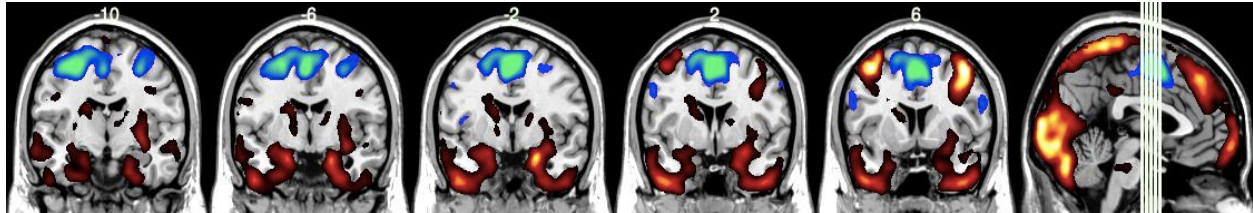
MS-SA



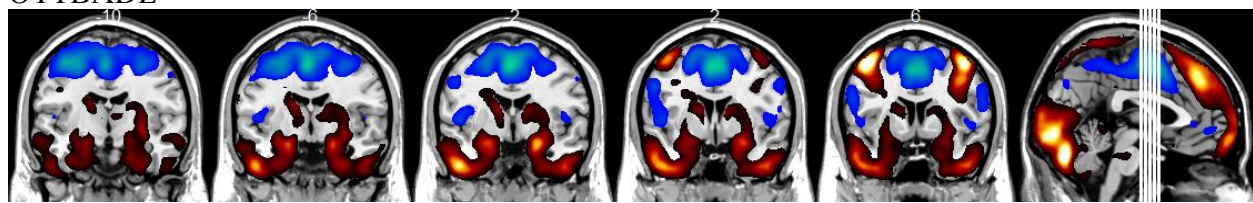
TSI-TGT



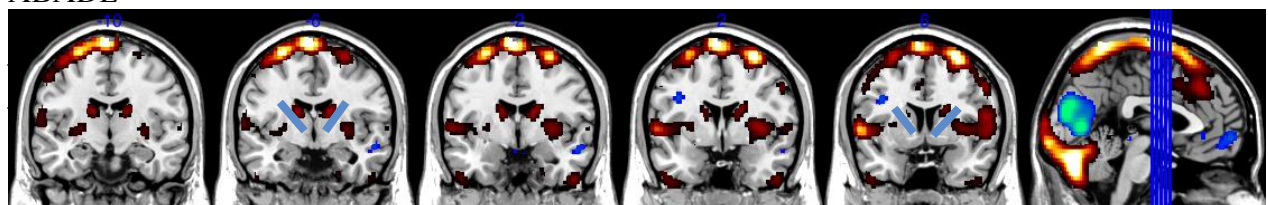
BADE



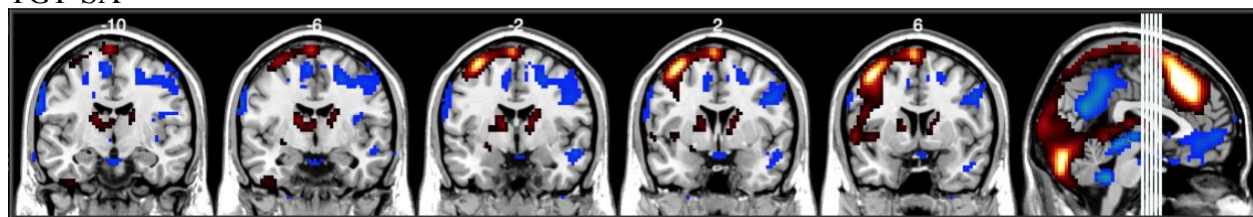
OTTB-ADE



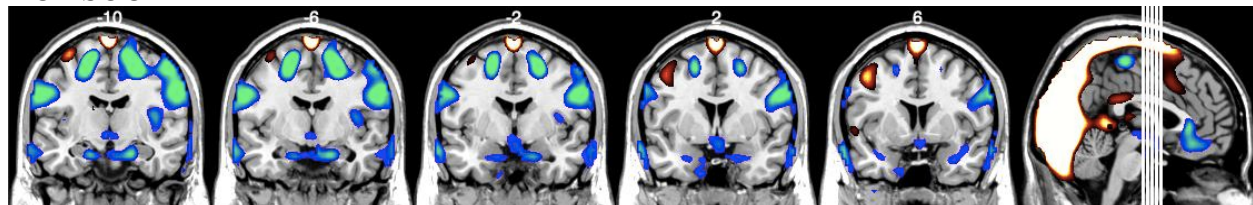
ABADE



TGT-SA

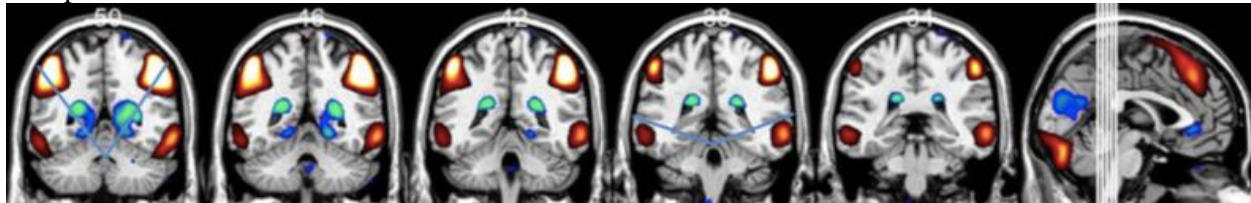


HCP-SOC

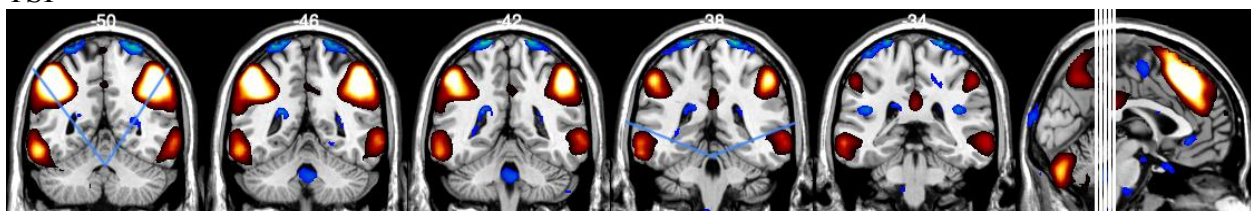


Sad Face Antennae & Flushed Cheeks: 76, 80, 84, 88, 92

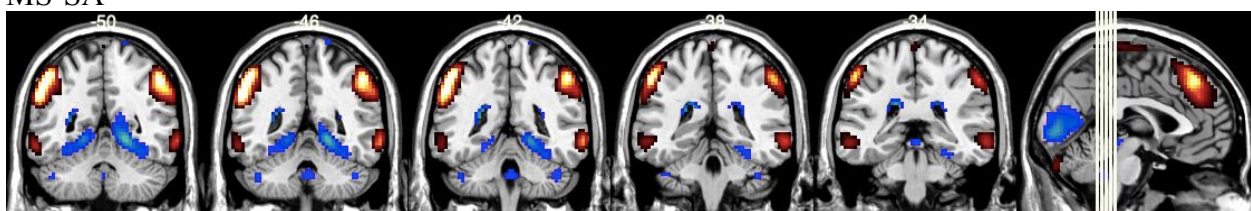
Template



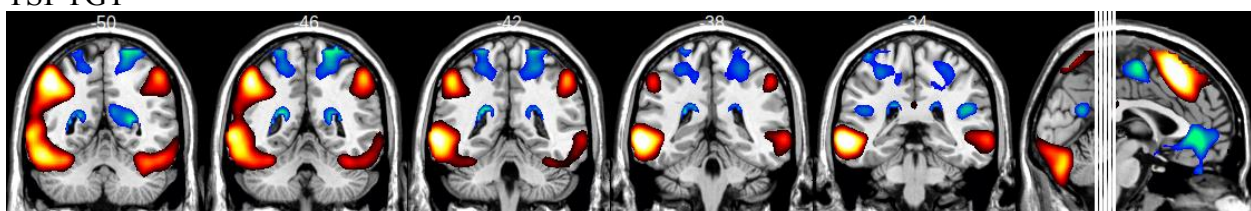
TSI



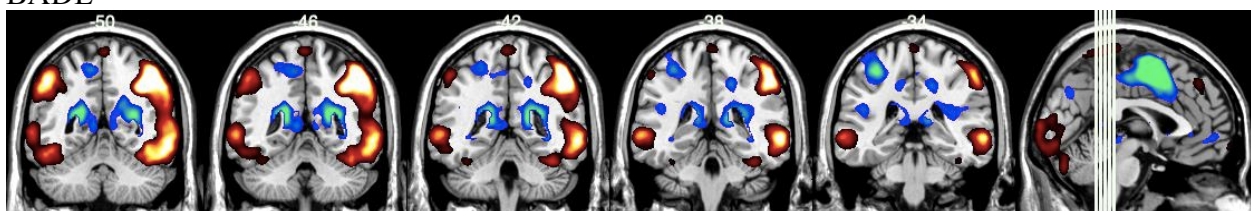
MS-SA



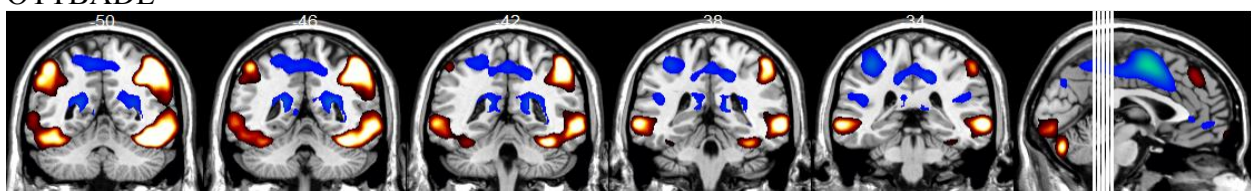
TSI-TGT



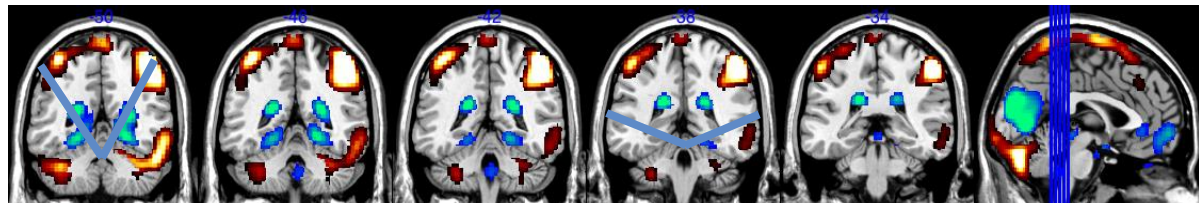
BADE



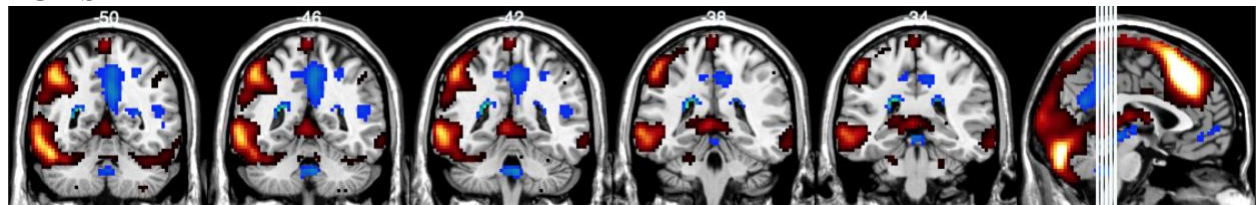
OTTBADe



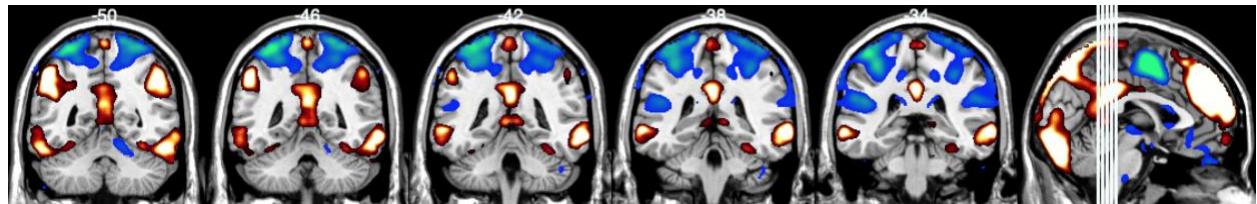
ABADE



TGT-SA

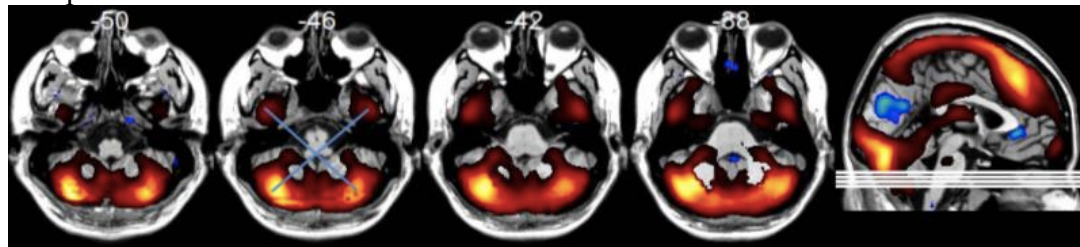


HCP-SOC

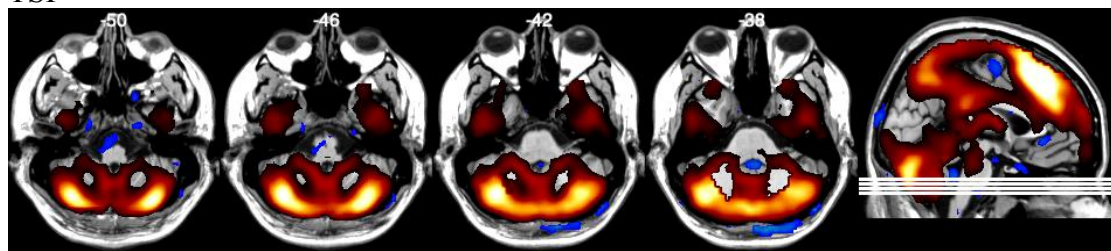


X Marks the Spot: 22, 26, 30, 34

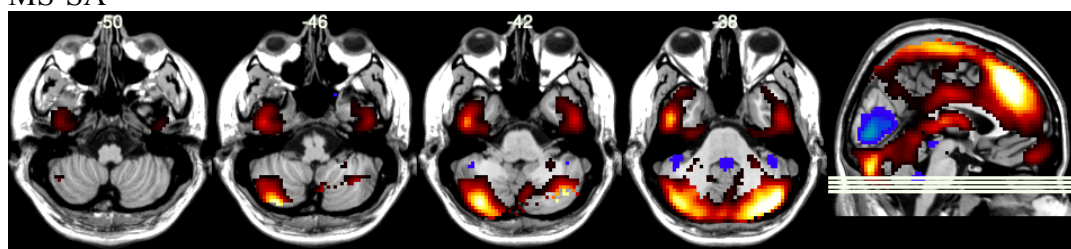
Template



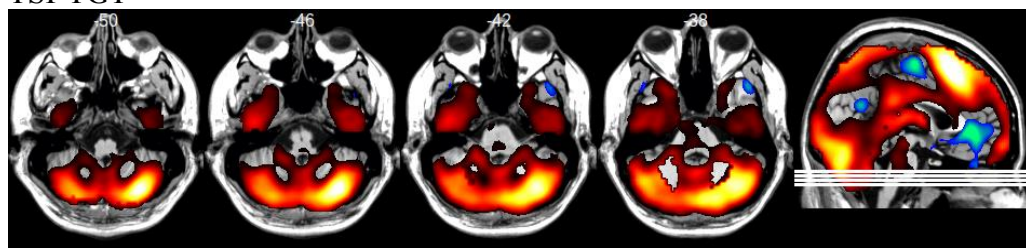
TSI



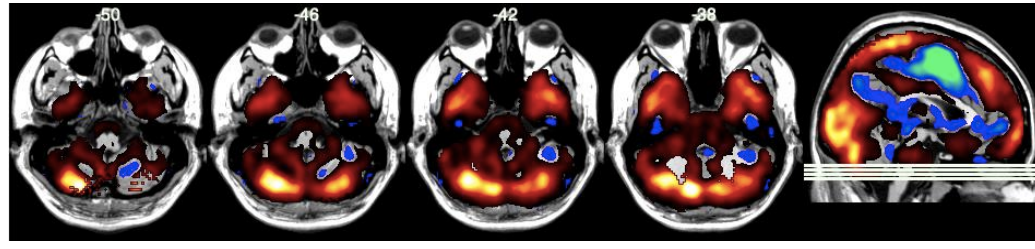
MS-SA



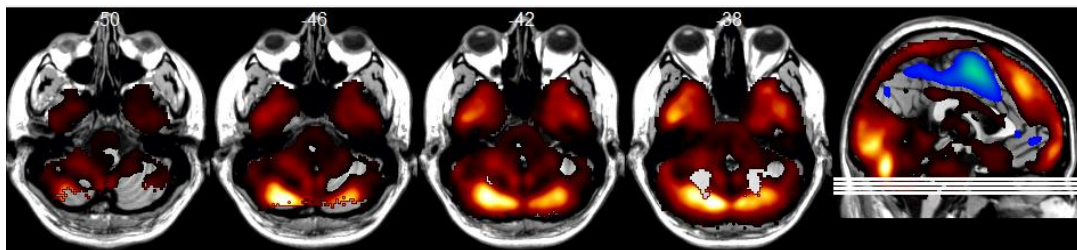
TSI-TGT



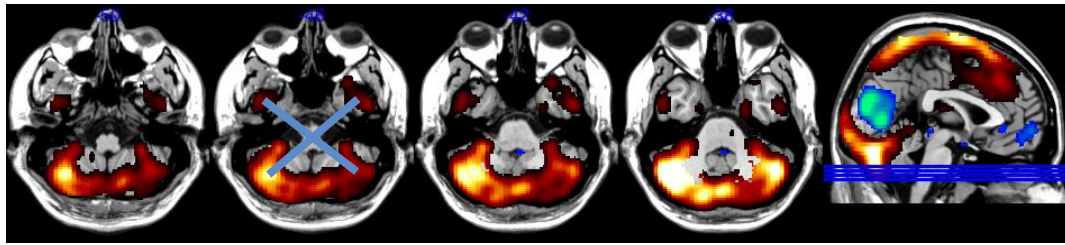
BADE



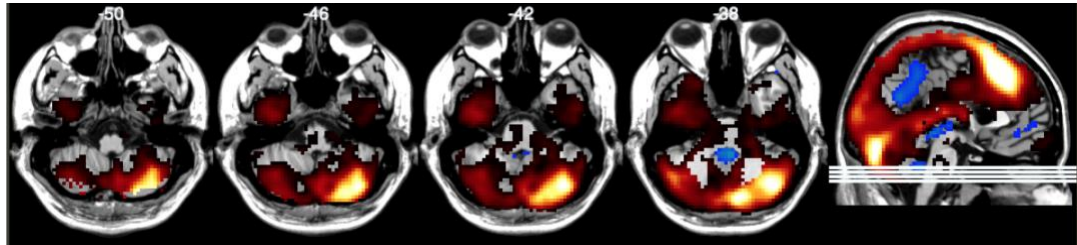
OTTBADE



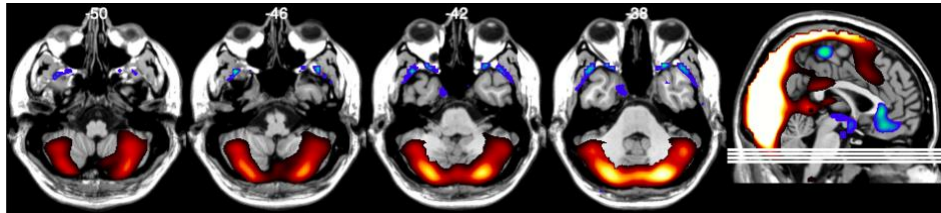
ABADE



TGT-SA



HCP-SOC



References

- Beck, A. T., Baruch, E., Balter, J. M., Steer, R. A., & Warman, D. M. (2004). A new instrument for measuring insight: the Beck Cognitive Insight Scale. *Schizophrenia research*, 68(2-3), 319-329.
- Boksa, P. (2009). On the neurobiology of hallucinations. *Journal of psychiatry & neuroscience: JPN*, 34(4), 260.
- Brown, R. E., Basheer, R., McKenna, J. T., Strecker, R. E., & McCarley, R. W. (2012). Control of sleep and wakefulness. *Physiological reviews*.
- Christoff, K., Ream, J. M., Geddes, L., & Gabrieli, J. D. (2003). Evaluating self-generated information: anterior prefrontal contributions to human cognition. *Behavioral neuroscience*, 117(6), 1161.
- Fitzsimmons, J., Kubicki, M., & Shenton, M. E. (2013). Review of functional and anatomical brain connectivity findings in schizophrenia. *Current opinion in psychiatry*, 26(2), 172-187.
- Friston, K., Brown, H. R., Siemerkus, J., & Stephan, K. E. (2016). The dysconnection hypothesis (2016). *Schizophrenia research*, 176(2-3), 83-94.
- Hadar, R., Bikovski, L., Soto-Montenegro, M. L., Schimke, J., Maier, P., Ewing, S., ... & Winter, C. (2018). Early neuromodulation prevents the development of brain and behavioral abnormalities in a rodent model of schizophrenia. *Molecular psychiatry*, 23(4), 943-951.
- Lavigne, K. M., Menon, M., Moritz, S., & Woodward, T. S. (2020). Functional brain networks underlying evidence integration and delusional ideation. *Schizophrenia research*, 216, 302-309.
- Lavigne, K. M., Menon, M., & Woodward, T. S. (2020). Functional brain networks underlying evidence integration and delusions in schizophrenia. *Schizophrenia bulletin*, 46(1), 175-183.
- Liddle, P. F., & Barnes, T. R. (1990). Syndromes of chronic schizophrenia. *The British Journal of Psychiatry*, 157(4), 558-561.
- Marek, S., & Dosenbach, N. U. (2018). The frontoparietal network: function, electrophysiology, and importance of individual precision mapping. *Dialogues in clinical neuroscience*, 20(2), 133.
- Metzak, P., Feredoes, E., Takane, Y., Wang, L., Weinstein, S., Cairo, T., ... & Woodward, T. S. (2011). Constrained principal component analysis reveals functionally connected load-dependent networks involved in multiple stages of working memory. *Human brain mapping*, 32(6), 856-871.
- Moritz, S., & Woodward, T. S. (2007). Metacognitive training in schizophrenia: from basic research to knowledge translation and intervention. *Current opinion in psychiatry*, 20(6), 619-625.
- Patel, K. R., Cherian, J., Gohil, K., & Atkinson, D. (2014). Schizophrenia: overview and treatment options. *Pharmacy and Therapeutics*, 39(9), 638.
- Percival C.M., Zahid H.B., and Woodward T.S. Set of task-based functional brain networks derived fro averaging results of multiple fmri-cpca studies.
- Rogers, B. P., Morgan, V. L., Newton, A. T., & Gore, J. C. (2007). Assessing functional connectivity in the human brain by fMRI. *Magnetic resonance imaging*, 25(10), 1347-1357.
- Sanford, N. A. (2019). *Functional brain networks underlying working memory performance in schizophrenia: a multi-experiment approach* (Doctoral dissertation, University of British Columbia).

FUNCTIONAL ASSESSMENT OF THE FMRI-DERIVED COGNITIVE EVALUATION NETWORK

- Sanford, N., Whitman, J. C., & Woodward, T. S. (2020). Task-merging for finer separation of functional brain networks in working memory. *Cortex*, 125, 246-271.
- Tanimizu, T., Kenney, J. W., Okano, E., Kadoma, K., Frankland, P. W., & Kida, S. (2017). Functional connectivity of multiple brain regions required for the consolidation of social recognition memory. *Journal of Neuroscience*, 37(15), 4103-4116
- Yeo, B. T., Krienen, F. M., Sepulcre, J., Sabuncu, M. R., Lashkari, D., Hollinshead, M., ... & Buckner, R. L. (2011). The organization of the human cerebral cortex estimated by intrinsic functional connectivity. *Journal of neurophysiology*.

Functional Assessment of the fMRI-Derived Maintaining Network

Ava Momeni^{1,2}, Dayana Stamboliyska^{1,2}, Todd Woodward^{1,2}

¹BC Mental Health and Substance Use Services

²Department of Psychiatry, University of British Columbia

Table of Contents

Abstract	3
Introduction	4
Methods.....	6
Tasks	8
1.1 Sternberg Item Recognition Paradigm (SIRP).....	8
1.2 Thought Generating Task (TGT)	10
1.3 Addis Task.....	12
1.4 The Spatial Capacity Task (SCAP).....	15
1.5 Task-Switch Inertia Task (TSI)	16
1.6 Semantic Integration Task (SIT)	18
1.7 Delusions of Reference (DOR).....	20
Results.....	22
1.1.1. Sternberg Item Recognition Paradigm (SIRP); Sanford et al. (2020).....	22
1.1.2. Sternberg Item Recognition Paradigm (SIRP); Sanford & Woodward (2020)	26
1.1.2. Sternberg Item Recognition Paradigm (SIRP); Metzak et al. (2012).....	30
1.2.1 Thought Generating Task (TGT); Sanford et al. (2020).....	33
1.2.2 Thought Generating Task (TGT); Sanford & Woodward (2020).....	35
1.3 Addis Task.....	38
1.4 Spatial Capacity Task (SCAP).....	40
1.5 Task-Switch Inertia Task (TSI)	46
1.6 Semantic Integration Task (SIT)	50
1.7 Delusions of Reference (DOR).....	56
Discussion.....	61
References.....	63

Abstract

The Maintaining network is one of 12 task-based networks that have been recently derived via a novel statistical data-driven approach called fMRI-CPCA. While applying this approach produces an anatomical characterization of the Maintaining network, the function of this network still remains to be fully interpreted. Across multiple studies, the Maintaining network has shown to be differentially recruited over a range of distinct tasks and task conditions. In the following chapter, the neuroimaging results of seven studies, analyzed with the fMRI-CPCA, that demonstrated BOLD activity classified as the Maintaining network with sufficient strength were considered. In addition, we identified the task conditions which promoted activity in the Maintaining network, as well as possible underlying commonalities between the various task conditions, in order to arrive at a better understanding of the network's function. We conclude that the Maintaining network is most likely involved in integrating different frontal functions, volitional attention to internal mental representations and conscious inner speech/language processing, while being non-specific to cognitive domain.

Introduction

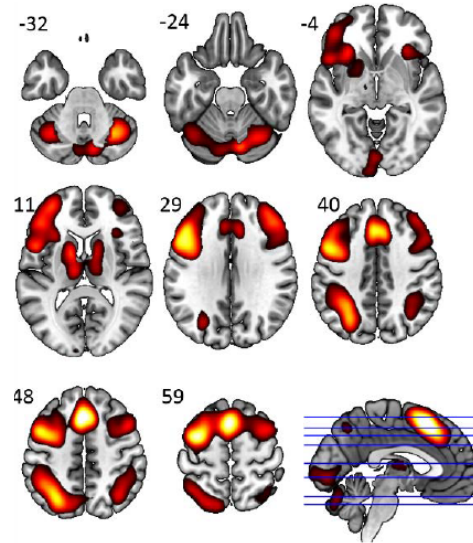
Large-scale brain networks, also known as intrinsic brain networks, are collections of widespread brain regions that show functional connectivity. The Cognitive Neuroscience of Schizophrenia (CNoS) lab has developed a novel statistical approach called fMRI constrained principal component analysis (fMRI-CPCA) and along with network classifications, it has discovered 10 task-positive and 2 task-negative functional networks (Percival et al., 2020).

The Maintaining network is one of the three networks that are involved in the cognitive processes of attending to internal representations (Percival et al., 2020). This network is characterized by activations in the frontoparietal regions as well as the cingulate cortex (Figure 1. Brain slices showing activation of the Maintaining network. Reprinted from Percival et al. (2020); Percival et al., 2020). These patterns of activations have been attributed to be load-dependent when recalling internal representations, including verbal and spatial working memory (Metzak et al., 2017, Sanford et al., 2020, Sanford & Woodward, 2020). The activation of the Maintaining network is also implicated in the recall of semantic knowledge of the to-be-associated word pairs, which also shows load-dependent activity meaning that there is a greater activation of the Maintaining network for distantly related word pairs as opposed to the closely related ones (Eickhoff & Woodward, 2021). The Maintaining network has also shown increased activation when one is imagining the past or the future relative to episodic recall (Addis et al., 2009). Lastly, it has been suggested that the activation of the Maintaining network may be linearly associated with increasing intensity of delusions of reference (Larivière et al., 2017).

Although, fMRI-CPCA has been successful in anatomically isolating characterized functional networks, such as the Maintaining network, how exactly each functional network relates to the different cognitive processes and conditions within the certain tasks that evoke it is

not yet clearly understood. Thus, the following chapter presents the published and unpublished studies from the lab which demonstrate components classified as the Maintaining network and attempt to explain the function(s) of this network and to identify which cognitive processes they may underlie.

Figure 1. Brain slices showing activation of the Maintaining network. Reprinted from Percival et al. (2020).



Methods

As mentioned earlier, the Maintaining network was identified with fMRI-CPCA and network classifications. CPCA combines multivariate multiple regression and principal component analysis to identify spatial configurations of brain networks (Sanford, 2019). Averaging component loadings from previous fMRI-CPCA studies, 12 exemplar networks were identified. Using a MATLAB-based algorithm, an automated classification program was developed which assigns 12 z scores to brain images input, indicating how closely the inputted images match with the exemplar networks (Percival et al., 2020). The higher the z scores, the greater the match between the image and the exemplar networks. In the current chapter, a Fisher transformed z score of ≥ 0.80 was considered a significant match, which approximately equates to $r = 0.85$.

In this chapter, the methods and hemodynamic response (HDR) plots for seven studies that contained a component extracted with fMRI-CPCA that best matched to the exemplar images for the Maintaining network via the classification program were considered to assess the functions of the Maintaining Network. Each study is summarized in Table 1 below, alongside information about its participant populations and task(s) used.

Table 1

List of Studies for Characterizing the Functions of the Maintaining Network

Study	Population(s)	Tasks	Component	z-score
Sanford et al. 2020	Healthy adults	WM; TGT	3	1.6
Klepel & Woodward 2021	Healthy adults	Addis	3	1.54
Sanford & Woodward 2020	Patients with schizophrenia; Healthy adults	SCAP; TGT; TSI; WM	2	1.37
Eickhoff & Woodward 2021	Patients with schizophrenia; Healthy adults	SA	5	0.91
Larivière et al. 2017	Patients with Delusions; Patients without delusions; Healthy adults	DOR	2	0.82
Metzak et al. 2012	Patients with schizophrenia; Healthy adults	WM	3	0.82

Note: TGT = Thought Generation Task; SIRP = Sternberg Item Recognition Paradigm; SCAP = Spatial Capacity Task; TSI = Task Switching Inertia Task; SIT = Semantic Integration Task; DOR = Delusions of Reference Task.

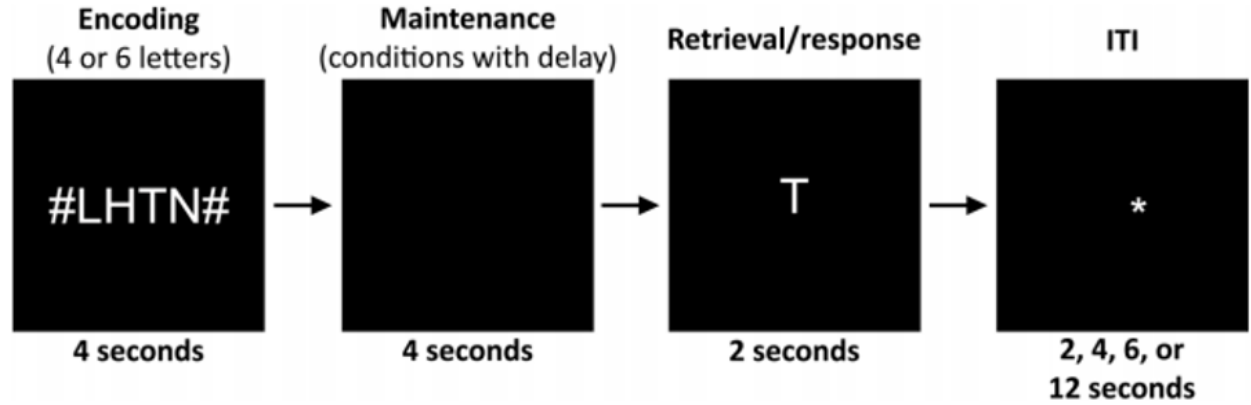
Tasks

1.1 Sternberg Item Recognition Paradigm (SIRP)

To test working memory (WM), a modified SIRP task (Figure 2. Sternberg Item Recognition Paradigm (SIRP); an example of a trial presented in the 4-letter condition with a 4-second delay (Sanford et al., 2020).) was administered in the Sanford et al. (2020) and Sanford & Woodward (2020) studies. In the Sanford & Woodward (2020) study, participants consisted of healthy adults ($n = 37$). In Sanford et al. (2020) study, participants included healthy controls ($n = 26$) and patients with schizophrenia ($n = 28$). In the SIRP task used in these studies, a string of 4 or 6 uppercase consonants was displayed for 4 seconds in each trial, followed by either a 0 or 4-second delay period. Then, a single probe letter was displayed for 2 seconds and participants were asked to respond “yes” or “no” with a button press as to whether this probe letter was part of the string of letters shown earlier. In the inter-trial intervals, a fixation marker was presented for either 2, 4, 6, or 12 seconds. The 2 experimental manipulations in this task consisted of Cognitive Load (presentation of either 4 or 6 letters) and Delay (either a 0 or 4-second delay period). There were a total of 2 runs, 4 conditions, and 112 trials (14 trials per condition per run, which were randomly generated within each run).

The Metzak et al. (2012) study also used the SIRP task. Participants consisted of healthy controls ($n = 15$) and patients with schizophrenia ($n = 15$). However, the SIRP task used in this study was slightly different from the one used in the Sanford et al. (2020) and Sanford & Woodward (2020) studies. In this variation of the SIRP task, in each trial, participants were presented with a string of 2, 4, 6, or 8 uppercase consonants and the delay period was held constant at 6 seconds. The rest of the procedure was similar to the previous studies.

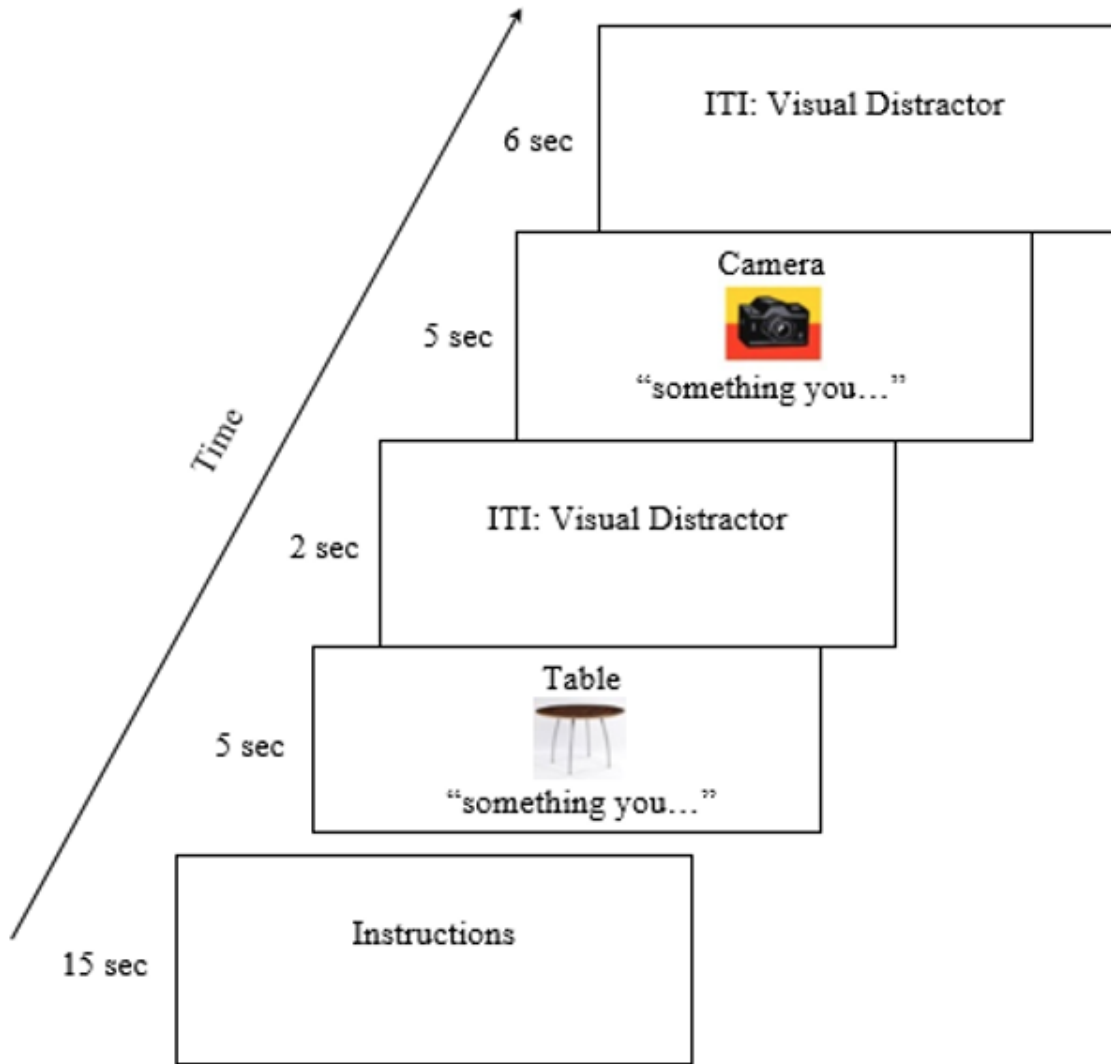
Figure 2. Sternberg Item Recognition Paradigm (SIRP); an example of a trial presented in the 4-letter condition with a 4-second delay (Sanford et al., 2020).



1.2 Thought Generating Task (TGT)

The TGT task (Figure 3. A Sample Trial in the TGT Task; Adapted from Sanford et al. 2020.) was used by Sanford et al. (2020) and Sanford & Woodward (2020) studies. In the Sanford et al. (2020) study, participants consisted of healthy adults ($n = 32$) and in the Sanford & Woodward (2020) study, participants included healthy controls ($n = 32$) and patients with schizophrenia ($n=28$). In the TGT task, participants were presented with an object noun and its' corresponding image for 5 seconds. They were instructed to either mentally generate or listen to a function of that object noun. Trials were cued with the words “something you ...” or “listen...” presented under the images in the generating and hearing conditions, respectively. The two experimental conditions (Generating and Hearing) were presented in alternating blocks of 15 trials (30 trials total for each condition across the 2 runs) with a 60-second rest period in between the 2 conditions. Post-scan, participants were asked whether, for each trial, they generated a definition and if so, what that definition was.

Figure 3. A Sample Trial in the TGT Task; Adapted from Sanford et al. 2020.



Note: ITI = inter-trial interval.

1.3 Addis Task

Data from Addis et al. 2009 using the Addis task (Figure 4. A Sample Trial with Sample Stimuli for Each Condition in the Addis Task; Reprinted from Klepel et al. 2021.) was analyzed by Klepel & Woodward (2021). Participants consisted of healthy right-handed adults (n=18). At least 4 days prior to the scanning session, participants were asked to complete a pre-scan stimulus collection session in which they completed a spreadsheet, detailing 170 memories of personal events that occurred in the last 5 years. For each event, the participants devised a title and 3 details including a person other than themselves, an object featured in the memory, and the location at which the memory occurred (Figure 4.A). The event title and the 3 details were then randomly selected from different memories and combined to create 60 trial-stimulus sets (Figure 4.B).

During the scanning session, 20 Imagine-Past, 20 Imagine-Future, and 20 Recall-Past event trials, each 35s in length, were presented randomly. Each trial began with a 24-second construction-and-elaboration phase. During the construction phase, a 4-line cueing slide was displayed. Line 1 described the task instructions and lines 2 to 4 contained the trial-stimulus-set (Figure 4.B). In the Imagine-Past and Imagine-Future conditions, participants were required to use the details specified on the cuing slide and imagine an event that might have occurred in the last 5 years or might occur in the next 5 years, respectively. In the Recall-Past conditions, participants were required to remember how the specified details on the cueing slide featured in the corresponding memories.

When they participants completed each task, they were asked to press a button on the response box. This response time was recorded and marked the end of the construction phase and the beginning of the elaboration phase. During the elaboration phase, participants were required

to elaborate and expand on the imagined events or the remembered events. Then, they had to complete two rating scales that were presented for 5 seconds: (1) a five-point scale concerning the amount of detail they retrieved or imagined (1 = vague with no/few details; 5 = vivid and highly detailed) and (2) a binary scale regarding whether the event was experienced primarily from a field or observer perspective (1 = saw the event through my own eyes; 5 = saw myself from an external perspective).

20 control trials were presented randomly across the scanning session as well. It began with a 24-second construction-and-elaboration phase. In the construction phase, a cueing slide was presented which contained four lines. Line 1 described the task and lines 2 to 4 specified the noun to be used in the sentence (Figure 4.B). Participants were required to order the three objects, as named by the three nouns, by physical size and insert them into the following sentence: “X is smaller than Y is smaller than Z”. Once participants had silently said the sentence to themselves, they made a button-press, marking the end of the construction phase. In the elaboration phase, participants elaborated on the representation of the nouns, generating as much detail about the meaning of the noun - including visually imagining the object. Then the participants had to complete two rating scales that were presented for 5 seconds: (1) a five-point scale concerning the amount of detail they retrieved or imagined (1 = vague with no/few details; 5 = vivid and highly detailed) and (2) a binary scale regarding task difficulty (1 = easy; 5 = difficult).

Figure 4. A Sample Trial with Sample Stimuli for Each Condition in the Addis Task; Reprinted from Klepel et al. 2021.

(A) EXAMPLES OF EVENTS & DETAILS RETRIEVED DURING PRE-SCAN SESSION

TITLE: Ring for Xmas PERSON: John LOCATION: John's place OBJECT: Ring	TITLE: Fall outside library PERSON: Katie LOCATION: Widener Lib. OBJECT: Hat	TITLE: Graduation Day PERSON: Mom LOCATION: Harvard Yard OBJECT: Gown
TITLE: Didn't finish exam PERSON: Prof. Smith LOCATION: William James Hall OBJECT: Clock	TITLE: Signing lease PERSON: Broker LOCATION: Broker's Office OBJECT: Contract	TITLE: Buying new TV PERSON: John LOCATION: Best Buy OBJECT: Flat screen TV
TITLE: \$100 on lottery PERSON: Jess LOCATION: Convenience store OBJECT: Lottery Ticket	TITLE: Fight with Maggie PERSON: Maggie LOCATION: Starbucks OBJECT: Scarf	TITLE: Meeting Cathy PERSON: Cathy LOCATION: Border's Café OBJECT: Chicken fajita

(B) EXAMPLES OF CUEING SCREENS FROM fMRI SESSION

IMAGINE FUTURE EVENT that involves:

Cathy: Meeting Cathy
Harvard Yard: Graduation Day
Ring: Ring for Xmas

(i) future-imagine

IMAGINE PAST EVENT that involves:

Broker: Signing lease
Best Buy: Buying new TV
Hat: Fall outside library

(ii) past-imagine

RECALL MEMORIES that involved:

Jess: \$100 on lottery
Starbucks: Fight with Maggie
Clock: Didn't finish exam

(iii) past-recall

CREATE SENTENCE start with smallest:

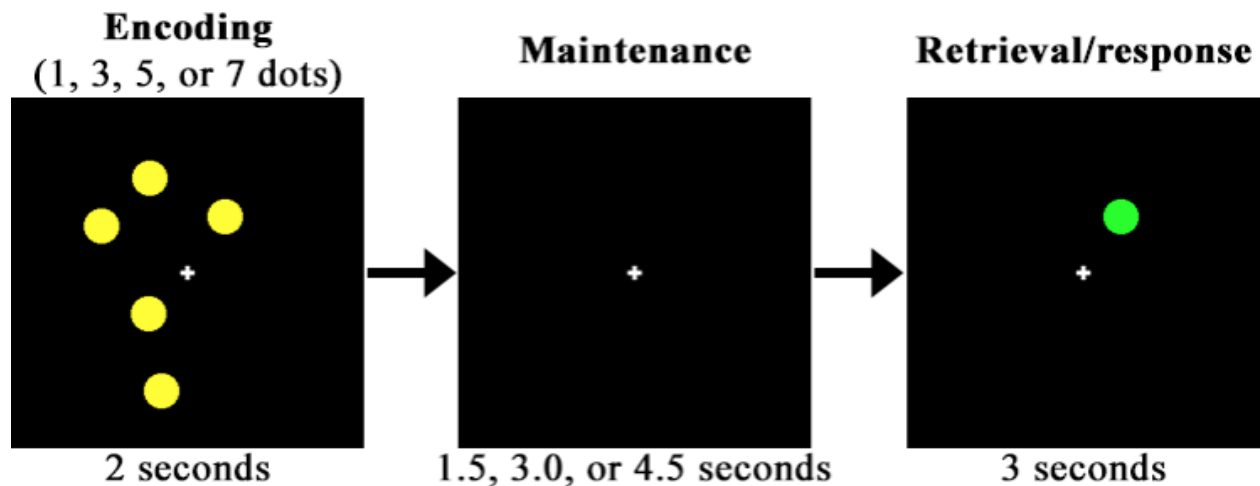
Bulb: Include bulb in sentence
Ice: Include ice in sentence
Tree: Include tree in sentence

(iv) control task

1.4 The Spatial Capacity Task (SCAP)

The Spatial Capacity task (SCAP) is another item-recall memory task used and described in Sanford & Woodward 2020 (Figure 5. A Sample Trial in the SCAP Task; Adapted from Sanford et al. 2020.). In this study, participants consisted of healthy controls (n=44) and patients with schizophrenia (n=44). The SCAP task is similar to the SIRP task except that it lacks any verbal content. Instead, it assesses visuospatial working memory by using dots randomly scattered across the screen whose locations are to be kept in mind. First, a target array of 1, 3, 5, or 7 yellow dots (positioned pseudo-randomly around a central fixation) was presented during a 2-second encoding period. After a 1.5, 3, or 4.5-second delay, a single green dot (i.e., the probe) was displayed for 3 seconds. Participants were asked to respond with a button-press as to whether the probe dot was in the same position as one of the target dots. The 2 experimental manipulations in this task include the Cognitive Load (the number of dots presented on the screen during the encoding phase) and Delay (the delay period between the encoding and response phase). 4 Cognitive Load levels \times 3 Delays resulted in 12 task conditions and in total, there were 4 trials per condition (total = 48 trials).

Figure 5. A Sample Trial in the SCAP Task; Adapted from Sanford et al. 2020.



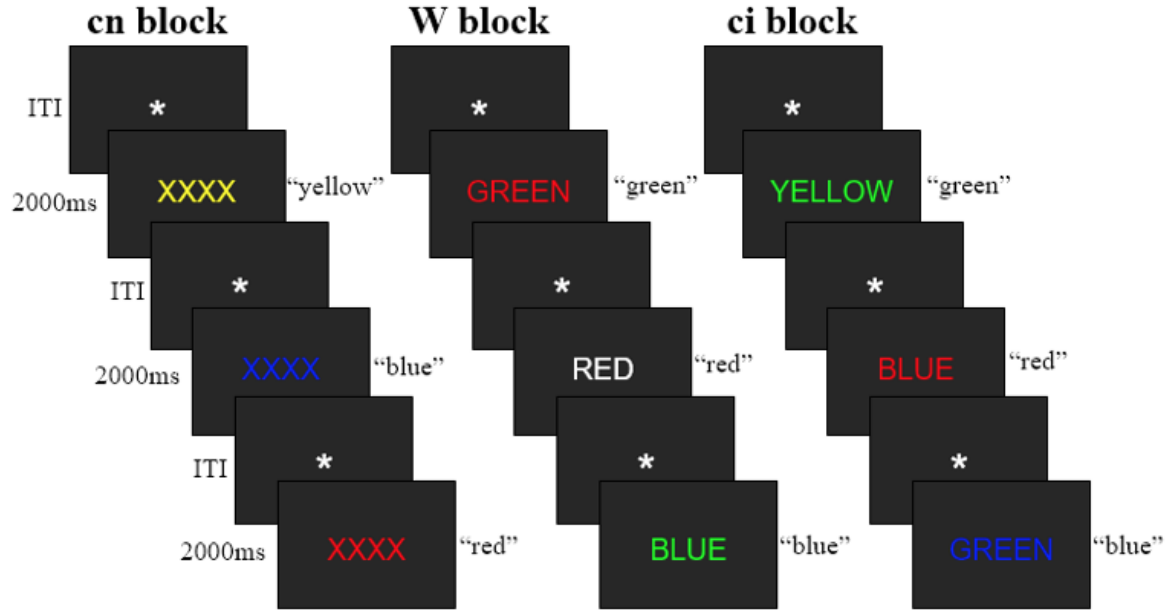
1.5 Task-Switch Inertia Task (TSI)

The Task-Switch Inertia (TSI) task (Figure 6. A Sample Trial in the TSI Task; Adapted from Sanford et al. 2020.) used in the Sanford & Woodward (2020) study is a set-switching Stroop task that involves responding to Stroop stimuli in alternating blocks of colour-naming (i.e., naming the font of the colour of the text displayed) and word-reading (i.e., reading the word displayed) of neutral and incongruent stimuli. In this study, participants consisted of healthy controls ($n = 26$) and patients with schizophrenia ($n = 28$).

Each block began with the instructions “NAME THE COLOUR” or “NAME THE WORD”, with reminders for which buttons to press at the bottom of the screen. In the neutral colour-naming blocks, a string of Xs was displayed in green, red, yellow, or blue font and participants were asked to name the colour of the text. In the word-reading blocks, colour words (“GREEN”, “RED”, “YELLOW”, “BLUE”) were displayed and the participants were asked to name the words. The word-reading blocks consisted of 5 neutral and 5 incongruent stimuli pseudo-randomly distributed throughout the block. A neutral word-reading stimulus is one in which colour words (“GREEN”, “RED”, “YELLOW”, or “BLUE”) were displayed in white font against a black background and participants were asked to name the words. An incongruent word-reading stimulus is one in which a colour word (“GREEN”, “RED”, “YELLOW”, or “BLUE”) is displayed in incongruent green, red, yellow, or blue font and participants were asked to name the words. In the incongruent colour-naming (ci) blocks, colour words (“GREEN”, “RED”, “YELLOW”, “BLUE”) were displayed in incongruent green, red, yellow, and blue fonts and the participants were asked to name the colour of the words. This task consisted of 12 blocks of 10 trials (3 neutral colour-naming, 3 incongruent colour-naming, and 6 word-reading). Sanford & Woodward (2020) only analyzed the word-reading blocks. The 2 experimental

manipulations in this task consisted of Stimulus Congruency (neutral (Wn) versus incongruent (Wi)) and Task-Switch (switching from neutral colour-naming (Cn) or incongruent colour-naming (Ci) blocks).

Figure 6. A Sample Trial in the TSI Task; Adapted from Sanford et al. 2020.



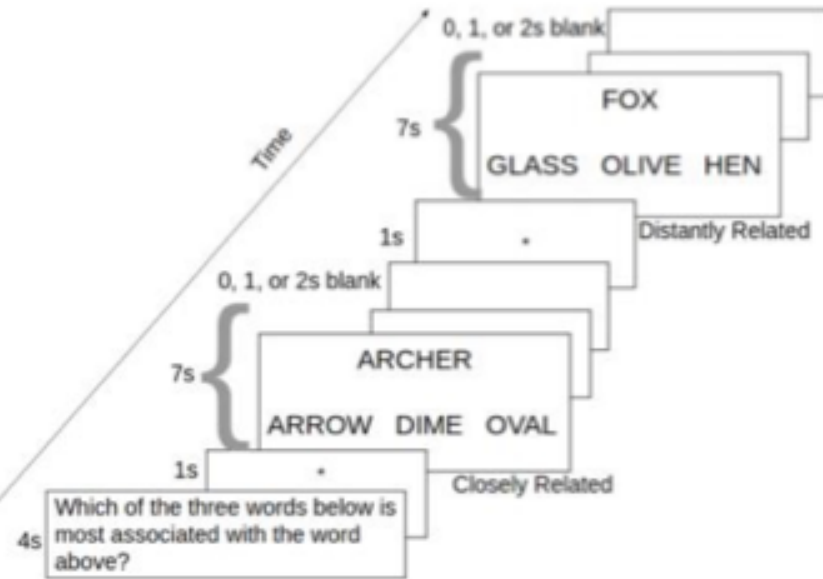
	Block 1	Block 2	Block 3	Block 4	Block 5	(Blocks 6-12)
Task	10 colour-naming	10 word-reading	10 colour-naming	10 word-reading	10 colour-naming	(etc.)
Stimulus	neutral	5 neutral + 5 incongruent	incongruent	5 neutral + 5 incongruent	neutral	

1.6 Semantic Integration Task (SIT)

In the Eickhoff & Woodward (2021) study, the SIT task was used, (Figure 7. Instructions and Two Sample Trials Showing Each Condition in the Semantic Integration Task; Reprinted from Eickhoff & Woodward 2021.). Participants consisted of healthy controls ($n = 24$) and patients with schizophrenia ($n = 21$). In the scanner, participants were presented with a prompt word (e.g. ARCHER) along with three potential match options (e.g. ARROW, DIME, and OVAL). They were asked to indicate, within 7 seconds, which of the three match options at the bottom of the screen was most related to the prompt word. They were instructed to indicate their response by using their index finger for the word on the left, middle finger for the word in the middle, or ring finger for the word on the right. If none of the 3 words fit with the prompt word, they were asked to choose a word that best fits according to any relationship that makes sense to them. Prior to each trial, a fixation screen with an asterisk was displayed for 1 second. In between trials, participants were presented by a blank screen lasting 0, 1 or 2 seconds to reset their thoughts. There was a total of 90 association trials. Following scanning, participants were asked to recall as many of the associated word pairs as possible. Only after completing the semantic association task were participants informed they would take part in a memory task to prevent them from actively trying to memorize word pairs inside the scanner (brain scans might reflect memory processes instead of semantic association processes). The encoding trials were sorted based on whether the associated word pairs were recalled or not-recalled. We were interested in examining whether a particular pattern of brain activity was more or less engaged for trials that were remembered later on (recalled) compared to trials that were not remembered (not-recalled). Trials were then analyzed in terms of both the degree of association between the

target word and the prompt word (high association or low association), and memory performance (whether the trials had been recalled or not).

Figure 7. Instructions and Two Sample Trials Showing Each Condition in the Semantic Integration Task; Reprinted from Eickhoff & Woodward 2021.



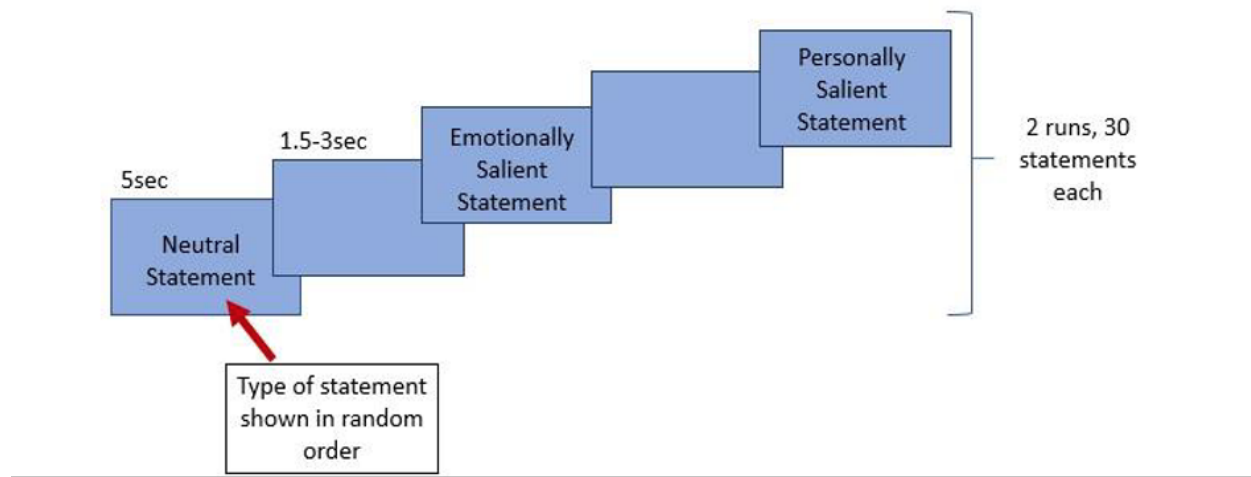
1.7 Delusions of Reference (DOR)

The Delusions of Reference task (DOR) was used by Larivière et al. 2017 (Figure 8). Sample trials from the Delusions of Reference Task (Reprinted from Woodward Lab.). This task aims to induce feelings of self-relevance which is typically seen in schizophrenic patients with delusions of reference. Delusions of reference are one of the most common symptoms in schizophrenic patients. They are misinterpretations of external stimuli in which neutral events trigger ideas of self-relevance. Schizophrenic patients with delusions of reference may mistakenly believe that an external stimulus somehow refers to them or that objects are specifically arranged in such a way that they are sending a message to them. In this study, the participants consisted of healthy controls ($n=15$), schizophrenic patients without the delusions of reference ($n=13$), and schizophrenic patients with prominent delusions of reference ($n=14$). In the DOR task, the participants were presented with 60 distinct statements (60 trials) over 2 separate runs. Of these 60 statements, 20 were “neutral” (e.g., she goes to school), 20 were “emotionally salient” (e.g., everybody loves her), and 20 were “personally salient” (personal statements about the participant). The “personally salient” statements were obtained from a screening interview conducted several weeks prior to the scanning session. However, the participants were not aware that they would see this information about themselves in the task. Each run consisted of 10 personalized statements and 20 generic statements (10 neutral and 10 emotional statements in random order. These 30 statements were presented twice, which resulted in a total of 60 trials per run. Each statement was presented for 5 seconds and between each statement, a jittered fixation cross was presented which lasted between 1.5 to 3 seconds. The participants were asked to respond with either “yes” (Endorsed condition) or “no” (Non-endorsed condition) with their right hand using a 2 button response box as to whether the

statement that was presented on the screen was written specifically about them— not merely that is was descriptive or true of them.

Figure 8. Sample trials from the Delusions of Reference Task (Reprinted from Woodward Lab).

Instruction: Press "yes" if you feel that the statement was written specifically about you (not just that it is true of you) and "no" if you don't.



Results

1.1.1 Sternberg Item Recognition Paradigm (SIRP); Sanford et al. (2020)

Component 3 was identified as the Maintaining Network with a z-score of 1.60 from increased activity at 89% of voxels. Repeated measure ANOVA revealed a significant main effect of Time, $F(9,324) = 25.20, p < .001$, (Figure 9). The Time factor was dominated by contrasts 1 to 2 ($p < .01$) for decreases from peak, and 3 to 4 ($p < .001$), 4 to 5 ($p < .05$), and 5 to 6 ($p < .001$) for increases to peak.

Repeated measure ANOVA also revealed a significant main effect of Cognitive Load, $F(1,36) = 69.64, p < .001$, where the average activity of the 6-Letter condition ($M = .12$) was significantly higher than the average activity of the 4-Letter condition ($M = .03$). Additionally, it showed a significant interaction between Cognitive Load x Time, $F(9, 324) = 15.76, p < .001$, (Figure 10). This interaction was dominated by a steeper increase for the 6-Letter condition relative to the 4-Letter condition Timebins 5 to 6, $F(1,36) = 8.24, p < .05$, which reflects a higher (positive) HDR peak for the 6-Letter condition than the 4-Letter condition.

In addition, repeated measure ANOVA revealed a significant main effect of Delay, $F(1, 36) = 48.48, p < .001$, where the average activity of the 0-second delay condition ($M = 0.03$) was significantly more suppressed than the 4-second Delay condition ($M = 0.11$). There was also a significant interaction between Delay x Time, $F(9, 324) = 30.61, p < .001$, (Figure 11). This interaction was dominated by a steeper increase for the 4-second Delay condition relative to the 0-second Delay condition from Timebins 6 to 7, $F(1,36) = 73.03, p < .05$, which reflects a higher HDR (positive) peak for the 4-second Delay condition relative to the 0-second Delay conditions.

Lastly, there was a significant interaction between Cognitive Load x Delay x Time, $F(9,324) = 4.47, p < .001$, (Figure 12). In both the 4-Letter and 6-Letter conditions, 4-second

Delay increased, while 0-second Delay decreased from Timebins 6 to 7, $F(1,36) = 4.761, p < .05$.

In both the 4-Letter and 6-Letter conditions, this interaction reflects a higher (positive) HDR peak for the 4-second Delay condition relative to the 0-second Delay condition.

Figure 9. Component 3 (C3_INT89_NDMN11_1.60_0.45) Varimax HDR averaged over Cognitive Load (4-Letter_6-Letter) and Delay (0s-Delay_4s-Delay).

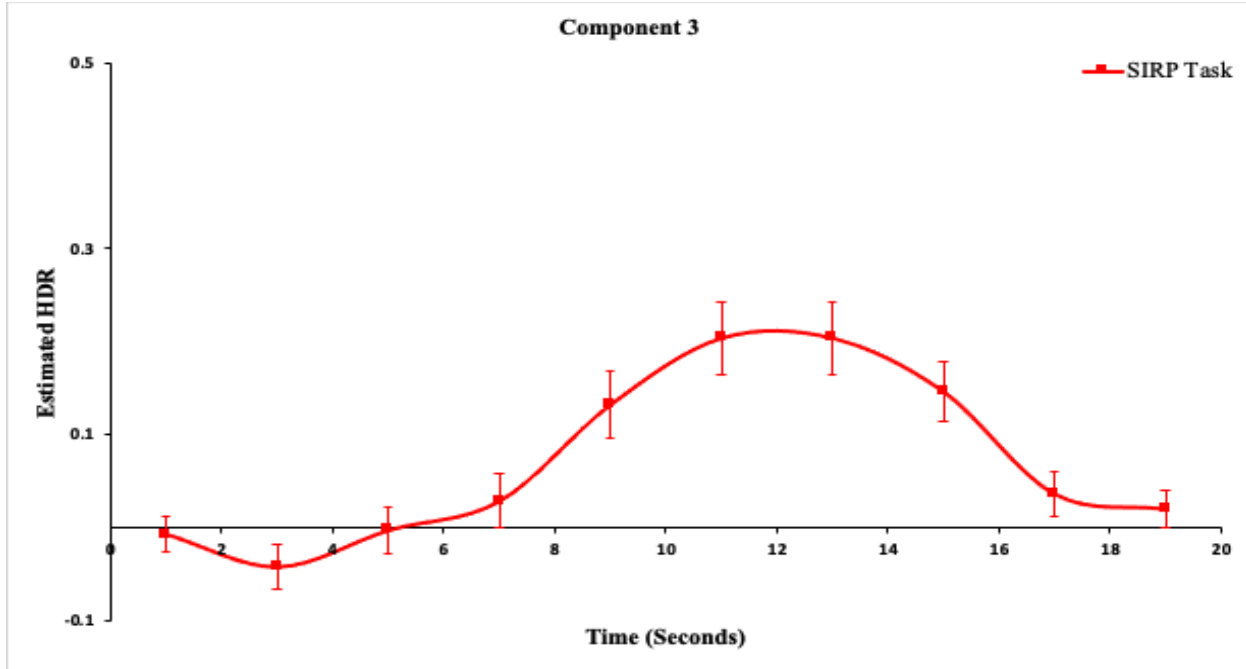


Figure 10. Component 3 (C3_INT89_NDMN11_1.60_0.45) Varimax HDR for Cognitive Load (4-Letter_6-Letter) x Time, averaged over Delay (0s-Delay_4s-Delay).

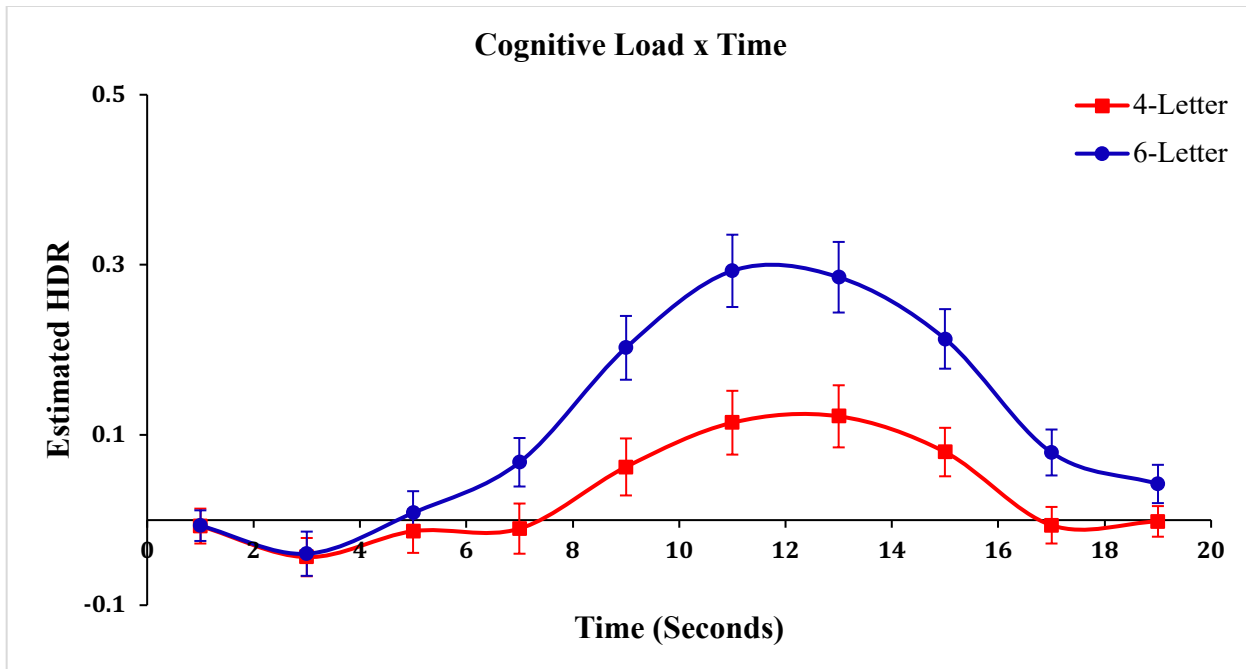


Figure 11. Component 3 (*C3_INT89_NDMN11_1.60_0.45*) Varimax HDR for Delay (0s-Delay_4s-Delay) x Time, averaged over Cognitive Load (4-Letter_6-Letter).

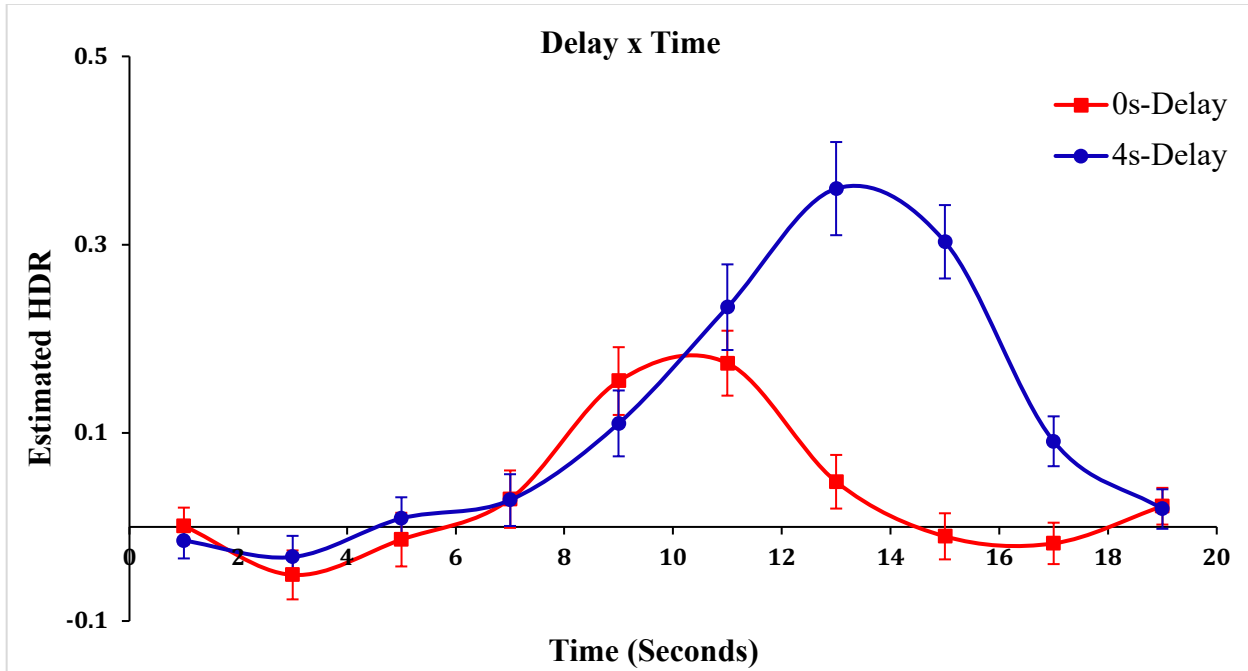
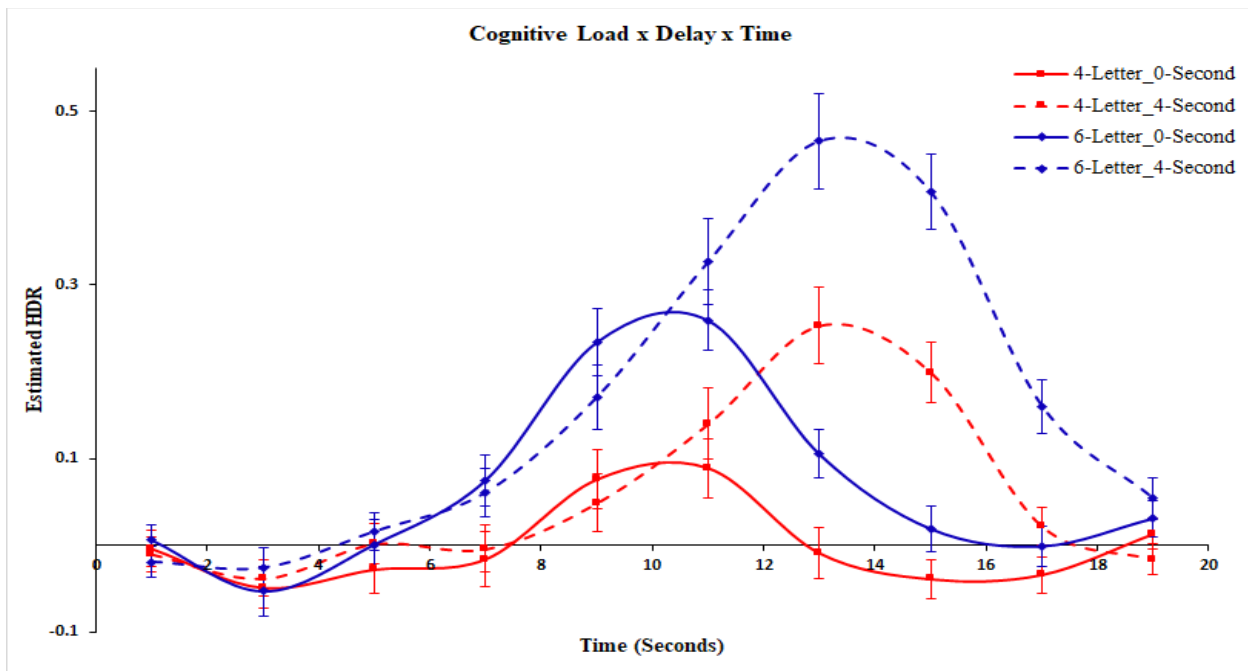


Figure 12. Component 3 (*C3_INT89_NDMN11_1.60_0.45*) Varimax HDR for Cognitive Load (4-Letter_6-Letter) x Delay (0s-Delay_4s-Delay).



1.1.1. Sternberg Item Recognition Paradigm (SIRP); Sanford & Woodward (2020)

Component 2 was identified as the Maintaining network with a z-score of 1.37 from increased activity at 91% of voxels. Mixed measure ANOVA revealed a significant main effect of Time, $F(9,468) = 52.56, p < .001$, (Figure 13). The Time factor was dominated by contrasts 3 to 6 for increases to peaks, and 7 to 10 for decreases from peak (all were $p < .001$).

Mixed measure ANOVA also revealed a significant main effect of Cognitive Load, $F(1,52) = 129.51, p < .001$, where the average activity of the 6-Letter condition ($M = 0.12$) is significantly higher than the 4-Letter condition ($M = 0.04$). Additionally, there was a significant interaction between Cognitive Load x Time, $F(9, 324) = 4.37, p < .001$, (Figure 14). The 4-Letter condition increased, while the 6-Letter condition very slightly decreased from Timebins 6 to 7, $F(1,52) = 5.25, p < .05$, which reflects a higher (positive) HDR peak for the 6-Letter condition relative to the 4-Letter condition.

In addition, mixed measure ANOVA revealed a significant main effect of Delay, $F(1, 52) = 59.86, p < .001$, where the average activity of the 0s-Delay condition ($M = 0.05$) was significantly more suppressed than the 4s-Delay condition ($M = 0.11$). It also revealed a significant interaction between Delay x Time, $F(9,468) = 84.20, p < .001$, (Figure 15). 0s-Delay decreased, while 4s-Delay increased from Timebins 6 to 7, $F(1,52) = 238.43, p < .001$, which reflects a higher (positive) HDR peak for the 4-second Delay condition relative to the 0-second Delay0 condition.

Lastly, there was a significant interaction between Cognitive Load x Delay x Time, $F(9,468) = 2.51, p < .01$,

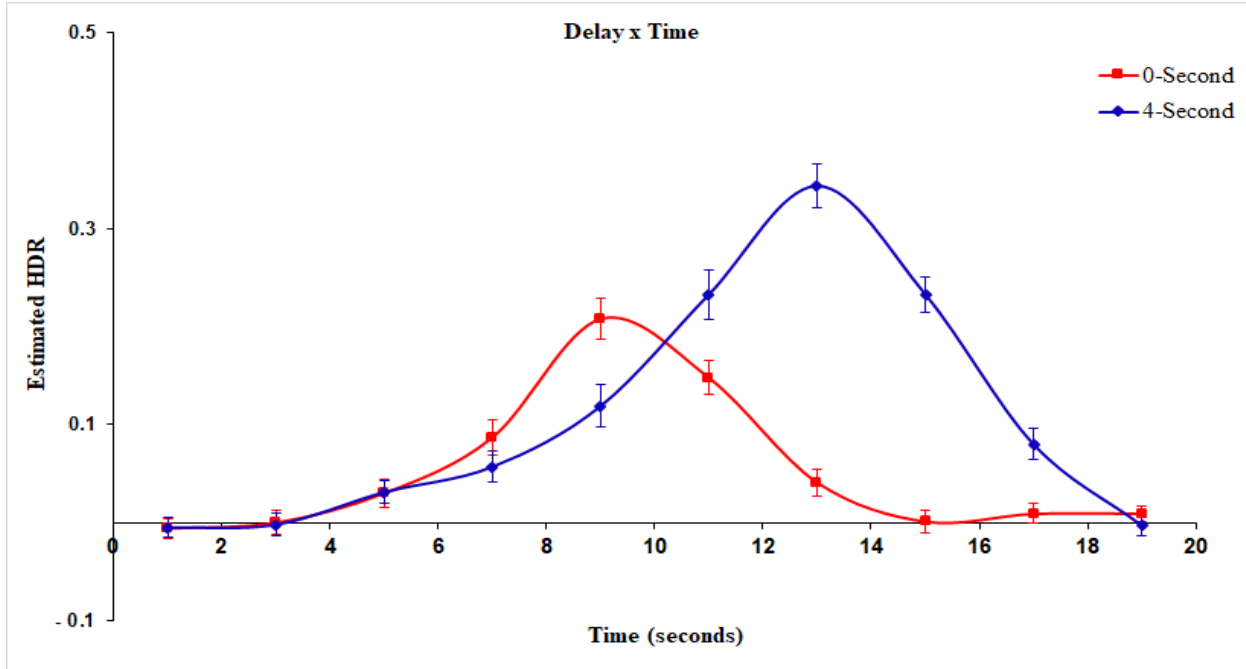


Figure 16). In both the 4-Letter and 6-Letter conditions, 4s-Delay increased, while 0s-Delay decreased from Timebins 5 to 6, $F(1,52) = 4.15, p < .05$. In both the 4-Letter and 6-Letter conditions, this interaction reflects a higher (positive) HDR peak for the 4s-Delay condition relative to the 0s-Delay condition.

Figure 13. Component 2 (C2_INT91_NDMN_1.37_0.31) Varimax averaged over Cognitive Load (4-Letter_6-Letter), Delay (0s_Delay_4s-Delay), and Group (Healthy_Schizophrenia).

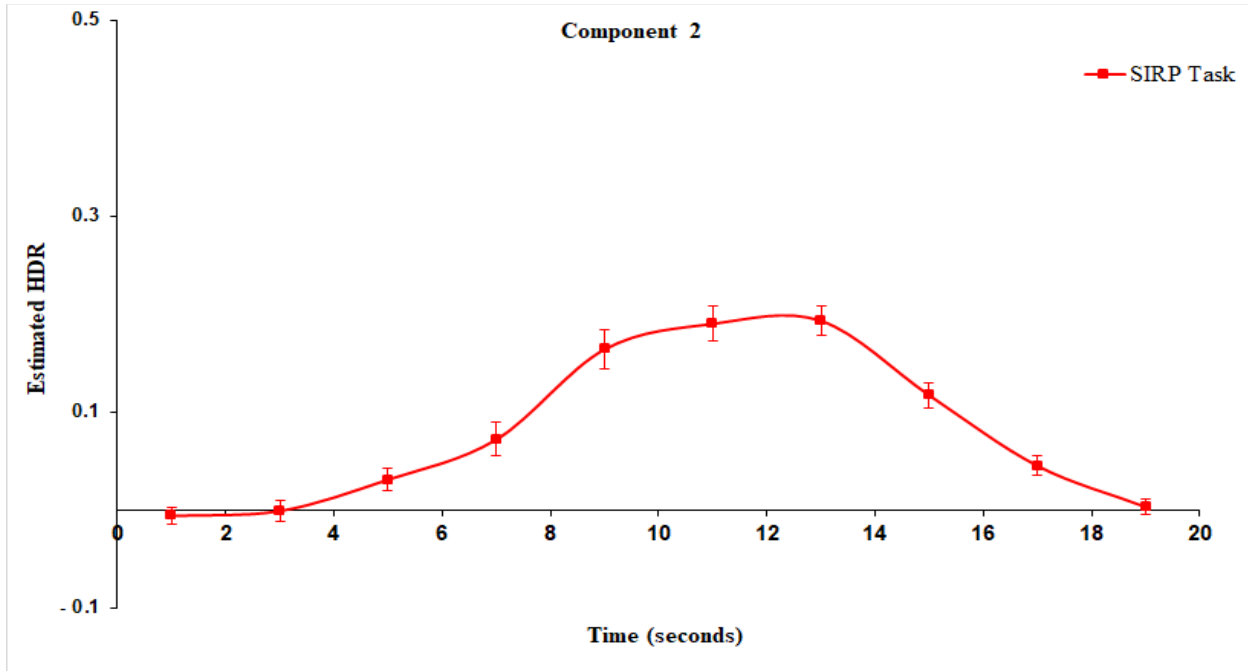


Figure 14. Component 2 (C2_INT91_NDMN_1.37_0.31) Varimax for Cognitive Load (4-Letter_6-Letter) x Time, averaged over Delay (0s_4s) and Group (Healthy_Schizophrenia).

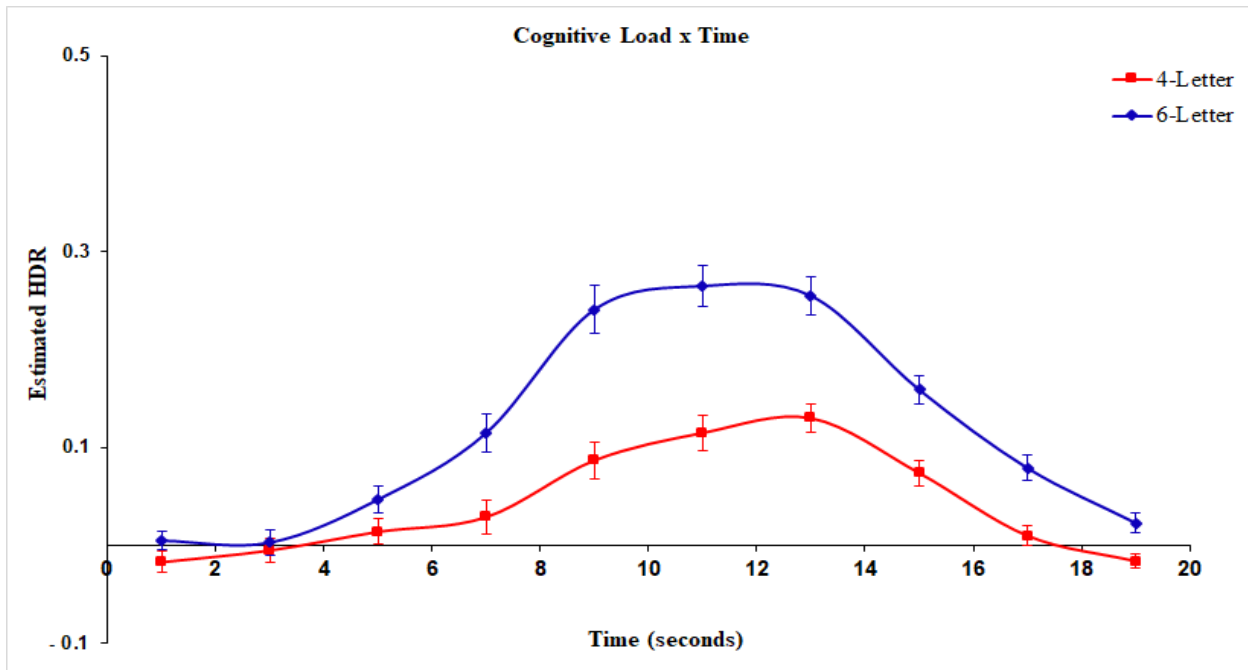


Figure 15. Component 2 (C2_INT91_NDMN_1.37_0.31) Varimax for Delay (0s-Delay_4s-Delay) x Time, averaged over Cognitive Load (4-Letter_6-Letter) and Group (Healthy_Schizophrenia).

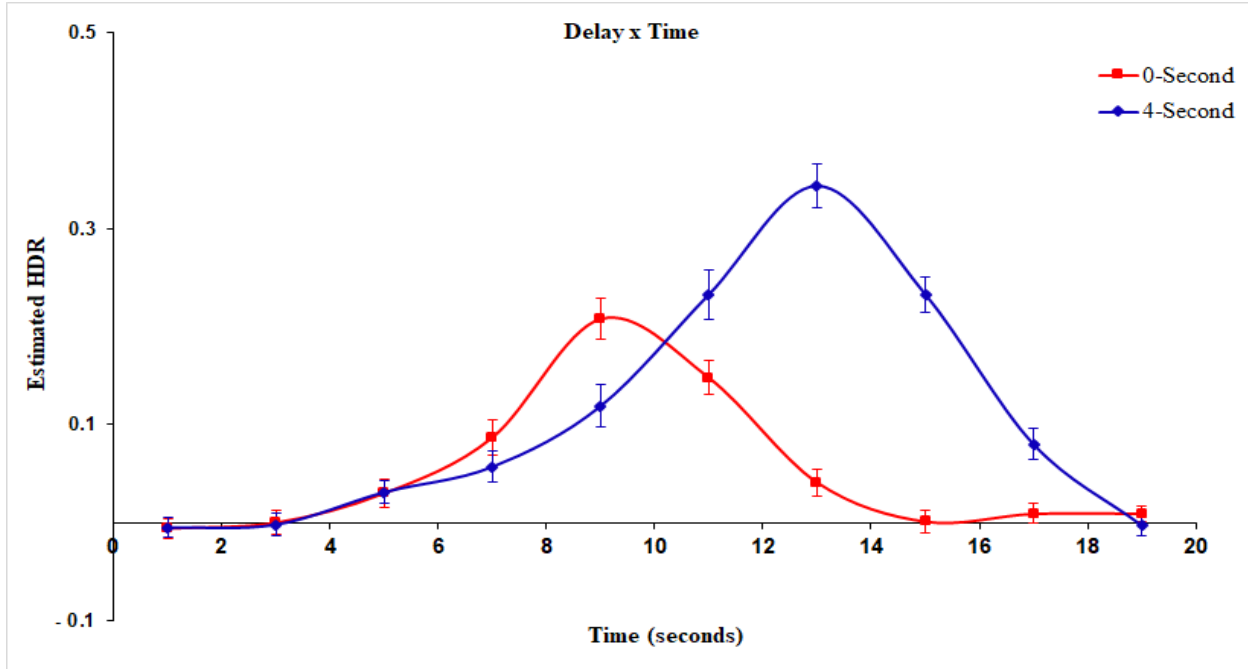
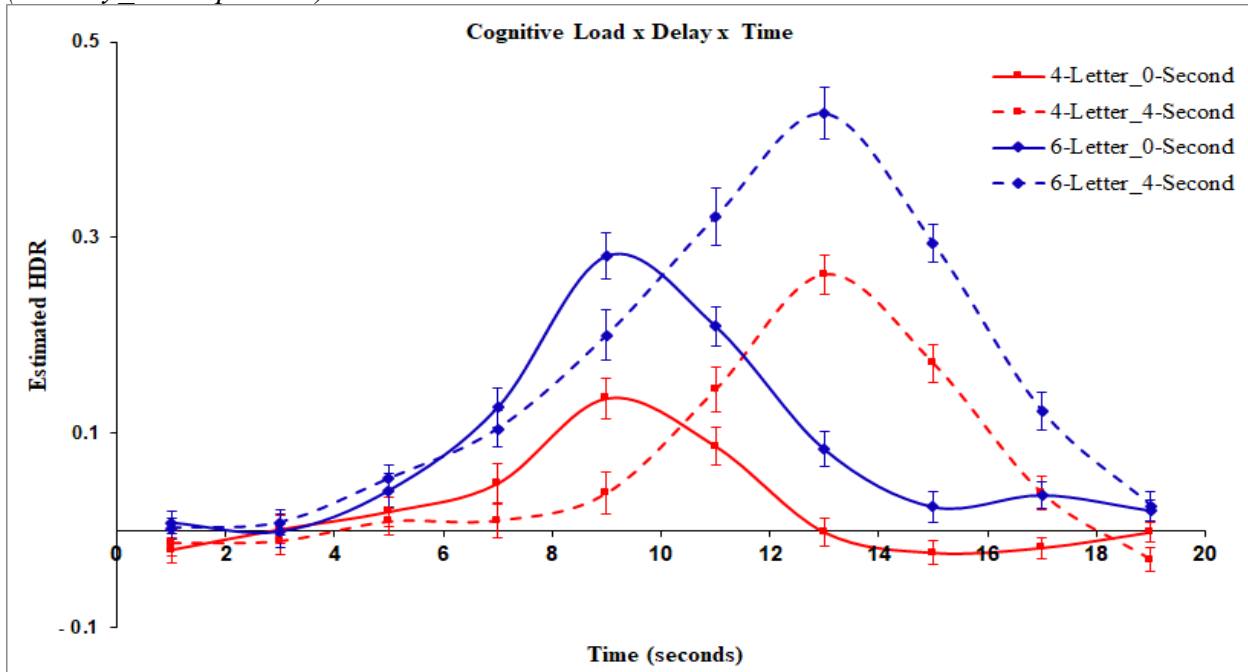


Figure 16. Component 2 (C2_INT91_NDMN_1.37_0.31) Varimax for Cognitive Load (4-Letter_6-Letter) x Delay (0s-Delay_4s-Delay) x Time, averaged over and Group (Healthy_Schizophrenia).



1.1.2. Sternberg Item Recognition Paradigm (SIRP); Metzak et al. (2012)

Component 3 was identified as the Maintaining network with a z-score of 0.82 from increased activity at 67% of voxels. Mixed measure ANOVA revealed a significant main effect of Time, $F(6, 174) = 58.33, p < .001$, (Figure 17). The Time factor was dominated by contrasts 1 to 5 for increases to peak and 5 to 7 for decreases from peak, (all were $p < .001$).

Mixed measure ANOVA also revealed a significant main effect of Cognitive Load, $F(3, 87) = 15.75, p < .001$, where average activity of the 8-Letter condition ($M = 0.185$) was significantly higher relative to the average activity of the 6-Letter ($M = 0.15$), 4-Letter ($M = 0.06$), and 2-Letter ($M = 0.05$) condition. It also showed a significant interaction between Cognitive Load x Time, $F(18, 522) = 9.51, p < .001$, (Figure 18). Both the 4-Letter and 6-Letter conditions showed an HDR increase from Timebins 4 to 5, $F(1, 29) = 10.30, p < .01$, which showed a higher HDR (positive) peak for the 6-Letter condition relative to the 4-Letter condition. The Cognitive x Load interaction was dominated by the 8-Letter condition relative to the 6-Letter condition from Timebins 4 to 5, $F(1, 29) = 8.09, p < 0.01$, which reflects a higher HDR peak for the 8-Letter condition relative to the 6-Letter condition.

Figure 17. Component 3 (C3_NDMN67_INT_0.80_0.69) Varimax HDR averaged over Cognitive Load (2-Letter_4-Letter_6-Letter_8-Letter) and Group (Healthy_Schizophrenia).

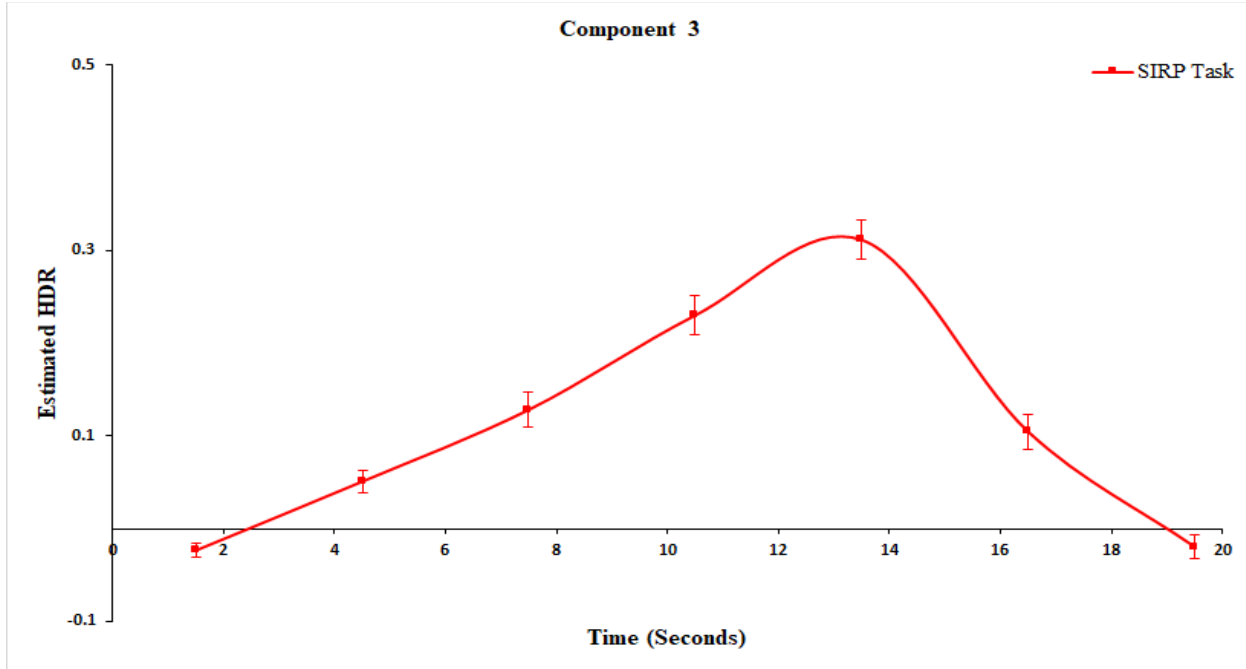
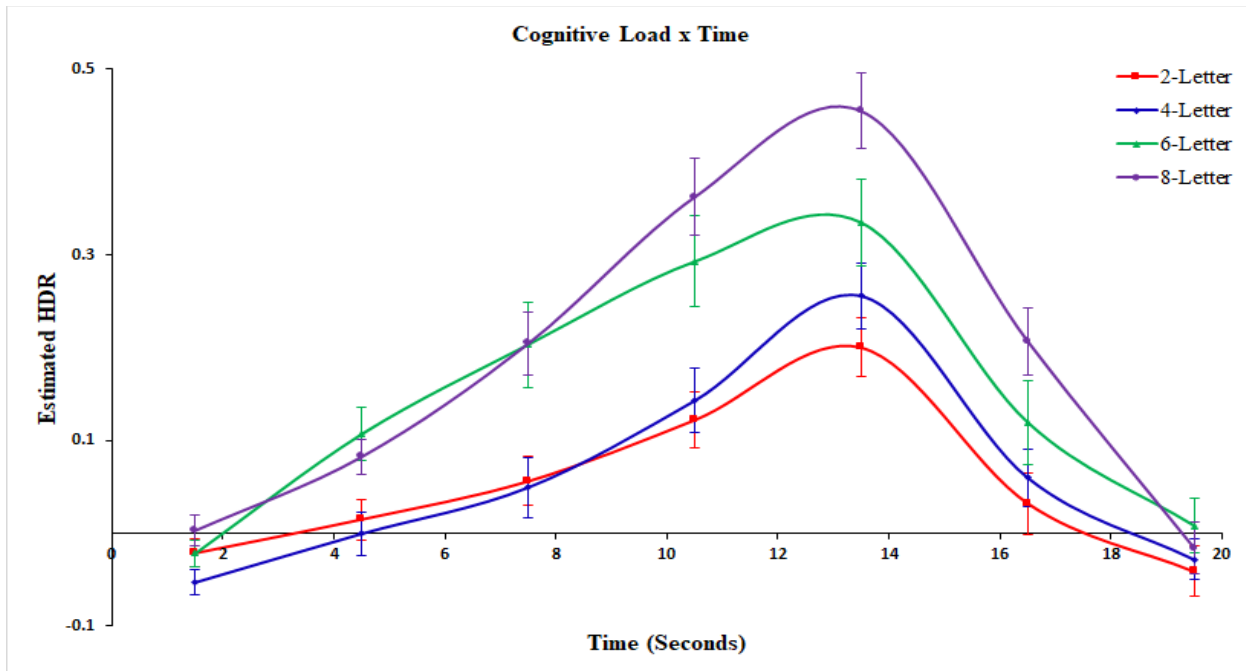


Figure 18. Component 3 (C3_NDMN67_INT_0.80_0.69) Varimax for Cognitive Load (2-Letter_4-Letter_6-Letter_8-Letter) x Time, averaged over Group (Healthy_Schizophrenia).



As shown by the results, different versions of the SIRP task elicited reproducible activation of the Maintaining network in 3 separate studies. These studies showed that the activation of the Maintaining network is affected by increasing both the cognitive load of the stimuli and the delay period between encoding and response phase. More specifically, increasing the cognitive load and the delay period elicited comparable increases in the activity of the Maintaining network. However, increasing the cognitive load and the delay period together yielded the highest activation of the Maintaining network. The timing of the HDR peaks suggests that the Maintaining network most closely underlies the maintaining/rehearsing phase of the SIRP task. Overall, these results suggest that the Maintaining network is involved in working memory, particularly the rehearsal phase of working memory which appears to be dependent on the cognitive and delay demands.

1.2.1 Thought Generating Task (TGT); Sanford et al. (2020)

Component 3 was identified as the Maintaining network with a z-score of 1.6 from increased activity at 89% of voxels. Repeated measure ANOVA revealed a significant main effect of Time, $F(9,279) = 15.53, p < .001$, (Figure 19). The Time factor was dominated by contrasts 2 to 4 for increases to peak (all were $p < .001$), and 5 to 6 ($p < .001$), 6 to 7 ($p < .05$), 7 to 8 ($p < .01$) for decreases from peak.

Repeated measure ANOVA also revealed a significant main effect of Condition, $F(1,31) = 9.96, p < .01$, where the average activity of Generating ($M = 0.04$) is significantly higher than the Hearing condition ($M = 0.02$), and a significant interaction between Condition x Time, $F(9,279) = 9.27, p < .001$, (Figure 20). Generating showed an HDR increase and then a decrease, while Hearing slightly increased from Timebins 4 to 5, $F(1,31) = 9.17, p < .01$, which reflects a higher HDR (positive) peak for Generating relative to Hearing.

Figure 19. Component 3 (C3_INT89_NDMN11_1.60_0.45) Varimax HDR averaged over Condition (Hearing_Generating).

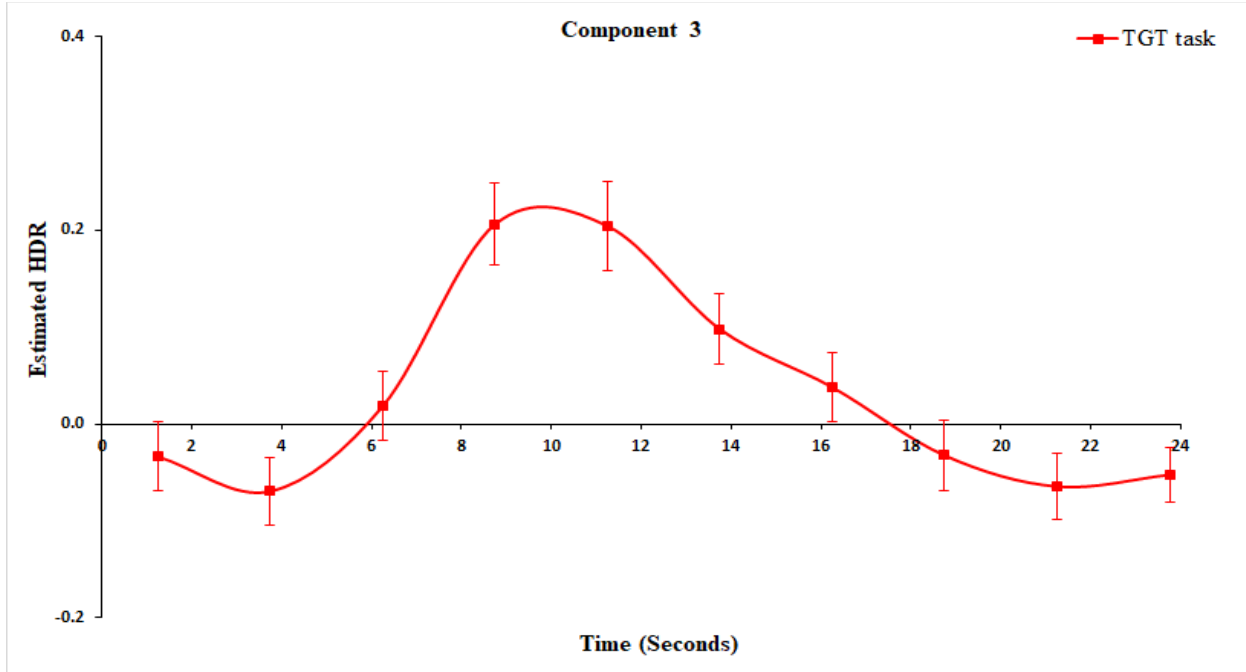
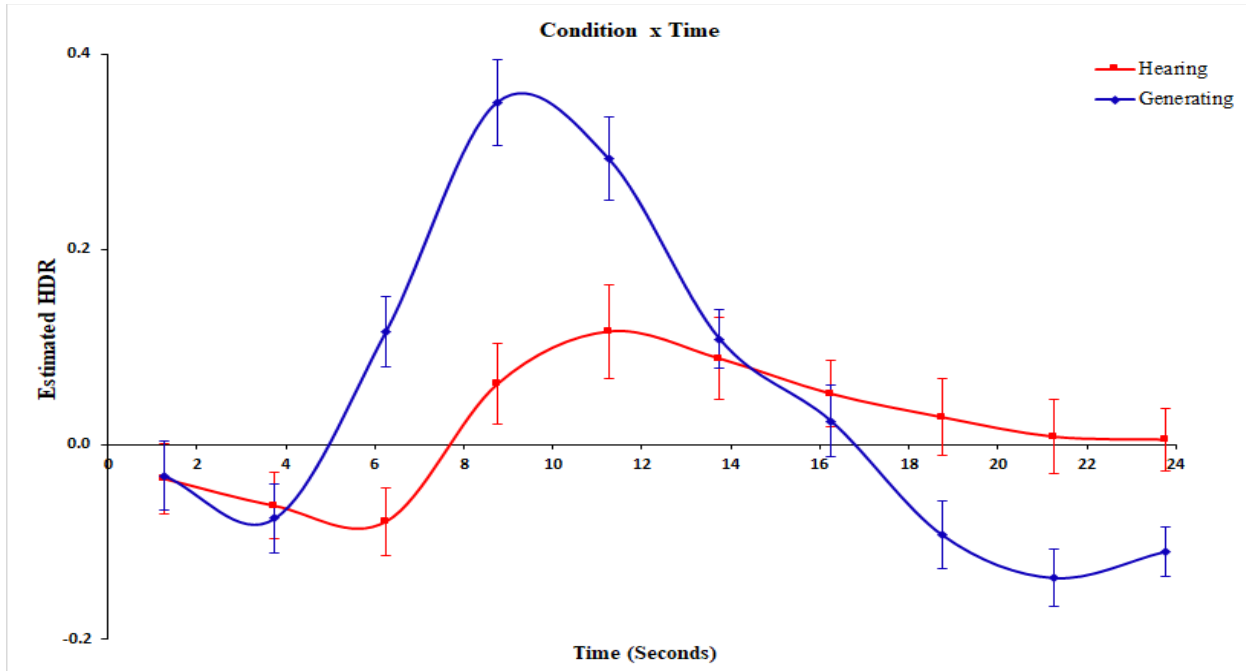


Figure 20. Component 3 (C3_INT89_NDMN11_1.60_0.45) Varimax HDR for Condition (Hearing_Generating) x Time.



1.2.2 Thought Generating Task (TGT); Sanford & Woodward (2020)

Component 2 was identified as the Maintaining network with a z-score of 1.37 from increased activity at 91%. Mixed measure ANOVA revealed a significant main effect of Time, $F(9,522) = 10.80, p < .001$, (Figure 21). The Time factor was dominated by contrasts 1 to 4 for increases to peak and 5 to 6 and 7 to 8 for decreases from peak (all were $p < .05$). Mixed measure ANOVA also revealed a significant main effect of Condition, $F(2,58) = 39.11, p < .001$, where the average activity of Generating ($M = 0.02$) is significantly higher than the Hearing condition ($M = -0.01$), and a significant interaction between Condition x Time, $F(9,522) = 21.13, p < .001$, (Figure 22). Generating showed an HDR decrease, while Hearing showed a small HDR increase from Timebins 4 to 5, $F(1,58) = 12.57, p < .001$, which reflects a positive HDR peak for Generating, but not for Hearing.

Figure 21. Component 2 (C2_INT91_NDMN_1.37_0.31) Varimax averaged over Condition (Hearing_Generating) and Group (Healthy_Schizophrenia).

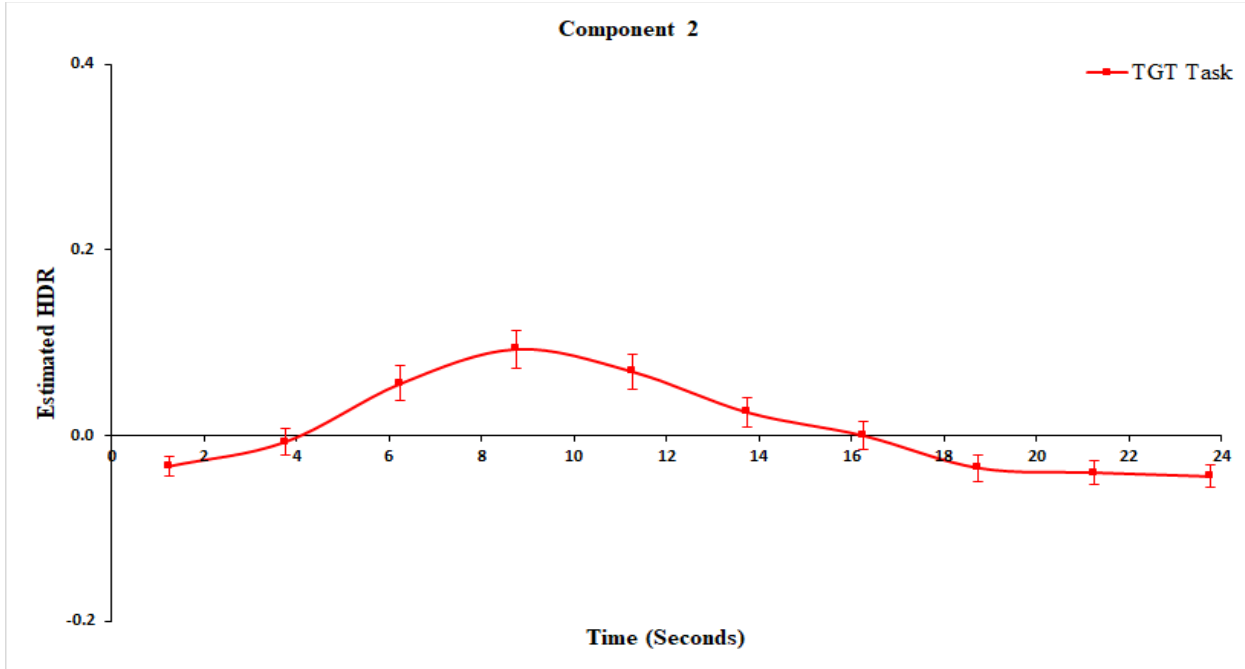
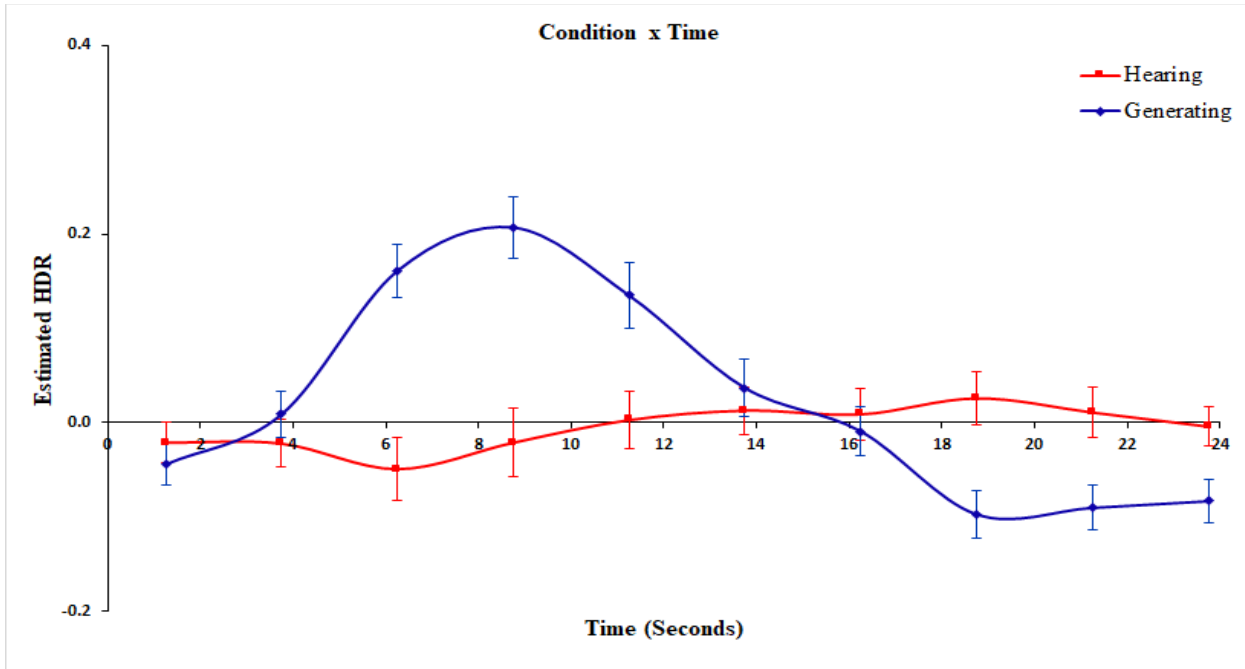


Figure 22. Component 2 (C2_INT91_NDMN_1.37_0.31) Varimax for Condition (Hearing_Generating) x Time averaged over Group (Healthy_Schizophrenia).



In both of the studies, the Generating condition evoked a greater activation of the Maintaining network than the Hearing condition, which implicates the Maintaining network in internally oriented cognition as opposed to externally oriented cognition. In the Sanford & Woodward (2020) study, the HDR peak for the Generating condition ($M = 0.21$) was much lower relative to the HDR peak for the Generating condition ($M = 0.35$) in the Sanford et al. (2020) study. This lower activation could be because in the Sanford & Woodward (2020) study, participants consisted of both healthy individuals and patients with schizophrenia, whereas the Sanford et al. (2020) study, participants included strictly healthy individuals. Therefore, the lower HDR peak in the Sanford & Woodward (2020) study could be because it represents the overall mean activation of the Maintaining network in both groups.

The timing trajectory of the estimated HDR plots for the Maintaining network in these 2 studies shows an increase and sustenance in the activation of Maintaining network that emerges at a time after a preceding component reaches its' peak, which suggests that the Maintaining network likely underlies the cognitive processes involved in generating representations of the stimulus in working memory, as opposed to the initial interaction and attention paid to the stimulus.

1.3 Addis Task

Component 3 was identified as the Maintaining network with a z-score of 1.54 from increased activity observed at 86% of voxels. Repeated measure ANOVA revealed a significant main effect of Time, $F(20,320) = 25.03, p < .05$, (Figure 23). The Time factor was dominated by contrasts 2 to 5 and 13 to 16 for increases to peaks, 7 to 12 and 17 to 19 for decreases from peak (all were $p < .05$).

Repeated measure ANOVA also revealed a significant main effect of Condition, $F(3,48) = 3.56, p < .05$ and a significant interaction between Condition x Time, $F(60,960) = 2.20, p < .05$, (Figure 24). Imagine-Past and Imagine-Future did not differ significantly in terms of main effects, $F(1,16) = 0.22, p = .64$. Therefore, these conditions were collapsed for the purpose of statistical testing to simplify the analyses. Comparing the Imagine and Control conditions did not result in a significant main effect of condition, $F(1,16) = 0.03, p = .88$. However, comparing the Imagine and Recall conditions resulted in a significant main effect of condition, $F(1,16) = 7.70, p < .05$, suggesting that the Condition x Time interaction is caused by the difference between Recall and the average of the other conditions, and none of the other conditions differ from each other.

All conditions produced similar HDR plots for the Maintaining network. Recall-Future condition showed the lowest HDR (positive) peak relative to the Imagine. Given that both the Imagine conditions involved some novel recombination and episodic construction in comparison to the Recall condition, the fact that the HDR peaks in the Imagine conditions differed from the Recall condition suggests that the activity of the Maintaining network discriminates between novel recombination of episodic details and the simple recall of episodic details.

Figure 23. Component 3 ($C3_INT86_NDMN_1.54_0.31$) Varimax averaged over Condition (Control_Imagine-Past_Imagine-Future_Recall-Past).

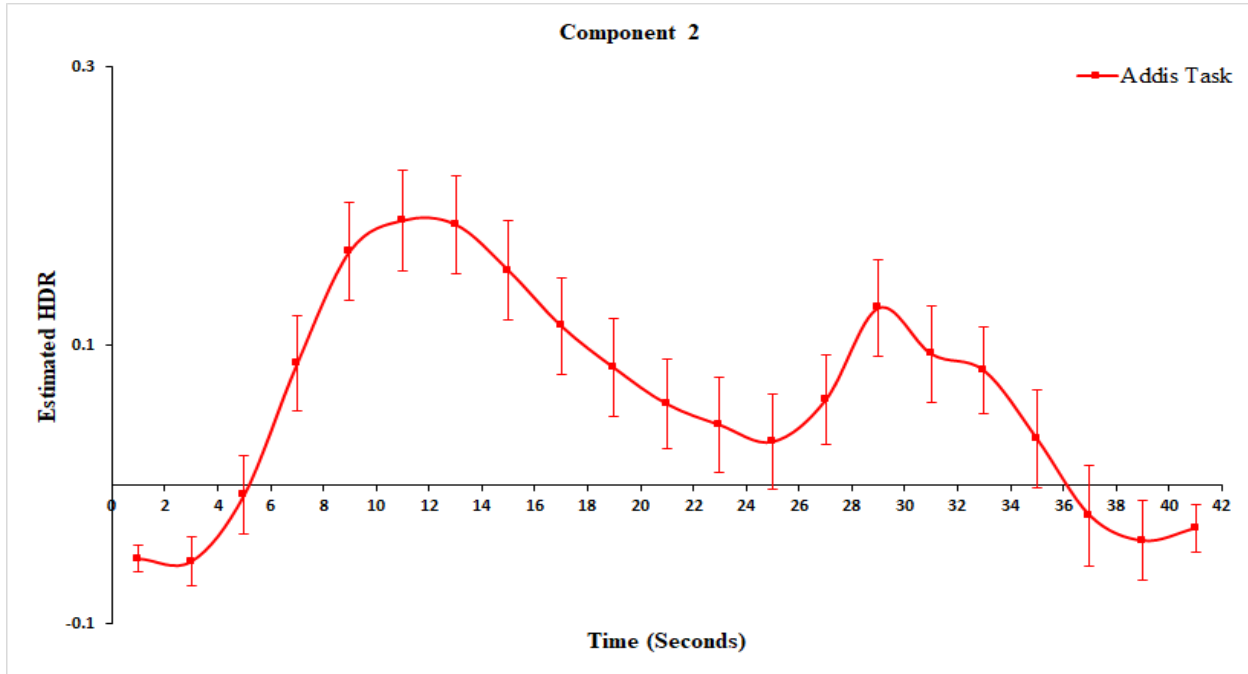
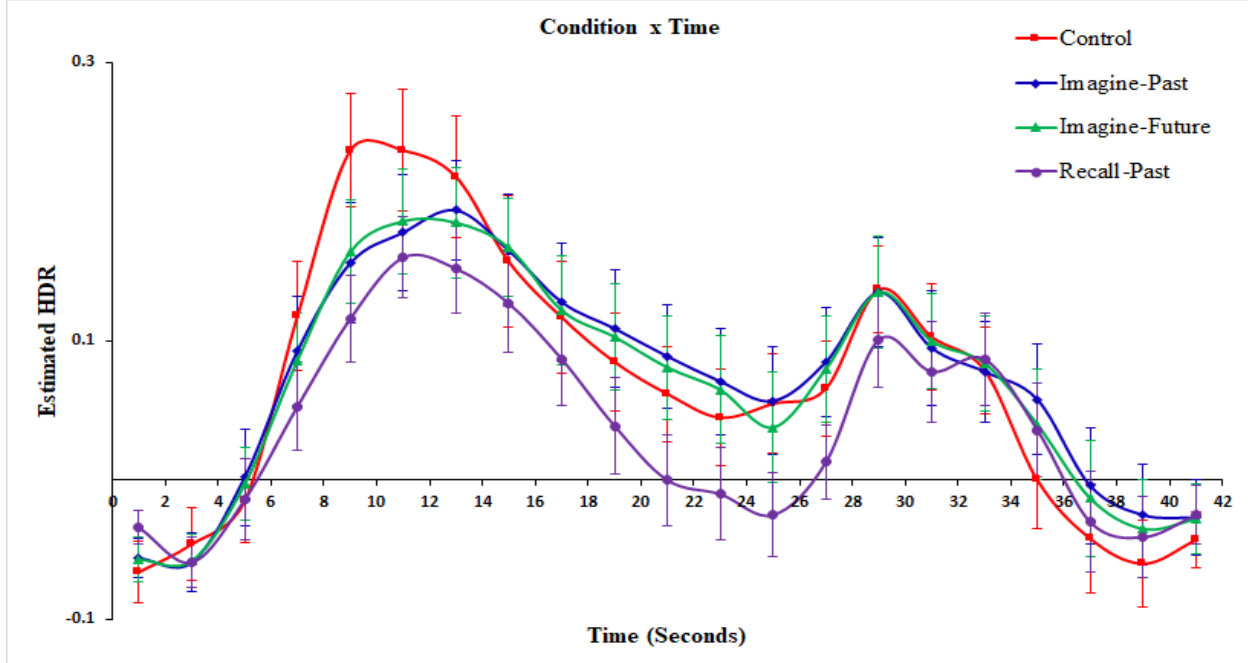


Figure 24. Component 3 ($C3_INT86_NDMN_1.54_0.31$) Varimax for (Control_Imagine-Past_Imagine-Future_Recall-Past) x Time.



1.4 Spatial Capacity Task (SCAP)

Component 2 was identified as the Maintaining network with a z-score of 1.37 from increased activity at 91% of voxels. Mixed measure ANOVA revealed a significant main effect of Time, $F(9,774) = 65.45, p < .001$, (Figure 25). The Time factor was dominated by contrasts 2 to 6 for increases to peaks and 6 to 10 for decreases from peak (all were $p < .001$).

Mixed measure ANOVA also revealed a significant main effect of Cognitive Load, $F(3,258) = 6.45, p < .001$, where the average activity of the 7-Dots condition ($M = 0.07$) was significantly higher than the average activity of 1-Dot ($M = 0.05$), 3-Dots ($M = 0.05$), and 5-Dots ($M = 0.05$) conditions. It also showed a significant interaction between Cognitive Load x Time, $F(27,2322) = 3.50, p < .001$, (Figure 26). The 7-Dots condition showed an HDR decrease, while the 5-Dots condition first showed a slight HDR increase followed by an HDR decrease from Timebins 6 to 7, $F(1,86) = 7.79, p < .05$. This reflects a higher and slightly earlier HDR peak for the 7-Dots condition relative to the 5-Dots condition.

Furthermore, a significant main effect of Delay, $F(2,172) = 16.82, p < .001$, where the average activity of the 4.5s-Delay condition ($M = 0.07$) was significantly higher than the 1.5s-Delay ($M = 0.04$) and 3.0s-Delay ($M = 0.06$) conditions, and a significant interaction between Delay x Time, $F(18,1548) = 20.14, p < .001$, (Figure 27), was observed. The Delay x Time interaction was dominated by a steeper increase for the 1.5s-Delay condition relative to the 3.0s-Delay condition from Timebins 4 to 5, $F(1,86) = 12.63, p < .01$. However, the 1.5s-Delay condition decreased, while the 3.0s-Delay increased from Timebins 5 to 6, $F(1,86) = 48.38, p < .001$. Then, the 3.0s-Delay conditions decreased, while Delay4.5s increased from Timebins 6 to 7, $F(1,86) = 88.34, p < .001$. Overall, this interaction reflects the earliest and smallest HDR peak

for the 1.5s-Delay condition, a later and higher HDR peak for the 3.0s-Delay condition, and the latest and highest HDR peak for the 4.5s-Delay condition.

Lastly, mixed measure ANOVA revealed a significant interaction between cognitive Load x Delay x Time, $F(54,4644) = 4.13, p < .001$, (Figure 28). In the 1-Dot condition, 1.5s-Delay condition showed an HDR decrease, while the 3.0s-Delay condition increased and the 3-Dot condition was dominated by a steeper increase for the 3.0s-Delay condition than the 1.5s-Delay condition from Timebins 5 to 6, $F(1,86) = 4.33, p < .05$. In both the 1-Dot and 3-Dots conditions, this reflects a higher (positive) HDR peak for 3.0s-Delay condition than the 1.5s-Delay condition. In the 1-Dot and 3-Dots conditions, 3.0s-Delay showed an HDR decrease, while 4.5s-Delay showed an HDR increase from Timebins 6 to 7, $F(1,86) = 13.98, p < .001$. In the 5-Dots and 7-Dots conditions, 3.0s-Delay showed an HDR decrease, while the 4.5s-Delay increased from Timebins 6 to 7, $F(1,86) = 4.44, p < .05$. Therefore, in all the Cognitive Load conditions (1-Dot, 3-Dots, 5-Dots, and 7-Dots), there is a higher HDR (positive) peak for the 4.5s-Delay condition relative to the 3.0s-Delay condition.

As shown by the results, activation of the Maintaining was dependent on cognitive load and the delay period. Timing-wise, this component peaked second among the other components in the study, so it is more likely to reflect rehearsal processes rather than initial encoding processes. The influence of the Delay conditions supports this interpretation, as the network's activation and rise of the HDRs plot begins at the same post-stimulus time for each delay condition (marking the beginning of the rehearsal phase) but ends at different times proportionate to the length of the delay period. Moreover, these results for visual working memory somewhat replicate the results seen in the studies with the verbal working memory task (SIRP) where the additional delay produced a higher peak.

Figure 25. Component 2 (C2_INT91_NDMN_1.37_0.31) Varimax averaged over Cognitive Load (1-Dot_3-Dots_5-Dots_7-Dots), Delay (1.5s-Delay_3.0s-Delay_4.5s-Delay) and Group (Healthy_Schizophrenia).

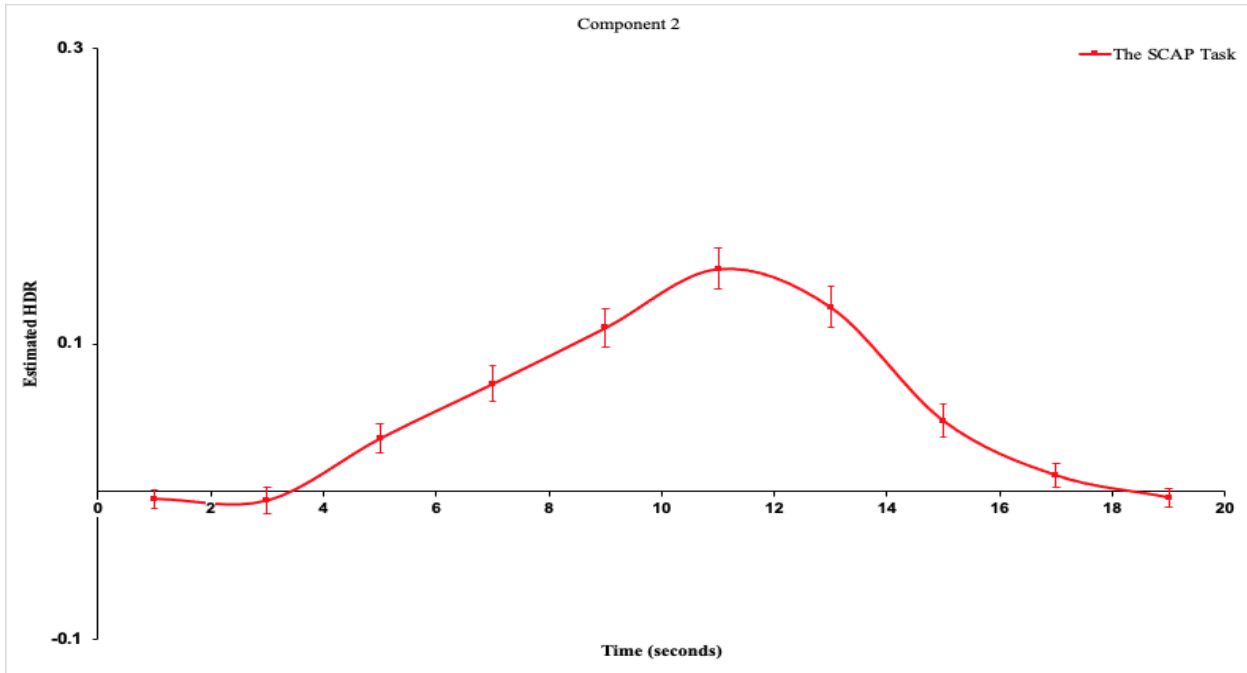


Figure 26. Component 2 (C2_INT91_NDMN_1.37_0.31) Varimax averaged for Cognitive Load (1-Dot_3-Dots_5-Dots_7-Dots) x Time, averaged over Delay (1.5s-Delay_3.0s-Delay_4.5s-Delay) and Group (Healthy_Schizophrenia).

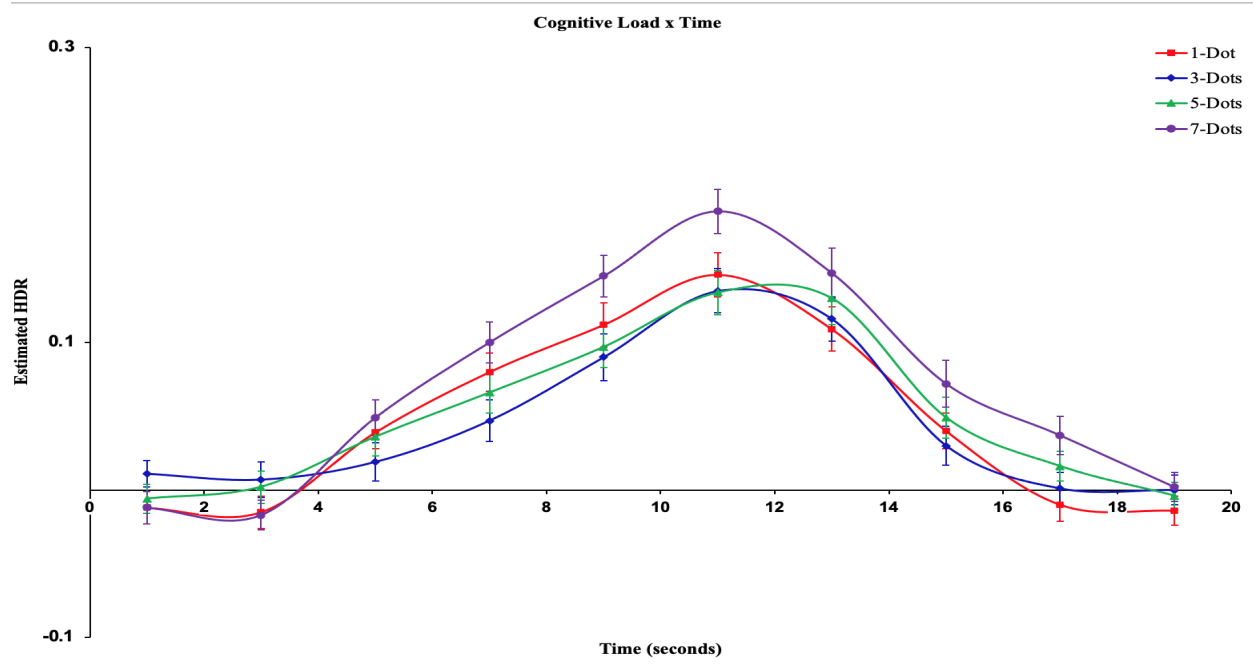


Figure 27. Component 2 (C2_INT91_NDMN_1.37_0.31) Varimax averaged for Delay (1.5s-Delay_3.0s-Delay_4.5s-Delay) x Time averaged over Cognitive Load (1-Dot_3-Dots_5-Dots_7-Dots) and Group (Healthy_Schizophrenia).

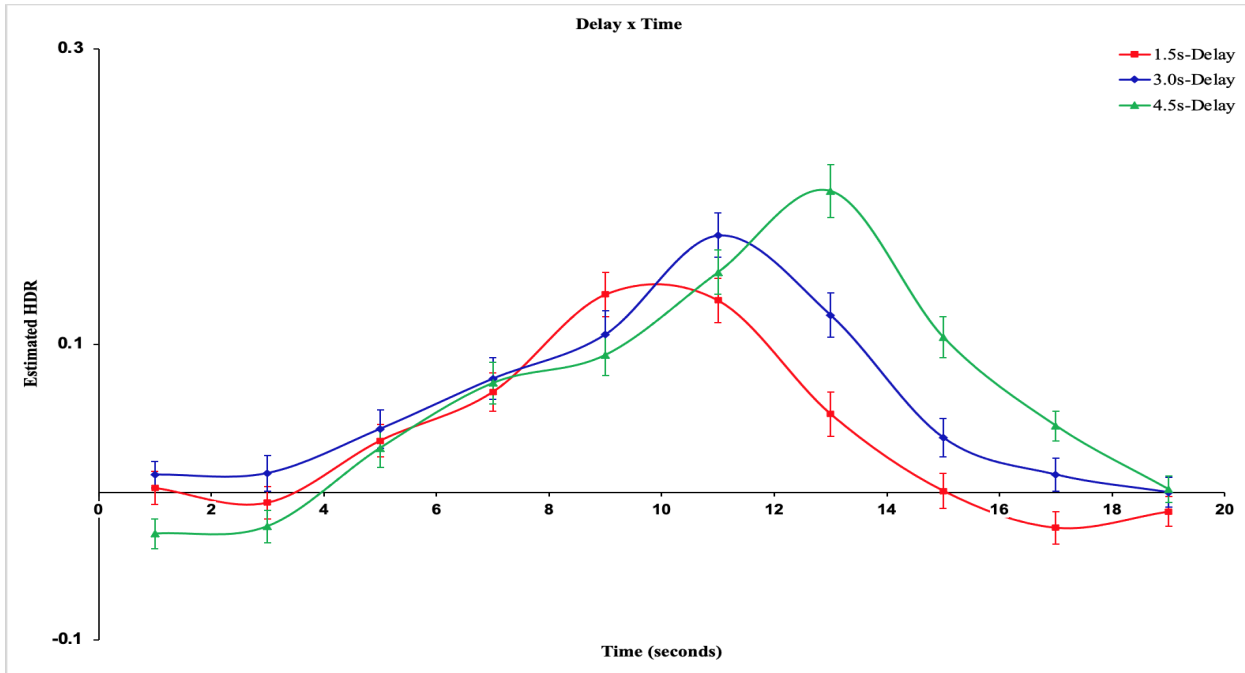
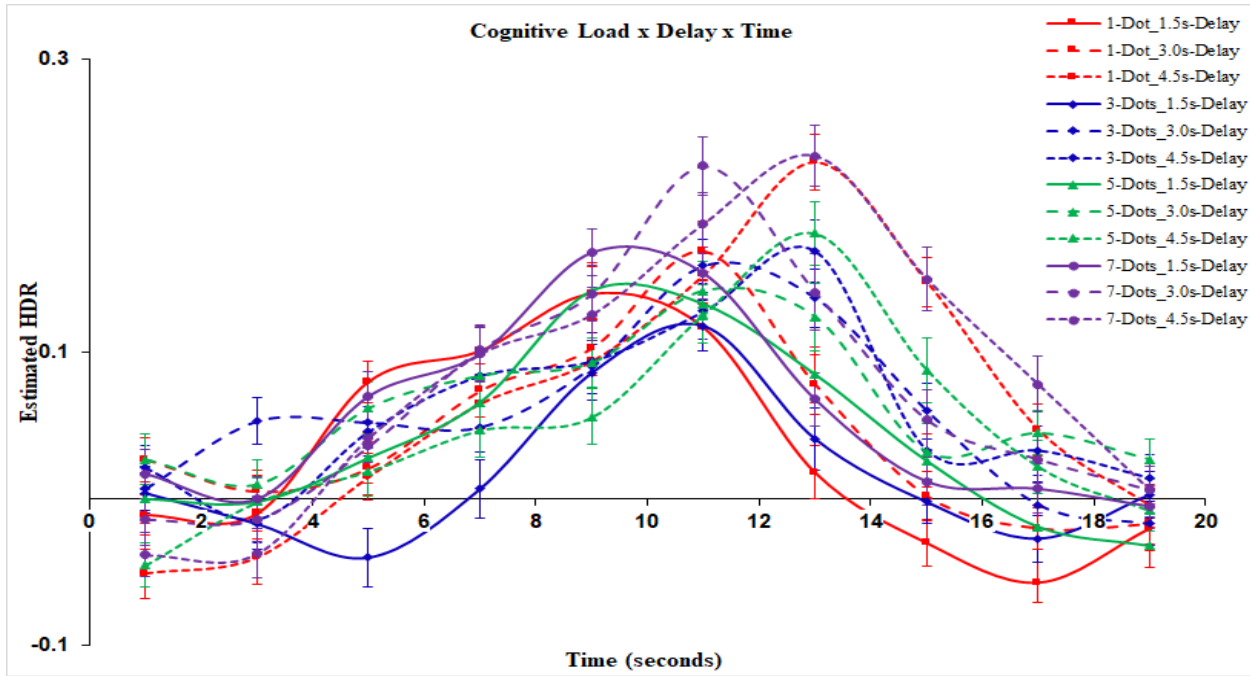


Figure 28. Component 2 (C2_INT91_NDMN_1.37_0.31) Varimax averaged for Cognitive Load (1-Dot_3-Dots_5-Dots_7-Dots) x Delay (1.5s-Delay_3.0s-Delay_4.5s-Delay) x Time, averaged over Group (Healthy_Schizophrenia).



1.5 Task-Switch Inertia Task (TSI)

Component 2 was identified as the Maintaining network with a z-score of 1.37 from increased activity at 91% of voxels. Mixed measure ANOVA revealed a significant main effect of Time, $F(9,468) = 16.94, p < .001$, (Figure 29). The Time factor was dominated by contrasts 1 to 3 for increases to peak, and 6 to 8 for decreases from peak (all were $p < .05$).

Mixed measure ANOVA also revealed a significant main effect of Task-Switch, $F(1,52) = 5.21, p < .05$ and a significant interaction between Task-Switch x Time, $F(9,468) = 13.73, p < .001$, (Figure 30). Cn showed an HDR decrease, while Ci slightly increased from Timebins 3 to 4, $F(1,52) = 7.24, p = .01$. This reflects a higher and slightly earlier (positive) HDR peak for Cn relative to the Ci.

In addition. Mixed measure ANOVA revealed a significant main effect of Stimulus Congruency, $F(1,52) = 24.65, p < .001$, where the average activity of Wi ($M = 0.04$) was significantly higher relative to the average activity of Wn ($M = -0.03$). There was also a significant interaction between Stimulus Congruency x Time, $F(9,468) = 13.73, p < .001$, (Figure 31). This interaction was dominated by a steeper increase for Wi relative to Wn from Timebins 2 to 3, $F(1,52) = 40.96, p < .001$, which reflects a higher (positive) HDR peak for Wi relative to the Wn.

Lastly, mixed measure ANOVA revealed a significant interaction between Task-Switch x Stimulus Congruency x Time, $F(9,468) = 6.42, p < .001$, (Figure 32). This interaction was dominated by a steep increase for the Wi-Cn and Wi-Ci relative to the Wn-Cn and Wn-Ci from Timebins 2 to 3, $F(1,52) = 5.97, p < .05$. This reflects a larger (positive) HDR peak for Wi-Cn and Ci-Wi conditions than the Cn-Wn and Ci-Wn conditions. However, the HDR peak for Cn-Wi was higher and occurred earlier than the peak for Ci-Wi.

As shown by the results, the incongruent trials (Wi) evoked a significantly higher and more sustained activation of the Maintaining network relative to the congruent trials (Wn). This likely reflects the increased cognitive demand in discerning between conflicting verbal information and visual information. Focusing on just the incongruent word-reading trials, switching from an incongruent colour-naming block (Cn) evoked more sustained HDR activation of the Maintaining network than switching from the neutral colour-naming block. Overall, word-reading blocks following neutral colour-naming blocks (Cn) seem to be associated with a faster return to baseline, greater magnitude of deactivation during the return and less sustained activity relative to word-naming blocks following incongruent colour-naming blocks (Ci).

These results together suggest that the Maintaining Network responds differently to demands of inhibition and cognitive flexibility on the PFC – inhibition requires reaching a greater maximal activity (i.e. greater HDR peak), whereas cognitive flexibility minimally increases activity, but evokes the greatest changes in the network's return to baseline instead.

Figure 29. Component 2 (C2_INT91_NDMN_1.37_0.31) Varimax HDR averaged over Stimulus Congruency (W_n _ W_i), Task-Switch (C_n _ C_i), and Group (Healthy_Schizophrenia).

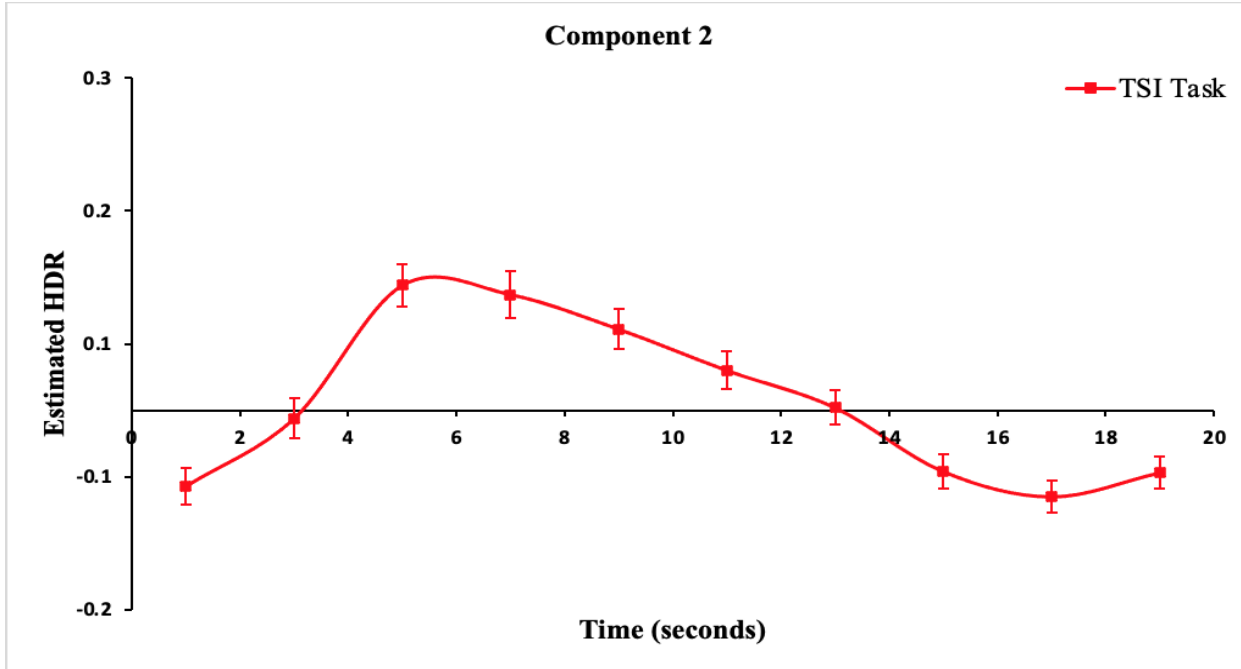


Figure 30. Component 2 (C2_INT91_NDMN_1.37_0.31) Varimax for Task-Switch (C_n _ C_i) x Time, averaged over Stimulus Congruency (W_n _ W_i) and Group (Healthy_Schizophrenia).

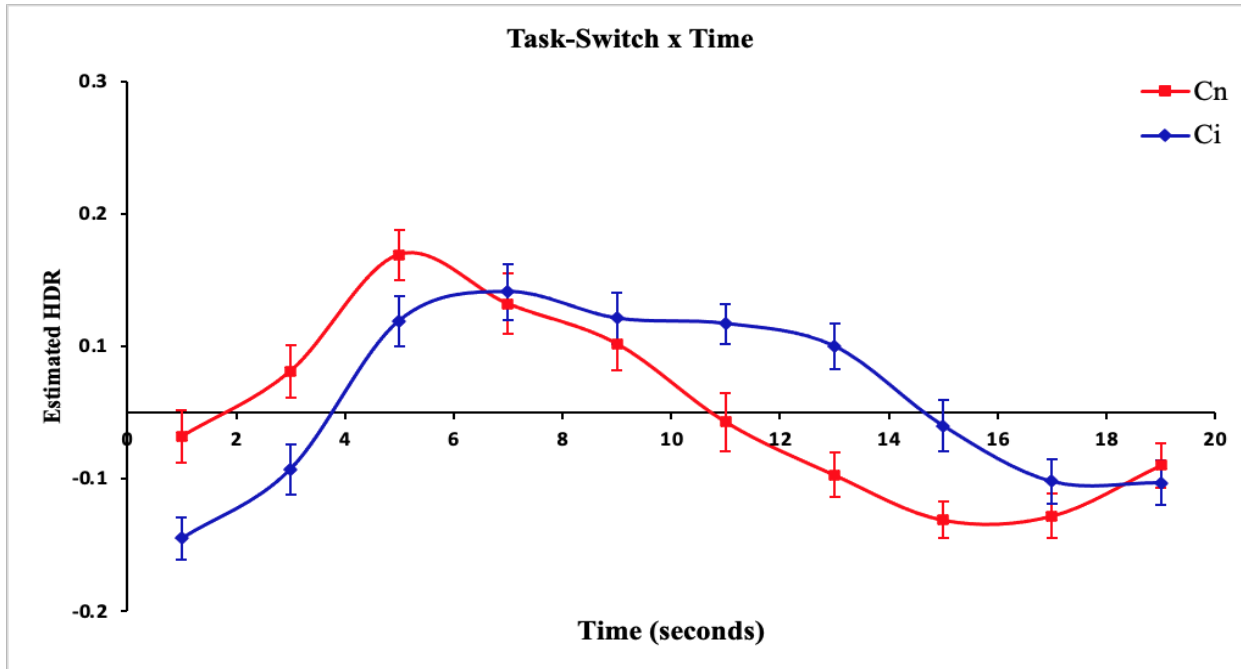


Figure 31. Component 2 (C2_INT91_NDMN_1.37_0.31) Varimax for Stimulus Congruency (W_n _ W_i) x Time, averaged over Task-Switch (C_n _ C_i) and Group (Healthy_Schizophrenia).

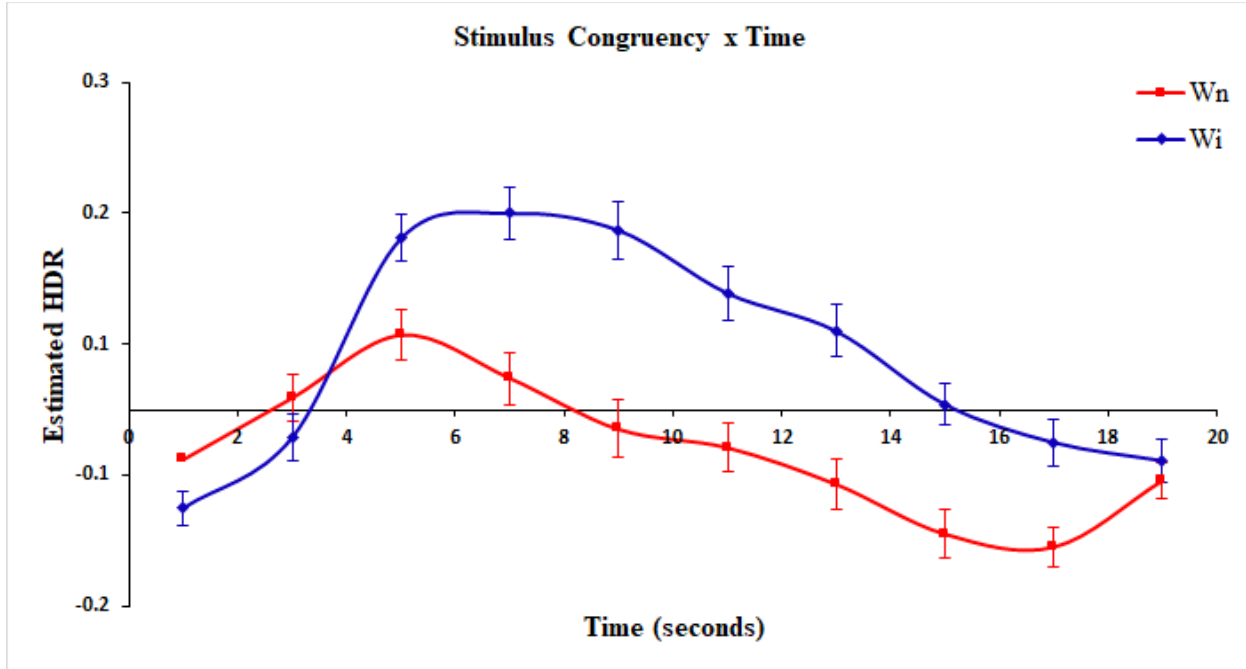
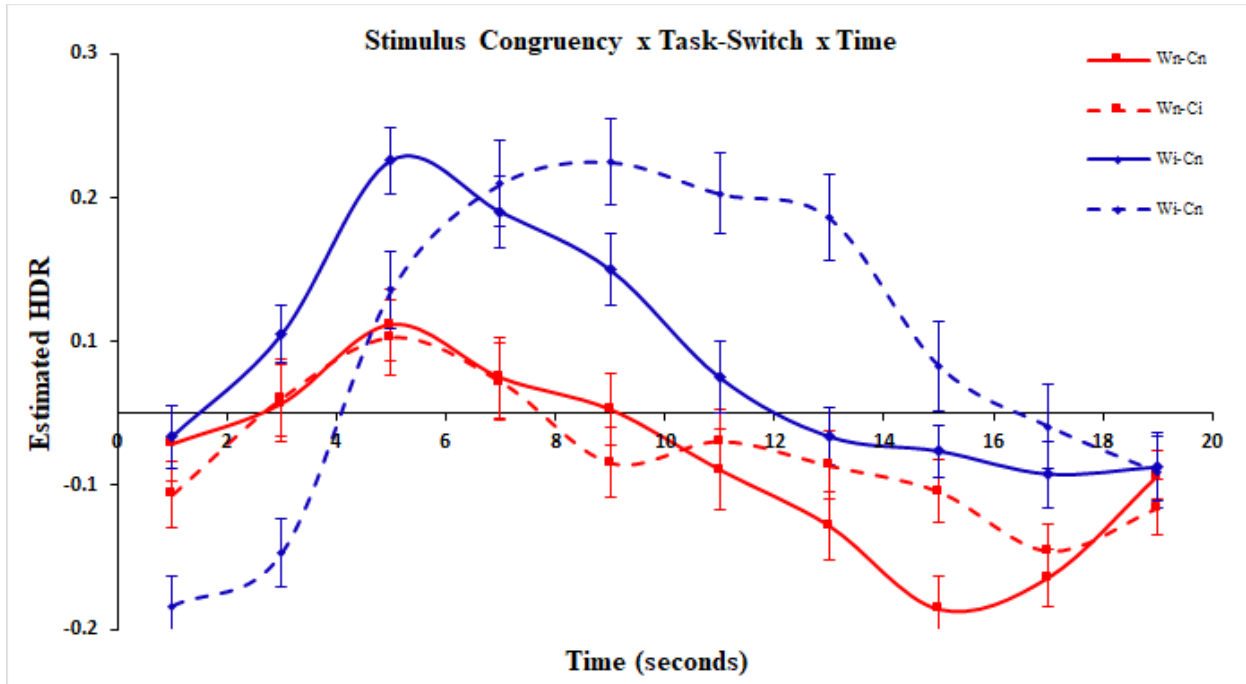


Figure 32. Component 2 (C2_INT91_NDMN_1.37_0.31) Varimax for Stimulus Congruency (W_n _ W_i) x Task-Switch (C_n _ C_i) x Time, averaged over Group (Healthy_Schizophrenia).



1.6 Semantic Integration Task (SIT)

Component 5 was identified as the Maintaining network with a z-sore of 0.91 from increased activity at 78% of voxels. Mixed measure ANOVA revealed a significant effect of Time, $F(19,817) = 32.80, p < 0.001$, (Figure 33). The Time factor was dominated by contrasts 2 to 5 for increases to peak and 6 to 14 for decreases from peak (all were $p < 0.05$).

Mixed measure ANOVA also revealed a significant main effect of Difficulty, $F(1,43) = 13.29, p < .001$, where the Low Association condition ($M = 0.10$) showed a significantly higher activity than the High Association condition ($M = 0.08$). Additionally, it showed a significant interaction between Difficulty x Time, $F(19,817) = 26.85, p < .001$, (Figure 34). High Association condition showed an HDR decrease, while the Low Association condition slightly increased from Timebins 5 and 6, $F(1, 43) = 20.13, p < .001$. This reflects a higher and slightly later (positive) HDR peak for the Low Association condition relative to the High Association condition.

Furthermore, mixed measure ANOVA revealed a significant main effect of Performance, $F(1,43) = 8.08, p < .01$, where the average activity of the No Recall ($M = 0.10$) was significantly higher than the Recall ($M = 0.07$), and a significant interaction between Performance x Time, $F(19,817) = 5.75, p < .001$, (Figure 35). This interaction was dominated by a steeper increase for the No Recall condition relative to the Recall condition from Timebins 4 and 5, $F(1, 43) = 6.27, p < .05$, which reflects a higher (positive) HDR peak for the No Recall condition than the Recall condition.

Lastly, mixed measure ANOVA revealed a significant interaction between Difficulty x Performance x Time, $F(19,817) = 6.81, p < .001$, (Figure 36). In the High Association condition, this interaction was dominated by a sharper decrease for the No Recall condition relative to the

Recall condition and in the Low Association conditions, No Recall showed a small HDR increase, while Recall showed a small HDR decrease from Timebins 5 and 6, $F(1, 43) = 4.90, p < .05$. In the Low Association conditions, this reflects a higher (positive) HDR peak for the No Recall relative to the Recall.

The task condition with the most influence on the network's activity was the degree of association between words, where low degree of association evoked the highest activity. This suggests the Maintaining Network supports cognitive processes underlying processing of linguistic and semantic information, and those that aid in assessing association between words, with its activity ramping up in response to higher cognitive demands in this domain. Interestingly, for the low association condition, word pairs that were not recalled later evoked significantly greater activity than word pairs that were recalled later in the same low association condition. This may suggest that the higher activation in processing linguistic demand and assessing word association might distract or take away from cognitive resources allocated to committing the stimuli words to short-term memory, and results in lower recall.

Figure 33. Component 5 (*C5_INT78_NDMN22_0.91_0.56*) Varimax HDR averaged over Difficulty (*High_Low*), Performance (*Recall_No Recall*), and Group (*Healthy_Schizophrenia*).

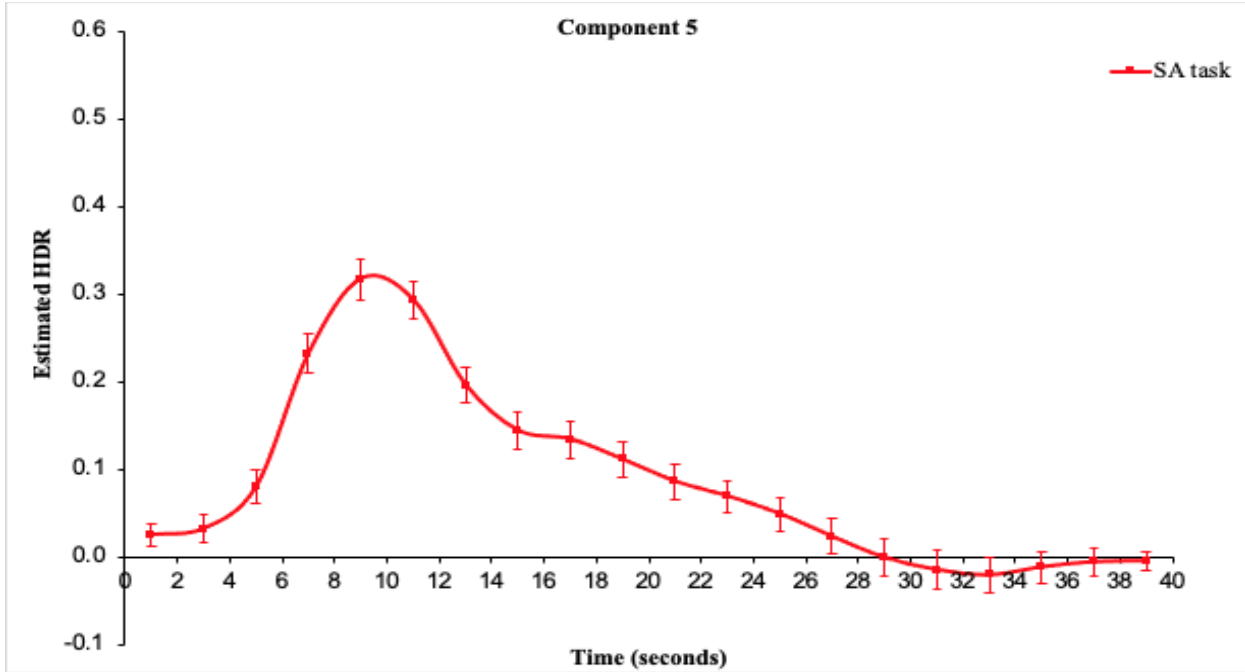


Figure 34. Component 5 (*C5 INT78 NDMN22 0.91 0.56*) Varimax HDR for Difficulty (High Association_Low Association) x Time averaged over Performance (Recall_No Recall) and Group (Healthy_Schizophrenia).

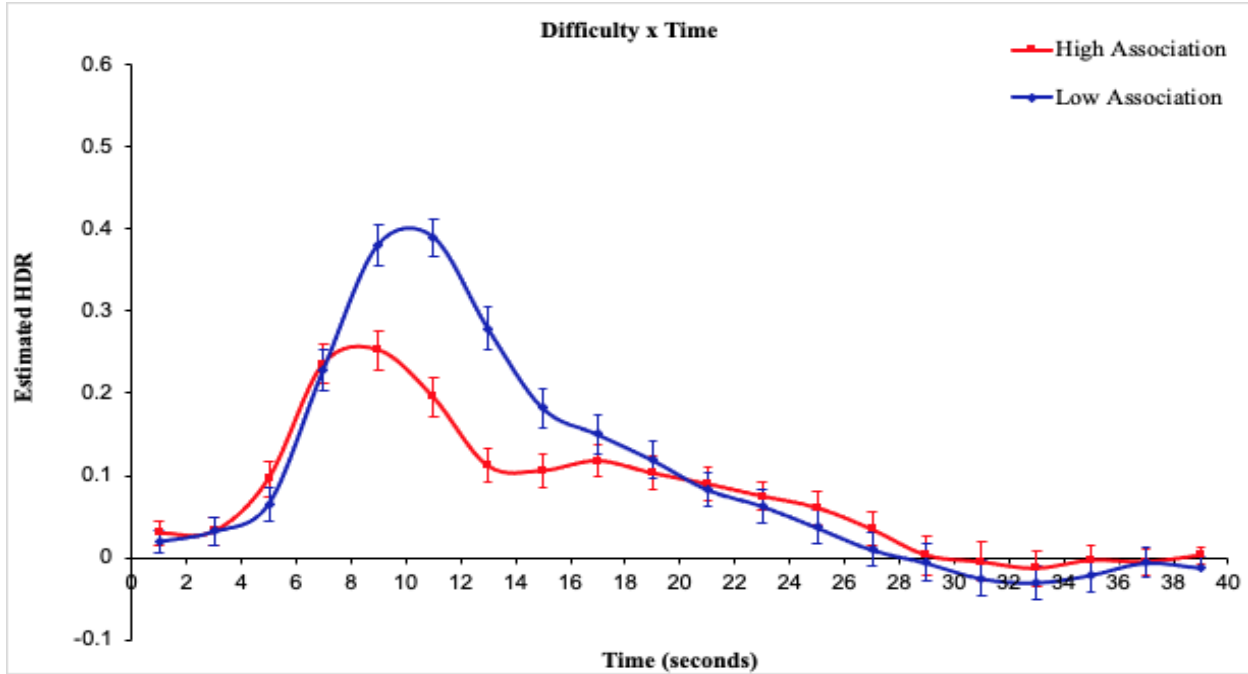


Figure 35. Component 5 (*C5_INT78_NDMN22_0.91_0.56*) Varimax HDR for Performance (Recall_No Recall) x Time, averaged across Difficulty (High Association_Low Association) and Group (Healthy_Schizophrenia).

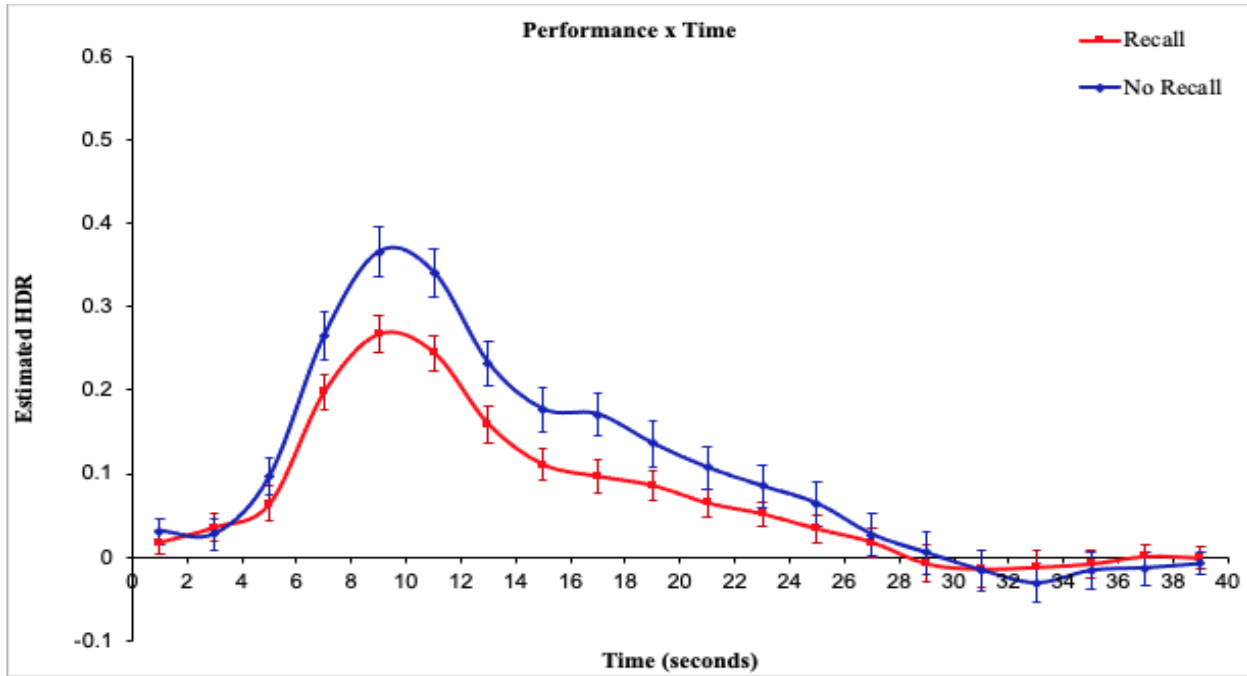
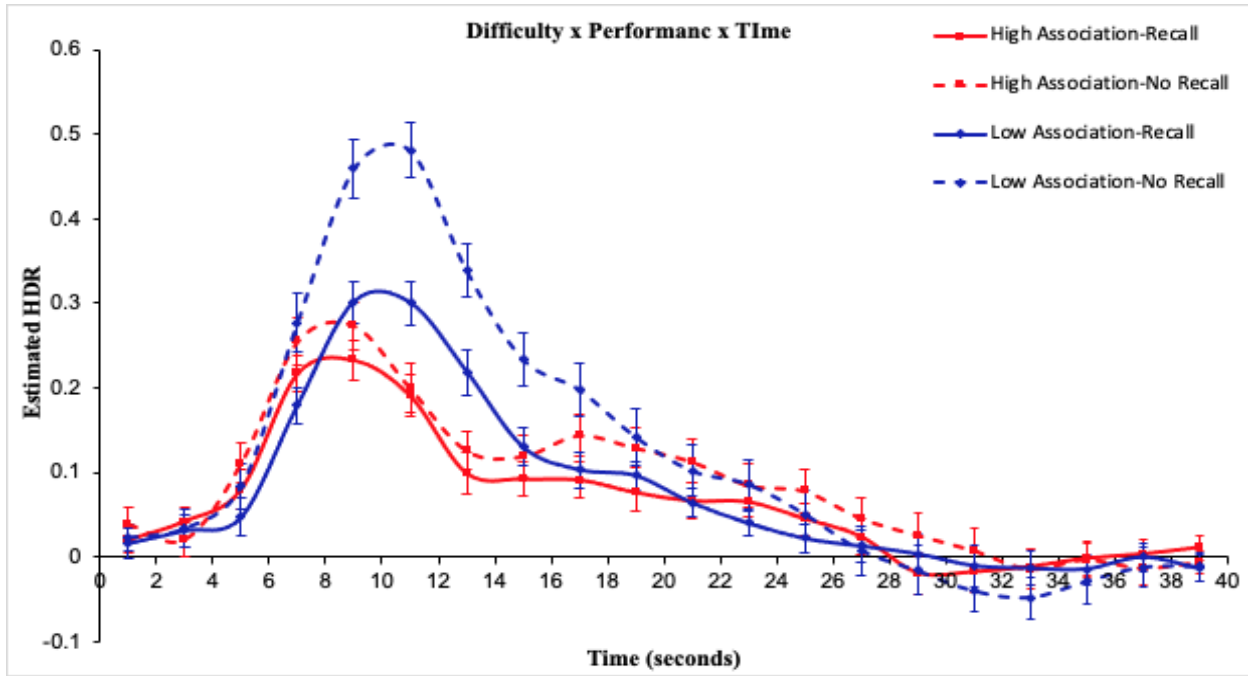


Figure 36. Component 5 (C5_INT78_NDMN22_0.91_0.56) Varimax HDR for Difficulty (High Association_Low Association) x Performance (Recall_No Recall) x Time averaged over Group (Healthy_Schizophrenia).



1.7 Delusions of Reference (DOR)

Component 2 was identified as the Maintaining network with a z-score of 0.82 from increased activity observed at 95% of voxels. Mixed measure ANOVA revealed a significant main effect of Time, $F(9,351) = 9.93, p < .001$, (Figure 37). The Time factor was dominated by contrasts 2 to 3 for increases to peaks and 6 to 7 for decreases from peak (all were $p < .001$).

Mixed measure ANOVA also revealed a significant main effect of Condition, $F(1,39) = 25.96, p < .001$, where the average activity of Endorsed ($M = 0.16$) is significantly higher than the average activity of Non-Endorsed ($M = 0.07$), and a significant main interaction between Condition x Time, $F(2,39) = 6.47, p < .01$, (Figure 38). Endorsed showed an HDR increase, while Non-endorsed decreased from Timebins 3 to 4, $F(1,39) = 27.18, p < .001$ which reflects a higher and later (positive) HDR peak for Endorsed than Non-endorsed. Additionally, Non-endorsed increased from Timebins 5 to 6, $F(1,39) = 21.28, p < .001$, which reflects a second small (positive) HDR peak for Non-endorsed but not for Endorsed.

Lastly, mixed measure ANOVA showed a significant interaction between Condition x Time x Group, $F(18,351) = 2.93, p < .001$, (Figure 39). Endorsed in the Healthy group and both Endorsed and Non-Endorsed in the Delusional group showed an HDR increase, while the Non-endorsed in the Healthy group and both Endorsed and Non-Endorsed decreased in the Non-delusional group from Timebins 3 to 4, $F(2,39) = 4.40, p < .05$. This interaction reflects that overall, the HDR peaks for the Endorsed conditions were higher than the Non-endorsed conditions in all groups. However, the Endorsed condition in the Healthy group showed the highest HDR peak relative to the Non-Endorsed-condition in the Healthy group and both the Endorsed and Non-Endorsed conditions in the Non-Delusional and Delusional groups.

This study showed a trend for greater activation in the Endorsed conditions relative to the Non-Endorsed, particularly in the control and patients with delusions of reference group. This component was the first to peak among the study's two components that showed an increase in activation, suggesting it underlies some of the encoding and probably maintaining of the task's stimuli in mind in order to make a decision about self-relevance. These results suggest the network could be involved in self-referential processing, especially comparing the control group's difference in HDR curves between the Endorsed condition and Non-Endorsed condition. The Endorsed condition clearly evokes a later and significantly higher peak, implicating the Maintaining network in judging statements as written about the self. However, an alternative and also likely explanation given the network's responsiveness to verbal task conditions and WM demand conditions is that the linguistic content and maintaining the goals of the task in mind could be partially responsible for provoking the activity. This interpretation may be supported by the somewhat conceptually challenging task instructions for participants to ensure they are not responding based on judging otherwise general statements to be simply relevant to them, and are instead responding to statements they believe to be written strictly and specifically about them. Given this subtle distinction, participants must make, they could have been spending a longer and more effortful time ensuring statements were actually self-referential and attending to task goals before endorsing them relative to non-endorsed statements.

Figure 37. Component 2 (C2_INT95_TDMN_0.82_0.16_DOR) HRF Procrustes averaged over Condition (Endorsed_Non-endorsed) and Group (Control_Non-delusional_Delusional).

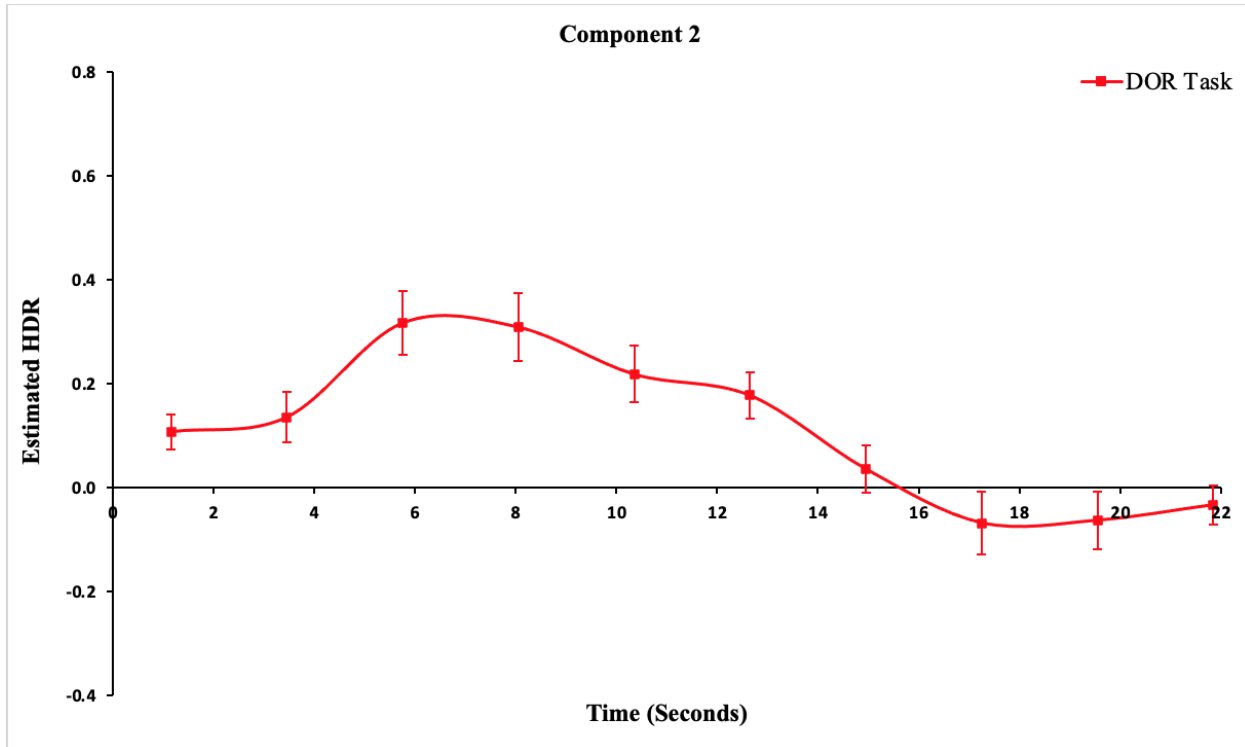


Figure 38. Component 2 (C2 INT95 TDMN 0.82 0.16 DOR) HRF Procrustes for Condition (Endorsed_Non-endorsed) x Time averaged over Group (Control_Non-delusional_Delusional).

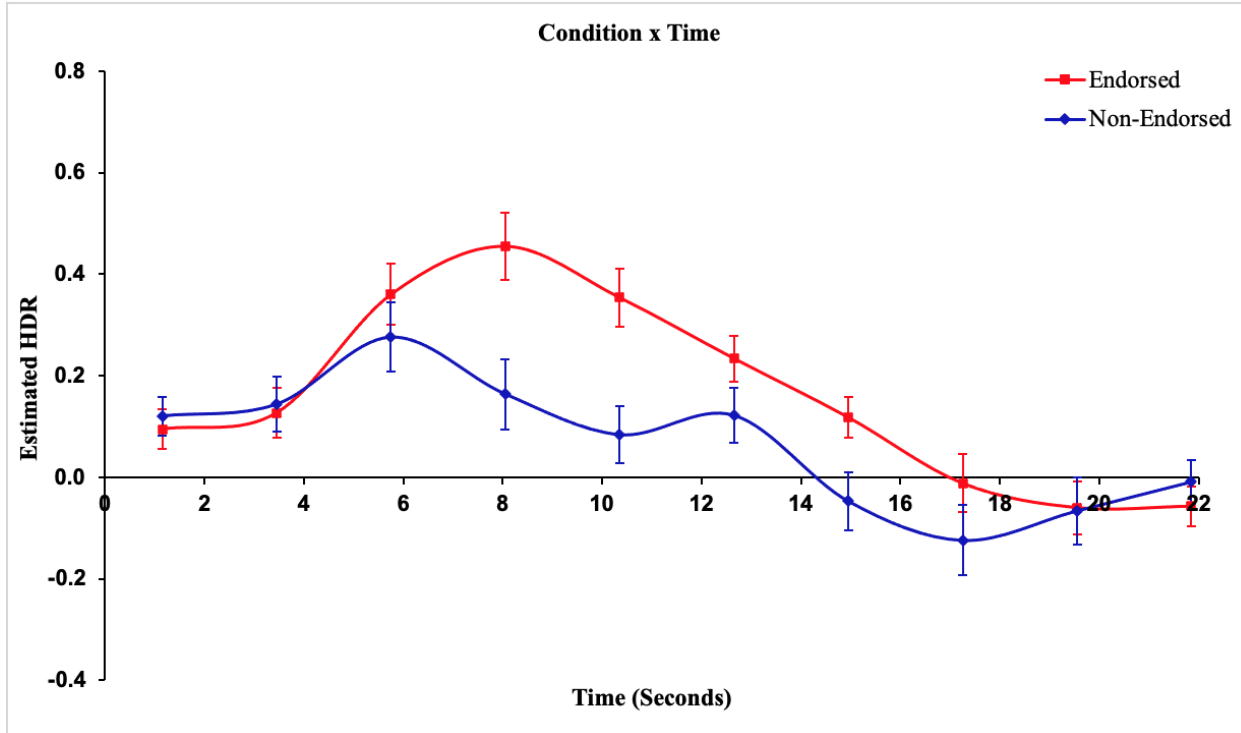
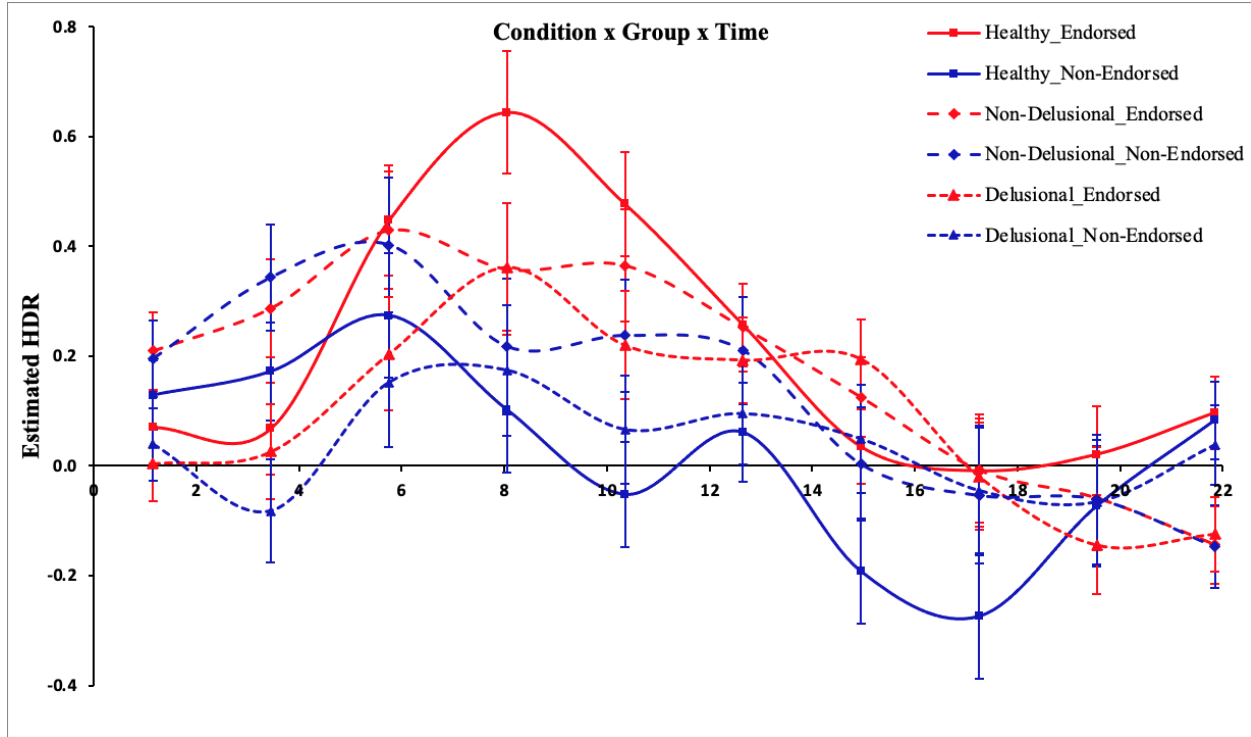


Figure 39. Component 2 ($C2_INT95_NDMN_{0.82_{0.06}}$) HRF Procrustes for Condition (*Endorsed_Non-endorsed*) \times Group (*Healthy_Non-delusional_Delusional*) \times Time.



Discussion

The Maintaining Network is implicated in a wide range of tasks. Its' presence can be observed in working memory, mental imagery, self-referential processing, and linguistic processing to various extents. Given its functional variety and distributed anatomy around the dorsolateral prefrontal cortex and anterior prefrontal regions, this network very likely underlies some functions associated with the prefrontal cortex, and more specifically, volitional attention to internal mental representations (Sanford & Woodward, 2020).

In the Sanford & Woodward (2020) study, the Maintaining network was interpreted to serve a broader integratory role for multiple frontal lobe functions as opposed to specifically underlying a particular executive function. This interpretation was supported in this study by showcasing the network did not predict working memory performance. A complementary network termed the “Energizing network” whose activity paralleled the Maintaining Network was predictive of working memory performance. The present report endorses this interpretation by appealing to the variability in the different tasks that evoked the Maintaining Network and highlighting that the studies that presented the highest match to the exemplar images for the network involved manipulations for working memory. All working memory tasks showed a graded response in the network dependent on cognitive load and delay conditions, reliably implicating the network in rehearsal processes. These tasks would presumably become more effortful with increasing cognitive load, more taxing on working memory, and thus require more brain activity. The strong activation of the Maintaining network evoked by the Addis task supplements the findings from working memory manipulations involving rehearsal and cognitive load as it suggests that the network is rightly named for its role of attention and volitional maintenance of mental content.

Furthermore, the role of the Maintaining network in tasks like TGT as well as its role in linguistic processing and the SIT cannot be overlooked. These results imply the network's role is not limited to one cognitive domain. Notably, the strong activation of the Maintaining network evoked by the DOR task may also implicate the network in self-referential processes and autobiographical cognition but could also be the result of the task's heavy reliance on verbal stimuli since other tasks have shown verbal content generally evokes Maintaining Network activity. In contrast, considering the SCAP task's results, the network seems less involved in visual rehearsal relative to a similar rehearsal of other content such as linguistic in the SIRP task, and the interpretation would benefit from more tasks manipulating strictly visual stimuli to deduce its role in response to visual stimuli.

Additional interpretive directions that may help characterize the functions of this network would include comparing studies using the same tasks that did not produce components from BOLD activity best characterized as the Maintaining Network and comparing the difference in task conditions. In addition, it would be useful to also look at correlating the Maintaining Network's activity with other networks' activity in the same tasks to discern where networks may be interacting to produce the same function or transition between functions. Lastly, it would also be helpful to look in more detail to the associated functions of the distinct brain regions included in the network's anatomical mapping.

Overall, the role of the Maintaining network is most likely in underlying the integration of various frontal functions, volitional attention to internal mental representations and conscious inner speech/language processing while being non-specific in cognitive domain.

References

- Addis, D. R., Pan, L., Vu, M.-A., Laiser, N., & Schacter, D. L. (2009). Constructive episodic simulation of the future and the past: Distinct subsystems of a core brain network mediate imagining and remembering. *Neuropsychologia*, 47(11), 2222–2238.
<https://doi.org/10.1016/j.neuropsychologia.2008.10.026>
- Eickhoff, S. & Woodward, T. S. (2021). *Semantic Association: Report (Varimax)* [Unpublished manuscript]. Department of Psychiatry, University of British Columbia.
- Klepel, F. & Woodward, T. S. (2021). *REPORT ADDIS DATA*. [Manuscript in preparation].
University of British Columbia.
- Larivière, S., Lavigne, K. M., Woodward, T. S., Gerretsen, P., Graff-Guerrero, A., & Menon, M. (2017). Altered functional connectivity in brain networks underlying self-referential processing in delusions of reference in schizophrenia. *Psychiatry research. Neuroimaging*, 263, 32–43. <https://doi.org/10.1016/j.psychresns.2017.03.005>
- Metzak, P. D., Riley, J. D., Wang, L., Whitman, J. C., Ngan, E. T., & Woodward, T. S. (2012). Decreased efficiency of task-positive and task-negative networks during working memory in schizophrenia. *Schizophrenia bulletin*, 38(4), 803–813. <https://doi.org/10.1093/schbul/sbq154>
- Percival, C., Zahid, H., & Woodward, T. S. (2020). *CNoS-Lab/Woodward_Atlas: Woodward Atlas November 2020 Release*. Zenodo. <https://doi.org/10.5281/zenodo.4274398>
- Sanford, N., Whitman, J. C., & Woodward, T. S. (2020). Task-merging for finer separation of functional brain networks in working memory. *Cortex*, 125, 246–271.
<https://doi.org/10.1016/j.cortex.2019.12.014>
- Sanford, N., & Woodward, T. S. (2020). *Functional Delineation of Prefrontal Networks Underlying Working Memory in Schizophrenia: A Cross-Dataset Examination*. [Doctoral dissertation submitted for publication]. Department of Psychiatry, University of British Columbia.

Abstract

Schizophrenia is a whole-brain disorder that is characterized by hallucinations, delusions, and impaired cognition. Network abnormality has been frequently associated with this psychiatric disorder. The current paper examined two functional task-negative networks, the Traditional Default Mode Network (TDMN) and the Novel Default Mode Network (NDMN). The methods and estimated hemodynamic responses (HDRs) of numerous studies that involved TDMN and NDMN were analyzed to better understand the cognitive processes that underlie these networks. It was found that as cognitive load increased, deactivations in the two default mode networks were also increased. Group differences between schizophrenia patients and healthy controls were also observed, where patients showed more NDMN deactivation. The task-positive networks that were commonly associated with NDMN include the maintenance/internal attention (INT) network, whereas TDMN was commonly found with the initiation (INIT) and 1-handed response (1RESP) networks. Both task-negative networks were often identified with the language (LANG) and the external attention (EXT) networks. Future areas should determine the connection between task-positive and task-negative networks to better understand the cognitive processes underlying different attention tasks, and how cognitive networks imbalances could contribute to the symptoms observed in schizophrenia.

Functional Connectivity of the Traditional and Novel Default Mode Networks

Using functional magnetic resonance imaging (fMRI), Raichle et al. (2001) described the default mode network (DMN) as a network that uses increased metabolic activity during rest and decreased activity during goal-directed tasks. Anatomically, the DMN consists of discrete cortical areas such as the ventral medial prefrontal cortex, precuneus cortex, angular gyrus, and the superior frontal gyrus (Buckner, Andrews-Hanna, & Schacter, 2008). Supporting Raichel et al.'s findings (2001), Fox et al. (2005) also found that the DMN routinely exhibits decreases in activity, which he termed as task-negative networks, while other frontal and parietal cortical regions showed increases in activity, which he termed as task-positive networks. The dichotomous relationship between task-positive and task-negative networks was first described by Fox et al. (2005): as the activity in positive regions is increased, activity in negative regions is simultaneously decreased. Moreover, when the attention to demand of the cognitive tasks increased, the dichotomy between task-positive and task-negative networks also became more pronounced (Fox et al., 2005).

In the Cognitive Neuroscience of Schizophrenia (CNoS) lab, 10 task-positive and 2 task-negative networks were discovered using fMRI constrained principal component analysis (fMRI-CPCA). In this paper, the focus is on the 2 task-negative networks: the Traditional Default Mode network and the Novel Default Mode Network. From our understanding, researchers in the field have been describing the DMN as a single, discrete network; the finding that there are two possible DMN is both novel and exciting. While TDMN activity is observed in the superior frontal gyrus and lateral occipital cortex, NDMN activity is observed in the precuneus cortex, cuneal cortex, and lingual gyrus (Buckner et al., 2008; Raichel et al., 2001). Although anatomical differences were observed between the networks, the functional differences between the two is

not clear. Thus, the primary goal of the present paper is to obtain a better understanding of the functional aspects of the two DMNs by analyzing studies of cognitive tasks where DMNs activities were exhibited.

Because schizophrenia is a whole-brain disorder, many researchers have compared the DMN functionality in healthy controls to schizophrenia patients. For example, Fox et al. (2017) found that fronto-parietal DMN connectivity may have implications on the social functioning deficits often seen in schizophrenia patients. As our understanding of the DMNs enhances on a neural level, it could have implications on treatment methods and interventions for these patients. Thus, the secondary goal of the present paper is to compare the activity of the 2 DMNs between healthy controls and schizophrenia patients.

Based on previous research that attentional demand and DMN activation are reciprocally correlated (Fox et al., 2005), it is hypothesized that as cognitive demand increases, TDMN and NDMN *deactivation* would increase. As numerous studies have also shown that schizophrenia patients show reduced/failure of task-related deactivations in the DMN (Jeong & Kubicki, 2010; Whitfled-Gabrieli et al., 2009; Salgado-Pineda et al., 2011), it is hypothesized that after controlling for performance, schizophrenia would show reduced deactivation in cognitive tasks, relative to healthy controls.

Methods

The DMNs were identified with fMRI-CPCA and network classifications. In order to understand the cognitive processes underlying these networks, I interpreted the study's methods and their respective estimated hemodynamic responses (HDRs). As HDR reflects changes in blood oxygen level dependent (BOLD), which ultimately reflects changes in neural activity,

analyzing the timing and duration of peaks allows for interpretation of different cognitive processes (Sanford, 2019).

fMRI-CPCA and Classification

Using BOLD activity from fMRI-CPCA, we can identify functional brain networks involved in specific tasks (Sanford, 2019). CPCA combines multivariate multiple regression and principal component analysis to identify spatial configurations of brain networks, estimates HDRs, and analyzes the difference in HDR shapes between controls and experimental groups (Sanford, 2019). Averaging component loadings from previous fMRI-CPCA studies, 12 exemplar networks were identified, of which two were task-negative networks.

Using a MATLAB-based algorithm, an automated classification program was developed. The program assigns 12 z scores to brain images input, which indicates how closely the inputted images match with the exemplar networks (Percival, Zahid, & Woodward, 2020). The higher the z scores, the greater the match between the image and the exemplar networks. In the present paper, a Fisher transformed z score of $z \geq 0.80$ was considered a good match, which approximately equates to $r = 0.85$. These studies were then further analyzed.

Results

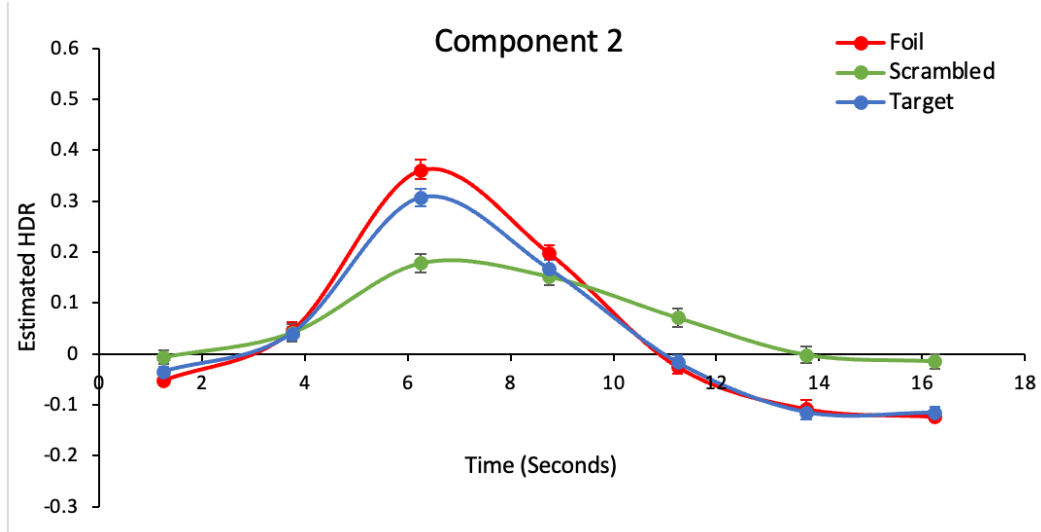
1. FDT HDR

TDMN deactivation was observed. Repeated measures ANOVA revealed significant main effects of Time, $F(6,402) = 127.63, p < .001$, Emotion $F(4,268) = 3.34, p < .05$, and Image type $F(2,134) = 3.95, p < .05$. Significant interactions were observed for Image Type \times Timebins, $F(12,804) = 38.042, p < .001$, where Foil showed greater HDR deactivation than Scrambled, dominated by changes over timebins 1-4 ($p < .001$;

Figure 1). The Target condition also showed greater HDR deactivation between timebins 2-4 than Scrambled, dominated by a flatter peak for Scrambled ($p < .001$; figure 1). A significant three-way interaction was also observed for Emotion \times Image Type \times Timebins $F(48,3216) = 3.53, p < .001$. Age Target and Anger Target increased and decreased more sharply than Age Scrambled and Anger Scrambled during timebins 1-5 ($p < 0.05$; Figures 2-3). Anger Target and Fear Target also decreased much more sharply than Anger Scramble and Fear Scramble between timebins 4 and 5 $F(1, 67) = 6.57, p < .05$. In general, greater TDMN deactivation was observed when the age/anger/fear image types were Target, relative to Scrambled.

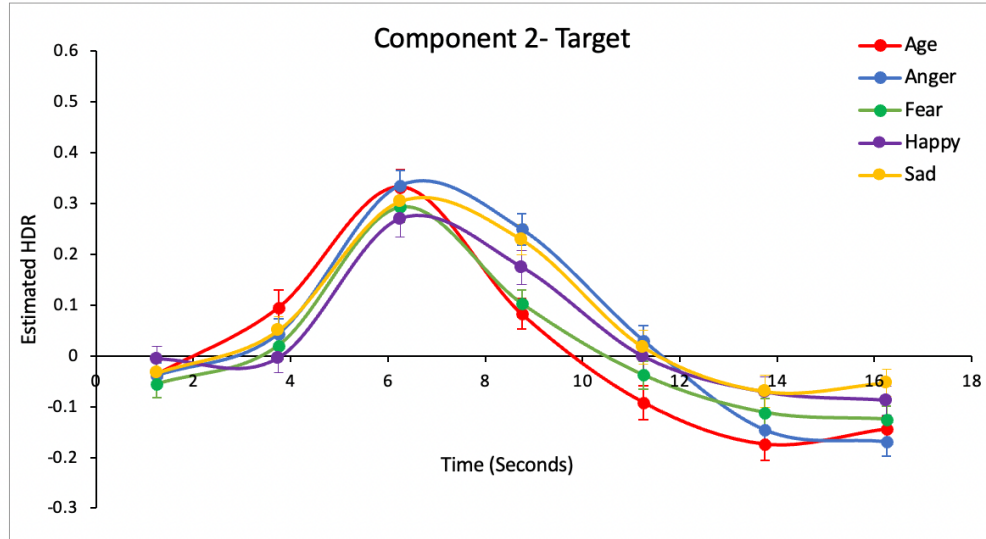
The main effect of Group was not significant, although a significant interaction of Group \times Timebins was observed, where relatives and patients showed sharper increases and higher peaks compared to controls between timebins 1 and 2, $F(2, 67) = 3.63, p < .05$. Relatives and patients also showed sharper decreases between timebins 3-5 ($p < .01$; Figure 4). Overall, controls showed decreased deactivation of TDMN, relative to the other two groups.

Figure 1



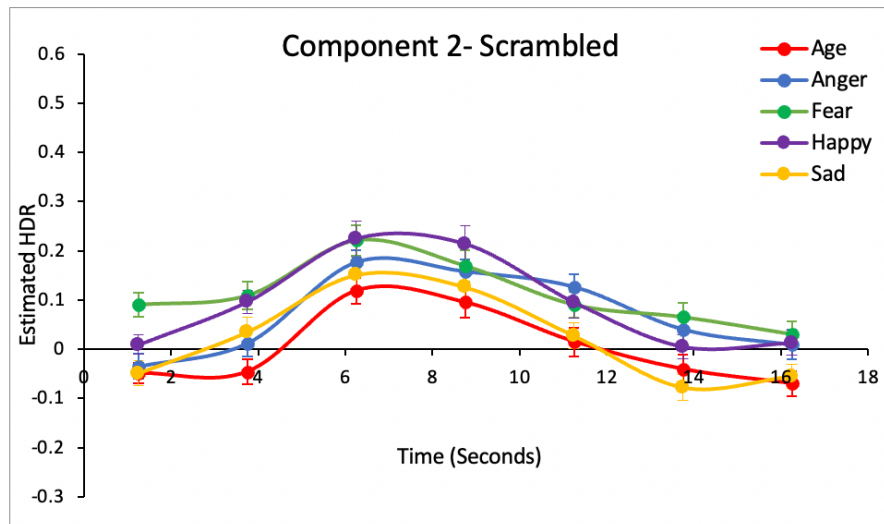
Note. HDR for Facial discrimination Image Type (Foil_Scrambled_Target) averaged over Condition (Age_Anger_Fear_Happy_Sad) and Group (Healthy_Relative_Schizophrenia).

Figure 2



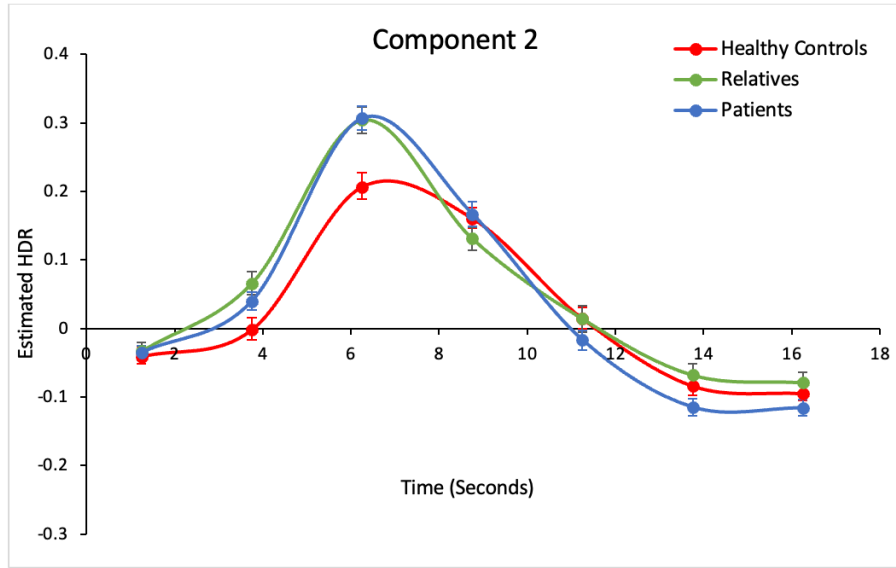
Note. HDR for Facial discrimination condition (Age_Anger_Fear_Happy_Sad), averaged over Group (Healthy_Relative_Schizophrenia), for Image Type.

Figure 3



Note. HDR for Facial discrimination condition (Age_Anger_Fear_Happy_Sad), averaged over Group (Healthy_Relative_Schizophrenia), for Scrambled Image Type.

Figure 4



Note. HDR for Group (Healthy_Relative_Schizophrenia), averaged over Facial discrimination condition (Age_Anger_Fear_Happy_Sad) and Image Type (Foil_Scrambled_Target).

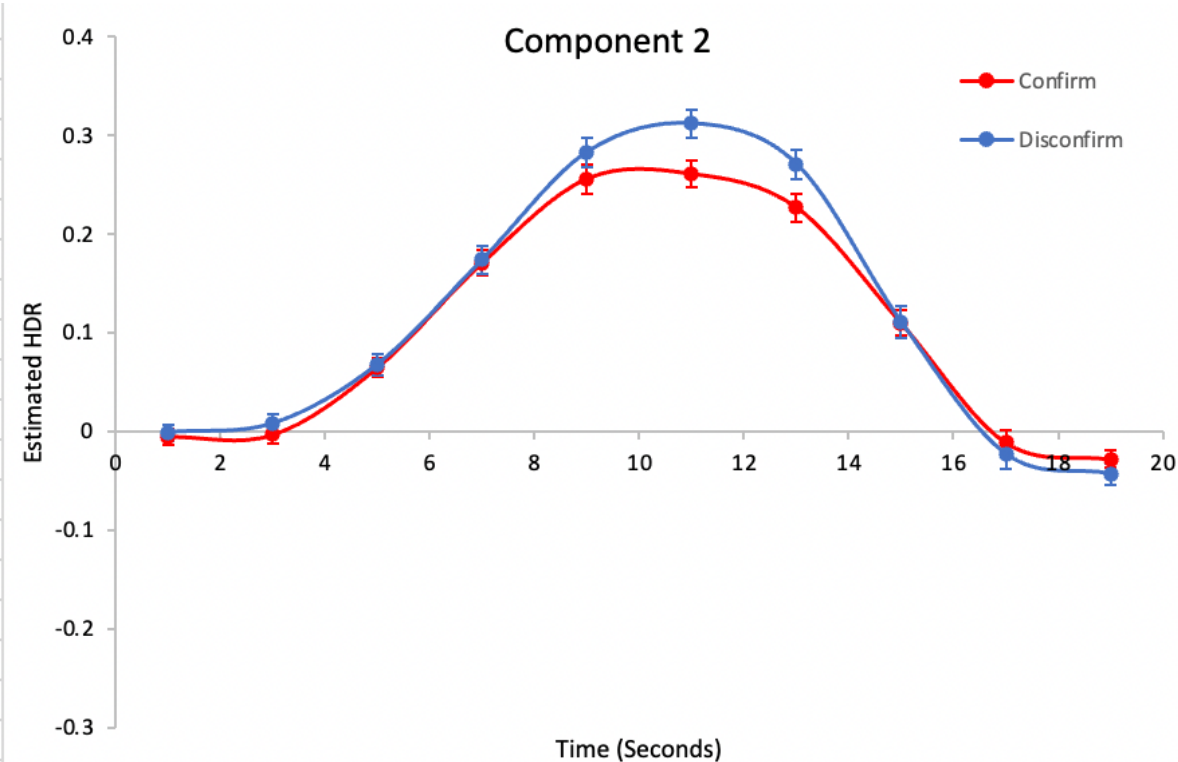
2. BADE

2.2.1 OTTBADE HDR

Repeated ANOVA measures revealed a significant main effect of Timebins, $F(9,981) = 180.86, p < .001$. A significant interaction emerged between Confirm_Disconfirm \times Timebins, $F(9,981) = 5.89, p < .001$. Between timebins 4 to 5, the Disconfirm condition showed a greater increase in TDMN deactivation compared to the Confirm condition, $F(1,109) = 7.76, p < .01$ (Figure 5). Between timebins 5 to 6, the Disconfirm condition increased in deactivation while the Confirm condition stayed relatively constant, $F(1,109) = 6.12, p < .05$. Between timebins 7 to 8,

the Disconfirm condition showed greater decrease in deactivation $F(1,109) = 22.92, p < .001$. Overall, disconfirm condition showed greater increase and decrease in TDMN deactivation.

Figure 5



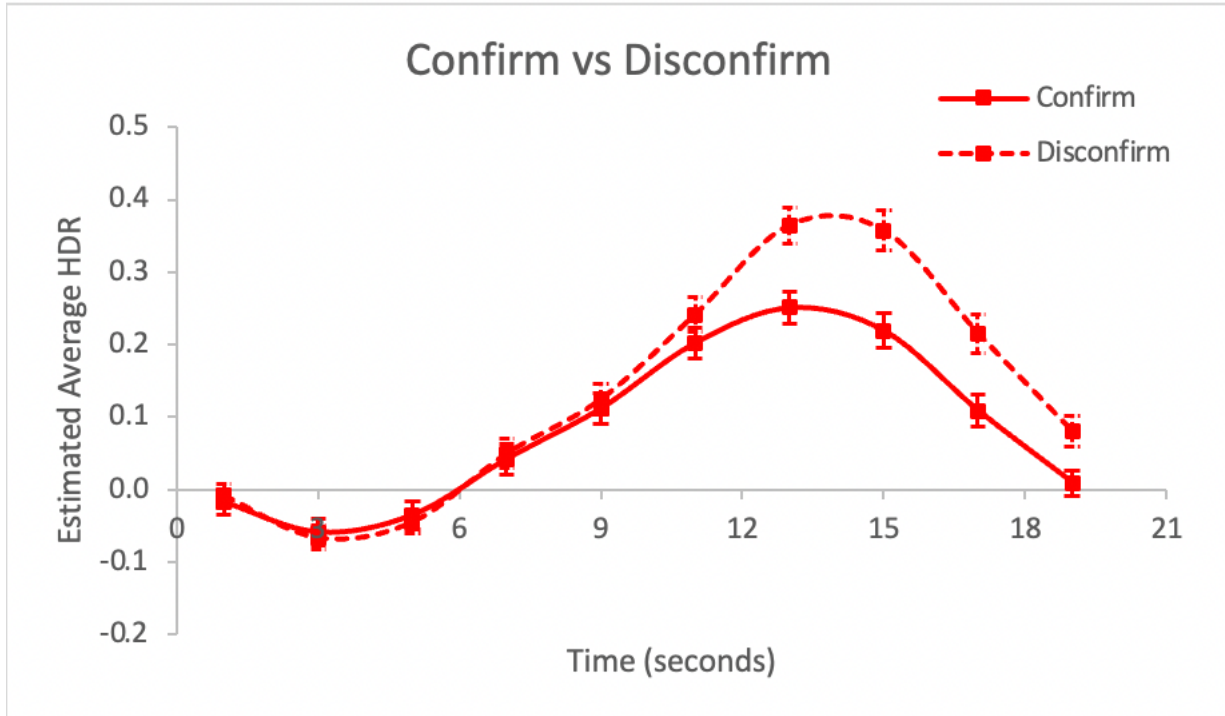
Note. Hrfmax HDR for Condition (Confirm_Disconfirm), averaged over Group.

In the SPQ-BADE study consisting of only healthy controls, similar results were observed (Lavigne, Menon, & Woodward, 2020). Repeated ANOVA measures revealed a significant main effect of Confirm_Disconfirm, $F(1,40)=28.13, p < .001$ and Yes First_No First, $F(1,40) = 15.10, p < .001$. A significant interaction emerged between Confirm_Disconfirm \times Timebins, $F(9,360)=15.82, p <.001$. Between timebins 6-7, the Disconfirm condition showed greater TDMN deactivation than the Confirm condition, $F(1,40)=32, p < .001$ (Figure 6). Overall, the Disconfirm condition showed greater activity. A significant three-way interaction also emerged between Confirm_Disconfirm \times Yes First_No First \times Timebins, $F(9,360)=15.82$,

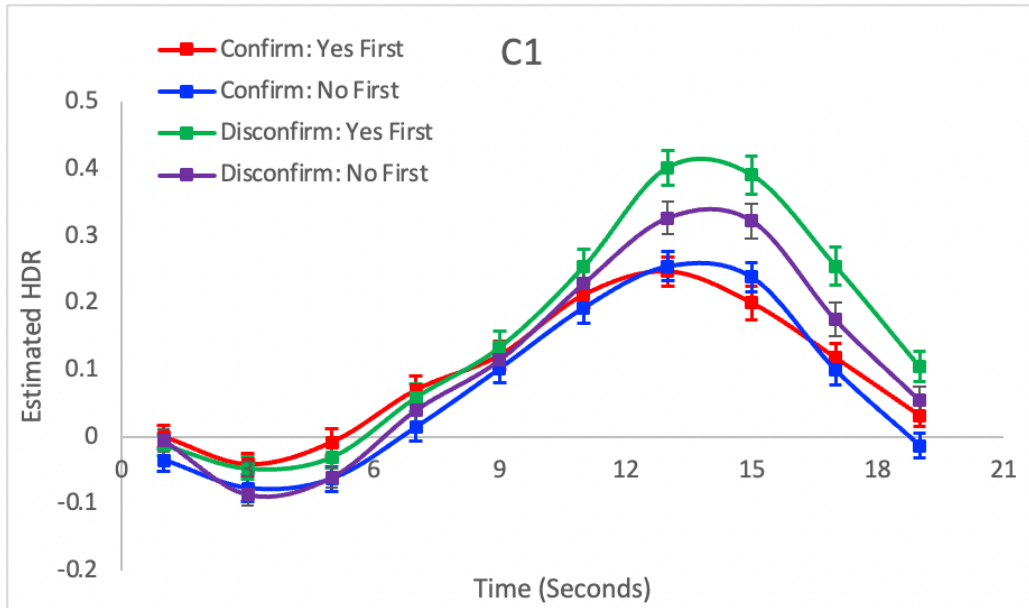
$p < .001$. Between timebins 6-7, the Disconfirm_Yes First condition showed a greater decrease in TDMN deactivation compared to the other conditions, $F(1,40) = 5.45, p < .05$ (

Figure 7).

Figure 6



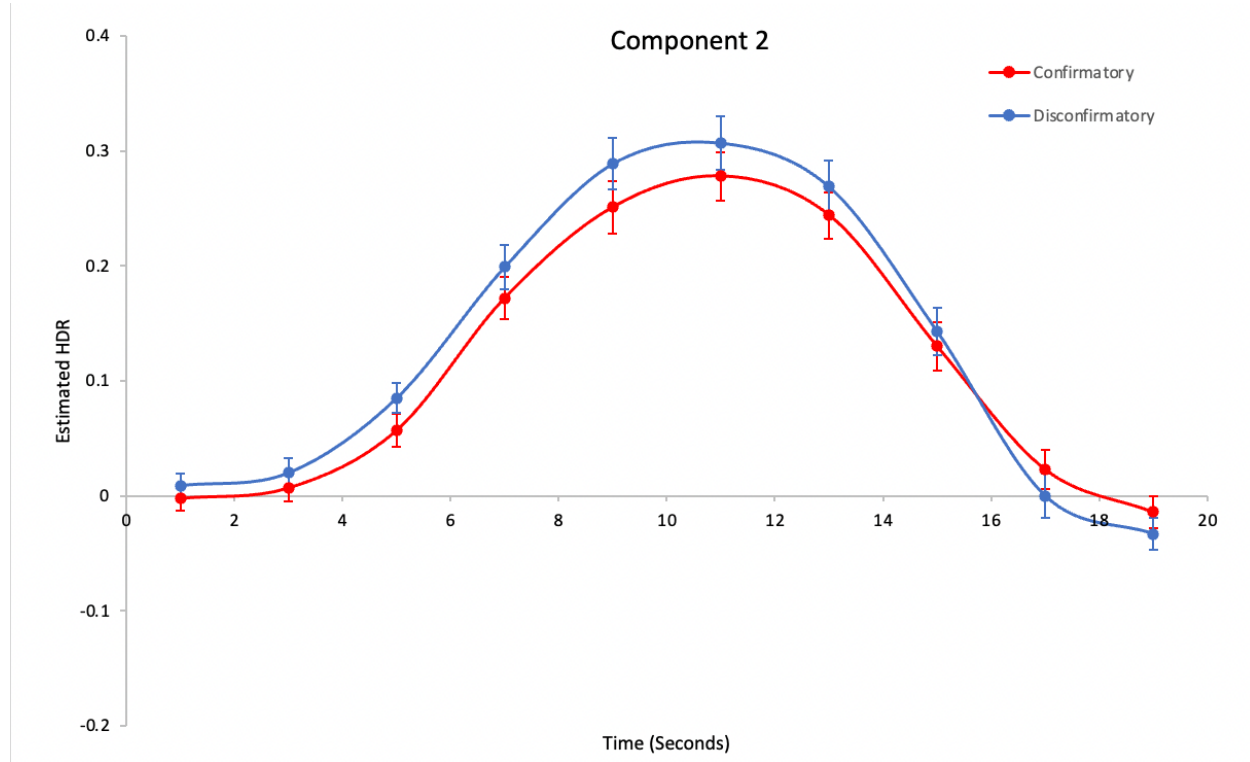
Note. HRFmax for Confirm_Disconfirm, averaged over YesFirst_NoFirst.

Figure 7

Note. HRFmax for YesFirst_NoFirst, averaged over Confirm_Disconfirm.

2.2.2 Changes in BADE Task HDR

TDMN was observed in this study. Repeated ANOVA measures revealed a significant main effect of Timebins, $F(9,513) = 101.70, p < .001$. A significant interaction between Confirm_Disconfirm \times Timebins emerged, $F(9,513) = 2.87, p < .01$. Between timebins 8-9, the Disconfirm condition showed a steeper decrease in TDMN deactivation than the Confirmatory condition, $F(1,57) = 9.04, p < .01$ (Figure 8). This is also seen in the OTTBADe study.

Figure 8

Note. HRFmax for Confirm_Disconfirm, averaged over YesFirst_NoFirst.

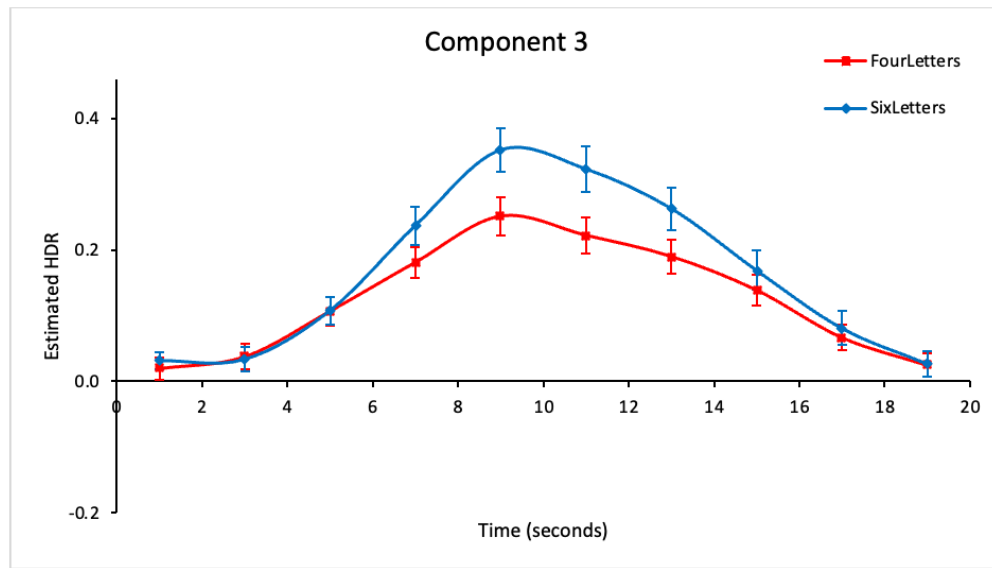
2.3 Working Memory

2.3.1 Sanford's WM HDR

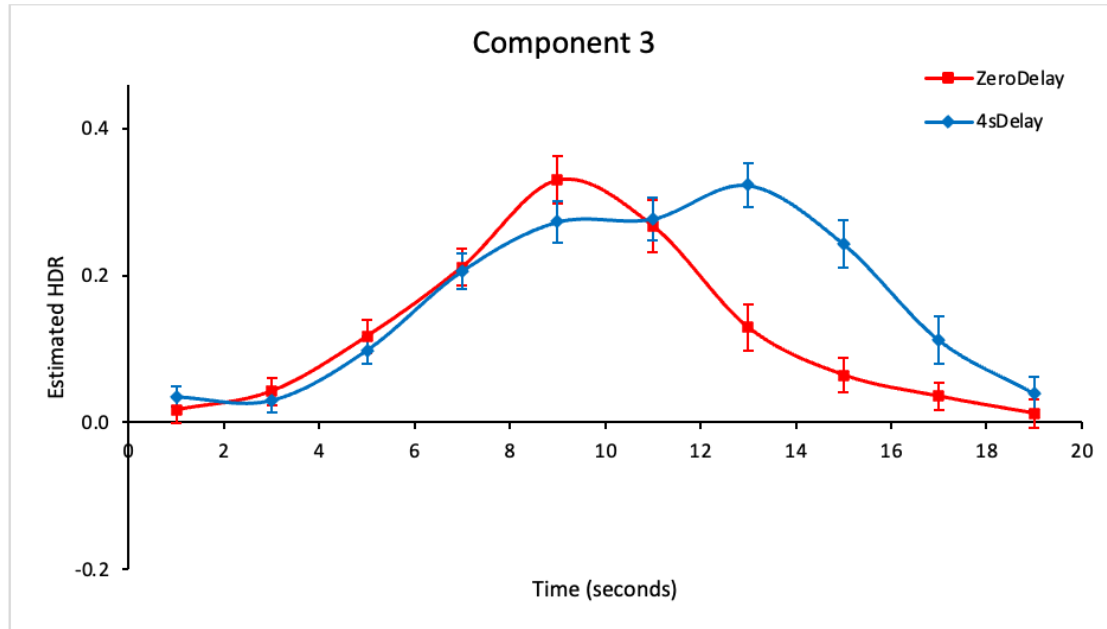
TDMN deactivation was observed in this study. Repeated ANOVA measures revealed a significant main effect of Cognitive Load (4 letters_6 letters), $F(1,36) = 17.30, p < .001$, Delay (0 second_4 seconds), $F(1,36) = 19.96, p < .001$, and Timebins, $F(9,324) = 34.23, p < .001$. A significant interaction was observed between Load \times Timebins (Figure 9), where more TDMN deactivation was seen in the 6-letter condition than the 4-letter condition between timebins 3-4, $F(1,36) = 8.43, p < .01$, timebins 4-5, $F(1,36) = 4.58, p < .05$, and timebins 7-8, $F(1,36) = 8.53, p < .01$. There was also a Delay \times Timebin interaction, $F(9,324) = 14.526, p < .001$ (Figure 10). Between timebins 1-2, 0s delay increased in deactivation while 4s delay decreased in deactivation, $F(1,36) = 4.40, p < .05$. Between timebins 4-5, 0s delay showed a sharper increase

than 4s delay, $F(1,36) = 9.924, p < .01$. Between timebins 5-6, 0s delay decreased in deactivation while 4s delay continued to increase in deactivation, $F(1,36) = 8.733, p < .01$. These observations showed that greater conditions with a higher cognitive load show greater TDMN deactivation and a later peak. A three-way interaction was also revealed between Load \times Delay \times Timebins, $F(9,324) = 14.526, p < .001$ (Figure 11). Between timebins 7-8, 4 letters_ 4s delay and 6 letters_ 4s delay decreased much quickly than 4 letters_ 0s delay and 6 letters_ 0s delay, $F(1,36) = 8.95, p < .01$. Similarly, greater delay, which uses greater cognitive resources, showed a later TDMN peak than 0s delay.

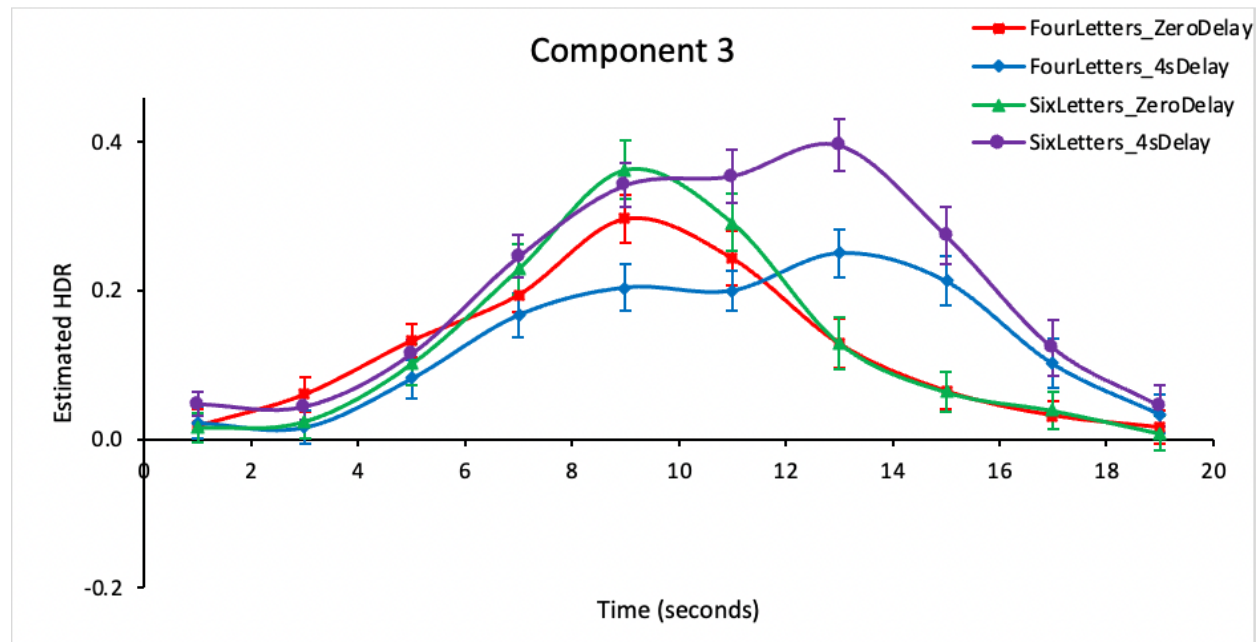
Figure 9



Note. Varimax HDR for Cognitive Load (Four Letters_Six Letters), averaged over Delay (Zero Delay_Four Seconds Delay).

Figure 10

Note. Varimax HDR for Delay (Zero Delay_Four Seconds Delay), averaged over Load (Four Letters_Six Letters).

Figure 11

Note. Varimax HDRs for Cognitive Load (FourLetters_SixLetters) x Delay Period (ZeroDelay_4sDelay).

In another study, WM was merged with TGT. (Sanford, Whitman, & Woodward, 2019). Repeated ANOVA measures revealed similar results: a significant main effect of Timebins, $F(9,324) = 38.57, p < .001$, Load, $F(1,36) = 22.26, p < .001$, and Delay, $F(1,36) = 24.83, p < .001$. Overall, the 4s Delay conditions showed a later HDR peak and the 6letter condition showed a higher HDR peak.

Analysis revealed similar results, where TDMN deactivation was load-dependent; there was greater TDMN deactivation for the 6-letter condition compared to the 4-letter condition. 4-s delayed conditions also showed a later peak compared to the no-delay conditions. These results corroborated Sanford's WM study (2019).

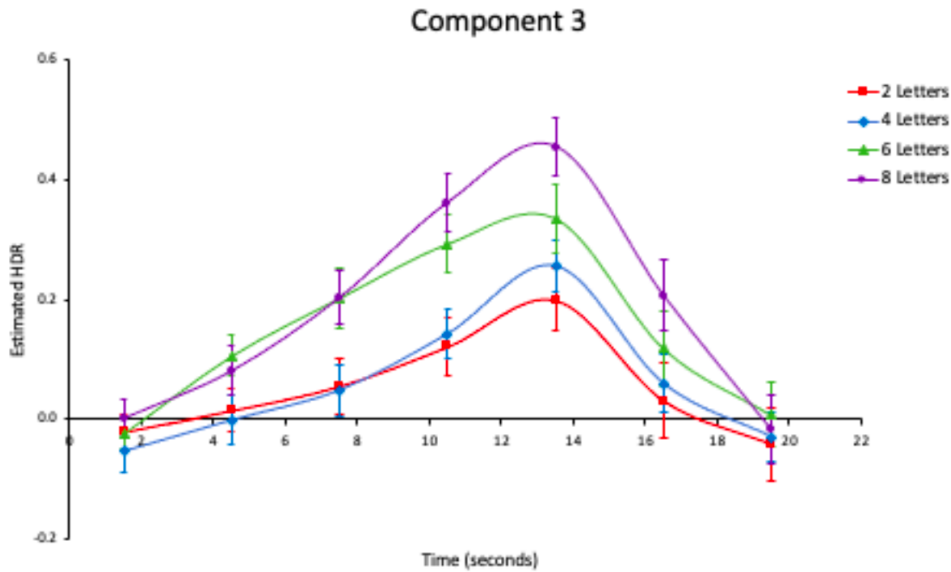
When the WM task was merged with SCAP, TGT and TSI (Sanford, 2019), similar results were observed. Similar to the WM task discussed above, there was a significant main effect of Cognitive Load, $F(1,52) = 39.86, p < .001$, Delay, $F(1,52) = 15.11, p < .001$, and Timebins, $F(9,468) = 61.99, p < .001$. Significant interactions were observed for Load \times Timebins, $F(9,468) = 17.19, p < .001$ and Delay \times Timebins, $F(9,468) = 39.70, p < .001$. There was greater TDMN deactivation for the 6-letter condition compared to the 4-letter condition. The 4s delay condition also showed greater TDMN deactivation compared to the 0s delay condition. A significant three-way interaction between Load \times Delay \times Timebins, was also observed, $F(9,468) = 2.21, p < .05$.

2.3.2 Metzak's WM Task HDR

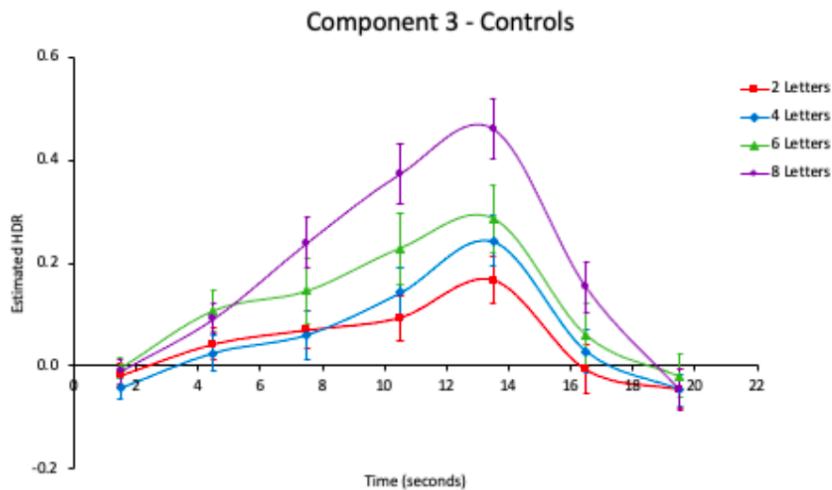
In Metzak et al.'s study (2011), NDMN deactivation was observed. Repeated ANOVA measures revealed a significant main effect of Cognitive Load, $F(3,84) = 15.62, p = .01$, and

Timebins, $F(6,168) = 59.62, p < .01$. A significant interaction was observed between Load \times Timebins, $F(18,504)=9.79, p = .01$. Between timebins 1-3 (Figure 12), the 6-letter condition showed a greater increase in NDMN deactivation than the 4-letter condition (both $p = .01$). Between timebins 4-5, the opposite was observed; the 4-letter condition showed a greater increase in deactivation. Between timebins 1-2, the 6-letter condition showed a greater increase in deactivation than the 8-letter condition, $F(1,28)=6.68, p=0.01$. The opposite was true during timebins 3-4, where the 8-letter condition showed a greater increase in NDMN deactivation. Between timebins 4-7, the 8-letter condition showed a greater increase and decrease in overall NDMN activity (all $p = .01$).

A significant three-way interaction also emerged between Load \times Group \times Timebins, $F(18,504)=1.85, p=0.01$. Between timebins 1-3 (Figure 13; Figure 14) the healthy controls showed greater NDMN deactivation than patients (all $p = .01$). Between timebins 3-4, controls showed a steeper increase in the 8-letter condition, relative to the 6-letter condition, $F(1,28)=12.39, p = 0.01$. In contrast, schizophrenia patients showed a flatter increase in the 6-letter condition, relative to the 8-letter condition. During timebins 6-7, both groups showed a greater decrease in the 8-letter condition than the 6-letter condition, $F(1,28)=23.20, p = 0.01$. Overall, controls showed greater NDMN deactivation.

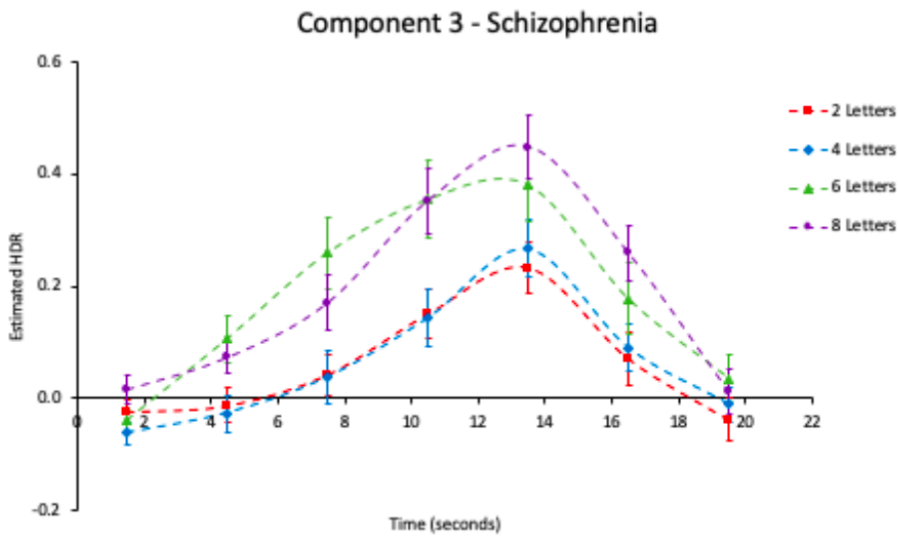
Figure 12

Note. Varimax HDR for Cognitive Load (2L_4L_6L_8L), averaged over Groups (Healthy_Schizophrenia).

Figure 13

Note. Controls' Varimax HDR for Load (2L_4L_6L_8L) \times Group (Healthy_Schizophrenia) \times Timebins.

Figure 14

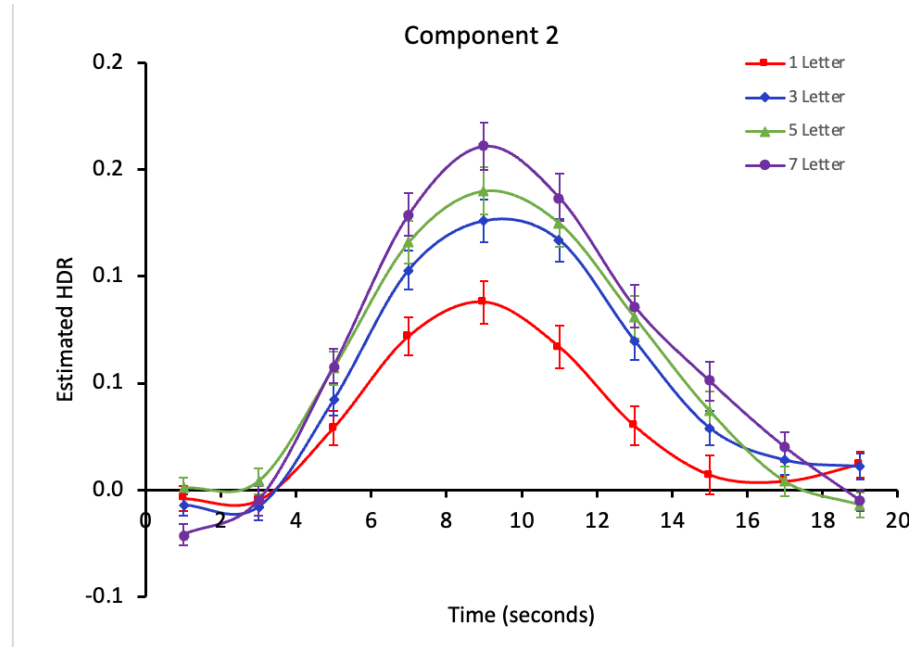


Note. Schizophrenia patients' Varimax HDR for Load (2L_4L_6L_8L) \times Group (Healthy_Schizophrenia) \times Timebins.

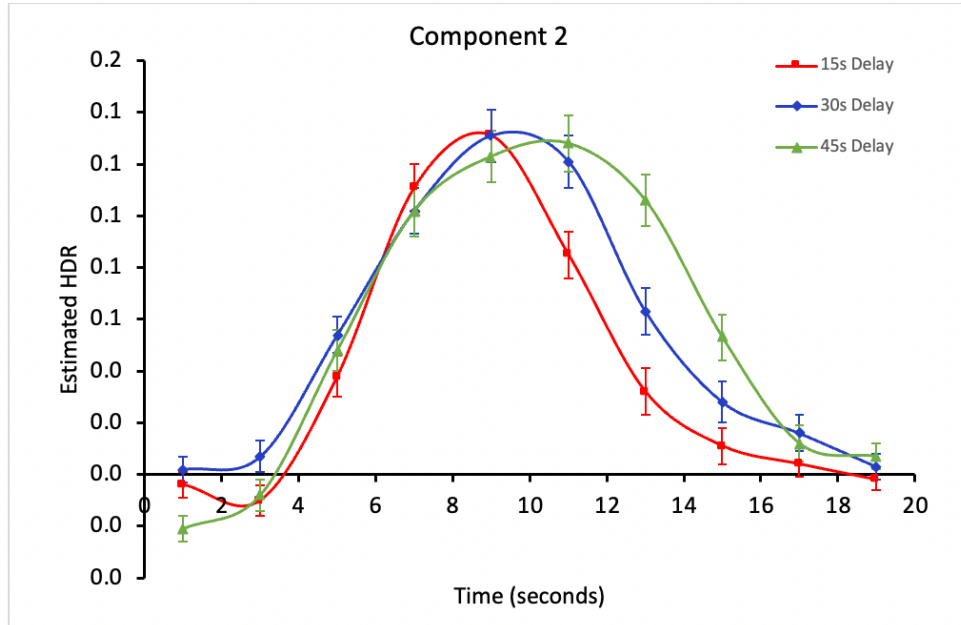
2.4 SCAP HDR

TDMN was observed in this study. Repeated ANOVA measures revealed a main effect of cognitive load, $F(3, 354) = 22.02, p < .001$, Delay $F(2, 236) = 15.86, p < .001$, and Timebins $F(9,1062) = 128.50, p < .001$. A significant interaction was observed between Load \times Timebins, $F(27,3186) = 12.58, p < .001$ (Figure 15). Between timebins 3-4, the 7-letter condition showed a sharper increase in deactivation compared to the 5-letter condition, $F(1,118) = 5.11, p < .05$. During the same time, the 3-letter condition also showed a sharper increase in deactivation compared to the 1-letter condition, $F(1,118) = 8.04, p < .01$. In general, greater TDMN deactivation

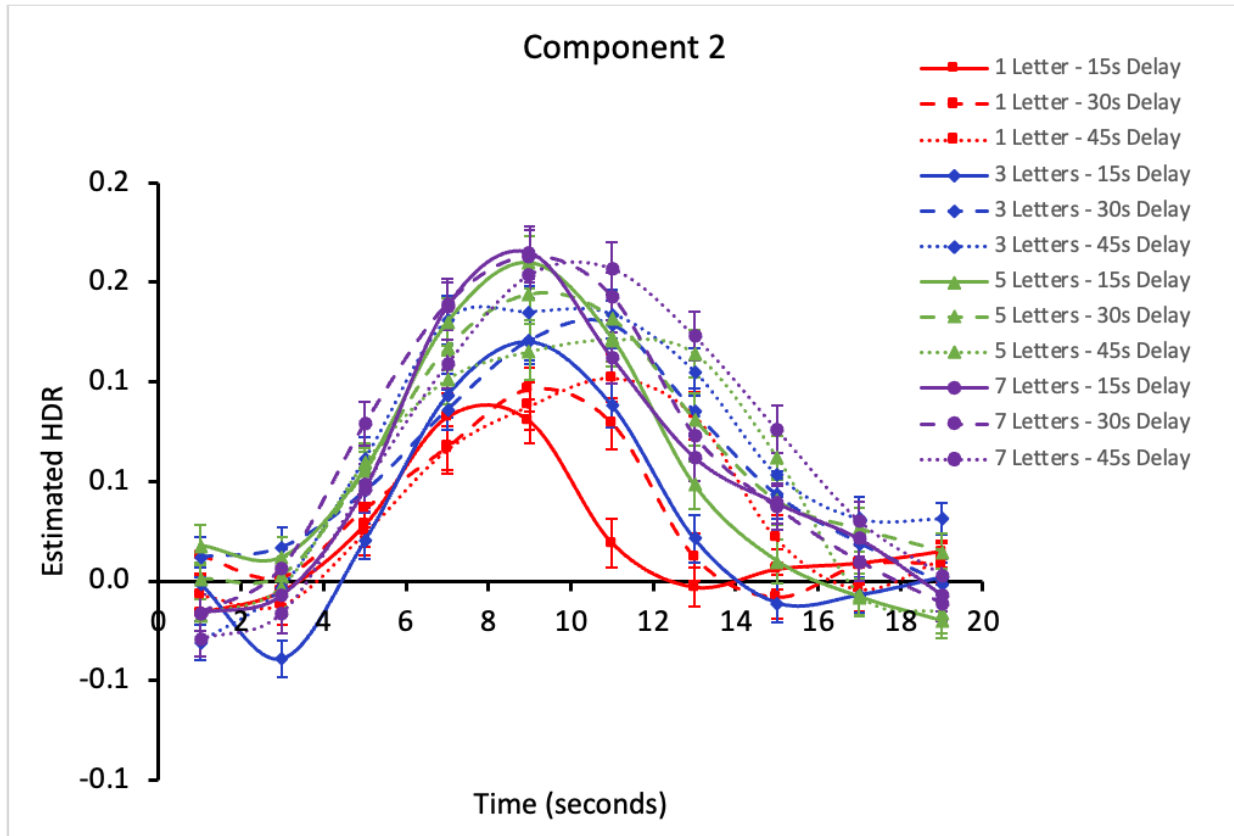
was observed with greater cognitive load. There was also a significant interaction between Delay \times Timebins, $F(18,2124) = 15.27, p < .001$ (Figure 16). Between timebins 5-6, the 30s condition showed a later decrease in deactivation compared to the 15s condition, $F(1,118) = 40.90, p < .001$. Similarly, between timebins 5-6, the 45s condition showed an increase to peak deactivation while the 30s decreased in deactivation, 30s and 45s between timebins 5-6, $F(1,118) = 9.29, p < .01$. The harder condition, 45s delay, showed a later peak, indicating that more difficult conditions tend to result in later DMN peaks. A three-way interaction was also observed between Load \times Delay \times Timebins, $F(54,6372) = 2.81, p < .01$ (Figure 17). Between timebins 8-9, a small positive increase in deactivation was observed in 1letter_15s and 1L_30s while the 3L_15s and 3L_30s conditions showed a steady decrease in deactivation.

Figure 15

Note. Cognitive load Varimax HDR averaged over Delay (15s_30s_45s).

Figure 16

Note. Delay Varimax HDR averaged over Load (1letter_3letters_5letters_7letters)

Figure 17

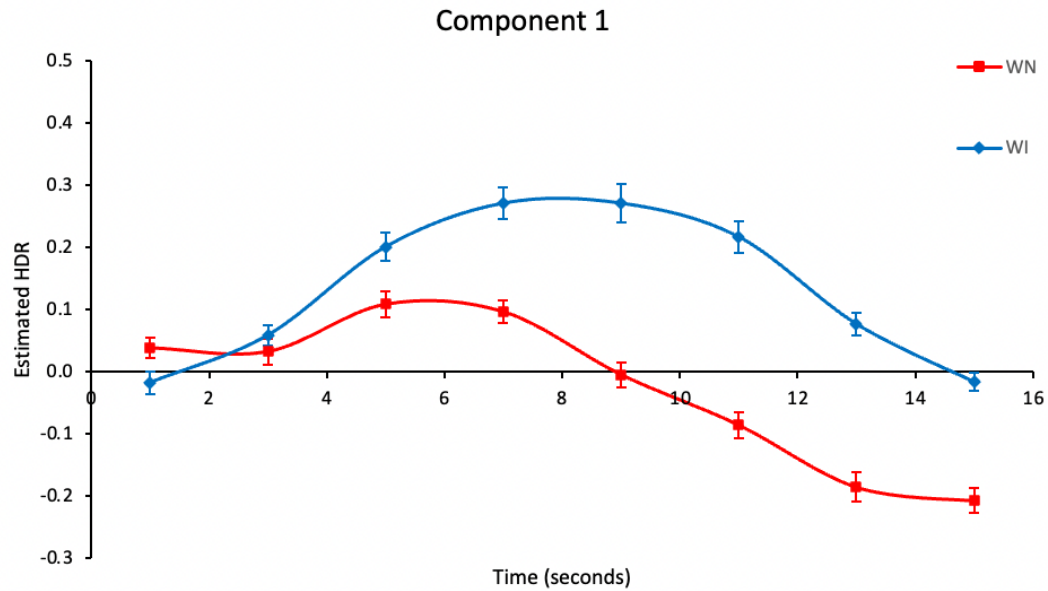
Note. Varimax HDR for Load \times Delay \times Timebins.

When the SCAP task was merged with WM, TGT and TSI (Sanford, 2019), similar results were observed. Repeated ANOVA measures revealed significant main effects of Cognitive Load, $F(3,258) = 13.37, p < .001$, Delay, $F(2,172) = 5.77, p < .01$, and Timebins, $F(9,774) = 77.06, p < .001$. Significant interactions emerged for Cognitive Load \times Timebins, $F(27,2322) = 6.17, p < .001$, and Delay \times Timebins $F(18,1548) = 10.19, p < .001$. A three-way significant interaction was also observed for Load \times Delay \times Timebins, $F(54,4644) = 2.21, p < .001$. A general trend of increased TDMN deactivation for increased cognitive load and increased delay was observed.

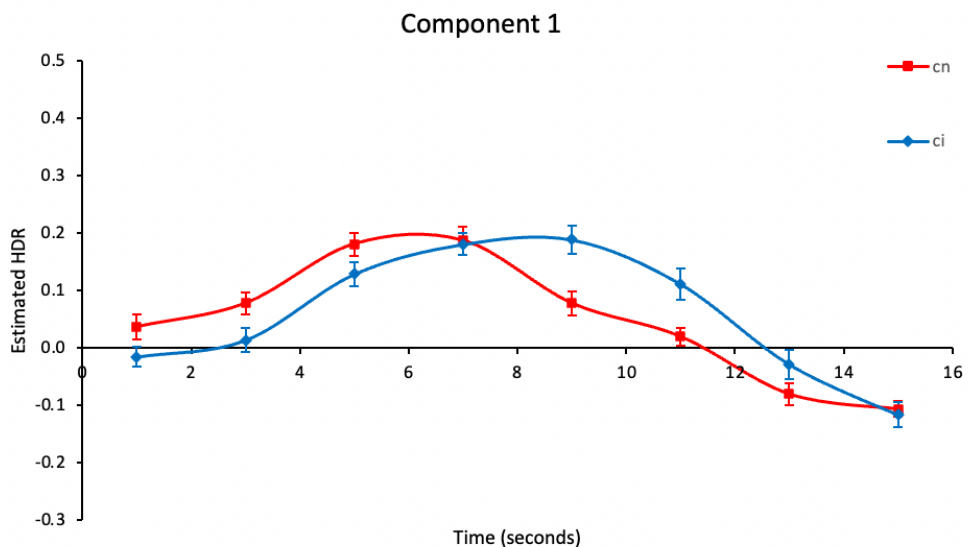
2.5 Task-Switching Inertia Task

2.5.1A Sanford's TSI Task HDR

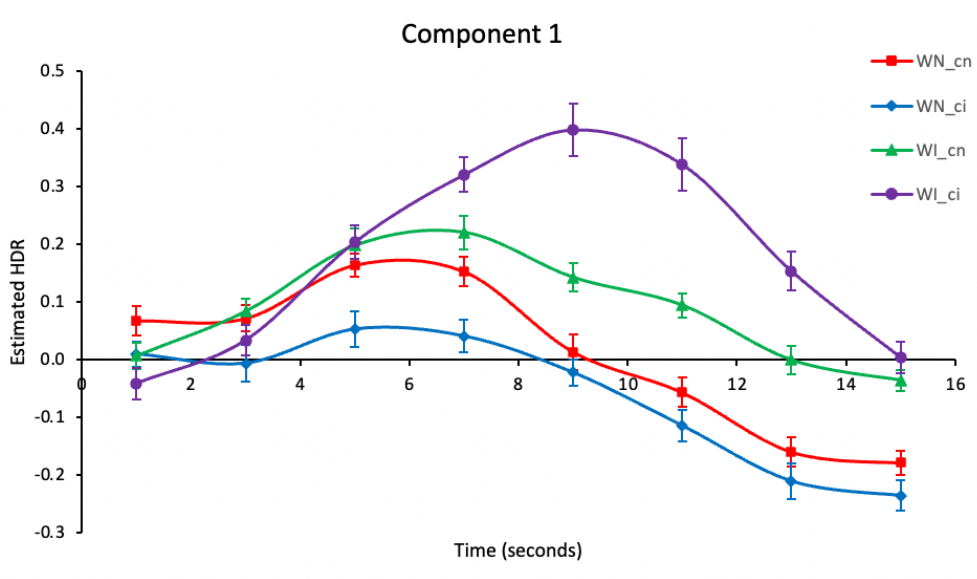
NDMN deactivation was observed. Repeated ANOVA measured reveal significant main effects of Timebins, $F(7,182) = 39.83, p < .001$, and Congruency, $F(1,26) = 66.64, p < .001$. The mean of WI was significantly higher than WN ($p < .001$), supporting the observation that greater cognitive load requires greater cognitive resources. A significant interaction was observed between Congruency \times Timebins, $F(7,182) = 43.21, p < .001$, and Task-switch \times Timebins, $F(7,182) = 6.22, p < .001$. Between timebins 1-2, WN decreased in deactivation while WI increased in deactivation $F(1,26) = 23.13, p < 0.001$ (Figure 18). Between timebins 3-4, WN decreased in deactivation while WI continued to increase, $F(1,26) = 23.23, p < .001$. WI, the more difficult condition, showed a later peak relative to the easier condition. The Task-switch \times Timebins interaction was observed timebins 4-5 when ci decreased while cn continued to increase $F(1,26) = 21.03, p < .001$ (Figure 19). Similar to the Congruency \times Timebins interaction, ci, the more difficult condition, also showed a later peak than ci, the easier condition. A three-way interaction was also observed between Congruency \times Task-switch \times Timebins, , $F(7,182) = 6.94, p < .001$. WI_ci increased in deactivation while all the other conditions decreased in deactivation between timebins 3-4, $F(1,26) = 4.59, p < .05$ (Figure 20). Wi_ci was the most difficult condition with incongruent words and incongruent task-switch. Again, there was a later peak in DMN deactivation in harder conditions.

Figure 18

Note. Varimax HDR for Congruency (WN_WI), averaged over Task-switch (cn_ci).

Figure 19

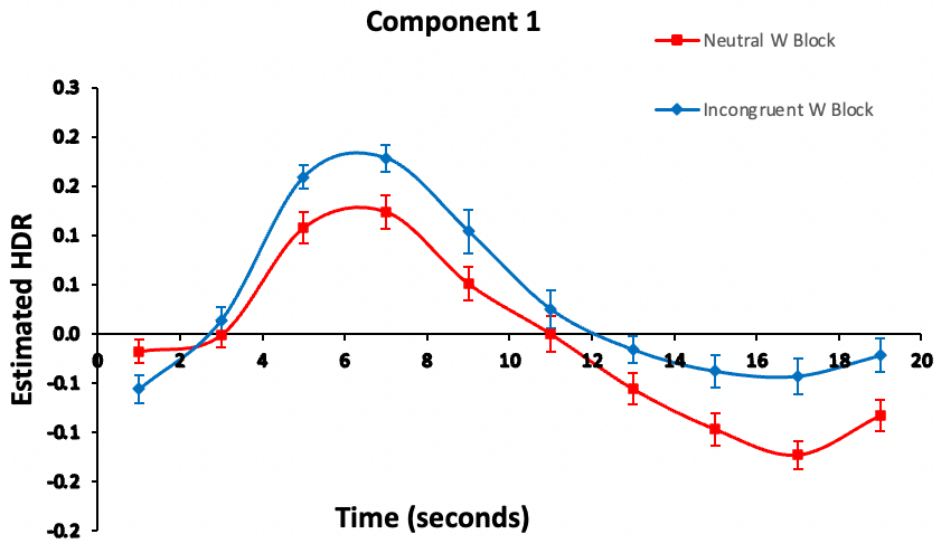
Note. Varimax HDR for Task-switch (cn_ci), averaged over Congruency (WN_WI).

Figure 20

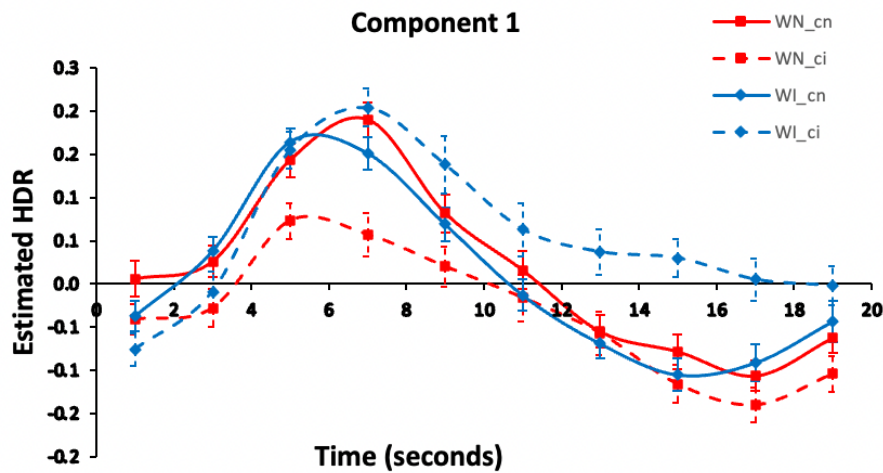
Note. Varimax HDR for Congruency (WN_WI) x Task-switch (cn_ci).

2.5.1B Sanford's TSI in SCAP-TGT-TSI-WM

When the TSI task was merged with the WM, TGT and SCAP tasks, TDMN deactivation was observed. Repeated ANOVA measures revealed significant main effects of Timebins, $F(9,468) = 50.06, p < .001$, and Congruency, $F(1,52) = 7.16, p = .01$. Overall, the main effect of Congruency was driven by an increase in TDMN deactivation in the Incongruent condition. A significant interaction was observed between Congruency \times Timebins, $F(9,468) = 3.75, p < .001$. Between timebins 1-2, the Incongruent condition increased in TDMN deactivation, relative to the Congruent condition, $F(1,52) = 15.73, p < .001$ (Figure 21). Between timebins 2-3, the Incongruent condition showed a steeper increase in TDMN deactivation compared to the Congruent condition, $F(1,52) = 4.13, p < .05$. A three-way interaction was also observed between Congruency \times Task-Switch \times Timebins, $F(9,468) = 3.72, p < .001$. Between timebins 3-4, WN_ci and WI_cn decreased from the deactivation peak while the other two conditions continued to increase, $F(1,52) = 15.99, p < .001$ (Figure 22)

Figure 21

Note. Varimax HDR for Congruency (WN_WI), averaged over Task-Switch (cn_ci), and Group (Healthy_Schizophrenia).

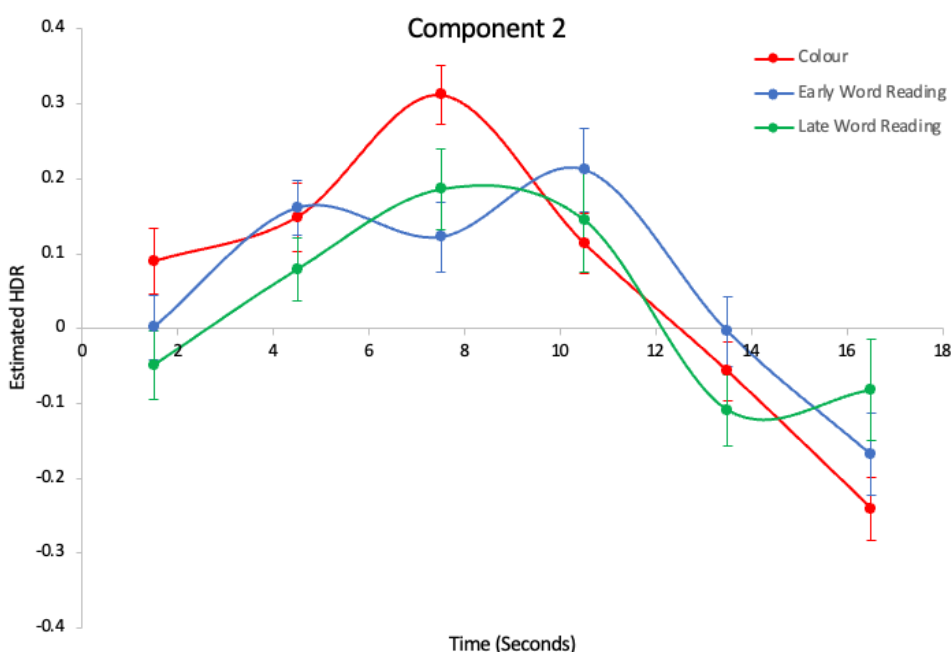
Figure 22

Note. Varimax HDR for Congruency \times Task-Switch \times Timebins, averaged over Group (Healthy_Schizophrenia).

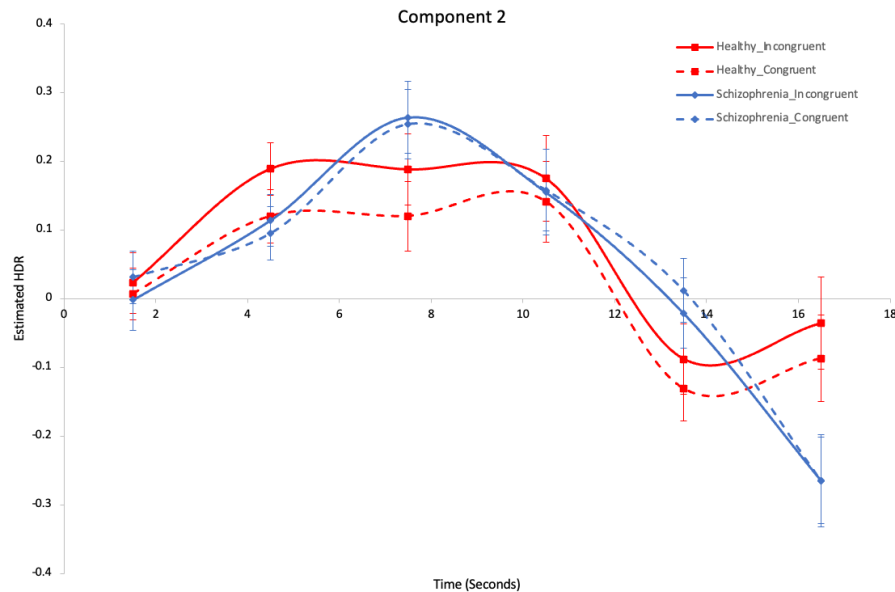
2.5.2 Woodward et al.'s TSI HDR

TDMN deactivation was observed in Woodward et al.'s TSI study (2016). Repeated ANOVA measures revealed a significant main effect of Task (Colour_EarlyWord_LateWord), $F(2,48) = 9.43, p < .001$, and Timebins, $F(5,120) = 15.23, p < .001$. Overall, the LateWord condition showed greater TDMN deactivation, $F(1,24) = 8.52, p < .01$. A significant interaction emerged between Task \times Timebins, $F(10,240) = 2.67, p < .01$. Between timebins 2-3, the EarlyWord condition decreased in deactivation while the Colour condition increased in deactivation, $F(1,24) = 5.54, p < .05$ (Figure 23). The opposite pattern was observed between timebins 3-4, where the Colour condition decreased in deactivation while EarlyWord increased in deactivation. Similarly, between timebins 2-3, the EarlyWord condition decreased in deactivation while LateWord increased in deactivation, $F(1,24) = 8.07, p < .01$. Between timebins 5-6, LateWord increased in deactivation while EarlyWord decreased in deactivation, $F(1,24) = 7.96, p < .01$. Overall, the HDR for the LateWord condition resembles that of Colour.

A significant Group interaction also emerged between Group \times Congruency, $F(1,24) = 5.47, p < .05$ (Figure 24). In general, the patient cohort showed greater TDMN deactivation.

Figure 23

Note. Hrf-Procrustes for Task (Colour_EarlyWord_LateWord) \times Timebins, averaged over Group (Healthy_Schizophrenia).

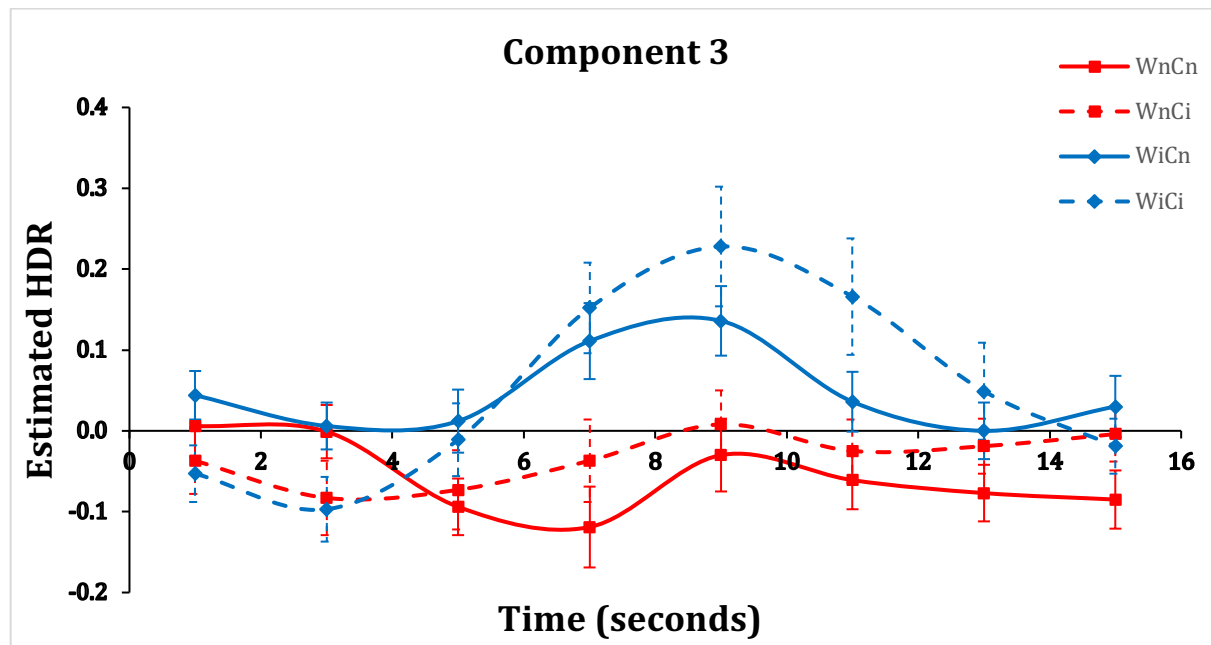
Figure 24

Note. Hrf-Procrustes for Group (Healthy_Schizophrenia) \times Congruency (Incongruent_Neutral), averaged over Task (Colour_EarlyWord_LateWord).

2.5.3 TSI-TGT Merge

Like all the studies discussed above, repeated ANOVA measures revealed a greater TDMN deactivation in incongruent TSI conditions, particularly for word-reading conditions, $F(3,78) = 3.96, p < .05$. A significant interaction between Congruency \times Timebins was also revealed, $F(21, 546) = 3.63, p < .001$. Between timebins 2-3, WN_CN showed a decrease in deactivation while WN_CI increased in deactivation, $F(1,26) = 4.78, p < .05$ (Figure 25).

Figure 25



Note. Varimax HDR for Congruency \times Timebins.

2.6 TGT

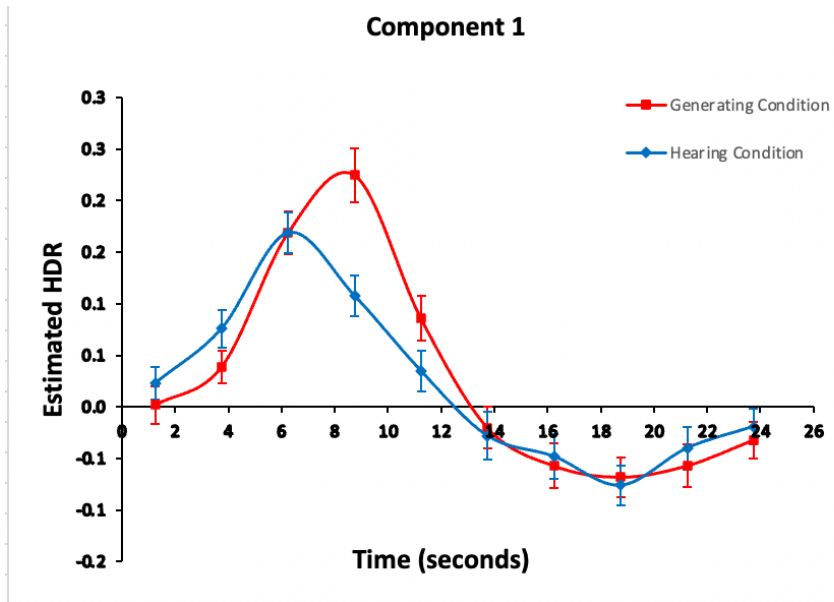
2.6.1 Lavgine's TGT HDR

TDMN was observed in this study. Repeated ANOVA measures revealed a main effect of Timebins, $F(8,552) = 94.81, p < 0.001$, and Group, $F(2,69) = 3.29, p < .05$. No significant interactions were found.

2.6.2 TGT in SCAP-TGT-TSI-WM HDR

When TGT was merged with SCAP, TGT, TSI and WM in another study, TDMN was also observed. Repeated ANOVA measures revealed a significant main effect of Timebins, $F(9,522) = 35.65, p < .001$. There was a significant interaction between Condition \times Timebins, $F(9,522) = 2.60, p < .01$. Between timebins 3-4, the Generating condition increased in TDMN deactivation while the Hearing condition decreased in TDMN deactivation, $F(1,58) = 19.65, p < .001$ (Figure 26). The more difficult condition, Generating, showed a later TDMN peak. Between timebins 4-5, the Generating condition showed a steeper decline in TDMN deactivation than the Hearing condition, $F(1,58) = 7.34, p < .01$. No significant between-subject factors were observed.

Figure 26



Note. Varimax HDR for Condition (Generating_Hearing), averaged over Group (Healthy_Schizophrenia).

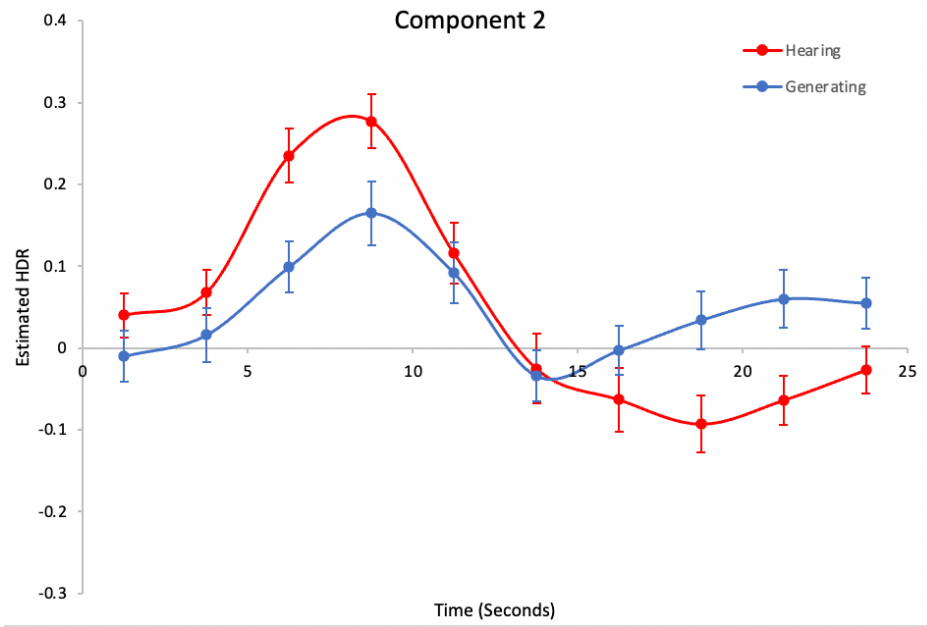
2.6.3 TGT in TSI-TGT HDR

Similar to SCAP-TGT-TSI-WM and in contrast to Lavigne's study, no significant main effect of group/condition nor interactions were observed. TDMN deactivation was seen.

2.6.4 TGT in MS-TGT-SA HDR

In Percival's study (2018a), repeated ANOVA measures revealed a significant main effect of Timebins, $F(9,423) = 14.10, p < .001$. A significant interaction between Condition \times Timebins was observed, $F(9,423) = 3.77, p < .001$. Between timebins 2-3, the Hearing condition showed a greater increase in TDMN deactivation than the Generating condition, $F(1,47) = 8.76, p < .01$ (Figure 27). Similarly, the Hearing condition showed a steeper decrease in deactivation between timebins 4-5, $F(1,47) = 5.62, p < .05$.

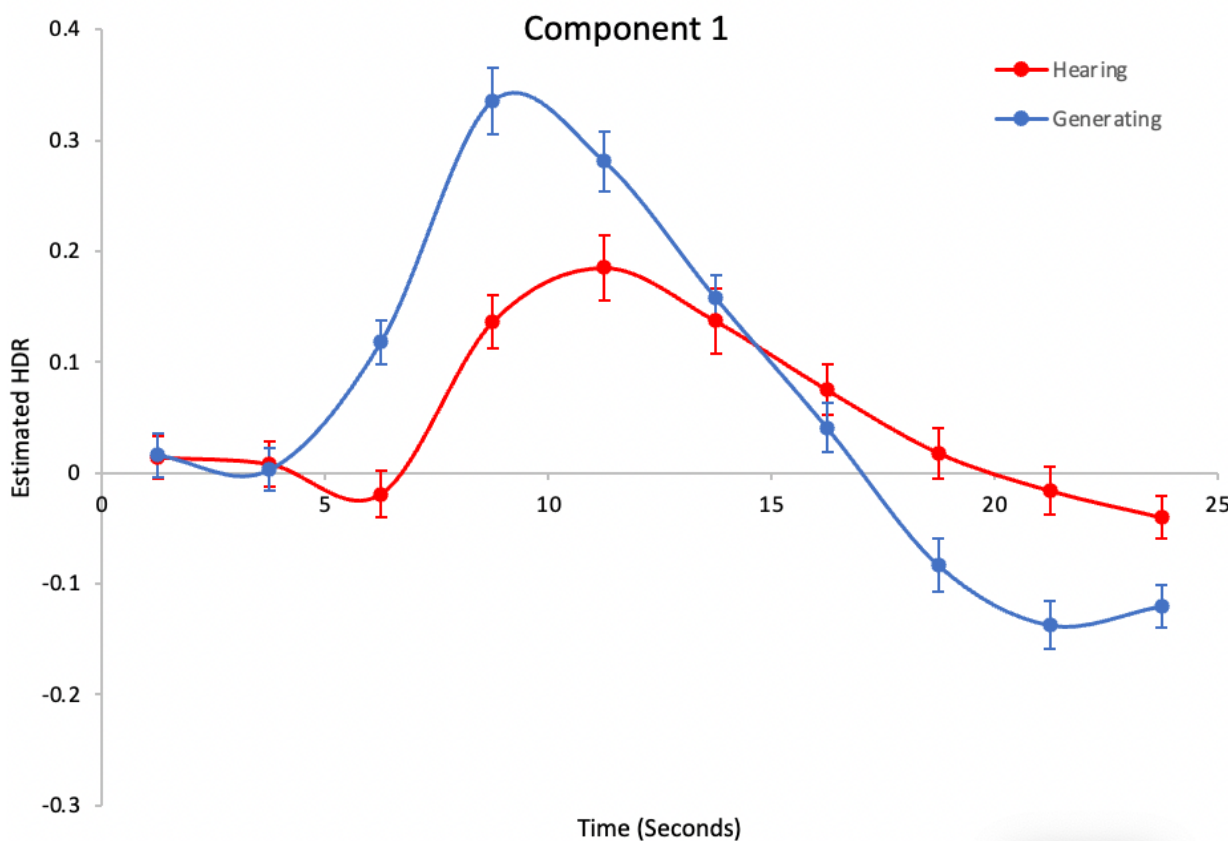
Figure 27



Note. Varimax HDR for Condition (Hearing_Generating) averaged over Group (Healthy_Schizophrenia)

In the same study, NDMN deactivation was observed in component 1. Repeated ANOVA measures revealed a main effect of Timebins, $F(9,423) = 47.17, p < .001$. A significant Condition \times Timebins interaction also emerged, $F(9,423) = 12.26, p < .001$. Between timebins 2-3, Hearing decreased in TDMN deactivation while Generating increased, $F(1,47) = 63.02, p < .001$ (Figure 28). Between timebins 4-5, Generating decreased from peak while Hearing continued to increase to in deactivation, $F(1,47) = 13.62, p < .001$. Between timebins 5-6 and 7-8, Generating showed a steeper decrease (both $p < .01$). Overall, Generating showed greater increases and decreases in HDR activity.

Figure 28



Note. Varimax HDR for Condition (Hearing_Geneering), average over Group (Healthy_Schizophrenia)

2.6.5 Other Merged TGT Studies

In another study, the TGT task was merged with the WM task, analysis revealed similar results to the studies discussed above, where there was a significant main effect of Timebins, $F(9,279) = 15.62, p < .001$, but no other significant main effects or interactions were observed. TDMN deactivation was seen in this study.

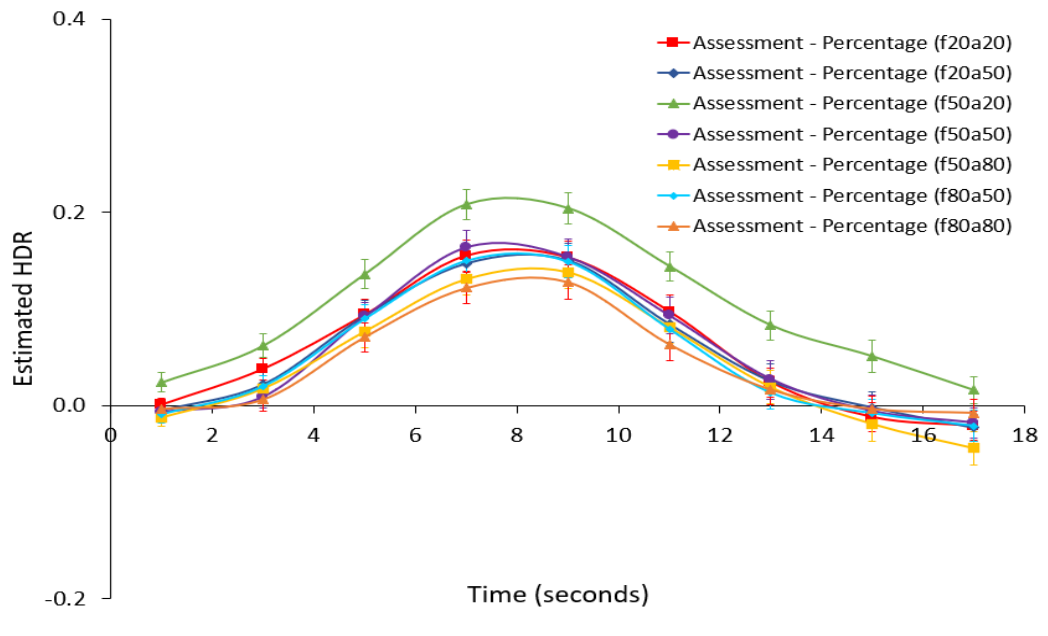
When TGT was merged with SA, repeated ANOVA measures revealed a main effect of Timebins, $F(9,225) = 8.03, p < .001$. No other significant interactions emerged.

When merged with MS, both TDMN and NDMN deactivation were observed. In the TDMN component, repeated ANOVA measured revealed no significant interactions. In the NDMN component, a significant Condition \times Timebins emerged, $F(7,329) = 5.65, p < .001$.

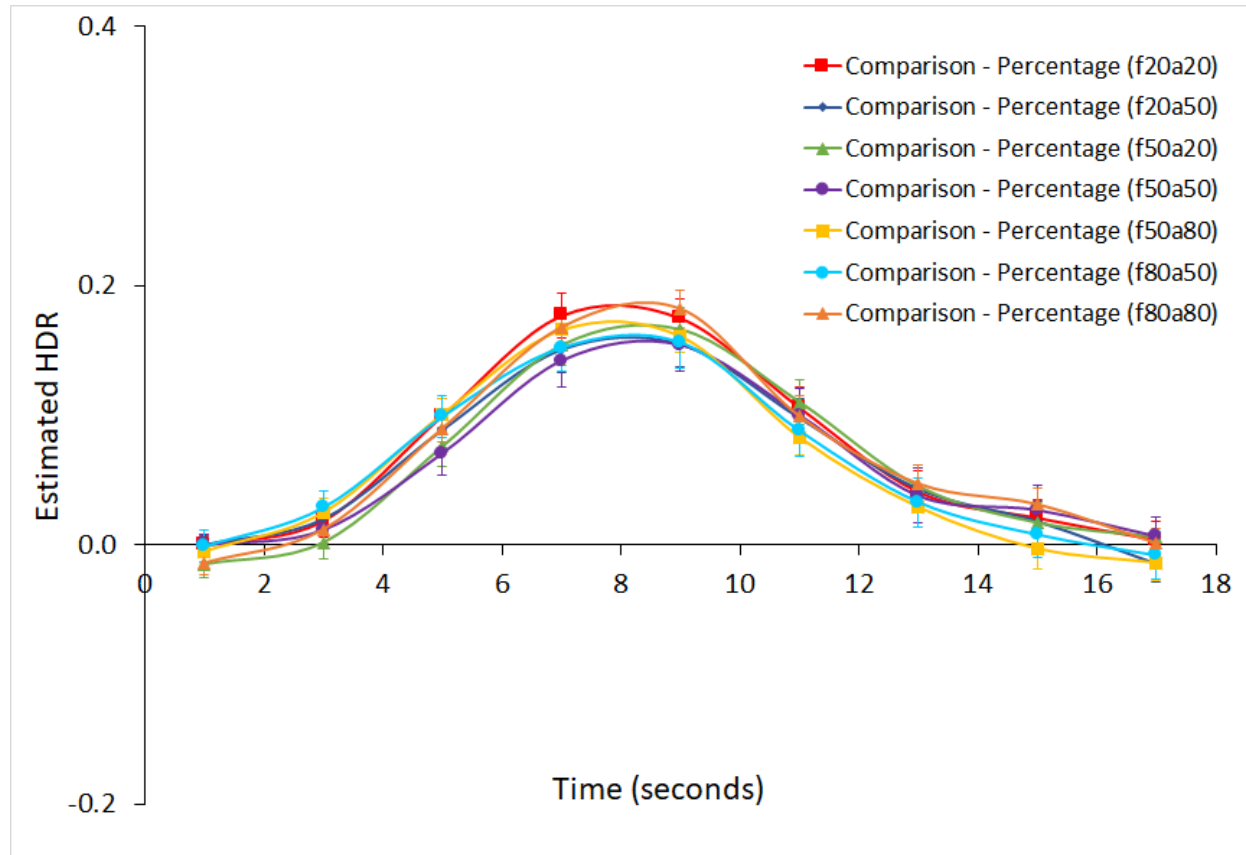
2.7 FISH Task

2.7.1 Whitman Fish Task

TDMN deactivation was observed in this task. Repeated ANOVA measures revealed a significant interaction between Assessment_Comparison \times Timebins, $F(8,360)=2.90, p < .05$. The Comparison condition showed greater increase in deactivation between timebins 3-4, relative to the Assessment condition, $F(1,45)=4.611, p < .05$ (Figure 29; Figure 30).

Figure 29

Note. Varimax HDRs for Evidence Assessment Task.

Figure 30

Note. Varimax HDRs for Hypothesis Comparison Task.

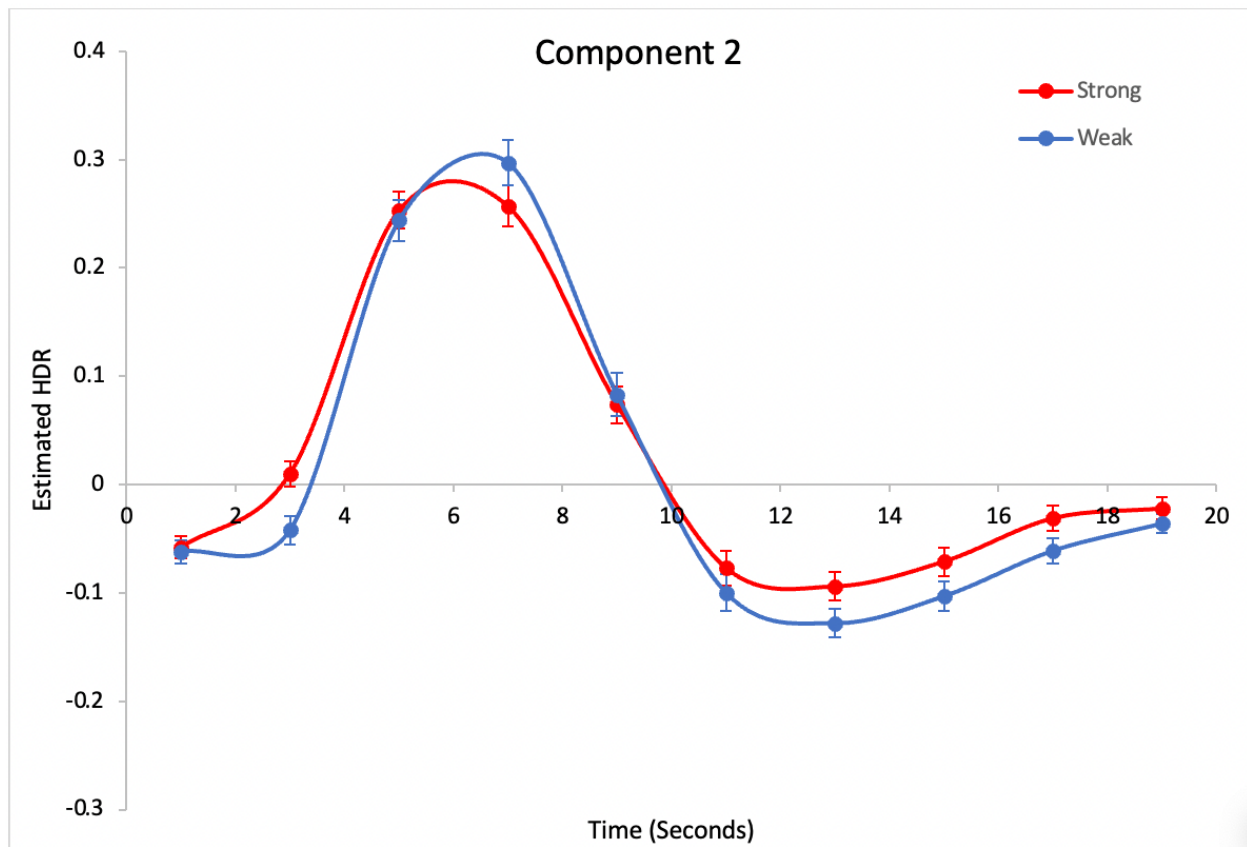
2.7.2 Fouladirad's Fish Task

TDMN was observed in this task. Repeated ANOVA measures revealed a significant main effect of Timebins, $F(9,981) = 124.58, p < .001$, and Strong_Weak, $F(1,109) = 7.09, p < .01$. A significant interaction emerged between Strong_Weak \times Timebins, $F(9,981) = 6.26, p < .001$. Between Timebins 1-2, Strong showed steeper increase in deactivation, relative to the Weak condition, $F(1,109) = 15.20, p < .001$ (Figure 31). The opposite was observed during Timebins 2-3, where the Weak condition showed steeper increase in deactivation, $F(1,109) = 10.79, p = .001$. Between Timebins 3-4, Strong showed slight increase then decrease from peak, while Weak continued to increase. Between timebins 4-5 and 5-6, the Weak condition showed

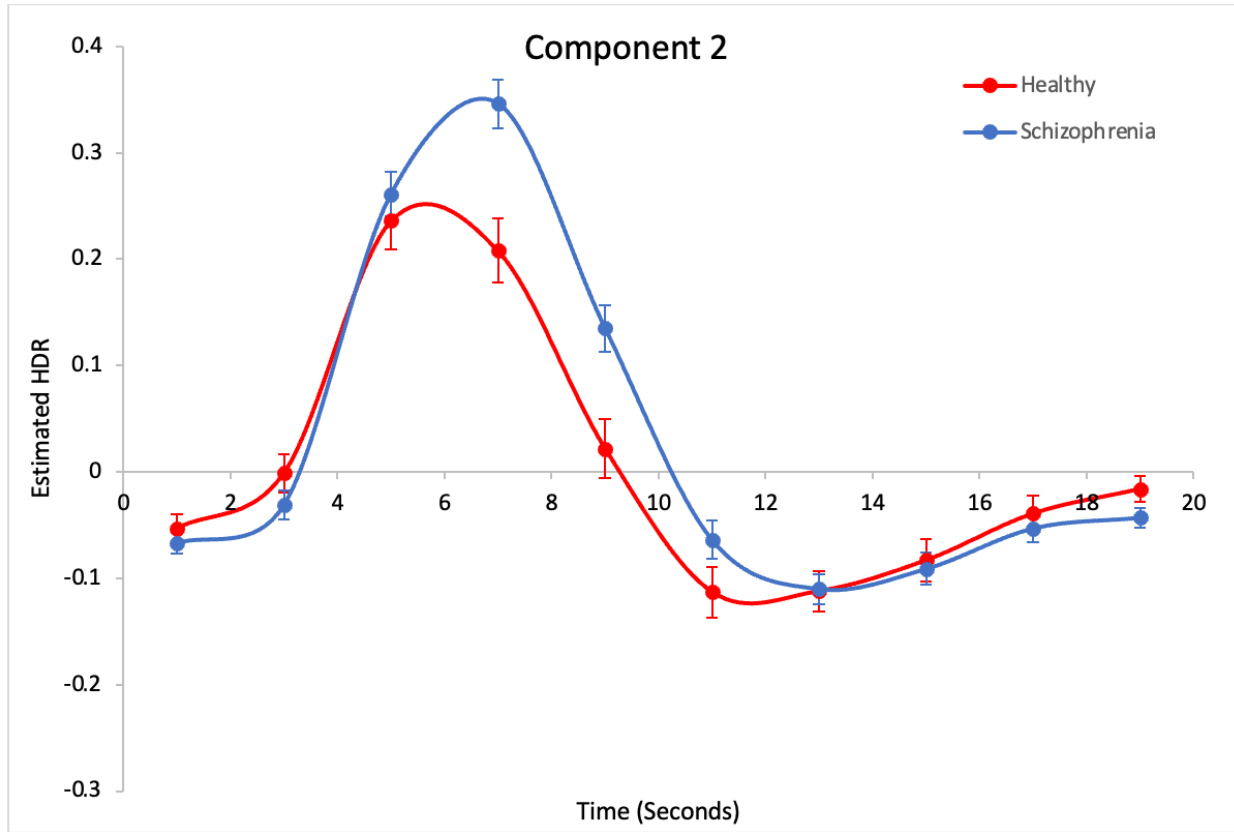
steeper declines in deactivation. ($p < .01$; $p < .05$). Overall, the Weak condition showed later peak.

A Group \times Timebins was also observed, $F(9,981) = 5.53, p < .001$. Between timebins 5-6, Schizophrenia patients continued to increase in deactivation while Healthy controls decreased from peak, $F(1,109) = 16.37, p < .001$ (Figure 32). The Schizophrenia patients showed a later HDR peak. Between timebins 6-7, Schizophrenia patients decreased in deactivation while controls showed a slight increase in deactivation.

Figure 31



Note. HRFmax HDR for Strong_Weak, averaged over Match_NonMatch and Group (Healthy_Schizophrenia).

Figure 32

Note. HRFmax HDR for Group (Healthy_Schizophrenia), averaged over Strong_Weak and Match_NonMatch.

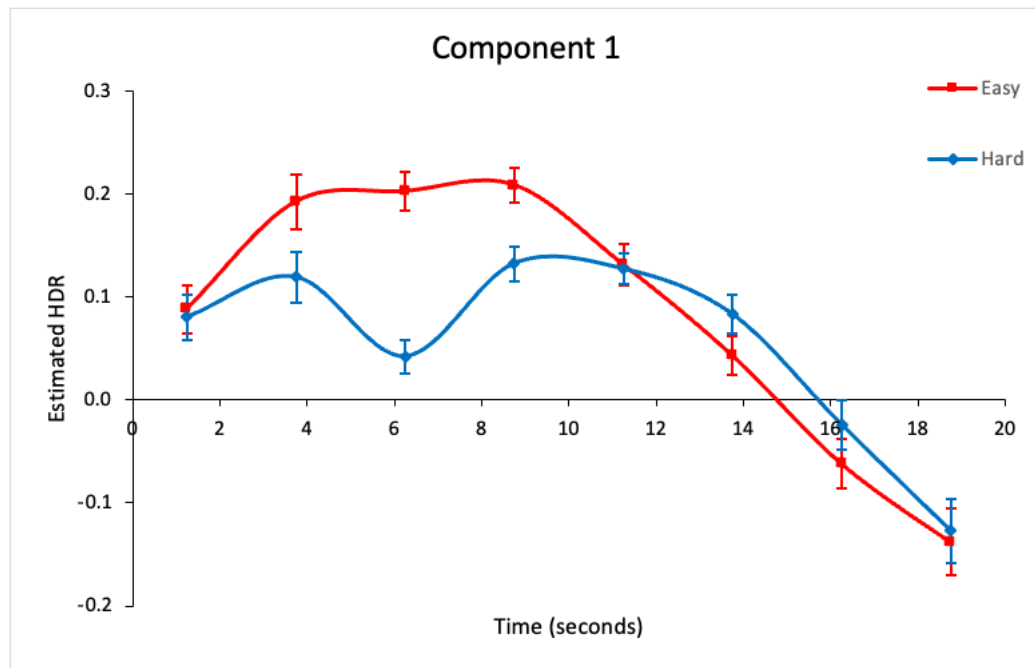
2.8.1 LDT

8.1 LDT HDR

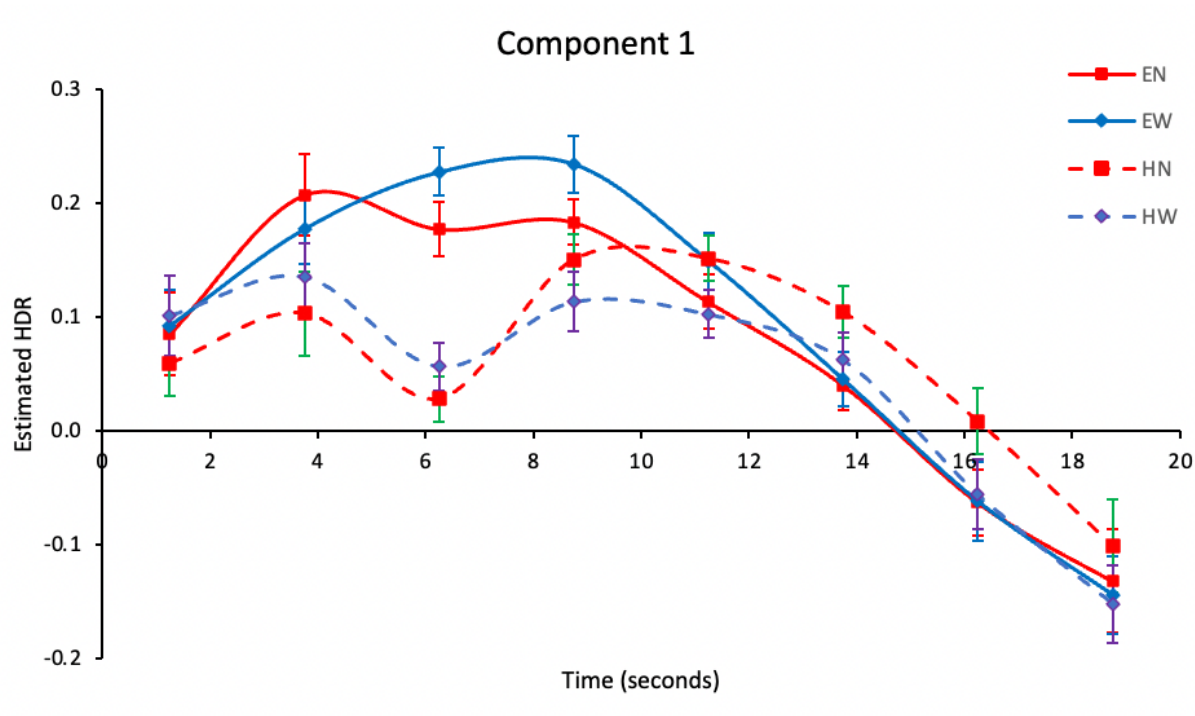
TDMN deactivation was observed in component. Repeated ANOVA measures revealed a significant main effect of Difficulty (Easy_Hard), $F(1,58) = 7.74, p < .01$, and Timebins, $F(7,406) = 26.89, p < .001$. A significant interaction between Difficulty \times Timebins was observed $F(7,406) = 18.55, p < .001$. Between timebins 1 and 2, the Easy condition showed a greater increase in deactivation than the Hard condition $F(1,58) = 19.79, p < .001$ (Figure 33). Between timebins 2 and 4, the Easy condition showed a relatively constant level of deactivation while the Hard condition showed a decrease in deactivation, followed by an increase in deactivation ($p < .001$).

Between timebins 5 and 6, the Easy condition showed a greater decrease in deactivation, relative to the Hard condition. A three-way interaction was also observed between Difficulty \times Lexicality \times Timebins, $F(7,406) = 3.44, p = .001$ (Figure 34). The Easy_Word condition showed an increase in deactivation while all other conditions decreased in deactivation. In general, the highest HDR peak was observed in the Hard_NonWord codnition.

Figure 33

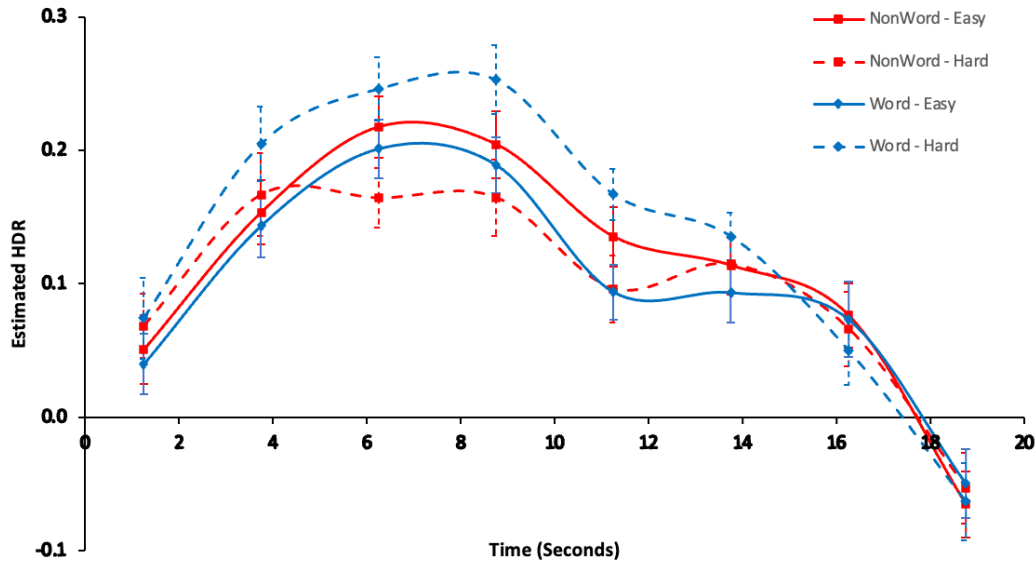


Note. HRFmax HDRs for Difficulty (Easy_Hard), averaged over Lexicality (Nonword_Word).

Figure 34

Note. *HRFmax HDRs for Difficulty (Easy_Hard) x Lexicality (Nonword_Word).*

In the same study, NDMN deactivation was observed in a different component. Repeated ANOVA measures revealed a main effect of Timebins, $F(7,817) = 34.65, p < .001$, and Difficulty, $F(1,58) = 7.96, p < .01$. A significant three-way interaction was observed between Timebins \times Difficulty \times Lexicality, $F(1,58) = 4.24, p < .05$. Between timebins 2-3, the NonWord_Hard condition decreased from peak NDMN deactivation while all other conditions continued to increase in deactivation, $F(1,58) = 4.43, p < .05$ (Figure 35). Between timebins 5-6, the Easy Conditions (NonWord_Easy and Word_Easy) decreased in deactivation while the Hard conditions (NonWord_Hard and Word_Hard) decreased slightly before a rebound in deactivation, $F(1,58) = 11.07, p < 0.01$. Between timebins 6-7, the Hard conditions showed a steeper decrease in NDMN deactivation compared to the Easy conditions.

Figure 35

Note. HRFmax HDR for Timebins \times Difficulty (Hard_Easy) \times Lexicality (Word_NonWord).

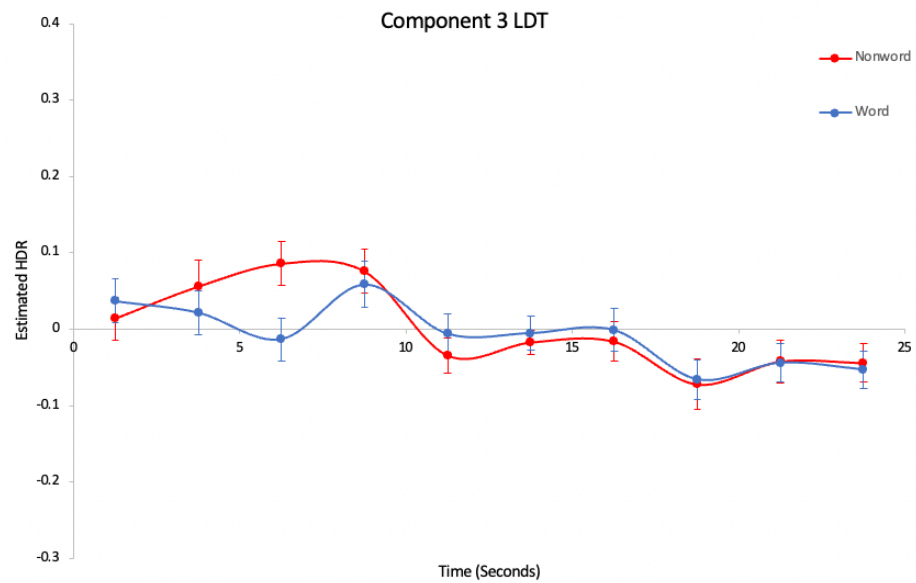
2.8.2 LDT in LDT-RSPM HDR

TDMN deactivation was observed in this component. Repeated measures ANOVA revealed significant main effects of Difficulty, $F(1,40) = 5.16, p < .05$ and Time, $F(9,360) = 2.92, p < .01$. Significant interactions were observed for Lexicality \times Time, $F(9,360) = 3.74, p < .001$, where NonWord showed an increase in TDMN deactivation while Word showed a decrease in deactivation during timebins 1-3 (both $p < .01$; Figure 36). Between timebins 3 and 4, NonWord showed slight decrease in TDMN deactivation while Word showed an increase in deactivation, $F(1,40)=22.22, p < .001$. Moreover, NonWord showed a larger decrease compared to Word during timebins 4-5 $F(1,40)=4.94, p < .05$ (Figure 36). These findings suggest that the TDMN deactivation patterns depends upon lexicality.

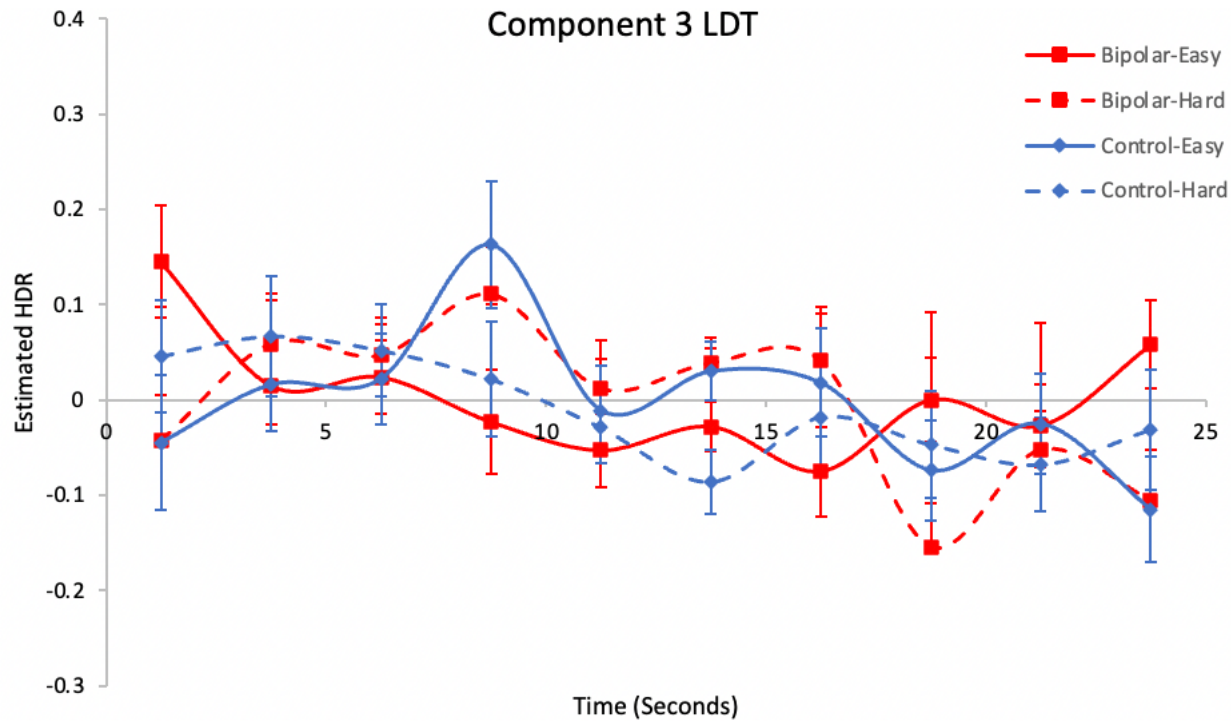
A three-way interaction was observed for Difficulty \times Timebins \times Group $F(9,360) = 3.16, p = .001$. Bipolar_Easy showed a decrease in TDMN deactivation while all other conditions showed increase in TDMN deactivation between timebins 1-2, $F(1,40)=4.50, p < .05$ (Figure 37).

This condition elicited the greatest TDMN deactivation when the stimulus was first presented and decreased thereafter. Bipolar_Easy also showed a slight increase in TDMN deactivation while all other conditions showed a decrease between timebins 7-8, $F(1,40)=7.09, p < .05$.

Figure 36



Note. LDT Varimax HDR for the Lexciality (Nonword_Word) condition, averaged over Difficulty (Easy_Hard) and Group (Bipolar_Ccontrol).

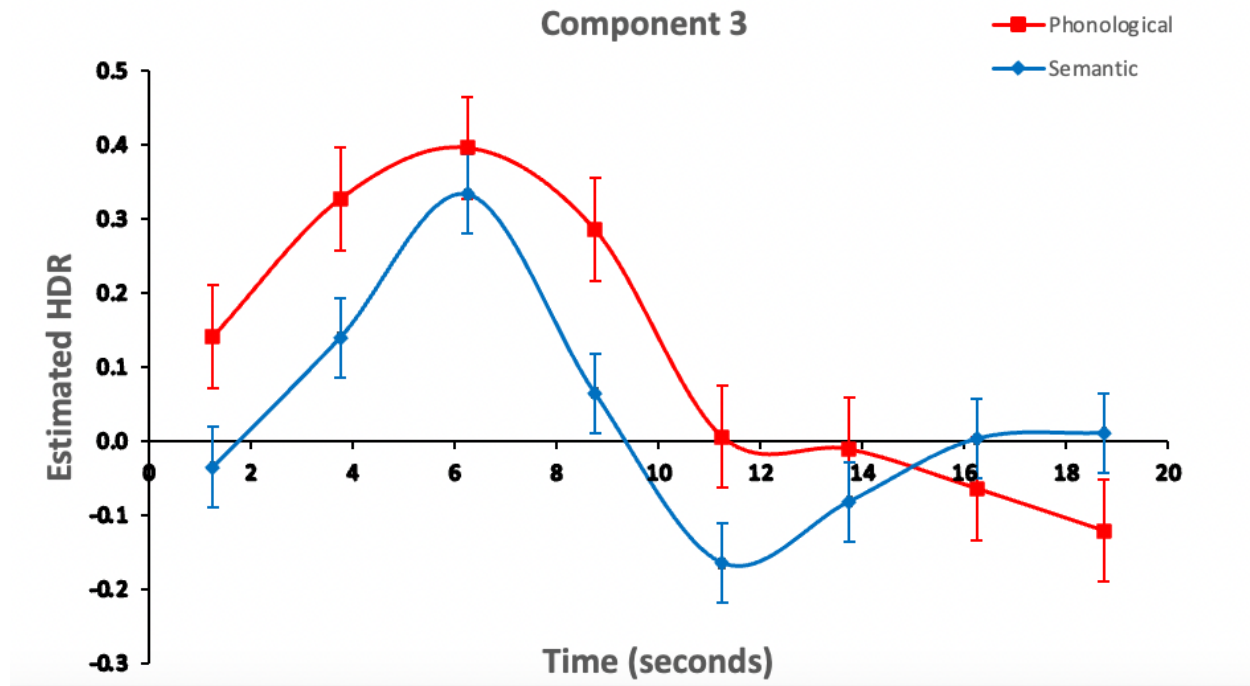
Figure 37

Note. LDT Varimax HDR for Difficulty (Easy_Hard) x Group (Bipolar_Control), averaged over Lexciality (Nonword_Word).

2.9 MS HDR

9.1 TDMN deactivation in the MS Task

TDMN deactivation was observed in one component of the study. Repeated ANOVA measures revealed a significant main effect of Timebins, $F(7,539) = 25.47, p < .001$ and Task $F(1,77) = 89.81, p < .001$. A significant interaction was also observed between Task \times Timebins, $F(7,539) = 6.29, p < .001$, where Semantic showed a greater decrease in deactivation than Phonological between timebins 3-4, $F(1,77) = 6.36, p < .05$ (Figure 38). No group differences were observed.

Figure 38

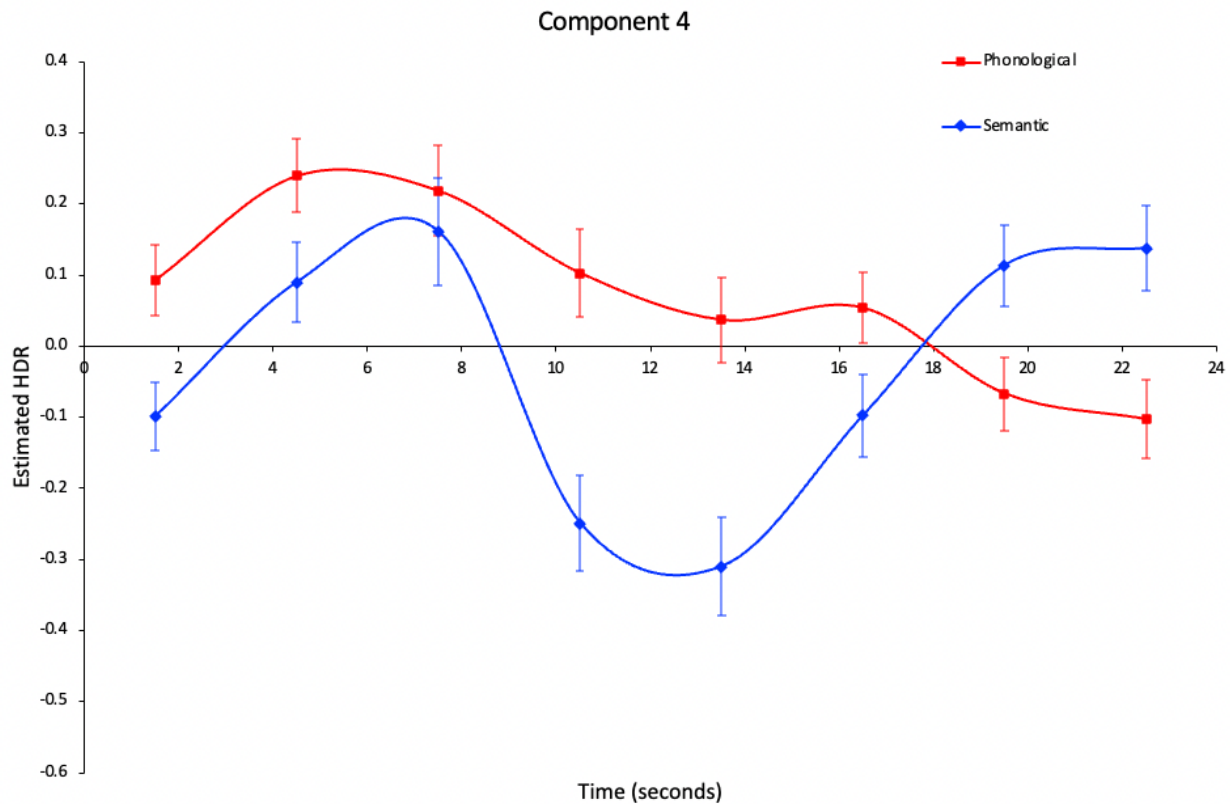
Note. HRFmax HDR averaged over Task (Phonolgoical_Semantic and Group (Healthy_Schizophrenia).

In the merged MS-TGT study, both NDMN and TDMN deactivation were observed. In the TDMN component, a significant main effect of Timebins, $F(7,539) = 5.78, p < .001$, and Condition, $F(1,77) = 68.03, p < .001$, were observed. A significant interaction between Condition and Timebins emerged, $F(7,539) = 7.61, p < .001$. Between timebins 3 to 4, the Semantic condition showed a steeper decrease in TDMN deactivation, $F(1,77) = 9.47, p < .01$ (Figure 39). During timebins 5-6, the Semantic condition also showed a steeper increase deactivation, Semantic showed a steeper decrease in TDMN deactivation $F(1,77) = 4.42, p < .05$. Between timebins 6-7, the Semantic condition increased in deactivation while the Phonological condition decreased in deactivation, $F(1,77) = 8.75, p < .01$. Overall, Semantic showed greater fluctuations in TDMN deactivation.

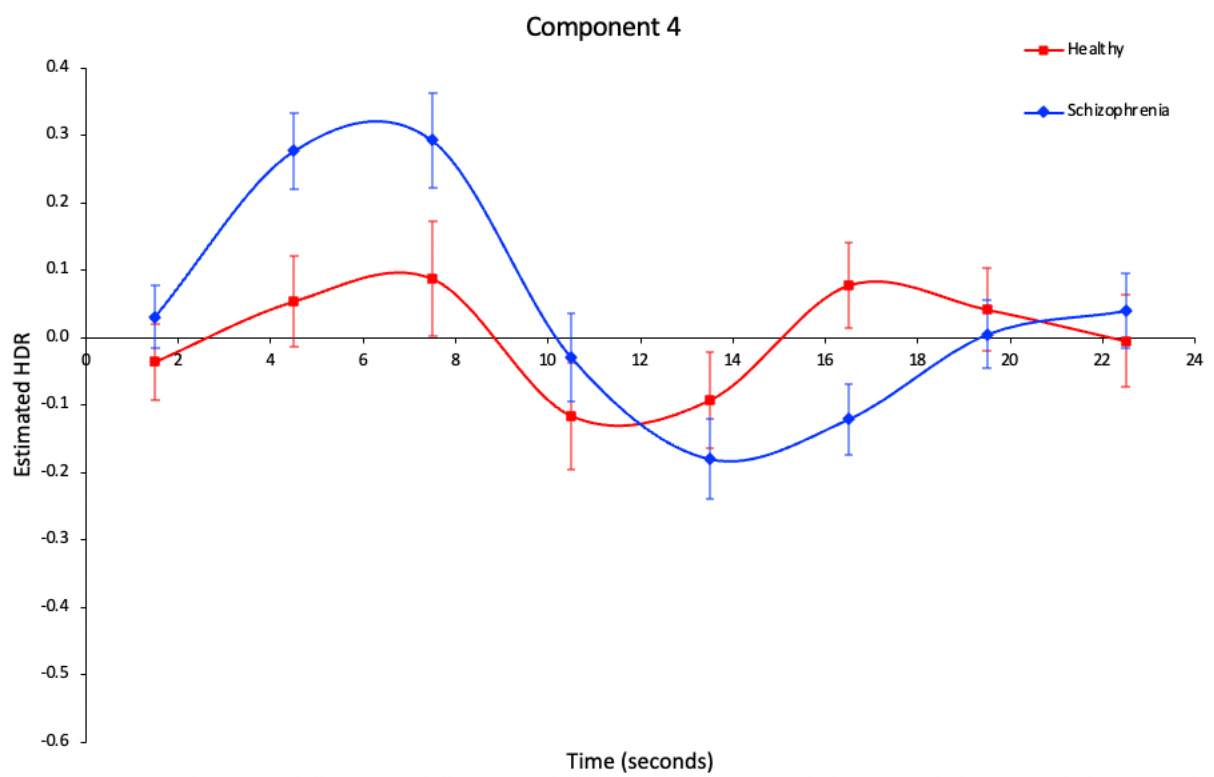
A group interaction was also observed between Group \times Timebins, $F(7,539) = 2.43$, $p < .05$.

Between timebins 1-2, the Schizophrenia showed greater increase in TDMN deactivation (Figure 40). Overall, the patients cohort showed greater TDMN Deactivation than the healthy controls.

Figure 39



Note. Varimax HDR for Condition (Phonological_Semantic) averaged over Group (Healthy_Schizophrenia).

Figure 40

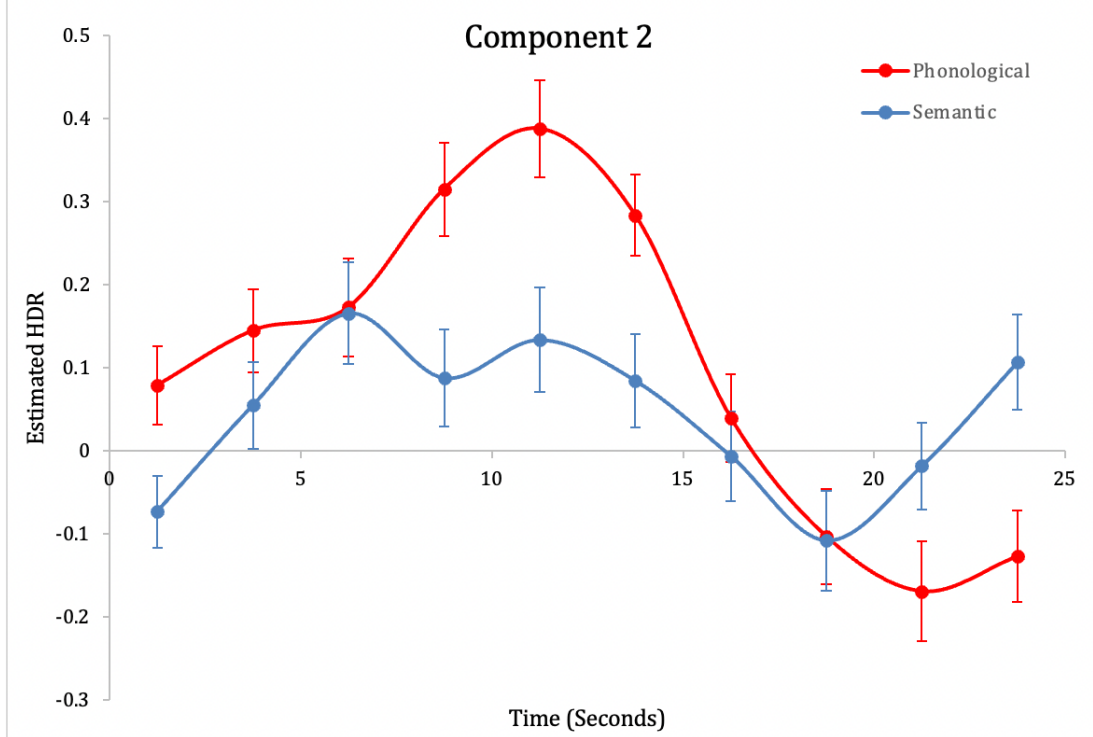
Note. Varimax HDR for Group (Healthy_Schizophrenia), averaged over Condition (Phonological_Semantic).

In the MS-TGT-SA, repeated ANOVA measures revealed a main effect of Timebins, $F(9,693) = 8.81, p < .001$, and Condition, $F(1,77) = 50.54, p < .001$. A significant interaction emerged between Condition \times Timebins, $F(9,693) = 4.66, p < .001$. Between timebins 3-4, the Phonological condition increased in TDMN deactivation while Semantic condition decreased (Figure 41), with the phonological condition reflecting a later HDR peak.

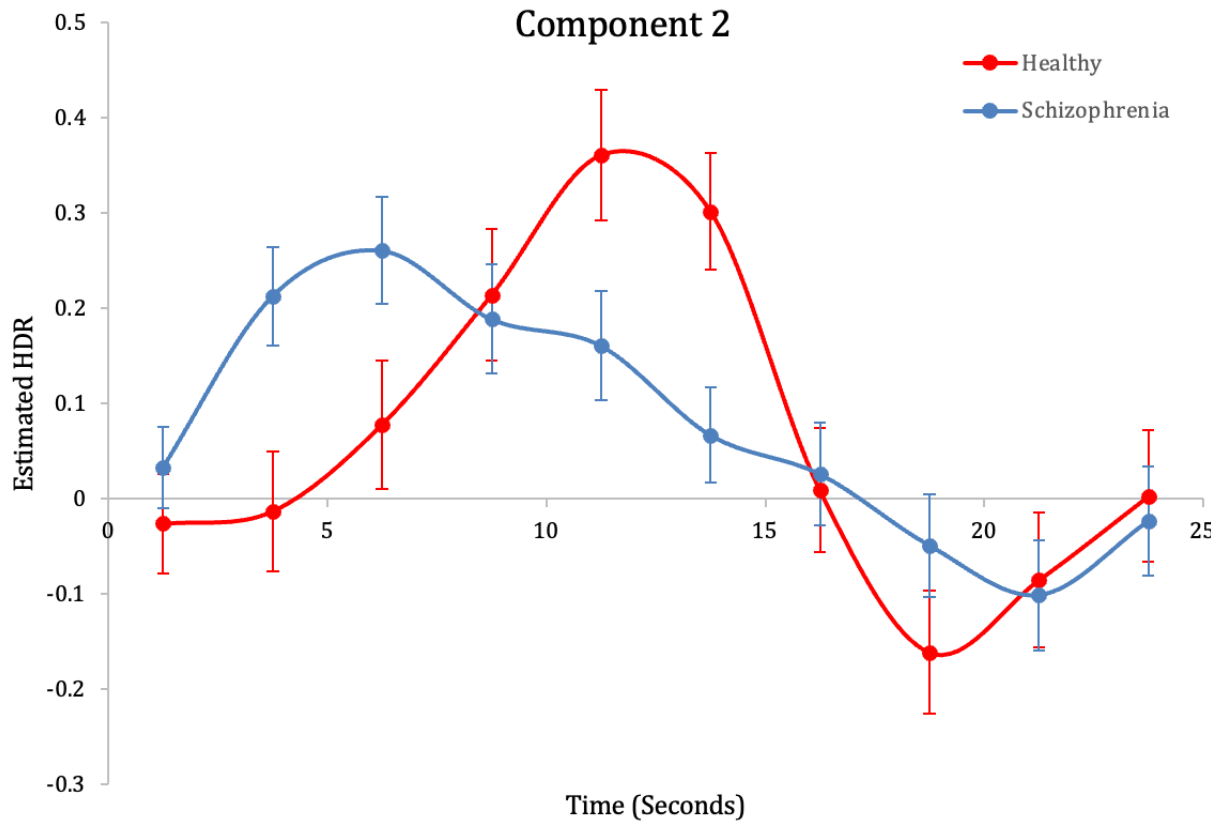
A Group \times Timebins also emerged, $F(9,693) = 2.91, p < .01$. Between timebins 1-2, schizophrenia patients showed a greater increase in TDMN deactivation, $F(1,77) = 6.66, p < .05$ (Figure 42). Between timebins 3-4, schizophrenia patients decreased in deactivation while healthy controls showed increase in deactivation. Between timebins 6-7, the healthy controls showed a

steeper decrease in deactivation, $F(1,77) = 8.06, p < .01$. In general, the healthy controls showed a delay HDR peak and greater deactivation.

Figure 41



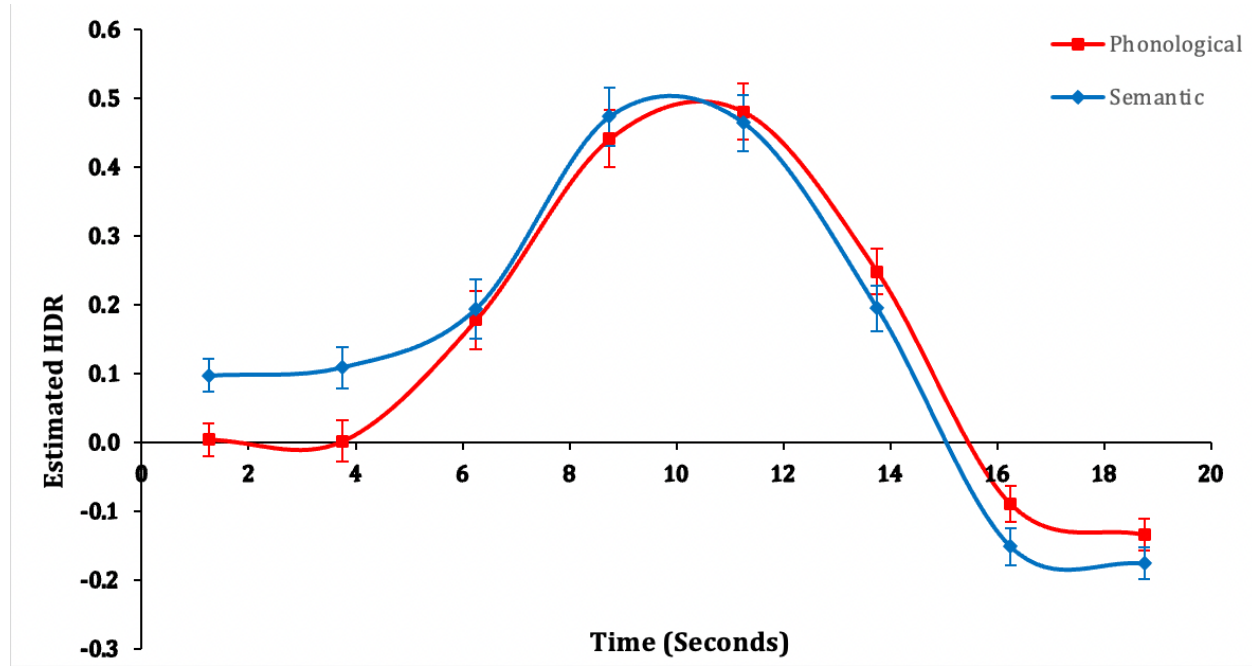
Note. Varimax HDR for Condition (Phonological_Semantic), averaged over Group (Healthy_Schizophrenia).

Figure 42

Note. Varimax HDR for Group (Healthy_Schizophrenia), averaged over Condition (Phonological_Semantic).

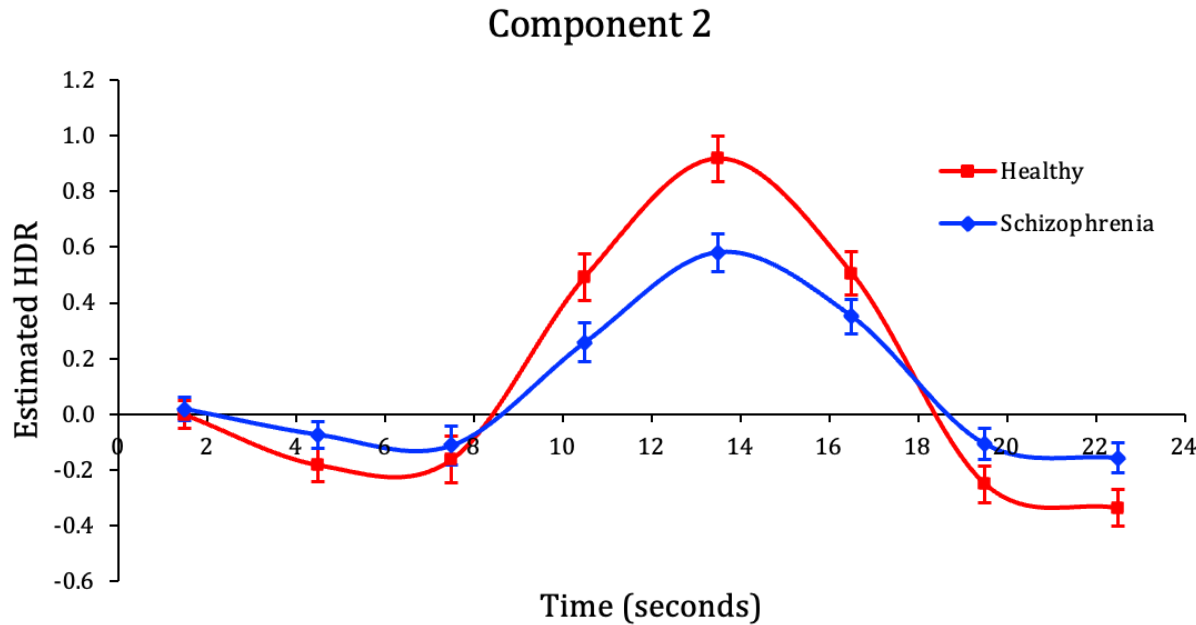
2.9.2 NDMN deactivation in the MS Task

In another component of Lariviere et al.'s study (2020), NDMN deactivation was observed. Repeated ANOVA measures revealed a significant main effect of Timebins, $F(7,539) = 77.43, p < .001$, and a significant interaction between Condition \times Timebins, $F(7,539) = 2.50, p < .05$ (Figure 43), suggesting that different NDMN deactivation levels were observed depending on the condition. No significant group effects were detected.

Figure 43

Note. Condition (Phonological_Semantic) HRFmax HDR averaged over Group (Healthy_Schizophrenia).

In the NDMN component of MS-TGT, a significant main effect of Timebins, $F(7,539) = 58.00, p < .001$, and Condition, $F(1,77) = 7.91, p < .01$, were observed. A significant interaction emerged between Group \times Timebins, $F(7,539) = 3.99, p < .001$. Between timebins 3-4, the Healthy controls showed a steeper increase in NDMN deactivation compared to schizophrenia patients, $F(1,77) = 6.05, p < .05$ (Figure 44). Similarly, the controls also showed a steeper decrease in deactivation between timebins 6-7 compared to patients, $F(1,77) = 6.40, p < .05$. Overall, the healthy controls showed a greater peak in NDMN deactivation.

Figure 44

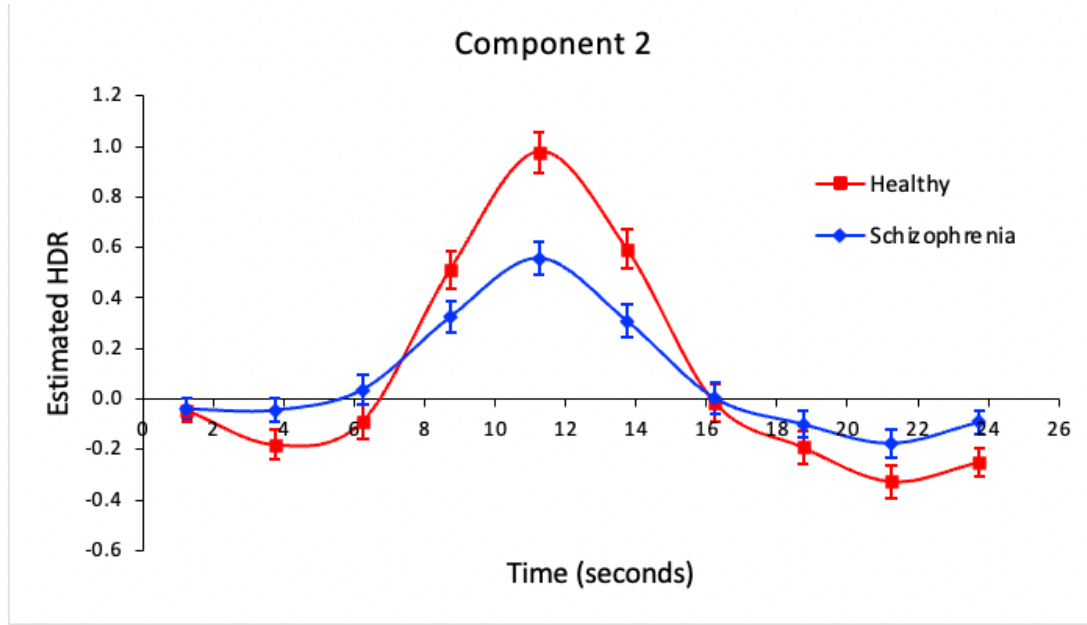
Note. Varimax HDR for Group (Healthy_Schizophrenia), averaged over Condition (Phonological_Semantic).

2.9.3 MS in MS-SA Task HDR

NDMN deactivation was observed in this study. Repeated ANOVA measures revealed a significant main effect of Timebins, $F(9,693) = 55.92, p < .001$, and Condition, $F(1,77) = 19.72, p < .001$. The average activity of the Phonological condition ($M = 0.101$) showed greater NDMN deactivation than the Semantic condition ($M = 0.075$). A significant interaction was observed between Timebins \times Group, $F(9,693) = 5.25, p < .001$. Between timebins 1-2, schizophrenia patients showed a relatively constant level of NDMN deactivation while the healthy controls showed a slight decrease, $F(1,77) = 4.02, p < .05$ (Figure 45). Between timebins 3-4, the healthy controls showed a sharper increase in NDMN deactivation than schizophrenia patients, $F(1,77) = 9.59, p < .01$. Similarly, between timebins 6-7, the healthy controls showed a sharper increase

relative to the patients cohort, $F(1,77) = 6.94, p < .05$. Relative to patients, the controls showed greater increase and decrease in NDMN deactivation, suggesting a group difference.

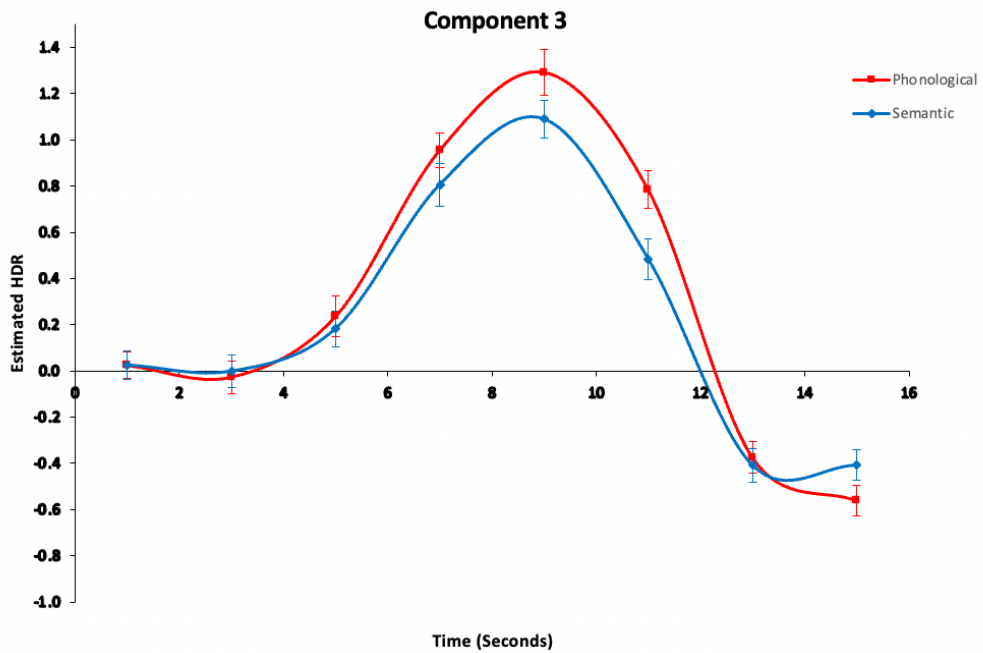
Figure 45



Note. Varimax HDR for Group (Healthy_Schizophrenia), averaged over Condition (Phonological_Semantic).

2.9.2 MS in fBRIN-MS-SA Task HDR

NDMN deactivation was observed in this task. Repeated ANOVA measures a significant main effect of Timebins, $F(7,546) = 91.67, p < .001$, and Condition, $F(1,78) = 39.06, p < .001$, where Phonological showed greater NDMN deactivation. This finding is consistent with MS-TGT and MS-TGT-SA. A significant interaction also emerged between Conditions \times Timebins, $F(7,546) = 2.11, p < 0.05$. Between timebins 6-7, the Phonological condition showed a steeper decline than the Semantic condition, $F(1,78) = 4.88, p < 0.05$ (Figure 46). Between timebins 7-8, the Semantic condition showed a slight increase in deactivation while the Phonological condition continued to decrease, $F(1,78) = 4.94, p < 0.05$. No group differences or interactions emerged.

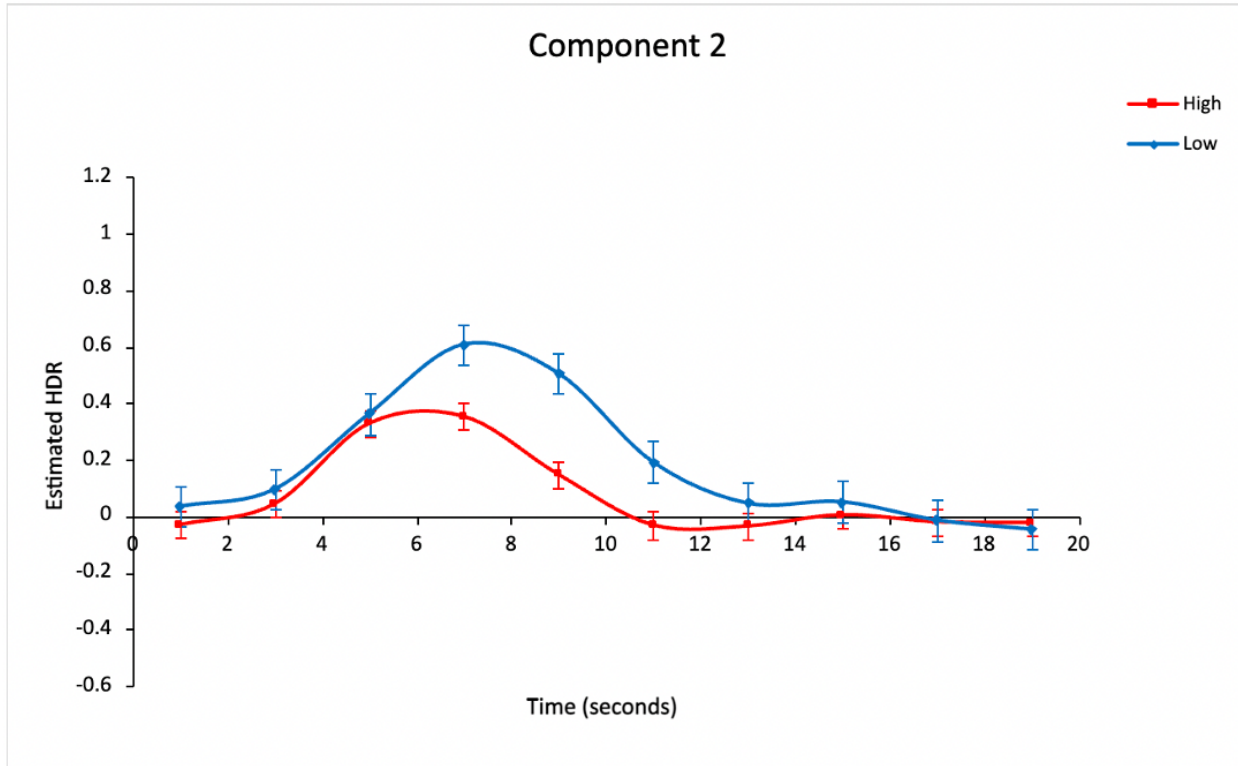
Figure 46

Note. Varimax HDR for Condition \times Timebins, averaged over Group (Healthy_Schizophrenia).

2.10 SA

2.10.1 Woodward et al.'s SA HDR

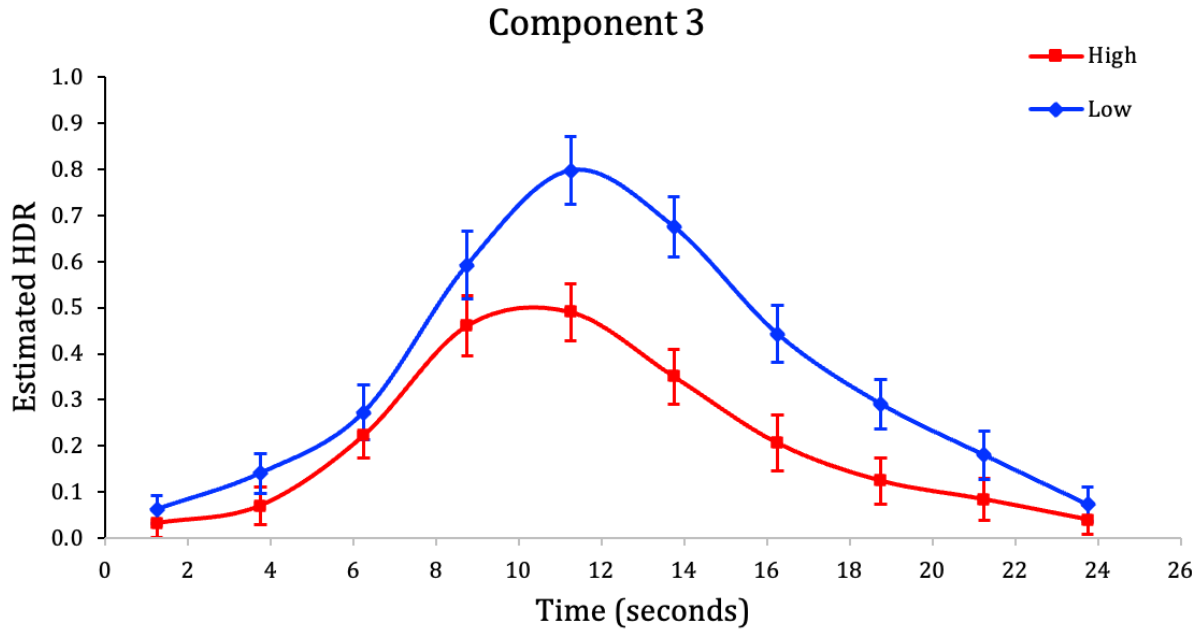
In Woodward et al.'s SA study (2015), TDMN deactivation was observed. Repeated ANOVA measures revealed a main effect of Timebins, $F(9,522) = 37.42, p < .001$, and Condition, $F(1,58) = 58.71, p < .001$. A significant interaction was observed between Conditions \times Timebins, $F(9,522) = 24.26, p < .001$. Between timebins 3-4, the Low SA condition continued to increase in TDMN deactivation while the High SA condition stayed relatively constant, $F(1,58) = 114.46, p < .001$ (Figure 47). Low SA the more difficult condition, showed a later peak than the easier condition. Between timebins 6-7, the Low SA condition decreased in TDMN deactivation while the High SA condition showed a slight rebound. No group differences emerged.

Figure 47

Note. Unrotated HDR for Condition (High_Low), averaged over Group (Healthy_Schizophrenia).

2.10.2 SA in TGT-SA HDR

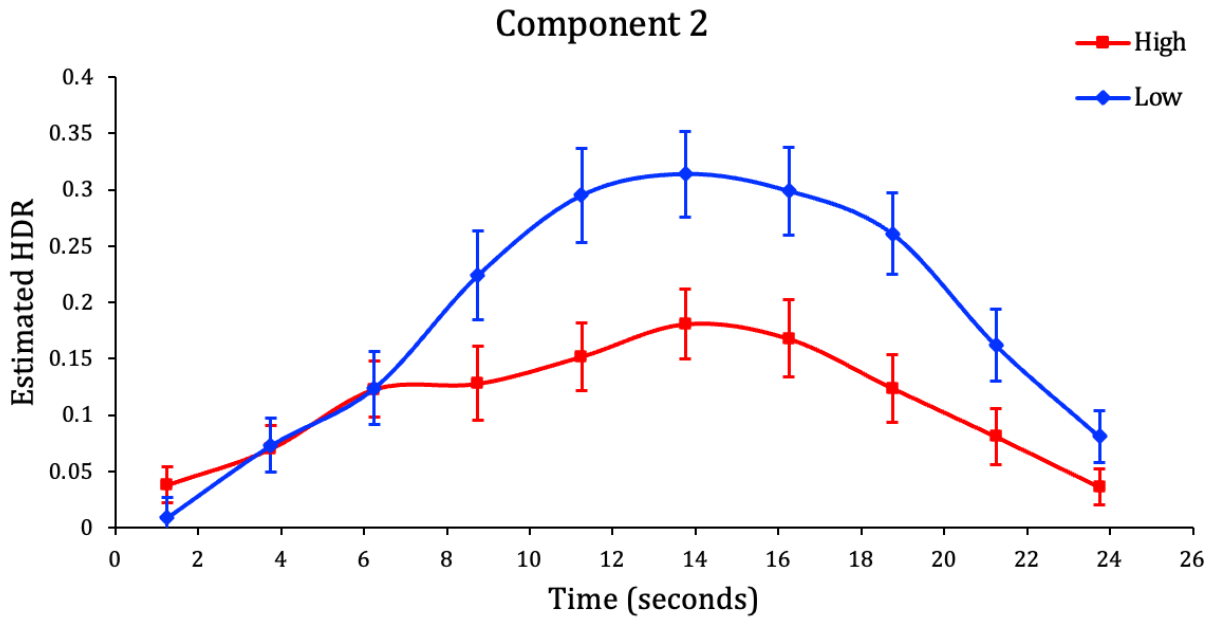
In the merged TGT-SA study, repeated ANOVA measures revealed a significant main effect of Timebins, $F(9,261) = 26.96, p < .001$, and Condition, $F(1,29) = 28.33, p < .001$. A significant interaction between Conditions \times Timebins, $F(9,261) = 8.79, p < .001$. Between timebins 3-4, Low SA showed a steeper increase in TDMN deactivation than High SA, the easier condition, $F(1,29) = 5.56, p < .05$ (Figure 48). Between timebins 4-5, a similar observation was observed, $F(1,29) = 30.61, p < .001$. Between timebins 6-7, the Low SA condition also showed a steeper decrease in TDMN deactivation than High SA, $F(1,29) = 4.31, p < .05$. Overall, the more difficult condition, Low SA, showed greater TDMN deactivation than conditions with a lighter cognitive load.

Figure 48

Note. Varimax HDR for Condition (High_Low), averaged over Group (Healthy_Schizophrenia).

2.10.3 SA in MS-SA HDR

NDMN deactivation was observed in this study. Repeated ANOVA measures revealed a significant main effect of Timebins, $F(9,495) = 9.88, p < .001$, and Condition, $F(1,55) = 37.35, p < .001$. The more difficult condition, Low SA ($M = 0.184$), showed greater NDMN deactivation than the High SA condition ($M = 0.110$). A significant interaction was observed between Conditions \times Timebins, $F(9,495) = 10.29, p < .001$. Between timebins 3-4, the High SA condition showed no change in deactivation showed an increase in deactivation, $F(1,55) = 23.15, p < .001$ (Figure 49). Between timebins 4-5, the Low SA condition showed a steeper increase in NDMN deactivation, relative to the High SA condition. Between timebins 8-10, the Low SA condition showed greater decreases in NDMN deactivation, $p < .05$.

Figure 49

Note. Varimax HDR for Condition (High_Low), averaged over Group (Healthy_Schizophrenia).

2.10.3 SA in fBIRN-MS-SA HDR

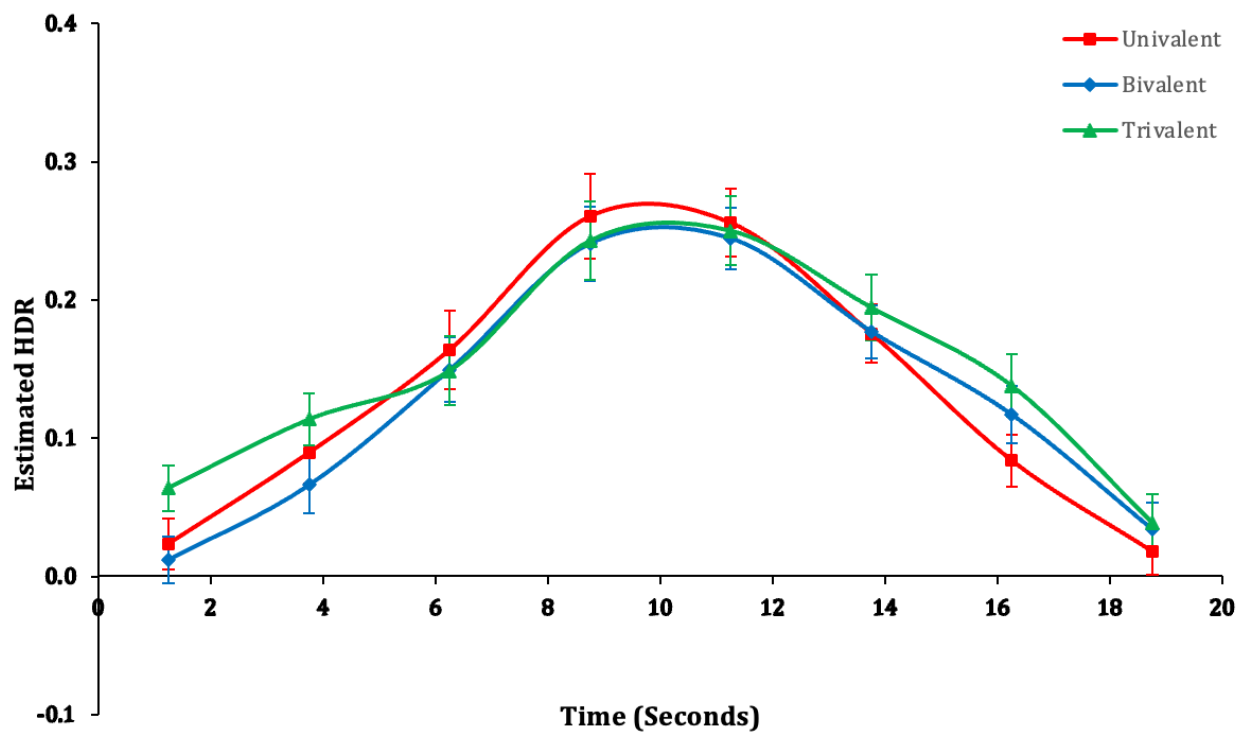
NDMN was observed. A main effect of Timebins, $F(7,399) = 37.85, p < .001$, and Condition, $F(1,57) = 56.27, p < .001$, were observed. The Low condition, the more difficult manipulation, showed greater NDMN deactivation. A significant interaction emerged between Conditions \times Timebins, $F(7,399) = 24.41, p < .001$. These findings are consistent with all the other SA studies analyzed in this report.

2. 11 MMCC HDR

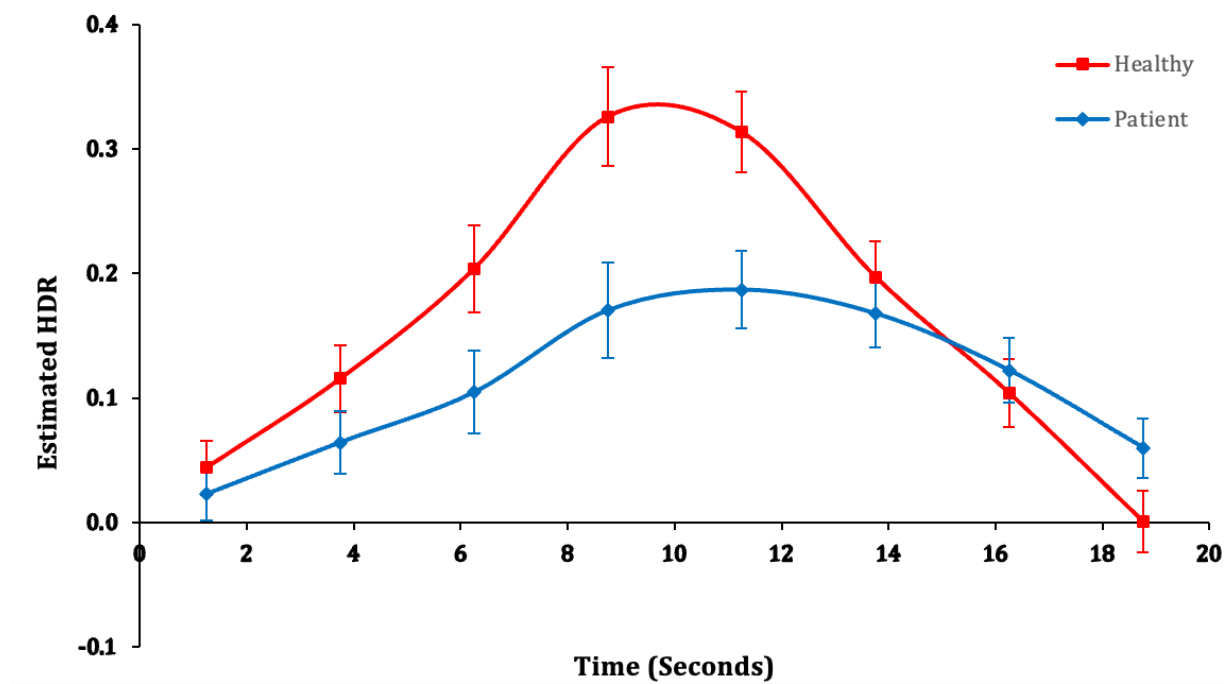
NDMN deactivation was observed in this component of the MMCC task. Repeated ANOVA measures revealed a significant main effect of Timebins, $F(7,294) = 24.91, p < .001$. A significant interaction was found between Valency \times Timebins, $F(14,588) = 3.01, p < .001$. Between timebins 6-7, the Univalent condition showed a steeper decrease in NDMN deactivation compared to the Bivalent condition, $F(1,42) = 5.24, p < 0.05$ (Figure 50). Between timebins 2-3,

the Bivalent condition showed a greater increase in deactivation compared to the Trivalent condition. A Group \times Timebins was also observed, $F(42) = 11.04, p < .01$. Between timebins 5-6, the Healthy group showed a greater decrease in deactivation, compared to the patient cohort, $F(42) = 11.04, p < .01$ (Figure 51). In general, the healthy controls showed greater NDMN deactivation.

Figure 50

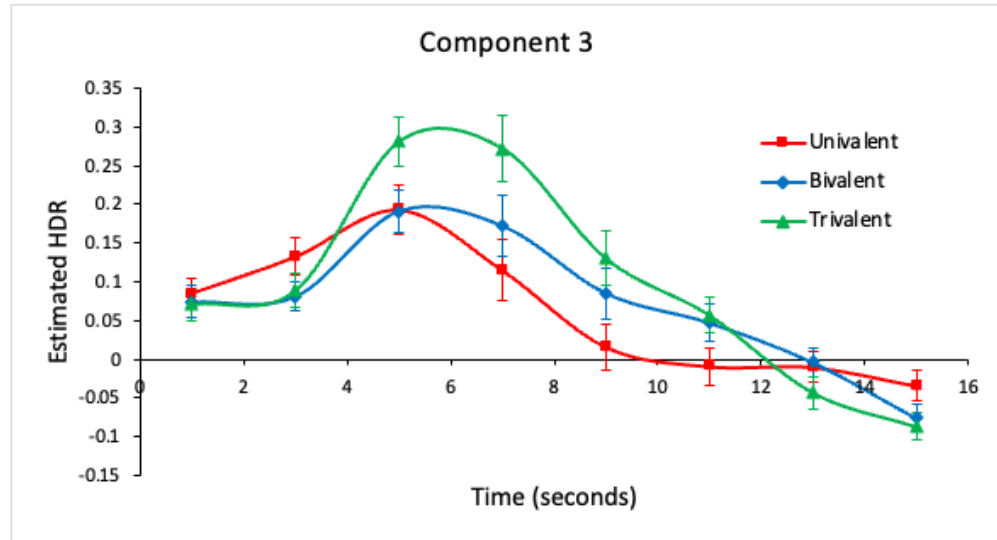


Note. Valency (Univalent_Bivalent_Trivalent) HRFmax HDR averaged over Groups (Healthy_Schizophrenia).

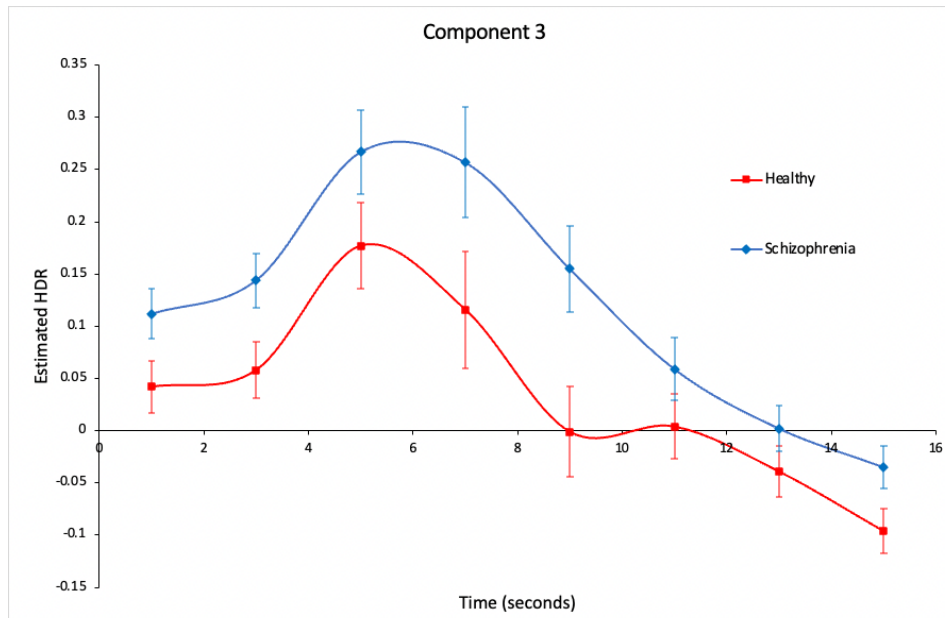
Figure 51

Note. Group HRFmax HDR averaged over Valency (Univalent_Bivalent_Triple).

In another component of the same study, TDMN deactivation was observed. A significant main effect of Timebins, $F(7,294) = 30.16, p < .001$, and Valency, $F(2,84) = 4.054, p < .05$ were observed. Repeated ANOVA measures also revealed a significant interaction between Valency \times Timebins, $F(14,588) = 15.18, p < .001$. Between timebins 1-2, the univalent condition showed an increase in deactivation while the other two conditions showed little changes, $F(1,42) = 8.04, p < .01$ (Figure 52). Between timebins 2-3, the trivalent condition showed a greater increase in deactivation than the bivalent condition, $F(1,42) = 15.48, p < .001$, suggesting that a higher cognitive load is associated with greater DMN deactivation. Although a main effect of group was observed $F(1,42) = 17.87, p < .05$ (Figure 53), there were no significant group interactions. Overall, the Schizophrenia patients showed greater TDMN deactivation, relative to the Healthy Controls.

Figure 52

Note. HRFmax HDR for Valency (Univalent_Bivalent_Trivalent) averaged over Group (Healthy_Schizophrenia).

Figure 53

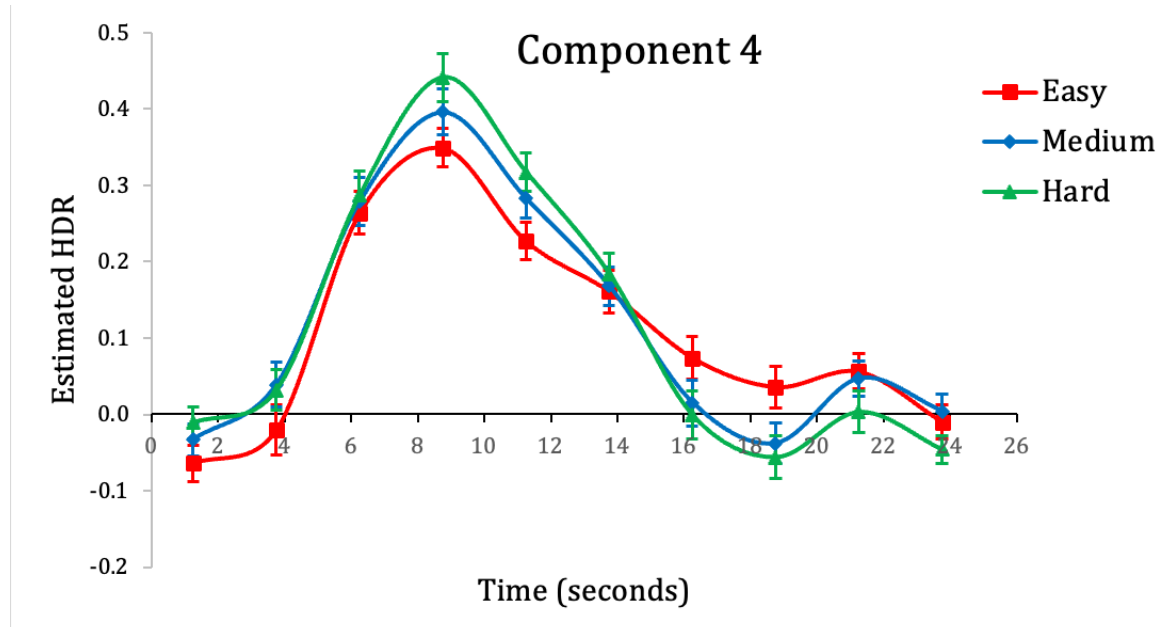
Note. HRFmax HDR for Group (Healthy_Schizophrenia), averaged over Valency (Univalent_Bivalent_Trivalent).

2.12 RSPM

2.12.1 Healthy RSPM HDR

TDMN deactivation was observed in this task. Repeated ANOVA measures revealed a significant main effect of Time, $F(9,495) = 52.90, p < .001$. A significant interaction between Difficulty \times Timebins was also observed, $F(18,990) = 2.35, p = .001$ (Figure 54). Between timebins 6-7, Medium difficulty showed a sharper decrease in condition compared to the Easy condition, $F(1,55) = 5.13, p < .05$. Between timebins 8-9, the Easy condition showed a smaller increase in deactivation than the Medium condition, $F(1,55) = 4.21, p < .05$.

Figure 54



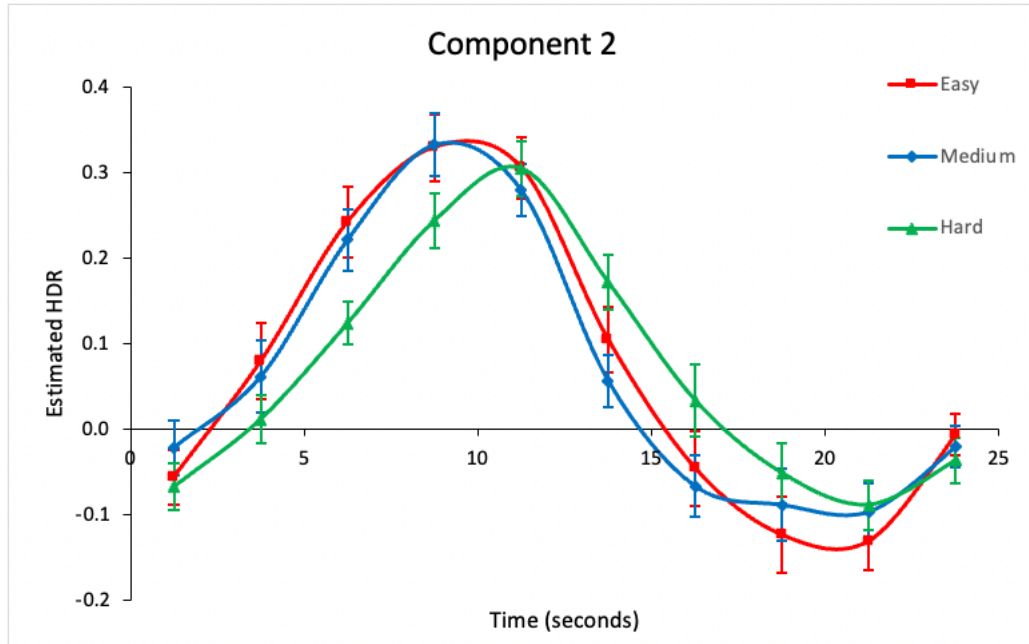
Note. HRFmax HDR for Difficulty (Easy_Medium_Hard).

2.12.2 Bipolar RSPM HDR

TDMN deactivation was observed in this study. Repeated ANOVA measures revealed a significant main effect of Time, $F(9, 387) = 49.51, p < 0.001$. There was a significant interaction between Difficulty \times Timebins, $F(18,774) = 49.51, p = 0.01$. Medium difficulty showed increase

in deactivation while the Hard condition showed a decrease in deactivation between timebins 4 and 5, $F(18,774) = 12.53, p < 0.001$, Figure 55). The Hard condition therefore showed a later peak. Between timebins 5 and 6, Medium difficulty also showed a greater decrease in deactivation compared to the Hard condition, $F(18,774) = 12.86, p < 0.001$.

Figure 55



Note. HRFmax HDR for Difficulty (Easy_Medium_Hard), averaged over Group (Bipolar_Control)

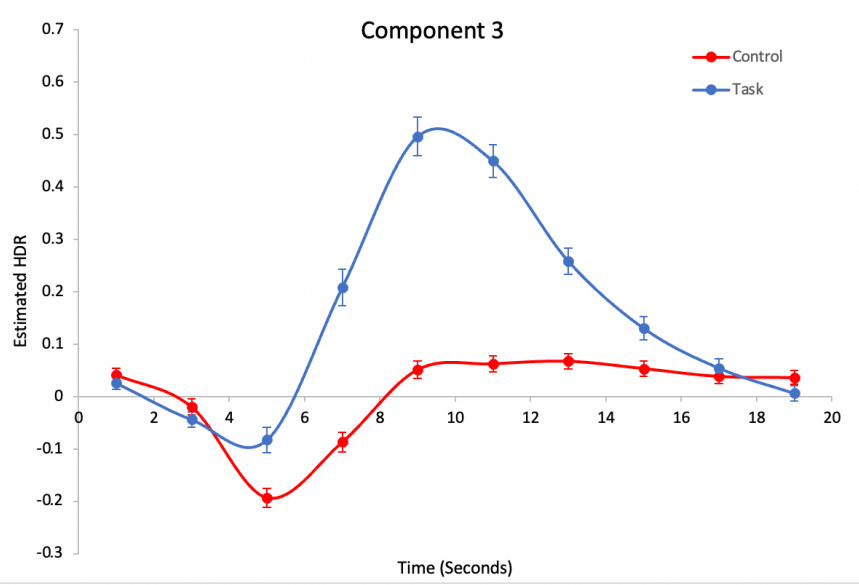
2.12.3 RSPM in LDT-RSPM HDR

TDMN deactivation was observed. Repeated ANOVA measures revealed a significant main effect of Time, $F(9, 360) = 21.09, p < 0.001$. No significant interactions/group effects were observed.

2.13 PAMENC HDR

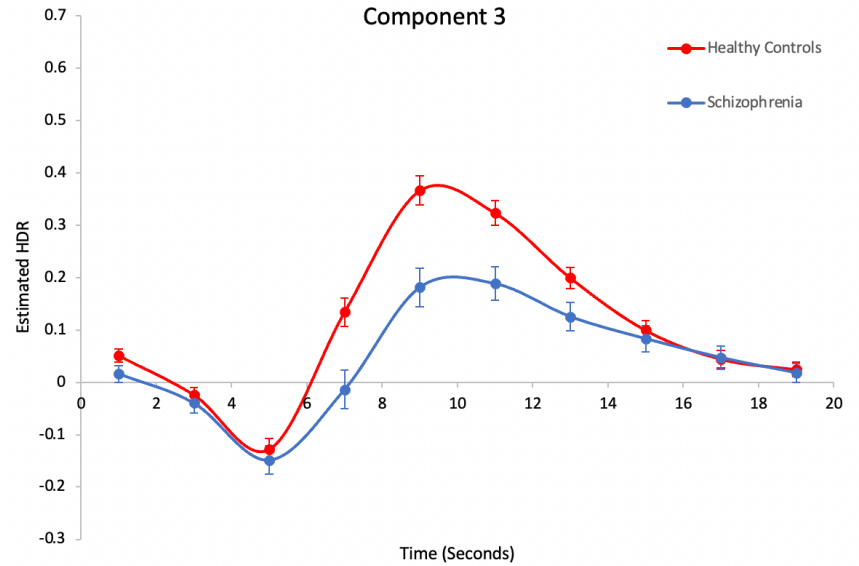
TDMN deactivation was observed in this task. Repeated ANOVA measures revealed a significant main effect of Timebins , $F(9,1080) = 84.54, p < .001$, and Condition, $F(1,120) = 91.64, p < .001$. A significant interaction emerged between Condition \times Timebins, $F(9,1080) = 78.92, p < .001$. Between timebins 3-5, the greater cognitive load condition, the Task condition, showed a greater increase in TDMN deactivation, $p < .001$ (Figure 56). Between timesbin 5-6, the Task condition showed a decrease in deactivation while the Control condition remained relatively constant. Between timebins 6-9, the Task condition continued to decrease in deactivation while the Control condition stayed relatively constant. Overall, a greater deactivation was observed in the Task condition, where participants had to actively form relationships between word pairs.

A main effect of Group was observed, $F(1, 120) = 8.93, p < .01$. A significant interaction also emerged between Group \times Timebins, $F(9,1080) = 6.25, p < .001$ (Figure 57). A three-way interaction was also seen between Group \times Condition \times Timebins, $F(9,1080) = 4.43, p < .001$. Between timebins 3-4, the Task conditions showed a greater increase in TDMN deactivation than the Control conditions, $F(1,120) = 4.20, p < .05$ (Figure 58). A similar pattern was observed between timebins 4-5, $F(1,120) = 4.02 p < .05$. Between timebins 7-8, the Schizophrenia_Control cohort showed a relatively constant level of deactivation while all other conditions continued to decrease in deactivation, $F(1,120) = 5.49, p < .05$. Overall, the patient cohort showed less TDMN deactivation in both conditions, relative to the Healthy cohort.

Figure 56

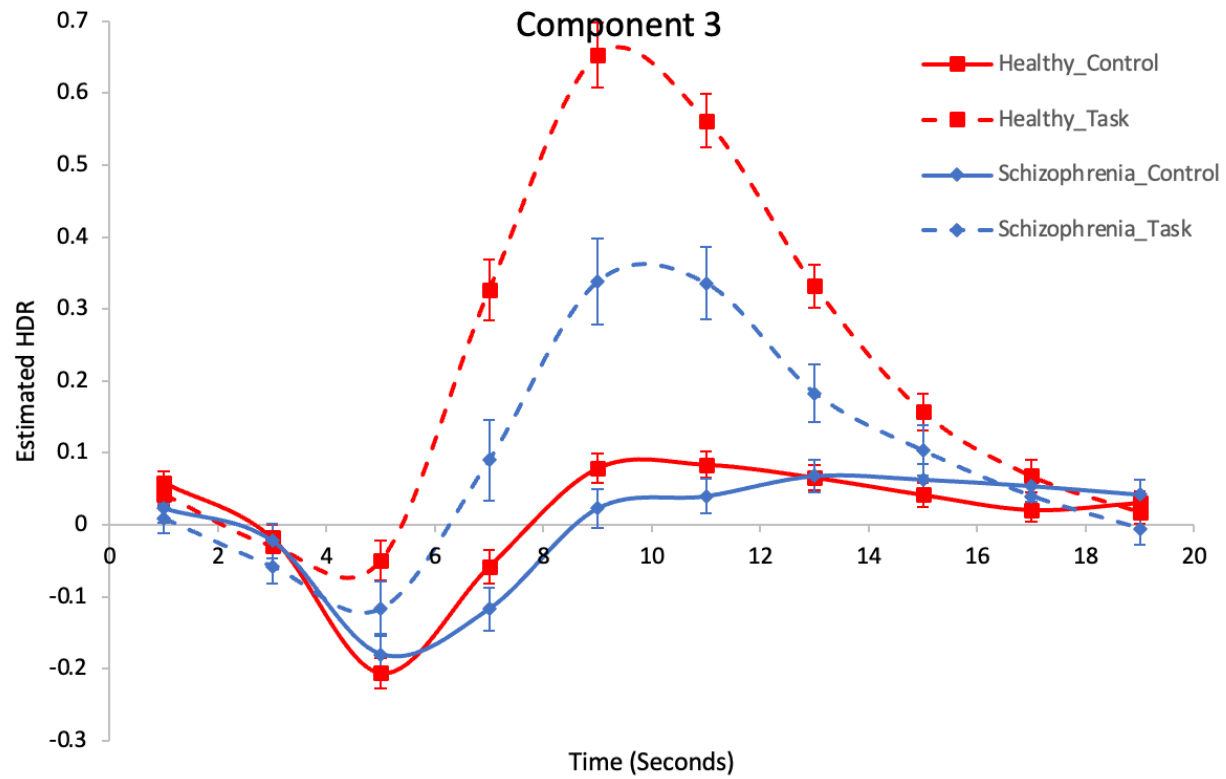
Note. HRFmax HDR for Condition (Control_Task) averaged over Group

(Healthy_Schizophrenia)

Figure 57

Note. HRFmax HDR for Group (Healthy_Schizophrenia) averaged over

Condition (Control_Task).

Figure 58

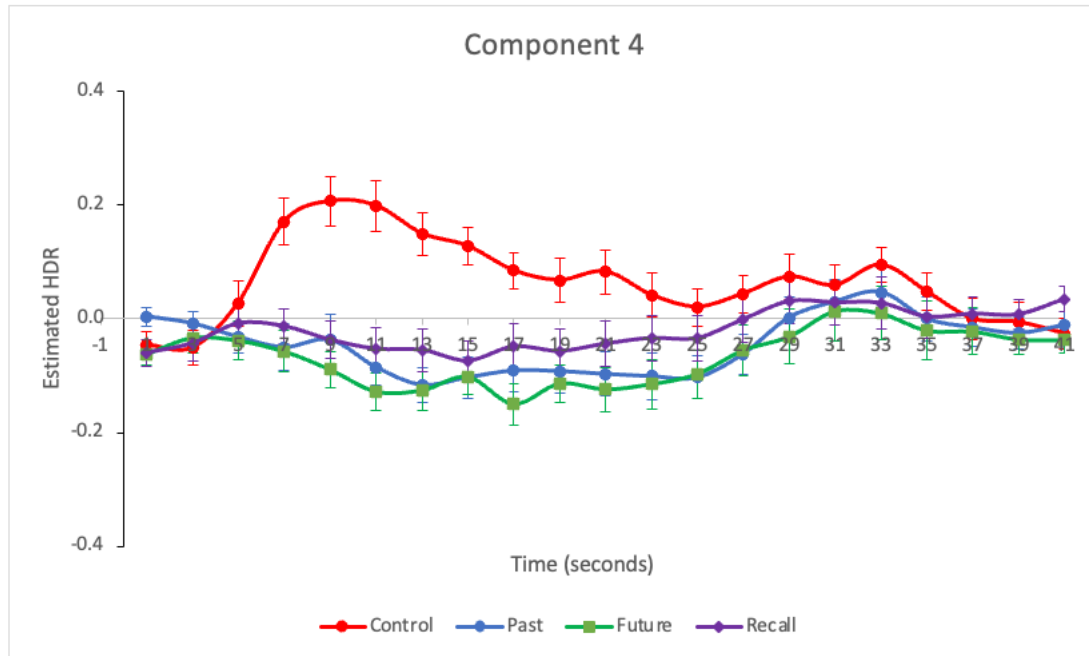
Note. HRFmax HDR for Group (Healthy_Schizophrenia) \times Condition (Control_Task) \times Timebins.

2.14 Addis HDR

TDMN deactivation was observed in this task. Repeated ANOVA measures revealed a significant main effect of Timebins, $F(20,320) = 4.26, p < .001$, and Condition, $F(3,48) = 35.92, p < .001$. A significant interaction emerged between Condition \times Timebins, $F(60,960) = 8.77, p < .001$. Between timebins 2-4, the Control condition increased in TDMN deactivation compared to the other conditions, $p < .001$ (Figure 59). Between timebins 4-5, the Past condition showed a slight increase in deactivation while the Future condition continued to decrease, $F(1,16) = 7.02, p < .05$. A similar trend was observed between timebins 8-9, $F(1, 16) = 4.86, p < .05$.

Simultaneously, the Future condition decreased in deactivation while the Recall condition increased in deactivation. Overall, the Control condition showed greater TDMN deactivation compared to the other 3 conditions, supporting the idea that the DMN is activated during daydreaming/recalling.

Figure 59



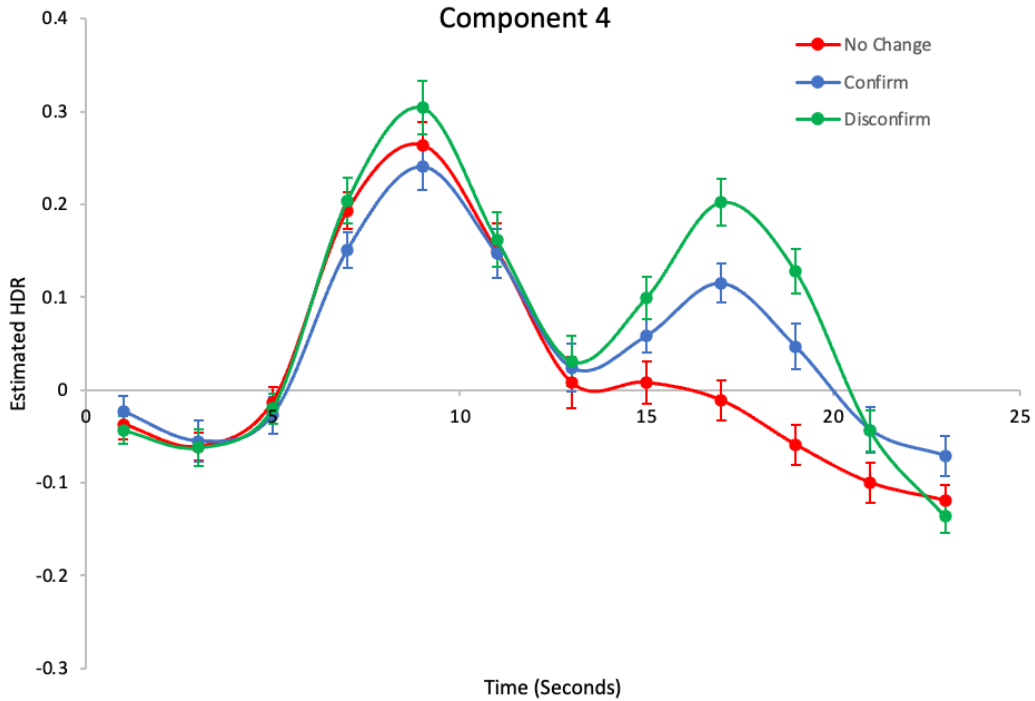
Note. Varimax HDR for Condition (Control_Past_Future_Recall).

2.15 ABADE HDR

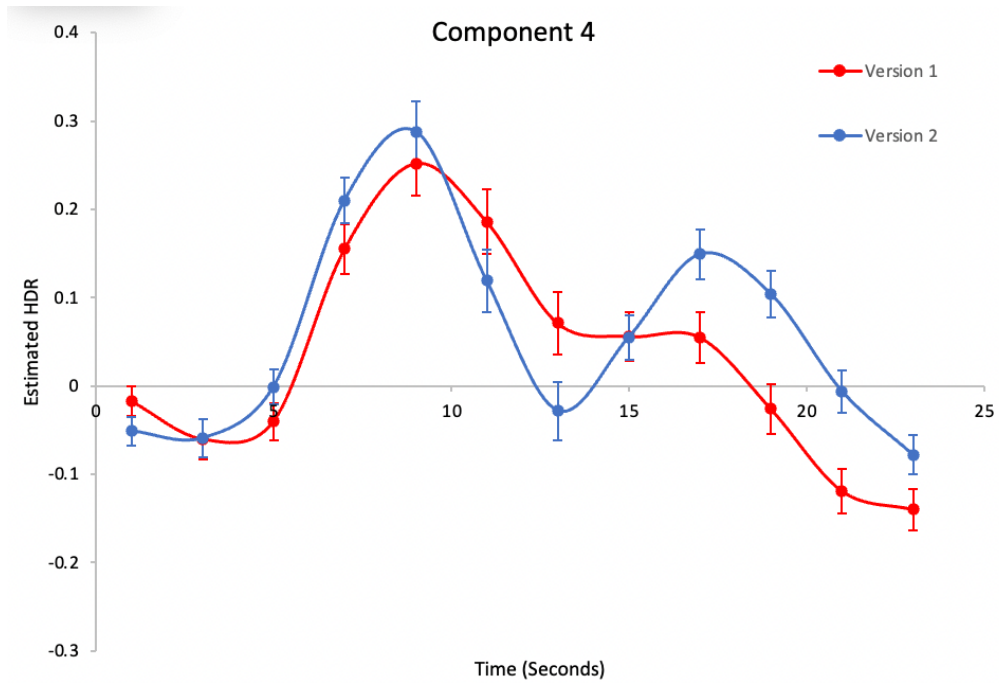
TDMN deactivation was observed in this task. Repeated ANOVA measures a significant main effect of Timebins, $F(11,374) = 56.30, p < .001$, and Condition, where the Disconfirm condition showed the greatest TDMN deactivation, $F(2,68) = 14.95, p < .001$. A significant Condition \times Timebins interaction emerged, $F(11,374) = 5.43, p < .001$. Between timebins 8-9, the No Change condition showed a slight decrease in TDMN deactivation while the Confirm condition increased to another peak, $F(1,34) = 16.23, p < .001$ (Figure 60). Between timebins 10-

11, the Confirm condition showed a steeper decline in deactivation relative to the No Change condition, $F(1,34) = 8.13, p < .01$. The Disconfirm condition showed a steeper increase in deactivation between timebins 3-4, $F(1,34) = 4.85, p < .05$, and timebins 7-8, $F(1,34) = 7.88, p < .01$. It also showed a steeper decline in deactivation relative to the Confirm condition between timebins 5-6, $F(1,34) = 9.09, p < .01$, and timebins 11-12, $F(1,34) = 11.20, p < .01$. Overall, the Disconfirm condition showed greater TDMN deactivation, as supported by the higher HDR peak.

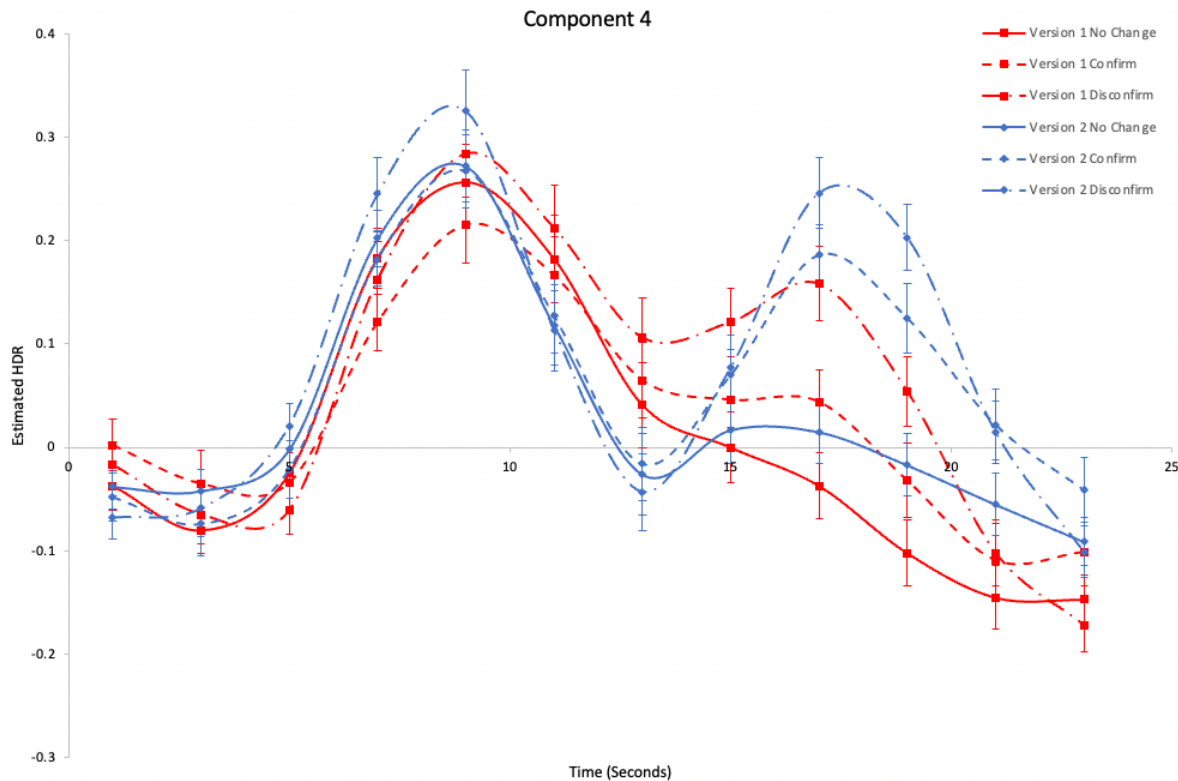
A Group \times Timebins interaction also emerged, $F(11,374) = 5.43, p < .001$. Between timebins 5-6, Version 2 showed a greater decrease in deactivation compared to the Version 1 cohort, $F(1,34) = 10.56, p < .01$ (Figure 61). During timebins 7-8, Version 2 showed an increase in deactivation while Version 1 stayed relatively constant, $F(1,34) = 12.21, p < .01$. Overall, Version 2 showed greater TDMN deactivation than Version 1. A three-way interaction was observed between Group \times Condition \times Timebins, $F(22,748) = 1.71, p < .05$. Between timebins 8-9, both Version 1_No Change and Version 2_No Change decreased in deactivation (Figure 62). However, Version 2_Confirm increased in deactivation while Version 1_Confirm decreased in deactivation, $F(1,34) = 4.96, p < .05$.

Figure 60

Note. HRFmax procrustes for Condition (No Change_Confirm_Disconfirm) averaged over Group (Version 1_Version 2).

Figure 61

Note. HRFmax procrustes for Group (Version 1_Version 2) averaged over Condition (No Change_Confirm_Disconfirm).

Figure 62

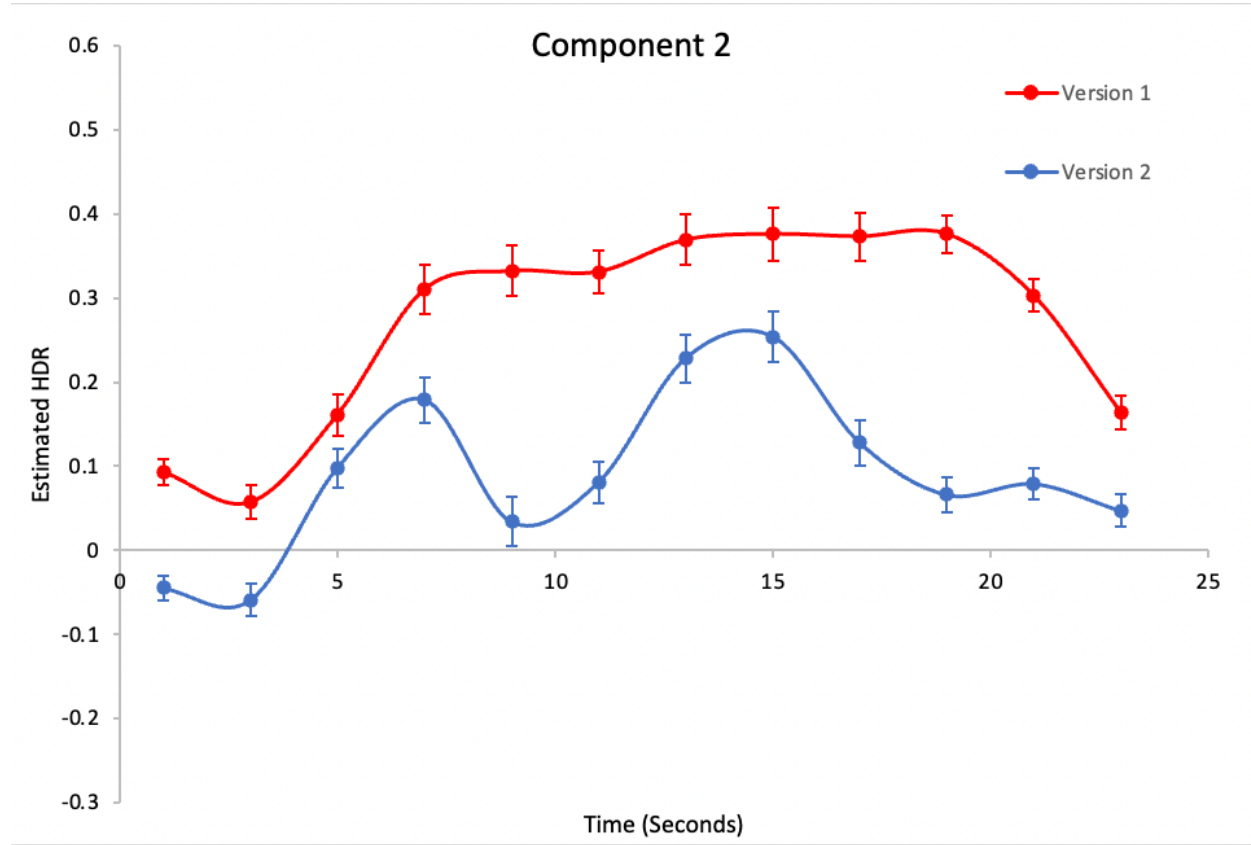
Note. HRFmax procrustes for Group (Version 1_Version 2) \times Condition (No Change_Confirm_Disconfirm).

In another component of the same study, TDMN was also observed. Similarly, a main effect of Timebins, $F(11,374) = 55.99, p < .001$, and a significant interaction between Condition \times Timebins, $F(22,748) = 3.57, p < .001$.

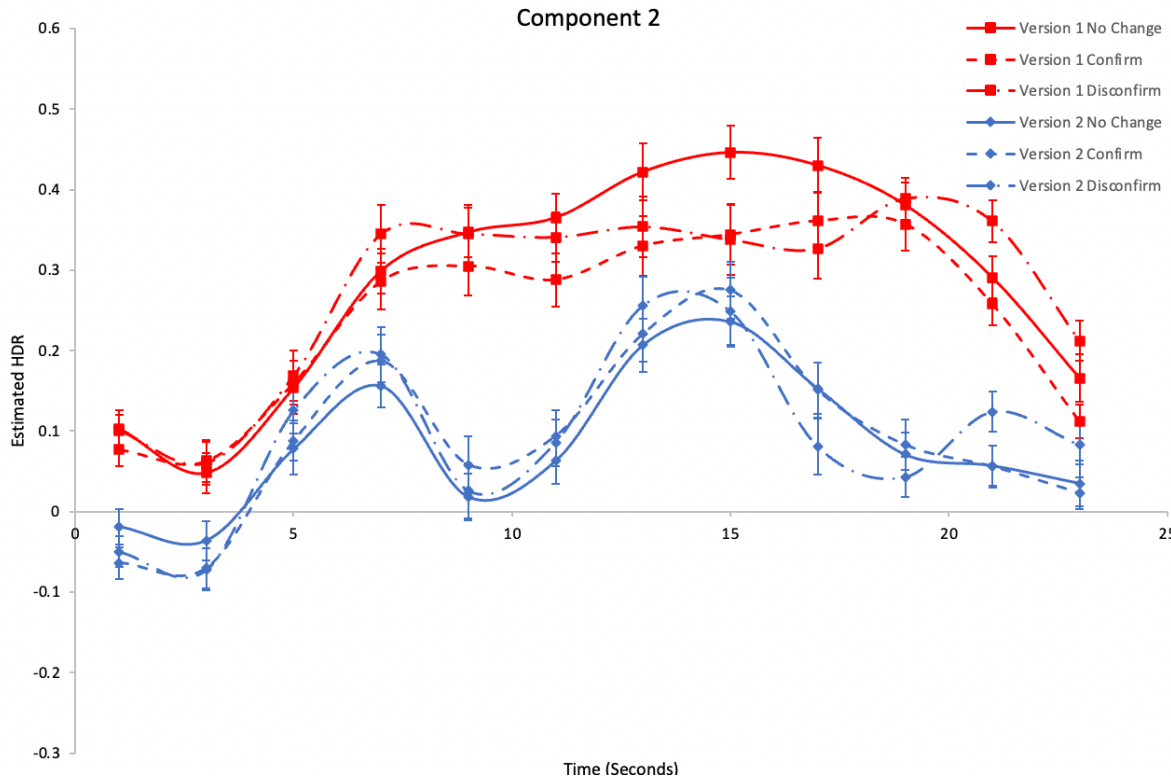
Unlike the other component, a significant main effect of Group was found, where TDMN deactivation was higher for Group 2, $F(1,34) = 58.39, p < .001$, as supported by the overall higher HDR activity (Figure 63). A three-way interaction between Group \times Condition \times Timebins was also observed, where Version 2 \times Condition showed steeper increases in

deactivation relative to Version 1 \times Condition between timebins 6-7, $F(1,34) = 6.17, p < .05$ (Figure 64).

Figure 63



Note. HRF-procrustes for Group (Version 1_Version 2), averaged over Condition (No Change_Confirm_Disconfirm).

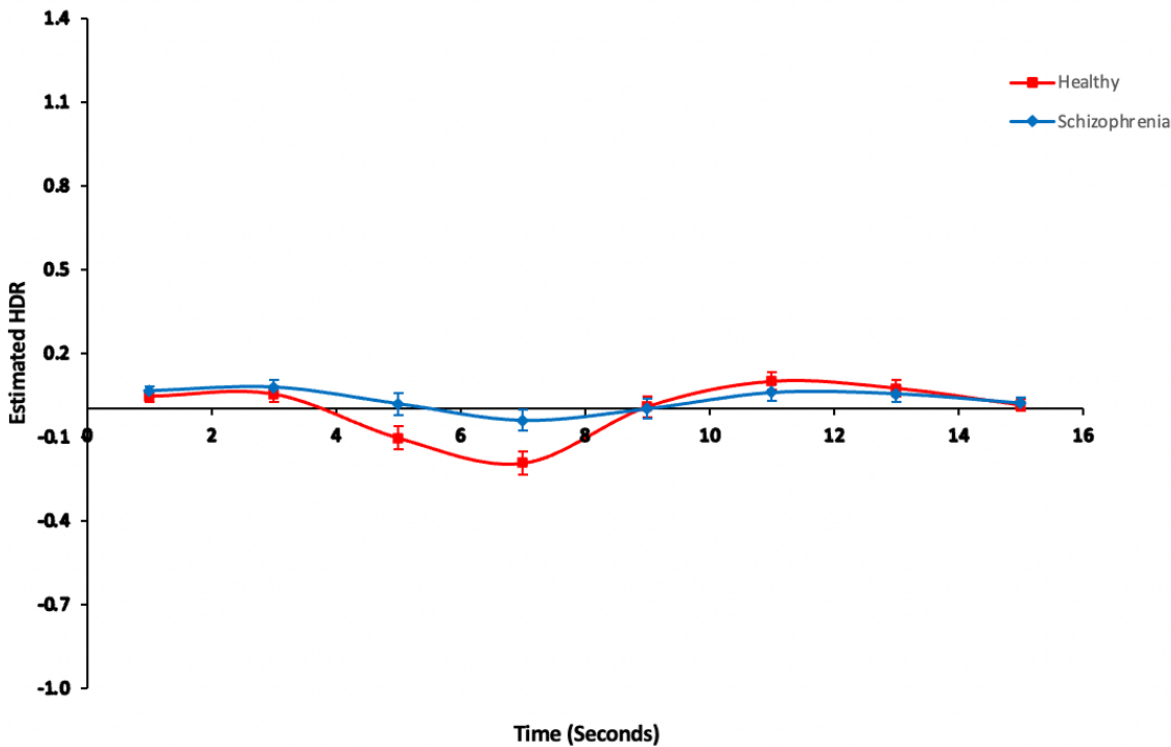
Figure 64

Note. HRFmax procrustes for Group (Version 1_Version 2) \times Condition (No Change_Confirm_Disconfirm).

2.16 fBIRN Oddball in fBIRN-MS-SA

Release of NDMN deactivation was observed when this task was merged with the MS and SA tasks. The analysis of fBIRN task revealed a z score < 0.20 . Therefore, the fBIRN stand-alone task is not analyzed in the present paper. When merged with the MS and SA tasks, ≥ 0.80 z scores were observed, so this is further discussed in the present paper.

The HDR plot showed an activation of the NDMN network until timebin 4. A significant interaction emerged between Group \times Timebins, $F(7, 742) = 3.00, p < .01$. Between timebins 4-5, the healthy controls patients showed a slightly greater release of NDMN activation compared to the patients, $F(1,106) = 12.46, p < .001$ (Figure 65).

Figure 65

Note. Varimax HDR for Group (Healthy_Schizophrenia) \times Timebins.

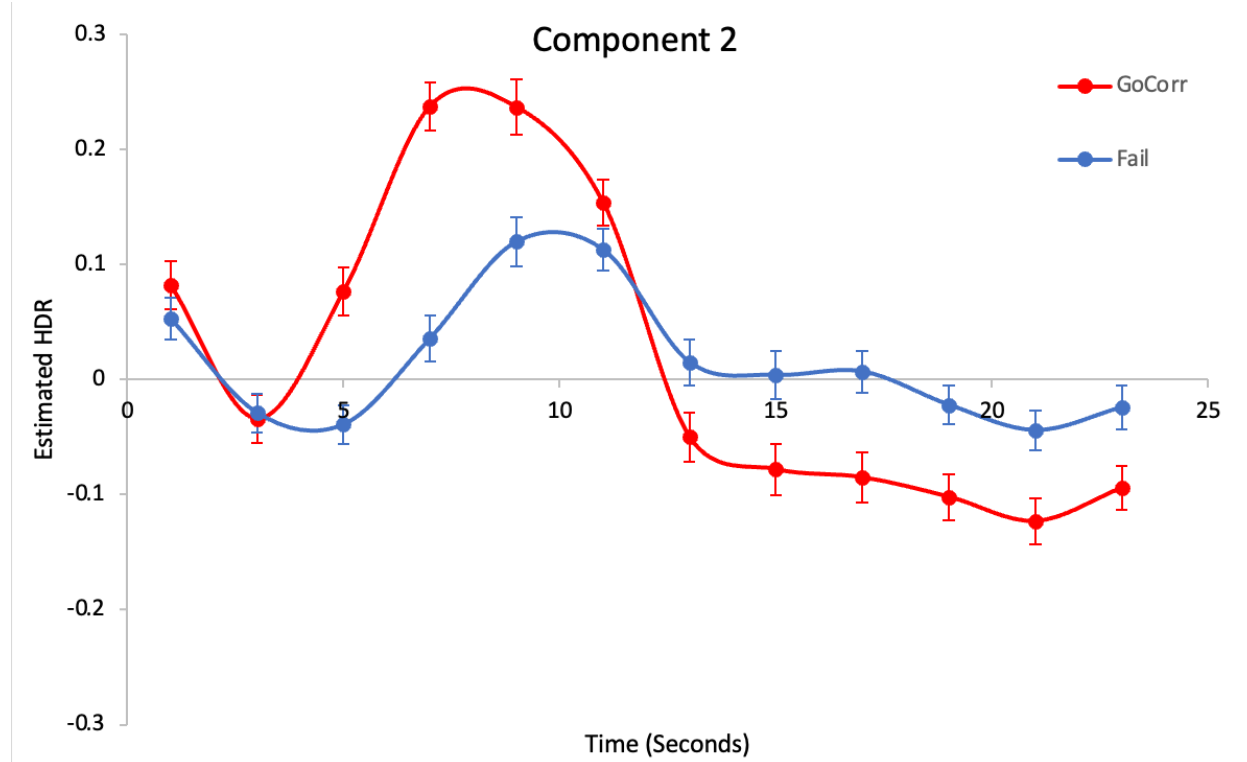
2.17 Alcohol STOP

NDMN was observed in this task. Repeated ANOVA measures revealed a main effect of Timebins, $F(11,1122) = 30.78, p < .001$. A significant interaction between GoCorr_Fail \times Timebins was observed, $F(11,1122) = 23.08, p < .001$. Between timebins 2-5, GoCorr showed greater NDMN deactivation compared to the Fail condition (all $p < .001$; Figure 66). This suggests NDMN was deactivated to a greater extent when the participants showed correct responses. Between timebins 5-6, GoCorr showed a greater decrease in deactivation compared to Fail, $F(1,102) = 10.26, p < .01$. A similar pattern was observed between timebins 6-7, $F(1,102) = 26.89, p < .001$.

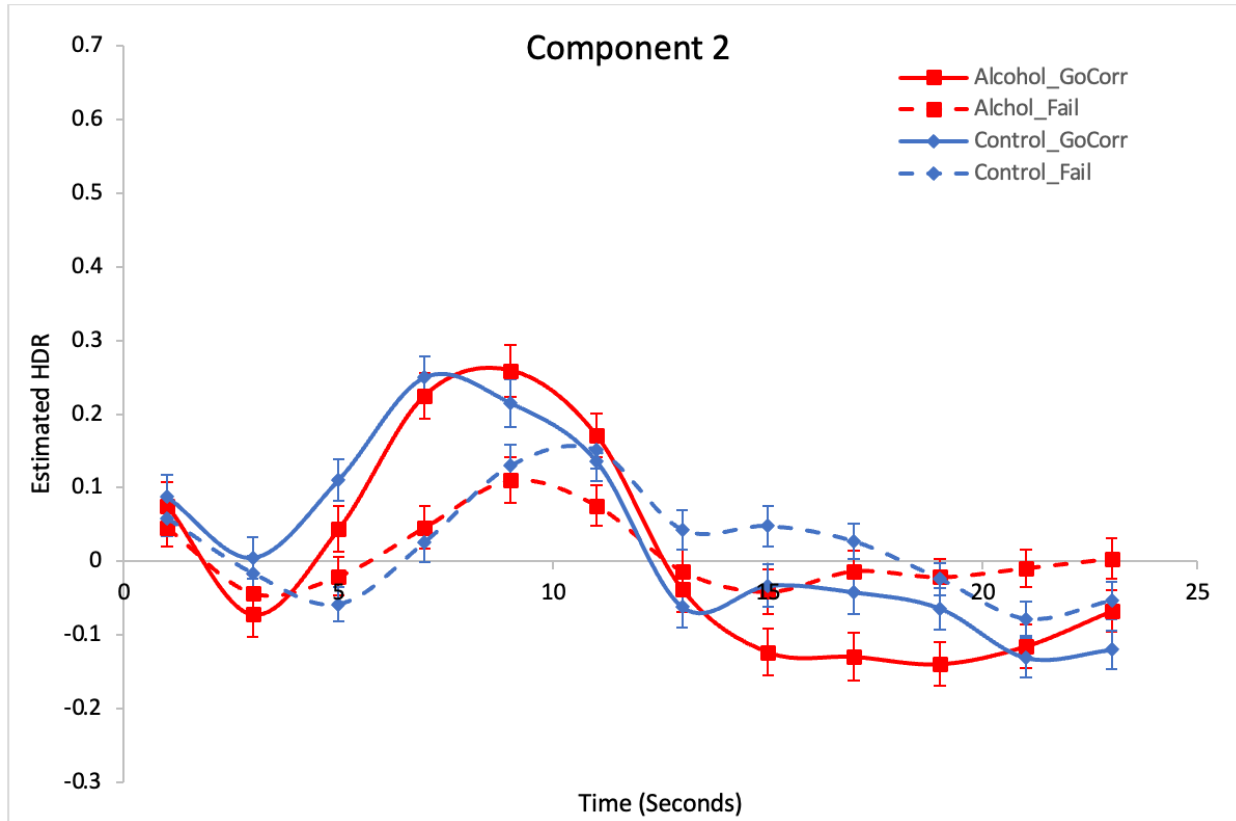
Although no significant main effect of Group was observed, a three-way interaction emerged between Group \times GoCorr_Fail \times Timebins, $F(11,1122) = 2.58, p < .01$. Between

timebins 4-5, Control_GoCorr showed a decrease in deactivation while all other conditions showed an increase, $F(1,102) = 5.91, p < .05$ (Figure 67). Between timebins 7-8, Control_GoCorr showed a slight increase while all the other conditions decreased in deactivation, $F(1,102) = 4.23, p < .05$

Figure 66



Note. Varimax HDR for GoCorr_Fail, averaged over Group (Alcohol_Control).

Figure 67

Note. Varimax HDR for GoCorr_Fail \times Group (Alcohol_Control).

Discussion

Classification Averages

An analysis of all the studies showed that when the components were categorized as 1RESP/INIT, the task-negative network that was often paired with them was the TDMN. This suggests that cognitive tasks that involve responses or initiation show TDMN deactivation simultaneously. In contrast, for tasks that involve internal attention, NDMN deactivation was often observed. For studies that involved LANG and EXT networks, both TDMN and NDMN deactivation were often seen. These findings suggest that depending on the task-positive network engaged, we are more likely to observe one DMN over the other (Table 1).

The Cognitive Load Hypothesis

As cognitive load increases, DMN deactivation increases. Numerous TDMN and NDMN studies analyzed in this paper support this hypothesis.

Cognitive Load and TDMN Deactivation

In Sanford's WM task (2019), greater TDMN deactivation was observed in the 6-letter condition, compared to the 4-letter condition (Figure 9). As the participants were required to hold more letters in their WM, greater TDMN deactivation was observed. This finding was also observed in the WM-TGT study, and the SCAP-TGT-TSI-WM study.

Sanford's SCAP task (2019) also showed greater TDMN deactivation with a greater delay and a greater number of dots (Figure 15). This supports the cognitive load hypothesis because a greater delay, in comparison to no delay, indicates that participants must hold the information longer, thereby exerting more cognitive resources. Similar to the WM task, the same effects were observed when SCAP was merged with three other tasks in the SCAP-TGT-TSI-WM study.

In the TSI-TGT study, the TSI portion showed greater TDMN deactivation for the incongruent conditions, particularly the word-reading ones (Figure 25). As word-reading is more cognitive-demanding, more deactivation was observed compared to the colour-naming trials. In the TSI portion of SCAP-TGT-TSI-WM, the Incongruent condition showed greater deactivation, as it was more cognitive-intensive.

In the SA study, greater TDMN deactivation was observed for word pairs that were further in semantic distance/lower association (Figure 47). As the relationships between word pairs become further and harder to associate with one another, cognitive demands proportionally increase, resulting in greater TDMN deactivation. Similar effects were seen when SA was

merged with TGT, where the Low conditions showed greater peaks compared to the High conditions (Figure 48).

In the PAMENC study, there was greater TDMN deactivation in the Task encoding condition relative to the Control condition (Figure 56). As the Control condition only involves identifying the side of the screen with an orange square, it does not involve any active encoding or memory processes. Thus, the Task encoding condition is the more difficult condition that involves active cognitive engagement.

From these studies, the hypothesis that TDMN deactivation increases with greater cognitive load is supported.

Cognitive Load and NDMN Deactivation

The same effects were observed when NDMN was detected in Sanford's TSI task, where the Incongruent condition showed greater deactivation.

In the MS task, greater mean NDMN deactivation was seen in the phonological condition, compared to the semantic one (Figure 43). This relates to the task condition where the participants have to pay attention to each syllable of the presented stimuli to determine where the metrical stress was placed on, as opposed to simply deciding if the word had a positive/negative connotation in the semantic condition. Thus, the MS task supports the cognitive load hypothesis.

In the LDT component where NDMN deactivation was observed, the greatest deactivation was observed in the Hard Word condition (Figure 35). While this may seem contradictory to the hypothesis, this phenomenon can be explained. The task-positive network engaged in this component, Language, is most strongly activated during the hard-word condition, and least activated in the non-word condition. As we interpret lexical representations, the language network should be engaged when real English words are encountered (Hard Word

condition) and suppressed when the stimuli do not represent real words (Non-Word condition). It is inferred that the activity of the language network dominates over that of the DMN in this component and NDMN was consequently masked by LANG. Therefore, it is unsurprising that the DMN activity observed in this component seems contradictory to the hypothesis.

Other experiments analyzed in the present paper also lend support to the cognitive load hypothesis. For instance, In Metzak's WM task, as cognitive load increased, more NDMN deactivation was also observed (Figure 12). Specifically, as the participants had to hold a greater number of letters in their WM, greater NDMN deactivation was seen. In MS-SA, greater NMDN deactivation was observed in the word pairs that were less closely-related to each other in the SA task, supporting the cognitive load hypothesis (Figure 49). In the TGT component of MS-TGT-SA, the Generating condition, the more difficult manipulation, showed greater increases and decreases in HDR activity (Figure 28).

In the Alcohol STOP study, GoCorr trials showed greater deactivation than Fail trials (Figure 66). As participants likely engaged more cognitive resources in correct trials, it is expected that they show more deactivation in GoCorr trials. The observation from the analysis of the study supports the hypothesis.

Overall, the cognitive load hypothesis is supported by many of the studies analyzed in the present paper. The relationship between cognitive demand and DMN deactivation is observed in both TDMN and the NDMN.

Patients vs. Controls Show Different Patterns of DMN Activity

An analysis of the studies revealed a general trend that when doing the same tasks, depending on the specific task design, patients showed greater/less TDMN deactivation compared to controls. For tasks that involve NDMN deactivation, schizophrenia patients showed

less NDMN deactivation compared to controls, supporting the hypothesis. Thus, the hypothesis is partly supported.

Controls Show Greater NDMN Deactivation

When MS was merged with SA, healthy controls showed steeper inclines and declines in NDMN deactivation (Figure 45). When merged with MS-TGT, a similar observation was noted (Figure 44). In Metzak's WM study, controls showed greater NDMN deactivation than patients between timebins 1-3 (Figure 13; Figure 14). In the MMCC task, healthy controls showed greater increases and decreases in deactivation compared to patients during timebins 5-6 (Figure 51).

Patients Show Greater TDMN Deactivation

In Lavigne's TGT task, a group effect was observed when comparing patients, which include both schizophrenia and bipolar groups, to healthy controls. Overall, patients showed greater TDMN deactivation.

In FDT, Fouladirad's FISH, MMCC and Woodward et al.'s TSI task, there was greater TDMN deactivation for schizophrenia patients compared to controls (Figure 4; Figure 32; Figure 53; Figure 24). A similar observation was found in the MS portion of the MS-TGT study (Figure 40)

Controls show Greater TDMN Deactivation in PAMENC

In the PAMENC task, controls showed greater TDMN deactivation during the Task encoding condition (Figure 57). Compared to the tasks where patients showed greater TDMN deactivation, PAMENC involves active memory encoding. The aforementioned tasks only involve analyzing the presented stimuli and responding based on given instructions, without any

active memorizing. This suggests that healthy controls and schizophrenia patients may differ in their use of cognitive resources when doing an active encoding/memorizing task.

Summary of TDMN vs. NDMN Deactivation

In the TSI and MMCC tasks where both DMNs were observed, patients showed more TDMN deactivation than controls, while controls showed more NDMN deactivation than patients. In the PAMENC task, controls showed more TDMN deactivation, which can be explained the active encoding cognitive processes involved in the task. This finding suggests that depending on the specific task design, different patterns of cognitive activity may be observed.

Other Patterns of DMN Activity Observed

In general, a later HDR peak is observed when cognitive demand increases/when the task is more difficult. This is true for both TDMN and NDMN deactivation. For example, the incongruent condition in Sanford's TSI, the more difficult manipulation, showed a later peak than the congruent condition (Figure 18). Similarly, when TGT was merged with other tasks in the SCAP-TGT-TSI-WM study, the thought generation showed a later peak than the speech perception condition, as participants had to actively generate definitions in the first condition (Figure 26). The same phenomenon was observed in the SA task, where words pairs that were most distant showed later peaks in the TGT-SA (Figure 48). In Fouladirad's FISH task, the Weak condition, which is also the more difficult one, showed a later peak than the Strong condition (Figure 31). As in the Bipolar RSPM task, the Hard condition also showed a later peak than the Easy and Medium conditions (Figure 55). Thus, these observations suggest that DMN deactivation peaks occur later for more difficult conditions, likely due to the fact that participants have to suppress more mind-wandering for a longer period.

Conclusion

An analysis of the classification averages show that the TDMN is often associated with task-positive networks, such as 1RESP, INIT, and EXT. On the other hand, NDMN is often associated with INT and LANG. These associations suggest that several brain networks may be working cooperatively during different cognitive processes, and imbalances in these network activities, such as increased/decreased DMN suppression could contribute to cognitive disorders.

Overall, the cognitive load hypothesis that as cognitive load increases, DMN deactivation also increases, is supported in this study. This finding was observed in studies that involved either TDMN and NDMN deactivation. Controls tend to show more NDMN deactivation than schizophrenia patients. For TDMN, depending on the specific cognitive processes involved, patients tend to show greater deactivation for tasks that involve following instructions on a screen. For tasks that involve active encoding, such as PAMENC, healthy controls showed more deactivation.

Moving forward, it would be valuable to analyze more studies that help to elucidate the relationship between task-positive and task-negative networks, and how abnormality/impairment in this area could contribute to schizophrenia symptoms. Also, more analyses of different task-designs that involve the DMNs would further contribute to our understanding of the specific networks underlying different cognitive processes.

References

- Buckner, R. L., Andrews-Hanna, J. R., & Schacter, D. L. (2008). The brain's default network: anatomy, function, and relevance to disease. *Annals of the New York Academy of Sciences*, 1124, 1–38. <https://doi.org/10.1196/annals.1440.011>
- Enz, R. (2019). *Identifying Impairment in Task-Related Functional Brain Networks in Schizophrenia: A Task-Merging Approach Using fMRI*. [Undergraduate thesis]. University of British Columbia
- Fox, J. M., Abram, S. V., Reilly, J. L., Eack, S., Goldman, M. B., Csernansky, J. G., Wang, L., & Smith, M. J. (2017). Default mode functional connectivity is associated with social functioning in schizophrenia. *Journal of Abnormal Psychology*, 126(4), 392–405. <https://doi.org/10.1037/abn0000253>
- Fox, M., Snyder, A., Vincent, J., Corbetta, M., Van Essen, D., & Raichle, M. (2005). The human brain is intrinsically organized into dynamic, anticorrelated functional networks. *PNAS*, 102 (27), 9673-9678. <https://doi.org/10.1073/pnas.0504136102>
- Goghari, V.M., Sanford, N., Spilka, M.J. & Woodward, T.S. (2017). Task-related functional connectivity analysis of emotion discrimination in a family study of schizophrenia. *Schizophrenia Bulletin*, 43(6), 1348–1362. <https://doi.org/10.1093/schbul/sbx004>
- Jeong, B., Kubicki, M. (2010). Reduced task-related suppression during semantic repetition priming in schizophrenia. *Psychiatry Research: Neuroimaging*, 181(2), 114-120. <https://doi.org/10.1016/j.pscychresns.2009.09.005>
- Klepel, F., & Woodward, T. S. (2019). *Report Addis Data*. University of British Columbia.

- Lariviere, S., Roes., M., Sanford, N., Percival, C., Damascelli, M., Lim. R., Enz, R., Moscovitz, A., Menon, M., Ćurčić-Blake, B., Aleman, A., & Woodward, T. (2020). *Brain Networks Involved in Hallucinations*. University of British Columbia.
- Lavigne, K. (2018). Cognitive biases and functional brain networks underlying delusions in schizophrenia. [Unpublished doctoral dissertation]. University of British Columbia.
- Lavigne, K., Menon, M., & Woodward, T. (2020). Functional brain networks underlying evidence integration and delusions in schizophrenia. *Schizophrenia Bulletin*, 46(1), 175-183.
<https://doi.org/10.1093/schbul/sbz032>
- Lavigne, K.M., Metzak, P.D., & Woodward, T.S. (2015). Functional brain networks underlying detection and integration of disconfirmatory evidence. *NeuroImage*, 112, 138-151.
<https://doi.org/10.1016/j.neuroimage.2015.02.043>
- Lavigne, K., Menon, M., Mortiz, S., & Woodward, T. (2020). Functional brain networks underlying evidence integration and delusional ideation. *Schizophrenia Research*, 216, 302-309.
<https://doi.org/10.1016/j.schres.2019.11.038>
- Metzak, P.D., Riley, J., Wang, L., Whitman, J.C., Ngan, E.T.C. & Woodward, T.S. (2012). Decreased efficiency of task-positive and task-negative networks during working memory in schizophrenia. *Schizophrenia Bulletin*, 38(4), 803-813. <https://doi.org/10.1093/schbul/sbq154>
- Metzak, P., Sanford, N., Percival, C., Gill., K., Noureddine, K., Ritchie, C., Hsiao, H., & Wong, S. (n.d.). *Functional Brain Networks involved in Attentional Biasing in Schizophrenia*. University of British Columbia.
- Percival, C. (2019a). *fMRI analysis of functional brain connectivity in two language tasks in schizophrenia*. [Unpublished undergraduate thesis]. University of British Columbia

- Percival, C. (2019b). *Merged Metrical Stress-TGT*. University of British Columbia
- Percival, C. (2018a). *Merged Analysis: Metrical Stress-Thought Generating Task-Semantic Association*. University of British Columbia.
- Percival, C. (2018b). *Merged Semantic Association-Metrical Stress*. University of British Columbia.
- Percival, C. M., Zahid, H. B., & Woodward, T. S. (2020). Task-Based Brain Networks Detectable with fMRI. *Zenodo*. <https://doi.org/http://doi.org/10.5281/zenodo.4274397>
- Raichle, M., MacLeod, a., Snyder, A., Powers, W., Gusnard, D., & Shulman, G. (2001). A default mode of brain function. *PNAS*, 98(2), 676-682. <https://doi.org/10.1073/pnas.98.2.676>
- Roes, M., Moscovitz, A., & Woodward, T. (n.d.). *Reduced Functional Connectivity in Brain Networks Underlying Paired Associates Memory Encoding in Schizophrenia*. University of British Columbia
- Salgado-Pineda, P., Fakra, E., Delaveau, P., McKenna, P., Pomarol-Clotet, E., Blin, O. (2011). *Schizophrenia Research*, 125(2-3). <https://doi.org/10.1016/j.schres.2010.10.027>
- Sanford, N. A. (2019). *Functional brain networks underlying working memory performance in schizophrenia : a multi-experiment approach [Unpublished doctoral dissertation]*. University of British Columbia. <https://open.library.ubc.ca/cIRcle/collections/ubctheses/24/items/1.0387449>
- Sanford, N. (n.d.). *TSI-TGT*. University of British Columbia.
- Sanford, N., Whitman, J.C. & Woodward, T.S. (2020). Task-Merging for finer separation of functional brain networks in working memory. *Cortex*, 125, 246-271.
<https://doi.org/10.1016/j.cortex.2019.12.014>
- Whitfield-Gabrieli, S., Thermenos, H., Milanovic, S., Tsuang, M., Faraone, S., McCarley, R., Shenton, M., Green, A., Nieto-Castanon, A., LaViolette, P., Wojcki, J., Gabrieli, J., & Seidman,

L. (2009). Hyperactivity and hyperconnectivity of the default network in schizophrenia and in first-degree relatives of persons with schizophrenia. *PNAS*, 106(4), 1279-1284.

<https://doi.org/10.1073/pnas.0809141106>

Whitman, J.C., & Woodward, T.S. (2012). Self-selection bias in hypothesis comparison.

Organizational Behavior and Human Decision Processes, 118(2), 216-225.

<https://doi.org/10.1016/j.obhdp.2012.02.002>

Woodward, T.S., Leong, K., Sanford, N., Tipper, C.M., & Lavigne, K.M. (2016). Altered balance of functional brain networks in schizophrenia. *Psychiatry Research: Neuroimaging*, 248, 94-104.

<https://doi.org/10.1016/j.pscychresns.2016.01.003>

Woodward, T.S., Tipper, C.M., Leung, A., Lavigne, K.M., Sanford, N., Metzak, P.D. (2015). Reduced functional connectivity during controlled semantic integration in schizophrenia: A multivariate approach. *Human Brain Mapping*, 36, 2948-2964.

<https://doi.org/10.1002/hbm.22820>

Wong, S., & Goghari, V. (n.d.a). *Bipolar Merged (RSPM and LDT): Report*. University of British Columbia.

Wong, S., & Goghari, V. (n.d.b). *Bipolar RSPM Report*. University of British Columbia.

Wong, S., & Goghari, V. (n.d.c). *Healthy RSPM: Report*. University of British Columbia.

Wong, S.T.S., Goghari, V.M., Sanford, N., Lim, R., Clark, C., Metzak, P.D., Rossell, S.L., Menon, M. & Woodward, T.S. (2020). Functional brain networks involved in lexical decision. *Brain and Cognition*, 138. <https://doi.org/10.1016/j.bandc.2019.103631>

Appendix

Table 1

Relative Strength of Patterns of Task-Positive and Default Mode Networks Within Individual Networks That Were Classified With Z-Scores ≥ 0.80

	> 50% Positive		> 50% Negative	
	TDMN	NDMN	TDMN	NDMN
1RESP	0.28 (12) ; 0.90 (6) m= 0.59	0.19 (12); 0.46 (4) m= 0.33	0.62 (2); 0.40 (27) m = 0.51	0.13 (2); 0.29 (6) m = 0.21
2RESP	0.07 (22); 0.86 (6) m = 0.47	0.05 (22); 0.43 (4) m = 0.24	N/A; 0.35 (27) m= 0.35	N/A; 0.23 (6) m= 0.23
AAR	-0.06 (11); -0.05 (6) m = -0.06	-0.02 (11); -0.03 (4) m = -0.03	-0.08 (2); -0.07 (27) m = -0.08	-0.12 (2); -0.09 (6) m = -0.11
AUD	-0.01 (8); -0.08 (6) m = -0.05	-0.01 (8); -0.11 (4) m = -0.06	N/A; -0.06 (27) m = -0.06	N/A; -0.17 (6) m = -0.17
CE	0.01 (14); 0.13 (6) m = 0.07	0.15 (14); 0.51 (4) m = 0.33	N/A; 0.03 (27) m = 0.03	N/A; 0.16 (6) m = 0.16
EXT	0.37 (22); 1.02 (6) m = 0.70	0.34 (22); 0.71 (4) m = 0.53	0.97 (2); 0.42 (27) m = 0.70	0.80 (2); 0.35 (6) m = 0.58

FVF	-0.06 (11); 0.13 (6) m = 0.04	-0.04 (11); -0.24 (4) m = -0.14	0.59 (6); 0.08 (27) m = 0.34	0.06 (6); -0.15 (6) m = -0.05
INIT	0.42 (13); 0.86 (6) m = 0.64	0.26 (13); 0.42 (4) m = 0.34	0.79 (1); 0.41 (27) m = 0.60	0.65 (1); 0.23 (6) m = 0.44
INT	0.30 (6); 0.44 (6) m = 0.37	0.42 (6); 0.87 (4) m = 0.645	N/A; 0.21 (27) m = 0.21	N/A; 0.36 (6) m = 0.36
LANG	0.44 (8); 0.63 (6) m = 0.54	0.73 (8); 1.48 (4) m = 1.1	1.06 (1); 0.34 (27) m = 0.70	1.41 (1); 0.64 (6) m = 1.03

Note. **Bolded** numbers are the **default-mode network (DMN) z-scores** averaged over networks that were classified as one of the ten task-positive networks with a z-value of ≥ 0.80 . (**Bracket**) indicates the number of studies that were classified as the task-positive network that contributed to the average DMN z-scores. *Italicized* numbers are the *task-positive network z-scores* averaged over networks that were classified as one of the two DMN (TDMN or NDMN) with a z-value of ≥ 0.80 . (*Bracket*) indicates the number of studies that were classified as DMN networks that contributed to the average of the task-positive networks. N/A indicates that there are no studies classified under that task-positive network had a z-value of ≥ 0.80 . The highlighted data were used to interpret the table.

Functional Assessment of the fMRI-derived One-Handed and Two-Handed Response Networks

Melody Li

FUNCTIONAL ASSESSMENT OF THE FMRI-DERIVED RESPONSE NETWORKS

Abstract

The Response Networks (RESPN)—2-Handed Response and 1-Handed Response—are two of the twelve fMRI-derived functional brain networks identified through Task-based Functional Magnetic Resonance Imaging (fMRI) and Constrained Principal Component Analysis (CPCA).

FUNCTIONAL ASSESSMENT OF THE FMRI-DERIVED RESPONSE NETWORKS

Keywords: Functional magnetic resonance imaging, constrained principal component analysis, canonical correlation analysis, 2-handed response network, 1-handed response network.

FUNCTIONAL ASSESSMENT OF THE FMRI-DERIVED RESPONSE NETWORKS

Table of Contents

Introduction to the One-Handed and Two-Handed Response Networks

In Uddin et al.'s (2019) paper, the Response Network (RESPN) is referred to as the Pericentral Network (PN) based on the anatomical region that best described the large-scale functional system. The broad cognitive domain the RESPN is most associated with is sensorimotor as there is well documented involvement of the network in motor processes and somatosensory processing due to the RESPN serving as the cortical component of primary sensory and motor pathways (Uddin et al., 2019). The RESPN is described as to having core regions in motor and somatomotor cortices, anterior and posterior to the central sulcus, in addition to the juxtapositional lobule (supplementary motor area) and secondary somatosensory cortices (Uddin et al., 2019; Smith et al., 2009; Zilles et al., 1995). The RESPN is also characterized by zones including the auditory cortex of the superior temporal gyrus to a lesser extent in studies employing resting state functional connectivity (RFSC) (Uddin et al., 2019).

Using independent component analysis (ICA), Smith et al. (2009) observed left and right subsystems in the RESPN as well as strong correspondence to action-execution and perception somesthesia paradigms. Yeo et al. (2011) observed dorsal (hand) and ventral (face) subsystems in some parcellations using resting-state functional connectivity MRI. With higher resolution resting-state and task-based fMRI, Kong et al. (2019) was able to observe separation of the auditory network and RESPN.

Both the One-Handed and Two-Handed RESPN are involved in motor responses and have HDRs that peak late in the trial; however, the One-Handed RESPN consisted of lateralized activation (Sanford et al., 2020) and the Two-Handed RESPN consisted of bilateral activation (Goghari et al., 2017; Sanford, 2019).

Methods

The 2-Handed Response Networks were identified with fMRI-CPCA and network classifications. Constrained Principal Analysis (CPCA) combines regression analysis and principal component analysis to derive images of functional neural networks when the analyzed blood-oxygenation-level-dependent (BOLD) is constrained to the predictable aspect of variance in the BOLD signal dependent on the stimuli presented (Metzak et al., 2011). An automated classification program developed using MATLAB algorithm was employed to assign Z-scores, which reflected how closely the inputted brain images matched a set of exemplar networks, with a higher Z-score indicating a greater match. In this paper, a Z-score ≥ 0.8 was considered a significant match.

To understand the cognitive processes underlying these networks, estimated hemodynamic response (HDR) plots were interpreted. HDR plots display changes in BOLD signals, which can be used to visualize brain function (Ogawa et al., 1990). The BOLD fMRI technique measures the changes in inhomogeneity of the magnetic field due to changes in blood oxygenation as haemoglobin and deoxyhaemoglobin are magnetically distinct. Subsequent analysis of the timing and duration of peaks on HDR plots can allow for interpretation of cognitive processes (Sanford, 2019).

Results

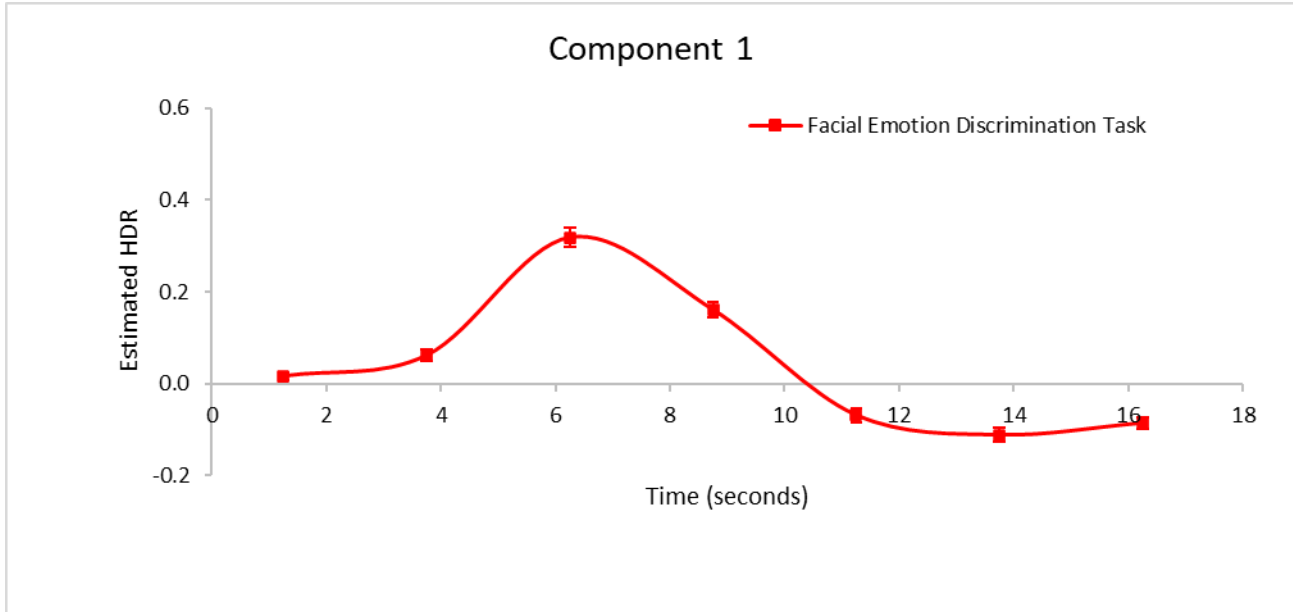
1. Ghogari's FDT HDR

Mixed ANOVA revealed significant main effects of Image Type, $F(2, 134) = 35.873, p < 0.001$, and Time, $F(6, 402) = 127.701, p < 0.001$ (Figure 1). A significant interaction was observed for Age_Anger_Fear_Happy_Sad \times Timebins, $F(24, 1608) = 2.185, p < 0.001$, where Age showed a higher HDR peak compared to Anger, dominated by changes over timebins 1-2 and 3-4 ($p < 0.05$; Figure 2). The Fear condition showed greater HDR post-activation suppression compared to Anger during timebins 3-4 ($p < 0.01$; Figure 2). Significant interactions were also observed for Foil_Scrambled_Target \times Timebins, $F(12, 804) = 19.097, p < 0.001$, where Foil showed a higher HDR peak compared to Scrambled during timebins 2-3 and 6-7 ($p < 0.001$; Figure 3). Target also showed a higher HDR peak compared to Scrambled during timebins 2-3 and 6-7 ($p < 0.001$; Figure 3). A significant three-way interaction was also observed for Age_Anger_Fear_Happy_Sad \times Foil_Scrambled_Target \times Timebins, $F(48, 3216) = 3.984, p < 0.001$. Foil Age decreased while Scrambled Age increased between timebins 1 and 2, $F(1, 67) = 12.362, p < 0.001$ (Figure 4-5).

The main effect of Group was not significant ($p = 0.199$). although a significant interaction of Group \times Timebins was observed, where relatives and controls showed a greater post-activation suppression compared to patients during timebins 3-4, $F(2, 67) = 6.568, p < 0.01$. Overall, patients showed decreased deactivation of the 2RESPN, relative to relatives and controls ($p < 0.01$; Figure 7).

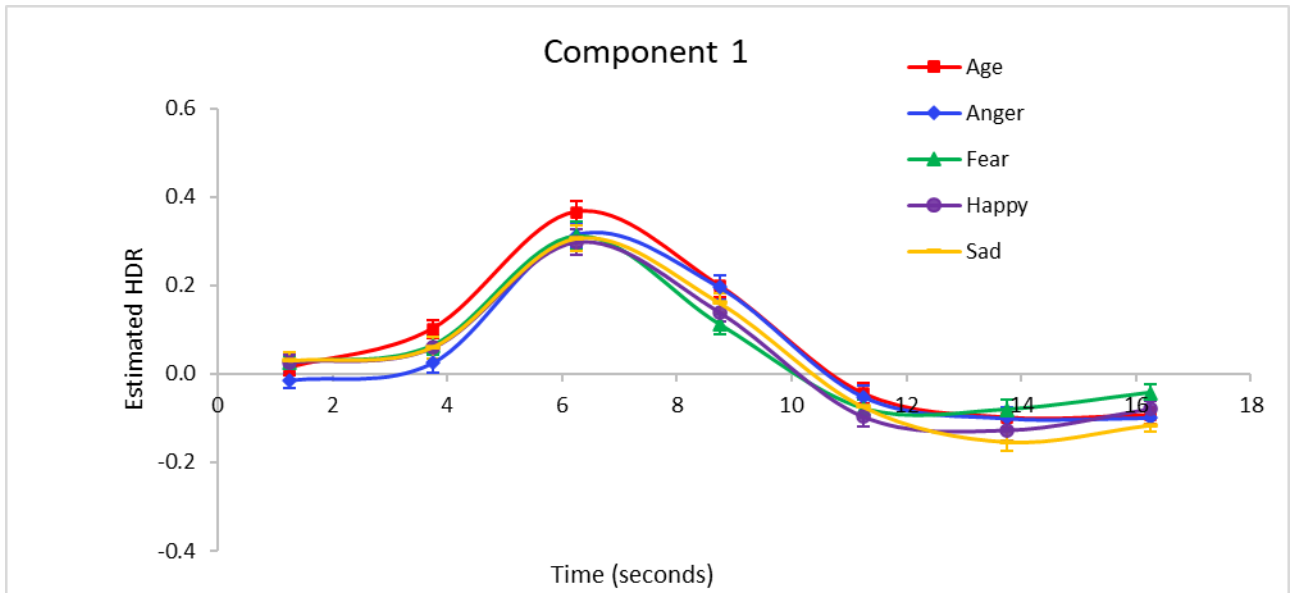
FUNCTIONAL ASSESSMENT OF THE FMRI-DERIVED RESPONSE NETWORKS

Figure 1

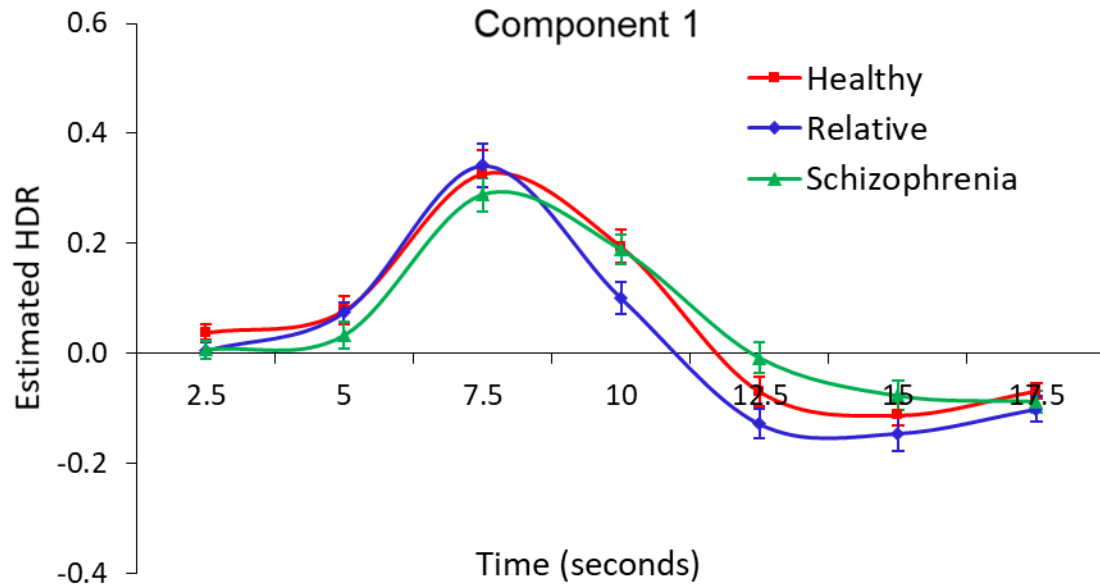


Note. HDR averaged over Facial discrimination condition (Age_Anger_Fear_Happy_Sad), Image type (Foil_Scrambled_Target), and Group (Healthy_Relative_Schizophrenia).

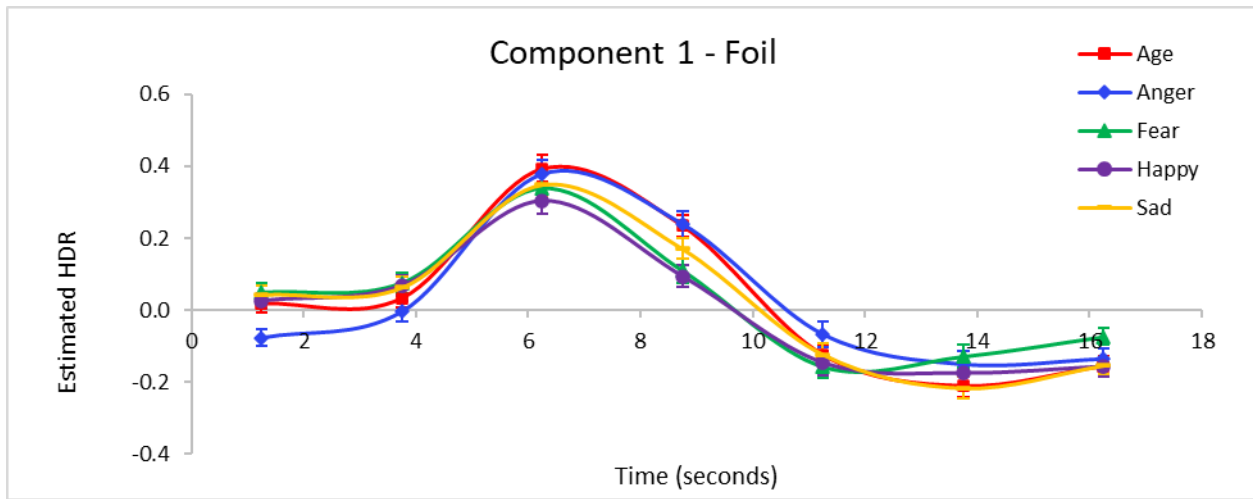
Figure 2



Note. HDR for Facial discrimination condition (Age_Anger_Fear_Happy_Sad), and averaged over Image Type (Foil_Scrambled_Target) and Group (Healthy_Relative_Schizophrenia).

Figure 3

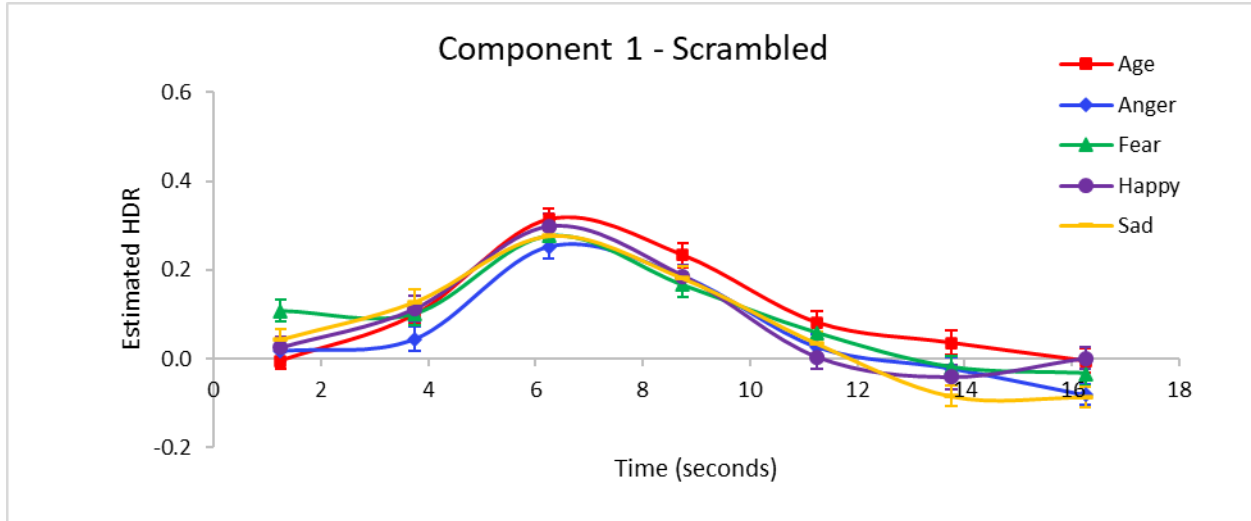
Note. HDR for Image Type (Foil_Scrambled_Target), and averaged over Facial discrimination condition (Age_Anger_Fear_Happy_Sad) and Group (Healthy_Relative_Schizophrenia).

Figure 4

Note. HDR for Facial discrimination condition (Age_Anger_Fear_Happy_Sad), and averaged over Group (Healthy_Relative_Schizophrenia), for Foil.

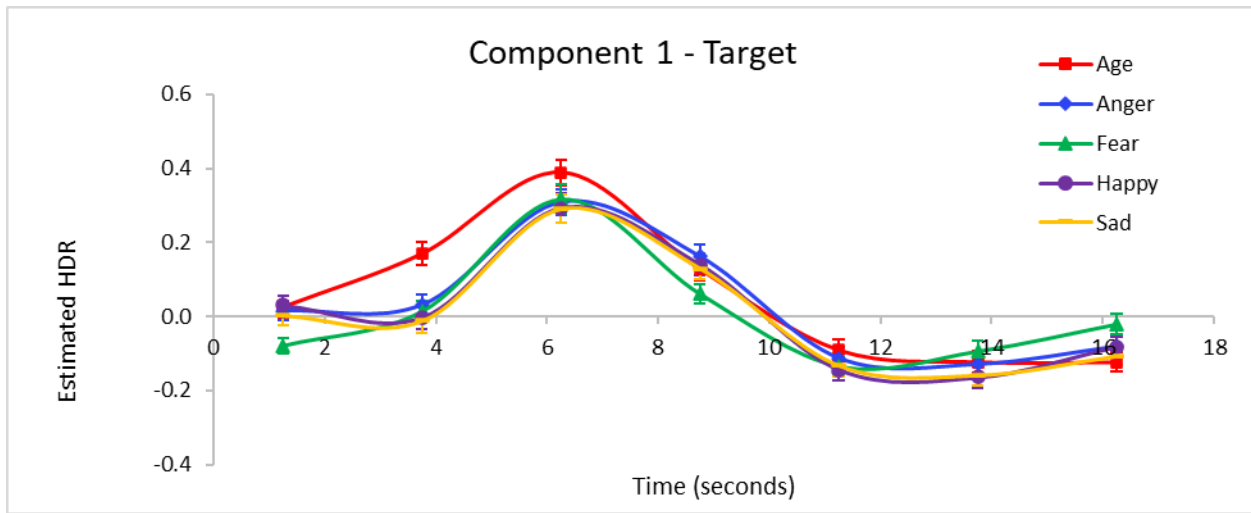
Figure 5

FUNCTIONAL ASSESSMENT OF THE FMRI-DERIVED RESPONSE NETWORKS



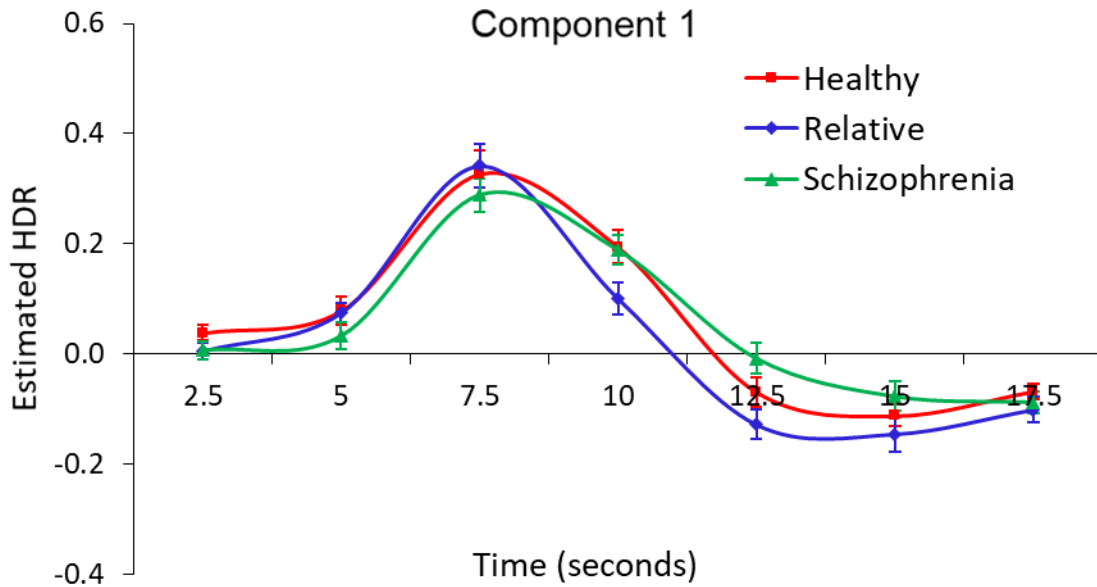
Note. HDR for Facial discrimination condition (Age_Anger_Fear_Happy_Sad), and averaged over Group (Healthy_Relative_Schizophrenia), for Scrambled.

Figure 6



Note. HDR for Facial discrimination condition (Age_Anger_Fear_Happy_Sad), and averaged over Group (Healthy_Relative_Schizophrenia), for Target.

Figure 7



Note. HDR for Group (Healthy_Relative_Schizophrenia), and averaged over Facial discrimination condition (Age_Anger_Fear_Happy_Sad) and Image Type (Foil_Scrambled_Target).

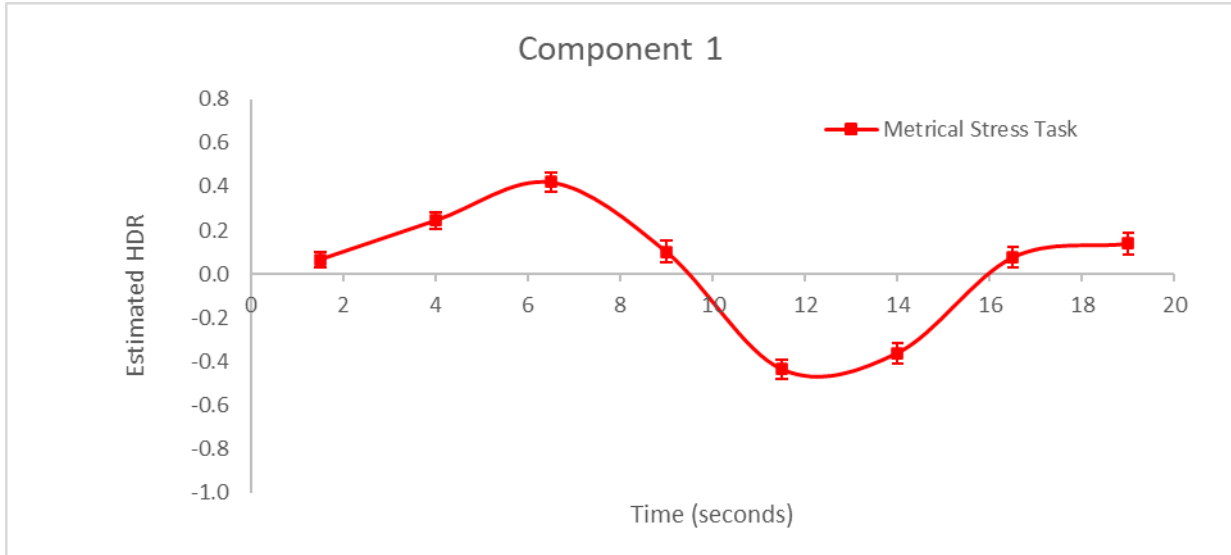
2. Lariviere's MST HDR

Mixed ANOVA revealed a significant main effect of Time, $F(7, 539) = 38.921, p < 0.001$ (Figure 8). There were no significant within-subject interactions.

The main effect of Group was not significant ($p= 0.629$); however, a significant interaction of Group \times Timebins was observed, $F(7, 539) = 7.470, p < 0.001$. Controls showed sharper decreases during timebins 3-4 and sharper increases during timebins 5-7 ($p=0.001$, Figure 9). Overall, controls showed a greater post-activation suppression from a higher activation peak of the 2RESPN compared to patients.

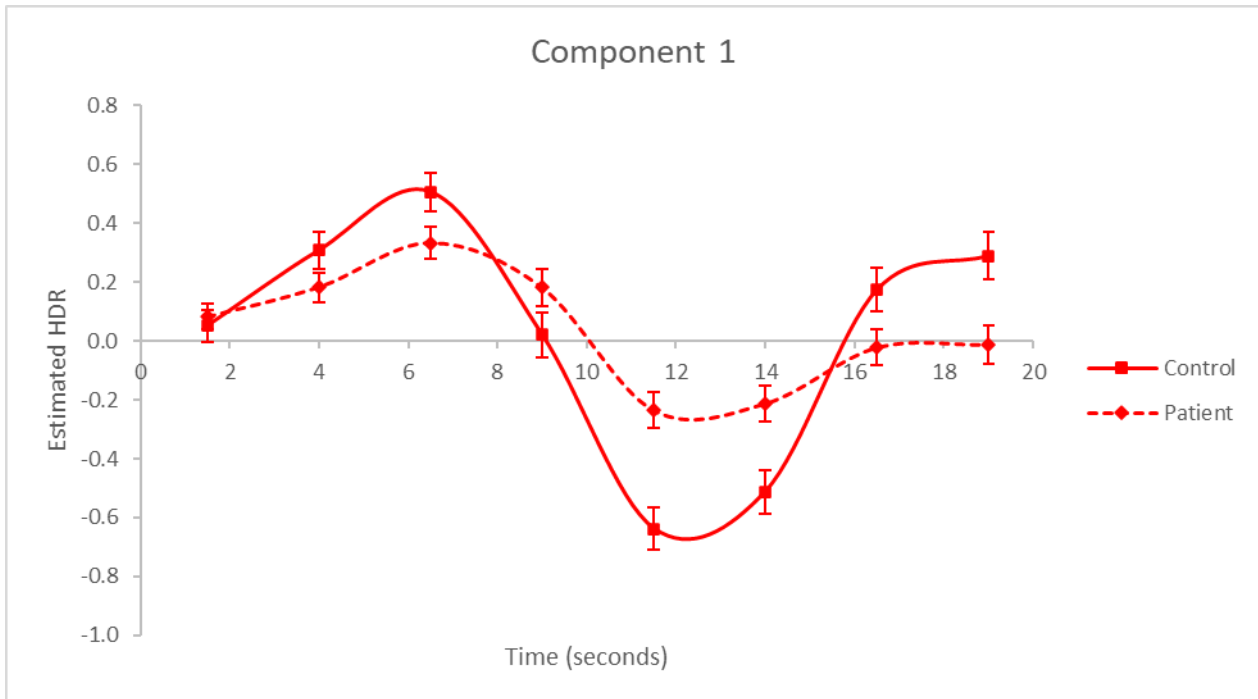
Figure 8

FUNCTIONAL ASSESSMENT OF THE FMRI-DERIVED RESPONSE NETWORKS



Note. HDR averaged over Task (Phonological_Semantic) and Group (Control_Patient).

Figure 9

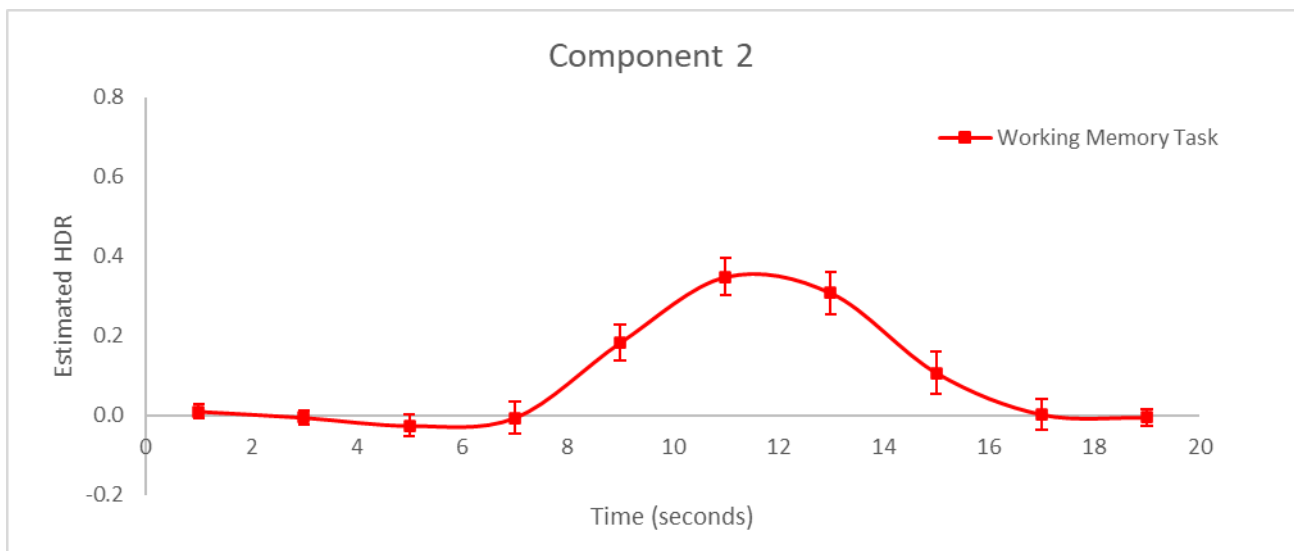


Note. HDR for Group (Control_Patient), and averaged over Task (Phonological_Semantic).

3. Manoach's WMT HDR

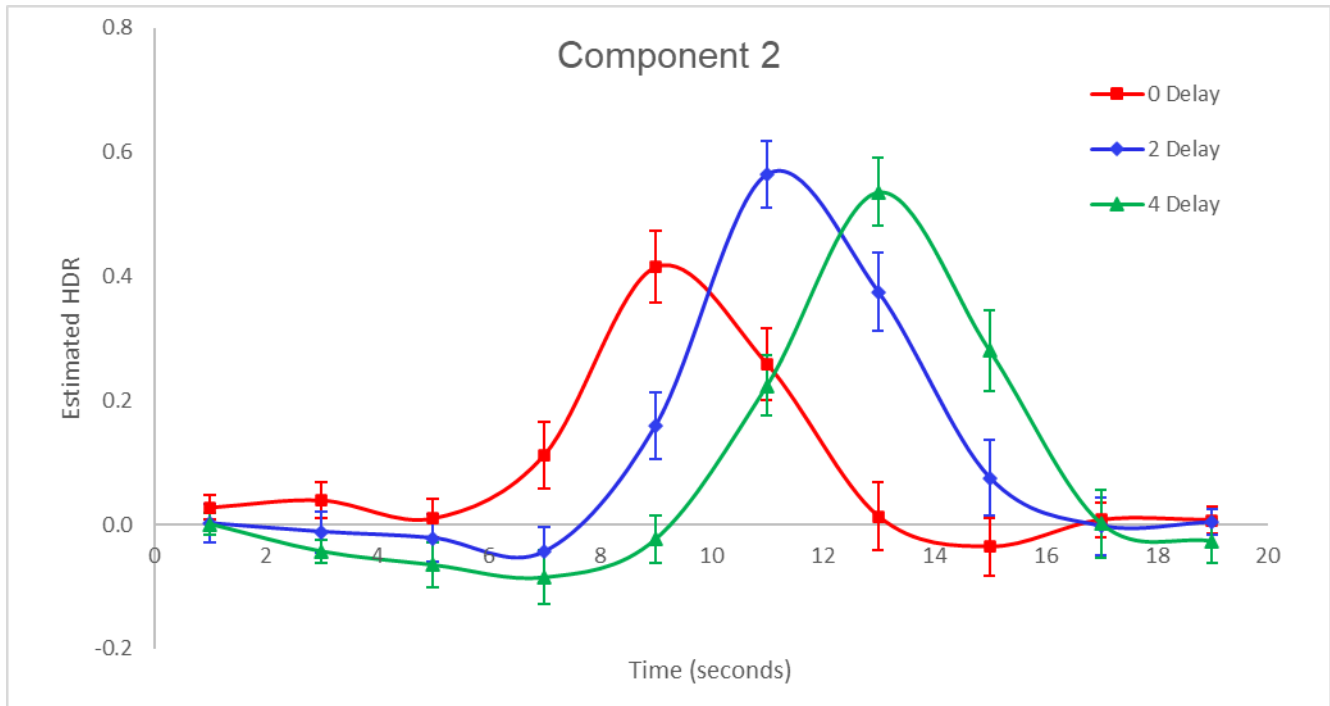
Repeated Measures ANOVA revealed a significant main effect of Time, $F(9, 81) = 27.774, p < 0.001$ (Figure 10). A significant interaction was observed between Delay \times Timebins, $F(18, 162) = 43.891, p < 0.001$, where D0 decreases while D2 increases during timebins 5-6 and D2 decreases while D4 increases during timebins 6-7 ($p=0.001$; Figure 11). In general, there were staggered peaks in 2RESPN activation for Delay.

Figure 10



Note. HDR averaged over Delay (D0_D2_D4).

Figure 11



Note. HDR for Delay (D0_D2_D4).

4. Metzak's RMT and SMT HDR

Repeated measures ANOVA revealed a significant main effect of Time, $F(9, 756) = 28.611, p < 0.001$.

5. Sanford's TSI-TGT HDR

2.6 Wong *et al.*, 2020

2.7 Woodward *et al.*, 2016

2.8 Wager Thermal Pain

2.9 Bipolar RSPM

2.10 Sanford, 2019

2.11 Toronto Alcohol WM

2.12 Toronto Alcohol STOP

2.13 MS-TGT-SA

FUNCTIONAL ASSESSMENT OF THE FMRI-DERIVED RESPONSE NETWORKS

2.14 Paired Associates Memory Encoding

Conclusion

Key Findings

Mixed with external attention normally

References

- Ogawa, S., Lee, T., Kay, A., and Tank, D. (1990). Brain magnetic resonance imaging with contrast dependent on blood oxygenation. Proc. Natl. Acad. Sci. U.S.A., 87:9868–9872.
- Sanford, N., Functional brain networks underlying working memory performance in schizophrenia: a multi-experiment approach, in Department of Psychiatry. 2019, University of British Columbia: Vancouver, Canada.
- Metzak, P. D., Feredoes, E., Takane, Y., Wang, L., Weinstein, S., Cairo, T., . . . Woodward, T. S. (2011). Constrained principal component analysis reveals functionally connected loaddependent networks involved in multiple stages of working memory. Human Brain Mapping, 32, 856-871. doi:10.1002/hbm.21072
- Goghari, V.M., Sanford, N., Spilka, M.J., and Woodward, T.S., Task-related fMRI network analysis of emotion recognition in a family study of schizophrenia. Schizophrenia Bulletin, 2017. 43: p. 1348–1362.
- Uddin, L.Q., Yeo, B.T.T. & Spreng, R.N. Towards a Universal Taxonomy of Macro-scale Functional Human Brain Networks. *Brain Topogr* 32, 926–942 (2019).
<https://doi.org/10.1007/s10548-019-00744-6>
- Smith SM, Fox PT, Miller KL et al (2009) Correspondence of the brain's functional architecture during activation and rest. Proc Natl Acad Sci USA 106:13040–13045 ->[Correspondence of the brain's functional architecture during activation and rest | PNAS](#)
<https://www.ncbi.nlm.nih.gov/pmc/articles/PMC3174820/>
- <https://www.ncbi.nlm.nih.gov/pmc/articles/PMC1167457/?page=11>
<https://link.springer.com/article/10.1007%2Fs10548-019-00744-6>
- Sanford, N., Whitman, J.C., and Woodward, T.S., Task merging for finer separation of functional brain networks in working memory. Cortex, 2020. 125: p. 246-271. ->[Task-merging for finer separation of functional brain networks in working memory - ScienceDirect](#)

Functional Assessment of the Initiation Network

Mehar Singh

Dr. Todd S.Woodward

Abstract

Twelve task-based brain networks detectable by functional magnetic resonance imaging (fMRI) have recently been derived using constrained principal component analysis for fMRI (fMRI-CPCA). While these networks have been anatomically identified, their comprehensive roles across varying conditions remain ambiguous. The current paper focuses on contextualizing the role and function of the Initiation Network (INIT) which is found across multiple studies over distinct tasks. Prior studies conducted by the Cognitive Neuroscience of Schizophrenia Lab (CNoS) in which INIT was found with sufficient strength were surveyed to better characterize the network's function. Examining these studies' methods and comparing hemodynamic response (HDR) patterns across studies where INIT activity emerged allows for a better understanding of the cognitive processes that underlie this network. In essence, by integrating the findings from the various tasks where INIT activity emerged, insight into the function of INIT can be determined under a variety of different conditions. By analyzing the various tasks where INIT was elicited, it can be seen that this network reflects strong initial engagement of cognitive processes following a cognitively undemanding period. The results of this interpretation reveal that INIT is particularly involved in various types of working memory tasks, followed by abstract reasoning tasks and even probabilistic reasoning tasks.

Keywords: initiation, fMRI-CPCA, hemodynamic response, working memory, abstract reasoning, probabilistic reasoning

1. Initiation Network

Currently, twelve recently derived networks have been categorized into the following general classes of function: internally oriented cognition, visually oriented cognition, auditorily oriented cognition, self-reflective oriented cognition and response based cognition. However, their unique roles remain to be contextualized in the context of varying task conditions (Percival et al., 2020). The focus of this exploration is the Initiation network (INIT), which is attributed to visually oriented cognition and encoding task-relevant information in working memory (Percival et al., 2020). Task-based fMRI studies have provided evidence that INIT shows positive load-dependence during the following tasks: verbal and visuospatial working memory, abstract reasoning (ability to discern meaning in confusion), and probabilistic reasoning (Percival et al., 2020). INIT is anatomically distinguished by bilateral activation in the occipital cortex (occipital poles, lateral occipital cortex and occipital fusiform gyri), precentral gyri, middle frontal gyri, supplementary motor area (SMA), superior frontal gyrus and thalamus (Sanford 2021). This network is largely localized in the occipital cortex, and the involvement of the SMA has been considered to be involved in restarting cognitive processes associated with visual stimuli after a break of a few seconds after a set of operations, and peaks sharply and early in trials (Percival et al., 2020).

2. Methods

In the Cognitive Neuroscience of Schizophrenia (CNoS) lab, fMRI-CPCA has been used to illustrate the presence of 2 task-negative networks and 10 task-positive networks, one of which was INIT. Out of 200 task-based fMRI datasets classified through fMRI-CPCA, eight components demonstrated positive loadings for INIT with a sufficiently high z-score (>0.80). INIT was not present in negative loadings with a z-score of 0.8 or higher in any of these past studies conducted by the CNoS Lab. These components were derived from 6 published

analyses and 2 unpublished studies. Each study is summarized in Table 1 below, accompanied by its participant populations and employed task(s). Each study's methods and associated estimated hemodynamic response plots (HDRs) were analyzed to contextualize the function of INIT. Analyzing the timing and duration of peaks of the blood oxygen level dependent (BOLD) response in an HDR plot can allow for the interpretation of cognitive processes associated with certain tasks (Sanford, 2019). Table 1 displays a comprehensive list of the studies used in this exploration. Table 2 displays those studies which were incorporated into INIT's mean exemplar.

Table 1: Comprehensive List of Referenced Studies

Study	Participant Populations	Task(s)	Component	z-score	Pos %
Woodward et al., 2012	Healthy adults	WM	1	1.25	100
Metzak et al., 2012	Schizophrenia patients; Healthy adults	WM	2	1.47	80
Sanford et al., 2019	Healthy adults	WM	2	1.25	79
Sanford et al., 2019	Healthy adults	WM, TGT	2	1.2	74
Zurrin et al., 2020	Healthy adults	RSPM	4	0.91	63
Sanford et al., 2020	Schizophrenia patients; Healthy adults	SCAP, TGT, TSI, WM	5	1.14	85
Sanford et al., 2020	Schizophrenia patients; Healthy adults	WM	2	1.21	79
FISH_T1_T2	Schizophrenia patients	FISH_T1_T2	3	0.92	65

The following tasks are included in Table 1: Working Memory (WM), Raven's standard progressive matrices (RSPM), Spatial Capacity Task (SCAP), Thought Generation Task

(TGT), Task Switch Inertia (TSI), and FISH Task. The highlighted rows are indicative of studies which were included in the mean exemplar for INIT.

3. Results

3.1 Woodward's WM HDR

This study was incorporated into INIT's mean exemplar. This study included analyses conducted for 10 healthy participants and 2 participants' data could not be retrieved. The task conditions are described in Section _. In this study, Component 1 was classified as the INIT network with a z-score of 1.25 from increased activity at 44% of the voxels. Positive loadings in Component 1 were found primarily in the visual cortex regions, including the primary visual cortex, as well as the left precentral gyrus and supplementary motor area, right angular gyrus, and bilateral hippocampi (Woodward et al., 2013). The increased signal in these brain regions largely reflects the activation of INIT for this study's working memory task.

A significant interaction between Delay (D0_D2_D4) and Timebin emerged, $F(18, 162) = 6.670, P < 0.001$. Significant interaction contrasts occurred where repeated contrast were dominated by Timebin 4-5, 6-7, 7-8, 8-9, and 9-10. The repeated contrasts were dominated by Timebin 4- 5 contrasts as D2 decreases faster than D0 at time bins 4 to 5 at $F(1, 9) = 13.603, p < 0.01$. D0 decreases faster than D2 at time bins 6 to 7 at $F(1, 9) = 16.442, p < 0.01$. D0 decreases faster than D2 at time bins 7 to 8 at $F(1, 9) = 6.438, p < 0.05$. D2 decreases faster than D0 at time bins 8 to 9 at $F(1, 9) = 11.690, p < 0.01$. D2 decreases faster than D0 at time bins 9 to 10 at $F(1, 9) = 5.734, p < 0.05$. This elicits the earlier flattening out of HDR at low delays. D4 decreases faster than D2 at time bins 4 to 5 at $F(1, 9) = 8.947, p < 0.05$. D4 increases while D2 decreases at time bins 7 to 8 at $F(1, 9) = 6.758, p < 0.05$. D4 decreases faster than D2

at time bins 9 to 10 at $F(1, 9) = 8.468$, $p < 0.05$. This elicits the addition of an HDR peak as delay increases, and earlier flattening out of HDR at low delays.

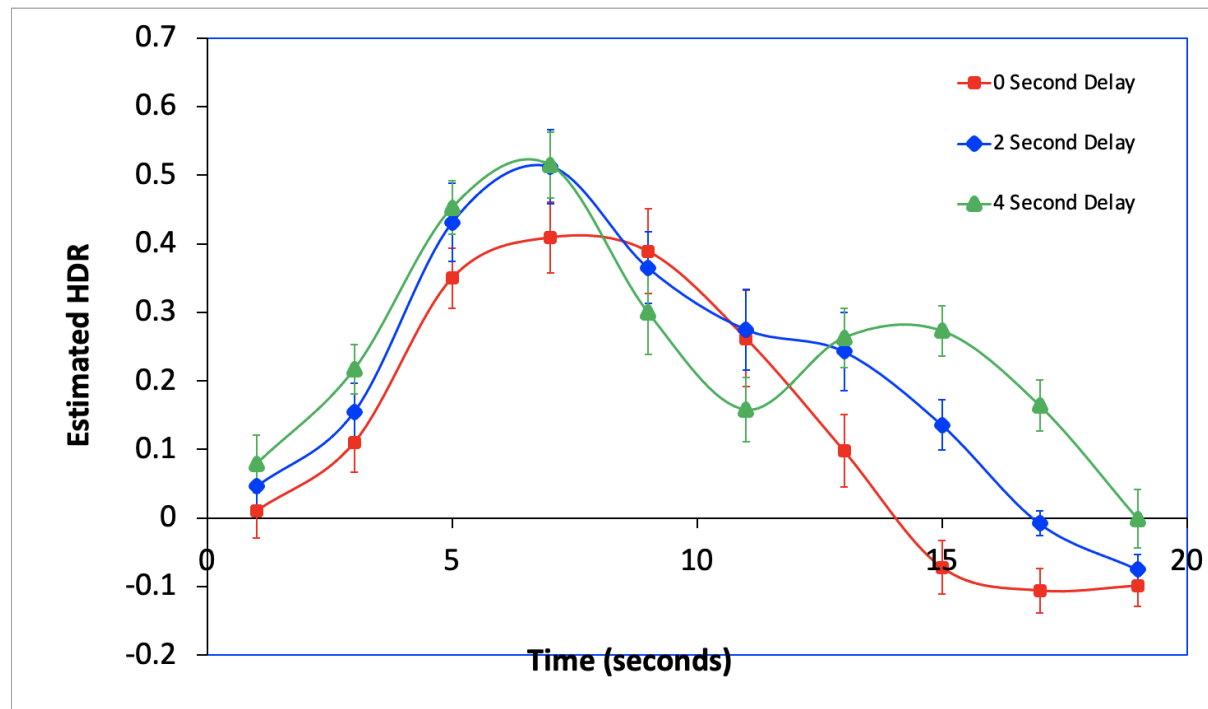
Through the visual examination of Figure 1 which displays the hemodynamic response plot (HDR) for Component 1, INIT activity corresponded with the onset of the trial with the highest activation seen early in the trial. The three working memory trials differed in that the D0 condition contained no delay period and the D2 and D4 conditions contained a 2 second and 4 second delay period, respectively. A bimodal peak is seen in the D4 condition; this is contrasted with the D0 condition where a unimodal peak is seen and with the D2 condition where the trend falls in between the pattern shown by D4 and D0. The D0 condition differs from D2 and D4 since it displays sustained activity with its peak at approximately 7 – 9 seconds before returning to baseline by 15 seconds. This is of particular interest since it contains no delay period, unlike the two other conditions. With the increase in the delay period in D2 and D4, the pattern shifts towards a more bimodal estimated HDR shape. In essence, with the display of a blank screen in the delay period, INIT activity decreases and with the continued display of stimuli, INIT activity is sustained until returning to baseline. Thus, in this working memory task, INIT responds to the visual demands of the encode and probe periods (Woodward et al., 2013). This coincides with the general view that the INIT network is a visually processing network (Sanford et al., 2019). However, this study also shows that INIT plays a key role in working memory which is over and above visual processing.

In the discussion of this study, INIT is labeled as the Encoding/Probe network as it displays activity mainly during the encoding and probe periods and not in the delay epochs. Essentially, the HDR's pattern of activation is expected for encoding epochs as they

correspond with the visual association and primary visual cortices. Furthermore, a notable finding was that INIT was also associated with bilateral hippocampus activation. The notion is that information held in the short term is activated with long-term memory representations. As such, encoding the digit stimuli into working memory and recognition and retrieval based processes appears to involve a network that involves the hippocampus, early visual cortex, frontoparietal areas (Woodward et al., 2013). Together these activated sets of regions form a core working memory network, which INIT is highly associated with (Woodward et al., 2013).

Figure 1

Woodward et al. WM HDR Plot



3.2 Metzak's WM HDR

This study was incorporated into INIT's mean exemplar. This study included 15 schizophrenia patients and 15 healthy participants who completed a modified Sternberg Item Recognition Paradigm WM task. In this study, Component 2 was classified as the INIT network with a z-score of 1.47 from increased activity at 80% of the voxels. Positive loadings in Component 2 were found primarily in the bilateral occipital cortex, left precentral gyrus and left supplementary motor area. The increased signal in these brain regions largely reflects the activation of INIT for this study's working memory task.

A significant main effect of task emerged (L2_L4_L6_L8), $F(3, 84) = 31.062, p < 0.001$. A significant interaction between Load x Timebins emerged, $F(18, 504) = 64.791, P < 0.001$. A significant interaction in Load occurred between: Levels 1 vs level 2 with $F(1, 28) = 9.497, p < 0.05$, Level 2 vs level 3 with $F(1, 28) = 18.937, p < 0.001$, and Level 3 vs level 4 with $F(1, 28) = 5.430, p < 0.05$. There were Load x Timebin interaction contrasts. This is due to a perfectly load dependent increase in HDR such that there is a higher peak and a right shift of peaks as there's a later activation as number of letters increase, and earlier flattening of HDRs at lower letter numbers.

By visually inspecting the HDR plot for Component 2 in Figure 2, it can be seen that INIT activity emerges soon in this task as shown by an increase in activity sharply, starting at approximately 4 seconds. Furthermore, an early peak can be seen in this component at approximately 10 seconds. This speaks to INIT's association with the encoding phase, which is the first phase of memory formation. INIT was strictly activated in only the encoding condition and not in the delay phase of this task as shown by the tapering off of activity by 17

seconds. The schizophrenia patients displayed overall lower INIT activations in comparison to the healthy control group, which suggests that working memory capacity in schizophrenia patients is indeed reached sooner. The fact that the schizophrenia group displayed greater performance deficits in the working memory task can be attributed to their corresponding decreased INIT activation. Since INIT activation is representative of encoding in this task, this demonstrates how the schizophrenia patients display a poorer ability to encode the stimuli presented compared to controls.

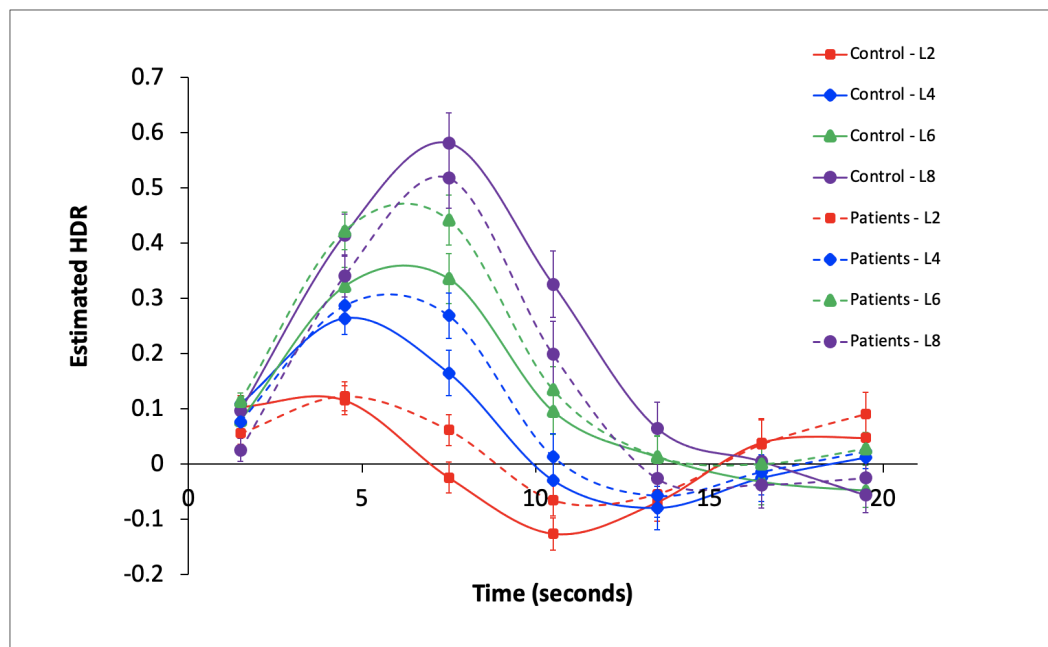
A particular point of interest is how the schizophrenia group displayed higher INIT activation in the 6 letter condition but lower INIT activation in the 8 letter condition relative to the healthy control group. In essence, the patient group may be more efficient at encoding moderate working memory loads but less efficient at encoding more complex working memory loads compared to controls. This could mean surpassing a certain working memory load limit leads to difficulties in accessing neural support to continue working on demanding tasks. INIT displayed reduced activation in the patient group when the task demands become sufficiently high (8 letters), demonstrating how schizophrenia patients show overall reduced efficiency in terms of working memory performance. This elicits how the patient group's performance was affected because of the ability to efficiently encode the stimuli. Furthermore, a significant interaction was observed where the highest BOLD activation in both groups can be seen in the 8 letter condition and the lowest activation can be seen in the 2 letter conditions. This demonstrates how INIT is more heavily operated when participants work on more cognitive demanding tasks. In essence, difficult conditions demonstrate larger peaks, indicating that greater initiation occurs for more difficult working memory tasks.

Due to its displayed early peak at approximately 7 seconds, its strong load dependence, and activation in the visual regions, INIT is primarily involved in the encoding phase of this modified Sternberg Item Recognition Paradigm working memory task. Thus,

INIT allows for the initial learning of information, which is the cognitive process of encoding.

Figure 2

Metzak et al. WM HDR Plot



3.3 Sanford & Woodward's WM HDR

This study produced a single-experiment WM analysis in addition to multi-experiment analysis (WM and TGT) results. Although the single experiment analysis was not included in the mean exemplar for INIT, the multi-experiment analysis was. In this study, 37 healthy participants were recruited to complete the Sternberg Working Memory task. The focus of this section is to elicit the function of INIT in terms of the Sternberg Working Memory task. In this study, Component 2 was classified as the INIT network with a z-score of 1.25 from increased activity at 79% of the voxels. Positive loadings in Component 2 were

found primarily in the bilateral occipital cortex (extending dorsally into parietal regions), supplementary motor areas, precentral gyrus, and thalamus (Sanford et al., 2019). Notably, the thalamus peaked relatively early on in the trials (Sanford et al., 2019). The increased signal in these brain regions largely reflects the activation of INIT for this study's working memory task.

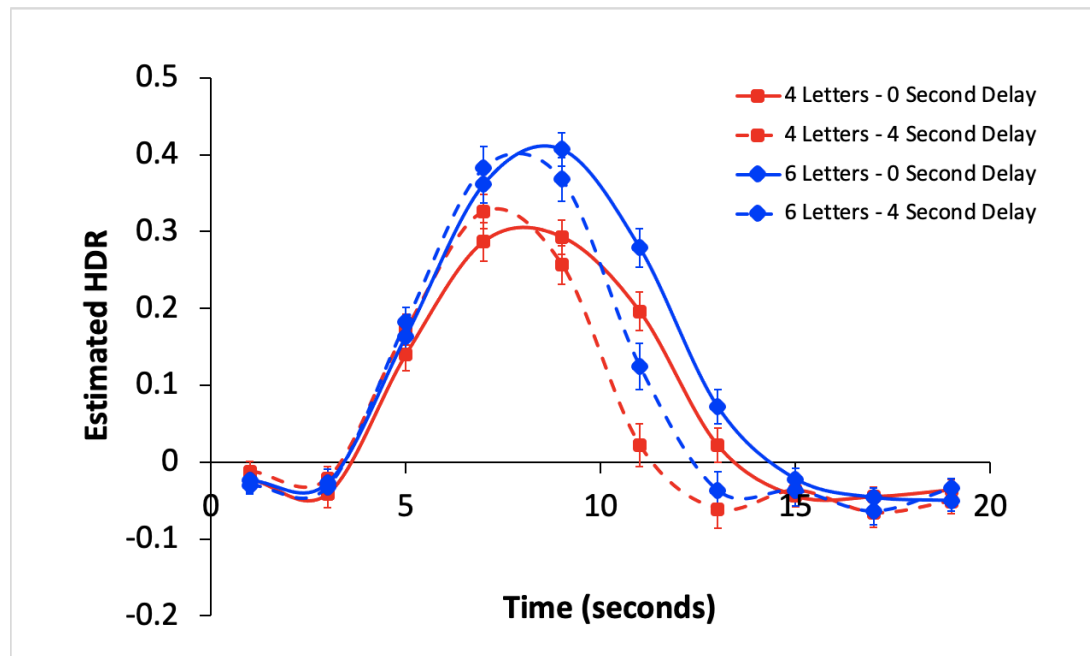
A significant main effect of Task (L4_L6) emerged, $F(1, 36) = 23.429, p < 0.001$. A significant main effect of Delay (NoDelay_4Delay) emerged, $F(1,36) = 15.482, p < 0.001$. A significant interaction between Task (L4_L6) x Timebin emerged, $F(9,324) = 15.971, p < 0.001$. A significant interaction between Delay (NoDelay_4Delay) x Timebin emerged $F(9,325) = 23.738, p < 0.001$. A significant interaction between Task (L4_L6) x Timebins dominated by Timebins 2-3, 3-4, 4-5, 6-7, 7-8 emerged. This is due to a load dependent increase in HDR such that there is a higher peak as numbers of letters increases. A significant interaction between Delay (NoDelay_4Delay) x Timebins, dominated by Timebins 2-3, 4-5, 5-6, 6-7, 7-8. This is due to a narrower HDR peak as delay increases.

By visually examining this component's HDR plot relative to other reported components, INIT activity corresponded with the onset of the trial with the highest INIT activation seen early in the trial. In essence, this earlier activation suggests the INIT network most closely underlies the encoding phase of this SIRP WM task. This study corroborates the findings suggested by Metzak et al. (2012) study which employed a modified Sternberg working memory paradigm. While the Metzak et al. (2012) study was done in both schizophrenia patients and healthy controls and contained four different letter conditions (2, 4, 6, 8 letters), Sanford et al was done in healthy patients, contained two letter conditions (4 and 6 letters) and had a variable delay condition (0 or 4 seconds). Yet, the findings which emerge can still be supported by prior research done by Metzak et al. (2012). The HDR provides evidence that the 6 letter condition produces more INIT activity; thus INIT follows a

pattern whereby increasing activation occurs with increasing demand until activation diminishes when working memory capacity is reached. This is evident as there is greater overall activation which can be seen in the 6 letter load condition in comparison to the 4 letter load condition. Furthermore, in terms of the delay condition, a 4-second delay results in a sooner increased-to-peak pattern in INIT compared to no delay. The presence of the delay condition, which produced a sooner activation in INIT, reinforces a previously considered notion that INIT requires a brief break to effectively encode stimuli to display earlier activation (Percival et al., 2020). The delay condition did not produce higher activation compared to the no delay condition but it did display an earlier activation in INIT. INIT can be said to play a role in visual perception in relation to this task but the absence of a second peak in the 4-second delay condition indicates that this network underlies another cognitive process in addition to visual processing. The attentional process that is likely to recruit INIT is the encoding phase of working memory, which is involved in visual attention.

Figure 3

Sanford & Woodward WM HDR Plot



3.4 Sanford & Woodward's WM and TGT HDR

This study was incorporated into INIT's mean exemplar. In this study, 69 adults were recruited to participate in one of two tasks: the Sternberg Working Memory task and the Thought Generation Task. 37 healthy adults completed the Sternberg Working Memory task and 32 healthy adults completed the Thought Generation task. In this study, Component 2 was classified as the INIT network with a z-score of 1.2 from increased activity at 74% of the voxels. Positive loadings in Component 2 were found primarily in the bilateral occipital cortex (extending dorsally into parietal regions), supplementary motor areas, precentral gyrus, and thalamus (Sanford et al., 2019). Notably, the thalamus peaked relatively early on in the trials (Sanford et al., 2019). The increased signal in these brain regions largely reflects the activation of INIT for this study's working memory task.

A significant main effect of Tasks (L4_L6) emerged, $F(1,36) = 6.615$, $p<0.05$. A significant main effect of Delay (NoDelay_4Delay) emerged, $F(1,36) = 34.362$, $p<0.001$. A significant interaction between Task (L4_L6) x Timebin emerged at $F(9,325) = 18.824$, $p<0.001$. A significant interaction between Delay (NoDelay_4Delay) x Timebin emerged at $F(9,324) = 24.463$, $p<0.001$. A significant interaction between Task (L4_L6) x Timebin emerged. This repeated contrast was dominated by Timebin 3-4, 4-5, 5-6, 6-7. *This is due to a load dependent increase in HDR such that there is a higher peak as numbers of letters increases.* A significant interaction between Delay (NoDelay_4Delay) x Timebin occurred. This repeated contrast was dominated by Timebin 4-5, 5-6, 6-7, 8-9, 9-10. *This is due to a narrower HDR peak as delay increases.* No significant interactions or effects observed with TGT.

The data in this multi-experiment analysis is nearly identical to the data in the aforementioned single-experiment analysis in terms of the working memory task. Essentially,

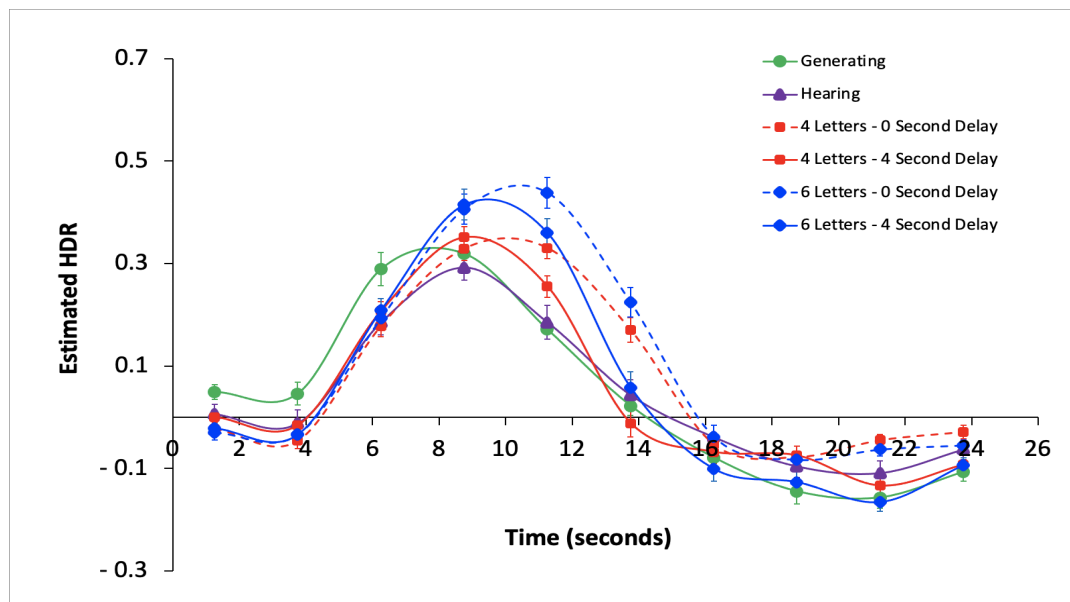
the findings are reproduced where INIT displays the earliest activation in comparison to the other components' HDRs. This pattern underscores how INIT is a key player in the encoding phase of working memory. Furthermore, INIT activation is shown to increase when load increases as shown by greater activation in the 6 letter condition compared to the 4 letter condition. Finally, the delay condition produces an even earlier INIT activation compared to the no-delay condition, but with no difference in the magnitude of activation. This could be attributed to how a greater delay, in comparison to no delay, indicates that participants have to hold the information longer. Thus, this analysis provides support for the argument that INIT is heavily involved in working memory encoding processes where that activation increases with load and activates earlier wherever more time is given to encoding.

This merged WM and TGT analysis does produce heightened INIT activity with sufficient strength ($z > 0.8$) but it is ambiguous whether or not TGT plays a significant role in recruiting INIT. Independent task analyses were not conducted for TGT in this study; the single task analysis was only conducted for WM. Thus, it is unclear whether TGT requires WM in order to demonstrate INIT with sufficient strength. No prior components, where TGT was the sole task, were derived from the CNoS Lab with sufficient strength ($z > 0.8$) where these studies did not display competition with the External Attention network (Section 4.3). In essence, merging tasks brought out INIT for TGT but on its own TGT does not seem to play a key role in recruiting INIT. Regardless, some information can be extracted from TGT in the context of the merged analysis. Indeed the thought generation task reveals differences between directing attention externally towards the environment (stimuli) and directing attention internally toward mental representations. Allowing to distinguish between externally oriented cognition and internally oriented cognition, this task is similar to the SIRP WM task which can allow researchers to differentiate between the cognitive processes of encoding versus maintaining/rehearsing. Through visually analyzing the HDR plot, this

component is more likely to underlie the mental operations involved in the initial interaction and attention paid to the stimulus in contrast to picturing and generating representations of the stimulus. This is consistent with the view that INIT plays a role in cognition earlier in trials. The greater activity elicited by the Generating condition compared to the Hearing condition suggests how INIT could be more active in internally oriented cognition relative to externally oriented cognition. Nonetheless, these hypotheses leave open the question of the extent to which INIT can be associated with internally oriented cognition and the precise type of this category of internally oriented cognition. Although INIT is categorized as a visually oriented cognition network, this does not prevent this network from displaying other properties which may be more reflective of internally oriented cognition. Ultimately, INIT is involved in this thought generation task in this merged task analysis, but it does not seem to sufficiently recruit INIT in studies where it is employed independently. Thus, it can be said that INIT is a non-dominant network for thought generation tasks.

Figure 4

Sanford & Woodward WM-TGT HDR Plot



3.5 Sanford's WM HDR

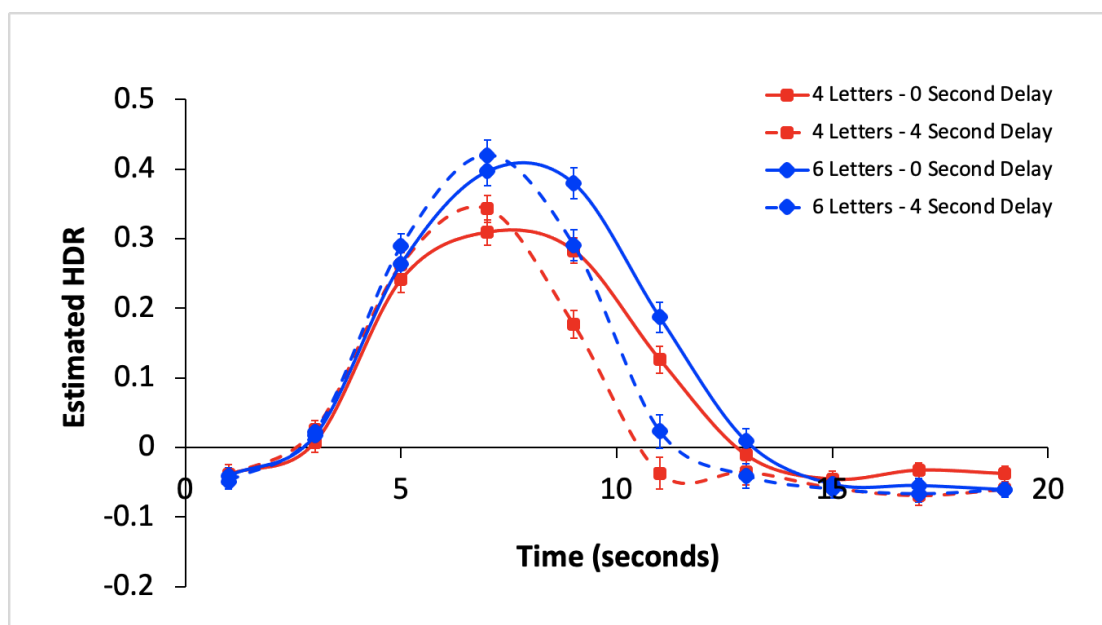
This study was not included in the mean exemplar for INIT. This section contains analyses of the single experiment of the Sanford et al. (2020) study which provided insights on the merged SCAP-TGT-TSI-WM analysis. This single experiment's focus is the Sternberg Item Recognition working memory task. This experiment included analyses conducted for 28 schizophrenia patients and 26 healthy controls who solely completed the working memory task. In this study, Component 2 was classified as INIT with a z-score of 1.21 from increased activity at 79% of the voxels. Positive loadings in Component 2 were found in the bilateral activation in the occipital cortex (occipital poles, lateral occipital cortex, and occipital fusiform gyri), precentral gyri, middle frontal gyri, supplementary motor area/superior frontal gyrus, and thalamus (Sanford et al., 2020). The increased signal in these brain regions largely reflects the activation of INIT for this study's working memory task.

A significant main effect of Task (L4_L6) emerged at $F(1, 53) = 19.054, p < 0.001$. A significant main effect of Delay (NoDelay_4Delay) emerged at $F(1, 53) = 31.072, p < 0.001$. A significant interaction between Task (L4_L6) x Timebin occurred at $F(9, 477) = 23.689, p < 0.001$. A significant interaction between Delay (NoDelay_4Delay) x Timebin occurred at $F(9, 477) = 33.278, p < 0.001$. A significant interaction between Task (L4_L6) x Timebins occurred. This contrast is dominated by timebins 2-3, 3-4, 4-5, 5-6, 6-7. *This is due to a perfectly load dependent increase in HDR such that there is a higher peak as numbers of letters increases.* A significant interaction between Delay (NoDelay_4Delay) x Timebins emerged. This contrast is dominated by timebins 1-2, 4-5, 5-6, 6-7, 7-8. *This is due to a wider HDR peak as delay decreases.*

Through visual examination of this component's HDR, INIT elicited some interesting properties. Overall early increased-to-peak activations followed by diminished activity were seen in the HDR across all conditions, which is characteristic of INIT. Controls in the 6 letter condition produced the highest increased-to-peak activation, followed by patients in the 6 letter condition, controls in the 4 letter condition and finally patients in the 4 letter condition. Thus, in terms of the load condition, INIT reaches the highest activation in more demanding tasks which may suggest that less exertion of neural processes is needed in dealing with less demanding tasks. In terms of participants, schizophrenia patients performed worse compared to controls in the respective load conditions. This is indicative of the impaired performance schizophrenia patients display in regards to working memory, which INIT may affect as it is a key player in encoding.

Figure 5

Sanford WM HDR Plot



3.6 Sanford's SCAP-TGT-TSI-WM's HDR

This study was not included in the mean exemplar for INIT. This section will explore the multi-experiment analyses (SCAP, TGT, TSI and WM) of the Sanford et al. (2020) study. This study included analyses conducted for 100 schizophrenia patients and 100 healthy controls who completed one of four tasks: a Sternberg verbal working memory task, a spatial capacity (visuospatial working memory) task, a Stroop set-switching task and a thought generation task. This multi-experiment analysis can provide insights into INIT's function through a merged task analysis perspective. In this study, Component 5 was classified as the INIT network with a z-score of 1.14 from increased activity at 85% of the voxels. Positive loadings in Component 5 were found in the bilateral activation in the occipital cortex (occipital poles, lateral occipital cortex, and occipital fusiform gyri), precentral gyri, middle frontal gyri, supplementary motor area/superior frontal gyrus, and thalamus (Sanford et al., 2020). The increased signal in these brain regions largely reflects the activation of INIT for this study's working memory task.

Sanford's SCAP HDR

The Spatial Capacity Task (SCAP) is an item-recall and visuospatial memory task with no verbal content. Across the conditions, there was a pattern for greater BOLD activation with a greater cognitive load, as evident by the greatest activation seen in the 7 dot condition. Activity in the INIT network appeared early in the task at approximately 4 seconds, during the encoding stage. Across each dot condition, greater activation was seen with increased delays; the 4.5-second delay had the highest peak for all conditions. Overall, the SCAP task showcased the role of visuospatial working memory tasks in the increased

activity in the INIT network. Similar to the results observed in the WM task, the conditions with more dots, and/or with greater delays exhibited the highest activations. Across all conditions, healthy controls performed better relative to schizophrenia patients in general. This supports the findings of Metzak et al. (2012) where patients displayed impaired working memory performance. Thus, according to the results of this study, it can be said that patients may also exhibit poorer visuospatial working memory performance where INIT may be playing a role. Overall, these findings reinforce the argument that INIT is a key player in working memory encoding processes as SCAP, another type of working memory task, supports these ideas.

A significant main effect of Load (L1_L3_L5_L7) emerged, $F(3, 258) = 48.089$, $p < 0.001$. A significant main effect of Delay (NoDelay_4Delay) emerged, $F(2, 172) = 15.610$, $p < 0.001$. A significant interaction between Load (L1_L3_L5_L7) x Delay (D15_D30_D45) emerged at $F(6, 516) = 3.785$, $p = 0.001$. A significant interaction between Load (L1_L3_L5_L7) x Timebin emerged at $F(27, 2322) = 39.679$, $p < 0.001$. A significant interaction between Delay (D15_D30_D45) x Timebin emerged at $F(18, 1548) = 10.548$, $p < 0.001$. A Significant interaction between Load (L1_L3_L5_L7) x Delay (D15_D30_D45) x Timebin occurred at $F(54, 4644) = 9.550$, $p < 0.001$. A significant interaction between Timebin x Group (Healthy_Schizophrenia) occurred, $F(9, 774) = 4.311$, $p < 0.001$. A significant interaction between Load (L1_L3_L5_L7) x Timebin x Group (Healthy_Schizophrenia) occurred at $F(27, 2322) = 1.864$, $p = 0.005$. A significant interaction of Load (L1_L3_L5_L7) occurred between L1 and L3 at $F(1, 86) = 51.633$, $p < 0.001$ and L3 and L5 at $(1, 86) = 11.199$, $p = 0.001$. A significant interaction of Delay (D15_D30_D45) emerged between D15 and D30 at $F(1, 86) = 19.841$, $p < 0.001$ and between D30 and D 45 at $F(1, 86) = 26.595$, $p < 0.001$. A significant interaction between Load (L1_L3_L5_L7) x Delay (D15_D30_D45)

occurred at L3 and L5 At D15 and D30 at $F(1, 86) = 4.590, p < 0.05$. Significant interactions between Load (L1_L3_L5_L7) x Timebin occurred, dominated by Timebins 1-2, 2-3, 3-4, 5-6, 6-7, 7-8, 9-10. An increase in load led to an increase in activation illustrated in the peak of the HDR as the number of letters increase, the activation increases. A significant interaction between Delay (D15_D30_D45) x Timebin, dominated by Timebins 1-2, 4-5, 5-6, 6-7, 9-10 occurred. Significant interactions between Load (L1_L3_L5_L7) x Delay (D15_D30_D45) x Timebin emerged. A significant interaction between Timebin x Group (Healthy_Schizophrenia) emerged. Significant interaction between Load (L1_L3_L5_L7) x Timebin x Group (healthy_Schizophrenia) emerged. Significant interaction differences between groups during L1 and L3 at Timebins 5 to 6 at $F(1, 86) = 3.959, p = 0.05$

Figure 6

SCAP Controls HDR Plot

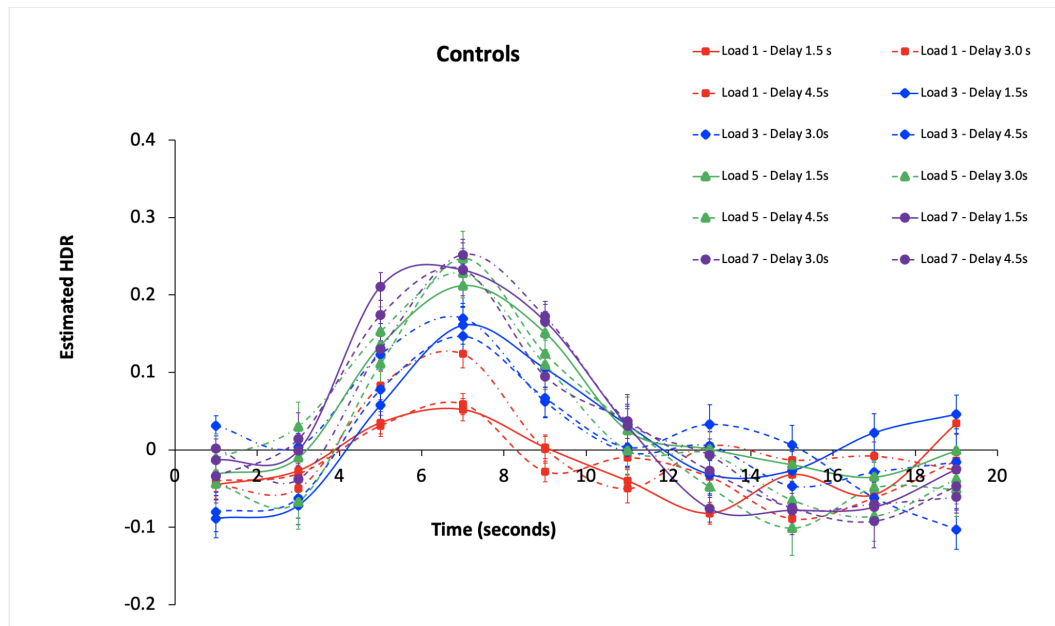
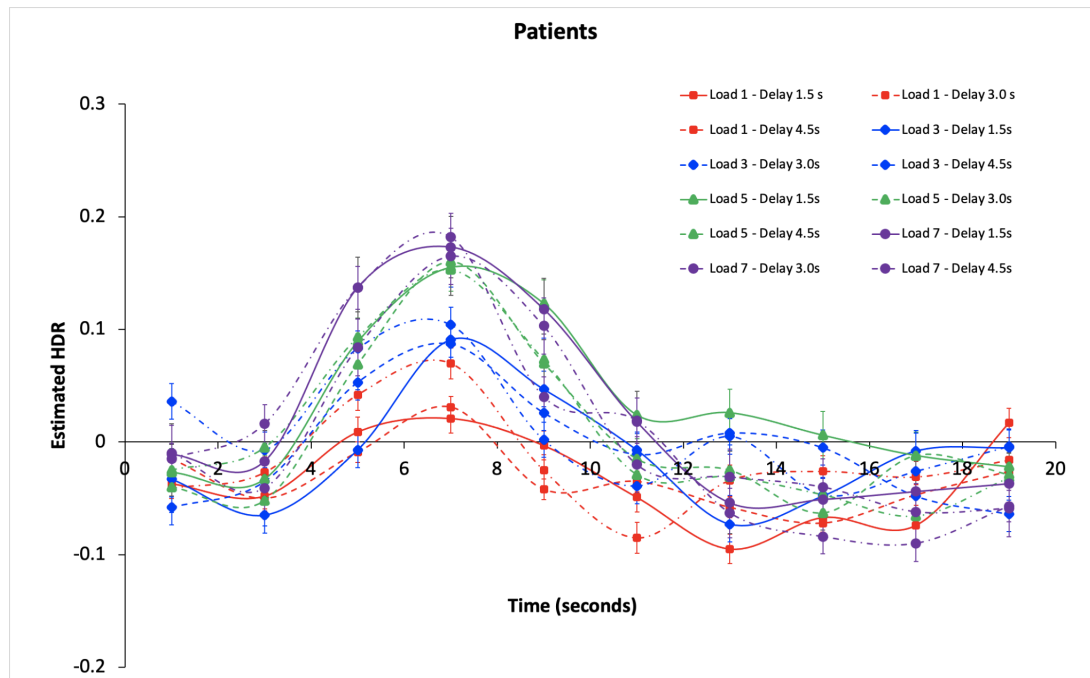


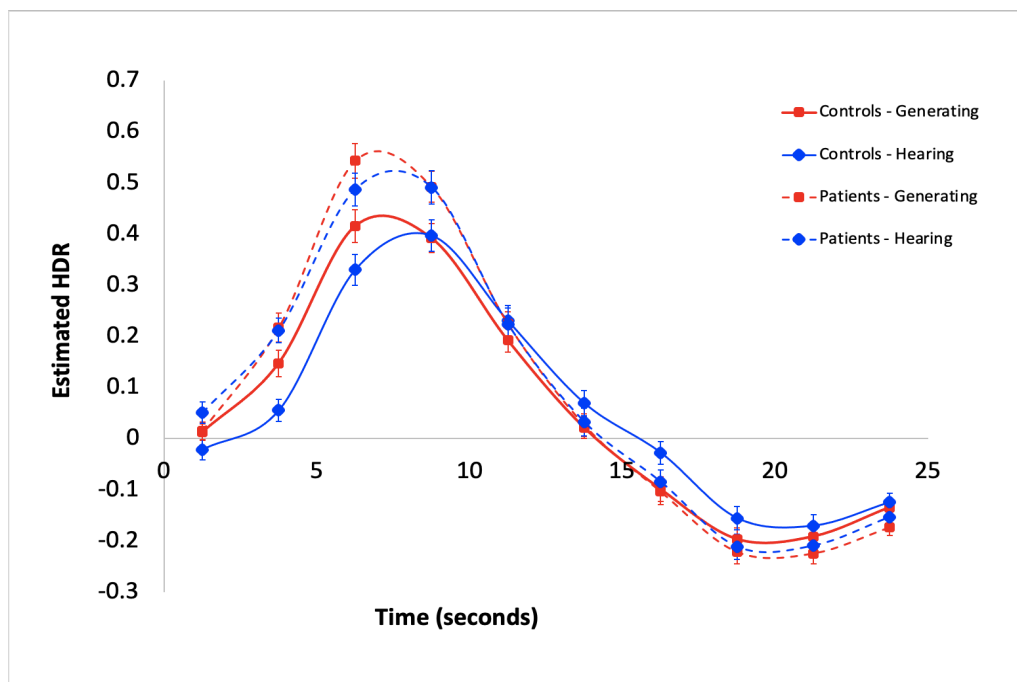
Figure 7*SCAP Patients HDR Plot***Sanford's TGT HDR**

The results of this TGT task are similar to the results of the Sanford et al. (2019) study where WM and TGT were merged. Essentially, the Hearing condition has a slower increase to peak activation compared to the Generating Condition. Significant differences were shown between healthy and schizophrenia groups; schizophrenia groups had significantly higher HDR peaks. The schizophrenia group had a faster and a greater initial increase in HDR compared to the control group. Altogether, thought generation tasks showcase how INIT, which is categorized as a visually oriented network, may be more active in internally oriented cognition relative to externally oriented cognition. This is because greater activity was evoked by the Generating condition compared to the Hearing condition. These are interesting results that further distinguish the contrast between INIT and the External Attention Network which are often found in competition with each other (Section 4.3).

A significant effect of group (Healthy_Schizophrenia) occurred at $F(1, 58) = 4.926$, $p < 0.05$. A significant interaction between Generating_Hearing x Timebin occurred at $F(9, 522) = 2.995$, $p < 0.05$. Significant Interaction between Group (Healthy_Schizophrenia) x Timebin emerged at $F(9, 522) = 6.259$, $p < 0.001$ (Figure 6). Higher activation in patient groups in both generating and hearing conditions compared to controls. Significant interactions between Generating_Hearing x Timebins occurred, dominated by Timebins 1-2. Generating increases faster than hearing at Timebin 1 to 2 at $F(1, 58) = 13.904$, $p < 0.001$.

Figure 8

Sanford TGT HDR Plot



Sanford's TSI HDR

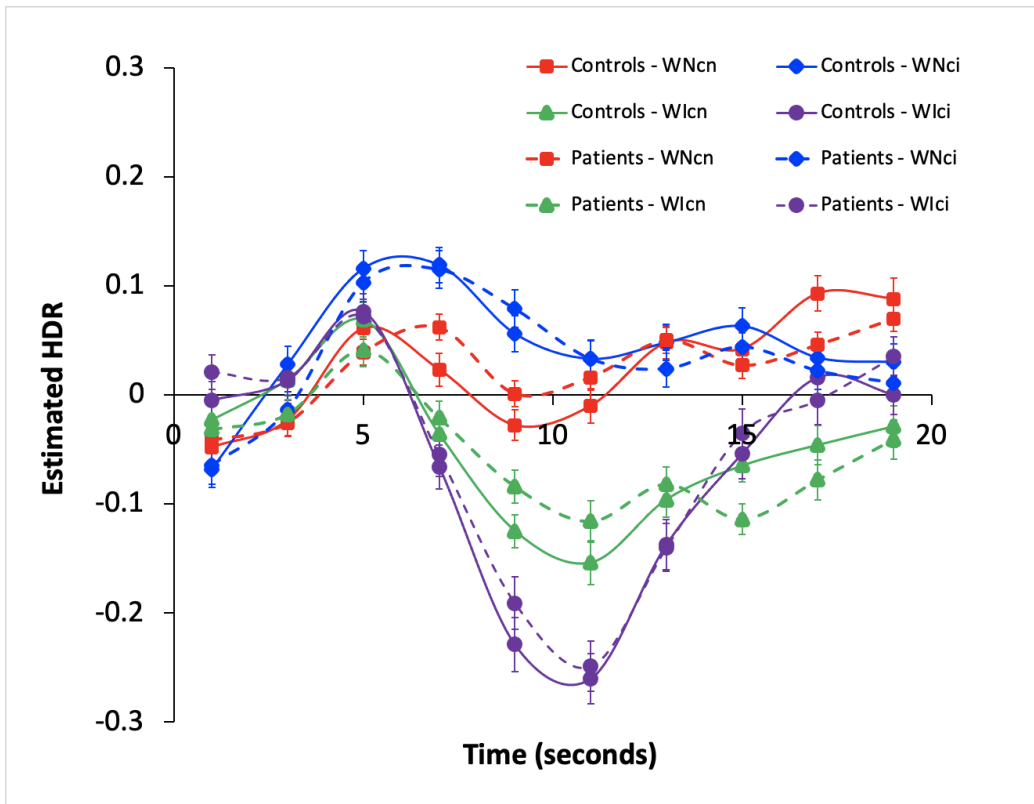
In this task-switch inertia (TSI) task, a strong suppression can be seen for INIT in this component's HDR (Figure 9). This coincides with the general understanding that INIT is not known to activate during rapid design tasks, such as TSI (Percival et al., 2020). Ultimately,

TSI does not play a significant role in the contextualization of INIT. The suppression associated with the TSI is notably the strongest in the WIci condition where participants were exposed to the incongruent word-reading preceded by incongruent colour naming. This condition is rather confusing since word-reading and incongruent colour naming utilize the same stimuli; thus, the suppression could be a result of INIT processes slowing down and deactivating due to the highly challenging nature of this task.

A significant main effect of Stimulus Type (WN_WI) occurred at $F(1, 52) = 96.571$, $p < 0.001$. A significant main effect of Color block (cn_ci) occurred at $F(1, 52) = 4.218$, $p < 0.05$. A significant interaction between Stimulus type (WN_WI) x Timebin occurred at $F(9, 468) = 82.180$, $p < 0.001$. A significant interaction between Color Block (cn_ci) x Timebin occurred at $F(9, 468) = 5.007$, $p < 0.001$. Significant interactions between Stimulus Type (WN_WI) x Color Block (cn_ci) x Timebin occurred at $F(9, 468) = 32.732$, $p < 0.001$. Significant interactions between Stimulus Type (WN_WI) x Timebin emerged, dominated by Timebins 1-2, 2-3, 3-4, 4-5, 5-6, 6-7, 7-8, 8-9, 9-10. This shows *suppression for WI stimulus and decrease in activation for WN stimulus*. Significant interaction between Block Color (cn_ci) x Timebin, Dominated by Timebins 4-5, 5-6, 7-8. Significant interactions between Stimulus Type (WN_WI) x Block Color (cn_ci) x Timebins emerged, dominated by Timebins 1-2, 3-4, 4-5, 5-6, 6-7, 7-8, 8-9.

Figure 9

Sanford TSI HDR Plot



Sanford's WM HDR

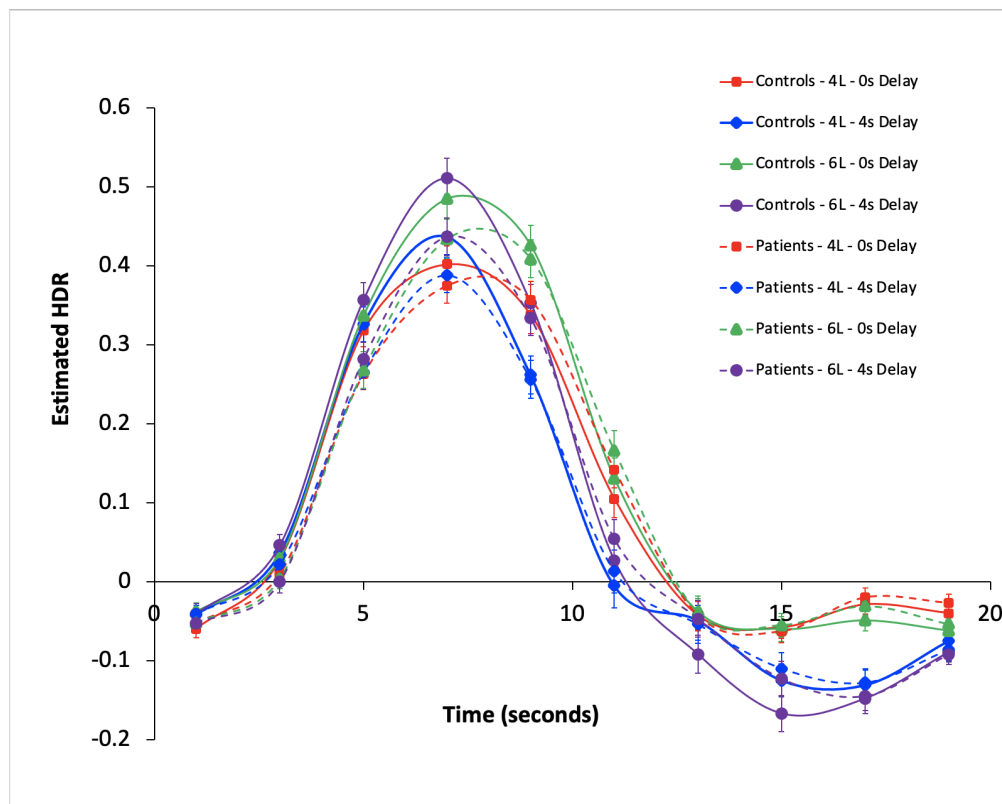
In terms of this study's SIRP WM task, Component 5's HDR plot (Figure 10), showcases how INIT was primarily engaged during working memory encoding and declined in participants later in the trials. This is a characteristic trend wherever INIT activity is seen, which remains consistent across studies with varying datasets. Due to the early responding nature of the INIT, it can be conjectured that working memory deficits in schizophrenia may arise from the disruption of INIT in encoding processes. The HDR plot also supports the idea that increased activation in INIT occurs with increasing demand until activation diminishes when working memory capacity is reached. This is evident as there is greater overall activation can be seen in the 6 letter load condition in comparison to the 4 letter load condition. This is interesting as the 4 letter condition was supplemented by pound “#” signs which did not seem to increase cognitive demand. In terms of the delay period, greater activation in the 0 second delay period can be seen relative to the 4-second delay condition.

The HDR shows that the increase to peak pattern was similar in delay conditions but the 0-second delay condition displays a gradual return to baseline. This can be attributed to the immediate presentation of the probe following the encoding period. In contrast, the 4-second delay condition is absent of a second peak which may have corresponded with the presentation of the probe after a delay. Thus, this indicates the importance of this activation for the encoding phase of the task. Ultimately, INIT is shown to be very predictive of working capacity due to its significant role in the encoding phase.

A significant main effect of Task (L4_L6) occurred at $F(1, 52) = 13.512, p < 0.001$. A significant main effect of Delay (NoDelay_4Delay) occurred at $F(1, 52) = 68.578, p < 0.001$. A significant interaction between Task (L4_L6) x Timebin occurred at $F(9,468) = 29.900, p < 0.001$. A significant interaction between Delay (NoDelay_4Delay) x Timebin occurred at $F(9,468) = 38.746, p < 0.001$. Significant interactions between Task (L4_L6) x Timebin emerged, dominated by Timebins 2-3, 3-4, 5-6, 6-7. This shows how an increase in load led to an increase in activation illustrated in the peak of the HDR as 6 letters had a higher peak than 4 letters. Significant interactions between Delay (NoDelay_4Delay) x Timebin emerged, dominated by Timebin 4-5, 5-6, 6-7, 7-8, 8-9, 9-10. In essence, a higher delay led to a narrower peak in the HDR indicating a shorter period of activation

Figure 10

Sanford TSI HDR Plot



3.7 Zurrin's RSPM HDR

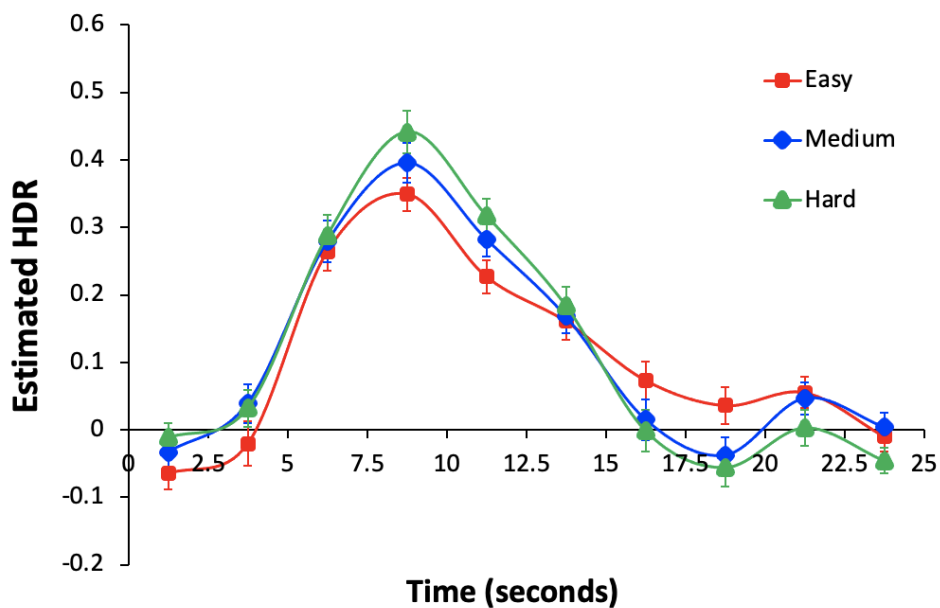
This study was not included in the mean exemplar for INIT. The Raven's Standard Progressive Matrices Task was conducted in an unpublished study, Health RSPM 5 on 56 healthy participants. In this study, Component 4 was classified as the INIT network with a z-score of 0.91 from increased activity at 63% of the voxels. Positive loadings in Component 4 were found primarily in the bilateral occipital cortex, supramarginal gyrus, middle frontal gyrus, postcentral gyrus, and bilateral activation in the precentral gyrus. These locations correspond with determined regions of INIT (Sanford et al., 2020). Thus, the increased signal in these brain regions largely reflects the activation of INIT for this study's RSPM task.

A significant interaction between difficulty (Easy_Med_Hard) x Timebin emerged at $F(18, 990) = 2.350, p = 0.001$. A significant interaction between Difficulty (Easy_Med_Hard) x Timebins occurred. This repeated contrast was dominated by Timebin 6-7 and 8-9. This is due to a difficulty dependent increase in HDR such that there is a higher peak as difficulty increases, in addition, as difficulty decreases, the activation towards the end maintains relatively high compared to higher difficulties.

Through visual inspection of the components' HDR plot, INIT is seen relatively earlier in the trial with its corresponding sharp peak. The early initiation of cognitive processes is demonstrated in this RSPM task, where participants decide which piece was missing from a certain set. As participants no longer need to recruit such cognitive processes, an absence of sustained INIT can be discerned.

There are three blocks within the RSPM task corresponding to difficulty level and it was found that a significant load interaction was present in relation to INIT. A higher INIT activity peak can be seen for the Hard condition followed by a more pronounced deactivation of the trend. Whereas the Easy condition displays a lower, main peak followed by more sustained yet lowering activity. The Medium condition falls in between the patterns shown by the Hard and Easy Condition. These patterns speak to a characteristic of INIT where greater initiation is needed in certain cognitive processes when attending to more difficult tasks.

The RSPM task tests participants' abilities to deconstruct problems in order to better deal with sets of sub-problems, and to reason abstractly. The activation of INIT may illustrate its role in visually attending to the RSPM task which aims to identify brain regions involved in intelligence (Zurrin et al. 2020). Thus, INIT may be a network associated with early visual attention and initial decision making in such abstract reasoning tasks.

Figure 11:*RSPM HDR Plot*

3.8 FISH HDR

This study was not included in the mean exemplar for INIT. In this unpublished study, participants consisted of both schizophrenia patients and healthy controls. The schizophrenia group consisted of 35 schizophrenia patients (non-delusional). In this study, Component 3 was classified as INIT with a z-score of 0.92 from increased activity at 65% of the voxels. Positive loadings in Component 3 were primarily found in the visual cortex regions of the occipital lobe and fusiform gyrus. The increased signal in these brain regions largely reflects the activation of INIT for this study's probabilistic reasoning, FISH task.

There is a significant main effect of match condition of $F(1,32) = 4.131$, $p=0.050$. A significant interaction occurs between Strong_Weak x Timebin ($F(9,288)=2.761$, $p=0.004$), where Weak starts off lower but becomes much higher than Strong at Timebin 4 and

onwards. Significant interactions between Match_Nonmatch x Strong_Weak x TAU_CRT_MCT occurs ($F(2,32)=3.660$, $p=0.037$). Significant interactions between T1_T2 x Match_Nonmatch x Strong_Weak x Timebin x TAU_CRT_MCT occur ($F(18,288)=1.891$, $p=0.016$). The average activity for Nonmatch is significantly higher than the average activity for Match, ($F(1,32)=4.131$, $p=0.050$).

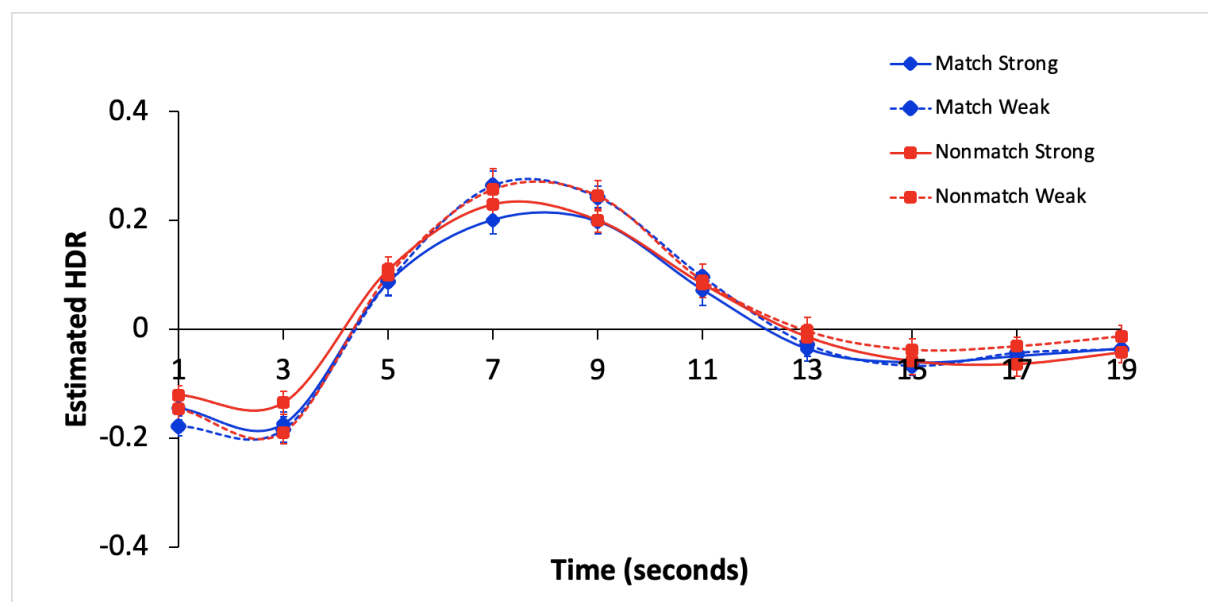
Previous studies have demonstrated that patients with delusions and schizophrenia may be willing to base decisions off of less evidence than patients with schizophrenia without delusions and healthy subjects; this effect is known as “jumping to conclusions” (JTC) bias. The JTC bias is explained by the hypersalience of evidence-hypothesis matches (EVH matches) account of delusions. An EVH match condition is created when the color of the central fish is congruent with the color of the majority of the fish in the lake to which it points. A probabilistic reasoning task, called FISH, assesses the involvement of functional brain networks in EVH matches. Based on the timing trajectory of the estimated hemodynamic response for INIT, the characteristic earlier peak pattern followed by a deactivation for the rest of the task is evident across all conditions. This may indicate how the INIT network generally attends to external visual stimuli in EVH matches and JTC bias. By further visually inspecting the HDR plot for Component 3, the nonmatch condition had a greater BOLD activation compared to the match condition. The FISH task required participants to make decisions based on evidence given to either accept (match-conditions) or reject (non-matching-condition) a hypothesis (Woodward et al., 2009). Overall, INIT can be said to play a role in visually attending to stimuli in probabilistic reasoning tasks.

An interesting finding associated with the presence of INIT in this FISH task is that INIT was not activated in any other study which included FISH. The FISH task is a rapid design task where stimuli are rapidly shown with brief breaks in between. INIT is typically

not activated in such task designs and so its presence in this task is quite intriguing. An explanation for this is that although the FISH task subscribes to this rapid task design style, it includes some breaks which are long enough between trials to justify that INIT would be elicited (2, 4, 6, 8-second breaks). Thus, INIT may be specifically involved in attending to stimuli in intertrial intervals.

Figure 12

FISH_T1_T2 HDR Plot



4. Discussion

4.1 Summary of Significant Task Findings

INIT is implicated in a wide range of tasks, and it emerges more in response to particular task conditions over others. Its presence can be observed substantially in working memory, followed by abstract reasoning, probabilistic reasoning, and visuospatial working memory. Indeed it is evident the function of INIT entails the initiation of cognitive faculties

due to its characteristic earlier increased-to-peak HDR activation and sharpness of its peak.

By examining prior studies conducted by the CNoS Lab where INIT was found with sufficient strength, it has been elicited that INIT strongly underlies cognitive processes in working memory tasks, followed by Raven's Standard Progressive Matrices, FISH task and working memory in combination with a visuospatial working memory task (SCAP).

Although the merged analysis with TGT and TSI did demonstrate INIT activity with sufficient strength, these tasks were not used to contextualize this networks' function after careful deliberation.

INIT's consistently strong presence in working memory tasks is of particular interest. Its initial engagement in working memory tasks exhibits its profound role in encoding in working memory. Furthermore, INIT was activated in many types of working memory tasks (Woodward's WM, Metzak's modified SIRP WM, Sanford's SIRP WM and Sanford's visuospatial working memory SCAP task). All of these working memory tasks showed a graded response in the network dependent on cognitive load and delay conditions, reliably implicating INIT in encoding processes. In essence, as Initiation activation becomes more effortful with increasing cognitive load, working memory processes are further taxed and thus greater brain activity is required. Considering the SCAP task's results, INIT is shown to also be as involved in visual encoding in addition to the encoding of linguistics in the SIRP WM task. All together these varied working memory tasks reinforce the conclusion that INIT is a key player in the encoding phase of working memory over a variety of working memory task conditions. This finding is significant, especially when considering schizophrenia, a psychiatric condition where working memory processes are impaired. Future research could be conducted to target INIT with the purpose of enhancing the encoding of memory sets in schizophrenia patients. Discerning the differences in activation and reduced activation of INIT in schizophrenia patients and healthy controls can expand the understanding of

functional connectivity in schizophrenia patients and be an instrumental factor in the future use of neuromodulation as a treatment option.

Furthermore, INIT's role in tasks like the RSPM and FISH, cannot be overlooked; these results imply the network's role is not limited to one cognitive domain. The networks' activation in the RSPM task reveals how INIT is implicated in attending to visual stimuli related to abstract reasoning. We can further characterize INIT with the RSPM task by recognizing that when the abstract reasoning task difficulty increases, INIT activation also increases. This demonstrates how INIT is recruited when initial attention must be paid to demanding abstract reasoning tasks. The FISH task's results further depict how INIT is a complex network with varied roles. The recruitment of INIT in the FISH task underscores its potential involvement in visually attending to probabilistic reasoning tasks especially during intertrial intervals .

TSI and TGT were found to demonstrate INIT, but confined to the context of merged analyses. Upon closer examination of these tasks, their associated HDRs and competition with other networks such as EXT, these tasks do not serve a profound role in the contextualization of INIT. Essentially, these studies would not provide great insight into the function of INIT as they are not the best or purest examples of INIT. In the multi-experiment, SCAP-TGT-TSI-WM Sanford et al. (2020) study, Component 5 was classified as the INIT network with a z-score of 0.85 from increased activity at 85% of the voxels. But since TSI's HDR displayed a strong suppression for INIT, the strong z score and positive percentage loadings for this component can be attributed to activity from other tasks, such as WM or SCAP. Contextually speaking, it makes more sense for INIT to be recruited in this study with sufficient strength because of the WM and SCAP tasks since it has led to the understanding that INIT is involved in the sub-process of encoding in working memory. In terms of thought generation, this task was found in two multi-experiment analyses, the Sanford & Woodward

(2019) study and the Sanford et al. (2020) study where the components display INIT activation with sufficient strength. In essence, merging tasks brought out INIT for TGT but on its own TGT does not seem to play a key role in recruiting INIT. In fact, independent thought generation tasks were excluded from this exploration after it was determined that they are actually reflective of External Attention activity (Section 4.3).

4.2 INIT and Load Dependency

As task difficulty increases, indicative of the increase in cognitive load, INIT activation is also shown to increase. All eight studies analyzed in this exploration revealed support for this finding. Metzak's modified SIRP WM task, Sanford & Woodward's SIRP WM task, RSPM task, Sanford's SCAP task and Sanford's SIRP WM task all demonstrated that a greater load condition (ie. 6 letters relative to 4 letters) displayed greater INIT activation. Notably it was also seen that as cognitive load increases, INIT activation decreases in the TSI task.

4.3 INIT and EXT Competition

Having shown involvement in the initiation of certain cognitive processes, this network has indeed been labeled as INIT. However, previously this network was labeled as the encoding network (Metzak et al., 2012, Woodward et al., 2013), energizing network (Sanford et al., 2020) and the visual attention network (Sanford & Woodward, 2019, Sanford et al., 2020). It is essential to understand that another task-based network, the External Attention network (EXT) was previously referred to as the visual attention network as well (Sanford et al., 2020). Due to the anatomical similarities between the Initiation Network (INIT) and External Attention network (EXT) and their involvement in visually oriented cognition, they are often activated in many similar tasks, such as evidence integration tasks, thought generation tasks and even paired associates memory encoding tasks (Table 2). There

were many studies classified as INIT, with a Fisher's z-score greater than 0.8, which needed to be excluded from this analysis as a detailed examination into the components' classification revealed heavy competition with the External Attention network. Thus, these studies would not provide great insight into the function of INIT as they are not the best or purest examples of INIT. Studies with tasks, such as Metrical Stress, Semantic Association, Thought Generation, Paired Associates Memory Encoding and Evidence Integration all displayed this competition with the external attention network (Table 2). What remained were the working memory tasks, Raven's standard progressive matrices task, FISH task, and working memory tasks in combination with thought generation, spatial capacity and task switch inertia (Table 3). A detailed depiction of the included and excluded studies in this exploration due to Initiation and External Attention competition has been provided in Table 2 and Table 3.

Two methods were used to distinguish whether the studies displayed INIT or EXT. Automated classifications have previously been conducted for all studies conducted in the Cognitive Neuroscience of Schizophrenia Lab. While most classifications are completed on the statistical basis of Fisher's z-score based on exemplar groupings, there are two other classification methods, which rely on the averages of exemplar-specific Fisher transformed z-scores and the average of all patterns' Fisher transformed z-scores. The studies which were maintained in this analysis displayed that INIT was the best match across all three classification methods or best match in at least two of the classification methods (Table 3). Furthermore, to further determine which network these components belonged to, MRIcron, a cross-platform brain image viewer was utilized. Certain slice numbers have previously been determined to be representative of either EXT or INIT activity. Comparing axial slice numbers 64 (indicative of INIT) with 54 (indicative of EXT) aided in the classification of these components where higher activation in slice 64 revealed stronger INIT activation.

Ultimately, these studies have been classified as EXT based on the above methods. Refer to Table 2 for the studies that were excluded from the analysis, including the computed z scores from the distinct classification methods and MRI-cron slice 64 and 54 activity levels.

Furthermore, INIT and EXT can be distinguished from their HDR shapes. There has been a general understanding that INIT typically demonstrates early activation followed by decreased activity and EXT displays sustained activation throughout trials (Sanford et al., 2020). Interestingly, an evaluation of INIT and EXT's HDRs in the Healthy RSPM 5 unpublished study (Figure 13) reveals how EXT can display earlier activation compared to INIT. This does not necessarily negate the fact that INIT is understood to display earlier activation; in fact, in all of the working memory tasks included in this exploration INIT does display the earliest activation. However, it should be recognized that EXT did not emerge in those studies. Thus, this could mean that EXT is the network which displays the earliest activation in trials. The fact that in the RSPM task, EXT is shown to activate first and is sustained throughout while INIT trails after EXT and peaks sharply around 8 seconds suggests that it cannot be broadly stated that INIT displays the earliest activation for all tasks where it is found with sufficient strength. Nonetheless, INIT is shown to display a sharp peak and absence of sustained activation, which is typically common for INIT. Altogether, its characteristic earliest activation can be definitively applied to working memory tasks but this generalization may not be the case for other tasks, such as RSPM, where INIT is found. In essence, INIT's HDR shape can be distinguished from EXT's HDR trend, such that a sharper peak is typically found with an absence of sustained activation. Ultimately, INIT's sharp peak and absence of sustained activation may suggest that the brief recruitment of intense cognition is all that is needed to bring an individual's attention to the task while EXT requires more sustained attention to effectively attend to a task.

Figure 13

Comparison of EXT and INIT's HDR in RSPM task

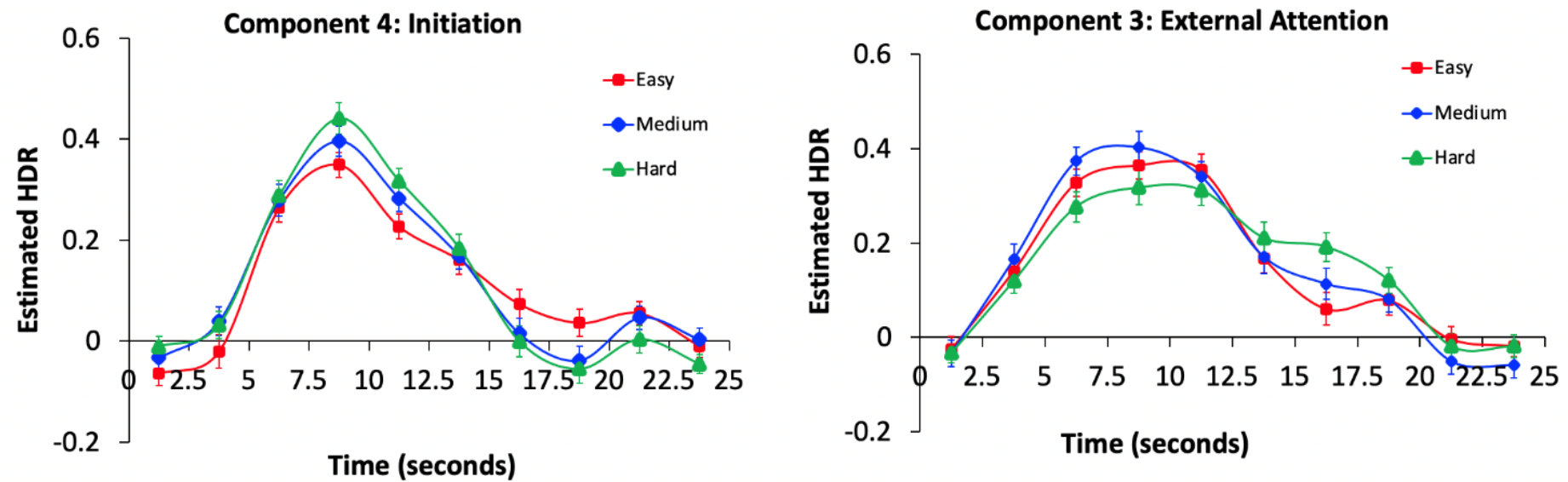


Table 2: Summary of Excluded Studies which elicit EXT Competition

Study	Lavigne et al., 2015a	Metzak et al. 2018	Lavigne et al., 2015b	Roes et al. 2021	Sanford et al. 2020	Percival et al. 2018	Percival et al. 2019a	Percival et al. 2019b
Task	ABADE	MMCC	TGT	PAMENC	TGT	MS-TGT-SA	TGT-SA	MS-TGT
Component	2	3	1	2	1	3	1	3
Fisher's z-score (from exemplar groupings) and Best Match	0.93/ INIT	0.96/ INIT	0.96/ INIT	0.89/ INIT	0.85/ INIT	0.88/ INIT	1.2/ INIT	0.83/ INIT
Mean exemplar specific pattern Fisher transformed z-scores and Best Match	0.84/ EXT	0.97/ One-handed response	0.86/ EXT	0.80/ EXT	0.81/ EXT	0.91/ INIT	1.17/ EXT	0.72/ INIT
All Mean patterns of Fisher transformed z-score and Best Match	0.97/ EXT	0.96/ EXT	0.87/ EXT	0.9/ EXT	0.86/ EXT	0.89/ EXT	1.22/ EXT	0.77/ EXT
Approximate 64 slice activation level (INIT)	0.01	0.18	0.21	0.26	0.24	0.16	0.21	0.19
Approximate 54 slice activation level (EXT)	0.11	0.20	0.30	0.29	0.28	0.27	0.29	0.25
Resulting Classification	EXT	Ambiguous	EXT	EXT	EXT	EXT	EXT	EXT

Table 3: Summary of Included Studies which elicit INIT Activation

The Lavigne et al. (2015) study and the Metzak et al. (2018) study were not included in this analysis for INIT even though they contained another component classified as EXT. In the Lavigne et al. (2015) study, Component 2 was classified as INIT while Component 5 was classified as EXT. In the Metzak et al. (2018) study, Component 3 was classified as INIT while Component 1 was classified as EXT. Although not common, some studies have been shown to recruit two components that can be classified as the same network. Examples of this would be where EXT was classified as C1 and C2 with a $z > 0.8$ in the Lavigne et al. (2018) study or where EXT was classified as C1 and C2 with $z > 0.77$ in the Lavigne et al. (2019) study. Furthermore, the Lavigne et al. (2015) study and the Metzak et al. (2018) study were further not utilized in this analysis to determine the function of INIT because they could be classified as EXT using the two other classification methods and using MRI-cron revealed greater activation in EXT. The studies utilized in this exploration are those that are considered to be the purest examples of INIT in order to provide meaningful insights into the functions of INIT. Ultimately, this ambiguous yet clearly present competition with EXT in the Lavigne et al. (2015) study and the Metzak et al. (2018) study warrants their exclusion from this analysis.

5. Conclusion

Indeed it is evident that the function of INIT entails the initiation of cognitive faculties due to its characteristic strong and earlier increased-to-peak HDR activation and absence of sustained activation. By examining prior studies conducted by the CNoS Lab where INIT was found with sufficient strength, it has been demonstrated that the INIT network is most strongly revealed by the cognitive processes of working memory tasks, abstract reasoning, probabilistic reasoning and visuospatial working memory. INIT's

consistently profound role in working memory encoding is of particular interest as it has been strongly associated with the sub process of encoding. Whether INIT is directly involved in encoding or encoding requires initiation of certain cognitive processes remains unknown. Thus, understanding the potential function of INIT to a greater extent may provide future insights into the biological underpinnings for schizophrenia impairment in working memory. Through the Raven's Standard Progressive Matrices task INIT was strongly activated early on, eliciting its role in visual attention in terms of abstract reasoning. In the probabilistic reasoning FISH task, INIT was found early in the trial, perhaps emphasizing the importance of visual attention to external stimuli particularly in intertrial intervals. Moreover, INIT's suppression discerned in the TSI task underscores how this network deactivates in tasks with a rapid design. This functional assessment of INIT can enhance current knowledge related to functional neural connectivity and contribute to the utilization of neuromodulation as a future treatment option in brain dysfunction, such as schizophrenia.

6. Acknowledgement

The research was supported by the Cognitive Neuroscience of Schizophrenia lab under the supervision of the principal investigator, Todd Woodward.

7. References

- Lavigne, K.M., Metzak, P.D., & Woodward, T.S. (2015). Functional brain networks underlying detection and integration of disconfirmatory evidence. *NeuroImage*, 112, 138-151. <https://doi.org/10.1016/j.neuroimage.2015.02.043>
- Lavigne, K.M., Rapin, L.A., Metzak, P.D., Whitman, J.C., Jung, K., E.T.C. & Woodward, T.S. (2015). Left-Dominant Temporal-Frontal Hypercoupling in Schizophrenia Patients With Hallucinations During Speech Perception. *Schizophrenia Bulletin*, 41, 259-267 <https://doi:10.1093/schbul/sbu004>
- Lavigne, K.M. (2018). Cognitive Biases and Functional Brain Networks Underlying Delusions in Schizophrenia. [Doctoral dissertation]. University of British Columbia.
- Lavigne, K.M., Menon, M., Moritz, S., Woodward, T.S. (2019). Functional Brain Networks Underlying Evidence Integration and Delusional Ideation. *Elsevier*, 216, 302-309 <https://doi.org/10.1016/j.schres.2019.11.038>
- Metzak, P.D., Riley, J., Wang, L., Whitman, J.C., Ngan, E.T.C. & Woodward, T.S. (2012). Decreased efficiency of task-positive and task-negative networks during working memory in schizophrenia. *Schizophrenia Bulletin*, 38(4), 803-813.
- Percival, C. (2019a). *fMRI analysis of functional brain connectivity in two language tasks in schizophrenia*. [Unpublished undergraduate thesis]. University of British Columbia.
- Percival, C. (2019b). *Merged Metrical Stress-TGT*. University of British Columbia.
- Percival, C. (2018a). *Merged Analysis: Metrical Stress-Thought Generating Task-Semantic Association*. University of British Columbia.
- Percival, C. (2018b). *Merged Semantic Association-Metrical Stress*. University of British Columbia.
- Percival, C., Zahid, H., & Woodward, T. S. (2020). *CNoS-Lab/Woodward_Atlas: Woodward*

Atlas November 2020 Release. Zenodo. <https://doi.org/10.5281/zenodo.4274398>

Roes, M., Chinchani, A., & Woodward, T.S. (2020). Reduced functional connectivity in brain networks underlying paired associates memory encoding in schizophrenia.

Manuscript in Preparation.

Sanford, N., Whitman, J.C. & Woodward, T.S. (2020). Task-Merging for finer separation of functional brain networks in working memory. *Cortex*, 125, 246-271.

Sanford, N. A. (2019). *Functional brain networks underlying working memory performance in schizophrenia : a multi-experiment approach [Unpublished doctoral dissertation]*. University of British Columbia.

<https://open.library.ubc.ca/cIRcle/collections/ubctheses/24/items/1.0387449>

Woodward, T.S., Feredoes, E., Metzak, P.D., Takane, Y., & Manoach, D.S. (2013). Epoch-specific functional networks involved in working memory. *NeuroImage*, 65: 529-539.

Zurrin, R., Wong, S., Goghari, V., & Woodward, T.S. (2021). *Functional Brain Networks Involved in Raven's Standard Progressive Matrices*. Manuscript in Preparation.

**Functional Analysis of the Volitional Attention to External Representations Network
through Task-Based fMRI**

Crystal Han^{1,2}, Jillian Rodger^{1,2}, Todd Woodward^{1,2}.

¹BC Mental Health and Substance Use Services

²Department of Psychiatry, University of British Columbia

Abstract

A large majority of previous research done to characterize brain networks focused primarily on the use of resting-state fMRI, which looks at brain activity in the absence of stimuli (Lee et al., 2013; Stanford et al., 2020), however, the specific relationship between regions of brain activity have yet to be identified. The current study utilized task-based fMRI to investigate the relationship between cognition and brain activity through the performance of certain tasks (Sanford et al., 2020; Zhang et al., 2016). Task-based fMRI allows for the observation of brain activity during performance of selected tasks and can be used to identify brain regions active during various tasks, using the blood-oxygen-level-dependent (BOLD) signals to create a hemodynamic response (HDR) pattern. The current study aimed to analyze HDR patterns in various studies which recruited the Volitional Attention to External Representations (EXT) network to identify a possible function for the EXT network. The EXT network has been hypothesized to be responsible for the maintenance of attention during the performance of tasks over a prolonged period (Fortenbaugh et al., 2017; Sarter et al., 2001), namely during tasks requiring attention to visual stimuli (Lavigne et al., 2020). With the knowledge of the hypothesized function of the EXT network, the current study analyzed 10 various studies involving the EXT network and compared the HDR patterns to identify an interpretation of the network's function to fit all studies.

Table of Contents

<i>Abstract</i>	1
<i>Introduction</i>	4
<i>Results</i>	5
1a. Raven's Standard Progressive Matrices Task (RSPM); Bipolar Merge.....	5
1b. Raven's Standard Progressive Matrices (RSPM); Healthy RSPM 5.....	7
2. Human Connectome Project Social Task	9
3. Lexical Decision Task (LDT); Bipolar Merge.....	11
4a. Evidence Integration Task (BADE); Lavigne Schizotypy SchizRes BADE	14
4b. Evidence Integration Task (BADE); Lavigne Prepost BADE	17
4c. Evidence Integration Task (BADE); Lavigne OTT BADE	19
5. Addis Task; Klepel in Prep Addis	23
6. Source Monitoring (SM).....	26
7.1. Semantic Association (SA); Woodward Human Brain Mapping Association	29
7.2 Semantic Association (SA); Metric Stress Semantic Association Merge	32
7.3 Semantic Association (SA); Triple Merge Thesis.....	34
8. MMCC; Metzak et al.....	36
9.1 Metrical Stress Task (MS); Metric Stress Semantic Association Merge.....	40
9.2 Metrical Stress Task (MS); Triple Merge Thesis.....	43
10. FISH task	45
11. fBIRN Oddball Task; Triple Merge Thesis	49
<i>Discussion</i>	51
<i>References</i>	55

Introduction

Previous research pertaining to brain network activation has focused solely on activation patterns of the brain during the absence of stimuli (Lee et al., 2013; Sanford et al., 2020), which does not provide sufficient information to characterize the function of various brain networks during the active performance of the brain during tasks. Zhang et al. (2016) noted task-based fMRI is advantageous in comparison to resting-state fMRI, as it reduces the variability in brain activity between participants by allowing more control over the focus of the participant's attention. Activity of networks vary based on the task being performed, thus requiring observation of the same network over various tasks to fully characterize it (Henson, 2006; Fortenbaugh et al., 2017). Task-based fMRI identified a novel network, which has since been named the Volitional Attention to External Representations network (EXT) (Percival et al., 2020), and the recruitment of this network is characterized by the activation in the anterior cingulate cortex, bilateral insula, and various sensorimotor regions (Lavigne et al., 2020). The current study is based on the analysis of previously completed tasks which involve the recruitment of the EXT network to identify the function of the network. It has been hypothesized according to previous studies which recruited the network that the EXT network is responsible for the direction of attention towards environmentally relevant stimuli and the recruitment of other large networks related to the stimulus for appropriate processing of the stimulus (Lavigne et al., 2015), also in tasks which require sustained attention to visual stimuli over prolonged periods of time (Fortenbaugh et al., 2017; Sarter et al., 2001; Lavigne et al., 2020), but further research needs to be done to characterize the function of the EXT network.

Results

1a. Raven's Standard Progressive Matrices Task (RSPM); Bipolar Merge

The EXT network was found to be deactivated during the identification of whether the answer presented was correct in comparison to the previously presented stimuli, and the HDR plot had the most deactivation at timebin 3. The Mixed ANOVA revealed a significant main effect of Time, $F(9,360) = 84.92, p < 0.001$. The time factor was dominated by timebins 1-3 for decreases to peak deactivation, and timebins 4-10 for increases from the peak deactivation ($p < 0.05$)

Mixed ANOVA also revealed significant interactions between Difficulty (Medium) \times Timebin, $F(1,40) = 4.78, p < 0.05$, where the medium difficulty condition showed decrease to peak suppression from timebins 3 to 4 followed by an increase in activity from peak suppression between timebins 5 to 6, $F(1,40) = 12.38, p = 0.001$ (Figure 1). The interactions between Groups \times Difficulty \times Timebins were significant for the Control: Easy difficulty condition from timebins 1 to 2 $F(1,40) = 4.92, p < 0.05$, where the Control: Easy difficulty showed a sharper decrease in activation compared to the other conditions and groups (Figure 2).

Overall, the EXT network is deactivated for both Control and Bipolar patient groups when participants are performing the task, and both groups showed sustained activity during the completion of the task, as indicated by the increase in activity when returning to baseline.

Figure 1. HDR for RSPM task averaged over Difficulty (Medium_Hard)

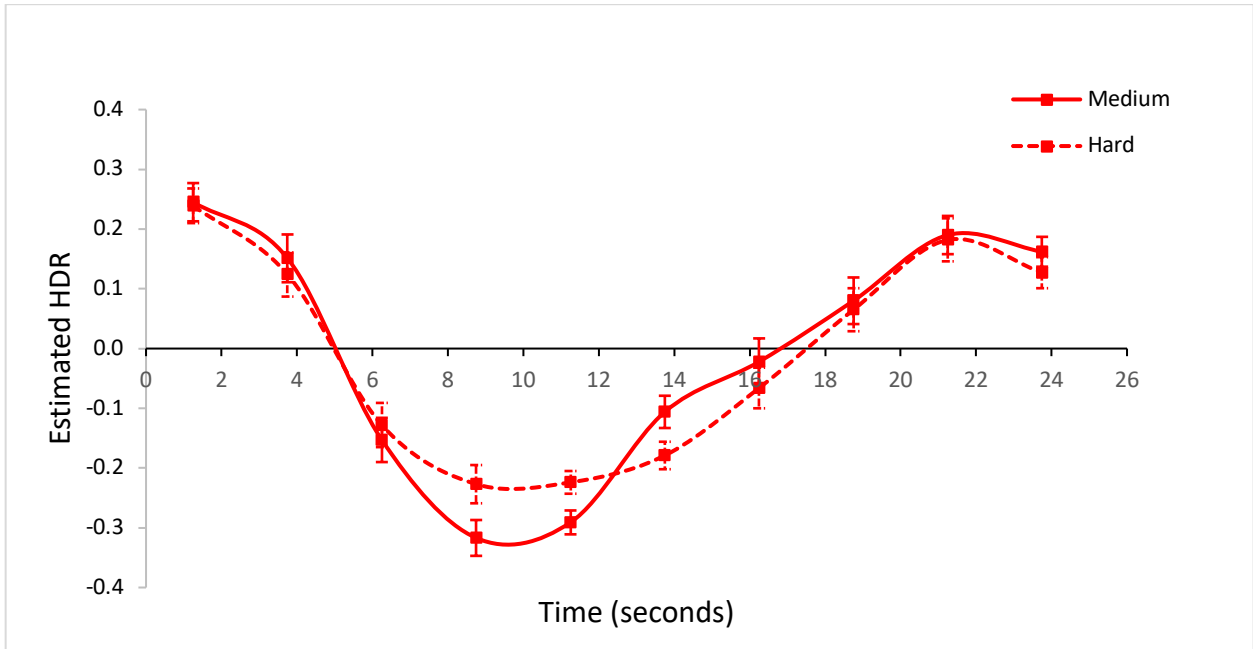
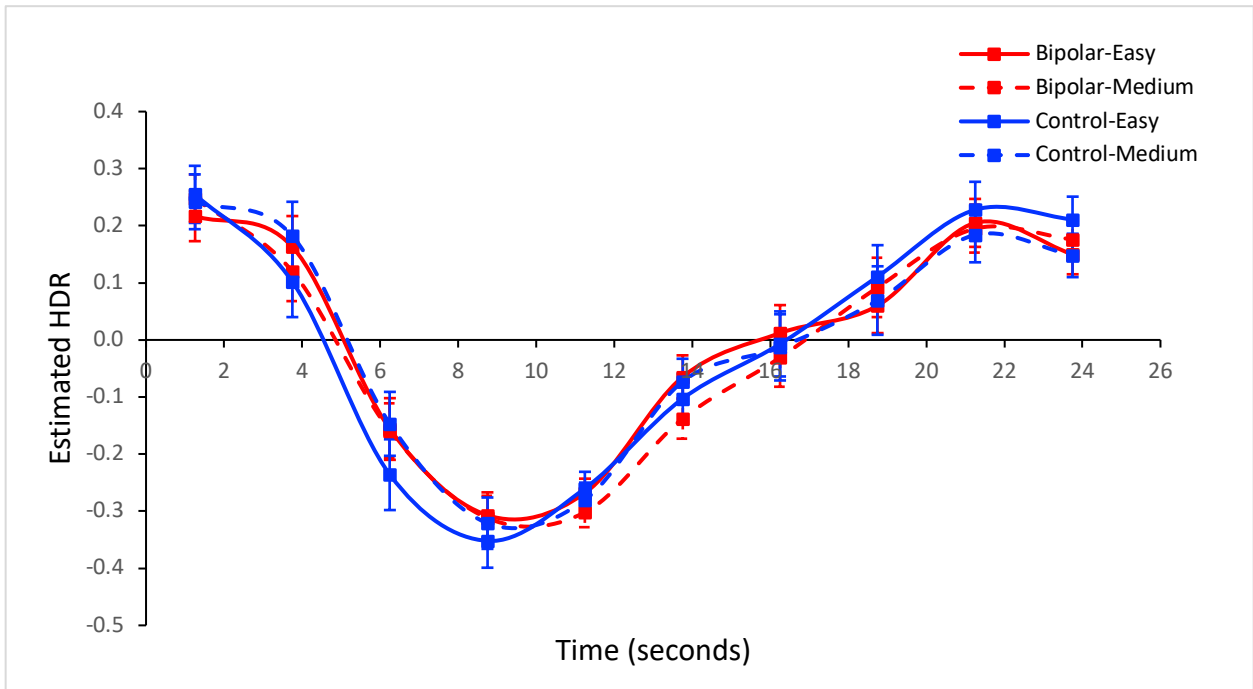


Figure 2. HDR for RPSM for Group (Controls_Bipolar), Difficulty (Easy_Medium), and Time.



1b. Raven's Standard Progressive Matrices (RSPM); Healthy RSPM 5

Repeated ANOVA revealed significant effects of the Difficulty of the task, $F(18,990) = 2.04, p < 0.01$, with the medium condition showing the peak suppression at the beginning of the task, before increasing to the peak activation and declining to baseline, (Figure 3). The effects of Time were also revealed to be significant, $F(9,495) = 138.11, p < 0.001$.

A significant 2-way interaction between Difficulty \times Timebins emerged, with significant interactions between the Easy vs. Medium difficulty between timebins 5 to 6, $F(1, 55) = 4.70, p < 0.05$, where the Easy difficulty showed a lower peak activation compared to the Medium difficulty. The Easy difficulty showed a lower rate of increase in activation between timebins 5 to 6 compared to the Medium difficulty (Figure 4)

The increased level of activation in the EXT network when the subjects were completing the more difficult matrix (Medium) suggests the increased level of difficulty requires increased attention to visual stimuli. Interestingly, this study contained only Healthy subjects, and showed an inverse activation pattern to that of the EXT network in the previous study.

Figure 3. Varimax HDR of Difficulty (Easy_Med_Hard) vs. Timebins

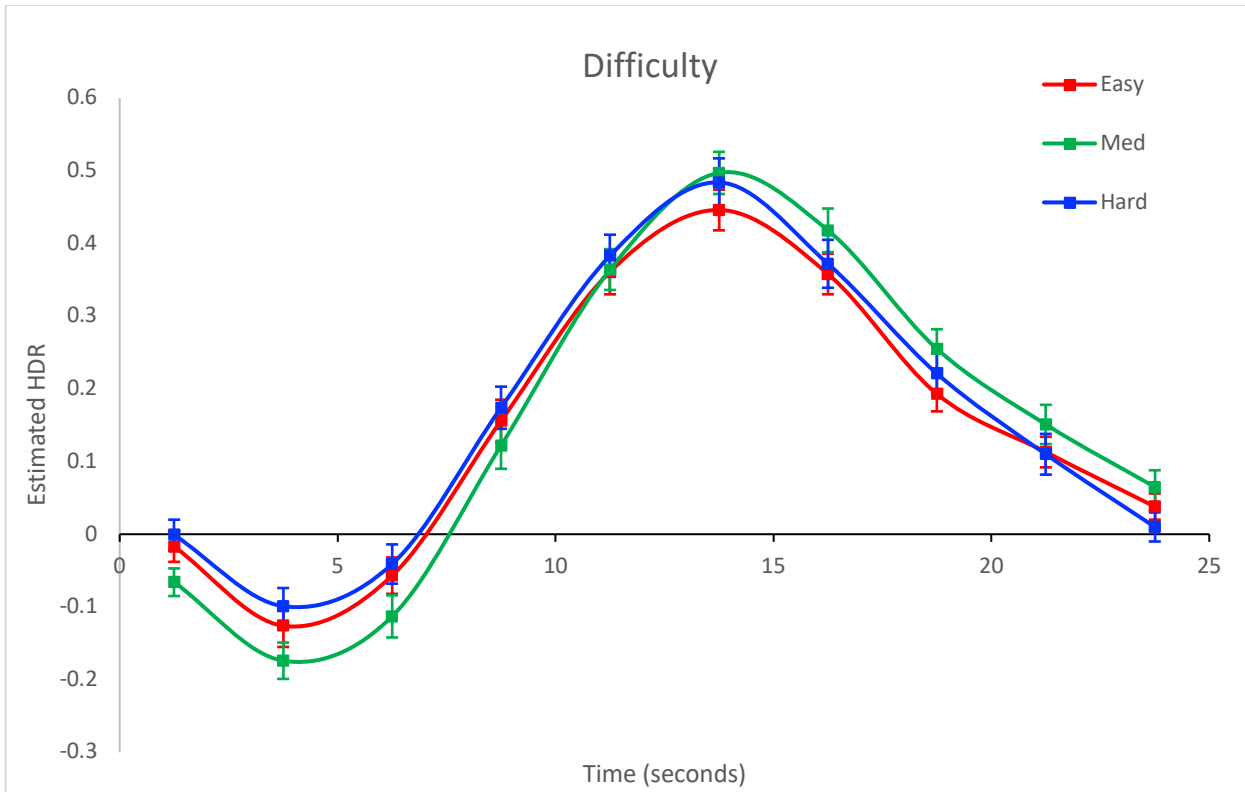
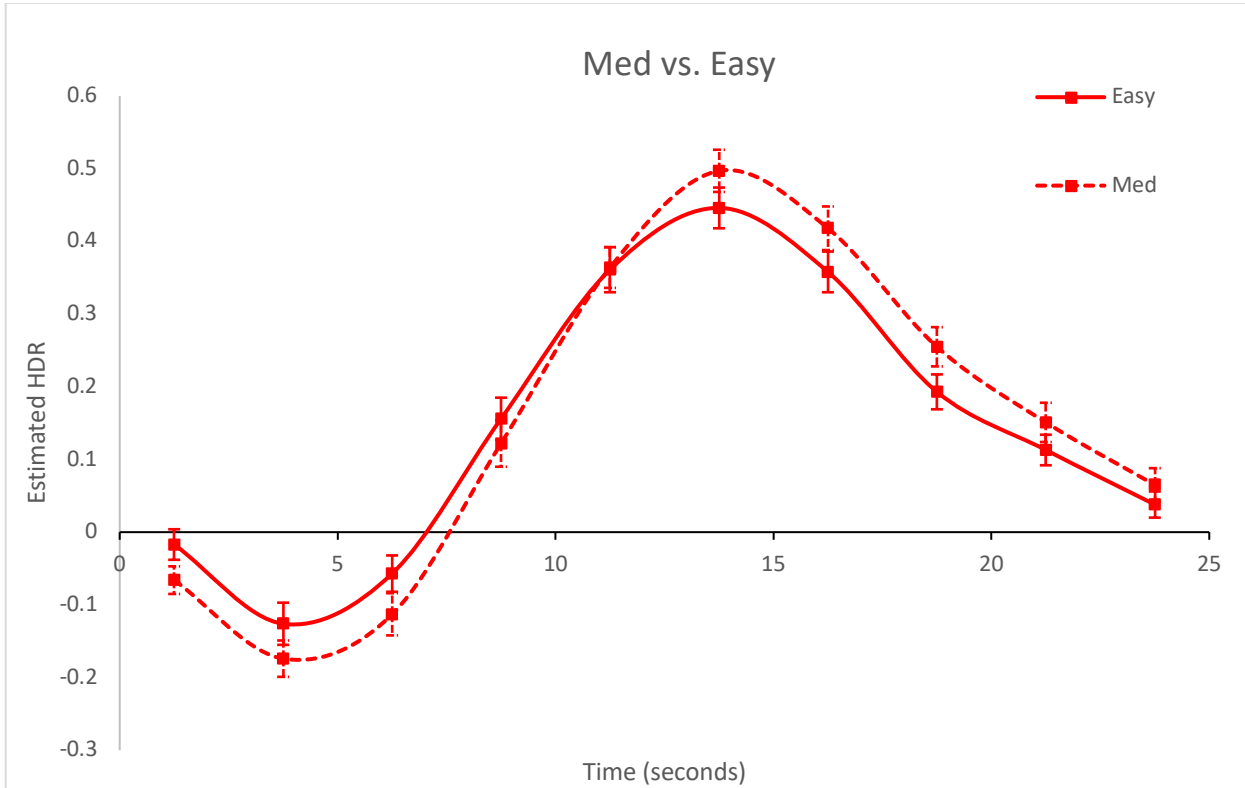


Figure 4. Varimax HDR of Difficulty (Easy_Med) vs. Timebins



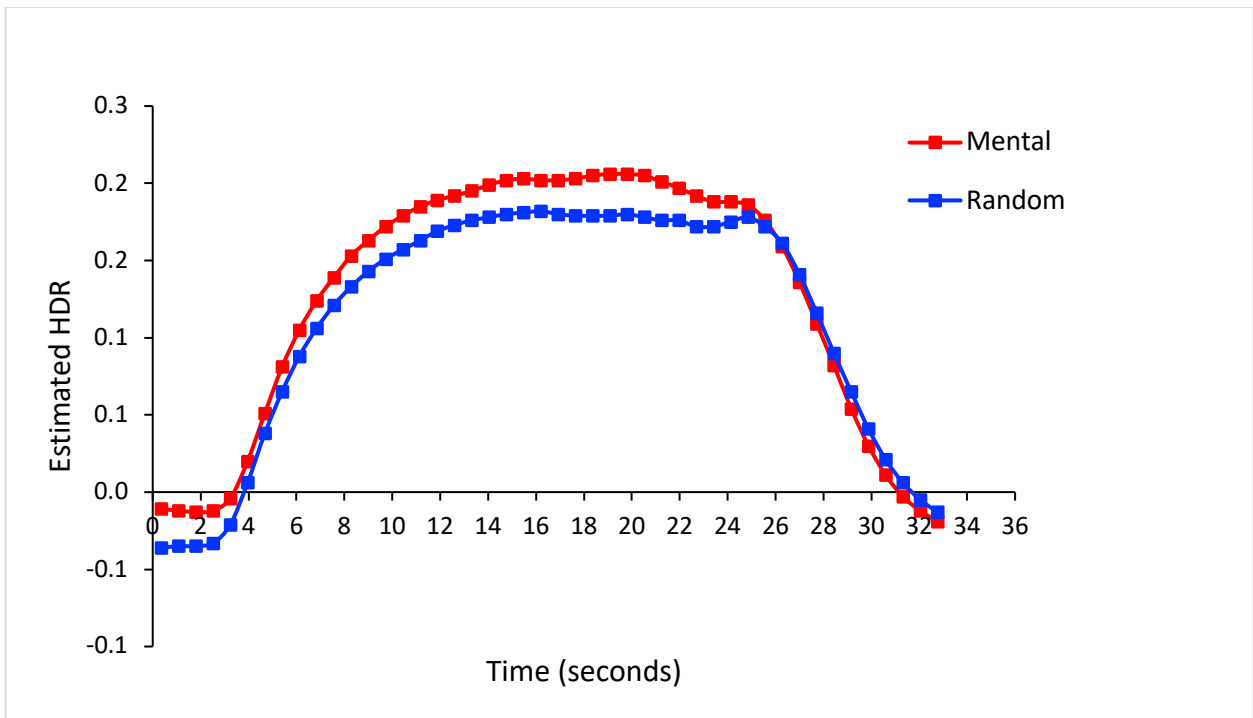
2. Human Connectome Project Social Task

The EXT network presented with increased activity for both conditions during the Social Task. Repeated ANOVA revealed significant main effects of Time, $F(45,22455) = 2611.23$, $p < 0.001$, as well as the average activity of the 2 task conditions (Mental vs. Random), $F(1,499) = 220.65$, $p < 0.001$.

Significant interactions between Conditions \times Timebins were identified, $F(45, 22455) = 40.82$, $p < 0.001$, where the Mental condition showed greater activation in comparison to the Random condition (Figure 5) from timebins 4 to 5, $F(1,499) = 15.13$, $p < 0.001$. The Mental condition continued to show an increase in HDR activity to peak, during timebins 7 to 8, $F(1,499) = 7.60$, $p < 0.01$. The Mental condition showed sustained EXT activation from timebins 24 to 33, $p < 0.05$. From timebins 33 to 38, $p < 0.01$, and timebins 40 to 41, $p < 0.05$, the Mental condition showed a sharp decline in HDR activity, until it reaches baseline.

Overall, both Conditions showed prolonged EXT activation, but the Mental condition had a higher level of activation and reached a higher peak HDR in comparison to the Random condition (Figure 5), suggesting greater EXT activation was required to attend to stimuli which had consistent social interactions. Both conditions had prolonged EXT activation, which supports the function of the EXT network, as it is activated to attend to a task requiring immense amounts of external visual attention.

Figure 5. HDR for the Social Task for the Condition (Mental_Random) and Time



3. Lexical Decision Task (LDT); Bipolar Merge

The EXT network showed significant deactivation during the lexical decision task throughout the Bipolar Merge study, regardless of lexicality, difficulty, and group. Significant effect of Time was determined, $F(1,40) = 117.65, p < 0.001$, along with the main effects of Difficulty (Easy vs. Hard), $F(1,40) = 24.51, p < 0.001$. Significant interactions between Lexicality \times Time were found, $F(1,40) = 21.01, p < 0.001$, where the level of EXT suppression for the Nonword condition reached peak suppression between timebins 2 to 3 (Figure 7)

A significant 3-way interaction between Lexicality \times Difficulty \times Timebin, $F(1,40) = 21.01, p < 0.001$, was determined, with the Nonword_Easy condition reaching peak suppression between timebins 2 to 3 (Figure 7). Another significant 3-way interaction emerged between Group \times Difficulty \times Timebin, where the Control_Easy condition showed a steep incline in EXT activity between timebins 3 to 4. The Control_Easy condition also showed a steep decline in EXT activity back to baseline, between timebins 9 to 10, $F(1,40) = 4.25, p < 0.05$ (Figure 8). Additionally, the Bipolar_Easy condition showed the least amount of decline in EXT activity between timebins 3 to 4 and had the lowest level of decline in activity back to baseline between timebins 9 to 10 (Figure 8).

Throughout the task, the suppression in the EXT network suggests that following the initial visual perception of the word, the subject's attention was no longer focused on the stimuli, but rather determining the lexicality of the word presented. The Nonword condition showed greater levels of suppression throughout the groups, suggesting the Nonwords required greater levels of activation in other networks to determine the lexicality, resulting in the higher level of suppression in the EXT network.

Figure 6. Varimax HDR for Difficulty vs. Lexicality, averaged over Group (Control_Bipolar)

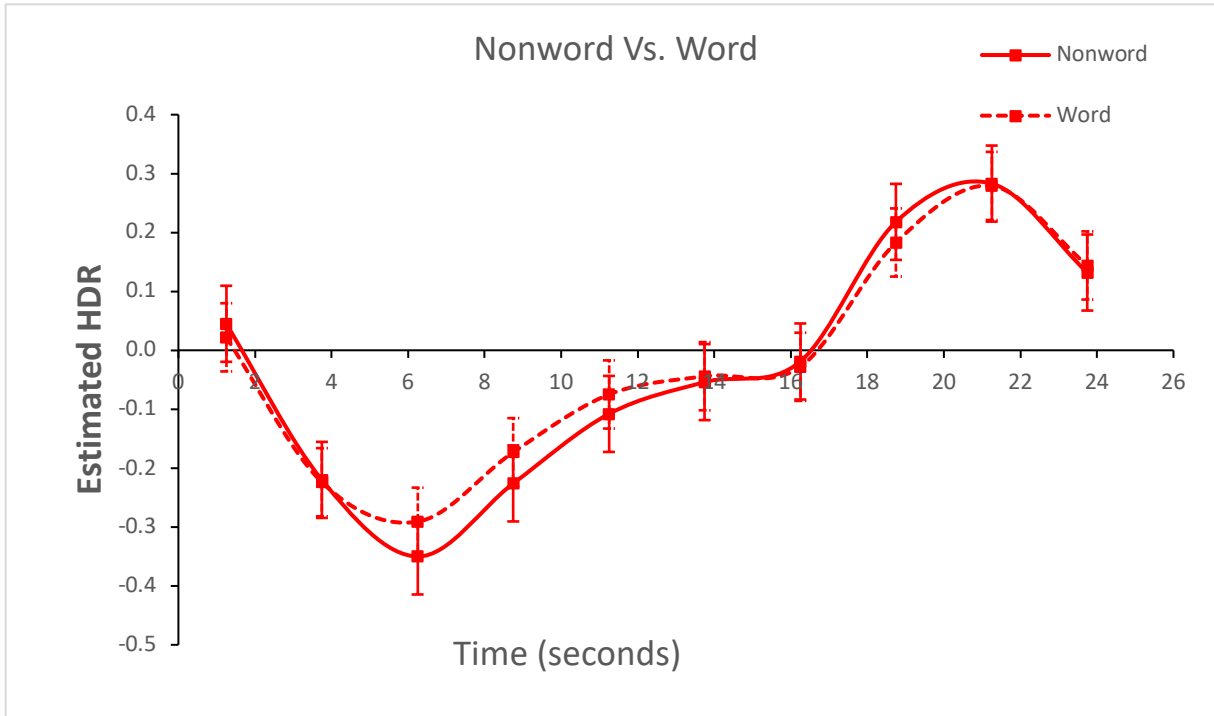


Figure 7. Varimax HDR Lexicality (Word vs. Nonword) averaged over Group and Difficulty

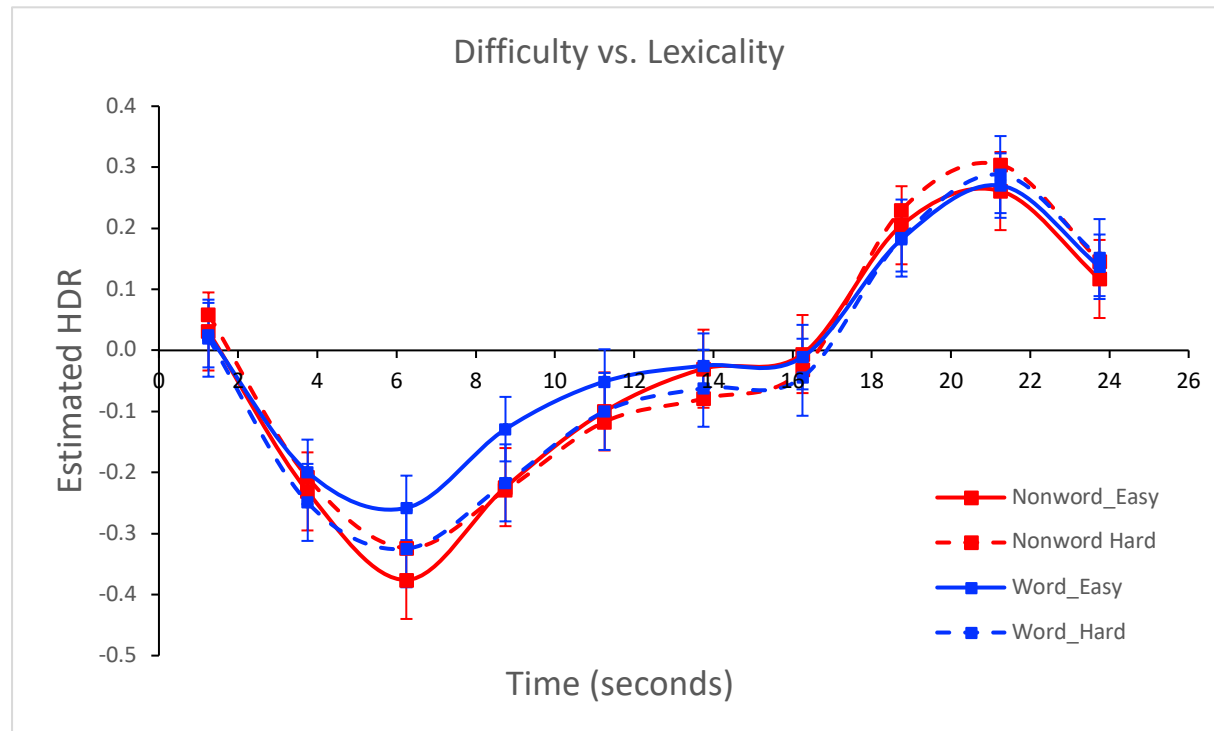
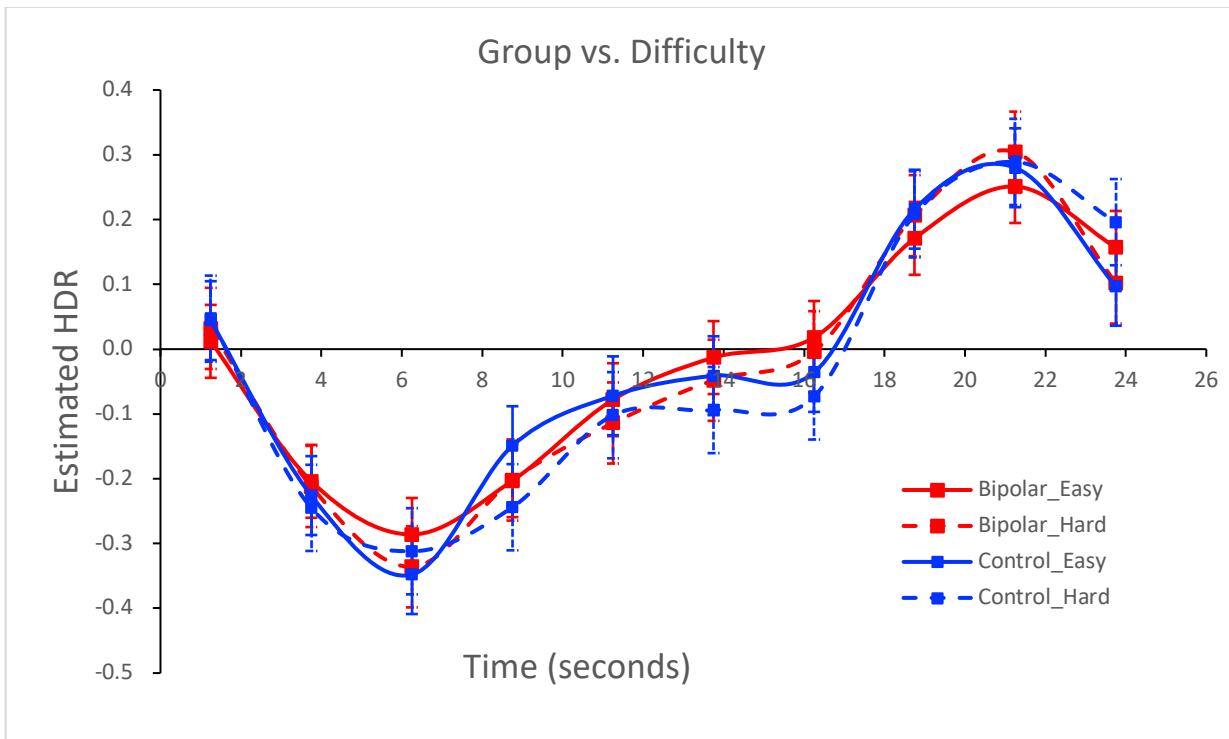


Figure 8. Varimax HDR Group (Bipolar_Control) vs. Difficulty (Easy_Hard)

4a. Evidence Integration Task (BADE); Lavigne Schizotypy SchizRes BADE

The EXT network showed increased activation during the Evidence Integration Task in all conditions. Repeated ANOVA revealed significant effects of Yes first vs. No first, where the Yes first condition showed significantly higher EXT activation throughout the task compared to the No first condition, $F(1,40) = 28.13, p < 0.001$, (Figure 11). Significant interactions between Confirm_Disconfirm \times Timebins were determined, $F(9,360) = 15.82, p < 0.001$, (Figure 9). The interactions between Confirm and Disconfirm were dominated by the Disconfirm condition from timebins 5 to 10, where the Disconfirm condition had significantly higher levels of activation to peak, and on the decrease from peak back to baseline.

A 3-way interaction was revealed between Yesfirst_Nofirst \times Confirm_Disconfirm \times Timebins, and was dominated by the Disconfirm: Yes first condition from timebins 5 to 10, where the Disconfirm: Yes first had higher significantly higher activation in the EXT network compared to the other conditions on the increase and decrease from peak, $F(9,360) = 3.28, p = 0.001$, (Figure 10).

Overall, the EXT network showed activation throughout the BADE task, with certain conditions showing more activation than others. Individually, the Disconfirm and Yes First conditions both had significantly higher activation compared to the Confirm and No First conditions, respectively, with the Disconfirm: Yes first condition having the most EXT activation throughout the task. The increased level of EXT activation in the Disconfirm condition suggests increased attention to visual stimuli in this condition, as the participant must integrate the evidence presented in the novel stimuli to identify a possibly alternative answer, to conclude the disconfirmation of their original answer.

Figure 9. Confirm vs. Disconfirm averaged over time

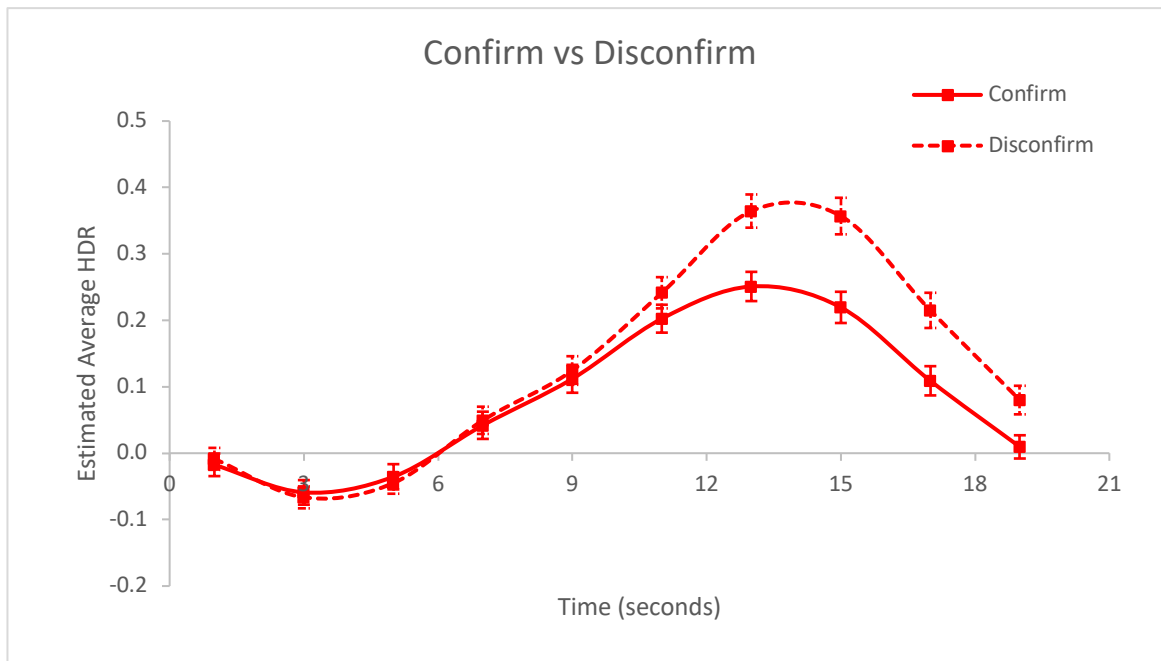


Figure 10. Confirm vs. Disconfirm, Yes first vs. No first

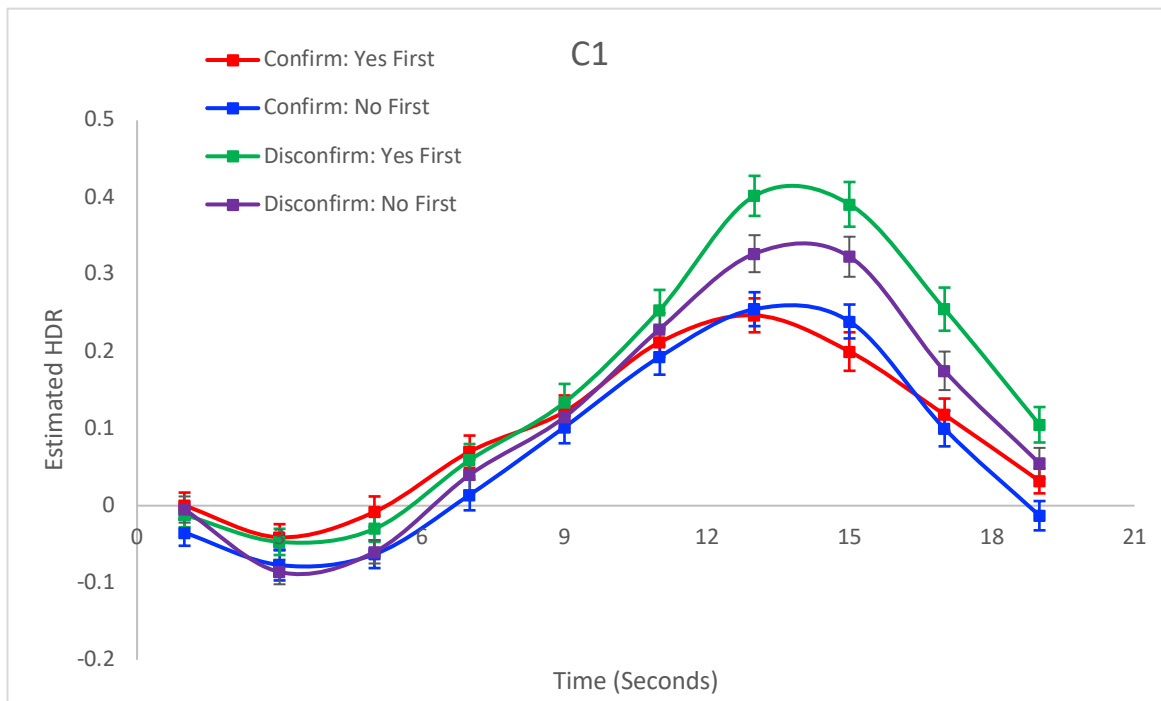
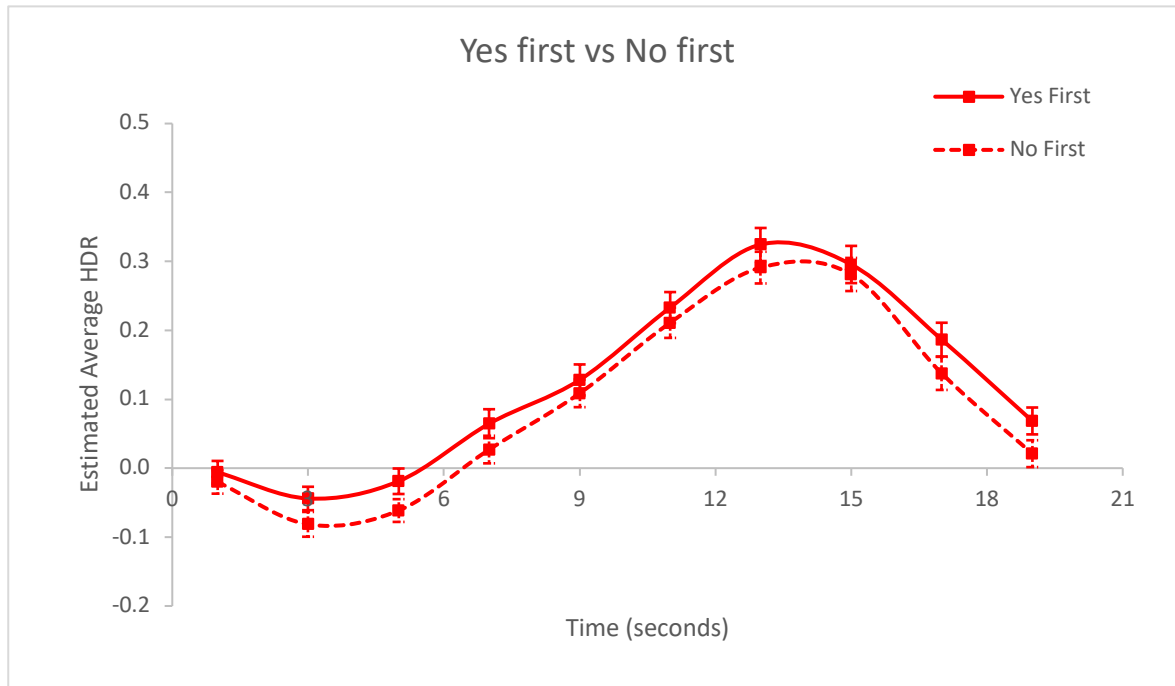


Figure 11. Yes first vs. No first averaged over time



4b. Evidence Integration Task (BADE); Lavigne Prepost BADE

Throughout the task, the EXT network showed significant activation. Repeated ANOVA revealed significant effects of the Conditions, $F(1, 57) = 6.14, p < 0.05$, as well as the effects of Time, $F(9, 513) = 93.42, p < 0.001$. Significant interactions between Conditions \times Timebins emerged for the Yesfirst_Nofirst conditions, $F(9, 513) = 2.38, p < 0.05$. The Yes first condition showed a greater rate of EXT activation compared to that of the No first condition, with both conditions showing increased activation from timebins 2 to 4, $p < 0.01$, (Figure 12). Between timebins 4 to 5, however, the Yes first condition showed a slower rate of activation and reached a lower peak activation (Figure 12).

A significant 3-way interaction between Yesfirst_Nofirst \times Confirm_Disconfirm \times Timebins also emerged, between the Yesfirst_Nofirst conditions vs. the Confirm_Disconfirm conditions and the timebin component, between timebins 1 to 2, $F(1, 57) = 4.55, p < 0.05$. The Disconfirm: No first vs. Confirm: Yes first conditions had a higher baseline level of EXT activation compared to that of the Confirm: No first vs. Disconfirm Yes first (Figure 13).

Similar to the previous study, the EXT network showed activation throughout the task, suggesting the increased level of visual attention was used to actively integrate visual evidence to determine if the image presented matches the description. The Disconfirm conditions dominated the interactions in this study as well, suggesting increased levels of visual attention is required when subjects must change their answer depending on the new visual evidence presented.

Figure 12. Varimax HDR for Conditions (Yesfirst_Nofirst) vs. Timebins

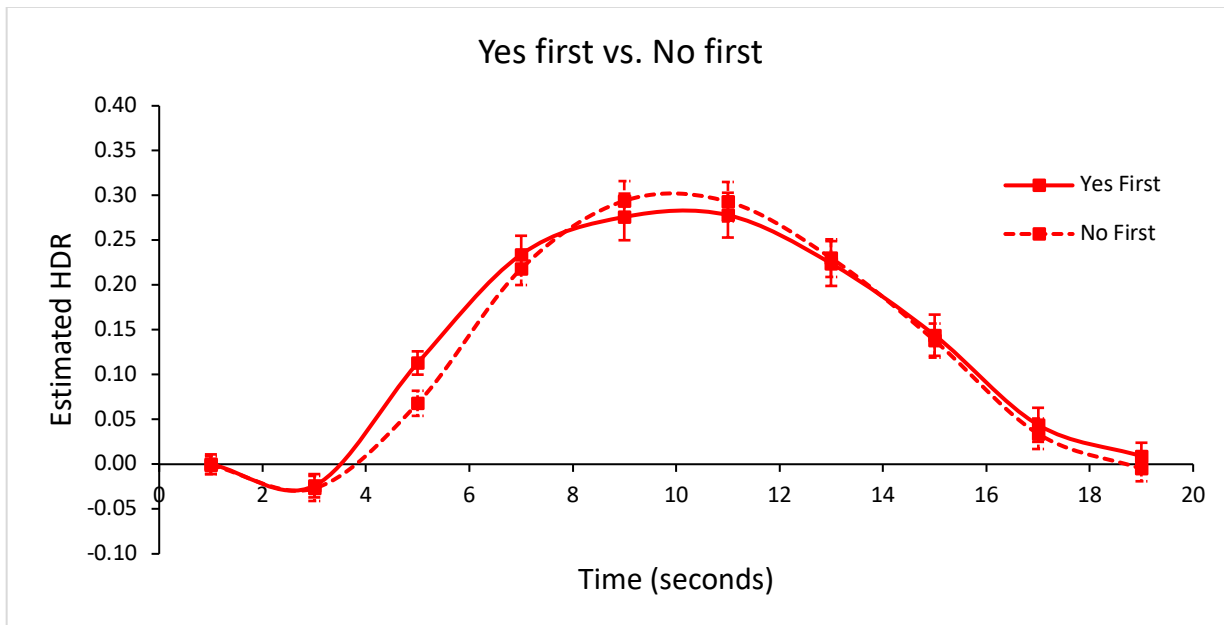
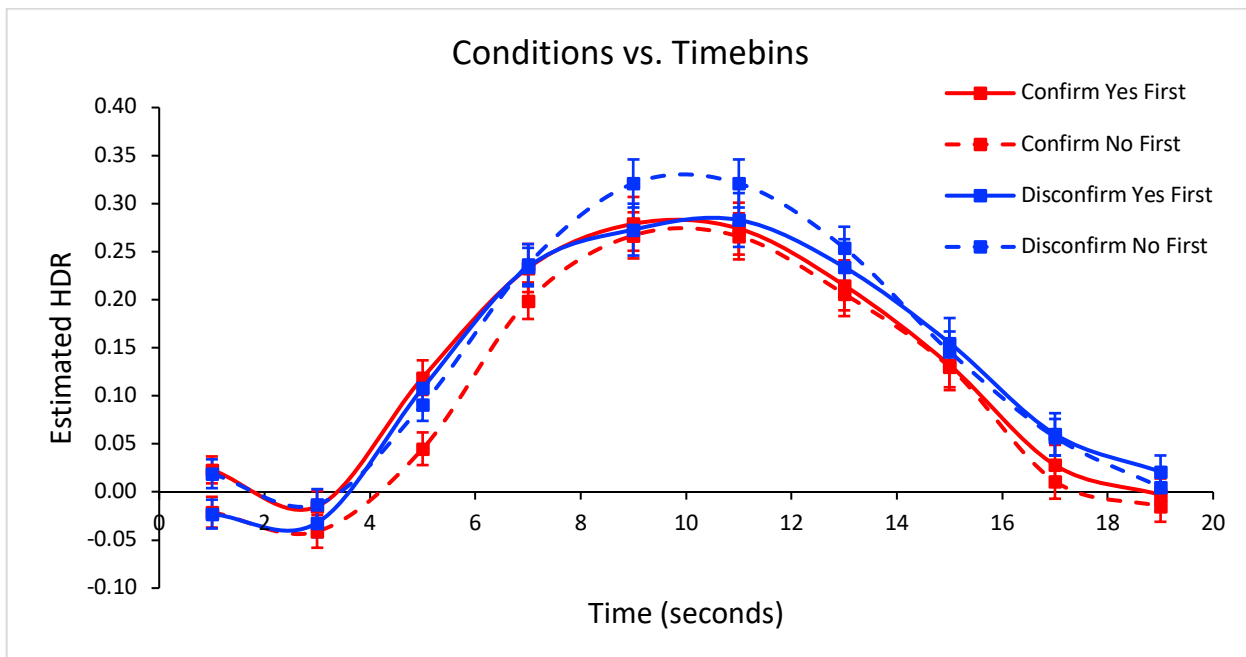


Figure 13. Varimax HDR Conditions (Yesfirst_Nofirst) vs. Conditions (Confirm_Disconfirm)



4c. Evidence Integration Task (BADE); Lavigne OTT BADE

Unlike the previous BADE task, this task involves both Schizophrenia and Control groups. Mixed ANOVA revealed significant effects of all conditions: Confirm vs. Disconfirm, $F(1, 109) = 64.67, p < 0.001$, Yes first vs. No first, $F(1, 109) = 63.03, p < 0.001$, and the effects of Time, $F(9, 981) = 214.24, p < 0.001$.

A significant 2-way interaction emerged between Confirm_Disconfirm \times Timebins, for Confirm vs. Disconfirm, $F(1, 109) = 64.65, p < 0.001$. The Confirm and Disconfirm conditions showed similar levels of activity between timebins 2 to 3, $p < 0.05$, with both conditions showing an initial suppression in activity from baseline (Figure 14). Between timebins 5 to 7, $p < 0.001$, both conditions showed an increase in activity, with the Disconfirm condition showing a greater rate of activation from timebins 5 to 7 compared to the Confirm condition. At timebin 8, both conditions reached peak activation, with the Confirm condition reaching a lower peak activation than the Disconfirm condition, before declining in activation back to baseline from timebins 8 to 10, $p < 0.001$, (Figure 14).

Another significant interaction was found between Yesfirst_Nofirst \times Timebins between timebins 8 to 9, $F(1, 109) = 5.01, p < 0.05$, where the Yes first condition reached a higher peak activation at timebin 8 compared to the No first condition, before both conditions showed decreased activation back to baseline (Figure 15).

A significant 3-way interaction was revealed between Confirm vs. Disconfirm \times Yes first vs. No first \times Timebins, where the Yes first conditions of both Confirm and Disconfirm were significantly higher than that of the No first conditions. All 4 conditions showed a steady increase in activation between timebins 4 to 5, $p < 0.05$, (Figure 16). Between timebins 6 to 7, the interactions were dominated by the steep increase in activity of Disconfirm conditions, with

the Disconfirm: Yes condition having the highest levels of activation, followed by the increase in activity of the Disconfirm: No condition, $p < 0.001$, (Figure 16). The Confirm conditions showed lower levels of activation, with the Confirm: Yes first condition showing a lower rate of increase in activity compared to that of the Confirm: No condition (Figure 16). At timebins 9 to 10, all conditions decreased in activity back to baseline, with the Confirm: No condition showing the steepest decrease, $p < 0.001$, (Figure 16).

Significant interactions between the subject groups were also revealed through Mixed ANOVA: a 3-way interaction emerged between Subjects \times Timebins \times Conditions. The Healthy and Schizophrenic groups had significant interactions with Confirm vs. Disconfirm, as well as Yes first vs. No first for timebins 6 to 7, $F(1,109) = 5.25, p < 0.05$, (Figure 17). Between timebins 6 to 7, all conditions showed an increase in activation of the EXT network, with the interactions dominated by the Healthy group. The Schizophrenia group showed the greatest rate of increase in activity as well as a delayed and lower level of peak activation. The Disconfirm conditions dominated the interactions between both the Healthy and Schizophrenic groups, with the Disconfirm: Yes first condition showing the greatest level of activation.

Like the previous studies, this BADE study showed greater levels of activation in the EXT network during the Disconfirm conditions, in both the Control and Schizophrenic groups, suggesting more visual attention is required during the Disconfirmation of the original answer. The Schizophrenic group in this study showed a delayed and lower peak activation of the EXT network in all conditions, suggesting a slightly delayed rate of processing of the visual evidence presented in this task compared to the Healthy group.

Figure 14. Varimax HDR Conditions (Confirm vs. Disconfirm) vs. Timebins

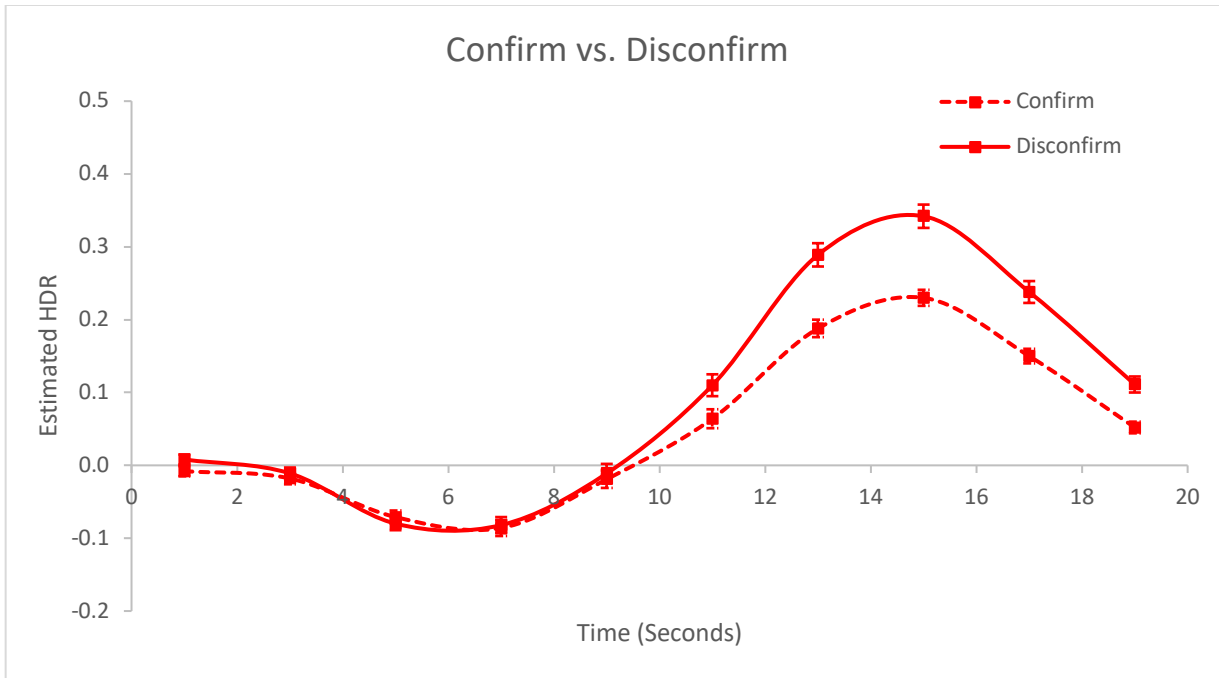


Figure 15. Varimax HDR for Conditions (Yesfirst_Nofirst) vs. Timebins

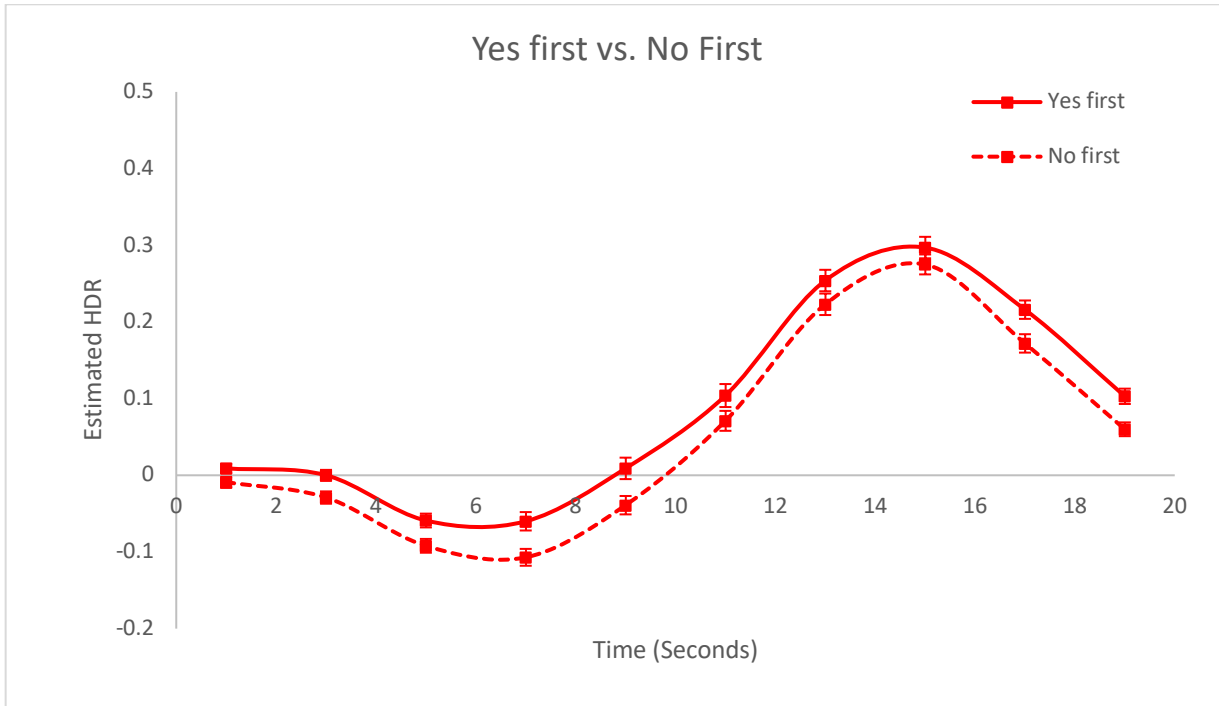


Figure 16. Varimax HDR for Conditions (Yesfirst_Nofirst) vs. Conditions (Confirm_Disconfirm) vs. Timebins

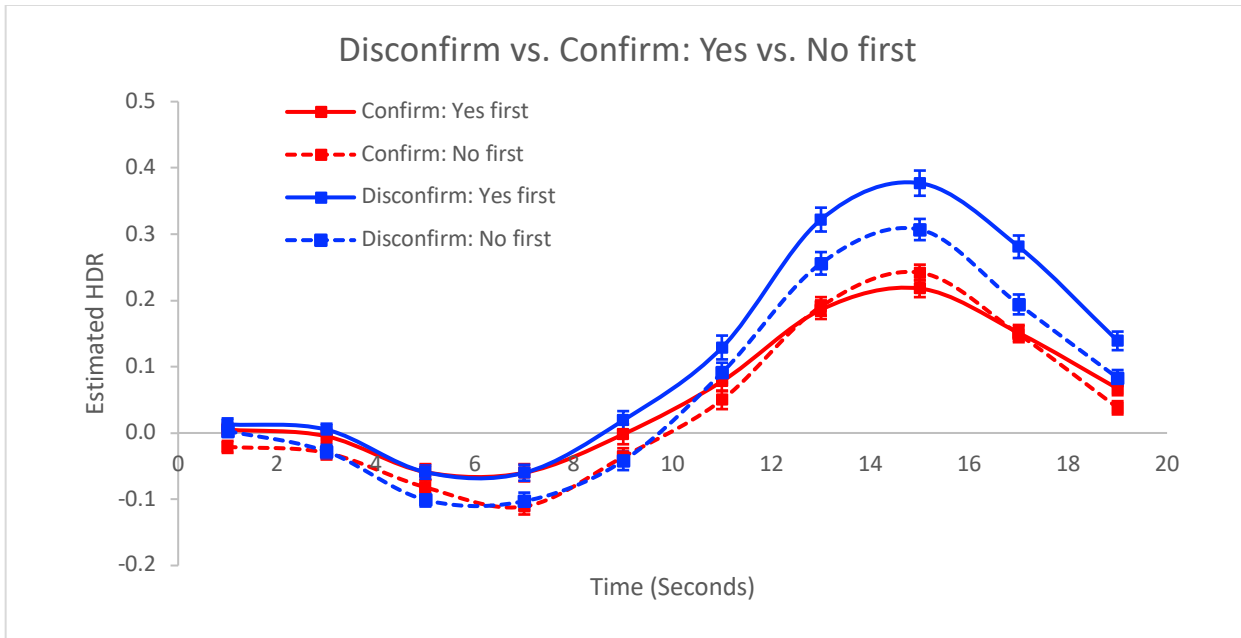
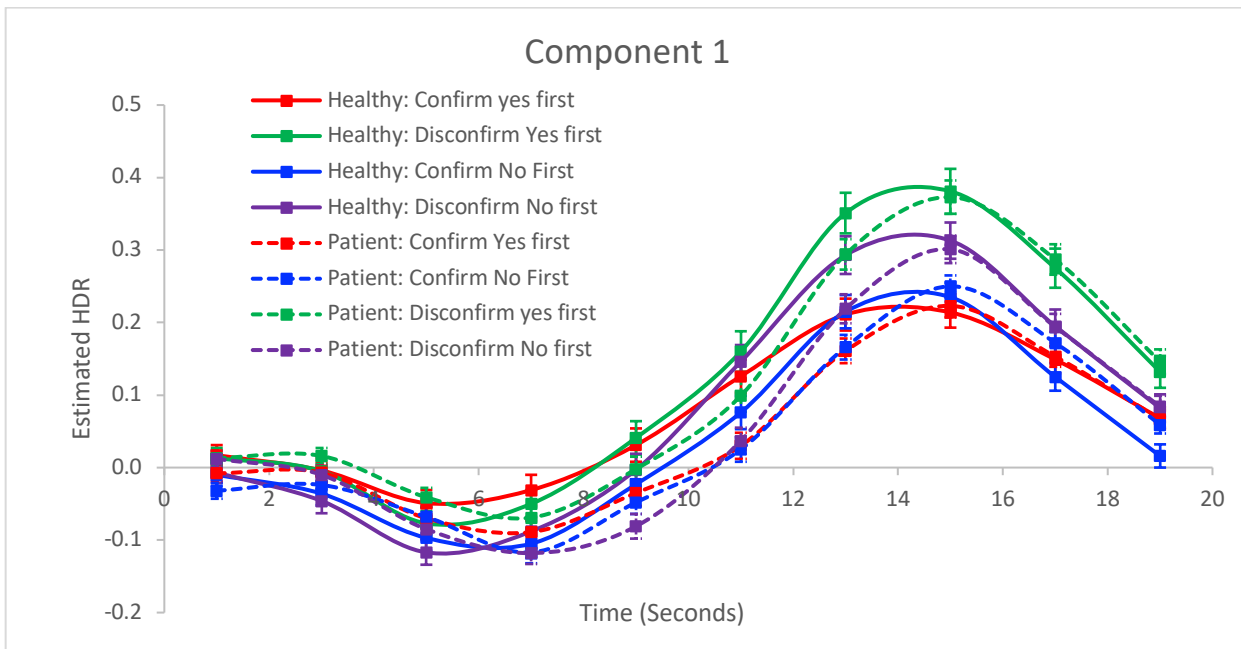


Figure 17. Varimax HDR of Group (Healthy_Schizophrenia) vs. Condition (Confirm_Disconfirm) vs. Condition (Yesfirst_Nofirst)



5. Addis Task; Klepel in Prep Addis

Repeated ANOVA revealed significant effects of the Time, $F(20,320) = 32.52, p < 0.001$, as well as the effects of the different conditions: Control, Past, Future, and Recall, $F(3,48) = 5.32, p < 0.05$, (Figure 20).

Several interactions were revealed to be significant between the Conditions \times Timebins, $F(60,960) = 5.14, p < 0.001$. The Control vs. Past conditions had significant interactions between timebins 3 to 4, $p < 0.05$, where both conditions reached peak activation, with the Past condition reaching a greater peak before the interactions were dominated by the decrease in activation in the EXT network of the Past-Imagine condition from timebins 4 to 5, and 6 to 7, $p < 0.05$, (Figure 18).

There were also significant interactions between the Future vs. Recall conditions, between timebins 4 to 6, $p < 0.05$, where the interactions were dominated by the decline in activation of the Future-Imagine condition from peak (Figure 19). The Future vs. Recall conditions also had significant interactions between timebins 14 to 15, $F(1,16) = 11.44, p < 0.01$, where both conditions showed an increase in activity, with the Future condition showing a greater rate of increased activation (Figure 19).

Since the task requires the participant to imagine a scenario which is not presented directly in front of them, the deactivation of the EXT network is required such that participant is able to focus on imagining a scenario rather than focusing on visual stimuli present in the room. Overall, the task conditions where the participant had to imagine a scenario rather than recalling a past occurrence had significantly higher levels of deactivation of the EXT network, suggesting the imagine condition requires increased levels of concentration and the EXT network must be deactivated to prevent distractions from other visual stimuli.

Figure 18. Varimax HDR of Control vs. Past

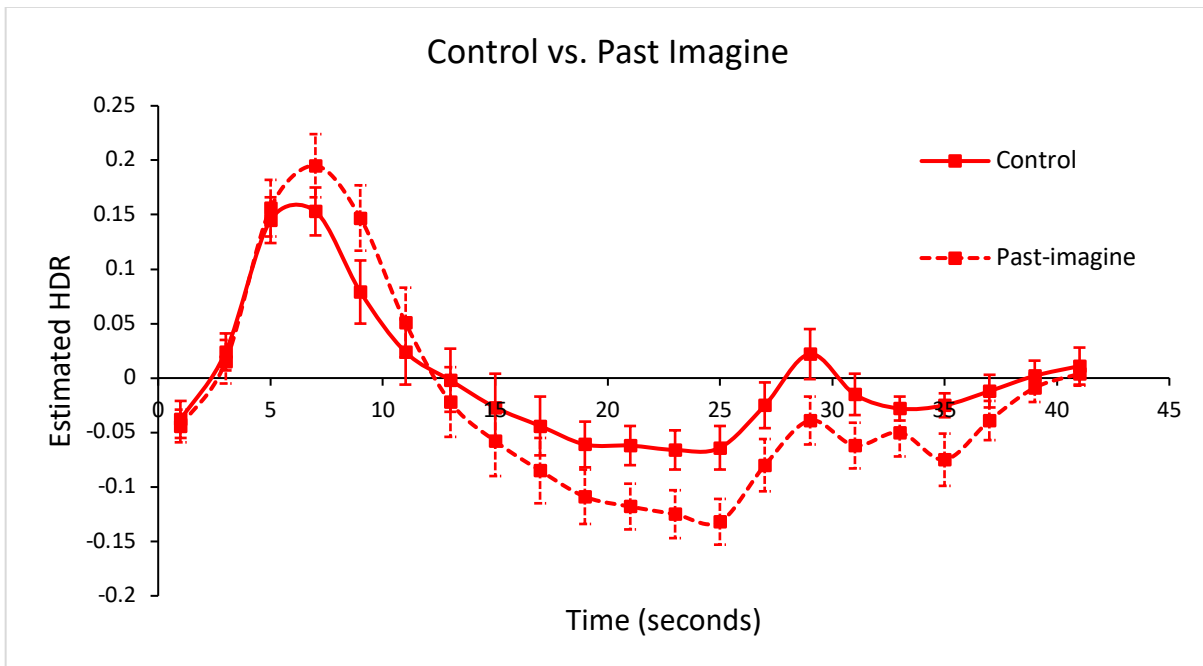


Figure 19. Varimax HDR of Future vs. Recall Imagine conditions.

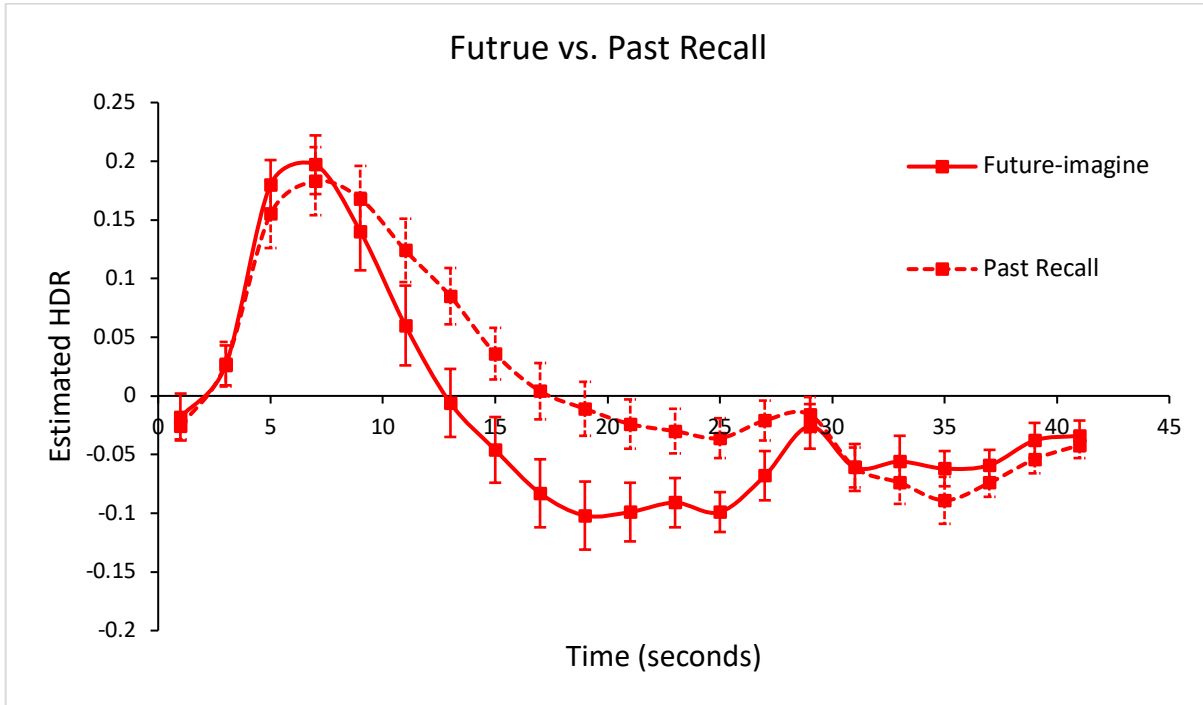
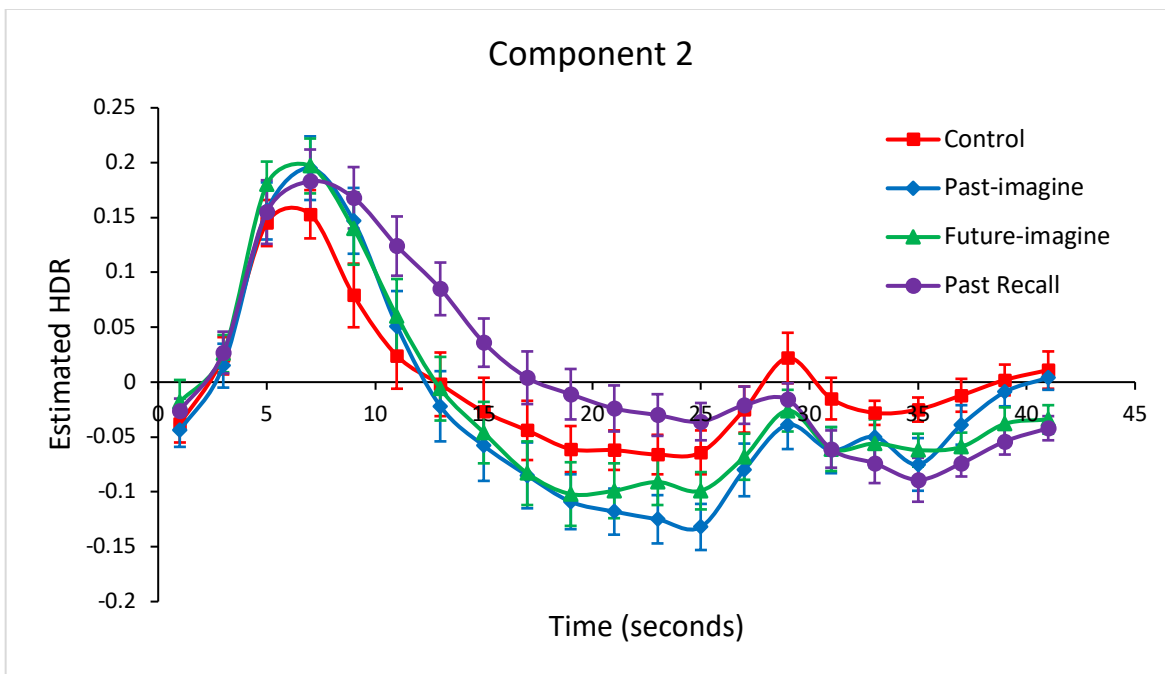


Figure 20. Varimax HDR for the Addis Task Averaged over Time



6. Source Monitoring (SM)

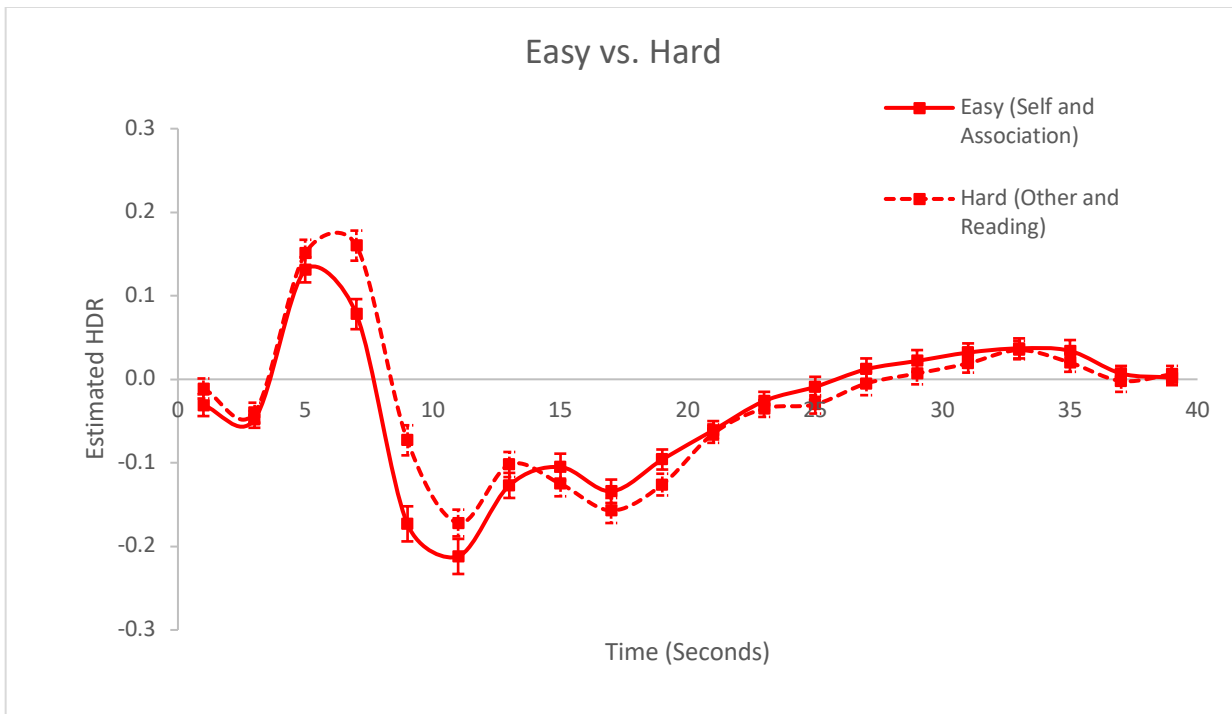
The EXT network showed initial increased activation during the Source Monitoring task, followed by deactivation of the network. The Mixed ANOVA revealed significant effects of the Time factor, $F(19, 817) = 52.90, p < 0.001$. There were significant interactions between the Easy vs. Hard conditions \times Timebins, but no significant interactions between the Controls or Schizophrenic groups.

The Hard to recall condition had an increase in EXT activation between timebins 3 to 4, whereas the Easy to recall condition showed a net decrease in activation within the same timebins, $F(1,43) = 17.90, p < 0.001$, (Figure 21). The Easy condition showed a greater rate of decrease in activation compared to the Hard condition, as well as greater levels of suppression in the Easy condition between timebins 5 to 6, $F(1,43) = 23.10, p < 0.001$, (Figure 21). The Hard and Easy conditions showed reciprocal levels of activation between timebins 7 to 8, with the Hard condition showing a decrease in activity while the Easy condition showed an increase, $F(1,43) = 14.67, p < 0.001$, (Figure 21). Both conditions showed an increase in activation, with the Hard condition showing a greater rate of increase in activity between timebins 10 to 11, $F(1,43) = 4.38, p < 0.05$, (Figure 21).

During the task, there was an initial increase in EXT activation in both conditions, followed by a steep suppression and a steady return to baseline. There was a greater and delayed peak EXT activation in the Hard condition, whereas the Easy condition had a lower peak EXT activation but a greater level of peak EXT suppression. This suggests the Hard condition consisted of trials which required more visual attention: the reading of the word required the participant to maintain their attention on the visual stimuli. The Easy condition, however, contained trials where the participant had to recall if the word was identified by themselves, or

by the computer, which requires more memory and less sustained attention on the visual stimuli, which was shown by the greater suppression of the EXT network in the Easy condition.

Figure 21. Varimax HDR for Easy vs. Hard to Recall conditions.



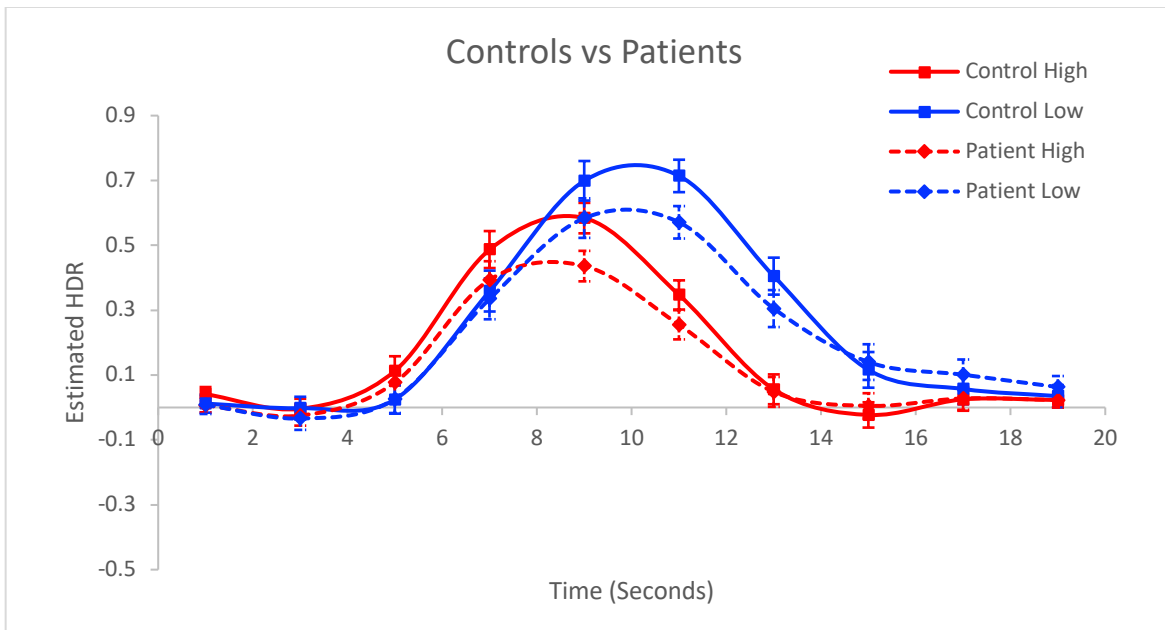
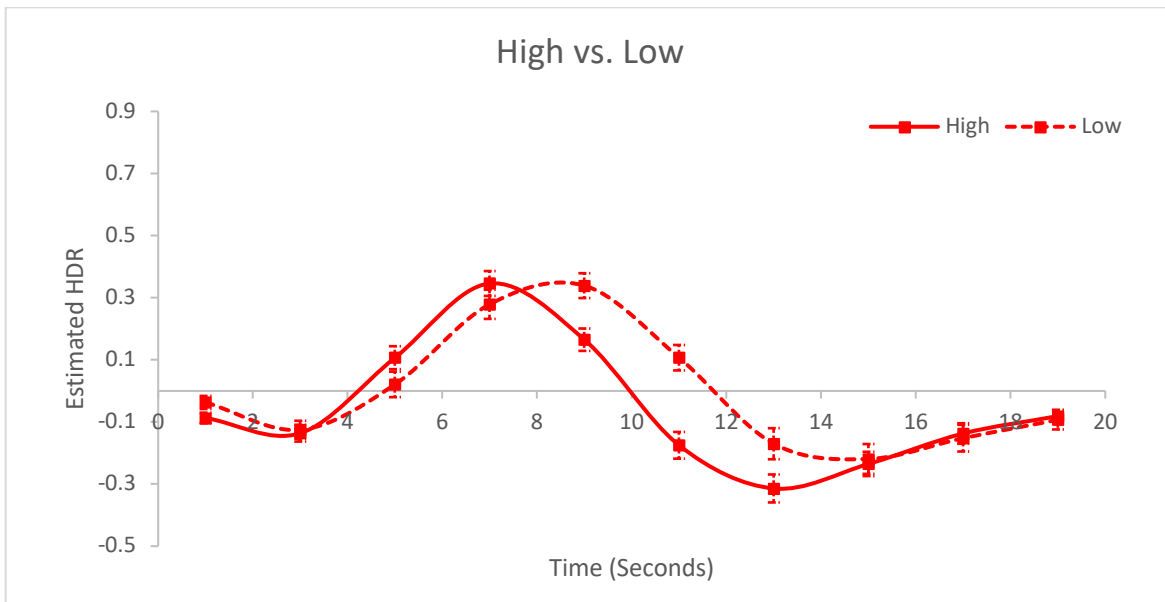
7.1. Semantic Association (SA); Woodward Human Brain Mapping Association

The EXT network showed increased activation to peak and then return to baseline for both conditions and between the subjects. Mixed ANOVA revealed significant effects of Conditions, $F(1,58) = 16.22, p < 0.001$, as well as the Time factor, $F(9,522) = 38.31, p < 0.001$. There were significant interactions between Conditions \times Timebins, where the High condition showed an increase in activity at a higher rate than the Low condition between timebins 2 to 3, $F(1,58) = 23.38, p < 0.001$, (Figure 23). Between timebins 4 to 5, the High and Low conditions showed inverse levels of activation, with the High condition decreasing from peak whereas the Low condition was increasing to peak, resulting a higher and delayed positive peak for the Low condition, $F(1, 58) = 104.23, p < 0.001$, (Figure 23). Between timebins 5 to 7, $p < 0.001$, both High and Low conditions showed decreases in activity, with the High condition reaching a greater peak suppression at timebin 7 (Figure 23). Between timebins 7 to 8, the High condition began to increase in activation whereas the Low condition continued to decline to peak suppression, $p < 0.001$, (Figure 23).

A 3-way interaction was revealed between Conditions \times Timebins \times Subjects between timebins 7 to 8, $F(1, 58) = 4.87, p < 0.05$, where the Controls and Patient: Low condition all showed a decrease in activation, however, the Patient: High condition showed increased activation (Figure 22).

The EXT network showed increased activation throughout the task before returning to baseline, suggesting that the EXT network is required to be active in participants to maintain their focus on the visual stimuli presented, and it allows for the participant to analyze each of the options before selecting the word which has the highest level of association to the target word. Additionally, the words with a high level of association with the target word had a lower peak

EXT activation compared to trials with words that had a lower level of association with the target word. This suggests words with a lower level of association with the target word requires increased levels of sustained visual attention due to the increased difficulty of identifying the word most closely associated the target word in the Low condition.

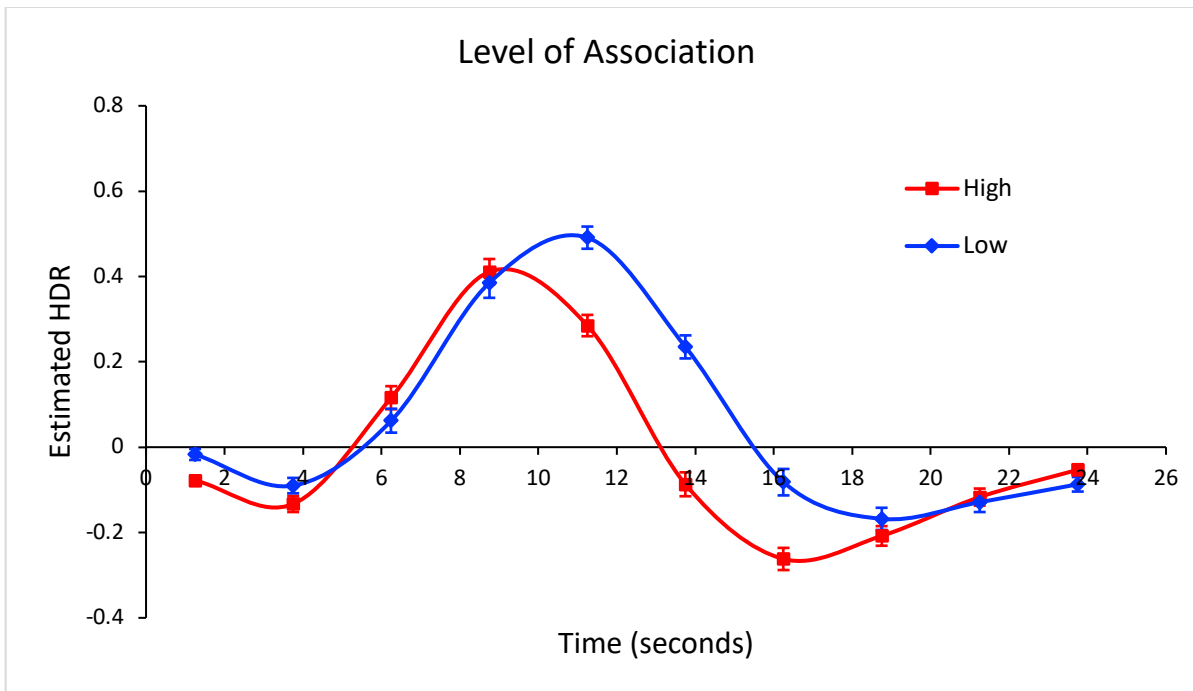
Figure 22. Varimax HDR for Conditions vs. Patients and Controls*Figure 23. High vs. Low averaged over groups*

7.2 Semantic Association (SA); Metric Stress Semantic Association Merge

Repeated measures ANOVA revealed significant effects of the Conditions, $F(1, 55) = 69.51, p < 0.001$, as well as significant effects of Time, $F(9, 495) = 114.28, p < 0.001$. Significant interactions were shown between Timebins \times Conditions, where the High condition showed a faster rate of increase in activity from timebins 2 to 3, $F(1, 55) = 47.80, p < 0.001$, compared the activity in the Low level of association (Figure 24). The High condition reached peak activation at timebin 4, $F(1, 55) = 158.25, p < 0.001$ before declining to peak suppression at timebin 7, $F(1, 55) = 80.80, p < 0.001$, and increasing back to baseline at timebin 9, $F(1, 55) = 14.61, p < 0.001$, (Figure 24). The Low condition exhibited a delayed and greater peak activation at timebin 5, $F(1, 55) = 23.63, p < 0.001$, before declining to a decreased level of peak suppression at timebin 8, $F(1, 55) = 14.61, p < 0.001$, and returning to baseline at timebin 9, $F(1, 55) = 14.61, p < 0.001$, (Figure 24).

The words which had lower levels of association with the prompt word showed increased levels of EXT network activation throughout the task, as distantly related words resulted in increased difficulty in finding the word with the closest association to the prompt. When words of higher levels of association were presented, the EXT network showed an earlier, and lower peak activation, suggesting the subject required less visual attention to identify the correct word, and was able to identify the correlation to the prompt faster than if the stimuli presented had lower association.

Figure 24. Varimax HDR of Association averaged over Group

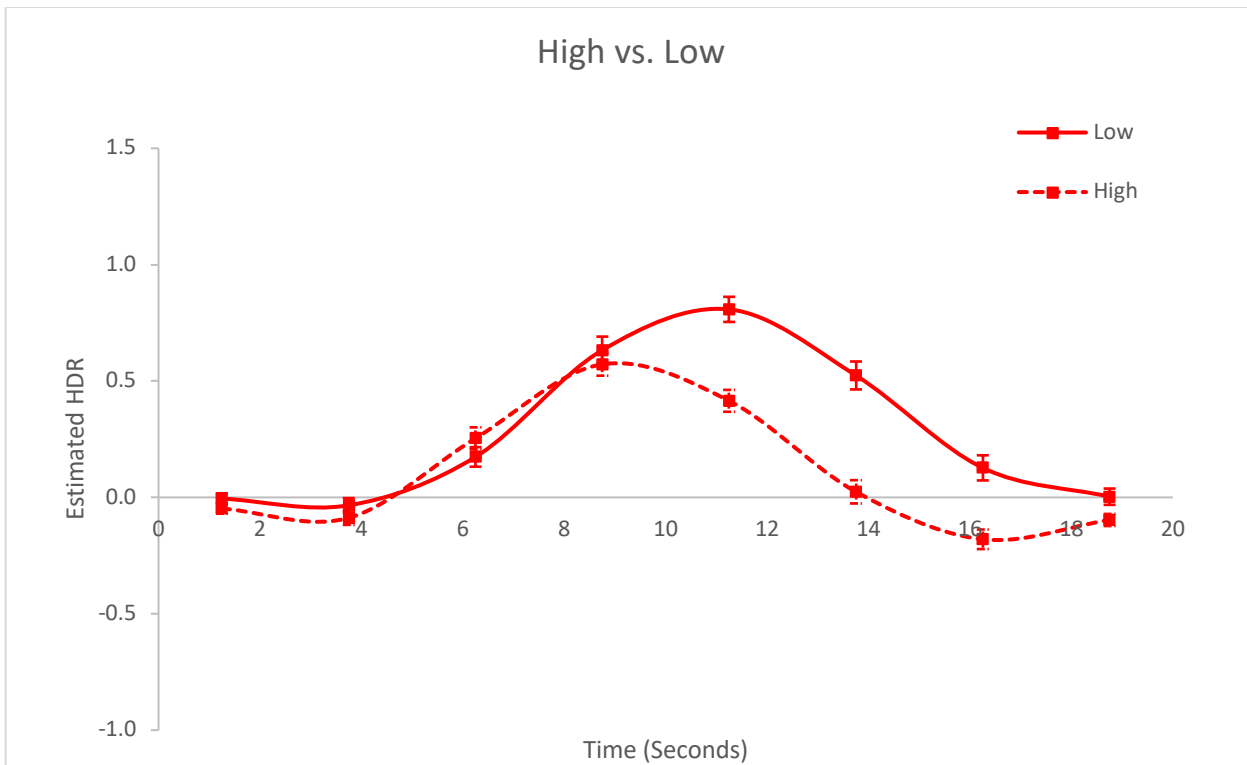
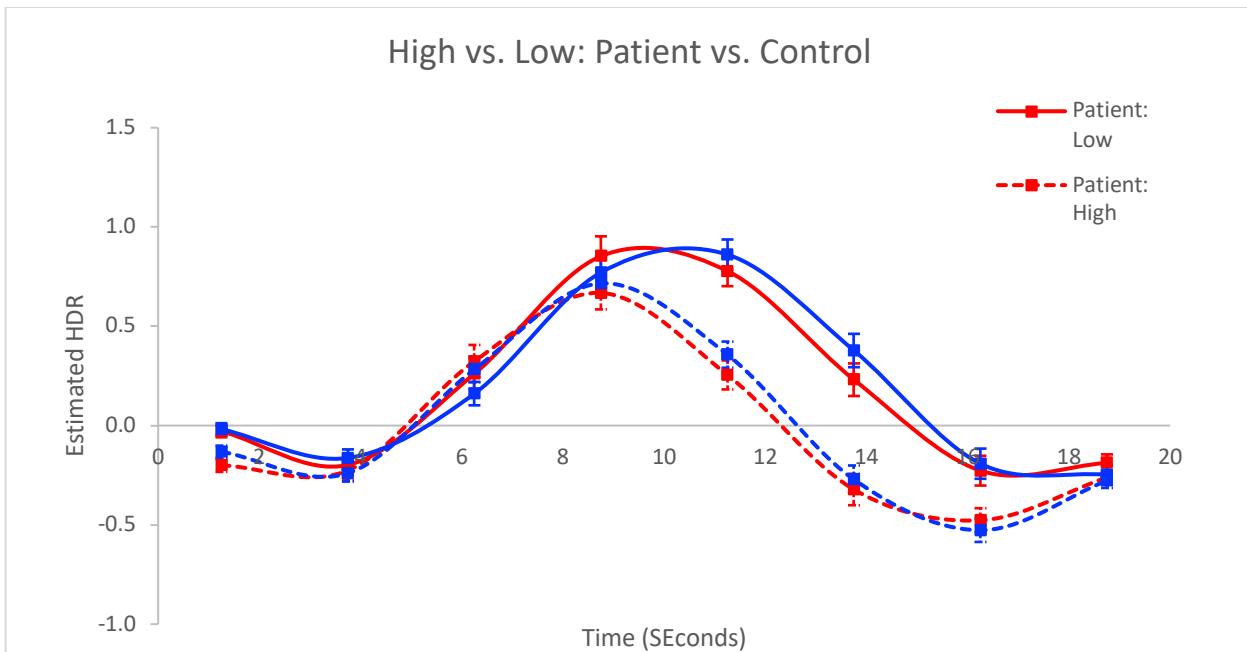


7.3 Semantic Association (SA); Triple Merge Thesis

Mixed ANOVA revealed significant effects of the Association Level, $F(1, 57) = 83.98, p < 0.001$ as well as Timebins, $F(7, 399) = 69.13, p < 0.001$. Significant interactions between Association Level \times Timebins also emerged, with significant interactions between timebins 2 to 6, all with $p < 0.05$. Between timebins 2 to 4, both conditions showed a steady increase in EXT activation (Figure 25). The Low condition showed a steep increase in activation to peak at timebin 5, with the High condition showing an earlier and lower level of peak activation at timebin 4, before declining in activation. From timebins 5 to 6, both the High and Low conditions showed decline in activation at similar rates (Figure 25).

A significant 3-way interaction emerged between Association Level \times Timebins \times Subjects, with the control and patient conditions showing similar levels of activation. At timebin 4, the High conditions reached a lower and earlier peak, whereas the Low condition showed a delayed and greater peak activation at timebin 5, all with $ps < 0.05$ (Figure 26). Overall, the control group showed slightly higher net activation on the decrease from peak in all conditions.

Similar to the previous Semantic Association tasks, the Low association condition showed a higher level of EXT activation compared to that of the High condition, due to the distantly related words requiring greater levels of visual attention to determine which word has the closest association to the prompt word. The High level of association showed lower rates of increase in EXT activation, suggesting the closely related words require less visual attention to identify the most correlated word to the prompt word.

Figure 25. Association Levels (High_Low) vs. Timebins*Figure 26. Subject vs. Conditions*

8. MMCC; Metzak et al.

Throughout the Task Switching Task, the EXT network showed a net increase in activation to peak, before declining steeply to peak deactivation. Mixed ANOVA revealed significant effects of Time, $F(7,294) = 19.98, p < 0.001$. Additionally, significant interactions between Valency \times Timebins emerged, where the interactions between the Valency conditions were dominated by the steady increase in EXT activation of the Bivalent condition to peak between timebins 1 to 2, $F(1, 42) = 5.17, p < 0.05$, whereas both the Univalent and Trivalent conditions showed an initial decrease in activity before gradually increasing to peak (Figure 27). The Trivalent condition presented with a delayed peak activation from timebins 3 to 4, $F(1, 42) = 4.37, p < 0.05$, whereas the Univalent and Bivalent conditions reached an earlier and greater peak activation (Figure 27).

Another significant interaction emerged between Subjects \times Timebins, which was dominated by the steep decline in activation from timebins 4 to 5 of the Healthy subjects from the peak activation at timebins 4, $F(1, 42) = 7.69, p < 0.01$, whereas the Patient subjects reached a lower peak activation at timebin 4 before gradually declining in activation from timebins 4 to 5 (Figure 28).

A 3-way interaction also emerged between Valency \times Subjects \times Timebins, which was significant for only the Bivalent vs. Trivalent conditions of Valency. Both Healthy conditions reached peak suppression between timebins 6 to 7, $F(1, 42) = 4.14, p < 0.05$, with the Healthy: Trivalent condition reaching a later, and greater level of suppression, at timebin 7, compared to the Healthy: Bivalent condition, which reached peak suppression at timebin 6 (Figure 29). Both Patient conditions, Bivalent and Trivalent, showed a steady rate of decline in activation between timebins 6 to 7 (Figure 29), however, did not reach peak suppression like the Healthy conditions.

Overall, the EXT network reached a higher level of peak activation in all Healthy conditions, compared to that of the Patient conditions, regardless of the Valency. As the task relies on both working memory and the ability to switch tasks following the analysis of an external visual stimuli, it is suggested the initial activation of the EXT network is due to the subject analyzing the presented visual stimuli for the task. The steep decline in EXT network activity and suppression of the network suggests subject was answering the presented question and had to recall the visual stimuli which they saw. Thus, the EXT network had to be suppressed so the subject was not distracted by any other external visual stimuli, and they can focus their attention to the recall of the visual stimuli they saw earlier to correctly answer the question. The decreased level of peak activation and late suppression of the EXT network in the schizophrenic subjects suggests a decreased ability to pay attention to the visual stimuli presented, as well as a decreased ability to suppress the EXT network during the recall phase which may result in distractions.

Figure 27. Valency averaged over Subjects

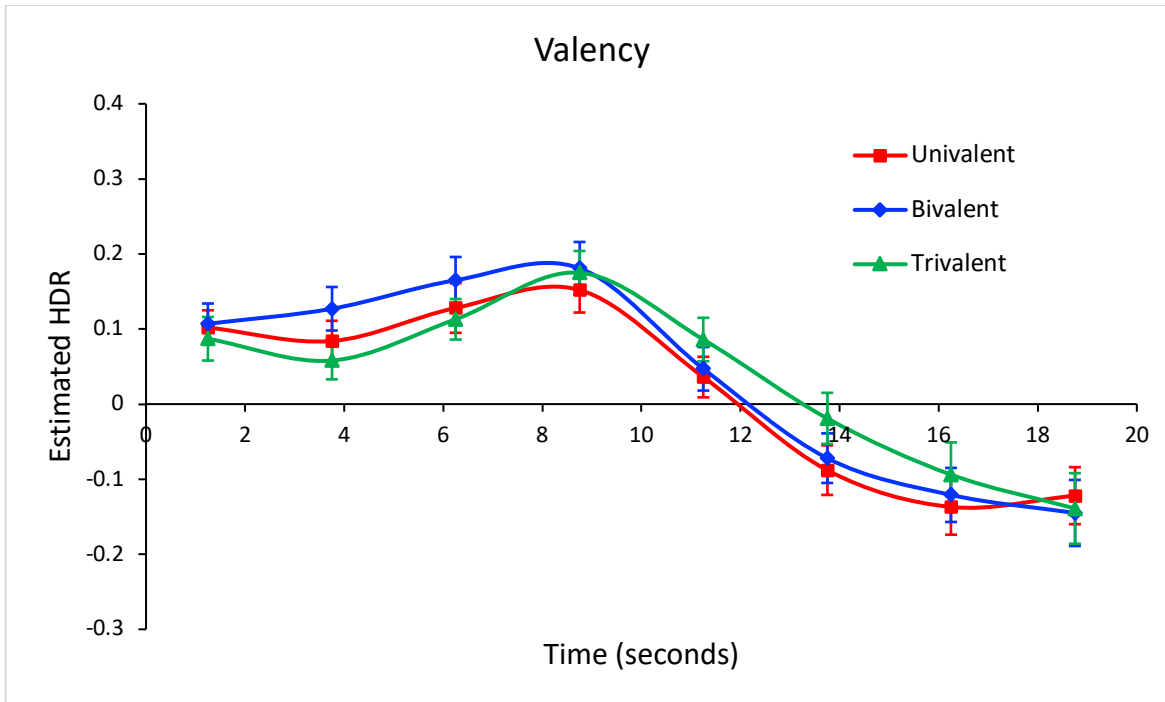


Figure 28. Varimax HDR of Healthy vs. Patient conditions

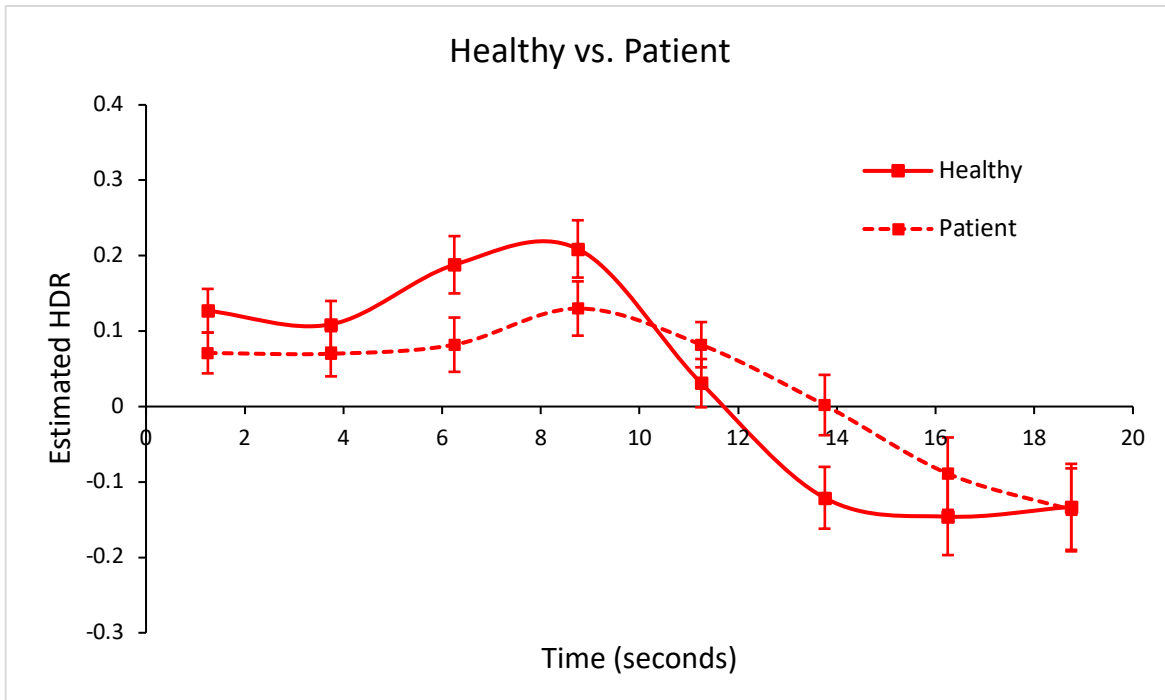
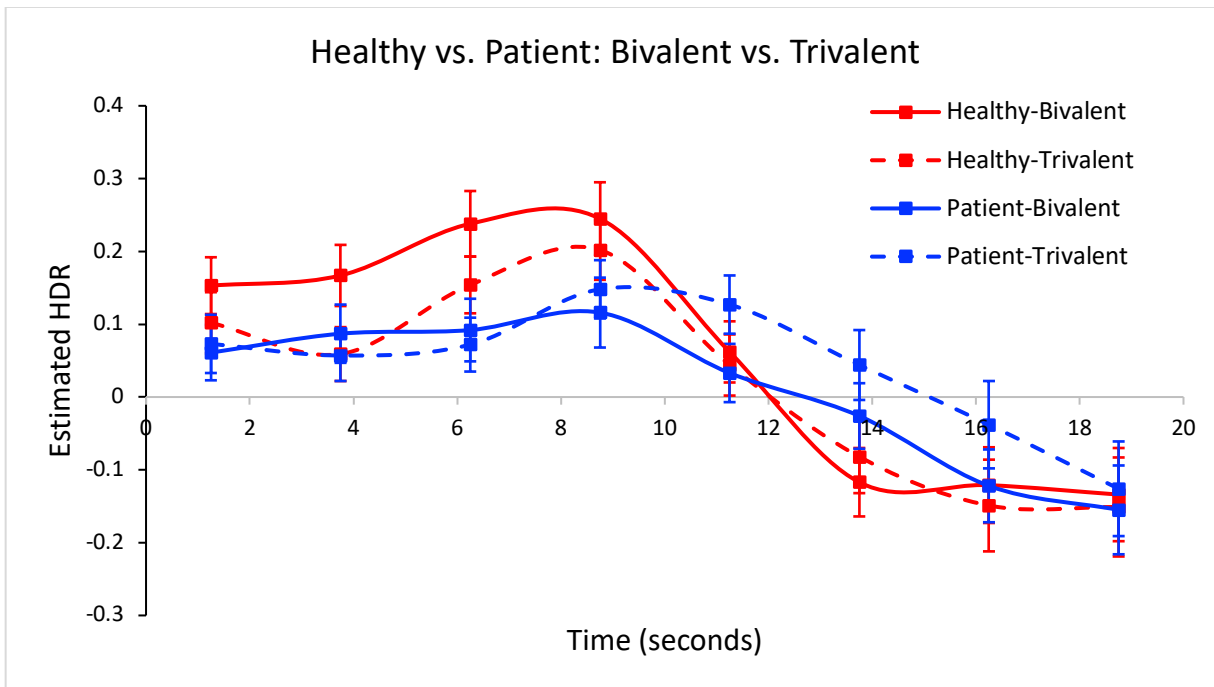


Figure 29. Bivalent vs. Trivalent for Healthy vs. Patient conditions

9.1 Metrical Stress Task (MS); Metric Stress Semantic Association Merge

The EXT network showed an initial increase in activation followed by a decrease from peak, and a net decline in activation throughout the Metrical Stress Task. Repeated ANOVA revealed significant effects of Time, $F(9,693) = 82.18, p < 0.001$, and significant effects of Conditions, $F(1,77) = 31.45, p < 0.001$. Significant effects of Conditions were also revealed, $F(1,77) = 31.45, p < 0.001$, with the phonological condition exhibiting a more gradual decline from peak and a higher level of EXT activation compared to the Semantic condition from timebins 3 to 4, $F(1,77) = 4.63, p < 0.05$, (Figure 30). The Semantic condition showed an earlier and greater peak suppression compared to the Phonological condition, and began to increase from peak suppression from timebins 5 to 6, $F(1,77) = 4.14, p < 0.05$, whereas the Phonological condition had just reached a later and less negative peak deactivation between those timebins (Figure 30). However, the Phonological condition showed greater levels of deactivation compared to the Semantic condition between timebins 8 to 9, $F(1,77) = 5.21, p < 0.05$, (Figure 30).

Significant interactions between Subjects \times Timebins were revealed, $F(9,77) = 4.27, p < 0.001$, where the Healthy condition showed a steep decline in EXT activation from peak between timebins 3 to 4, $F(1,77) = 5.84, p < 0.05$, and reached an earlier and greater suppression compared to that of the Schizophrenia condition (Figure 31). The Schizophrenic participants, however, dominated the interaction between timebins 6 to 7, $F(1, 77) = 4.57, p < 0.05$, where the Schizophrenic participants showed a higher level of EXT activation compared to Healthy participants (Figure 31). The Schizophrenic participants also showed a steeper decline in EXT activation between timebins 8 to 9, $F(1, 77) = 4.16, p < 0.05$, compared to the Healthy participants.

The EXT suppression suggests the linguistic processing of the word following stimuli presentation no longer requires sustained visual attention to the formation of the letters itself. The deactivation of the EXT network allows for the subject to focus on determining either the connotation or the stress placement of syllables of the word by shifting their attention to using other networks.

During the Phonological condition, the EXT network exhibited greater levels of activation, suggesting increased level of external attention required to determine where the stress should be placed on which of the two possible syllables. The Semantic condition, however, required less sustained attention on the external visual stimuli due to the task requiring the subject to identify the connotation of the word, rather than reading the word to determine the placement of stress on the syllables. Overall, the participants showed relatively similar levels of activation of the EXT network, however, the Schizophrenic participants showed fewer extreme ranges of activation and deactivation of the EXT network compared to the Healthy condition.

Figure 30. Varimax HDR for Conditions averaged over Subjects

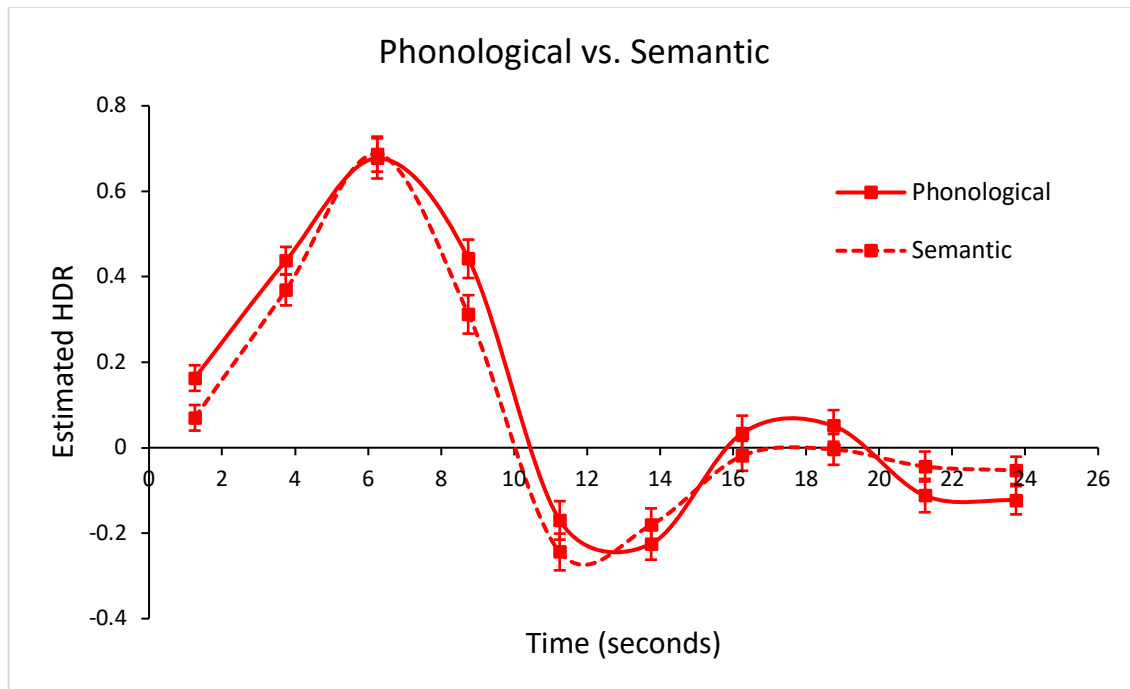
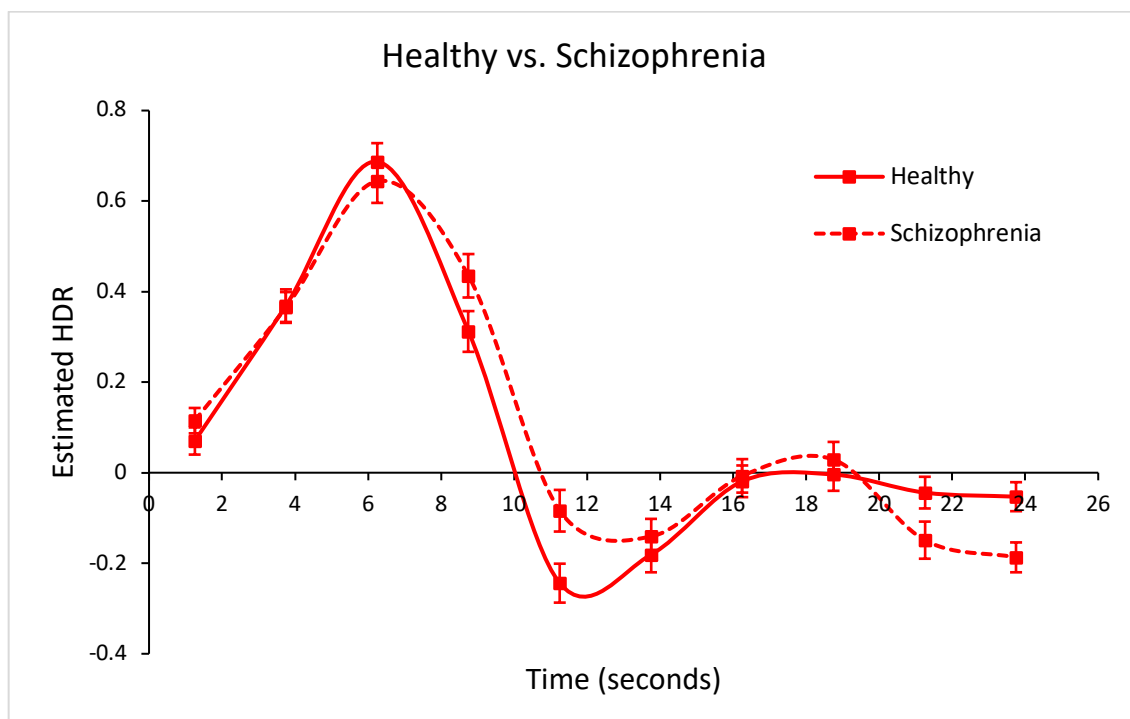


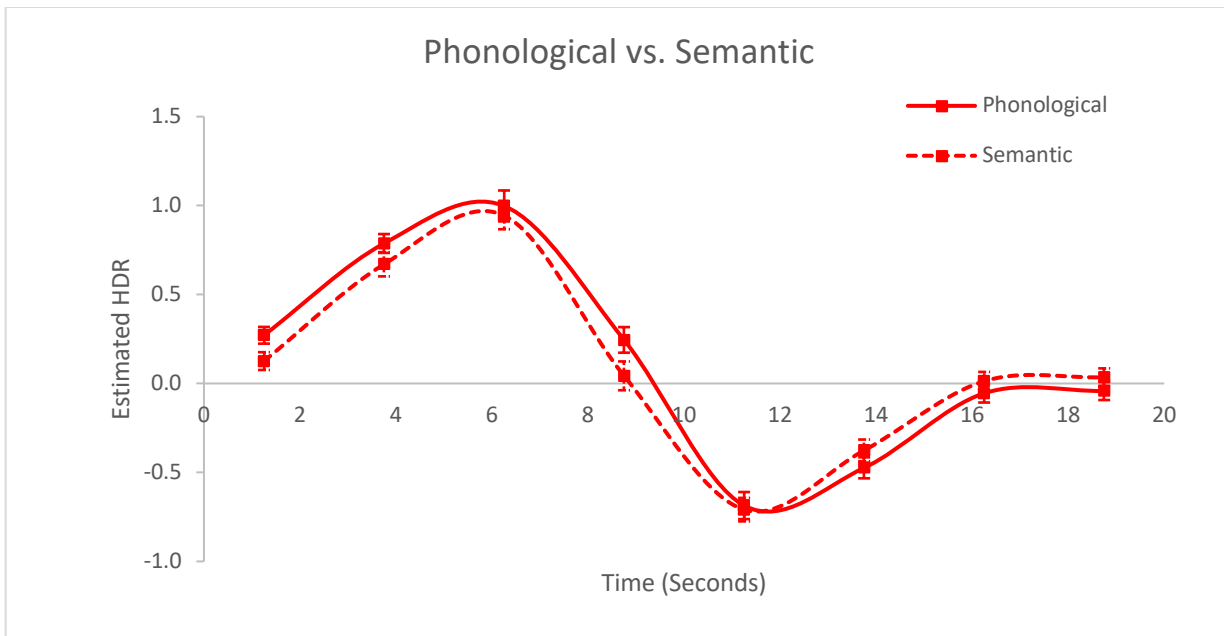
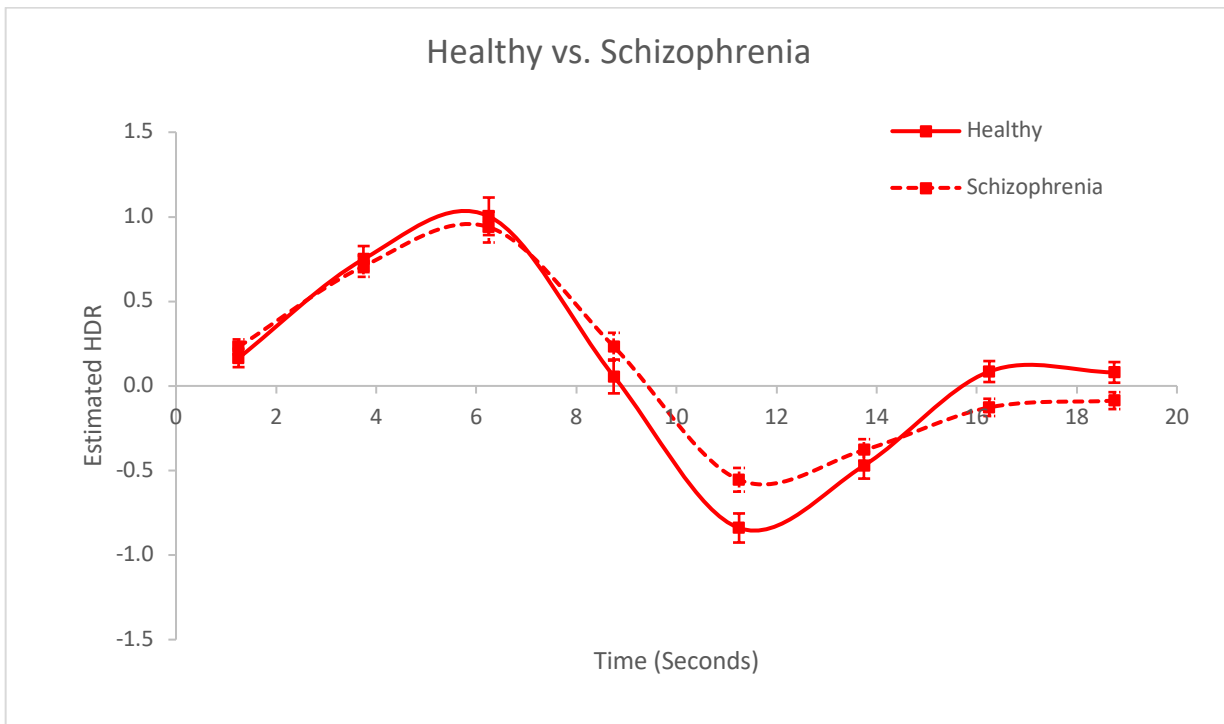
Figure 31. Varimax HDR for Subjects averaged over Conditions



9.2 Metrical Stress Task (MS); Triple Merge Thesis

The EXT network showed net increase in activity to peak activation before declining to peak suppression throughout the task. Repeated ANOVA revealed significant effects of Time, $F(7,546) = 101.82, p < 0.001$, as well as significant effects of Conditions (Phonological_Semantic), $F(1,78) = 14.94, p < 0.001$. Significant 2-way interactions were revealed between Conditions \times Timebins, with the Phonological condition showing significantly greater levels of activation throughout the task until reaching peak suppression, after which the Semantic condition showed greater level of activity on the return to baseline (Figure 32). Another significant interaction was revealed between Group \times Timebins, where the Schizophrenia group showed an increase in activity at a lower rate compared to that of the Healthy group between timebins 6 to 7. The Healthy group showed a steep increase in activation on the return to baseline, whereas the Schizophrenia group showed a slower rate of increase in activity on the return to baseline activation (Figure 33).

Overall, the EXT network showed increased activation during the initial task, before declining to peak suppression. Like the previous Metrical Stress task, the EXT network activation suggests the increased attention required to identify the word, with the suppression suggesting the deactivation of the EXT in order for the activation of other networks to identify the word's connotation or syllable stress placement.

Figure 32. Conditions (Phonological_Semantic) vs. Timebins*Figure 33. Varimax HDR for Subjects (Healthy_Schizophrenia) vs. Timebins*

10. FISH task

Mixed ANOVA revealed significant effects of Time factors, $F(9, 981) = 80.16, p < 0.001$, as well as a significant 2-way interaction between Match Status \times Timebins for various timebins. The Match condition showed a faster rate of increase in activation compared to the Nonmatch condition between timebins 2 to 3, $F(1, 109) = 5.40, p < 0.05$ (Figure 34). The Match condition reached an earlier, but lower peak activation at timebin 4 and begins to decline from peak at timebin 5, whereas the Nonmatch condition showed a delayed, but greater peak activation at timebin 5, $F(1, 109) = 12.511, p = 0.001$, before declining from peak (Figure 34). Another significant interaction between Strength of Evidence \times Timebins also emerged, with the Weak condition showed an increase in activation at a faster rate to peak compared to the Strong condition between timebins 3 to 4, $F(1, 109) = 13.19, p < 0.05$, before reaching peak activation between timebins 4 to 5, $F(1, 109) = 5.33, p < 0.05$, with the Weak condition reaching a higher level of activation compared to the Strong condition (Figure 35).

A significant 3-way interaction also emerged between Strength of Evidence \times Match Status \times Timebins, where both Strong conditions (Match and Nonmatch) showed similar levels of activation to peak from timebins 4 to 5, $F(1, 108) = 19.29, p < 0.001$, and the Weak conditions showing various levels of peak activation. The Nonmatch: Weak condition showed a delayed, and greater level of peak activation at timebin 5, whereas the Match: Weak activation showed an earlier and lower level of peak activation, at timebin 4 (Figure 36).

Another significant 3-way interaction emerged between the Subjects \times Match Status \times Timebins, with all conditions decreasing from peak activation from timebins 5 to 6, $F(1, 109) = 4.08, p < 0.05$, (Figure 37). The Healthy conditions reached the highest levels of peak activation, with the Healthy: Match condition reaching the highest level of peak activation. The Healthy:

Nonmatch condition exhibited an earlier, but lower peak activation. Both Schizophrenia conditions showed lower levels of peak activation compared to the Healthy conditions, with the Schizophrenia: Nonmatch condition showing a delayed, peak activation compared to that of the Schizophrenia: Match condition (Figure 37).

The EXT network showed increased activation during the Weak conditions of the Strength of Evidence, as lower levels of evidence require increased levels of visual attention to the fish stimulus, so the subject can correctly categorize the visual stimuli into one of the two ponds shown. Significant interactions between the subject groups were also identified, as the Schizophrenic subjects showed lower levels of activation in the EXT network for both conditions of Match Status, suggesting the Control groups had greater levels of EXT activation when focusing on the quantities of the fish in the two ponds during the task.

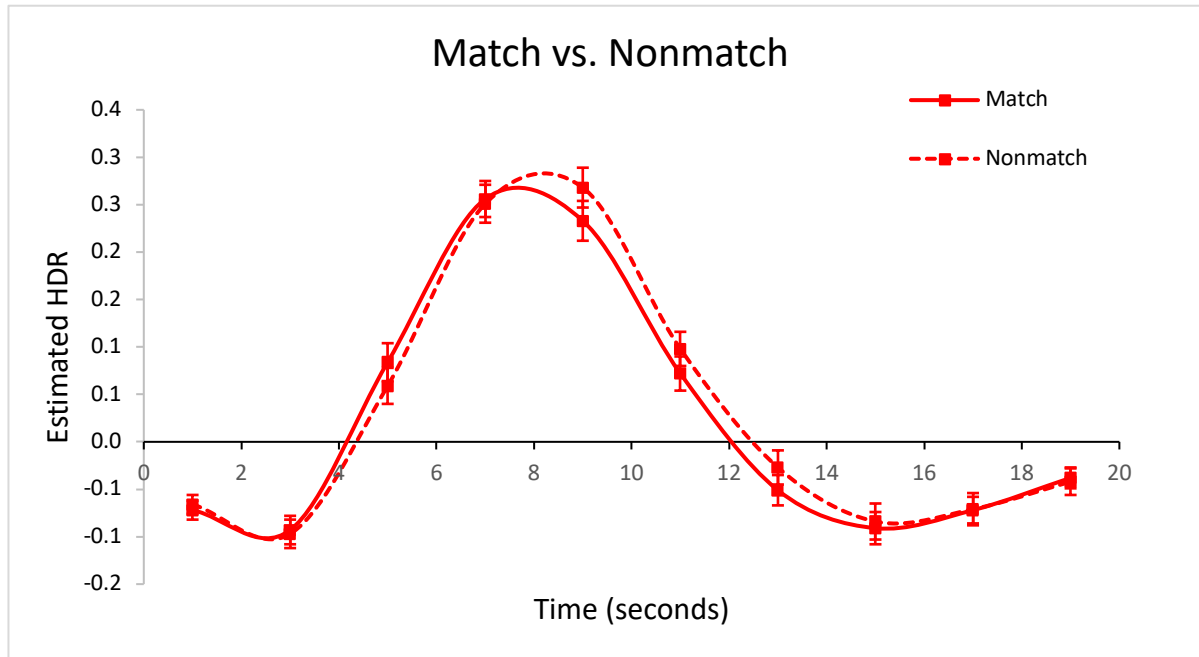
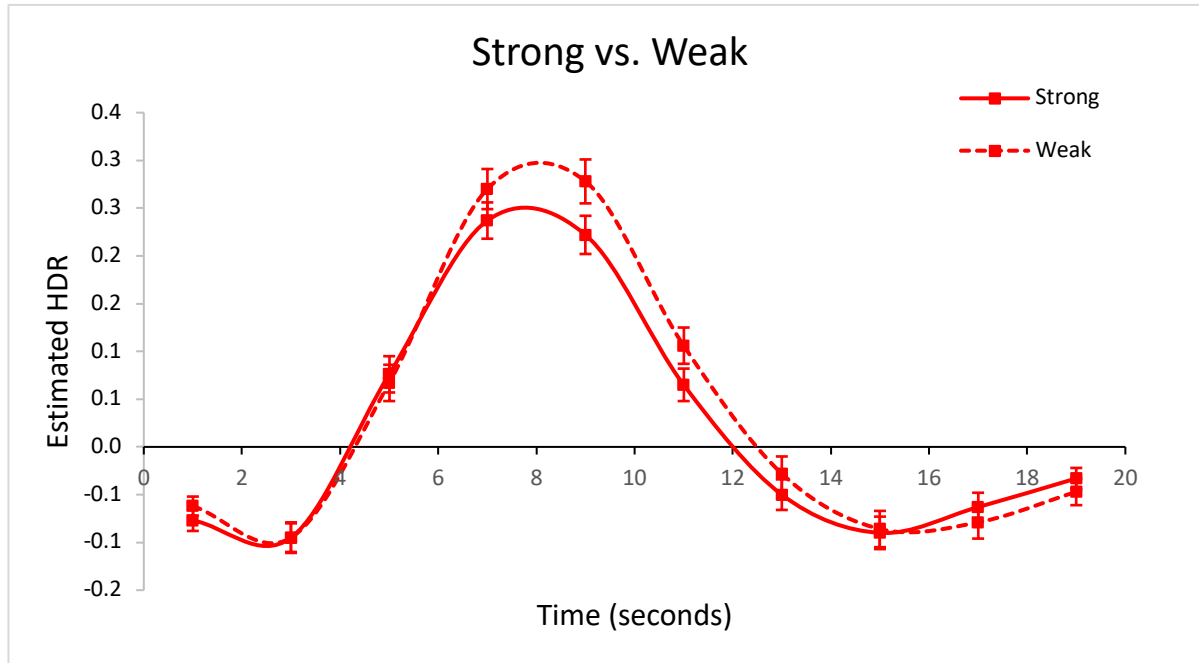
Figure 34. Varimax HDR of Orientation*Figure 35. Varimax HDR for Strength*

Figure 36. Varimax HDR of Match Status vs. Strength averaged over subjects

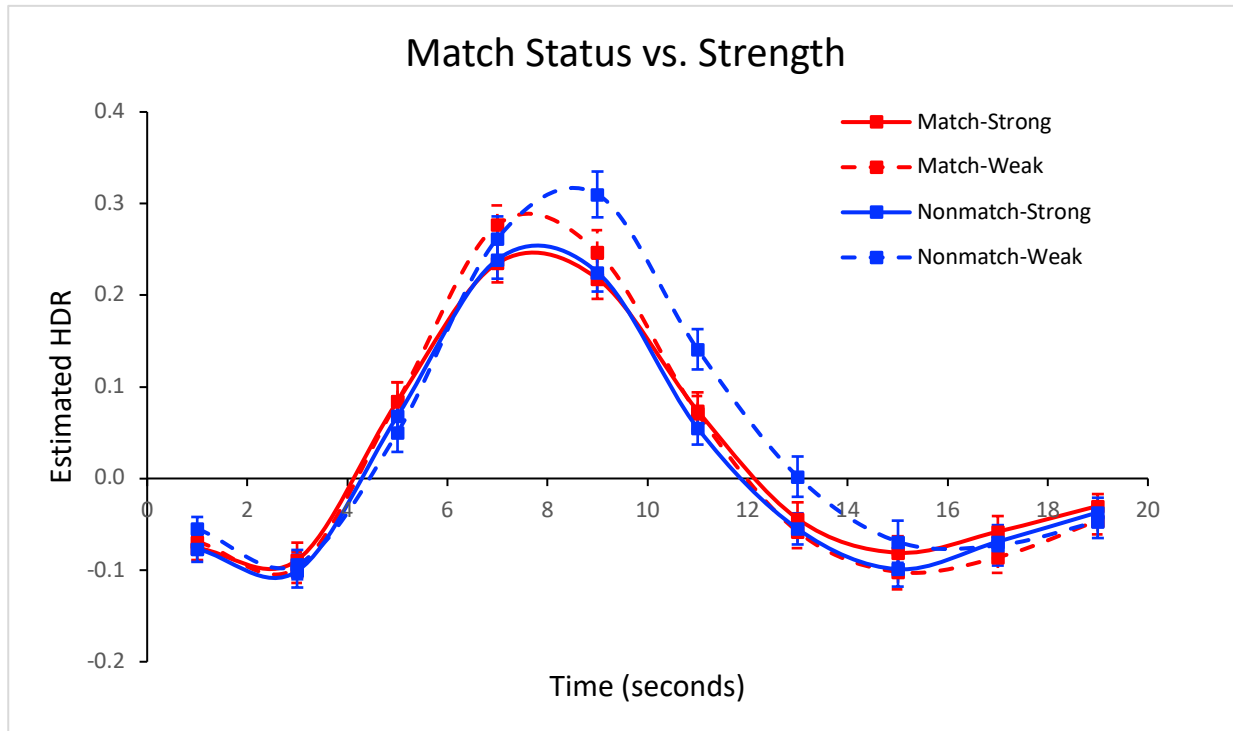
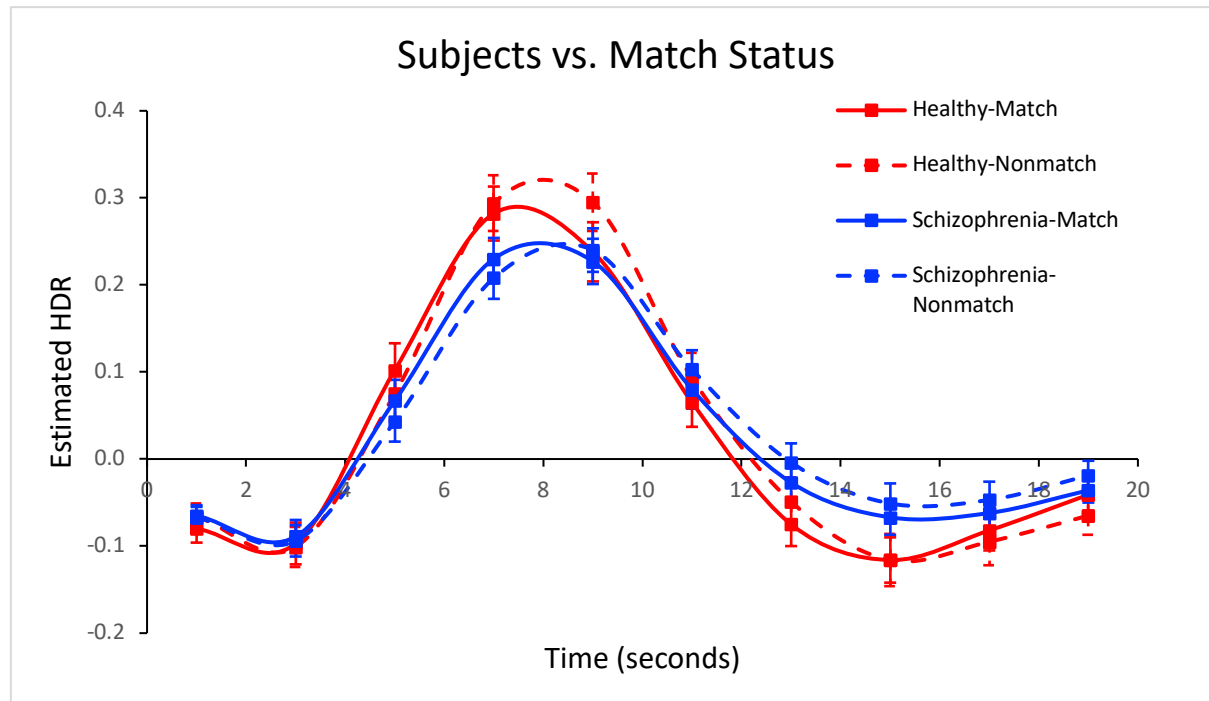


Figure 37. Varimax HDR of Subjects vs. Match Status averaged over Strength

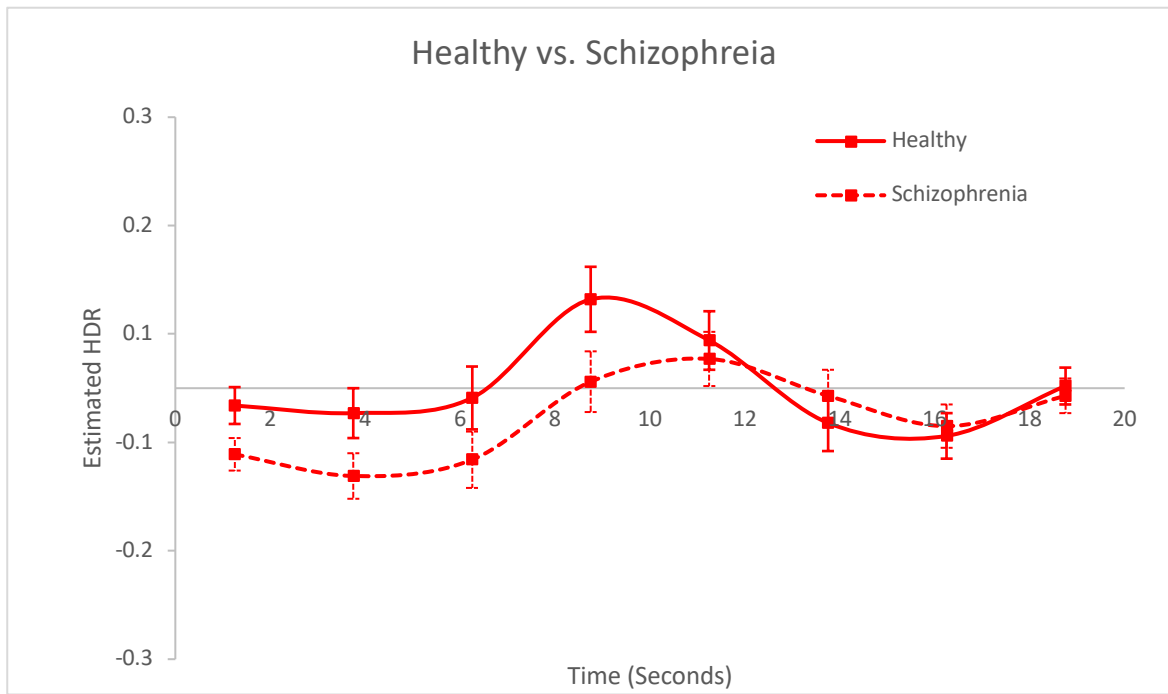


11. fBIRN Oddball Task; Triple Merge Thesis

Mixed ANOVA revealed significant effects only in the Time factor, $F(7, 742) = 5.902, p < 0.001$. The Time factor was significant between timebins 3 to 4, $F(1, 106) = 36.04$, timebins 5 to 6, $F(1, 106) = 16.73$, and timebins 7 to 8, $F(1, 106) = 15.39$, all with $p < 0.001$. There were no significant interactions shown between controls and patient groups.

Due to the lack of significant interactions between the patient and control groups, it is not possible to conclude whether there was a significant difference in EXT network activation during this task. However, the patient group did show a slightly lower level of activation of the EXT network throughout the task, suggesting possible reduced activation in the visual attention network during this task in those with schizophrenia, but this cannot be concluded confidently. The EXT network showed low levels of activation throughout, with one peak activation between timebins 3 to 5 in both groups (Figure 38), suggesting an increased activity in the EXT network when the subject was looking to select the correct answer through button press, however, when completing the auditory task the participants showed baseline levels of EXT activation, as the task primarily involves the auditory processing networks.

Figure 38. Varimax HDR for Groups (Healthy_Schizophrenia) vs. Timebins



Discussion

Through the analysis of the hemodynamic response curves of all tasks which recruited the Volitional Attention to External Representations network, an overall understanding of the function of the network can be formulated as a result. It can be concluded that the four main factors which are affect the level of activation in the EXT network are the degree of cognitive demand, degree of significance of the visual stimuli, the degree of visual attentional demand, and the demand for visual memory.

Increased levels of cognitive demand on tasks involving a language component appear to be directly correlated with the level of activity in the EXT network, possibly due to regions of the EXT network being involved in general attention and visual word recognition (Lavigne et al., 2020), as well as more difficult tasks requiring sustained and greater levels of visual attention prior to response. In both the Hard condition of the MS task and the Low condition of the SA task there was an increased level of EXT activation required to scan both options presented when the difficulty of the task increased regardless of subject group. Interestingly, the MS task in the Triple Merge Thesis (Enz, 2019) did not show significant levels of activity in the EXT network between the Patients and Controls. Regardless of group, the Phonological condition in both studies showed greater levels of activity compared to the Semantic condition, suggesting the identification of the syllable stress placement requires greater visual attentional demand compared to identification of the connotation of the word. Patients presented with hypoactivity in the EXT network compared to controls in both the High and Low conditions in the SA task as well as that of the MS task, suggesting a decreased level of sustained visual attention during word association tasks in those with schizophrenia. Overall, these studies suggests that greater levels of EXT activation are seen during more cognitively demanding tasks.

The degree of significance in the visual stimuli presented is directly correlated with the level of activation in the EXT network. In the Human Connectome Project Social Task, visual stimuli appearing to have social interactions elicited greater EXT activation compared to that of random motion of visual stimuli. Given that Lavigne noted increased EXT activation during environmentally salient stimuli presentation, it can be suggested that social interactions are considered environmentally salient, whereas random motion is not deemed significant enough for the participant to actively pay attention to it. In all Evidence Integration tasks, the EXT network exhibited increased activation in all Disconfirm conditions, regardless of group. The disconfirmation of a belief with presented visual stimuli requires increased attention towards the newly presented visual evidence, as this stimulus is now determined to be more significant in confirming the new response, followed by the rejection of the original response. The increased activation in the Disconfirm condition is supported in the literature by Lavigne et al., (2020) which stated the disconfirmation of the original answer requires increased visual attention to significant visual evidence, which is contradictory to the original belief, before concluding the rejection of the initial answer. Overall, the EXT network shows increased levels of activation when visual attention is directed towards visually significant stimuli, with the visually significant stimulus varying depending on the context of the task.

Tasks which require processing of visual stimuli immediately followed by immediate recall of the stimuli involved greater activation of the EXT network during the visual processing phase, followed by immediate and steep deactivation in the network during the recollection of the stimuli. During the MMCC task, the EXT network demonstrated a delayed and lower peak activation in the Patient group, as well as a reduced decrease from peak. Like the activation pattern seen in the SM and MS studies, hypoactivity in the EXT network of the patient group

supports the theory of reduced levels of visual attention to stimuli. The reduced decline from peak suggests inefficient suppression of the EXT network to prevent distraction by external stimuli during the recall phase of the task, supporting the hypothesis presented by Metzak et al. (2019), which suggested patients had an inefficient suppression of motor responses which are not involved in the task.

Tasks involving non-visually presented stimuli resulted in minimal activity of the EXT network, where the network showed a steady baseline level of activation throughout the task, as seen in the fBIRN Auditory Oddball Task. Between subjects and patients, there were no significant differences, suggesting the ability for patients to attend to auditory stimuli are like that of the controls, which rejects the hypothesis by Collier et al, (2014) that auditory processing sees higher levels of attentional deficits compared to visual processing in those with schizophrenia. By looking at the plot, it can be identified that the patient group shows a slightly lower level of activation in the EXT network, but not enough to be considered significant. This suggests due to the nature of the task being mostly reliant on auditory processing, the level of activity in the EXT network is steadily maintained at baseline due to the visual stimuli not being complex enough to require attentional demand in this task, therefore it is not possible to conclude a deficit in EXT network activation during this auditory task.

Overall, the level of cognitive demand and level of significance of visual stimuli are directly correlated with the level of EXT activation, whereas the involvement of visual memory or auditory processes are inversely correlated with the level of EXT activation. The findings from this study provide valuable information regarding levels of sustained attention in relationship to the type of stimuli which is presented to the participant, with the results suggesting any tasks with greater levels of cognitive demand and visually significant stimuli,

there will be greater levels of EXT activation. It can also be inferred that deactivation of the EXT network occurs when there's a strong level of attention directed towards auditory stimuli, as seen in the Auditory Oddball task. Additionally, tasks which do not require immediate visual attention will also show a deactivation in the EXT network, such as the MMCC task involving visual memory. Further studies regarding the connection between deviant tones and sustained visual attention, such as the Auditory Oddball task, should be performed to identify whether there is a significant difference between controls and patients in EXT network activation. With a better understanding of EXT network function through various task-based fMRIs, we can use this information to infer how aberrant activation patterns, or malfunction in certain brain regions involved in the EXT network can result in certain symptoms, and how to mediate those symptoms.

References

- Collier, A. K., Wolf, D. H., Valdez, J. N., Turetsky, B. I., Elliott, M. A., Gur, R. E., & Gur, R. C. (2014). Comparison of auditory and visual oddball fmri in schizophrenia. *Schizophrenia research*, 158(1-3), 183–188.
- Enz, R. (2019). *Identifying impairment in task-related functional brain networks in schizophrenia*. [Thesis for Cognitive Science, University of British Columbia].
- Fortenbaugh, F. C., DeGutis, J., & Esterman, M. (2017). Recent theoretical, neural, and clinical advances in sustained attention research. *Annals of the New York Academy of Sciences*, 1396(1), 70-91.
- Henson, R. (2006). Forward inference using functional neuroimaging: Dissociations versus associations. *Trends in Cognitive Sciences*, 10(2), 64-69.
- Lavigne, K. M., Metzak, P.D., Woodward, T.S. (2015). Functional networks underlying detection and integration of disconfirmatory evidence. *Neuroimage*, 112, 138-151.
<https://doi.org/10.1016/j.neuroimage.2015.02.043>
- Lavigne, K. M., Menon, M., Moritz, S., & Woodward, T. S. (2020). Functional brain networks underlying evidence integration and delusional ideation. *Schizophrenia Research*, 216, 302-309.

Lee, M. H., Smyser, C. D., & Shimony, J. S. (2013). Resting-state fMRI: A review of methods and clinical applications. *American Journal of Neuroradiology : AJNR*, 34(10), 1866-1872.

Metzak, P.D., Sanford, N., Percival, C., Gill, K., Noureddine, K., Ritchie, C., Hsiao, H., Wong, S., Woodward, T.S. (2019). Functional brain networks involved in attentional biasing in schizophrenia.

Percival, C. M., Zahid, H. B., Woodward, T. S. (2020). Task-Based Brain Networks Detectable with fMRI [fMRI image]. Github.com.

https://github.com/CNoS-Lab/Woodward_Atlas/tree/main/Network_Images

Sanford, N., Whitman, J. C., & Woodward, T. S. (2020). Task-merging for finer separation of functional brain networks in working memory. *Cortex*, 125, 246-271.

Sarter, M., Givens, B., & Bruno, J. P. (2001). *The cognitive neuroscience of sustained attention: Where top-down meets bottom-up*. Elsevier B.V.

Zhang, S., Zhang, S., Li, X., Li, X., Lv, J., Lv, J., Jiang, X., Jiang, X., Guo, L., Guo, L., Liu, T., & Liu, T. (2016). Characterizing and differentiating task-based and resting state fMRI signals via two-stage sparse representations. *Brain Imaging and Behavior*, 10(1), 21-32.

Characterization of a Novel Task-Based fMRI Functional Brain Network: Focus on Visual Features

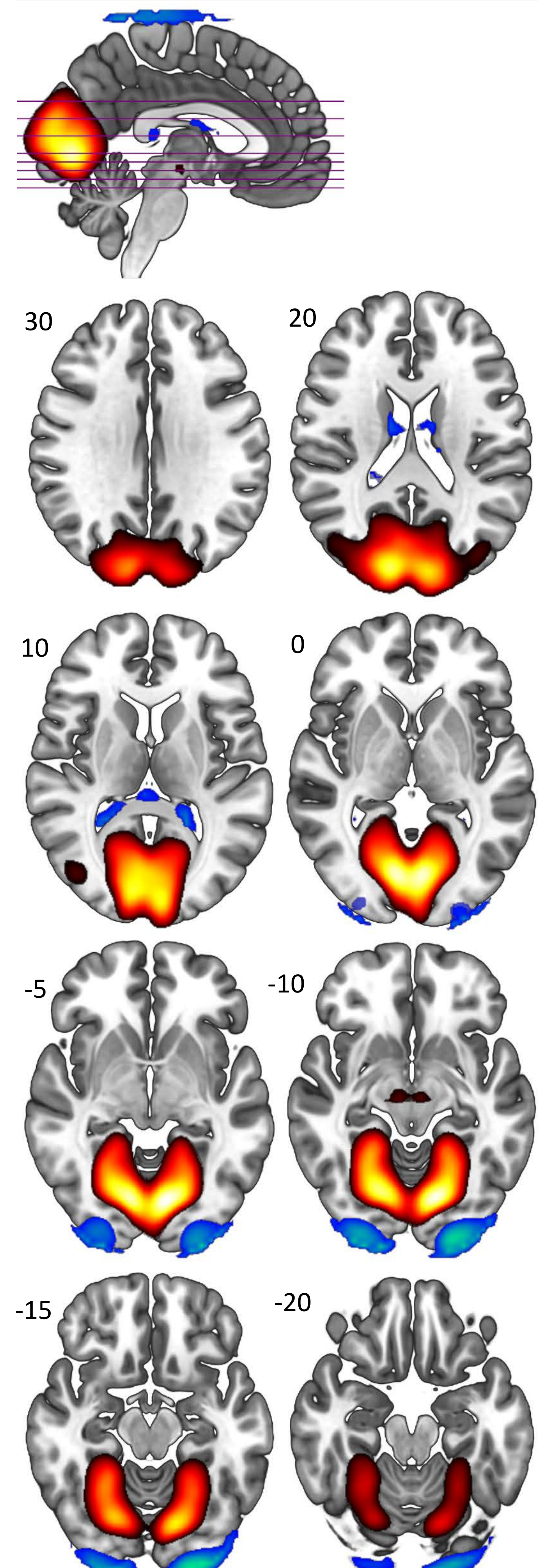
Chantal M. Percival^{1,2} & Todd S. Woodward^{1,2}

¹Department of Psychiatry, University of British Columbia, Vancouver, BC ²BC Mental Health & Substance Use Services, Vancouver, BC

INTRODUCTION

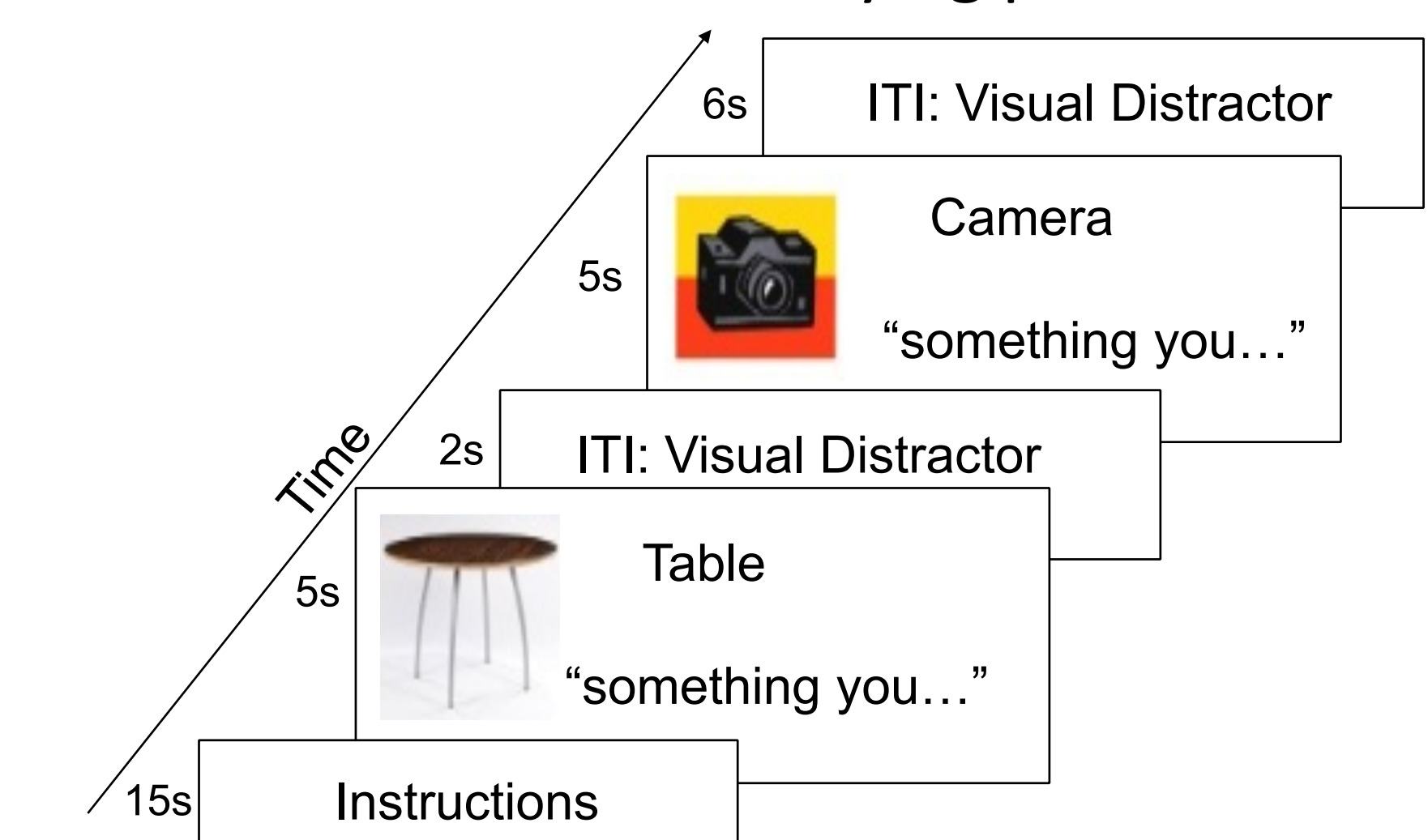
The novel focus on visual features (FVF) functional brain network has emerged in several task-based fMRI studies. FVF displays activation in the medial occipital and parietal cortex, with reciprocal suppression in the lateral occipital cortex (Sanford et al., 2020). However, the influence of task demands and conditions on activity remains ambiguous. Estimated hemodynamic responses (HDRs) may help contextualize FVF function.

RESULTS



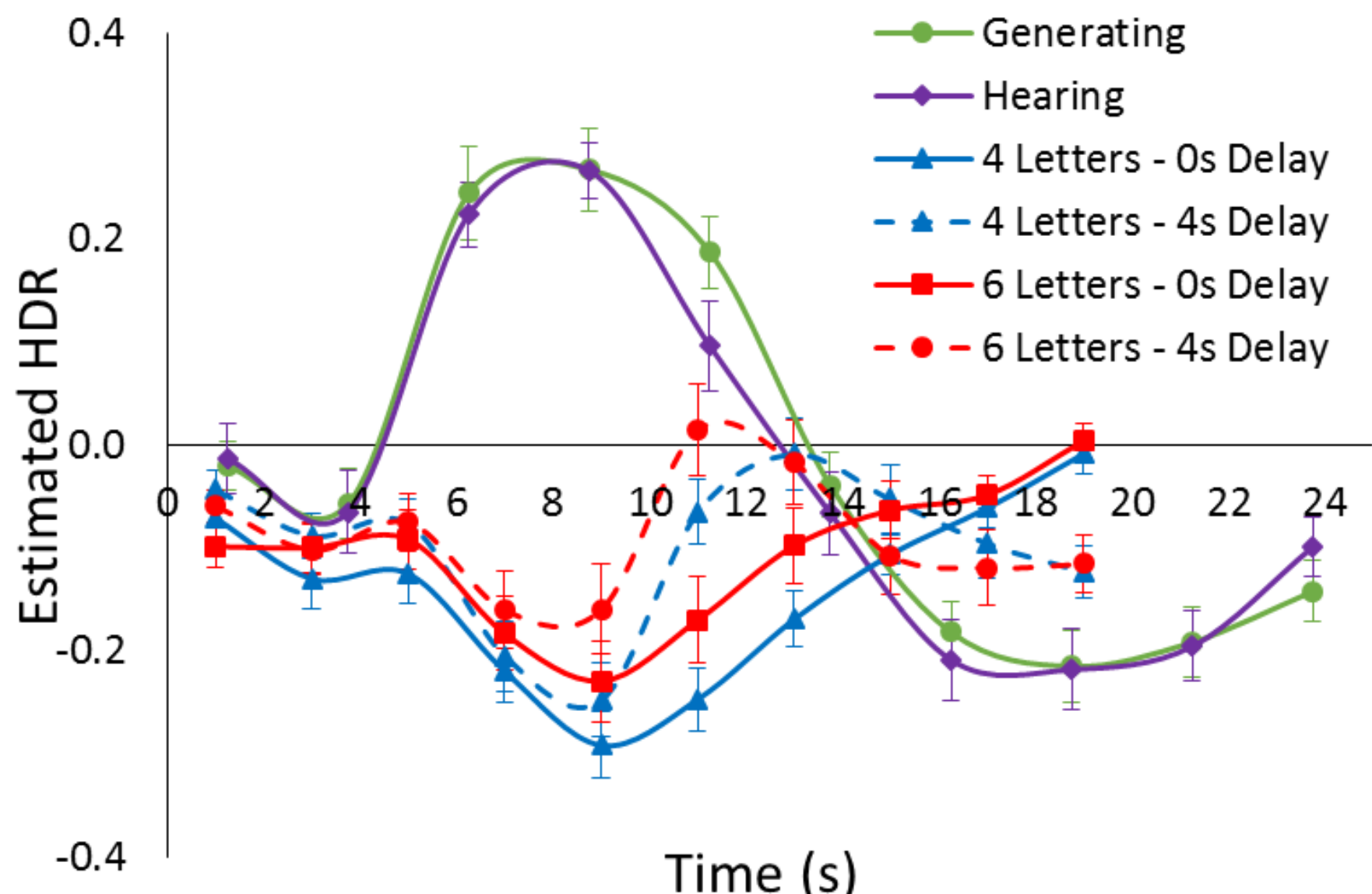
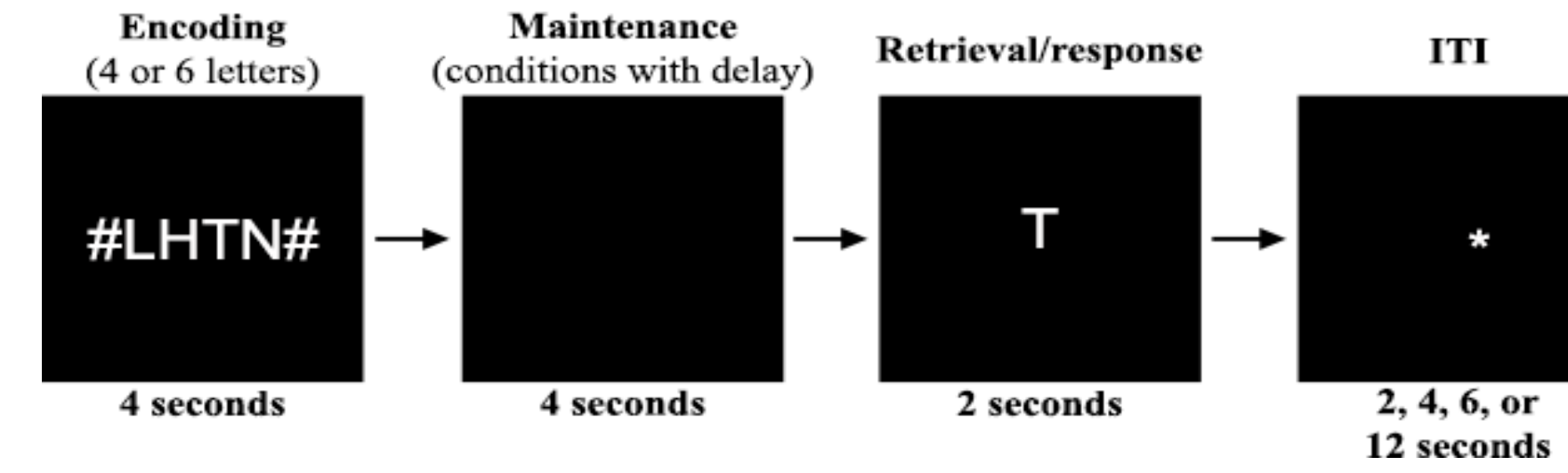
Thought Generating Task [3]

- Participants (n=32) either mentally generated or listened to a definition of a noun.
- FVF activation when studying pictures.



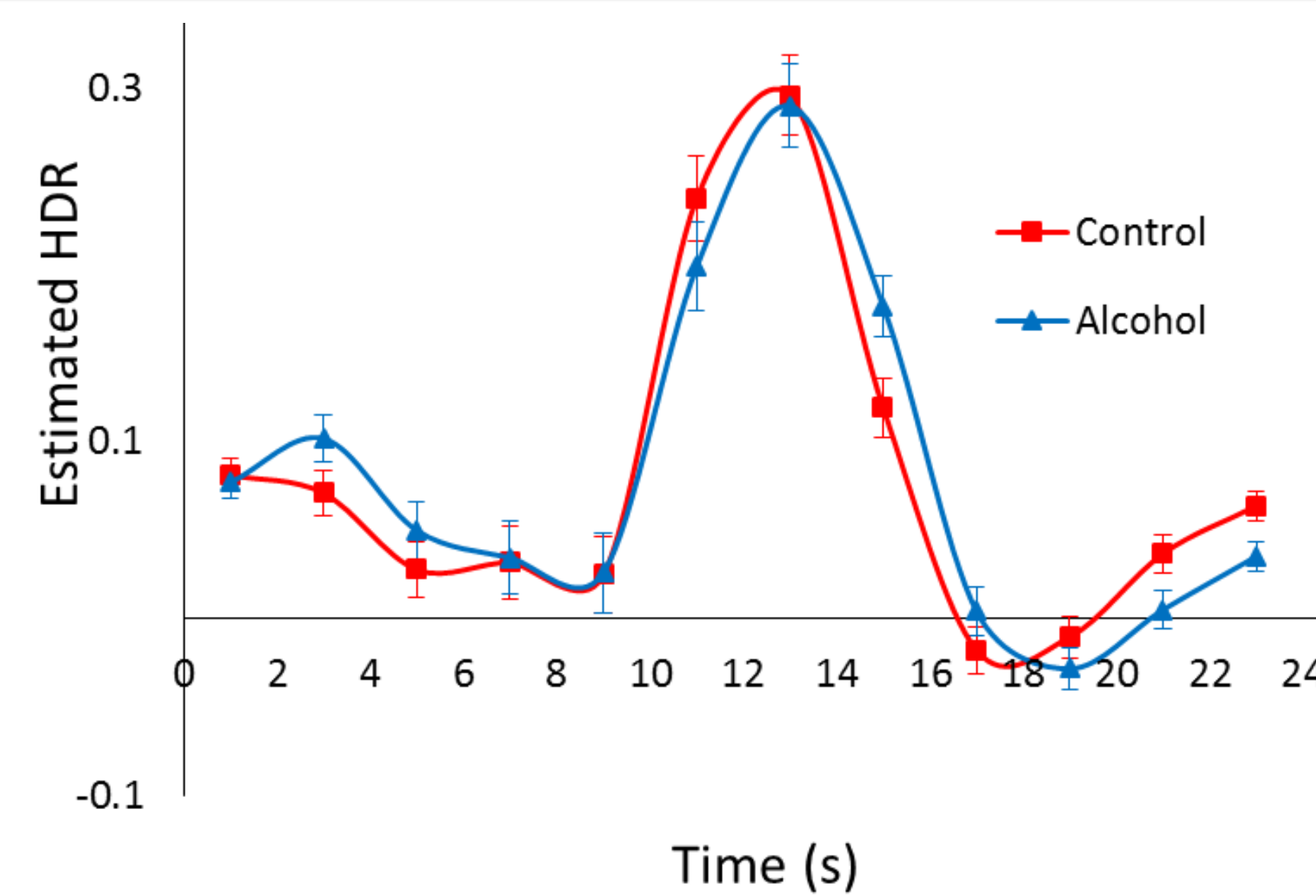
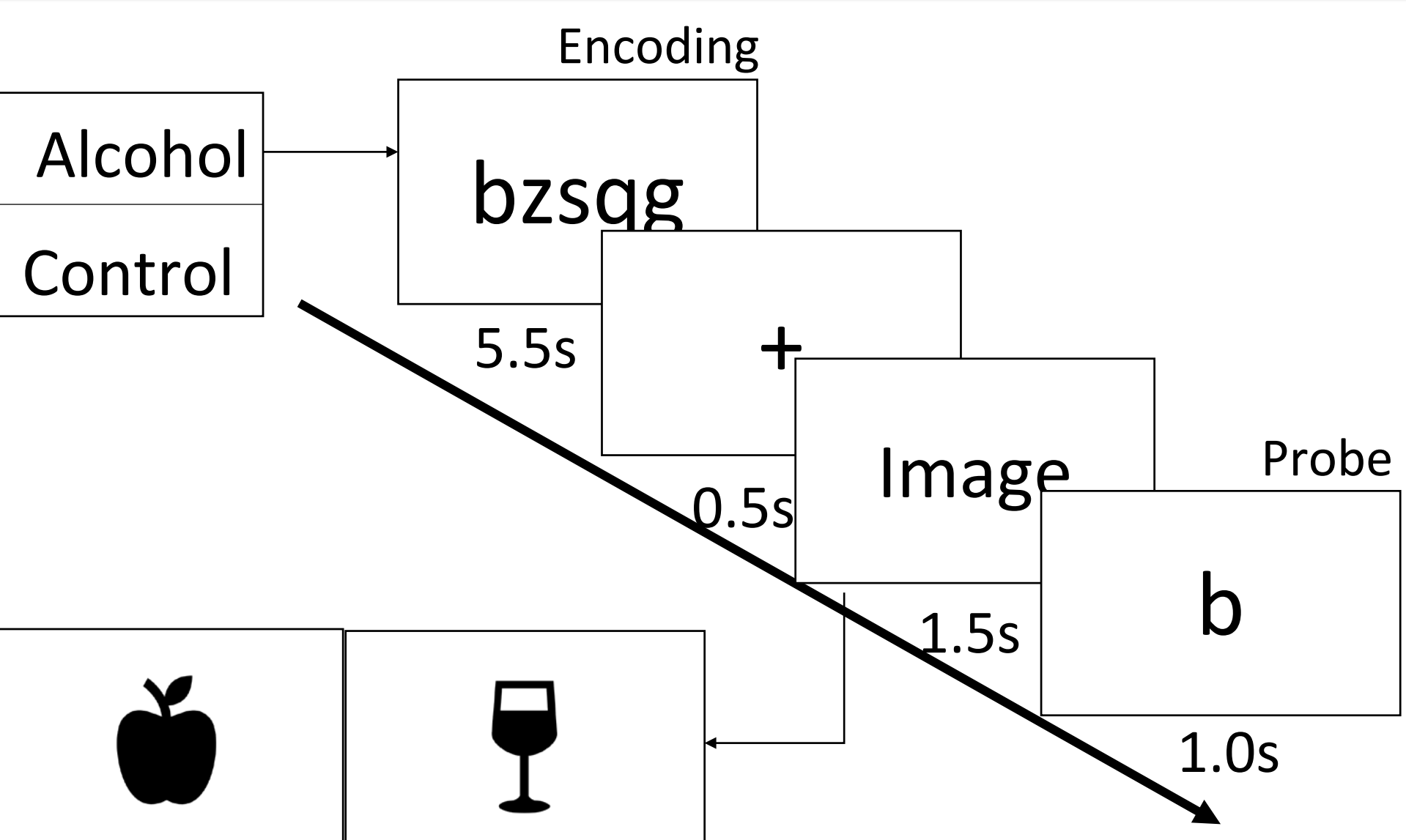
Working Memory [3]

- Participants (n=37) were presented with 4 or 6 letters, then were asked if a probe letter was found in the initial string immediately after, or after a 4 second delay.
- FVF suppression when remembering previously viewed letters.



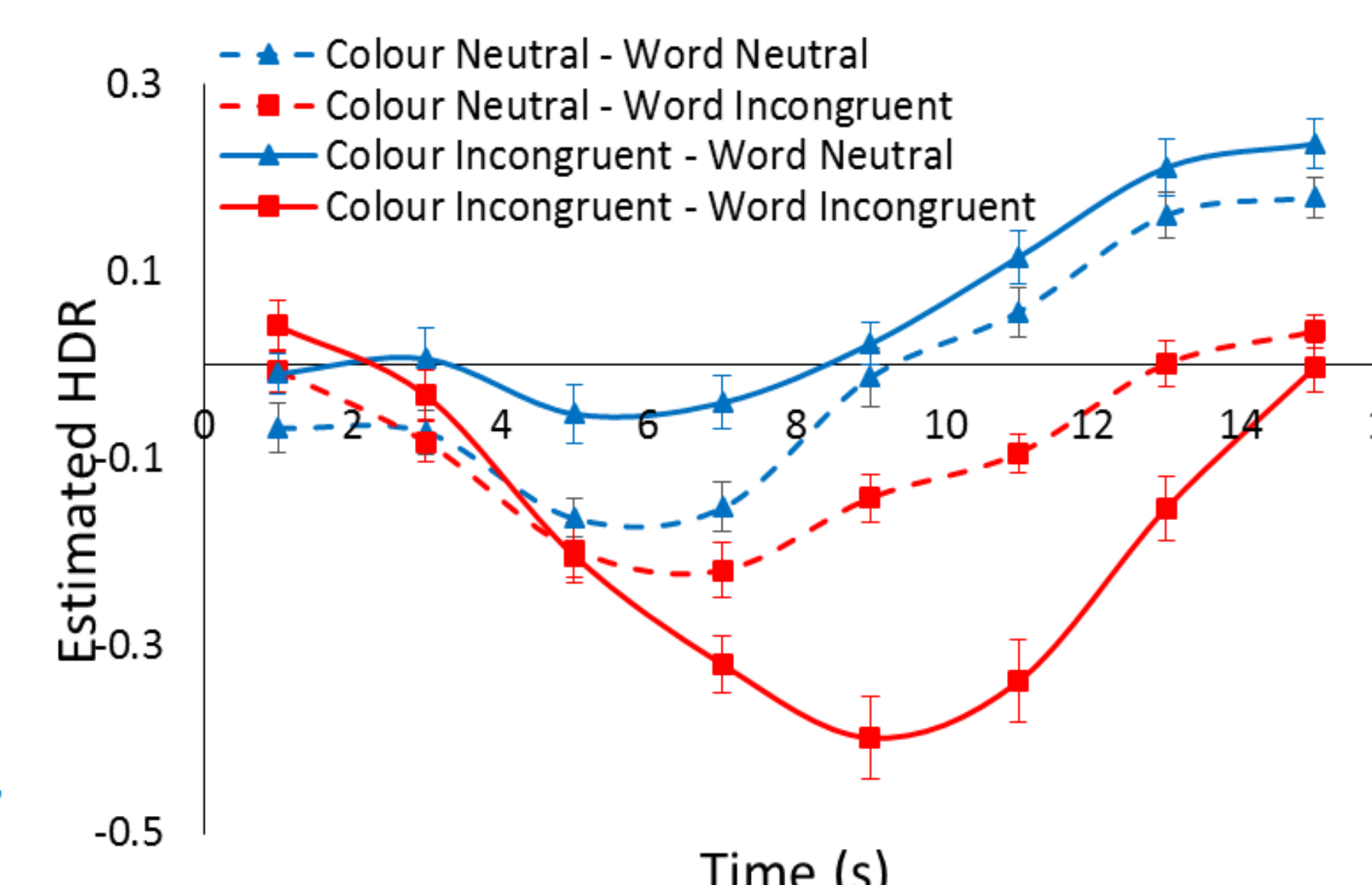
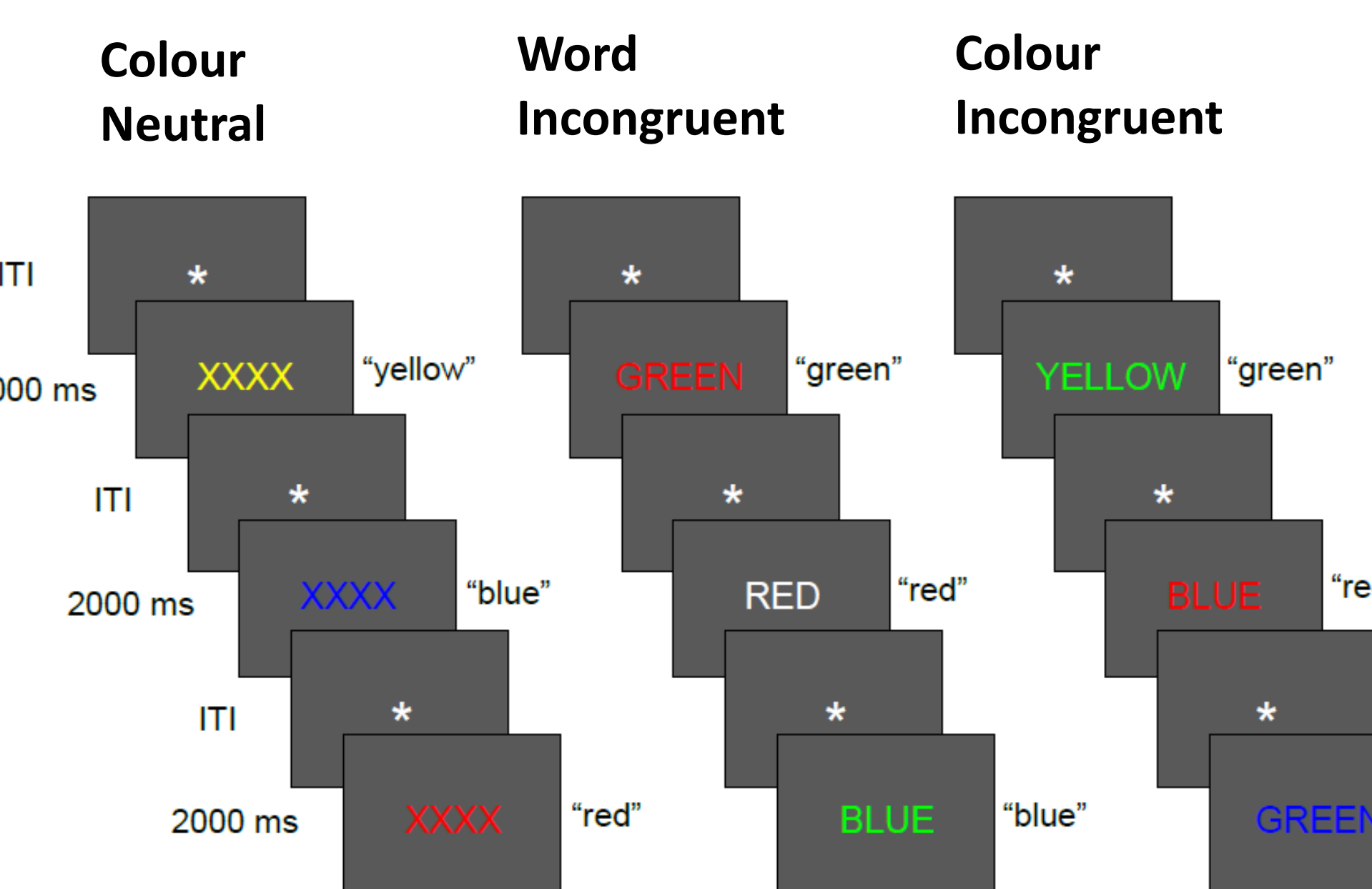
Alcohol Working Memory [1]

- Participants (n=71) were presented with 5 letters, then an image for 1.5 seconds. They were then asked if a probe letter was found in the initial string.
- Alcohol group received alcohol infusion, controls received saline infusion.
- Increased FVF activation upon presentation of image.



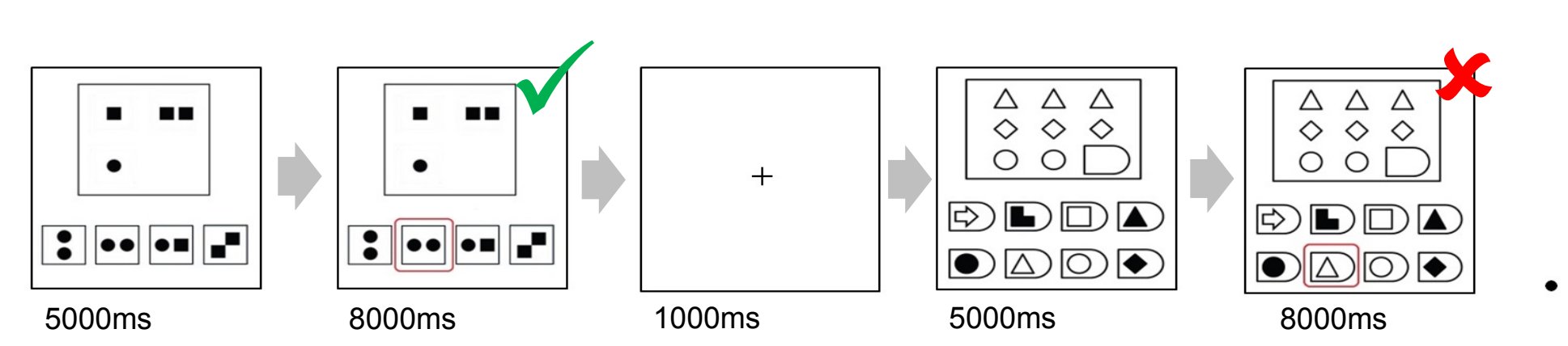
Task Switch Inertia [2]

- Participants (n=27) read colour words presented in neutral (white font) or incongruent coloured fonts. This followed blocks of colour naming with neutral (letter X) or incongruent (incongruent colour word) conditions.
- FVF suppression greatest in word incongruent conditions, when the visual features of presented stimuli had to be ignored.



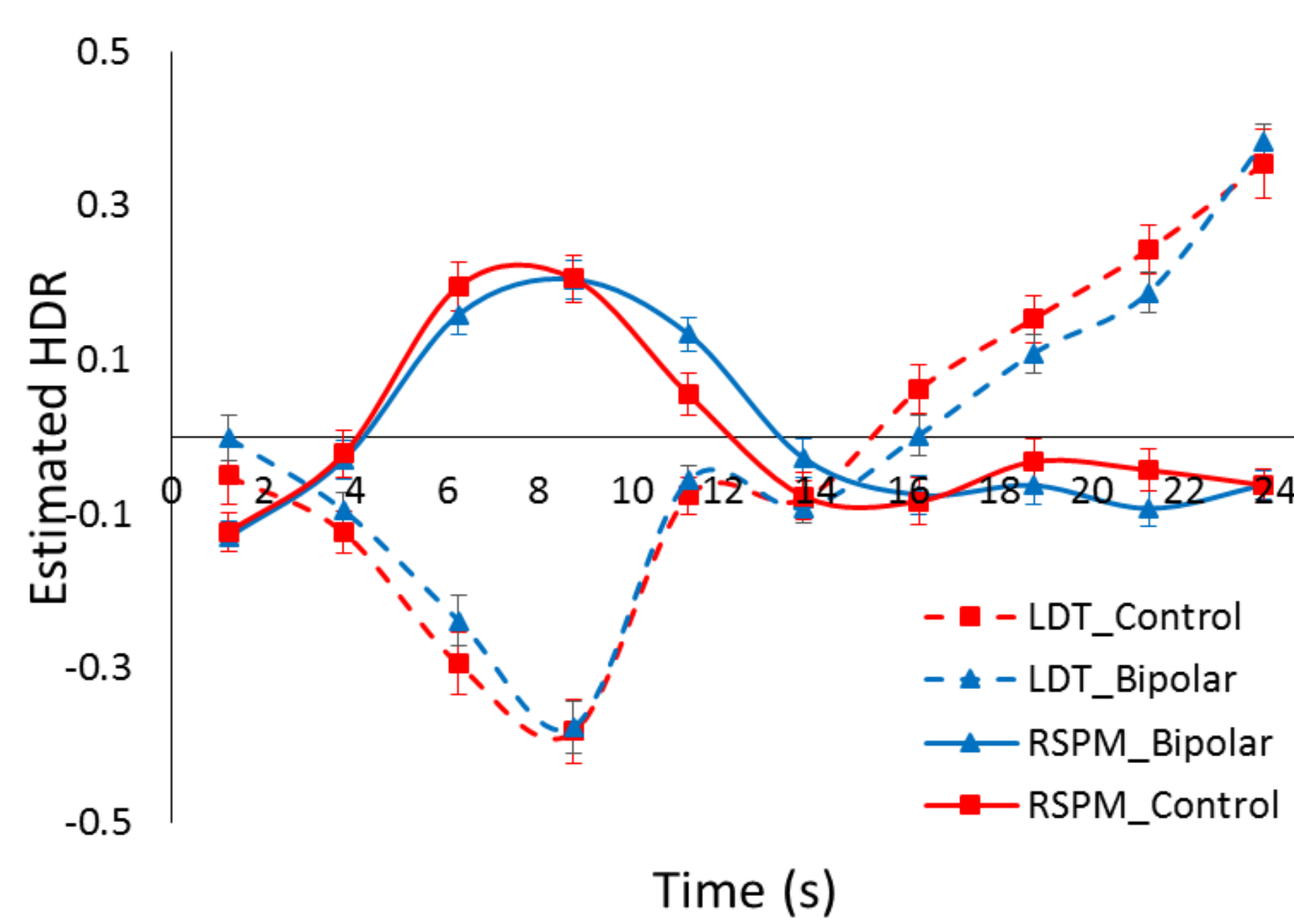
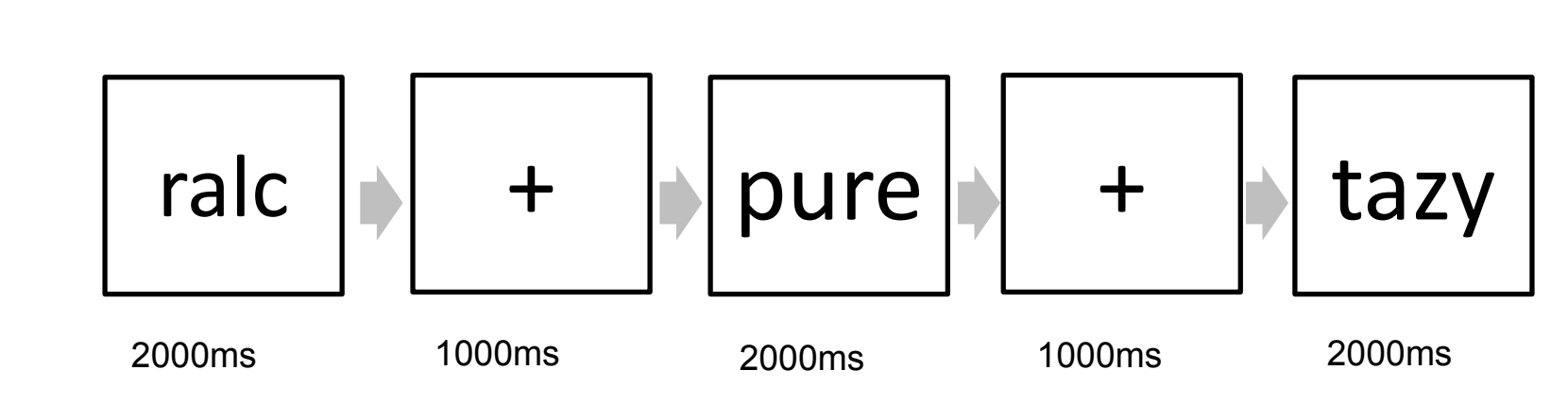
Raven's Standard Progressive Matrices

- Participants (control: n=18, bipolar: n=24) viewed matrix for 5 seconds before being given 8 seconds to determine if a suggested answer was correct.
- FVF activation when examining matrices.



Lexical Decision Task

- Participants decided whether four-letter sequences were real English words or not.
- FVF suppression when thinking of word formation rather than visual details.



CONCLUSION

- Results suggest that FVF activation occurs when having to focus on presented visual features, or in the presence of an image irrespective of task relevance.
- FVF appears to be suppressed when removing focus from presented visual features in order to perform task demands, such as focusing on semantic meaning of presented word, word formation, or encoding and maintaining in working memory.

REFERENCES

- [1] Brotchie, J. (2020). The Effect of Alcohol on the Functional Brain Networks Underlying Working Memory. [Unpublished]. University of British Columbia.
- [2] Sanford, N. (2019). Functional Brain Networks Underlying Working Memory Performance in Schizophrenia: A Multi-Experiment Approach. [Unpublished doctoral dissertation]. University of British Columbia.
- [3] Sanford, N., Whitman, J. C., & Woodward, T. S. (2020). Task-merging for finer separation of functional brain networks in working memory. Cortex, 125, 246-271. doi:10.1016/j.cortex.2019.12.014